5101-222
Flat-Plate
Solar Array Project

DOE/JPL-1012-88
Distribution Category UC-63b

Progress Report 21

for the Period April 1982 to January 1983

and Proceedings of the 21st Project Integration Meeting

Prepared for
U.S. Department of Energy
Through an Agreement with
National Aeronautics and Space Administration
by
Jet Propulsion Laboratory
California Institute of Technology
Pasadena, California

JPL PUBLICATION 83-48

Prepared by the Jet Propulsion Laboratory, California Institute of Technology, for the U.S. Department of Energy through an agreement with the National Aeronautics and Space Administration.

The JPL Flat-Plate Solar Array Project is sponsored by the U.S. Department of Energy and is part of the Photovoltaic Energy Systems Program to initiate a major effort toward the development of cost-competitive solar arrays.

This publication reports on work done under NASA Task RE-152, Amendment 66, DOE / NASA IAA No. DE-AI01-76ET20356.

ABSTRACT

This report describes progress made by the Flat-Plate Solar Array Project during the period April 1982 to January 1983. It includes reports on polysilicon refining, thin-film solar-cell and module technology development, central-station electric utility activities, silicon sheet growth and characteristics, advanced photovoltaic materials, cell and processes research, module technology, environmental isolation, engineering sciences, module performance and failure analysis and project analysis and integration. It includes a report on, and copies of visual presentations made at, the 21st Project Integration Meeting held at Pasadena, California, on January 12 and 13, 1983.

NOMENCLATURE

A	Ampere(s)
Å	Angstrom(s)
ac	Alternating current
AESD	Advanced Energy Systems Division (Westinghouse Electric Corp.)
AG	Allocation Guideline
AM	Air mass (e.g., AM1 = unit air mass)
AR	Antireflective
AR&D	Advanced research and development
ASEC	Applied Solar Energy Corp.
a-Si	Amorphous silicon
AS/ISES	American Section, ISES (q.v.)
ASME	American Society of Mechanical Engineers
ASTM	American Society for Testing and Materials
BA	Butyl acrylate
BOS	Balance of System (non-array elements of a PV system)
BPU	Basic Process Unit
BSF	Back-surface field
BSR	Back-surface reflection
BTU	British Thermal Unit
CAA	Computer-aided analysis
CER	Controlled-environment reactor
CFF	Cell fill factor
CLEFT	CLEaved Film Technique
cm	Centimeter(s)
CPVC	Chlorinated polyvinyl chloride
c-Si	single-crystalline silicon
CVD	Chemical vapor deposition

PRECEDING PAGE BLANK NOT FILMED

Cz	Czochralski (classical silicon crystal growth method)
dc	Direct current
DCS	Dichlorosilane
DOE	U.S. Department of Energy
EBIC	Electron-beam-induced current
EFG	Edge-defined film-fed growth (silicon ribbon growth method)
EMA	Ethylene methyl acrylate
EPDM	Ethylene-propylene-diene monomer
EPRI	Electric Power Research Institute
EPSDU	Experimental process system development unit
ESP	Edge-supported pulling (silicon-sheet production process)
EVA	Ethylene vinyl acetate
FBR	Fluidized-bed reactor
FEM	Finite-element method
FF	Fill factor
FOB	f.o.b., free on board
FSA	Flat-Plate Solar Array Project
FSR	Free-space reactor
GE	General Electric Co.
GFCI	Ground-fault circuit interruptor
HEM	Heat-exchange method (silicon-crystal ingot-growth method)
I_{sc}	Short-circuit current
I-V	Current-voltage
ID	Inside diameter
IEEE	Institute of Electrical and Electronics Engineers
IIT	Illinois Institute of Technology
IITRI	IIT Research Institute
Inv	Invar

IPEG	Improved Price Estimation Guidelines
IPEG2	IPEG, non-computerized
IPEG4	IPEG, computerized
IR	Infrared
ISES	International Solar Energy Society
ITO	Indium-tin oxide
ITW	Illinois Tool Works
J_{sc}	Short-circuit current
JPL	Jet Propulsion Laboratory
kcal	Kilocalorie(s)
kg	Kilogram(s)
kW	Kilowatt(s)
LAPSS	Large-area pulsed solar simulator
LASS	Low-angle silicon sheet growth method
LIN	Distance from bottom of web furnace lid to web growth front
LOI	Letter of interest
LPE	Liquid-phase epitaxy
m	Meter(s)
MBE	Molecular-beam epitaxy
MCCC	Mississippi County Community College (Arkansas)
MCS	Monochlorosilane
MEPSDU	Module experimental process system development unit
mgSi	Metallurgical-grade silicon
MIS	Metal-insulator-semiconductor (cell configuration)
mm	Millimeter(s)
mod	Module
MPFA	Module Performance and Failure Analysis Area (of FSA)

MSEC	Mobil Solar Energy Corp.
m-Si	Microcrystalline silicon
MT	Metric ton(s)
MW	Megawatt(s)
NASA	National Aeronautics and Space Administration
NEC	National Electrical Code
NMA	Non-mass-analyzed
NOC	Nominal operating conditions
NOCT	Nominal operating cell temperature
ODAS	On-site data acquisition system
OFHC	Oxygen-free hard copper
O&M	Operating and maintenance
P	Power
P	Probability
P_{max}	Maximum power
PA&I	Project Analysis and Integration Area (of FSA)
P/FR	Problem-failure report
PC	Power conditioner
PCF	Power-conditioning system
PCS	Power-conditioner system
PC/TS	Performance Criteria/Test Standards (SERI)
PDU	Process development unit
PE	Polyethylene
PEBA	Pulsed electron beam annealing
PIM	Project Integration Meeting
PMMA	Polymethyl methacrylate
PnBA	Poly-n-butyl acrylate

PPG	Pittsburgh Plate Glass Co.
PRDA	Program Research and Development Announcement
psia	Pounds per square inch, absolute
psig	Pounds per square inch, gauge
PU	Polyurethane
PV	Photovoltaic(s)
PVB	Polyvinyl butyral
PVC	Polyvinyl chloride
PVD	Physical vapor deposition
QE	Quantum efficiency
R&D	Research and development
RCA	RCA Corp.
RES	Residential Experiment Station
RFP	Request for proposal
RFQ	Request for quotation
RH	Relative humidity
ROI	Return on investment
RTV	Room-temperature vulcanized
S	Incident solar energy
SAMIS	Standard Assembly-Line Manufacturing Industry Simulation
SCE	Southern California Edison Co.
SD	Standard deviation
SDG&E	San Diego Gas and Electric Co.
SDSU	San Diego State University
Secco	Etching technique
SEM	Scanning electron microscope
SERI	Solar Energy Research Institute
SIMRAND	SIMulation of Research ANd Development Projects

SIMS	Secondary ion mass spectroscopy
SMUD	Sacramento Municipal Utility District
SoCal	Southern California
SOA	State of the art
SOC	Silicon on ceramic (crystal growth method)
SOC	Standard operating conditions (module performance)
Sohio	Standard Oil Co. of Ohio
SOLMET	Solar radiation surface meteorological observations
SS	Stainless steel
STC	Silicon tetrachloride
STC	Standard test conditions
SYSGEN	A computer program
T	Temperature
TCS	Trichlorosilane
TEM	Transmission electron microscope
TMY	Typical meteorological year
TREI	Texas Research and Engineering Institute
TTU	Texas Tech University
UCC	Union Carbide Corp.
UCP	Ubiquitous crystallization process
UL	Underwriters Laboratories
UV	Ultraviolet
V	Volt(s)
V_{oc}	Open-circuit voltage
W	Watt(s)
W_p	Peak watt(s)
η	Greek letter eta: efficiency
μm	micrometer

METRIC CONVERSION FACTORS

Approximate Conversions to Metric Measures

Symbol	When You Know	Multiply by	To Find	Symbol
		LENGTH		
in	inches	*2.5	centimeters	cm
ft	feet	30	centimeters	cm
yd	yards	0.9	meters	m
mi	miles	1.6	kilometers	km
		AREA		
in^2	square inches	6.5	square centimeters	cm^2
ft^2	square feet	0.09	square meters	m^2
yd^2	square yards	0.8	square meters	m^2
mi^2	square miles	2.6	square kilometers	km^2
	acres	0.4	hectares	ha
		MASS (weight)		
oz	ounces	28	grams	g
lb	pounds	0.45	kilograms	kg
	short tons (2000 lb)	0.9	tonnes	t
		VOLUME		
tsp	teaspoons	5	milliliters	ml
Tbsp	tablespoons	15	milliliters	ml
fl oz	fluid ounces	30	milliliters	ml
c	cups	0.24	liters	l
pt	pints	0.47	liters	l
qt	quarts	0.95	liters	l
gal	gallons	3.8	liters	l
ft^3	cubic feet	0.03	cubic meters	m^3
yd^3	cubic yards	0.76	cubic meters	m^3
		TEMPERATURE (exact)		
°F	Fahrenheit temperature	5/9 (after subtracting 32)	Celsius temperature	°C

*1 in = 2.54 (exactly). For other exact conversions and more detailed tables, see NBS Misc. Publ. 286, Units of Weights and Measures, Price $2.25, SD Catalog No. C13.10:286.

Approximate Conversions from Metric Measures

Symbol	When You Know	Multiply by	To Find	Symbol
		LENGTH		
mm	millimeters	0.04	inches	in
cm	centimeters	0.4	inches	in
m	meters	3.3	feet	ft
m	meters	1.1	yards	yd
km	kilometers	0.6	miles	mi
		AREA		
cm^2	square centimeters	0.16	square inches	in^2
m^2	square meters	1.2	square yards	yd^2
km^2	square kilometers	0.4	square miles	mi^2
ha	hectares (10,000 m^2)	2.5	acres	
		MASS (weight)		
g	grams	0.035	ounces	oz
kg	kilograms	2.2	pounds	lb
t	tonnes (1000 kg)	1.1	short tons	
		VOLUME		
ml	milliliters	0.03	fluid ounces	fl oz
l	liters	2.1	pints	pt
l	liters	1.06	quarts	qt
l	liters	0.26	gallons	gal
m^3	cubic meters	35	cubic feet	ft^3
m^3	cubic meters	1.3	cubic yards	yd^3
		TEMPERATURE (exact)		
°C	Celsius temperature	9/5 (then add 32)	Fahrenheit temperature	°F

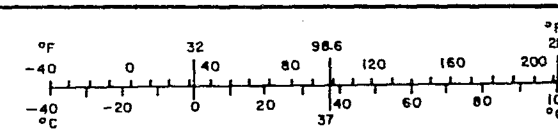

ORIGINAL PAGE IS
OF POOR QUALITY

CONTENTS

PROGRESS REPORT

Tables

PRECEDING PAGE BLANK NOT FILMED

PROJECT INTEGRATION MEETING

PROCEEDINGS

PROGRESS REPORT

Project Summary

INTRODUCTION

This report describes the activities of the Flat-Plate Solar Array Project (FSA) from May 1981 to January 1983, including the 21st FSA Project Integration Meeting (PIM), held on January 12 and 13, 1983.

FSA, sponsored by the U.S. Department of Energy (DOE), has the responsibility for advancing solar array technology while encouraging industry to reduce the price of arrays to a level at which photovoltaic (PV) electric power systems will be competitive with more conventional power sources. This responsibility has included developing the technology for producing low-cost, long-life photovoltaic modules and arrays. More than 100 organizations have participated in FSA-sponsored research and development of low-cost solar module manufacturing and mass-production technology, the transfer of this technology to industry for commercialization, and the development and testing of advanced prototype modules and arrays. Economic analyses were used to select, for sponsorship, those research and development efforts most likely to result in significant cost reductions. Set forth here is an account of the progress that has been made during the reporting period.

SUMMARY OF PROGRESS

Silane was successfully produced in early January 1983 in the experimental process system development unit (EPSDU) at Washougal, Washington, by Union Carbide Corp. (UCC), where operation continues under UCC funding. The silane EPSDU equipment title was transferred to UCC in exchange for EPSDU operational data. UCC has achieved complete conversion of silane into silicon during fluidized bed reactor (FBR) steady-state experiments. The FBR is being installed for operation in conjunction with the EPSDU, with JPL funding.

An advanced research 6-in.-dia FBR has been successfully operated by JPL in studies aimed at the characterization of the silicon deposition process using high concentrations of silane.

Initial results indicate that deposition of silicon on the reactor walls has been reduced significantly in cold-wall tests conducted by Hemlock Semiconductor Corp. during research on its polysilicon process.

A new silicon dendritic web furnace configuration at Westinghouse Electric Corp. has resulted in wider ribbons grown at higher growth rates with less stress.

Both Mobil Solar Energy Corp. and Westinghouse Electric Corp. are working on reduction of stresses induced in ribbons during growth.

PROGRESS REPORT

Solar cells made from three types of cast silicon wafers (Wacker Silso, Semix Inc. UCP, and Crystal Systems, Inc., HEM) had similar efficiencies, which were lower than those of Czochralski (Cz) cells, when fabricated using an advanced process.

Ethylene vinyl acetate (EVA) formulation A-9918 has been exposed to weatherometer ultraviolet light (UV) and temperature for more than 30,000 hours without significant change in properties.

Mild steel coated with polymeric coatings has withstood 3,000 hours of salt spray without corrosion.

Application of liquid dopants by use of a new meniscus coating machine has resulted in cell efficiencies equal to or greater than those of baseline gaseous-diffused cells. In making these cells, Westinghouse used a belt furnace instead of the usual tube furnace. In production, this technique would permit continuous cell processing.

Underwriters Laboratories (UL) published a document titled Proposed Standard for Safety, Flat-Plate Photovoltaic Modules and Panels.

An FSA paper on PV array--power conditioner interfaces titled "Characterization of the Electrical Output of Flat-Plate PV Arrays" was published at an IEEE meeting, and numerous other reports and documents on module reliability, design, and safety have been published.

Block IV module design, fabrication, and qualification testing activities, including publication of a User Handbook for Block IV Silicon Solar Cell Modules, have been completed.

Most of the Block V Group I Phase modules have been delivered to JPL.

The portable array data logger became operational in July 1982 and is being used to monitor numerous PV field arrays.

An economic analysis of 1982 PV module industrial practices using Cz technology compared well with a 1980 estimate of possible technologies that could be used in 1982, including f.o.b. factory prices and an actual late-1982 module price quote of less than $\$5.00/W_p$.

Economic analysis of module fabrication using today's dendritic web technology at a 25 MW/year production rate indicated that the f.o.b. price could be about $\$2.00/W_p$. Expected technology improvements should allow the price to be reduced to less than $\$0.60/W_p$ in a few years. Potential additional improvements might reduce the price to less than $\$0.50/W_p$ (1980 \$).

Economic analysis of lower-bound costs of encapsulation materials and processes for thin-film modules indicated that these costs can contribute from $\$0.12/W_p$ (large, 12%-efficiency modules) to $\$0.30/W_p$ (small, 8%-efficiency modules) to the total module price.

Studies of silicon abrasion by the University of Illinois indicate that cutting-fluid properties dictate whether the silicon surface is brittle or ductile and that microhardness correlates with the dielectric constant of the fluid.

Area Reports

PHOTOVOLTAIC COMPONENTS RESEARCH AREA

Advanced Materials Research Task

INTRODUCTION

The objective of the Advanced Materials Research Task is to identify the critical technical barriers to low-cost silicon (Si) purification and sheet growth that must be overcome to produce a photovoltaic cell substrate material at a price consistent with FSA objectives and then to perform and support research and development to address those barriers.

Present solar-cell technology is based on the use of silicon wafers obtained by ID slicing of Czochralski (Cz)-grown ingots from Siemens-reactor-produced semiconductor-grade Si. This method of obtaining single-crystal Si wafers is tailored to the needs of semiconductor device production (e.g., integrated circuits and discrete power and control devices other than solar cells). The small market offered by present solar-cell users does not justify industry's development of the high-volume Si production techniques that would result in low-cost photovoltaic electrical energy.

It is important to develop and demonstrate the feasibility of several processes for producing refined Si and sheet material suitable for long-life, high-efficiency solar photovoltaic energy conversion. To meet FSA objectives, sufficient research must be performed on a number of processes to determine the capability of each of producing large quantities of pure Si and large areas of crystallized Si at a low, competitive cost. The form of the refined Si must be suitable for use in the sheet-growth processes, and these must in turn be suitable for direct incorporation into automated solar-array industry schemes.

Silicon purification processes involving deposition of the material from silane and dichlorosilane are being pursued because these two substances can be purified relatively easily and, because of their high reactivity, they can be more readily decomposed or reduced to form Si than can trichlorosilane, which is used today in the conventional process.

FSA-funded improvements of the standard Czochralski ingot-growth process by reduction of expendable material costs and improvement of ingot growth rate together with improved slicing techniques have developed the technology so that large areas of Si can be produced. Growth of large ingots by casting techniques, such as the Ubiquitous Crystallization Process (UCP), may reduce sheet costs further.

Growth of crystalline Si material in a geometry that does not require cutting to achieve proper thickness is an obvious way to eliminate costly processing and material waste. Growth techniques such as edge-defined film-fed growth (EFG) and dendritic-web growth are candidates for such solar-cell material.

ADVANCED MATERIALS RESEARCH TASK

SUMMARY OF PROGRESS

Semiconductor-Grade Silicon Refinement Processes

Silicon Refinement Using Silane (Union Carbide Corp.)

Union Carbide Corp. (UCC) is conducting research on the pyrolysis of silane in a fluidized-bed reactor (FBR), this being a critical step in the process sequence of metallurgical-grade Si to silane to semiconductor-grade Si. Silane synthesis is under active investigation in UCC's own pilot plant at Washougal, Washington.

A 6-in.-dia FBR process development unit (PDU) was operated with silane-fed concentrations up to about 24 mole % in hydrogen. A total of 33 hours consecutive run duration was accumulated, during which time approximately 26 kg of silicon product was withdrawn in batches, while fresh seed material was added to replenish the bed. The longest single run was 13 hours in steady state. A suitable operating window was identified with a gas distributor temperature below 300°C.

After completion of these tests, an FBR technology review was held. It was concluded that (1) a suitable operating window for the UCC FBR had been identified as a result of the long-duration tests in which steady-state operation was achieved; (2) greater than 20 mole % silane feed concentration could be maintained with total conversion to Si within the bed, making the process economically attractive; (3) further work is necessary to demonstrate product purity and to improve reactor performance.

The PDU, which was located in Tonawanda, New York, was dismantled and shipped to the Washougal site, where it is being reinstalled for further R&D using high-purity silane.

UCC completed construction of the silane pilot plant, using equipment from the DOE-supported EPSDU (Experimental Process System Development Unit) program. Title to this equipment had been transferred to UCC in exchange for silane operation data. The plant was checked out and early in January 1983 it produced silane for the first time.

Silicon Refinement Using Dichlorosilane (Hemlock Semiconductor Corp.)

Hemlock is conducting research on the critical portions of a process for making semiconductor-grade Si, in which dichlorosilane (DCS) is made from trichlorosilane (TCS) by a redistribution reaction using an organic amino functional catalyst, and the DCS is then reduced by hydrogen to produce Si in a chemical-vapor-deposition step using Siemens-type reactors.

In June 1982, Hemlock completed the Phase II effort, which consisted of checkout and operation of a DCS PDU integrated with intermediate-size and large-size Si-deposition reactors. In this program, an Si deposition rate of 2 g/h per cm of deposition rod length and a conversion efficiency of 38.7% (DCS to Si) were attained simultaneously, almost achieving the goals for these parameters (2 gm/h · cm and 40%, respectively). However, the reactor power consumption was 89.5 kWh/kg Si, appreciably above the goal of 60 kWh/kg.

ADVANCED MATERIALS RESEARCH TASK

When the PDU was shut down, the batch of catalyst in the redistribution reactor, which converts TCS to DCS, had produced 68,500 lb of DCS at a 13.6% molar conversion efficiency during its entire period of use, corresponding to 2090 lb of DCS/lb of catalyst. At this usage figure, the catalyst cost contributes a negligible amount to the product cost.

A major problem that was encountered was excessive deposition of Si on the reactor vessel (bell jar) wall, resulting in frequent bell-jar breakage and loss of Si product. Efforts to reduce this deposition had mixed results. Use of mixed feed -- i.e., feeds consisting of DCS mixed with either TCS or silicon tetrachloride (STC) -- reduced wall deposition and increased bell-jar life. However, the deposition rate on the Si rods was also reduced and does not allow program goals to be met. Post-run etching of Si from the bell jar by hydrogen chloride increased bell jar life by a factor of two. This technique appears to be both feasible and practicable as a method to control wall deposition.

The draft final report on the program since its inception in October 1979 was completed and delivered to JPL in January 1983.

With completion of the Phase II effort, Hemlock undertook an 18-month program in which, at its own expense, the output of the PDU was approximately tripled to 200 lb DCS/hr and this DCS was fed to various combinations of mid-size and large Siemens-type deposition reactors. The purpose is to characterize further and to optimize the performances of the PDU and the reactors. The enlarged PDU has operated well, achieving high on-line times.

In September 1983 a contract modification was executed for a research effort on a cold-metal-wall Si deposition reactor. The objective is to eliminate the excessive Si deposition on the inside surfaces of the reactor bell jar and thereby allow operation at optimum efficiencies, so as to increase DCS-to-Si conversion efficiency, increase Si deposition rates, and decrease reactor energy consumption.

The cold-wall reactor, which had been designed for use on TCS, was converted to DCS use and put into operation. Baseline tests were conducted to allow comparison with performance of similar-sized reactors having conventional (hot-wall) quartz bell jars. There were essentially no differences in Si deposition rate on the rods and in conversion efficiency of DCS to Si. The amounts of Si wall deposition were considerably lower for the cold-wall reactor than for the conventional reactor, a promising result.

Economic analysis of the DCS CVD process coupled with a hydrochlorination process indicates a manufacturing cost of $15.60/kg Si (1000-MT/yr plant, 1980 $), and product price of about $20/kg (1980 $, 10% return on investment) or about $25/kg for 20% ROI.

Silicon Refinement Process Supporting Studies

Hydrochlorination Reaction Investigation (Solarelectronics, Inc)

A research and development program is being carried out to study the hydrochlorination of STC and metallurgical-grade silicon to TCS in a 2-in.-dia reactor.

In this period, the contract was extended with the goal of providing basic understanding of the hydrochlorination reaction. The revised program plan includes a systematic study on reaction kinetic measurements to develop a rate equation, measurements on thermodynamic functions, and study of the reaction mechanism for the hydrochlorination reaction.

A number of kinetic models for the hydrochlorination reaction were developed and tested with previous and current kinetic measurements. Preliminary results showed that the rate of formation of TCS fits reasonably well in a pseudo-first-order rate equation. The rate constant, k_1, was measured over a temperature range of 450°C to 550°C. The activation energy, ΔE, was determined by plotting ln k_1 versus 1/T in the Arrhenius equation to give a value of 13.2 kcal/mole. Variation of the hydrogen and STC concentrations showed a small effect on the reaction rate. The rate constants decrease slightly with a decreasing H_2/STC feed ratio. The effect of pressure on the reaction rate was studied over the range from 25 to 500 psig. The pseudo-first-order rate constant decreases with increasing reaction pressure.

Experiments were also carried out to measure the equilibrium constant, K, for the hydrochlorination reaction for the temperature range of 500°C to 575°C. The heat of reaction, ΔH, was calculated by the Second Law method by plotting ln K versus 1/T in the Van't Hoff equation to give a value of 10.6 kcal/mole.

A new quartz hydrochlorination reactor was designed and built to study the mechanism of the hydrochlorination reaction, using the deuterium isotope. This quartz reactor will also be used for experiments at temperatures of 600°C and above.

Fluidized-Bed Reactor Research (Oregon State University)

A study of radiantly heated fluidized-bed reactors for silicon production was undertaken in this period by Oregon State University. The effort, consisting of non-reactive studies, is intended to form the basis of an engineering study to develop an internally heated reactor with relatively cool walls to minimize silicon deposition on the walls. Experiments were designed to obtain information concerning the effective absorptivity and the flow rate of heat; to determine the heating characteristics of the internal heat source; to investigate the means of maintaining the distributor plate below the critical temperature to prevent clogging; and to measure the effective absorptivity, heat flux, and bed-plate heat transfer coefficient at high temperatures. An analysis based on the experimental results will be done to evaluate the characteristics and capabilities of this reactor.

The initial objectives of determining low-temperature values for the effective absorptivity and flow rate of heat are being conducted in a 6-in. reactor with square cross section. The first series of experiments is under way using a variable matrix of the parameters of source power input, bed height, and gas velocity. An HP85 computer and a data logger are incorporated in the apparatus.

ADVANCED MATERIALS RESEARCH TASK

Silicon Particle Growth Research (California Institute of Technology)

An investigation of the reaction system of silane pyrolysis in a free-space reactor was undertaken in this period at Caltech. It was begun with the objectives of characterizing the reaction system and attempting to develop the conditions for the production of usable Si particles. (Early studies of the operation of free-space reactors by UCC under a JPL contract and in-house at JPL resulted in making submicrometer powder that is difficult to use.) Theoretical studies led to a description of the experimentally-obtained particle size distribution and then to calculations that suggested the experimental conditions for obtaining substantially larger particles.

The theory of gas-phase nucleation quenching by aerosols was extended from the continuum regime into the transition and free molecular-particle-size ranges. Using this theoretical basis, a new reactor was designed and constructed with the objective of extending the particle-diameter range from submicrometer to 10 μm. The efficiency of this reaction for producing one-μm mass mean diameter particles in the first reactor stage was 30% to 50%. A second-stage reactor to grow particles to diameters of 10 to 20 μm by direct chemical vapor deposition was designed and fabricated. It was intended that the production rate would be 6 to 10 gm/h in a 10-mm-ID, 300-mm-long externally heated quartz reactor. The first experiments operated in the free-space reactor mode have produced between 2×10^7 and 8×10^{18} particles cm^{-3}; these particles were in the 0.1 to 1.0-μm range. The product from the second stage was particles as large as 20-μm diameter in a concentration of 6×10^4 particles cm^{-3}. Modifications in the apparatus and way of operation have led to the production of particles having a volume mean diameter of 35 μm.

Investigation will continue under the original plan of characterizing this reaction system and with the additional objective of producing particles that can be used as seed for a fluidized-bed reactor.

Research on Silane Pyrolysis in Fluidized-Bed Reactors (JPL)

JPL is conducting FBR research with the objective of characterizing the deposition of Si from silane and providing bases for significant improvements in this process. The 6-in.-dia FBR that was designed, constructed, and checked out in the last period was operated and found to have certain deficiencies; for example, incomplete conversion to Si was obtained. Modifications were made to provide bed temperatures above 600°C while keeping the distributor temperature below 400°C, and operation of the modified FBR was successful. A test program consisting of 18 tests was completed. For clean seed particles of about 200-μm-diameter size, 650°C bed temperature, U/U_{mf} (ratio of superficial velocity to minimum fluidization velocity) of 5, and a bed height of 60 cm, the following results were obtained: (1) for 20 mole % silane in hydrogen feed over a 90-min period, the Si deposition rate was 1 kg/h; (2) for silane feed concentrations ranging from 20% to 100% over a 2-h period (average silane concentration of 57%), the Si deposition rate was 3 kg/h; (3) for 80% silane feed for a 3-h period, the deposition rate was 3.5 kg/h. The effluent dust level was 11% or lower in all cases, and no wall deposit or bed agglomeration occurred. Complete conversion of silane to Si was obtained at 650°C. The

product is being analyzed to provide information on particle growth mechanisms. These results confirm the promising feasibility of the FBR to attain the $14/kg Si price goal. Further research to explore the high-concentration silane region and to characterize growth mechanisms and product is planned.

Some preliminary experiments were conducted to investigate improved methods of FBR seed material preparation. A limited study on cracking heated Si particles by rapid cooling gave negative results, so no further effort on this approach will be conducted. A set of experiments was performed to investigate the feasibility of employing fluid jet milling. The results indicated that 20% to 40% of the mass of particles originally about one mm in diameter was reduced to particles in the 400 to 500-μm-diameter range in each 10 to 15-minute pass, warranting further study of this method.

Shaped-Sheet Technology

Edge-Defined Film-Fed Growth (Mobil Solar Energy Corp.)

A new contract titled "Stress Studies in EFG" was initiated in July, 1982. The effort will require research on defining growth-induced stresses in Si ribbons, specifically EFG ribbons.

The work plan focuses on the development of a computer model for temperature field-stress relationships in dynamic ribbon-growth situations. The relevant ribbon-temperature field data and boundary conditions will be obtained experimentally from existing growth stations and used to refine and confirm the theoretical analyses. The modeling effort will be directed toward generating an optimum ribbon growth condition that allows high-speed growth with acceptable residual stresses.

The computer code for residual stress calculation is operational. Sensitivity analyses involving growth parameters such as speed, temperature, stress boundary conditions, and strain rate are in progress. Experimental data on temperature profiles of static 10-cm-wide EFG ribbon at growth conditions have been obtained and integrated into the computer analysis.

Other ongoing work includes development of a high-resolution fiber-optic-based system for measuring ribbon temperature; analysis of the liquid/solid interface shape and composition; high-temperature measurement of creep behavior for EFG ribbons; and laser interferometric in-situ measurement of ribbon-surface topology during growth.

Dendritic Web Ribbon Growth (Westinghouse Electric Corp.)

Westinghouse is investigating the key problems that are associated with a process for making a thin, wide-ribbon form of single-crystal Si directly from the melt. "Dendritic" refers to the wirelike supporting dendrites on each side of the ribbon, and "web" refers to the Si sheet that results from the freezing of the liquid film between the bounding dendrites as the latter are raised from the molten Si.

ADVANCED MATERIALS RESEARCH TASK

The main thrust of the effort in this period was directed toward understanding and implementing the control of thermally generated stress, which is the factor limiting the area rate of ribbon growth, not only for dendritic web but for other forms of Si ribbon. To this end, development continued on computer models that are being used to characterize critical elements of web growth and to define growth system configurations that produce ribbon with reduced stress at increased throughput rates.

Early in the period, the model for web temperature was modified by incorporating a graphics output that prints the information into a curve, providing a capability of evaluating a larger number of thermal cases and reducing cost per case. Also, the buckling model was evaluated and verified for application to the wider web that is now being developed.

Using the models, various configurations for increased area growth were defined. One particularly promising one, designated J460, was built and experimentally evaluated both at the R&D Center and at Westinghouse's Advanced Energy Systems Division pre-pilot facility. The J460 hardware has produced undeformed ribbon of up to about 5.5 cm width, the widest low-stress ribbon grown to date. A second set of this furnace configuration was fabricated to include provisions for melt replenishment so that longer runs could be made, and runs as long as 90 hours were conducted. The growth behavior was reproducible, usually producing web of 150-μm thickness and in excess of 4-cm width. A growth rate of about 13 cm^2/min was achieved.

The use of Si pellets produced by the Kayex Corp. shotting tower was introduced into the replenishment system. This tower, which was developed under a subcontract with Kayex by UCC as part of the latter's FSA silane-to-silicon program, was acquired by Westinghouse for the Module Experimental Process System Development Unit (MEPSDU). The modified melt replenishment system eliminates oxide accumulation and thereby permits both long-term continuous operation (for at least 90 hours) and interruptions in operation for extended periods (i.e., overnight), thus greatly increasing flexibility. In November 1982 growth runs were made with width-limiting versions of the J460 furnace design; with such a feature, ribbon of constant width is grown. The tests showed that the width was controlled to about the 4-cm design target.

Recently, further analysis of modeling results indicated that elastic buckling stresses can be reduced to very small values by the use of configurations with higher shield stacks. Modeling of one such configuration indicated that some elements of the growth system affect ribbon growth in an essentially independent manner. For example, it was found that the top shield temperature had almost no effect on the growth speed and relatively small effect on residual stress, but had considerable effect on buckling stress. On the other hand, the furnace lid parameters such as temperature and slot width affected both growth speed and residual stress, but had little effect on the buckling stress. Such independence of these parameters is expected to facilitate further improvements in the growth systems.

Since further sizeable improvements in ribbon growth rates are considered not likely to be attained with static furnace configurations, the contract was recently modified to provide for an effort in which dynamic control of the

furnace elements will be studied. With such a system, ribbon growth can be started with an appropriate set of conditions, and the furnace configuration can be changed during operation to that required for high growth rates.

To summarize some of the significant progress in this period, the quasi-steady-state (for ribbon lengths of 30 to 100 cm) area growth rate was increased by 60% (from 8 cm^2/min to 13 cm^2/min), the maximum ribbon width at standard thickness (150 μm) was increased by 30% (3.8 cm to 4.9 cm), and the maximum low-stress ribbon width was increased by 12% (4.9 cm to 5.5 cm).

Shaped-Sheet Technology Supporting Studies

Modification of Silicon Surface Properties by Fluid Adsorption (University of Illinois at Chicago)

The purpose of this study is to provide an understanding of the abrasion and wear of Si through modification of its surface properties by interaction with fluids.

The fundamental mechanisms of surface property modification of Si by fluid adsorption are being investigated by the University. Effects of abrasion by diamond, and of microhardness and fracture of Si in fluids, are being studied. The abraded surfaces are examined by scanning electron microscopy to deduce the material fracture and removal mechanism; micro-hardness tests are used to determine the changes in surface hardness due to fluid adsorption; and fracture of the Si abraded in fluids is being studied to determine how the subsurface damage due to abrasion is affected by fluid adsorption.

Diamond abrasion tests were made in deionized water, 5 wt % sodium chloride in water, acetone, and ethanol for normal forces of 5 gf and 10 gf. The results indicated that the abrasion rate of Si in ethanol is twice as high as in water, all other experimental conditions being held constant. The data were compared with two models: one by Rabinowicz et al, who describe the wear rate as a function of material hardness only, and one by Evans, who describes the material removal rate as a function not only of hardness but also of fracture toughness; the Rabinowicz model is based on the elastic/brittle fracture of ceramic materials, and the Evans model is based on the elastic/plastic properties of materials. The experimental results indicate that the abrasion rate in the aqueous liquids and acetone are within the range of the result predicted by the Rabinowicz model. Examination by scanning electron microscopy indicated little plasticity. However, the wear rate in ethanol appears to be more consistent with the Evans model. In addition, greater plasticity was observed on the surface abraded in ethanol.

The surface hardness of Si was tested in toluene, acetone, ethanol, methanol, glycerol, and deionized water, and it ranged between 1374 $\pm$ 89 kg/mm^2 for ethanol and 1845 $\pm$ 150 kg/mm^2 for deionized water. The microhardness correlates with the dielectric constant, ϵ, of the fluid.

The subsurface damage due to abrasion of Si in fluids is being investigated by fracture-strength test of Si wafer samples. A linear multiple-scratch

groove generated in ethanol and acetone was used as a "thumbnail" crack in a three-point bend test. The fracture strength varies for the grooves generated in the two fluids, and a measure of the mirror radius, r, on the 110 fracture surface and fracture strength, σ_F, yields the constant A in $\sigma_F r^{1/2} = A$. The constant A is 1.87 and 2.20 $MN/m^{3/2}$ for grooves formed in ethanol and acetone, respectively. This difference in A confirms that chemomechanical effects are dominant in the fracture behavior of Si.

Materials Properties Modification (JPL)

In order to study the effect of environments on the mechanical properties and/or cracking of Si, double torsion (DT) and microhardness indentation testing methods were recently undertaken. The environments of interest include light, heat, chemical (contact fluids), and electrical and magnetic fields. Initial efforts were focused on studying the effects of light, heat, and electric fields.

Baseline data were generated on Cz Si fractured along $\{111\}$ in air at room temperature (23°C). The fracture toughness (K_{IC}) measured by the DT method was found to be 0.715 to 1.0 $MNm^{-3.2}$. These values are within the scatter of the previously published data measured by the controlled-flaw/bend-bar method. The DT test data provide higher precision and are more useful for design application than data from the controlled-flaw/bend-bar method.

Preliminary tests on the effect of light on the mechanical strength of Si were made. It was found that the strength of Si increased appreciably under infrared irradiation (IR) in comparison with that of Si tested in darkness. However, the strength of Si remained unchanged (compared to darkness strength) when tested under intensified visible light. A better, controlled IR light source and testing setup are being prepared for the detailed testing on the effects of light irradiation.

Preliminary microhardness tests have begun on single-crystal Cz material with and without an applied current/voltage passing through the samples. An initial test consisting of 30 microhardness indentations indicated a softening effect in the $\{211\}$ Si surface when impressed with 10 volts at the time of indentation. A reduction in hardness of approximately 25% was recorded. However, subsequent tests have failed to reveal this same electromechanical softening effect. These results are somewhat consistent with reports in the literature, where there is no consensus on the existence of an electromechanical effect in semiconductors. Ongoing work at JPL includes new sample configurations, standardized surface preparation techniques, and an optimized electric-circuit arrangement for studying the effects of electric fields on silicon.

Ingot Technology

Semicrystalline Casting (Semix Inc.)

The semicrystalline casting development effort with Semix is a continuation of the cooperative agreement established in 1980 between Semix and the

Department of Energy. Technical assistance in the monitoring of this agreement is being supplied by JPL. The initial agreement envisioned a large-scale development of the technology for casting and wafering semicrystalline Si. Philosophical changes in the scope and direction of the Department of Energy program have resulted in a reduction of scope of the effort with Semix to three elements. These are non-destructive evaluation of cast ingot quality, high-speed wafering developments, and modeling and experimental control of the casting process. This latter element includes confirmation of cell efficiencies. Each of these technical elements will be reviewed in turn.

The approach to quantitative determination of ingot quality before wafering would permit rejection of unsatisfactory bricks before the added value of wafering. Such bricks could be remelted in total to minimize yield losses. The approach under investigation involves generation of free carriers by means of a brief laser pulse into the bulk of the Si ingot. Decay time for the free carriers generated is then analyzed by a laser capable of penetrating entirely through the brick and determining the absorption of this laser by the carriers in the Si as a function of time. Decay time in absorption can thus be correlated with free-carrier lifetime in the brick. Work has largely involved investigations of various available lasers in terms of relative power and absorption at the Center for Laser Studies in Philadelphia, Pennsylvania. The choice of laser powers and absorptions is critical, since penetration must be great enough to provide meaningful bulk measurements but not so great as to provide inadequate signal for detection. Results suggest that the technique is feasible, and experimentation continues.

The second element of the program involves high-speed wafering. This effort is a result of earlier studies that indicated that multiblade wafering as presently practiced was inadequate in both conventional and high-speed forms as a result of excessive use of expendable materials, limited rates, and equipment inadequacies. The details of the new technique are proprietary. As a result of experimental difficulties and termination of wafering efforts throughout the FSA program, this experimentation has largely been concluded within the Semix effort. No experimental results were obtained at the conclusion of the effort.

The final element of the program involves the use of a computer thermal model to describe heat flows during the casting process. This thermal model is to be correlated experimentally with crystalline behavior during the process. Variations in crystallization would be imposed by varying the thermal configuration within the casting furnace. Details of crystallization-front behavior would be determined from the crystallization structure observed in the ingot. Finally, implications of the ingot structure would be confirmed by solar-cell measurements on wafers. Such a program contains many subelements that are not described in detail here; such description is available in Semix quarterly reports. All elements of the analysis are now proceeding, but none has progressed to the point that the total effectiveness of the approach can be evaluated. Major results have been attained in the portion of the work involving structure and its relation to performance. These are described in detail in the Proceedings of the 21st Project Integration Meeting in this document.

Devices and Measurements Research Task

INTRODUCTION

The objective of this task is to identify and implement research and development activities in the photovoltaic device and measurements area to meet the near-term and long-term objectives of FSA. Task activities encompass research in device physics, device structure, material-device property interaction, and measurement techniques for physical, chemical and electrical evaluation of devices and materials.

Technical Approach, Organization and Coordination

To meet FSA objectives, efforts are now directed toward characterization of various silicon-sheet materials, material-device property interaction investigation, and measurement techniques. The program of the Task is structured accordingly.

Ongoing research contracts awarded for material and device evaluation are listed in Table 1.

The program of the Task also includes JPL in-house activities to conduct basic research in materials and devices characterization to support contractor needs and other Tasks of the Photovoltaic Components Research Area.

SUMMARY OF PROGRESS

Cornell University

Studies using scanning transmission electron microscopy (TEM) and electron-beam-induced current (EBIC) techniques were used to evaluate dislocation networks in processed EFG ribbon. The networks appear to provide nucleation sites for small precipitates. The electrical activity of the dislocation networks in the twin planes in web decreases sharply after cell processing. An algorithm has been developed to determine the orientation of twin boundaries by visual inspection of Si surfaces after preferential etch. Ribbons using a method of quenching liquid Si on a rotating wheel have been made to improve the understanding of structural defects in silicon grown at high speed.

A general theory of the structure of $\langle 110 \rangle$ tilt boundaries has been worked out in terms of repeating structure unit.

An extension of the contract has been approved for one year. The milestone final report originally scheduled for late June 1982 has been rescheduled for late June 1983.

DEVICES AND MEASUREMENTS RESEARCH TASK

Table 1. Devices and Measurements Research Task Contracts

Contractor	Research Area
Applied Solar Energy Corp. City of Industry, CA JPL Contract No. 955089	Cell fabrication and silicon-sheet evaluation
Cornell University Ithaca, NY JPL Contract No. 954852	Characterization of silicon-sheet properties
Materials Research, Inc. Centerville, UT JPL Contract No. 957977	Quantitative analysis of defects and impurity evaluation technique
University of California Los Angeles, CA JPL Contract No. 956233	High-efficiency solar-cell structures by molecular-beam epitaxy
C.T. Sah Associates Urbana, IL JPL Contract No. 954685	Effects of impurities on solar-cell performance
Applied Solar Energy Corp. City of Industry, CA JPL Contract No. 956369	Microcrystalline silicon growth for heterojunction solar cells
University of Pennsylvania Philadelphia, PA JPL Contract No. 956290	Development and analysis of silicon solar cells of near 20% efficiency

Applied Solar Energy Corp.

Studies have been made to evaluate new silicon cast material (the oscillating carbon crucible technique with Bridgman directional solidification) and silicon cast materials: UCP (Semix Inc.), HEM (Crystal Systems, Inc.), and Silso (Wacker Siltronic Corp.). The average results for the UCP, HEM, and Silso cast materials indicate the their efficiency is about the same (HEM 11.1, UCP 10.4, Silso 10.2). This contract expired in December 1982. An add-on effort to the contract is being negotiated. A final report is scheduled for February 1983. Future activities are expected to include dark current-voltage data on cast silicon.

Material Research, Inc.

Characterization by quantitative microscopy of processed and unprocessed semiconductor material has been completed. A final report containing

information on both the processed and improcessed material was submitted to JPL in November 1982. Negotiations are under way for an add-on effort to this contract.

C.T. Sah Associates

This project started seven months ago and contains two interrelated tasks: (1) theoretical and experimental studies of impurities-related energy levels, densities of the levels, and carrier capture probabilities; (2) generation of a mathematical model to describe the experimental results and to specify the material property requirements for high-efficiency cells. This project includes studies on thick and thin cells. Work is continuing on developing the model for thin-film high-efficiency solar cells. This model will allow for both single-crystalline and polycrystalline materials, and will include the effect of drift field on allowable impurity concentration.

Applied Solar Energy Corp.

The purpose of this contract is to investigate a new heterojunction structure for silicon solar cells, consisting of microcrystal (m-Si) with a 1.72 eV band gap grown on single-crystal (c-Si) sublayers, with band gap ≈1.1 eV. N-type silicon wafers were supplied by ASEC to Boston College for evaporation of a microcrystalline silicon layer (p-type) for formation of a heterojunction. Of the cells made from the heterojunction material, most showed interface shorts with very low open-circuit voltages. Ion microprobe analysis is under way to evaluate the interface.

University of Pennsylvania

The project started in September 1982; purpose is to explore the capabilities of certain process approaches with respect to yielding material properties adequate for the preparation of very-high-efficiency silicon solar cells. A multi-variable experiment has been designed to study the process parameters including type of gas and dopants that yield the highest minority carrier lifetimes in CVD-deposited epitaxially grown silicon layers. Suitable p-type substrate wafers with minority carrier lifetime are due to be received from Microwave Associates in January 1983. High-minority-carrier-lifetime samples are also expected from Wacker Chemie.

University of California at Los Angeles

During the first seven months of this program, emphasis has been on characterizing molecular-beam epitaxy (MBE)-grown silicon films and junctions. Studies of carrier concentration and Hall mobility in n-type (Sb) and p-type (Ga) films shown near bulk-like properties. SEM and etch-pit studies indicate low dislocation concentrations. Diffusion lengths in substrates did not degrade during MBE processing. SIMS analyses of MBE films showed unexpected carbon and boron impurities. One solar cell was made from and MBE-grown n-film on a p-substrate with the contact added at JPL. Solar-cell parameters could be measured but were poor due to high reverse leakage. Causes of the latter are being studied.

Environmental Isolation Task

ORIGINAL PAGE IS
OF POOR QUALITY

INTRODUCTION

The objective of the Environmental Isolation Task is the development and qualification of the total encapsulation system required to protect the active optical and electrical elements of a photovoltaic array from the effects of the field environment. The most challenging technical problem has been the development of high-transparency materials for the photoactive side of the module that meet the Project's low-cost and 20-year-life objectives. The approach to the objective includes a combination of contractor and JPL in-house efforts, which can be divided into two technical areas:

(1) Materials and Process Research. This effort includes all of the work necessary to develop, demonstrate, and qualify one or more encapsulation systems to met FSA cost and performance goals. It includes the testing of off-the-shelf materials, formulation and testing of new and modified materials, identification of automated processes to handle these materials during formulation and fabrication of modules, and systems analysis and testing to develop optimal module designs.

(2) Material Durability and Life Testing. This work is directed toward the attainment of the FSA 20-year-minimum life goal for modules. It includes research aimed at the development of a life-assessment method applicable to terrestrial photovoltaic modules, and validation of that method by specific application to photovoltaic demonstration sites. Material degradation studies are being conducted to determine failure modes and mechanisms. This effort supports both the materials and process development work and the degradation model development.

SUMMARY OF PROGRESS

Isolation Materials and Process Research

Module encapsulation material systems and configurations that meet the original FSA performance and cost goals and have the potential of meeting the service-life goal of 20 to 30 years have been developed and are being evaluated extensively. Major PV module manufacturers, including ARCO Solar, Inc., Solar Power Corp. and Solarex Corp. are using and evaluating the FSA-developed pottant (EVA) and primer materials (silanes) in their current product lines.

More advanced encapsulation concepts as well as work on some identified problem areas with EVA have been worked on during this reporting period.

PRECEDING PAGE BLANK NOT FILMED

ENVIRONMENTAL ISOLATION TASK

Encapsulation Materials and Process Research and Evaluation (Springborn Laboratories, Inc.)

New compounds were evaluated by Springborn for efficiency in curing both ethylene vinyl acetate and ethylene methyl acrylate pottants intended for vacuum-bag lamination of solar cells. One compound in particular, designated Lupersol-TBEC (Lucidol Division of Pennwalt Corp.), was found to be unusually effective in promoting the rapid cure of both these materials. Formulation of these resins with TBEC resulted in compositions of very high gel content, lower temperatures of activation, and much lower cure times, even in the ethylene methyl acrylate polymer that is more difficult to cure. It is expected that TBEC-modified pottant formulations may permit the lamination-encapsulation step to be operated at lower temperatures, higher speed, higher throughput and with a much wider tolerance for intentional or accidential variations in the cure schedule. Investigations of this new curing agent will be emphasized in the development of future of formulations.

Two component aliphatic urethane casting syrups were evaluated for suitability as solar-module pottants on the basis of optical, physical and fabrication characteristics. One formulation was selected as being acceptable for industrial evaluation. This compound, designated Z-2591, is a prototype solar-cell encapsulant manufactured by Development Associates, Inc., North Kingstown, Rhode Island, and is available in pilot-plant quantities. This urethane is characterized by high transparency, low mix viscosity, fast cure time and surprising lack of the moisture sensitivity that has given trouble with previous urethane compositions. This material is produced with an ultraviolet (UV) stabilizer system already blended in; similar formulations have a history of use in outdoor applications. Commercial quantities are available for module fabrication.

Mild steel is a readily available and easily worked material that holds the promise of being a cost-effective substrate. Its major deficiency is corrosion sensitivity. Experiments are under way to access the durability and cost effectiveness of coatings for protection of steel. Test specimens were prepared with a variety of films, paints and pottants and then exposed to 35°C salt spray (ASTM B-117) and outdoor weathering conditions. The specimens were evaluated for degree of corrosion, delamination and other destructive effects at regular intervals. The salt spray and outdoor results generally correlated well, except for the degree of attack, which was much more severe in the heated salt fog. Untreated control specimens survived only three hours under salt spray before extensive corrosion became apparent. The most successful coating identified so far is lamination with an EVA/Scotchpar polyester combination, which has endured 5,000 hours of salt spray with no sign of change. Other coatings based on EVA modified with zinc chromate have also survived this period without change. These coatings are currently too expensive to be practical (approximately $10/m^2$), but they serve to demonstrate proof of concept and show the effectiveness of chromate modification.

Investigations are continuing with commercial maintenance coatings based on fluorocarbon and silicone-alkyd chemistries. Tests of these coatings show good salt-spray resistance to 4,000 hours and the cost, including the steel and both sides coated, is in the order of $3.50/m^2$. This is well within the $7.00/m^2$ upper limit for substrate cost.

ENVIRONMENTAL ISOLATION TASK

Wood products, such as hardboard, are potentially the lowest-costing candidate substrates identified to date. The high modulus (0.5 to 1.0 x 10^6 lb/in.^{2}) and low cost (approximately \$0.14/ft^2) satisfy cost and load-deflection requirements. The difficulty with the use of these materials lies in their very high hygroscopic expansion coefficients. Periods of dryout followed by subsequent moisture regain cause large expansions and contractions that result in cell fracture when these materials are used as substrates. Experiments were conducted to determine the effectiveness of occlusive coatings to prevent this effect. Both metal foils and organic films bonded to the hardboard with appropriate adhesives were found to decrease the hygroscopic response dramatically and to lower the expansion coefficient by four orders of magnitude. These results improve the position of wood products as potentially useful substrates and future experiments will continue to assess this approach and identify cost-effective coating materials and techniques.

An experimental program continued to determine the usefulness of soil-resistant coatings. These coatings are intended to be surface treatments applied to the sunlight side of solar modules to prevent the persistent adhesion of soil to the surface, to aid in its removal, and thus to maintain high power output. These treatments have been applied to Sunadex glass, Tedlar and oriented acrylic film. The treatments are based on silicone, acrylic, and fluorosilane chemistries. After 15 months of outdoor exposure, the most effective treatment for Sunadex glass appears to be a fluorosilane designated L-1668. For both the organic films, a silane-modified adduct of perfluoric acid gave the best results. These treatments gave improvements of 2.5% to 4% in power transmission, measured with a standard cell. The surface treatments were found to be self-cleaning during rainfall periods. After one year there is evidence that the treatments are slowly being lost; consequently, a maintenance schedule may be required to maintain effectiveness over long periods of time.

Primers were evaluated for effectiveness in bonding candidate pottants to outer covers, glass and substrate materials. The bond strengths were determined by standard peel-test methods and measured in lb/in. of bond line. Successful primers were also tested after two weeks of water immersion and two hours in boiling water. Good primers have been identified for bonding EVA (A-9918) to almost all candidate materials and a new primer that is effective with polyester films, that gave bonds of 35 lb/in.^{2}, was identified. Despite the similarity in chemistry, EMA is much more difficult to bond and successful results have been obtained only with glass and mild steel. Polyurethane casting syrup has been effectively bonded to Sunadex, Tedlar and Korad but additional work is required on steel and polyester. Butyl acrylate syrup is the most difficult pottant of all to bond; this limitation is additionally complicated by its inherently low tensile strength. Bonds to Tedlar and Sunadex glass that survive the water immersion and boiling tests have been achieved; however, they are both low in bond strength, not exceeding 1 to 2 lb/in. of width.

The RS/4 Sunlamp exposure is a widely used industrial method of assessing the relative stability of plastics subjected to the degrading effects of ultraviolet light. The results are useful for the ranking and comparison of the stabilities of polymeric materials and the effectiveness of additives and formulations. The EVA formulation A-9918 is performing extremely well and has survived more than 30,000 hours' exposure to date with no significant change in

properties. In comparison, the uncompounded EVA resin begins to degrade in about 500 hours. The other pottants are also surviving without change, but they have not yet accumulated as many test hours. The fully compounded EMA has endured 10,000 hours, and the casting syrups, polyurethane and butyl acrylate, have been exposed for 8,600 and 5,700 hours, respectively. Pigmented back-cover films of Tedlar and Scotchpar and outer-cover films of transparent Tedlar (100BG30UT) show no signs of deterioration. The low-cost biaxially oriented acrylic film, Acrylar (3M Corp.), has been exposed to 12,000 hours and shows no change in useful properties, except that a 40% decrease in tensile strength (from 24,000 $lb/in.^2$ to 14,500 $lb/in.^2$) occurred within the first 1,500 hours.

Fabrication of outdoor heating racks has been completed, and the racks have been roof-mounted. The heated surface of each of these racks is a thin-walled aluminum plate, 3 feet on a side (9 ft^2 of heating area), behind which will flow a Dow-Therm commercial heating fluid, regulated in a separate heating chamber hot enough to yield the desired surface temperature. The racks were designed to operate at surface temperatures as high as 125°C to 130°C.

The intent of these racks is to achieve exposure of materials and modules to natural outdoor conditions of UV, oxygen, humidity, etc., and to accelerate aging with temperature. The racks can be operated at constant temperature on a 24-hour basis, or can be cycled to turn on at sunrise and shut off at sunset. The latter operation would generate diurnal thermal-stress cycles in experimental modules.

Initially, the plans are to operate the racks in the cyclic mode, with one rack at 80°C, a second at 95°C, and the third at 110°C. Identical samples, yet to be selected, will be mounted on each rack, to yield data on temperature dependence of property changes.

Module Design Analysis and Verification (Spectrolab, Inc.)

The breakdown voltage of electrical insulation is a function of many parameters, but the dominant ones appear to be the dielectric strength of the insulation material and the geometry of the metal conductors separated by the insulation. For real-world solar-cell assemblies that have sharp points, corners, or edges with very small radii of curvature, electrical breakdown of insulation will initiate at these geometric locations, rather than from flat surfaces of the conductors, and electrical breakdown will occur at values of volts/mil less than the dielectic strength of the insulator.

A computer program for the analytical modeling of electrical stress (isolation) has been generated. This model will initially interrelate the dielectric properties of encapsulation pottants, pottant thickness, and geometry and thickness of electrodes and solar cells. The program is designed to analyze both thick-film and thin-film PV modules.

In analytical work involving computer stress modeling, a reduced-variable master curve has been developed for calculating deflection stresses in cells due to module bending. This master curve, similar in concept to the previously generated thermal-stress master curve, provides the design interrelationships

between mechanical properties of the pottant, cells, and structural panel to provide encapsulation design criteria for reducing solar-cell stresses when a module is deflected into an arc by wind pressure. As with the thermal-stress master curve, this deflection master curve was generated for a 4-foot square module bearing 15-mil-thick, 4 in.-square silicon solar cells with a 30-mil separation distance. For both master curves, the effects of cell dimensions (length and width) will be included, and solar-cell stresses generated by the combined actions of module thermal and deflection stressing will be analyzed.

Synthesis of UV Absorbers
(Polytechnical Institute of New York)

A contract has been let to the Polytechnical Institute of New York for the development and demonstration of synthetic procedures for polymeric ultraviolet stabilizers and absorbers. Professor Otto Vogl and his associates will test and scale up synthesis of previously developed ultraviolet absorbers and antioxidant additives that can be incorporated permanently into PV encapsulation materials. This effort will continue the work on new stabilizer formulations initially synthesized at the University of Massachusetts under JPL Contract No. 955531.

Ion-Plated Coatings
(Illinois Tool Works)

This contract was scheduled to terminate October 31, 1982, and ITW is preparing its final report. A draft copy is expected during January. ITW will close out its experimental activities by measuring the I-V performance of ion-plated n-on-p solar cells and by evaluating the antitarnish properties of ion-plated AR coatings over copper metallization. Both are in progress.

Edwin P. Plueddemann
(Dow Corning)

E.P. Plueddemann has developed candidate primer systems for bonding EVA and EMA to Acrylar, and for bonding EVA to Tedlar. He has also developed a candidate primer system for bonding the Z-2591 castable polyurethane to Tedlar, and continues work to develop primers for bonding this polyurethane to Acrylar and polyester films.

Separately, JPL, Springborn, and some PV manufacturers have observed that EVA will not bond to solder. Efforts to achieve and EVA-solder bond with primers developed to bond EVA to other materials such as glass, copper, aluminum, and the various plastic films have not worked. Plueddemann will initiate development of an EVA/solder primer system.

ENVIRONMENTAL ISOLATION TASK

MATERIAL DURABILITY AND LIFE TESTING

Interface Degradation (Rockwell Science Center)

Experimental studies to establish the mechanical and viscoelastic requirements for interface bond stability (IBS) of FSA-advanced encapsulated PV systems have been carried out using reactive silane adhesion promoters. Three reactive silanes, Z-6020, Z-6030 and Z-6031, which are used in Springborn primers for EVA encapsulants, were selected for detailed bulk property studies. Bulk polymerized films were prepared and studied by differential scanning calorimetry. Results supported an important hypothesis that reactive silane polymers retain chemical reactivity under long-term aging.

Jack Koenig at Case Western Reserve University has pioneered experimental techniques based on Fourier-transform infrared and Raman spectroscopy for the direct interrogation of a chemically bonded interface for fundamental chemical information. His techniques offer the promise of being tools to qualitatively and quantitatively monitor changes, at an interface, that may result from accelerated aging tests or from natural outdoor aging. A consultant arrangement to explore the potential of these techniques for FSA has been negotiated.

Springborn has supplied Koenig with test specimens of EVA bonded to glass by means of the EVA-glass primer (A-11861) developed by Plueddemann, and has also supplied control specimens without the primer. Koenig's test methods for chemically interrogating a chemically bonded interface are sensitive to sample configuration. The Springborn test specimens were of various sizes and material thicknesses in order to determine the optimum test configuration. This activity is expected to be completed by January and to provide preliminary chemical information about the chemically bonded EVA-glass interface. After that, EVA-glass test specimens will be aged at Springborn and Koenig will investigate properties of the resulting interfaces.

Degradation Computer Modeling (University of Toronto)

Work is continuing on refining EVA photodegradation model to allow for the inclusion of substituent groups, the reactivity of secondary and tertiary C-H bonds, and the influences of temperature cycling and dark reactions. These modeling studies will provide a general understanding of polymer photooxidation phenomena that can lead to a new understanding in the study of controlled lifetimes for polymers.

Work is continuing to investigate the effects of moisture and crosslink density on diffusion processes in EVA and how they influence the chemical degradation process. Modification of the overall chemical mechanism on which the computer program is modeled can then be evaluated to make allowance for the appropriate choice of diffusion rates in the solid state.

Photothermal Degradation of Polymers (JPL)

Efforts to investigate electrical properties of encapsulation materials are continuing. The initial objective is to monitor leakage current of

candidate materials under various environmental conditions. Monitoring of leakage current of PVB as a function of temperature and salt-solution concentration has been performed.

Preliminary results demonstrate that PVB becomes more conductive by a factor of two when soaked in a salt solution, as compared with tap water. Data on thermally aged PVB samples have also been obtained. Samples were aged at 50°C and 135°C in a dark oven for 2 days. Current versus soaking time was monitored. Results indicated that PVB had become a better insulator as a result of dry-oven thermal aging, when compared with the control sample.

The mechanical behavior of a polymer sample can be influenced by the extent of the sample's crystallinity. A particularly effective way of examining partially crystalline polymers, of which EVA is one, is by X-ray diffraction.

Samples of EVA placed in the Controlled Environmental Reactor (CER) at 135°C for various periods of exposure are being tested using X-ray diffraction. Sample crystallinity will then be estimated from the X-ray pattern by plotting the intensity of the scattered beam against the angle of incidence. Any changes in the morphological network can be determined by the degree of crystallinity. Results will be evaluated.

Quantifying Degradation Research Forum

This Research Forum, held at Williamsburg, Virginia, December 6-8, 1982, was organized to address critical issues related to the identification and quantification of photovoltaic module life-limiting degradation rates and mechanisms. This forum focused on current industrial practices and potential new approaches to identifying, characterizing, and modeling mechanisms such as corrosion, cyclic fatigue, photochemical aging, surface soiling, debonding, and electrical isolation breakdown. The meeting was attended by 66 representatives of some 27 different industrial, government and academic organizations. The experience and approaches of 10 non-photovoltaic-related industries in achieving and assuring hardware durability were reviewed and their application to photovoltaics discussed. These presentations were by 13 representatives of such companies as Ford Motor Co., PPG Industries, 3M Co., Eastman Kodak, Bell Telephone, and Underwriters Laboratories, Inc. The Forum Proceedings, including discussion comments, is in press.

A conclusion reached as a result of this forum was that the task of predicting and assuring photovoltaic module life is a very complex undertaking, but the current FSA approach is consistent with the best current industrial practice in other fields.

Process Research Task

INTRODUCTION

The objective of this task is to conduct research and technology development in critical areas of photovoltaic-device fabrication processes and module formation to minimize technical barriers in those areas.

Process research is grouped in four categories for reporting convenience: surface preparation, junction formation, metallization, and module completion.

SUMMARY OF PROGRESS

The Process Research Task was incorporated into the Photovoltaics Components Research Area to provide greater visibility for the redirected Cell and Module Formation Research Area contracts. Increasing emphasis on reduction of technology barriers has resulted in the preparation of numerous technical papers. No new requests for proposals have been issued; however, unsolicited proposals were reevaluated in accordance with DOE guidelines and two contracts were awarded to Spire Corp. for ion implantation of non-Czochralski silicon-sheet materials and development of a hermetically sealed module.

A Photovoltaic Metallization Systems Research Forum has been organized, to be held March 16-18, 1983, at Callaway Gardens, Pine Mountain, Georgia. Speakers from different organizations and backgrounds have been engaged along with a meeting place offering off-season rates and an atmosphere conducive to concentrated discussion and the equally important informal exchange of information.

Surface Preparation

The Photowatt International, Inc., effort to develop a thick-film metallization system for application over a silicon nitride antireflection coating was only partially successful. Even though the results of this small contract were mixed, there were indications that a base-metal system could be developed. No additional funding is being considered. RCA completed the final report on its process-sequence development contract. PV cells were to be made on silicon sheets that had been epitaxially grown on low-cost substrates. This contract was cancelled before completion.

Junction Formation

Non-mass-analyzed (NMA) ion implantation tests by Spire Corp. have demonstrated 15.5% cell efficiency. This equipment is designed to have a throughput capability of 10 MW per year with lower capital investment, utility costs and maintenance requirements.

PROCESS RESEARCH TASK

NMA efforts at JPL have been concentrated on back-surface field (BSF) formation using boron trifluoride. This effort is aimed toward defining the implantation parameters and process sensitivity.

Westinghouse Electric Corp.'s work on liquid dopants and masks has been successful. Liquid dopant cells have shown photovoltaic conversion efficiency equal to or greater than that of baseline gaseous-diffused cells. Part of this excellent cell performance (15% to 16%) is due to the high quality of the film applied by the new meniscus coating machine. Another advance is the demonstration that belt-furnace-diffused cells are as good as tube-furnace cells. This allows a continuous process approach in all areas of cell production.

Solarex Corp. efforts on polycrystalline devices have shown that thin cells show BSF improvements. Unfortunately, thin polycrystalline materials still exhibit poor mechanical properties and therefore have high process handling losses.

A JPL in-house pulsed-plasma ion source has been fabricated and tested. Early results were mixed but the concept was successfully demonstrated.

Metallization

During this period Bernd Ross Associates demonstrated a successful copper thick-film ink back-contact system. An adherent front copper contact system was also shown but lack of a diffusion barrier prevented valid evaluations.

Spectrolab, Inc. also was successful with its tin/molybdenum/titanium-hydride thick-film system. Cells equal to silver thick-film cells were produced. Inherent in this system is a higher series resistance loss due to lower metallic conductivity in the grid lines. This contract has been redirected to include a conductive transparent oxide coating to reduce series resistance.

Photowatt International was unable to develop a nickel-based thick-film ink that would have good electrical and mechanical properties when fired through a silicon nitride antireflection coating. A silver-based ink was developed and successfully demonstrated.

Electrink succeeded in the development of a silver-based thick-film ink that can be applied directly to as-sintered aluminum back-surface metallization. This saves an expensive cleaning step and makes interconnect attachment easier.

Caltech researchers have formulated a general rule for the creation of amorphous metal films. This work involved the creation of a number of different binary amorphous metal films by ion mixing and co-sputtering. Seven papers were published in this subject area.

JPL in-house metallization research centered on development of an improved measurement technique for determination of the contact resistance of the metal-to-semiconductor interface. A new approach has been found and two papers submitted. Another area of interest is the use of thermogravimetric analysis for development of improved thick-film ink formulations. A paper on this new application has been submitted.

PROCESS RESEARCH TASK

Module Completion

Spire Corp. started on a new contract to develop an electrostatically bonded, ultrasonically sealed module. This hermetic sealing approach could provide reliable modules in remote or extreme environment locations.

Investigation of the process parameters required for vacuum lamination of large modules was achieved by the in-house design, fabrication, testing and operation of the 4 x 4 in. laminator. A report has been written and a patent application submitted.

A cooperative effort with Spectrolab and the Encapsulation Task resulted in successful fabrication of 4-foot square, flexible "credit card" modules needed for low-cost module substrate development.

General

The silicon shot tower transferred to Westinghouse from Kayex Corp. has been operated with a 93% yield.

Solarex has obtained fill factors on polycrystalline cells equal to those on single-crystal control cells.

PROJECT ANALYSIS AND INTEGRATION AREA

INTRODUCTION

The objective of the Project Analysis and Integration Area (PA&I) is to support the planning, analysis, integration, and decision-making activities of FSA. Accordingly, PA&I supports the Project by developing and documenting Project plans, and by contributing to the generation and development of alternative plans through the assessment of technology options. The analysis function of PA&I generally involves the establishment of standards for the economic comparison of options under Project study, and development of the analytical capabilities to perform the trade-offs required. Supporting the integration of FSA entails integrating tasks within the Project, and interfacing between the Project and other elements of the National Photovoltaics Program. Coordinated assessments of progress toward achievement of goals are performed to guide decision-making within the Project, the project goals having been established to reflect the requirements of the solar-array manufacturing industry and the National Photovoltaics Program.

SUMMARY OF PROGRESS

Assessing the state of the art of single-crystalline technologies and extrapolating results to a future production environment are ongoing activities of PA&I. Recently, a comparison of 1982 industrial practices was made with economic estimates projected in 1980 for Czochralski technology. Interestingly, all processes, equipment, and module design factors assumed in the projections made in 1980 had been adopted by industry by the end of 1982, and technical and performance parameters had all equaled or exceeded the 1980 projection with the exception of sawing. (The technology had been in existence in 1980, but had not been adopted for use in full-scale commercial production.) The f.o.b. factory price estimates made in 1982 (for factories ranging in size from 2 MW/year to 30 MW/year) agreed remarkably well with the projections for 1982 made in 1980. Even more to the point, the required market price projected for the industrialized technologies ranged from $\$7/W_p$ to $\$8/W_p$ (1980 \$) at the 2 MW level of production. These price estimates are, of course, in close agreement with actual market prices quoted in 1982. Results of this study were presented at the 21st PIM (see the Proceedings section of this document).

Single-crystalline technology was assessed for its cost reduction potential over the next decade. Estimates were made for ribbon technology (dendritic web) in existence today but not yet used in full-scale production, and longer-term projections were generated based on a program of realistic ongoing technical innovation and development. If the state of the art in ribbon technology were to be scaled up to a 25 MW/year level of production, an f.o.b. factory-dock-required module price of about $\$2/W_p$ was indicated by the analysis. To date, thermally induced stresses have inhibited ribbon growth rates and a conservative estimate of 10 cm^2/min was therefore assumed in the analysis. As our understanding of thermally induced stresses improves,

28 PRECEDING PAGE BLANK

however, higher growth rates can be expected to reduce module prices significantly. Results of the silicon ribbon assessment are reported in the proceedings section of this document.

A silicon cost-sensitivity study was initiated. The purpose of the study is twofold: (1) to verify Improved Price Estimation Guidelines (IPEG2) for silicon manufacturing processes by comparing IPEG2 results with those provided by a Lamar University study. (The IPEG price was within an average of 2.5% of the Lamar University price for the processes studies); (2) to perform a probabilistic cost analysis of the Union Carbide Corp. and Hemlock Semiconductor Corp. processes in order to access the uncertainty in silicon cost. Although the prospects for lower-cost silicon are promising, the results of the study should be regarded as preliminary. Further probability cost analysis of silicon refining processes is scheduled. Results to date are reported in this document.

New Allocation Guidelines (AGs) have been prepared. The AGs are a project management tool for FSA that provide consistent and meaningful targets for R&D. These guidelines are revised when necessary to reflect new information and new programmatic direction. They replace the Price Allocation Guidelines, which were last issued in January of 1980 (JPL Publication 80-51, JPL Document No. 5101-68, Rev. A). Significant changes include the following: (1) the Allocation Guidelines are now generic in that they are not identified with particular sheet technologies; (2) efficiency is treated parametrically, with cells and sheet receiving larger allocations if they can provide greater efficiency; (3) advanced PV module concepts have also received a set of Allocation Guidelines (see the Proceedings section of this document).

A preliminary study assessing the state of the art of metallization techniques and the potential impact of R&D in this area has been completed. The Grid Optimization Model was used to analyze the 12 metallization approaches studied. Results of the analysis will be used to identify preferred metallization techniques. The study, however, is not yet complete. Necessary steps towards completion include analyzing a larger number of metallization techniques and incorporating reliability analysis into the study. The study methodology and preliminary results were presented at the 21st PIM.

Encapsulation requirements consistent with long-life, high-performance systems, which have been extensively researched by FSA, were applied to thin-film modules. Lower-bound encapsulating costs were found to be comparable in magnitude to projected cell deposition costs, casting some doubt on recent estimates of extremely low-cost PV modules (i.e., 15¢/W). The lower-bound estimates of thin-film encapsulating costs were presented at the 21st PIM.

The Gross National Product deflator models used within FSA have been updated. Copies of the revised tables have been sent to DOE, SERI, and Sandia.

ENGINEERING SCIENCES AREA

ARRAY REQUIREMENTS

The Array Requirements activity addresses the identification and development of detailed design requirements and test methods at the array level. Continuing areas of activity that addressed improved definition of array requirements included the establishment of module and array electrical safety criteria and the development of array-to-power-conditioner electrical interfaces.

Safety Requirements

In support of array safety, Engineering Sciences Area and Procurement staff members attended a Design and Contract Status Review on Protective Bypass Diode Chip Encapsulation at General Electric Corp., Valley Forge, Pennsylvania, on October 26. The objective of this contract is to research techniques for using p-n junction or Schottky diode chips (dies) as bypass diodes within glass-laminate type PV modules with current ratings from 2 A to 20 A. The program is divided into three parts: requirements definition, design synthesis, and component and module mockup evaluation. Emphasis of the status review was on the third part, addressing specific design layouts to be fabricated.

Research aimed at developing module/panel and array subsystem electrical and fire safety requirements continued with the publication in August 1982 of UL's draft final report, which emphasizes work at the module level (first phase) and includes UL's "Proposed Standard for Safety, Flat-Plate Photovoltaic Modules and Panels." The final draft supersedes JPL Document 5101-164 (same title).

Engineering Sciences Area staff members participated in the first meeting of Underwriters Laboratories' Industry Advisory Group (IAG) for photovoltaics in Chicago on June 29-30. The seven PV-industry persons who make up the IAG provided a non-UL in depth review of UL's Standard for Safety for FlatPlate PV Modules and recommended a variety of changes to the draft standard before its final publication.

Power-Conditioning Interface

Specific areas of activity on the array--power-conditioner task during this reporting period included: (1) Submittal of final revisions for the array--power-conditioner interface requirements document to Sandia National Laboratories for their Power Conditioning Specification. Revisions stemmed from discussions generated during a joint meeting with Sandia representatives at JPL on April 9, 1982, and corresponding expansion of the written input and tabulated data has provided an improved format for the specification. (2) The

ENGINEERING SCIENCES AREA

December 1982 release of the final report draft that summarizes the array--power-conditioner interface studies conducted by the Engineering Sciences Area. The final report presents the computer simulation study results used to define the array operating characteristics and extreme output limits necessary for the systematic design of array-load interfaces under a wide variety of U.S. climatic conditions.

A paper titled "Characterization of the Electrical Output of Flat-Plate Photovoltaic Arrays" by C.C. Gonzalez, G.M. Hill and R.G. Ross Jr. was given at the 16th IEEE Photovoltaics conference in San Diego, September 27-30, 1982. The paper presents the above computer simulation study results as normalized ratios of power-conditioning parameters to array parameters to make the results universally applicable to a wide variety of system sizes, sites and operating modes.

Hot-Spot Heating

Work continued to focus on final additions to, and major revisions of, the task report draft submitted for review late in September, which summarizes Engineering Sciences Area hot-spot heating research. Detailed discussions of the analytical model developed for the task and specific conclusions comparing model results and laboratory hot-spot test data are being incorporated into the report. The report was rescheduled for release in April 1983 to provide additional time for reformatting and revising specific sections.

ARRAY SUBSYSTEM DEVELOPMENT

Array Subsystem Development activity is focused on the development of conceptual designs for integrated flat-plate array and module support structures as a key approach to minimizing total array costs. An important output of array conceptual designs is the definition of specific design requirements addressed to functional performance, interface and maintainability (at the array level).

Integrated Residential Arrays

Supporting the development of cost-effective residential array support structures, JPL Engineering Sciences Area in-house efforts have focused on the environmental durability of black PVC extrusions for direct-mounted residential array designs. The concept test model, which used black PVC extrusions to support 12 frameless 2 x 4-ft Block IV modules on a portable 45-deg-slope roof section, was placed on a JPL field site for weathering studies. In addition, accelerated UV aging tests were conducted on black polycarbonate (PC) and chlorinated polyvinyl chloride (CPVC) extrusions. These extrusions have shown no changes in mechanical properties. However, a linear weight loss with time after an equivalent 6-year exposure was recorded. Both CPVC and PC extrusions are experiencing obvious cosmetic degradation on the sunlit surfaces. The tests are scheduled for 40 weeks and use biweekly inspections, which are equivalent to a year's exposure of UV, to gather a 20-year-life performance assessment of these materials.

ENGINEERING SCIENCES AREA

RELIABILITY AND DURABILITY RESEARCH

Reliablity and durability development efforts are addressed to provide the technical base required to achieve reliable modules with 20-year lifetimes. Activities are conducted to clarify design tradeoffs, to develop analysis tools and test methods, and to provide generalized design solutions for the PV community. Specific activities during this reporting period included: (1) cell temperature and humidity testing, (2) module voltage isolation, (3) interconnect fatigue, (4) array soiling, (5) module temperature and humidity testing, and (6) module and array reliability.

Cell Temperature and Humidity Endurance (Clemson University)

The encapsulated cell testing program, which includes six different cell types and eight different encapsulated systems and combinations, have shown no electrical degradation after completing 250 hours of exposure at 85°C/85% RH. However, noticable physical changes were observed on two Springborn Laboratories EVA-encapsulated test samples. Springborn has been contacted and will participate in the followup investigation on physical changes in EVA samples.

A draft Progress Report for the 1981 calendar year from Clemson University was released in September 1982. It includes a report on cell reliability testing leading up to the current Encapsulated Cell Test Program.

Module Voltage Isolation

Voltage isolation studies continue to focus on the source and magnitude of leakage currents to ground caused by material aging. Ongoing tests include voltage breakdown of polymeric back-cover films that have been thermally aged at 85°C for 700 hours and for 1400 hours. The probability versus voltage profiles generated for these materials will be used to predict module life and to identify voltage-withstand capability of PV design materials after thermal aging.

Several modules featuring copper cells, EVA or EMA encapsulants and various polymeric back cover films have been tested in the ac-corona mode of the Biddle Partial Discharge Detection System, a key research tool in studying degradation processes in PV insulation systems. Location and quantization of discharges for improved sample voltage-withstand capability plus the determination of electrical discharges in module insulation are some of the operational features of the Biddle.

Interconnect Fatigue

Examination of the mechanical-fatigue life of cell interconnects is continuing in an effort to obtain a 20-year-life predictive model. Fractograph photos were used to show that crack propagation initiates on the concave surface of a fatigued interconnect, which analysis revealed to be the most highly stressed surface. The result suggested the use of bimetallic interconnect or clad-laminant interconnects with the more highly fatigue-resistant metal on the

outside for an improved operating life. Mechnical fatigue life testing of thick-clad laminates followed, with sample copper Invar materials supplied by Texas Instruments, Inc., in an effort to obtain a 20-year-life predictive model. Two clad Cu-Invar-Cu materials used in the fatigue tests had the same cladding ratios, but different metallurgical treatments.

A reliability design procedure was completed that includes tradeoffs of design, fatigue resistance, electrical performance and economic costs for copper, aluminum, copper-clad Invar and copper-clad stainless steel interconnects. A paper describing the procedure, titled "Design Solutions for Solar Cell Interconnect Fatigue Fracture Problem," by G.R. Mon and R.G. Ross Jr., was presented at the 16th IEEE PV Specialists Conference in San Diego.

Module Temperature and Humidity Testing (Wyle Laboratories)

A total of 90 minimodules, including Block III and IV designs, have been incorporated into the temperatures and humidity test series at Wyle Laboratories. Six environmental tests in progress include 85°/85% RH, 85°C/70% RH, 70°C/85% RH, 40°C/93% RH, 85°C and 100°C chambers with half of the test lot in a forward-voltage-bias mode. The reduction of visual and electrical performance data is being used in the development of degradation-rate curves for various failure mechanisms. The Wyle accelerated environments will be correlated through use of the degradation rates to 20-year equivalent site environments based upon temperature data from SOLMET weather tapes.

Initial observations from the Wyle tests have revealed: (1) the importance of foil back covers over Tedlar in protecting PVB-encapsulated modules; (2) that electrochemical degradation of grid-line ends occurs on both print-Ag and Ti-Pd-Ag metallizations and (3) the high resistivity of silicone over PVB and EVA encapsulants to discoloration from long temperature exposure.

Array Soiling

Tests were conducted on smooth- and stippled-glass superstrate modules to measure power losses from shadowing of soiling particles as well as losses from Fresnel effects and cosine (of angle of incidence) effects. Results showed that estimates of annual energy output can be overestimated by 6.5% for smooth glass modules (10% soiling) and 6.2% for stippled glass modules (15% soiling) if only cosine effects are considered and Fresnel and soiling losses are ignored. Dramatic overestimates of up to 20% in annual power output were obtained with heavily soiled stippled-glass superstrate modules.

Module and Array Reliability

IIT Research Institute (IITRI), Chicago, completed its final report, titled "Reliability Engineering Analysis Research for Flat-Plate Photovoltaic Modules/Arrays." The IITRI research was performed as a support effort within the FSA Engineering Sciences Area and consists of an overview of component failures and reliability within modules and arrays. The report was distributed to the PV community and DOE National Laboratories.

ENGINEERING SCIENCES AREA

ENGINEERING SUPPORT

Engineering interface activities that provide for transfer of array requirements, design guidelines, analysis tools and test methods to the overall photovoltaic community continued in several areas.

Engineering Sciences Area supported the development of the Sacramento Municipal Utility District (SMUD) Project in several key areas, which included reviews of design criteria and module specification drafts, the establishment of the electrical and mechanical subsystem functional requirements, natural frequency analysis of the tracking array, design reviews and an array--power-conditioner interface analysis for concept selection. JPL conducted a Safety Workshop and participated in a Power-Conditioner Workshop involving representatives from SMUD, Acurex, California Energy Council, DOE, Sandia, EPRI and Aerospace Corp. In addition, JPL installed a field-test experiment to measure variations in soiling rates at the SMUD PV System Rancho Seco site. Plans also include acquiring an On-Site Data Acquisition System (ODAS) from Sandia for SMUD to record local insolation and weather data. These data will aid in the design of photovoltaic systems for SMUD; weekly telephone transmissions of ODAS data will be made to JPL for storage and analysis.

Engineering Sciences Manager R.G. Ross Jr. participated in a meeting of the U.S. Technical Advisory Group to the International Electrotechnical Commission (IEC) photovoltaic technical committee (TC-82) in Phoenix, Arizona, on August 2-3. Ross was nominated as a candidate for the U.S. delegate to Working Group 2 on Module Environmental Testing and Electrical Measurements.

Engineering Sciences staff members participated in the ASTM meeting of Subcommittee E 44.09 on Photovoltaics held September 13-16, 1982 in Reno, Nevada. Meeting highlights included reviews of three newly revised Draft Standards and a Subcommittee vote to resolve "negatives" received on another Draft Standard which had been through subcommittee-committee ballot. An Action Item was taken to have FSA play an active role in the development of a Draft Standard on "Standard Method for Performing Hail Test on Photovoltaic Modules" at the next ASTM meeting in March, 1983.

Members of the Engineering Group participated in a Research Forum on Quantifying Degradation of Materials and Material Systems for Terrestrial Service held in Williamsburg, Virginia, December 6-8. The miniconference of about 75 researchers covered many degradation disciplines including fatigue, glass breakage, soiling, polymer degradation and corrosion. R.G. Ross Jr. made the theme presentation for the conference. Technical presentations were made by G.R. Mon, D.M. Moore and Ross, all of the FSA Engineering Sciences Area.

Recent Engineering Sciences Area Publications

"Characterization of the Electrical Output of Flat-Plate Photovoltaic Arrays," C.C. Gonzalez, G.M. Hill and R.G. Ross, Jr., 16th IEEE Photovoltaic Specialists Conference, September 27, 1982.

"An Accelerated Stress Testing Program for Determining the Reliability Sensitivity of Silicon Solar Cells to Encapsulation and Metallization Systems," J.W. Lathrop and E.L. Royal, 16th IEEE Photovoltaic Specialists Conference, September 27, 1982.

ENGINEERING SCIENCES AREA

"Design Solutions for the Solar Cell Interconnect Fatigue Fracture Problem," G.R. Mon and R.G. Ross Jr., 16th IEEE Photovoltaic Specialists Conference, September 27, 1982.

"Development of a Photovoltaic Module Qualification Test Based on Combined-Environment Accelerated Stress Data," S.E. Trenchard, E.L. Royal and R.T. Anderson, 16th IEEE Photovoltaic Specialists Conference, September 27, 1982.

"Photovoltaic Array Power Conditioner Interface Requirements," C.C. Gonzalez, ISES Annual Meeting, June 1982.

"Advanced Residential Photovoltaic Array Designs," R.S. Sugimura, N.E. Shepard and G. Royal, ISES Annual Meeting, June 1982.

"Photovoltaic Array Grounding and Electrical Safety," A. Levins and R.S. Sugimura, ISES Annual Meeting, June 1982.

"Solar Cell Interconnect Design for Terrestrial Photovoltaic Modules," G.R. Mon and D.M. Moore, JPL Publication 81-111; JPL Document No. 5101-173, presented at ASME Annual Meeting, April, 1982.

PERFORMANCE CRITERIA AND TEST STANDARDS

Active interfaces were maintained between FSA Engineering Area activities and the SERI Performance Criteria/Test Standards (PC/TS) project to establish Performance Criteria and Test Standards covering both flat-plate and concentrator arrays. Interim Performance Criteria (IPC) Issue 2, containing Performance and Criteria (Volume I) and Test Methods (Volume II) for both flat-plate and concentrating photovoltaics was published and released by SERI to the PV community. Environmental test methods included in the document were compiled by FSA Engineering Sciences Area and represent a consensus of FSA Block V Procurement and PV industry qualification test methods.

State of Arizona representatives chaired an Electrical Performance Subgroup meeting August 18, 1982, to finalize reformatted copies of electrical performance test methods for concentrating photovoltaics.

MODULE PERFORMANCE AND FAILURE ANALYSIS AREA

INTRODUCTION

The overall objective of the Module Performance and Failure Analysis Area (MPFA) is to evaluate the reliability and durability of modules that are constructed using the improved techniques researched in the other FSA Tasks and Areas. This is accomplished through a structured program of:

(1) Procurement of modules to a specification.

(2) Environmental stress testing.

(3) Detailed failure analysis.

(4) Operation in a field environment to obtain data that will:

   (a) Confirm the reliability and durability of the tested article.

   (b) Confirm the validity of the environmental test regimen imposed in item (2).

Accomplishment of this work also requires implementation of an accurate, repeatable, and reliable performance measuring system. Work activities and accomplishments in all of these activities of the Area during the reporting period are described below.

MODULE DEVELOPMENT

Block IV Design and Qualification

The last open contract for Block IV module designs was completed with qualification of the Photowatt International, Inc., module, and delivery of the final report. Qualification had been delayed by failure of the final hi-pot test. The problem was solved by substitution of a continuous rather than a pieced vinyl gasket around the periphery of the laminate.

The performance characteristics and physical descriptions of 12 different modules are given in the User Handbook for Block IV Silicon Solar Cell Modules, JPL Document No. 5101-214 (DOE/JPL-1012-75), by M. I. Smokler, dated September 1, 1982. Included are eight successful Block IV designs and four other designs that also were submitted to Block IV tests.

Block IV Production Orders

All block IV production orders have been completed with the delivery of intermediate-load and residential modules from Solarex Corp. and of intermediate-load modules from Applied Solar Energy Corp. (ASEC) and Photowatt International, Inc. The Solarex deliveries were completed after JPL approval of a module repair procedure. The ASEC production had awaited completion of environmental

tests to determine whether delamination problems in early production were solved. Photowatt could not start production until successful completion of the Design and Qualification contract.

Block V Group I Phase

The six contractors for the Block V designs were invited to bid on supplying 10 modules each for Block V testing. ARCO Solar, Inc., General Electric Co. (GE), Mobil Solar Energy Corp. (MSEC), Solarex Corp. and Spire Corp. elected to bid and were awarded purchase orders. RCA declined to participate.

GE delivered 10 modules, of which four are in a roof section. ARCO also delivered 10, but four have been returned for investigation of the cause of failure in the hi-pot test. MSEC has delivered six modules (with EFG cells) and is installing the other four in a roof section.

Solarex has delivered seven of the 20 due (two types). The Spire modules are due by February 1, but will be several months late as have been those from MSEC and Solarex. These late deliveries are not unreasonable, since the modules represent the first attempt to manufacture the Block V designs.

Block V Group II Phase

Requests for proposals were issued for a Group II phase of the Block V effort to obtain design and inspection documentation, design review presentations, submission of 10 more modules and a final report. Fabrication of these 10 modules will not be permitted until the contractor presents acceptable corrections to cure deficiencies arising in the qualification tests on the Group I modules. This procurement effort resulted in contracts with ARCO, MSEC, Solarex and Spire, with contract issue dates ranging from September through January. However, no activity other than preliminary documentation has been possible because none of the Group I modules has completed qualification testing.

A report on the Block I through Block V experience was presented at the AS/ISES 1982 Annual Meeting, Houston, Texas, June 1-5, titled Experience in Design and Test of Terrestrial Solar-Cell Modules, by M. I. Smokler and L. D. Runkle.

MODULE TEST AND EVALUATION

Performance Measurements

The selection, fabrication and identification of 12 new reference cells have been completed in support of Block V and Georgetown module testing. Spectral response and temperature coefficient measurements have also been completed. Final calibration and sealing of the cells has been awaiting good weather and repair of the data acquisition equipment.

MODULE PERFORMANCE AND FAILURE ANALYSIS AREA

JPL has given DSET Laboratories, Inc., a contract to fabricate and calibrate three types of reference cells: Spire, ASEC (BSR), AND MSEC (production). DSET has completed the fabrication of four reference cells of each type. These cells are presently scheduled for calibration in sunlight at DSET and are expected to be returned to JPL for evaluation in May 1983.

Since the 20th PIM, further evaluations have been made of the Schott GG-4 filter presently in use with the LAPSS systems to simulate AM1.5 spectral irradiance. A paper on the results was presented at the 21st PIM. Some refinements were made on the location and the height dimension of the intensity slot in the lamp assembly to improve illumination uniformity. Uniformity is now better than $\pm$ 1% over a 4 x 6-ft area at the target plane. In addition, temporal stability tests have shown that about 1500 lamp flashes over a two-month period have had no detrimental effect on the filter's transmission characteristics. Tests to determine long-term filter stability are in progress.

The Field Test effort required an improved means of normalizing module electrical performance data for evaluating the long-term electrical degradation of modules. To provide this means, intensity and temperature-dependent correction factors, including series resistance, were measured for all modules to be fielded, using the LAPSS and hot box. Knowledge of the module series resistance was particularly important to normalize sunlight electrical performance measurements correctly. Using these correction factors, module data taken over a wide range of temperatures (28°C to 60°C) and intensities (50 to 122 mW/cm^2) were normalized to 100 mW/cm^2 intensity at 45°C. The results showed excellent agreement with empirical data taken at 100 mW/cm^2 at 45°C and provided a means of considerable improvement in the normalization of field-test data.

Last year, an in-depth study of the cause of random LAPSS flash failures (failure to record data properly) was conducted. The conclusion is that there are deficiencies in the ac source and in the LAPSS controller circuitry. The ac source has higher-than-normal impedance, allowing LAPSS-generated pulses to form. The LAPSS controller does not include adequate isolation between signal circuitry and power circuitry to be independent of these pulses. Consideration will be given to the tradeoff between LAPSS data recording failures and the cost of correcting the problem.

Progress continues on the PDP-11/60 computer-LAPSS interface. The SYSGEN phase is complete and documented. It is now possible to develop system software with minimum interruption of normal LAPSS operations. When complete, each LAPSS facility will be equipped with a printer/plotter and the disk access time and storage capabilities of the PDP-11/60 will be much improved.

Environmental Testing

Another three sets of Georgetown University modules (for four prime contractors) were tested in this period. (Problems with the first set tested last winter, January - April, 1982, had resulted in rejection of all bid proposals and reissuance of the RFQ.)

MODULE PERFORMANCE AND FAILURE ANALYSIS AREA

In the current series of Georgetown module tests, one of the three sets of modules passed the environmental tests. The other two types had various problems including encapsulant bubbles and/or delamination, mounting-frame failure, and electrical degradation.

A variety of other modules were tested, including:

(1) Block IV prototypes and other special modules procured for testing to Block IV specs

(2) Block IV production modules tested to Block V specs

(3) Block V and commercial modules tested to Block V specs.

Results are given in Table 2.

Field Testing

Field-test activities during this period consisted of completing the restructuring plan, getting the portable array I-V logger to an operational state and initiation of data collection at all sites. The main effort consisted of the installation of modules to complete the remaining three arrays at the JPL site and to start the daily data acquisition process for all modules in the field. The modules for the newly established site at the Florida Solar Energy Center (FSEC) in Cape Canaveral, Florida, were installed and baseline I-V data were obtained.

Installation of the remaining three arrays at the JPL site brought the total at the site to six in accordance with the restructuring plan. The new arrays were made up of modules from ASEC, Photowatt, and GE. The GE array consists of 80 modules, wired four modules in parallel by 20 in series, resulting in a system with an output in the 1200 W to 1300 W region. The ASEC array consists of 12 modules in series yielding 800 W to 900 W. The Photowatt array is made up of 11 modules with an output of 350 W to 400 W. All of the arrays, including the three arrays installed during the last reporting period, are connected to the data acquisition system and data are being taken daily for all modules, except those in the GE array. Since the GE array consists of the hexshingle type modules (on which module interconnections are inaccessible) only array data can be sampled. Four months of data have been acquired to date.

The portable array data logger became operational in mid-July, 1982. Since that time the logger has been used to obtain data for the arrays at the JPL site, at Mississippi County Community College in Blytheville, Arkansas and at two residential installations near San Diego, California. The results of the non-JPL site tests were presented to the managers of the systems in the form of tabulated and plotted data.

A test site was established at FSEC consisting of 36 modules, six each from ARCO, ASEC, Motorola, Photowatt, Spire, and Solarex. These modules were individually wired to fixed resistors that represent peak power output loads. The modules are visully inspected weekly by FSEC personnel on a contractual

Table 2. Results of Environmental Tests

Vendor Code	No. of Modules Tested	Test Spec.	Tests Completed	Results
Block IV				
S/Prod	4	V	Final Tests	Satisfactory
S/Repaired	2	IV	T~, H~, Hi-Pot	Satisfactory
UR/Proto	4	IV	H~, Wind, Hail~	Many more cell cracks
US/Prod	4 2	V	T~, HF, T-200~	A few cell cracks, cell movement, acceptable interconnect fatigue; edge sealant extruding, grid discoloration on all modules
V/Prod	6	V	T~	Laminates loose in frame, gaskets shrunk, back-skin wrinkled, cell cracks
V/Prod	1	V	Hot-spot	Satisfactory
YR/Prod	6/4	V	T~, HF	1 cell crack, 1 back surface split, 1 loose gasket; amber discoloration and cloudiness over cells from HF
YS/Prod	6/4	V	T~, HF	Air bubbles at edges and corners; back-surface splits (2); amber discoloration, cloudiness; splits in RTV edge sealant
M/Prod (Exchange)	3	IV	T~, H~	Small air bubbles at module edges; marginal electrical degradation (1 module)
Special				
F	6/4	IV	All	Frame seal delamination, 360°; brown discoloration, terminal corrosion (2), cover glass cracks, cell crack (1)
F	1		NOCT	Heavy brown/gray discoloration, 1 in. wide inboard of edge, 360°; edge delam, cloudiness

Table 2. Results of Environmental Tests (Cont'd)

Vendor Code	No. of Modules Tested	Test Spec.	Tests Completed	Results
<u>Block V</u>				
US1	5/4	V	T~, HF, MI	4 cracked cells; discoloration of grids; mild extrusion of edge sealant and yellowing of RTV terminal cover cement
<u>Commercial</u>				
M	6/4	V	T~, HF	3 electrical failures due to corroded terminals; drop in resistance to ground during test; 1 cell crack; yellowing of terminals and Tedlar
M	1		Hot-spot	Failed
Q	4/2	V	Final Testing	2 of 6 failied final hi-pot; some problems with delam, cell crack (1), yellow discoloration; hot-spot wrinkled back surface
R	4/2	V	Final Testing	J-boxes loose (2), cover screw inserts cracked, delam between cells (1 at 2.5 x 4 cm); Tedlar splits and peeling
X	6	V	All	Galvanized frame corrosion, mounting board (plastic) cracked; some encapsulant yellowing
<u>Foreign</u>				
I	1	IV	T~, H~	Delam front and back of cells, edge delam, discolored metallization

Test Code:

- T~ = 50 temperature cycles
- H~ = Blk IV humidity test
- HF = 85°/85% humidity-freeze
- HS = Hot-spot test
- MI = Mechanical integrity
- Prod = Production module
- Proto = Blk IV prototype

basis and monthly reports are sent to JPL describing the condition of the modules. Electrical measurements will be made every six months by JPL, using the portable module I-V logger.

FAILURE ANALYSIS

The quarterly problem/failure reports (PFRs) and summaries have been issued to the module manufacturers in May, August and November, 1982. These reports are intended to keep the manufacturers abreast of environmental, field-test and application problems. Causes of problems are investigated to establish failure modes resulting both from design inadequacies and from workmanship.

The problem/failure reporting system now includes recorded problems/failures on 35 manufacturers' products, both domestic and foreign. The reporting system has accumulated a total of 1217 PFRs of which 1067 have been closed.

The laser-scan equipment developed to support the solar project has been used extensively to record the condition of modules before environmental test and to select specific cells to be subjected to hot-spot testing. The laser-scan test has been successful in identifying shorted, partially shorted, and cracked cells that affect the cell output.

The Block IV, Block V and commercial modules that are generally contained in metallic frames have often exhibited problems in ability to meet the high-voltage-withstanding tests. Failure analysis indicated that the breakdowns were caused by either point-to-plane discharge or leakage current between the active solar cell string and the frame, as a result of voids.

The failure modes of modules investigated during this reporting period are summarized as follows:

(1) High-voltage-withstanding problems

(2) Shorted cells

(3) Cracked cells

(4) Fractured/overstressed interconnects

(5) Discolored encapsulation

(6) Voids in encapsulation

(7) Loose junction boxes/terminals

(8) Poor solder joints at terminals or bus interconnections

(9) Delamination of encapsulant at the edges of module

(10) Discolored cell collector grids.

PRECEDING PAGE BLANK NOT FILMED

ORIGINAL PAGE IS
OF POOR QUALITY

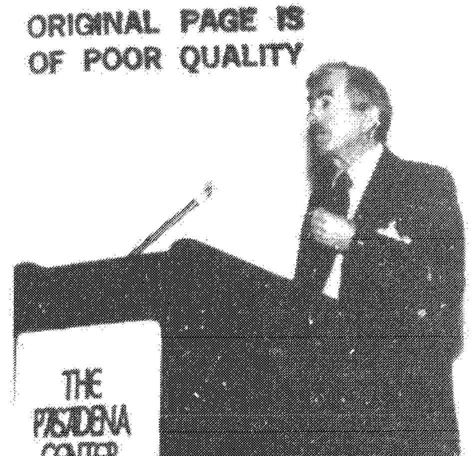


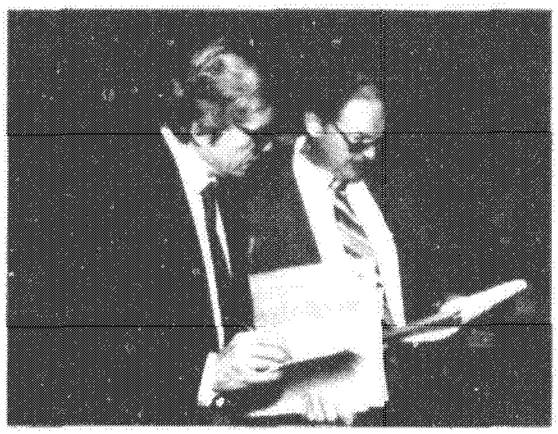



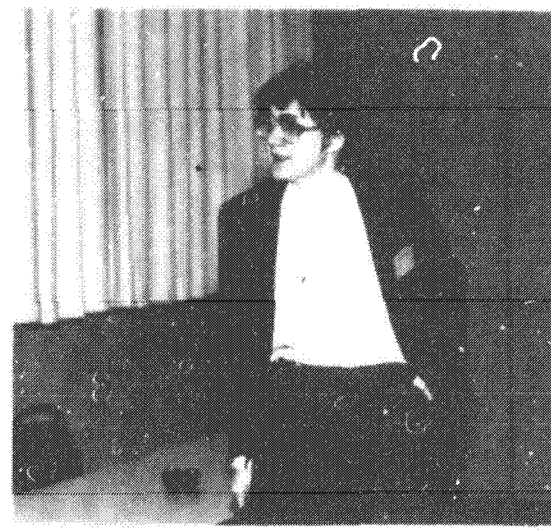


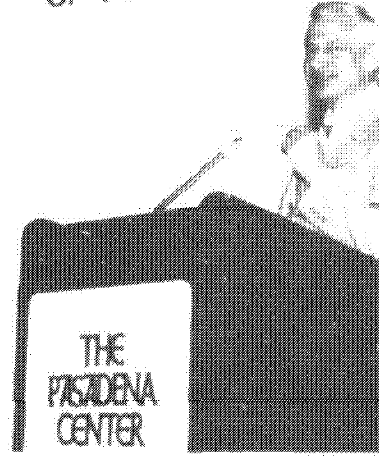
THE
PASADENA
CENTER



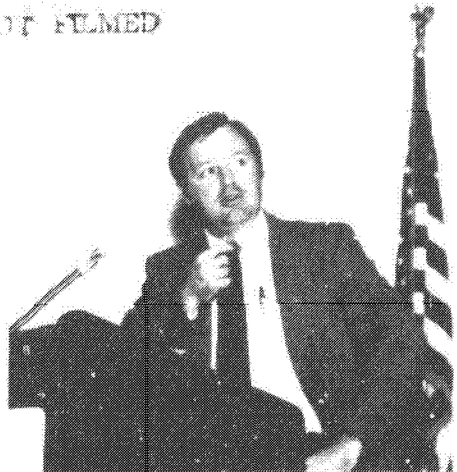


PROCEEDINGS

INTRODUCTION

The 21st Project Integration Meeting (PIM) of the Flat-Plate Solar Array Project (FSA) of the Jet Propulsion Laboratory (JPL) was held at the Pasadena Center, Pasadena, California, on January 12 and 13, 1983. The theme, "FSA Progress and Plans," highlighted three subjects in addition to covering the usual presentations and discussions of FSA photovoltaic activities: thin-film solar cell and module technology development needs, polysilicon activities, and central-station activities.

During the January 12 plenary session, presentations were made on each of the three highlight topics as were summaries of the Silicon Material Workshop and the Quantifying Degradation Research Forum, which were held after the 20th PIM. On January 13, thin-film deposition technologies for photovoltaics were discussed by four speakers.

The three topics were highlighted because:

Excellent progress has been achieved in thin-film cell research during the past few years. Increasingly efficient cells that can be duplicated have been fabricated in laboratories. A few of these devices now have the efficiency and quality to warrant the application of resources to begin their transformation from laboratory devices into practical and economically manufacturable products for large-scale use. The development of the necessary technology requires a long-range commitment, the involvement of a broad spectrum of talented people, considerable financing, and years of consistent and productive labor. A vital factor is the stimulation and involvement of people with diverse talents and capabilities who can contribute to this new thrust in photovoltaics.

Significant progress has also been made in developing the technology required for the production of polysilicon. More research in the silane-to-silicon deposition technology is needed to acquire knowledge before a commercial plant can be built that can produce high-quality low-cost silicon. Assessment of the status of the competing low-cost silicon refining technologies and the current silicon refining research activities is necessary for guiding the remaining DOE-sponsored technology efforts.

Significant progress has been made in photovoltaic central-station studies, designs, and an actual installation. It is important to understand how these achievements relate to future module and array considerations.

A summary of plenary session presentations follows.

Plenary Sessions

ORIGINAL PAGE IS OF POOR QUALITY

SUMMARY

Mort Prince, Chief of the Collector Research & Development Branch (Photovoltaic Division) of the U. S. Department of Energy (DOE), presented the latest thinking within DOE regarding the FY83 photovoltaic budget. He discussed the fact that the ARCO Solar, Inc. bid on the Sacramento Municipal Utility District (SMUD) project of $4.95/W$_p$ for modules (f.o.b.) compares well with the DOE 1982 goal of $2.80/W$_p$ (1980 $) when inflation, production levels, and markets costs are considered. He also discussed DOE's initiation of a Thin-Film Study Task Force.

W.T. Callaghan, manager of the Flat-Plate Solar Array Project, was chairman of the first plenary session, titled Polysilicon Refining Progress, Problems and Promise.

Silicon Material:

James McCormick of Hemlock Semiconductor Corp. described the status of Hemlock's polysilicon process. Dichlorosilane (DCS) is made from trichlorosilane (TCS) by a redistribution reaction using an organic amino functional catalyst, and the DCS is then pyrolyzed to produce silicon in a chemical-vapor-deposition (CVD) step using Siemens-type reactors. In June 1982 Hemlock's contract effort was completed with promising results, which indicated that work should continue. Hemlock has since tripled the output of the DCS process development unit (PDU) by company-funded activities. JPL is funding experiments with a cold-metal-wall silicon-deposition reactor to reduce excessive silicon deposition on the reactor walls. Initial results are promising.

James Lorenz, recently retired from Union Carbide Corp. (UCC), described the status of the UCC silane process for producing low-cost semiconductor-grade silicon. The silane portion of the 100 MT/yr experimental process system development unit (EPSDU) has produced its first silane. The quality of the silane will be determined during the next stage of the effort. The operation of the EPSDU will permit optimizing the design of a commercial UCC 1200 MT/yr plant under construction at Moses Lake, Washington, with completion scheduled for 1984. A fluidized-bed reactor for conversion of the silane to silicon is now being installed.

A Science of Silicon Material Workshop, sponsored by FSA, was held August 23 to 25. The objectives of this Workshop, which was chaired by R. Lutwack of JPL, were to discuss the chemistry, physical chemistry, and chemical engineering involved in the preparation of semiconductor-grade polysilicon; to review the status of preparation technologies, and to identify critical barriers to improved processes and experimental programs to address the technical problems. Six sessions were held: Silicon Production and Purity; Thermodynamics, Kinetics and Mechanisms; Particle Formation and Growth; Deposition in Fluidized-Bed Reactors; Chemical Vapor Deposition, and Alternative Polysilicon Processes. The 22 invited papers and the discussions

48

provided a stimulating forum for the exchange of information, the pinpointing of problem areas, and the introduction of research ideas. A large part of the Workshop dealt with the chemistry of, and the problems encountered in the use of, silane for the deposition of silicon. Proceedings have been published.

Thin-Film Solar Cell and Module Technology Development:

K.M. Koliwad of JPL summarized a photovoltaic thin-film viewpoint: with the recent excellent progress in thin-film PV materials and device research by both government and privately funded efforts, it is now time to initiate development of the technology required to make a competitive product. Some industrial organizations are now funding product-oriented thin-film technology development. However, thin-film module design and fabrication processing is sufficiently different from crystalline silicon technology that extensive new technology and techniques must be developed before inexpensive and reliable products can be produced. Therefore, a comprehensive well-planned approach is required to explore systematically the many technical options and parametric tradeoffs in order to understand the complex interactions involved in good module design and reliable, long-life module operation.

FSA's thin-film activities are in abeyance until the DOE Thin-Film Task Force has submitted its report and decisions are made regarding future activities and responsibilities.

J. Stone of the Solar Energy Research Institute (SERI) presented a comprehensive overview of promising thin-film solar cells, including a chronology of significant events in the DOE-sponsored thin-film program. He set forth a number of reasons for the development of thin-film solar cells, and he developed a general rationale for the advantages of thin-film technology. He presented plots of cell-conversion efficiency improvements against time, and sketches of cell configurations for amorphous silicon cells, Cu binary and ternary cells, $CdS/CuInSe_2$ cells, CdTe cells and gallium arsenide cells. He explained key AR&D problems and discussed a possible future federal government role in thin-film photovoltaics.

A concise overview of the thin-film deposition technologies was presented by J. Thornton of Telic Co., covering the basic deposition processes and their general applicability to high-efficiency thin-film PV cells. He discussed physical vapor deposition (PVD), including evaporation and sputtering CVD and plasma-assisted CVD (glow discharge), and presented sketches representing the basic process parameters and equipment functions. He described the major limitations and problems involved in making photovoltaic cells.

The entrance of Ametek, Inc., into photovoltaics was described by R.E. Russell. Ametek has been doing research on CdTe thin-film solar cells and is now building a small pilot plant for fabricating prototype modules. The company has electro-deposited CdTe on areas of up to 20 square inches, which are then cut into smaller cells for encasement in glass tubes. Ametek seeks understanding of a number of technical aspects of fabricating and measuring the performance of CdTe cells, which could be aided by government effort.

PLENARY SESSIONS

R. Gillette of Boeing Engineering and Construction discussed Boeing's R&D priorities as the company initiates its activities in producing $CdZnS/CuInSe_2$ thin-film solar cell modules. He discussed the four areas of Boeing's development plan: cell and material characterization, cell and module design, process development, and testing. Boeing realizes that considerably different technical approaches and different types of personnel are required to produce a product than are required to perform research; consequently, Boeing has established a new, separate organization for its production activities.

R. Blieden of Energy Conversion Devices (ECD) described ECD's entrance into commercial thin-film PV production, started by its joint venture with Sharp Corp. A one-foot-plus-wide, 0.008-inch-thick, 1,000-ft-long stainless-steel roll has been coated with amorphous silicon PV materials by glow-discharge-induced decomposition of silane. The automatic processor equipment that continuously deposits the PV cell layers was designed and fabricated by ECD. Initially the rolls of material will be cut into cells for use in solar-powered calculators. Later the rolls of material will be used to make PV modules for greater power generation.

"Chemical Reaction Engineering" was a presentation on the need for, and the value of, using existing chemical-reactor technology for use in developing future thin-film PV manufacturing capabilities. T.W.F. Russell of the University of Delaware explained the steps that today's profitable thin-film manufacturing operations have passed through as they evolved from laboratory to commercial production. Each new process requires adaptation and an evolution to a practical, profitable operation.

Module Degradation:

A major question in the large-scale use of photovoltaics is: How long will photovoltaic modules and arrays function reliably? The answer has a significant influence on power-generation economic projections. E.F. Cuddihy of JPL presented a summary of an FSA-sponsored Research Forum on "Quantifying Degradation," of which he was chairman. The Forum addressed the challenge of assessing long-term durability by short-term field testing and/or accelerated testing. Topics included current and potential approaches to identifying and characterizing degradation mechanisms such as corrosion, cyclic fatigue, photothermal aging, soiling, debonding and electrical-stress effects. Many of the 25 invited speakers were from other industries; their presentations and discussions related this broader experience to photovoltaics.

Central-Station Activities:

Three speakers offered presentations on progress in PV central-station studies and designs and on an actual installation.

M. Anderson, manager of the SMUD photovoltaic plant, presented SMUD's plan for a 100-MW PV station and the status of the first 1 MW plant. For the first 1 MW, ARCO modules, selling for under $\$5.00/W_p$ f.o.b., have been selected from competitive bids. These modules will be mounted on a 134-foot-long, 8-foot wide array that rotates on a north-south axis, enabling

more PV power to be generated during the utility's late-afternoon peak-load period. The modules are to be installed in 1983 and 1984 after a 10-kW test array has been tested satisfactorily.

A 1-MW PV power station in Hesperia, California, designed, built, owned and operated by ARCO Solar Electric Power, Inc., became fully operational on December 15, 1982. This was 38 weeks after an agreement was signed with Southern California Edison Co. (SCE). SCE buys the electric power from the ARCO Solar subsidiary at a competitive rate. The plant was financed through federal and state tax incentives, using a third-party arrangement. R.E.L. Tolbert, manager of the site, presented a sequence of slides showing the effort in planning and installing the 1-MW plant. It has 58 arrays, each 32 ft square, which are mounted on dual-axis tracker pedestals. The station is automatic and is unmanned.

The economic viability of tracking flat-plate photovoltaic arrays was presented by G. Jones of Sandia National Laboratories. He showed that at today's module prices, two-axis tracking arrays are more economical than fixed flat arrays, because the extra energy generated is worth more than the costs of tracking and of the additional land requirements. Analysis shows that two-axis tracking can be more economical, even at $\$1/W_p$ module prices, although land costs are the key factor at low module costs. Cost analyses for single-axis tracking arrays were not presented.

Thin-Film Deposition Technology Presentations:

The growth of thin films using a variety of materials and/or layers at relatively low temperatures can be accomplished relatively easily by CVD. V. Dalal explained how Chronar Corp. has used this technology to make amorphous-silicon PV devices. Chronar is planning to start thin-film PV commercial module manufacturing.

The advantages of depositing amorphous silicon by the glow-discharge technique in comparison with silicon deposition by evaporation or sputtering was presented by A. Madan of Chevron Research Co. for SERI. Amorphous silicon produced by the glow-discharge-induced decomposition of silane (SiH_4) gas onto substrates (at 200°C to 300°C) has high photoconductivity and an optical band gap of the range of 1.7 eV. Amorphous silicon deposited by evaporation or sputtering tend to have more dangling bonds that act as recombination centers for photogenerated carriers and consequently do not have as high cell-conversion efficiency. The decomposition of silane by glow discharge results in amorphous Si-H and H, in which the substrate temperature affects the amount of hydrogen incorporated in the film and the amount of dangling bonds. Further research and development to improve our understanding of the characteristics of amorphous silicon materials and devices can lead to higher-efficiency devices and is required to develop the technology for inexpensive mass-production capabilities.

The commercial aspects of physical vapor deposition (PVD) by sputtering and physical evaporation as appropriate for photovoltaics was presented by R. Hill of Airco Temescal. PVD is used today for coating large areas in

quantity production; coated architectural glass is an example. Millions of square feet of glass per year are coated by use of planar magnetron sputtering facilities, which have the capability of depositing multilayer coatings. Sophisticated thin-film PV coatings with stringent compositional, structural, and stability requirements, which are required to yield high-efficiency modules, will still require considerable research and development. A typical sequence required to plan and design a machine for producing thin-film products, which includes consideration of the many parameters required for a high-quality, high-yield product was presented. Even with extensive planning and development effort, there is a need to operate and fine-tune new process equipment.

The thin-film sessions were concluded by a presentation on the Characteristics of Thin Film by J. Thornton of Telic Co. The presentation included thin-film characteristics versus bulk materials, properties versus deposition conditions, and scale-up considerations. The general character of thin films is that they grow with a columnar structure, which has structural flaws induced by the many deposition parameters. Knowledge of the effects of parameters such as geometry, departures from stoichiometry, multimaterial fluxes, pressures, temperatures and many other conditions must be developed and they must then be controlled adequately. In the scale-up procedure after theoretical device development, deposition modeling, scaling laws, bench type tests, and identification of critical issues must be addressed before production equipment is designed.

Polysilicon Refining Progress, Problems and Promise

ORIGINAL PAGE IS OF POOR QUALITY

W.T. Callaghan, Chairman

HEMLOCK DICHLOROSILANE CVD PROCESS

HEMLOCK SEMICONDUCTOR CORP.

J. McCormick

Dependence of Array Power Cost ($\$/W_p$) on Solar-Cell Efficiency and Polycrystalline Silicon Cost

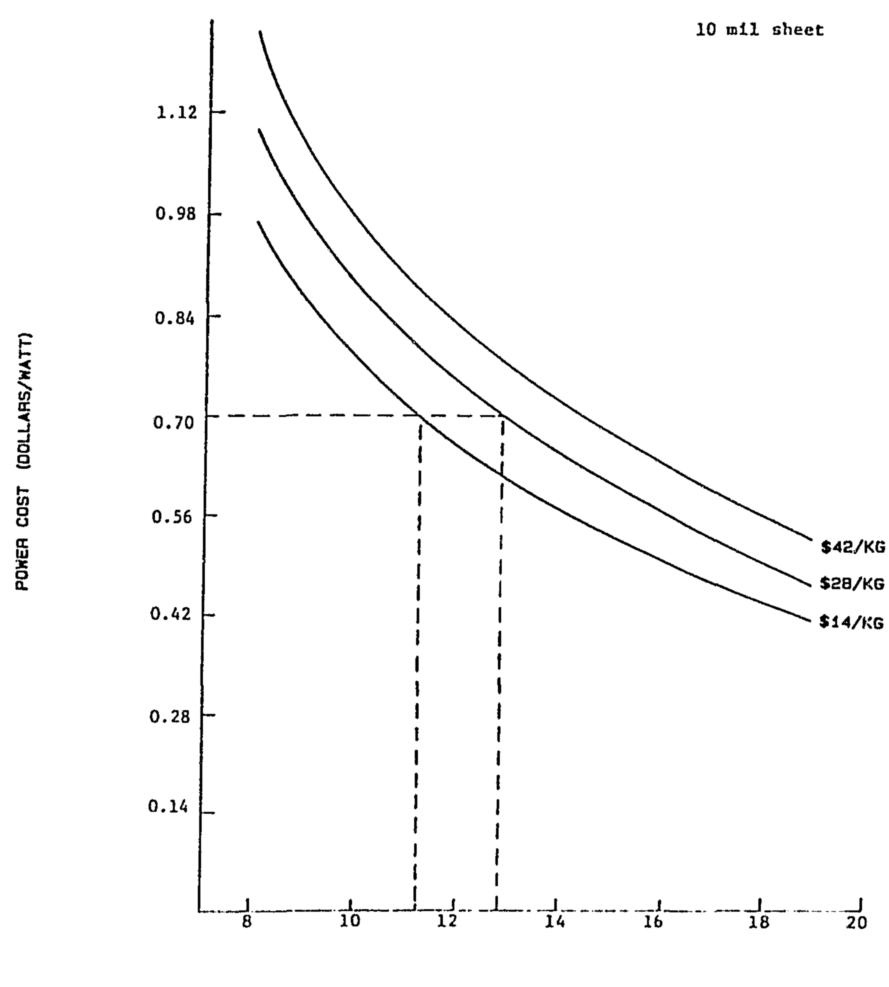

PRECEDING PAGE BLANK NOT FILMED

PAGE 54 INTENTIONALLY BLANK

Process Flow Diagram for Hemlock Dichlorosilane-Based CVD Process

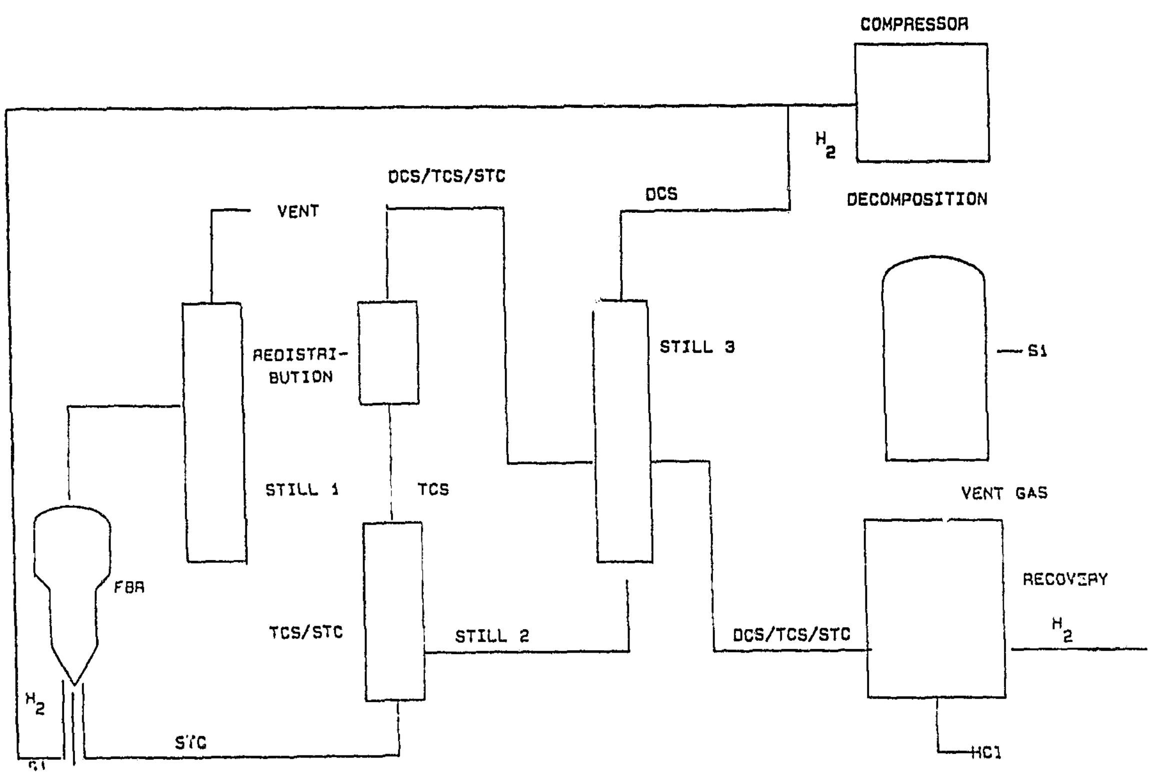

Relative Importance of Independent Variables on Response Function in DCS Decomposition

Silicon Deposition Rate	Conversion Efficiency	Power Consumption
1. Flow	1. % DCS	1. Flow
2. Temp.	2. Temp.	2. % DCS
3. % DCS	3. Flow	3. Int. of Temp. X % DCS
4. Int. of Flow and Temp.	4. Int. of Temp. and % DCS	4. Temp.
5. Int. of Flow and % DCS	5. Int. of Flow and Temp.	5. Int. of Flow and Temp.
6. Int. of Temp. and % DCS	6. Int. of Flow and % DCS	6. Int. of Flow and % DCS

ORIGINAL PAGE IS OF POOR QUALITY

Comparison of Experimental Reactor and Pilot-Scale Reactor Performance With JPL/DOE Contract Goals

	Deposition Rate $gh^{-1}cm^{-1}$	Conversion Mole Percent	Power Consumption kWh/kg
JPL/DOE Goal	2.00	40	60
Experimental Design	1.60	35.2	96
Modified Production Reactor	2.00	35.1	82

Summary of Solar-Cell Performance Using DCS

Cell Designation	V_{oc} (Ave.) mV	I_{sc} (Ave.) mA/cm^2	CFF (Ave.) %	η (Ave.) %
Applied Solar DCS	590	29.0	75	12.84
Applied Solar Baseline	583	28.2	75	12.40
Westinghouse DCS	571	21.18	70	9.11
Westinghouse Baseline	553	21.10	71	8.9

UNION CARBIDE SILANE PROCESS

UNION CARBIDE CORP.

J. Lorenz

UCC 100-MT/yr Pilot Plant for Silane Process (Washougal, Washington, June 1982)

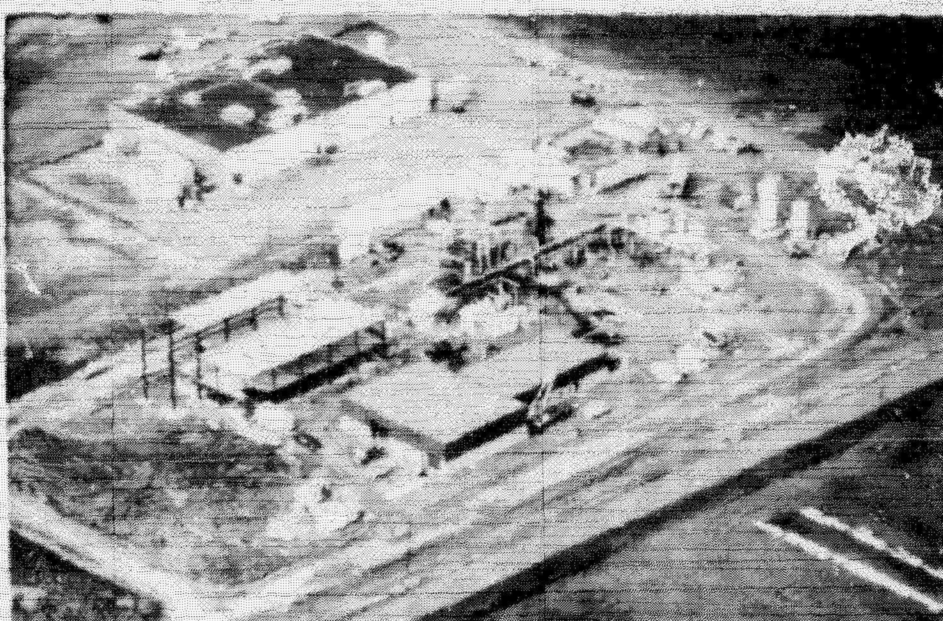

UCC Silane Process Pilot Plant for Producing Low-Cost Semiconductor-Grade Polysilicon

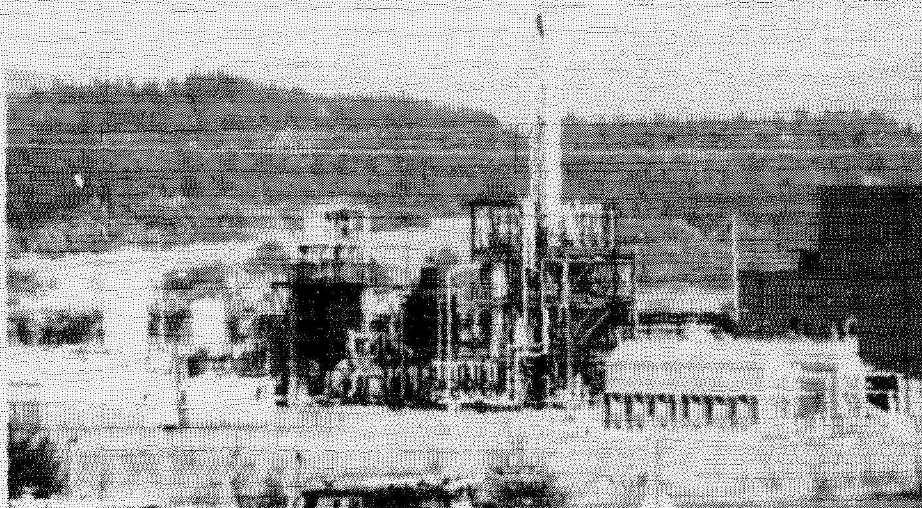

Silane Section of the Plant (Late 1982)

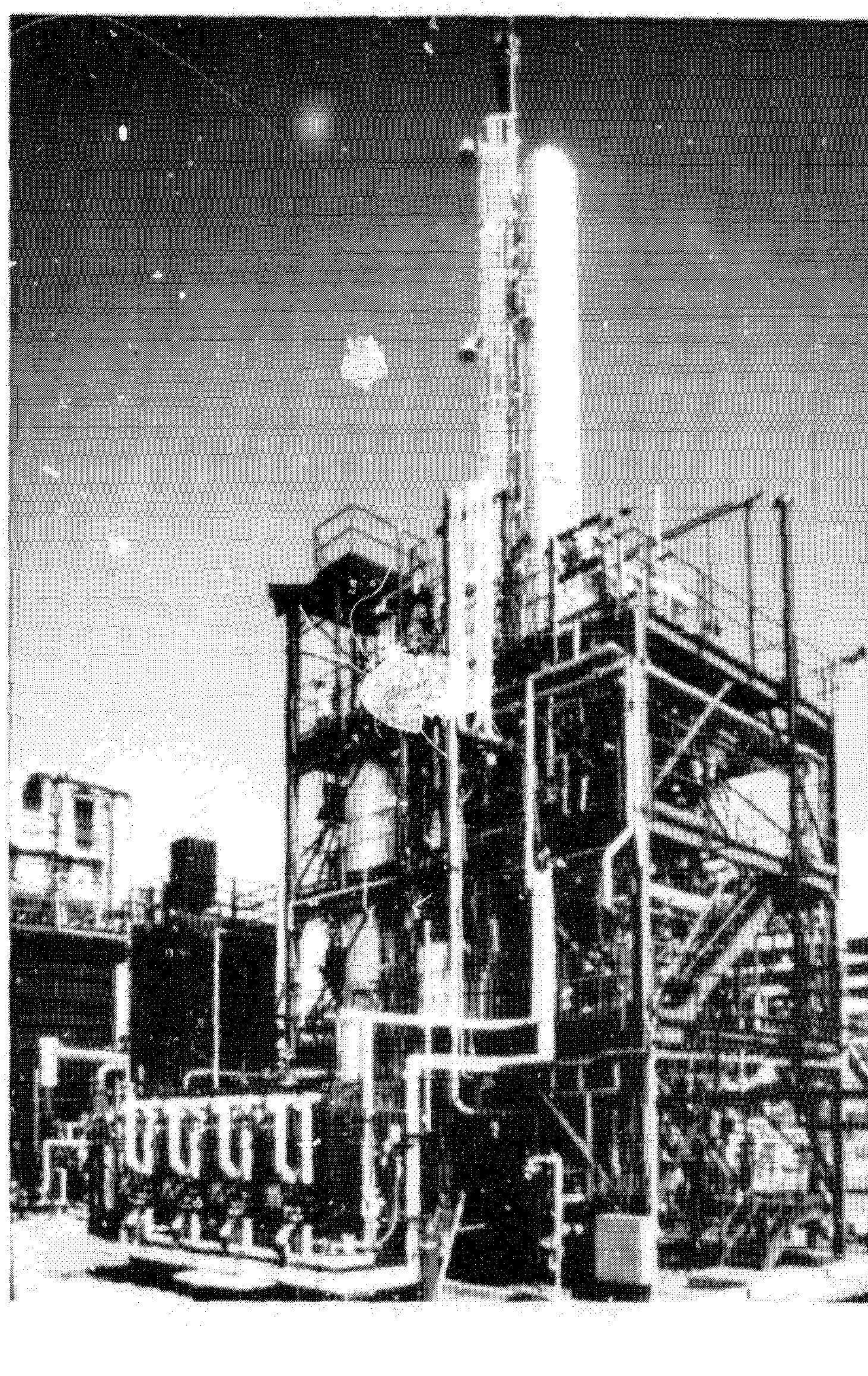

Site of Future 1200-MT/yr Silane Process
Plant at Moses Lake, Washington

Moses Lake Plant Site (October 1982)

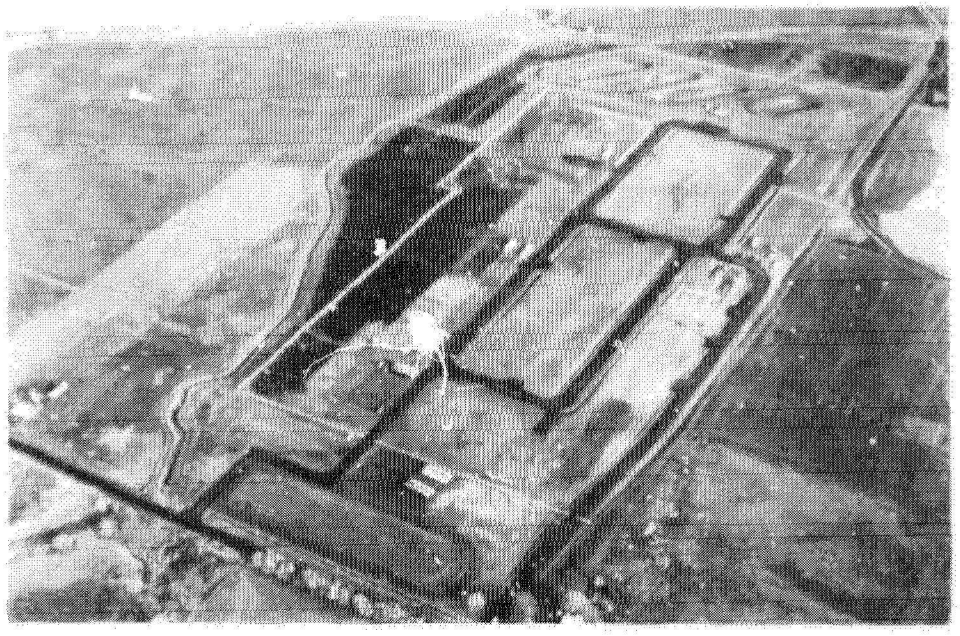

POLYSILICON REFINING PROGRESS, PROBLEMS AND PROMISE

THE SCIENCE OF SILICON MATERIAL PREPARATION WORKSHOP

August 23 to 25, 1982, at Phoenix, Arizona

JET PROPULSION LABORATORY

R. Lutwack

PROGRAM

Session I: Silicon: Production and Purity

(R. Lutwack, Chairman)

- THE SILICON CHALLENGE
  (JAMES LORENZ, UNION CARBIDE CORPORATION)

- SILICON PURITY: IMPACT ON CRYSTAL GROWTH AND SILICON PROPERTIES
  (RICHARD HOPKINS, WESTINGHOUSE RESEARCH CENTER)

Session II: Thermodynamics, Kinetics and Mechanisms

(D. Bailey, Chairman)

- CHLOROSILANE THERMODYNAMIC EQUILIBRIA CALCULATIONS WITH APPLICATIONS TO HIGH PURITY SILICON PREPARATIONS
  (HENRY F. ERK, MONSANTO CORP.)

- KINETICS AND MECHANISMS OF CHLOROSILANE DECOMPOSITION
  (DONALD BAILEY, CONSULTANT)

- KINETICS AND MECHANISM OF SILANE DECOMPOSITION
  (MORRIE RING, SAN DIEGO STATE UNIVERSITY)

- SESSION II - DISCUSSION

Session III: Particle Formation and Growth

(R. Flagan, Chairman)

- Homogeneous Gas - Phase Condensation of Silicon by Shock-Wave-Induced Decomposition of Silane (Jurgen Steinwandel, University of Stuttgart)
- Kinetics of Particle Growth in Silane Systems (William Felder, AeroChem Research Laboratory)
- Submicron Particle Size Measurement (Donald Pettit, University of Arizona)
- Factors Governing Particle Size in the Free Space Reactor (Richard Flagan, Californa Institute of Technology)
- Coherent Detection of Scattered Light from Submicron Particles (Donald Pettit, University of Arizona)
- SESSION III - Discussion

Session IV: Deposition in Fluidized-Bed Reactors

(T. Fitzgerald, Chairman)

- THE MECHANISM OF THE CHEMICAL VAPOR DEPOSITION OF CARBON IN A FLUIDIZED BED OF PARTICLES
(JAMES KAAE, GENERAL ATOMIC CO.)

- A MODEL FOR THE GROWTH OF DENSE SILICON PARTICLES FROM SILANE PYROLYSIS IN A FLUIDIZED BED
(THOMAS FITZGERALD, TRW, INC.)

- PARTICLE SIZE DISTRIBUTION IN FLUIDIZED BED REACTORS
(FERHAN KAYIHAN, WEYERHAUSER TECHNICAL CENTER)

- AN UPDATE ON A MATHEMATICAL MODEL WHICH PREDICTS THE PARTICLE SIZE DISTRIBUTION IN A FLUIDIZED BED PROCESS
(EARL GRIMMET, CONSULTANT)

- SESSION IV - DISCUSSION

Session V: Chemical Vapor Deposition

(M.P. Dudukovic, Chairman)

ORIGINAL PAGE IS
OF POOR QUALITY

- Reactor Models for CVD of Silicon
(Milorad Dudukovic, Washington University at St. Louis)

- The Deposition of Low Defect Density Amorphous Semiconductors by Homogeneous Chemical Vapor Deposition
(Bruce Scott, IBM Thomas J. Watson Research Center)

- Mechanisms in Plasma Enhanced Deposition of Silicon
(Kalluri Sarma, Solavolt International)

- Chemical Vapor Deposition of Epitaxial Silicon
(Rafael Reif, Massachusetts Institute of Technology)

- Chemical Vapor Deposition of Silicon for Optical Uses
(Michael Jacobson, University of Arizona)

- SESSION V - Discussion

Session VI: Alternative Silicon Processes

(A. Briglio, Jr., Chairman)

- Kinetics of Silicon Electrodeposition
(Jerry Olson, Solar Energy Research Institute)

- The Hemlock Semiconductor Dichlorosilane CVD Process
(James McCormick, Hemlock Semiconductor Corporation)

- Production of Silicon by the Reduction of Silicon Tetrafluoride with Sodium
(Angel Sanjurjo, SRI International)

- SESSION IV - Discussion

- WORKSHOP DISCUSSION AND CLOSING REMARKS
(Chairman, Ralph Lutwack)

Thin-Film Solar Cell and Module Development

K.M. Koliwad, Chairman

PROMISING THIN-FILM SOLAR CELLS: OVERVIEW

SOLAR ENERGY RESEARCH INSTITUTE

Jack L. Stone

Chronology of Significant Events

FY 78:
- Amorphous thin film for solar cell applications (DOE/PRDA)
- Thin film polycrystalline silicon solar cells (DOE/PRDA)
- Emerging materials systems for solar cell applications (DOE/PRDA)
- Photovoltaic mechanisms in polycrystalline thin-film solar cells (DOE/PRDA)
- SERI Photovoltaic AR&D Lead Center established

FY 79:
- Electrochemical photovoltaic cells (RFP)
- Advanced photovoltaic concentrator cells (RFP)
- Spray/screen print solar cell research (RFP)
- Low-cost substrates for polycrystalline silicon solar cells (RFP)
- Innovative concepts for photovoltaic converion (LOI)
- Thin film gallium arsenide solar cell research (RFP)
- Innovative concepts for photovoltaic conversion (LOI)
- Future supply of gallium (RFP)

THIN-FILM SOLAR CELL AND MODULE DEVELOPMENT

FY 80:
- Exploratory development of thin film polycrystalline silicon PV devices (RFP)
- Stability of cadmium sulfide/copper sulfide solar cells (RFP)
- Investigations of electronic properties of polycrystalline GaAs (RFP)

FY 81:
- Investigations of edge-supported pulling of silicon ribbon (RFP)
- Advanced photovoltaic system simulator (RFP)
- Module optimization methodology for advanced PV cells and devices (RFP)

FY 82:
- Basic understanding of high efficiency in silicon solar cells (RFP)
- Selected electrically active defects in polycrystalline silicon (RFP)

FY 83:
- Advanced high efficiency concentrator cells (RFP)
- New ideas for photovoltaic conversion (LOI)
- High efficiency single-junction monolithic thin-film amorphous silicon solar cells (planned RFP)
- High efficiency stacked multi-junction amorphous silicon alloy thin-film solar cells (planned RFP)

Why Thin Films?

- Material Conservative (typically <10 micrometers)
- High Absorption (typically >10 times crystalline silicon)
- More Optimum Bandgap for Efficient Solar Conversion (1.3-1.7 eV)
- Bandgap can be Synthesized in Many Material Systems
- Monolithic Approaches can be Used to Avoid Costly Conventional Interconnects
- Potentially Scaleable to Large Areas Using High Throughput Deposition Approaches
- Relaxes Encapsulation Requirements by Integrating the Substrate or Superstrate as Part of the Encapsulation
- Unique Structures are Possible Analogous to Integrated Circuit Fabrication
- Processes are Energy Conservative
- Material Utilization can be High
- Low Cost Potential

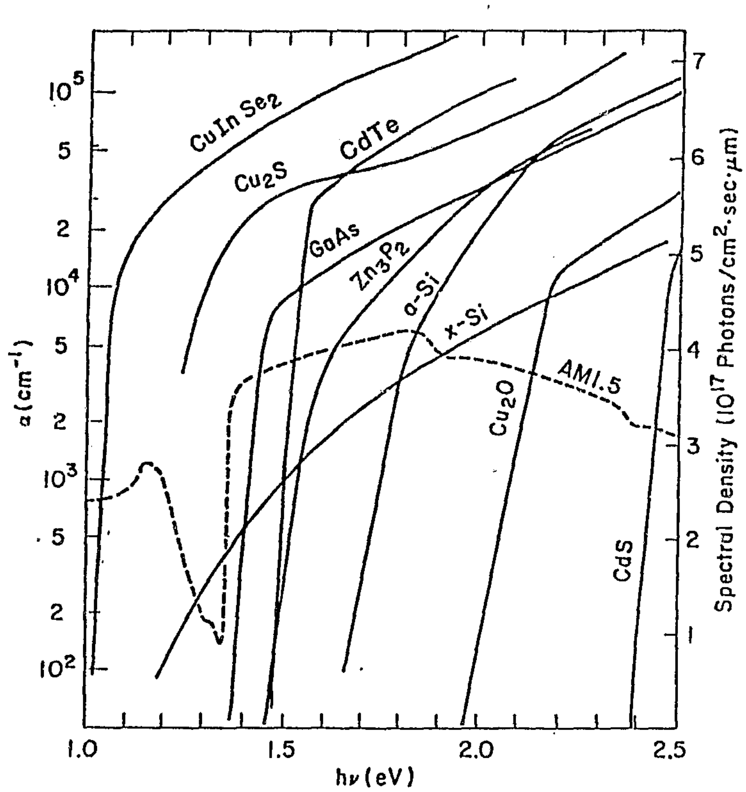

Actual and Projected Amorphous Silicon Solar-Cell Conversion Efficiency

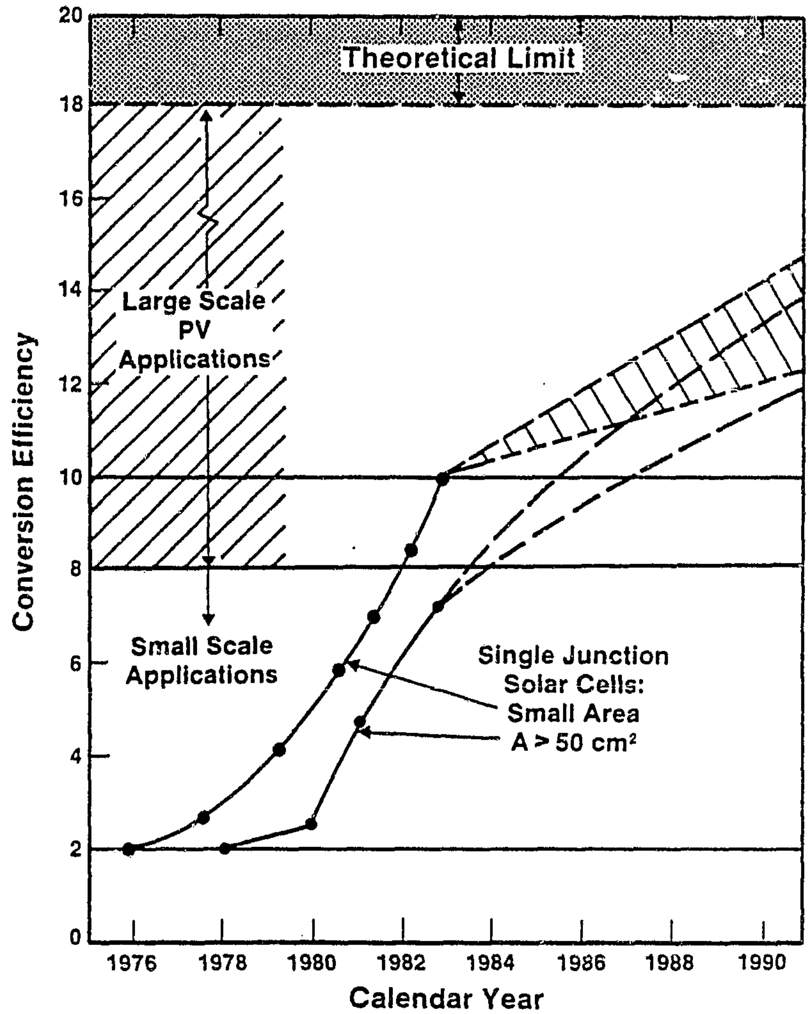

a-Si:H Solar Cell Structure

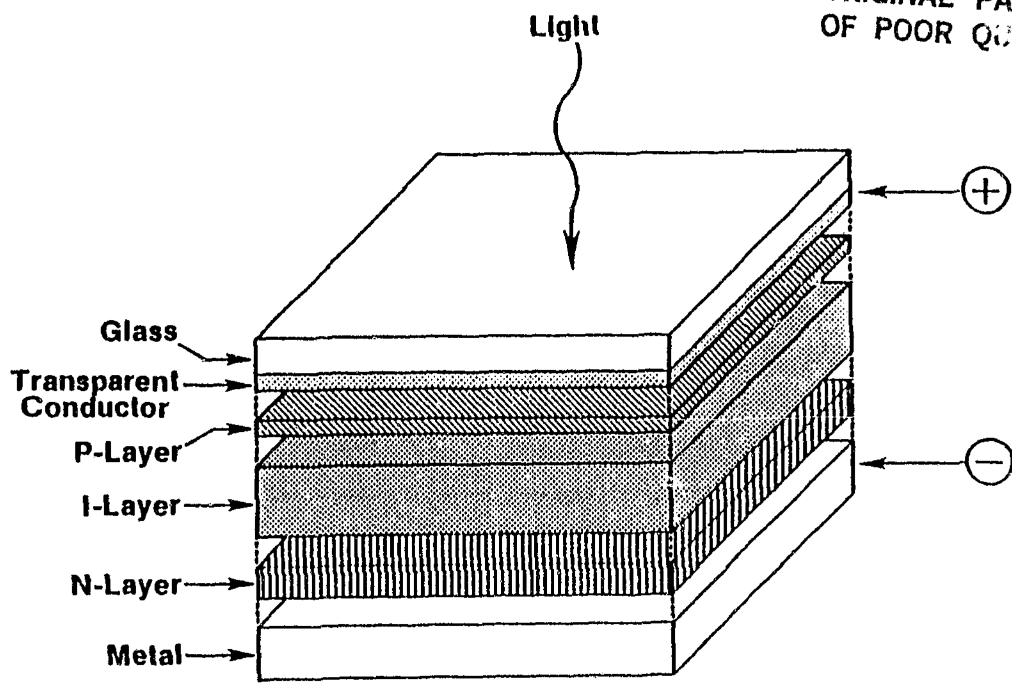

Integrated Cell Module

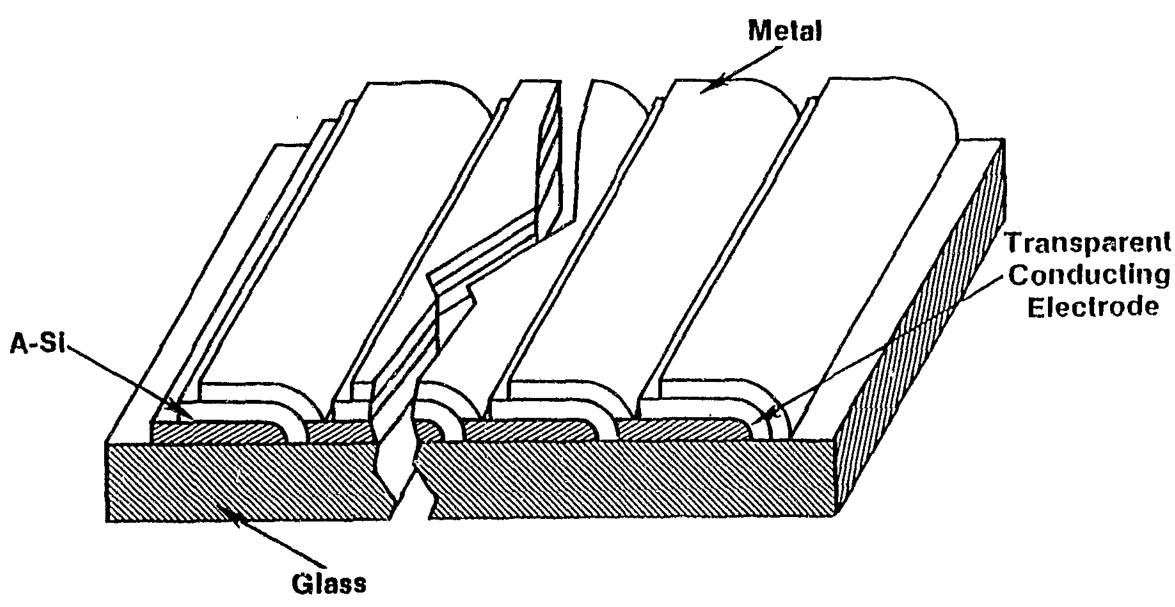

Process Sequence for a-Si Module Using Series-Connected Cells

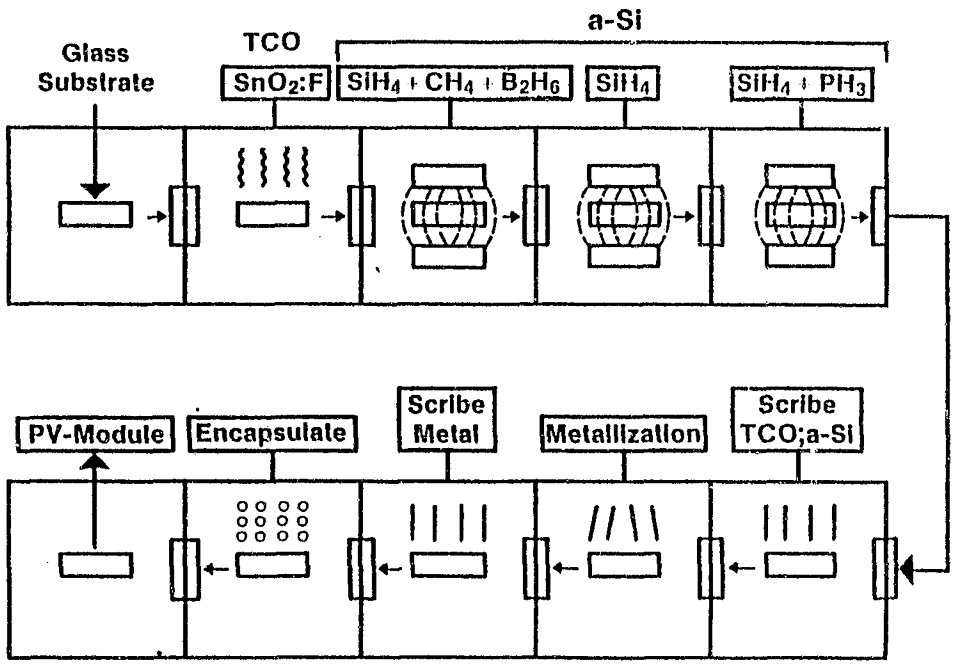

Colors of the Rainbow

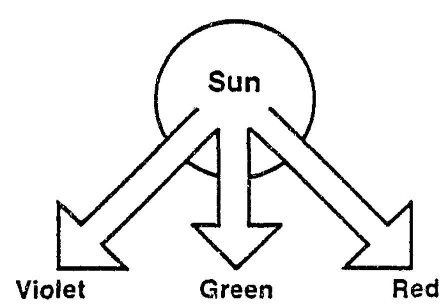

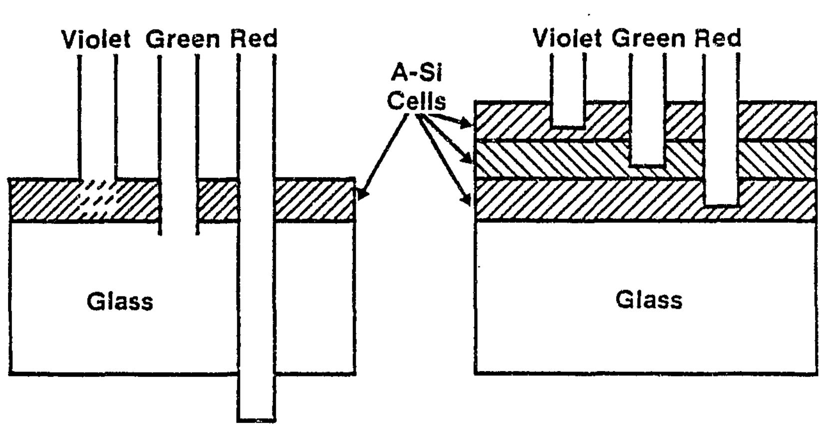

Single-Junction Cell **Triple-Junction Cell**

ORIGINAL PAGE IS OF POOR QUALITY

SERI PV AR&D Thrusts in Amorphous Thin Films in FY83

- Research on high efficiency single-junction monolithic thin-film amorphous silicon solar cells
- Research on high efficiency stacked multi-junction amorphous silicon alloy thin-film solar cells:
- Competitive solicitations planned in Spring 1983 for multi-year research programs

Efficiency of Cu Binary and Ternary Solar Cells

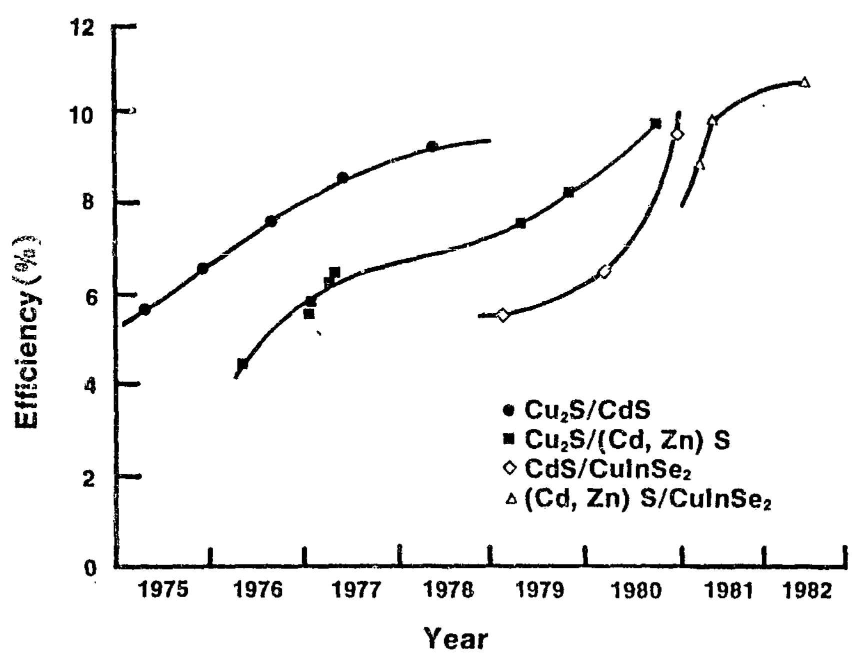

ORIGINAL PAGE IS
OF POOR QUALITY

CdS/CuInSe$_2$ Cell: Cross Section

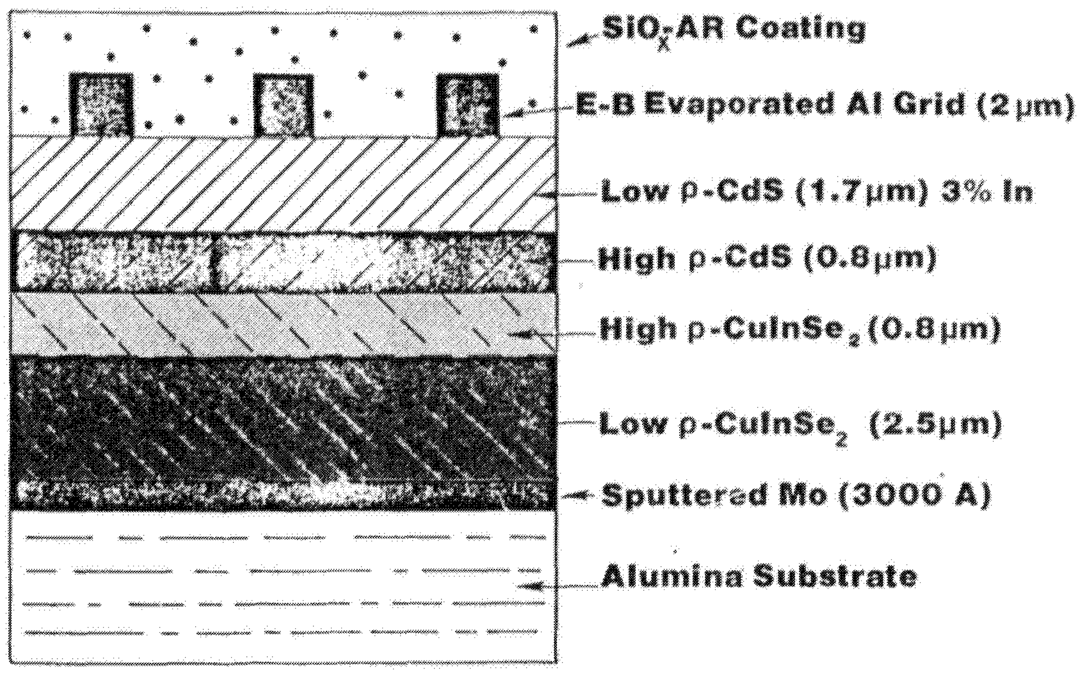

Development of CdTe and Zn$_3$P$_2$ Solar Cells

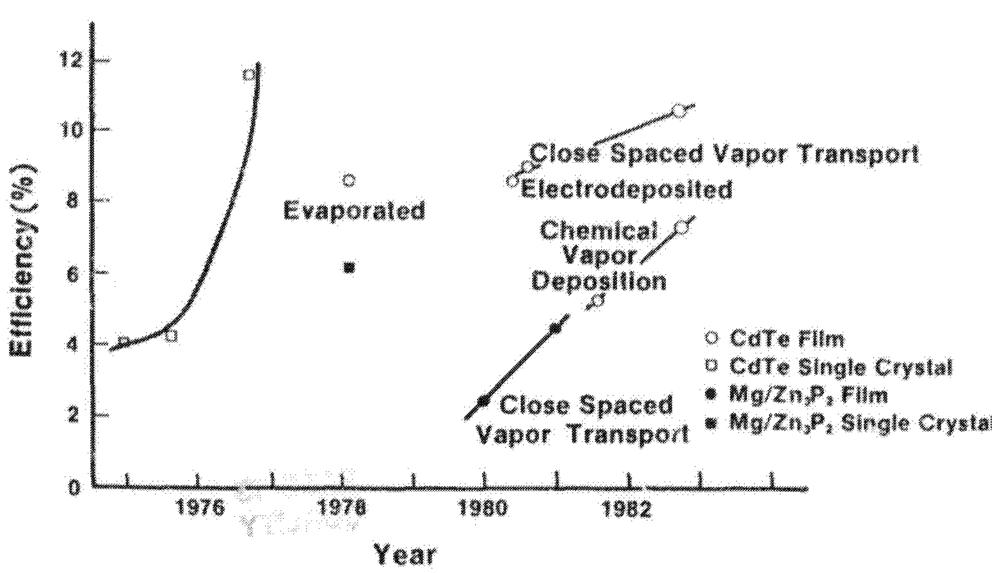

ORIGINAL PAGE IS
OF POOR QUALITY

Development of Gallium Arsenide Solar Cells

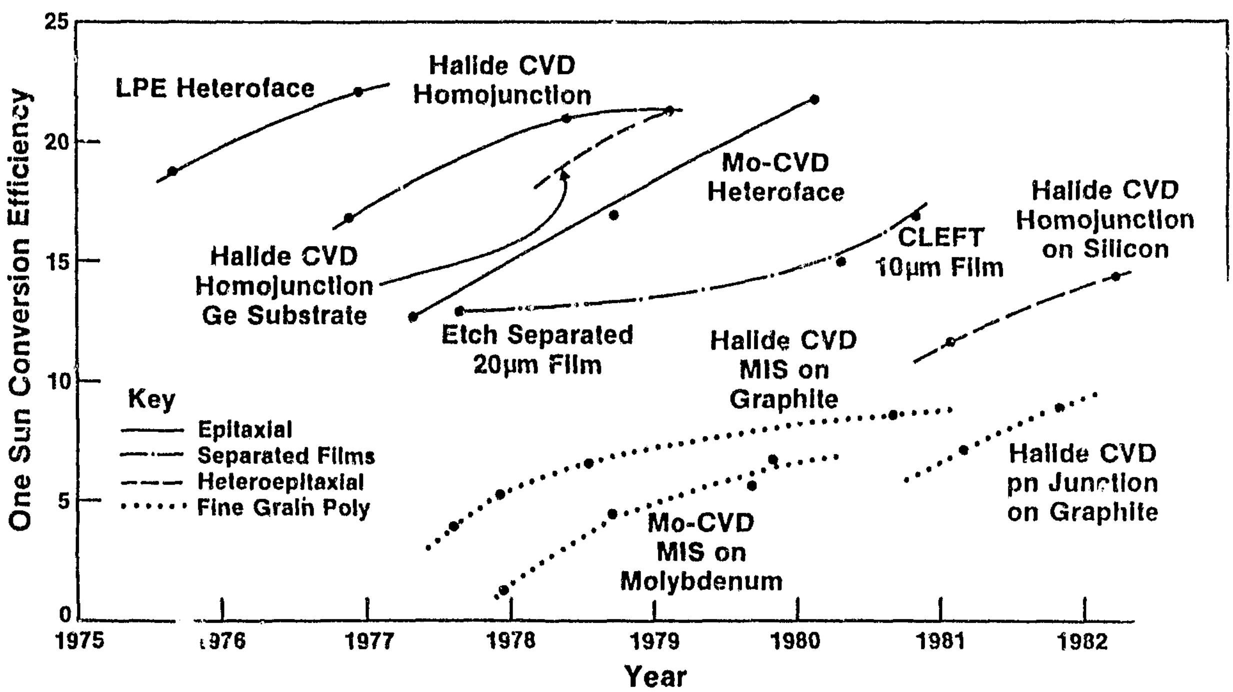

ORIGINAL PAGE IS OF POOR QUALITY

Commercial Ventures in Thin Films

- **Amorphous Silicon**
  - Energy Conversion Devices
  - Chronar
  - ARCO Solar
  - SANYO
  - Fuji Electric
  - ~15 other Japanese Companies
  - Siemans (Germany)
  - SOLEMS (France)
  - Phillips (Great Britain)
  - British Petroleum (Great Britain)
  - RACAL (Great Britain)
  - MBB (Germany)

- **Cadmium Sulfide Based Materials**
  - SES
  - Photon Power
  - SOVOLCO
  - Nukem (Germany)
  - ARCO Solar
  - SOHIO
  - Poly Solar

- **Cadmium Telluride Based Materials**
  - Eastman Kodak
  - Ametek
  - Monogram Industries

THIN-FILM SOLAR CELL AND MODULE DEVELOPMENT

Key AR&D Problem Areas

- Improvement in efficiency
- Stability
- Investigation of new deposition approaches with rates exceeding 10 Å/second
- Research on scaleability to at least 100 cm^2
- New cell structure, with >20% conversion efficiency potential
- Basic understanding of plasma discharge chemistry
- Creation of a firm theoretical base

Federal Role in Thin Films

- Continue aggressive AR&D program addressing the key problem areas within a priority group of thin film materials with SERI as lead laboratory
- Investigate high efficiency structure/materials which have potential of penetrating the central utility market in the 1990's
- Continue to pursue those high risk ideas which industry will not address
- Develop a technology base which will allow U.S. photovoltaics to be competitive with the international competition
- Carry out the recommendation, of the thin film task force established by DOE headquarters to define the federal role in thin film, beyond the research and development stages

THIN-FILM DEPOSITION TECHNOLOGIES OVERVIEW

TELIC CO.

J. Thornton

PHYSICAL VAPOR DEPOSITION
- EVAPORATION
- SPUTTERING

CHEMICAL VAPOR DEPOSITION
- CVD
- PLASMA ASSISTED CVD (GLOW DISCHARGE)

High-Efficiency Thin-Film Solar Cells

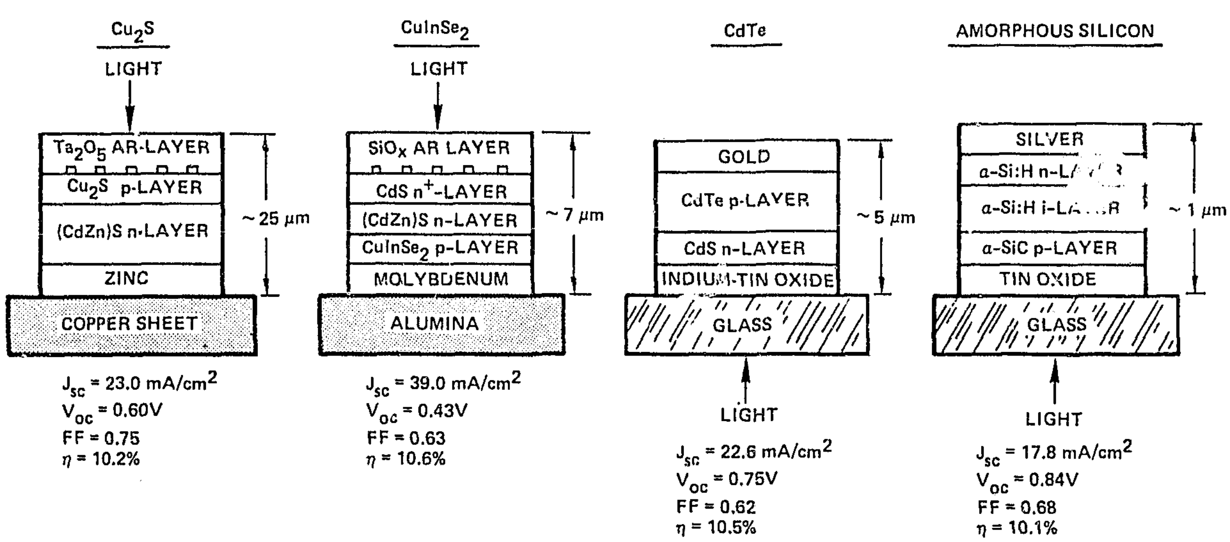

The Scale-up Challenge

- PRODUCTION GOAL - \$0.25 TO \$0.50/Watt (MODULE COST)
- CAPACITY GOAL - 10 GW/Year
- THIN FILM AREA - 100 Million m^2/Year (10% EFFICIENT CELL)
- PRODUCTION PLANT SIZE - 1-10 Million m^2/Year
- MATERIAL AVAILABILITY - ~700 Tons
  100 Million m^2
  1 Micron Thick
  Specific Weight - 7

In-Line Deposition Apparatus

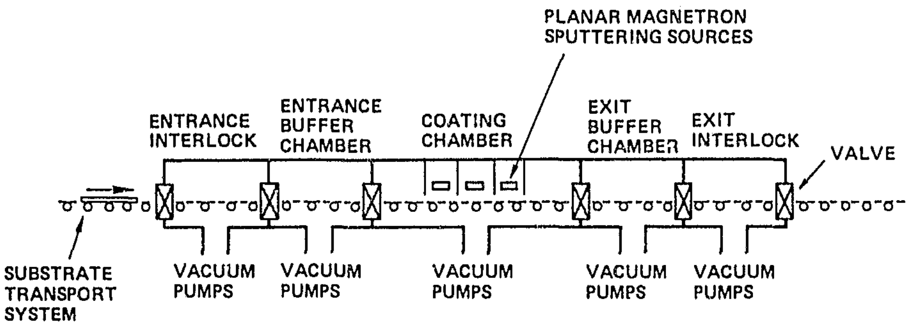

Basic Deposition Process

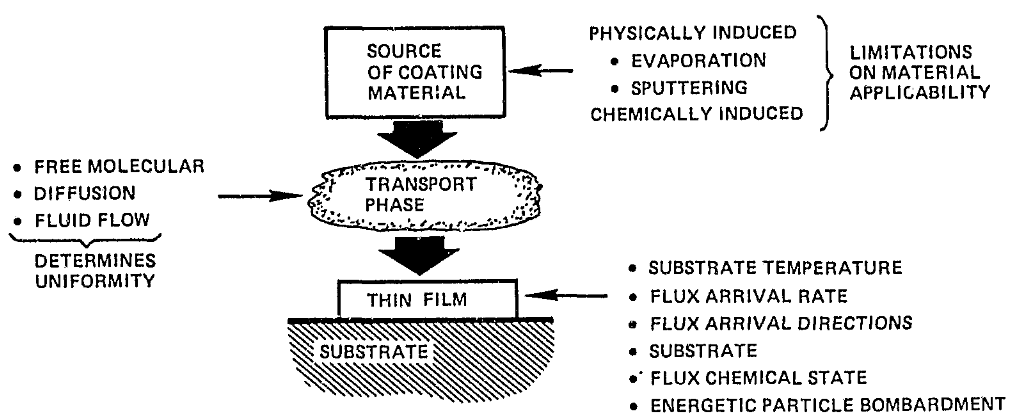

Two-Source Evaporation

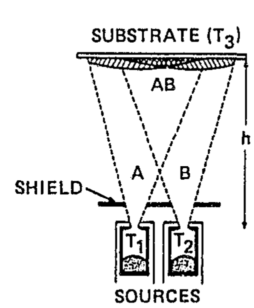

ORIGINAL PAGE IS OF POOR QUALITY

ROM:
HANDBOOK OF THIN FILM TECHNOLOGY
LEON I. MAISSEL AND REINHARD GLANG, Ed.
McGRAW-HILL BOOK COMPANY
NEW YORK (1970)

Close-Spaced Sublimation

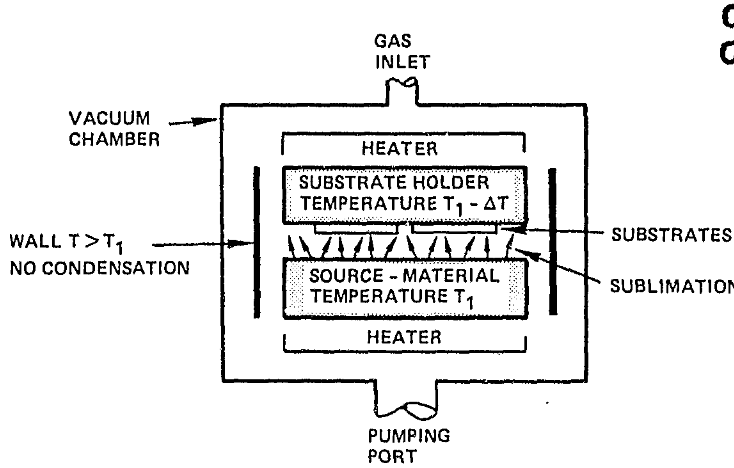

Basic Sputtering Process

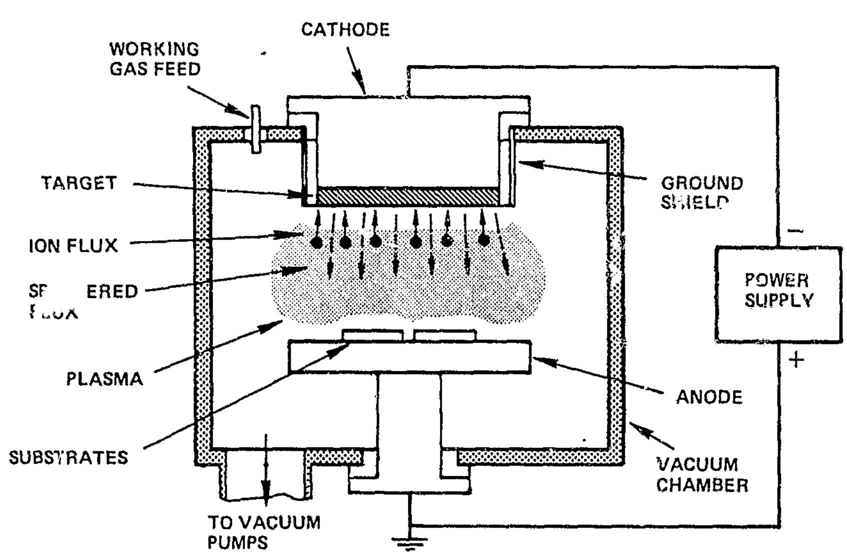

Planar Magnetron

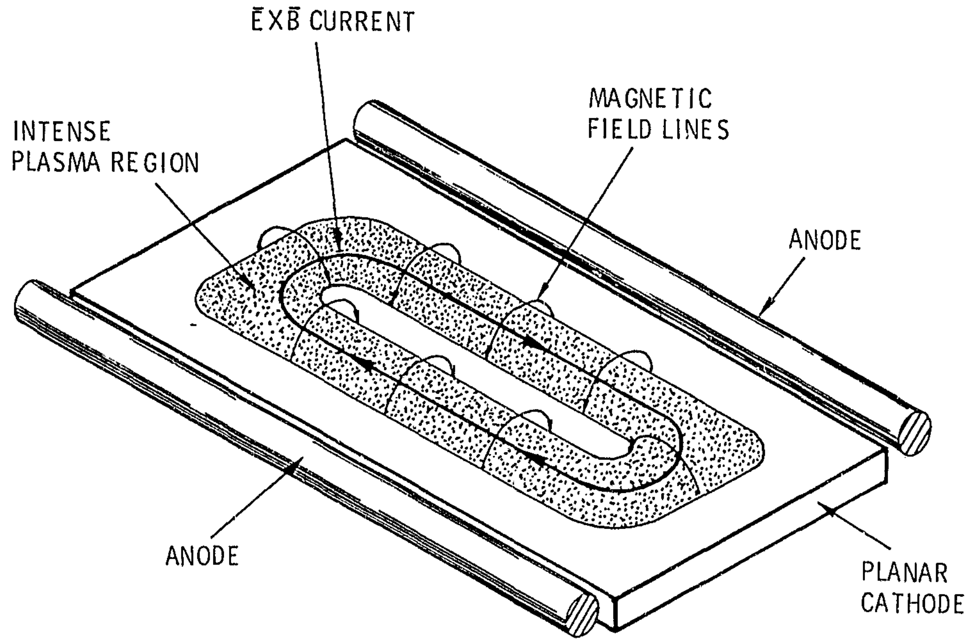

Basic CVD Process

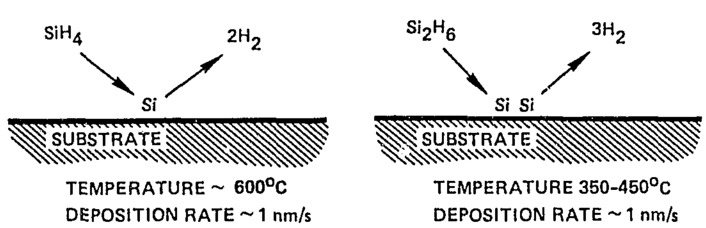

CVD Deposition Apparatus

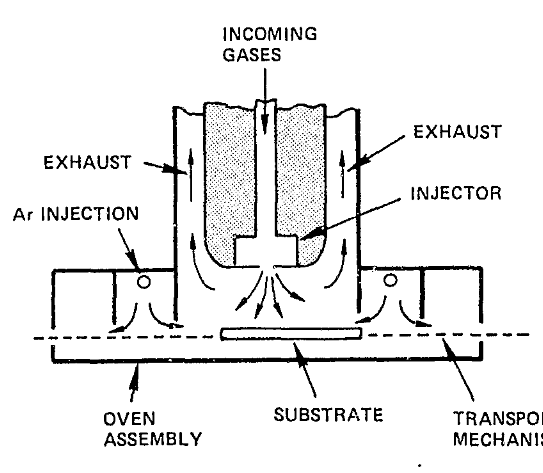

ORIGINAL PAGE IS OF POOR QUALITY

Plasma-Assisted CVD

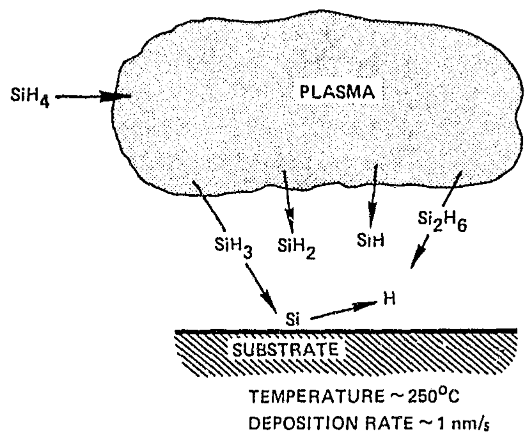

Planar Reactor

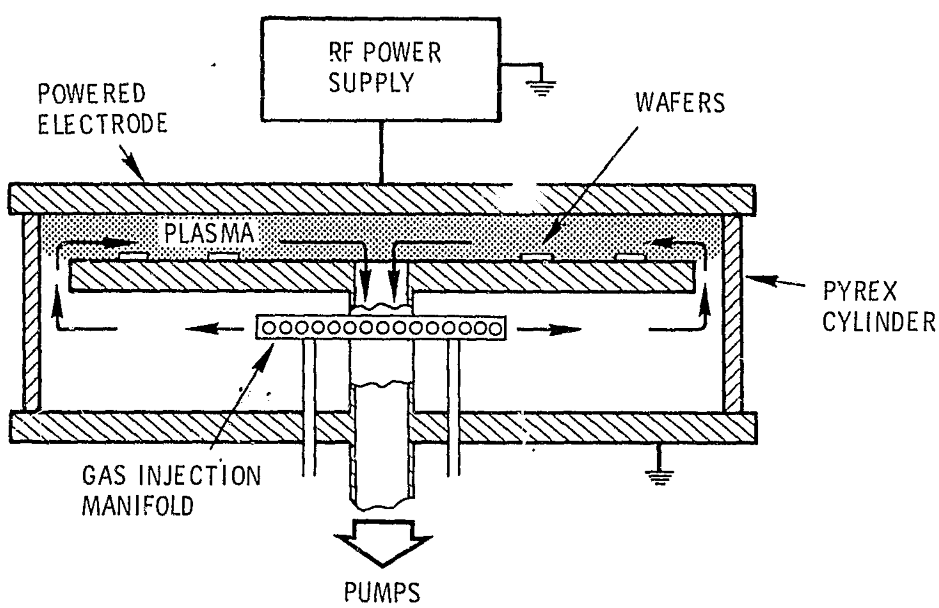

Summary of Processes

• EVAPORATION	–	• PROVEN PROCESS FOR DEPOSITING $CuInSe_2$, CdTe, CdS AND (CdZn)S. • QUESTIONABLE FOR LARGE AREAS.
• SPUTTERING	–	• EXCELLENT LARGE AREA CAPABILITY. • CAN DEPOSIT ALL MATERIALS REQUIRED FOR CELL FABRICATION. • HIGH EFFICIENCY (>10%) CELLS FABRICATED BY SPUTTERING ARE YET TO BE DEMONSTRATED.
• CHEMICAL VAPOR DEPOSITION	–	• RELATIVELY LOW COST EQUIPMENT. • POTENTIAL FOR HIGH DEPOSITION RATES. • RELATIVELY HIGH, BUT REASONABLE, SUBSTRATE TEMPERATURES ARE REQUIRED. • HIGH EFFICIENCY (>10%) CELLS FABRICATED BY CVD ARE YET TO BE DEMONSTRATED.
• PLASMA ASSISTED CVD	–	• PROVEN PROCESS FOR DEPOSITING AMORPHOUS SILICON. • QUESTIONABLE FOR LARGE AREAS. • HIGH PERFORMANCE CELLS DEPOSITED AT LOW RATE.

Problem Areas

- DEPOSITION UNIFORMITY
- SUBSTRATE QUALITY
- WALL CONDITIONS
- PINHOLES
- MASKING METHODS

THIN-FILM TECHNOLOGY DEVELOPMENT PRIORITIES

AMETEK, INC.

R.A. Russell

The AMETEK Corporation has been involved in the development of solar powered energy apparatus since late 1974. The initial activities were in the field of thermal solar energy and resulted in the development of a high efficiency solar collector which utilized an electrodeposited selective coating of non-stoichiometric lead oxide. In addition to its superior absorptive and emissive optical characteristics this electrodeposit was found to exhibit thin film photovoltaic properties.

The research program which was initiated to investigate these properties and to fabricate functioning devices has continued to the point where we are now producing thin film photovoltaic cells in pilot quantities for assembly into test modules and arrays.

During the initial period of the technical program it was judged that the evolution of the lead oxide based photovoltaic device from a laboratory demonstration to functional commercial hardware would require an extended and expensive research and development program. Since the AMETEK program is supported solely by corporate funding and since the principal objective of such corporate sponsored technical activities is the development of marketable commercial hardware in some reasonable time period, methods of obtaining this objective in a more expeditious manner were evaluated.

The major technological strength upon which our then existant state of development was based was the knowledge and experience of our scientists, engineers and consultants in the field of specialized electrodeposition, especially the codeposition of elements. We, therefore, began a search for other photovoltaic materials with which our technological strength could be utilized.

The choice of cadmium telluride as a candidate material was based on its known physical, chemical and semiconductor properties. These properties as well as other considerations had led many investigators to cite cadmium telluride as a potentially superior semiconductor for use in thin film photovoltaic devices. Our initial experimentation did indicate that cadmium telluride could be formed utilizing our electrodeposition technology and the present development project was initiated.

———— o ————

At this point, I should like to briefly describe the key aspects of our process and use this background to lead into a discussion of some recommended technological development activities which we feel could be of value in advancing the progress of thin film devices from their current status to practical, low cost commercial products.

The AMETEK cadmium telluride cell has an MIS configuration consisting of a substrate of nickel plated steel, an electrodeposit of cadmium telluride semiconductor, an insulating layer which consists of mixed oxides of tellurium and cadmium and a nickel Schottky. The overall dimensions of the present pilot cells are approximately 1 inch by 2 inches. The collecting fingers are applied either by vacuum deposition of aluminum or the silk screening of silver based inks. (Figure I)

The open circuit voltage of these cells have exhibited maximum values of about 700 millivolts with typical values in the vicinity of 630 millivolts. The short circuit current has exhibited maximum values in excess of 16 milliamps per square cm. based on the irradiated Schottky area with typical values in the 13 to 14 milliamps per sq. cm. range. The highest fill factors obtained on large area samples are about 60 percent with typical values slightly above or below 55 percent depending on the specific collecting finger technique used. In our research and development laboratories small experimental devices have exhibited efficiencies in excess of 8 percent under AM-1 illumination.

The present module design utilizes glass fluorescent tube blanks as the surrounding envelope into which are inserted metal supports on which a line of cells are mounted and interconnected in series. One end of the glass tube is closed with a formed glass piece through which the electrical leads pass and which also contains a small diameter tubular stem through which the tube can be evacuated after it is closed at the other end. The stem is closed by heating the glass and pinching it shut after the desired interior atmosphere is established. Prior to this assembly step the metal support and interconnected cells are inserted through the opposite open end and connected to the electrical leads. This end is closed with an adhesively bonded plastic cap or the glass is heated and rotated to form a hemispherical end closure. The tube is then evacuated to remove all residual volatiles and moisture and then backfilled with an inert gas at slightly less than atmospheric pressure.

The tube currently in use has an inside diameter of 2 inches and a length of about 75 inches. The tubes are designed to be compatible with 12 volt systems and have a peak output of 2 watts, however other design parameters are possible. Tubes can be grouped together in a simple rack support to form an array of any size. (Figure II)

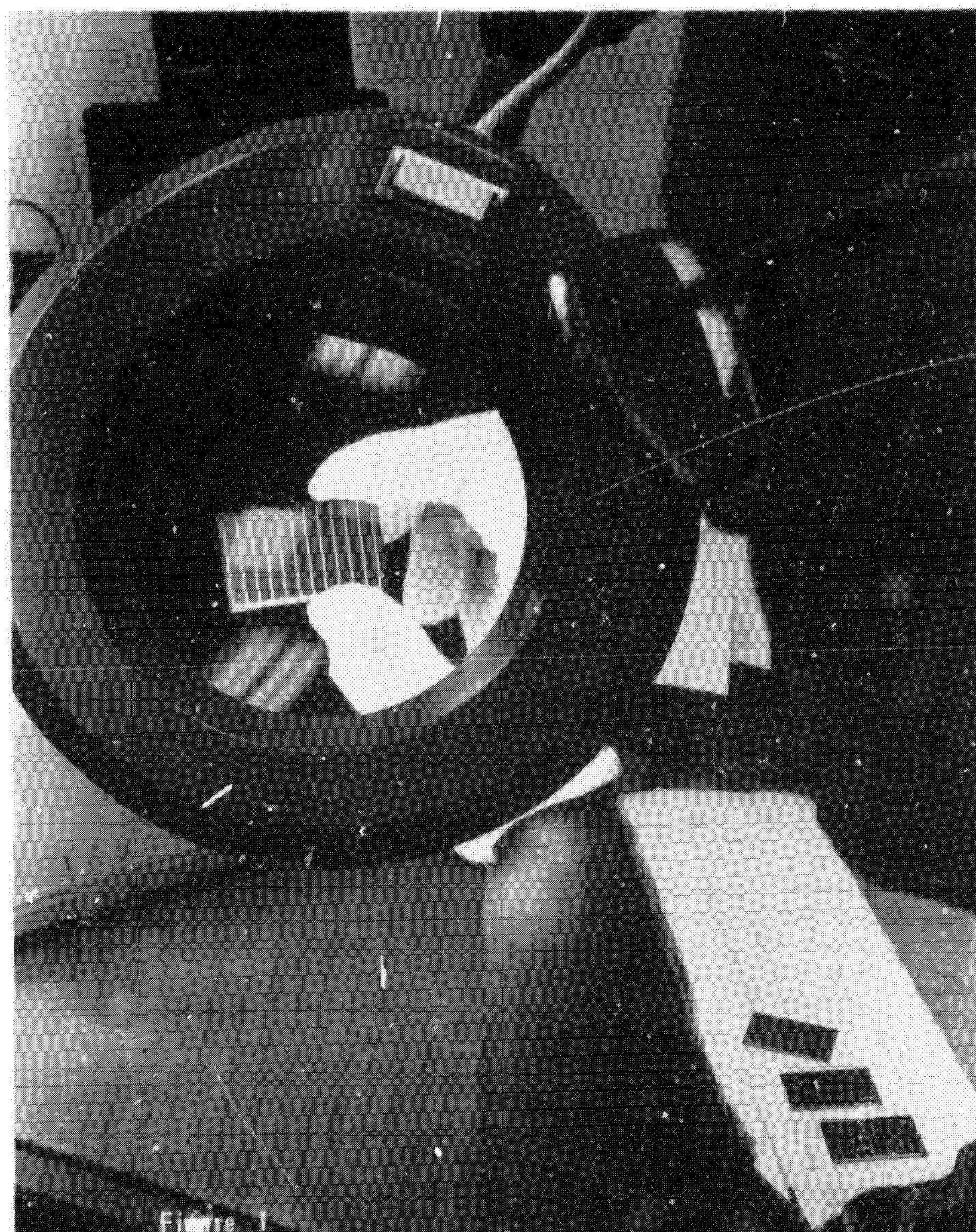

Figure 1

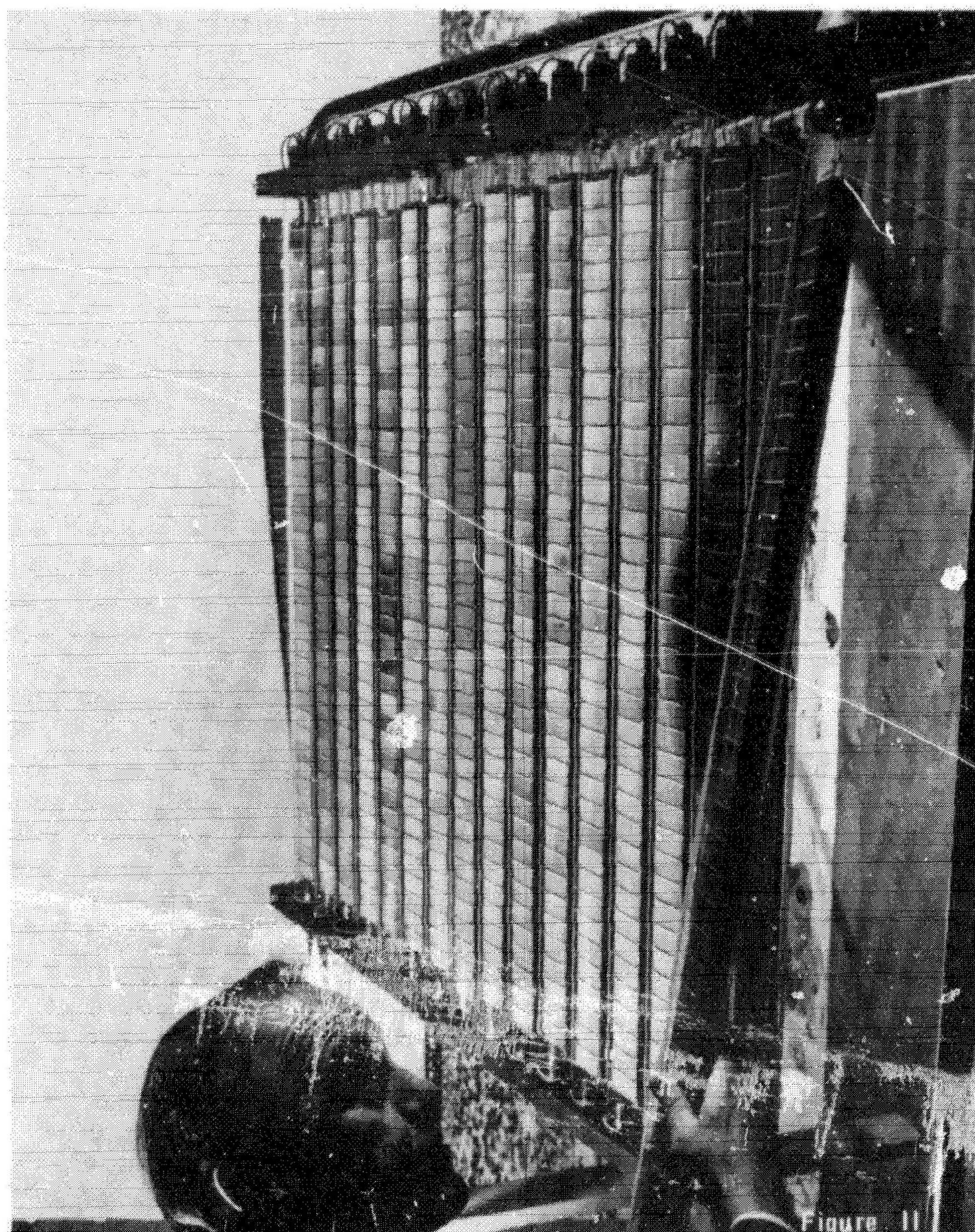
Figure 11

In addition to the tube module, we have produced prototype flat plate modules but have not currently established firm design criteria. The cell size we judge to be best suited for this type of module would have approximate dimensions of 4 inches by 4 inches -- that is about 100 sq. cm. in area.

To summarize the photovoltaic cell pilot production process currently being practiced -- we begin with the cleaning and surface preparation of nickel plated steel sheets. A critical step at this stage is the deposition of a very thin layer of cadmium metal on the surface of the substrate.

The next step is the electrodeposition of two microns of cadmium telluride on this substrate. At the present time the total area plated is approximately 20 sq. in. (Figure III) The electroplating tanks, which are about the size of a large dishpan with high sides, are designed to accommodate substrates having twice this area. In our present arrangement up to ten units could be run simultaneously in the pilot line. (Figure IV)

Following electrodeposition, the large substrates are cut or sheared to cell size and oven annealed in a controlled atmosphere at several hundred degrees centigrade, followed by the vacuum deposition of the nickel Schottky, which in turn is followed by a chemical etching or treatment step and a final heat treatment.

o

At this point, I should like to note three characteristics which distinguish our and many other thin film photovoltaic devices from conventional silicon modules and relate these differences to some proposed technical projects which may help advance the rate of development of commercially viable hardware.

The differences are:

<u>First</u> - The microscopic dimensions and lack of any significant long range order in the thin film semiconductor.

<u>Second</u> - The predominant use of either a surface barrier junction or a heterojunction, both of which exhibit a significantly greater degree of structural and compositional discontinuity when compared to silicon homojunctions.

<u>Third</u> - A spectral response typically greater in the shorter wave lengths than silicon.

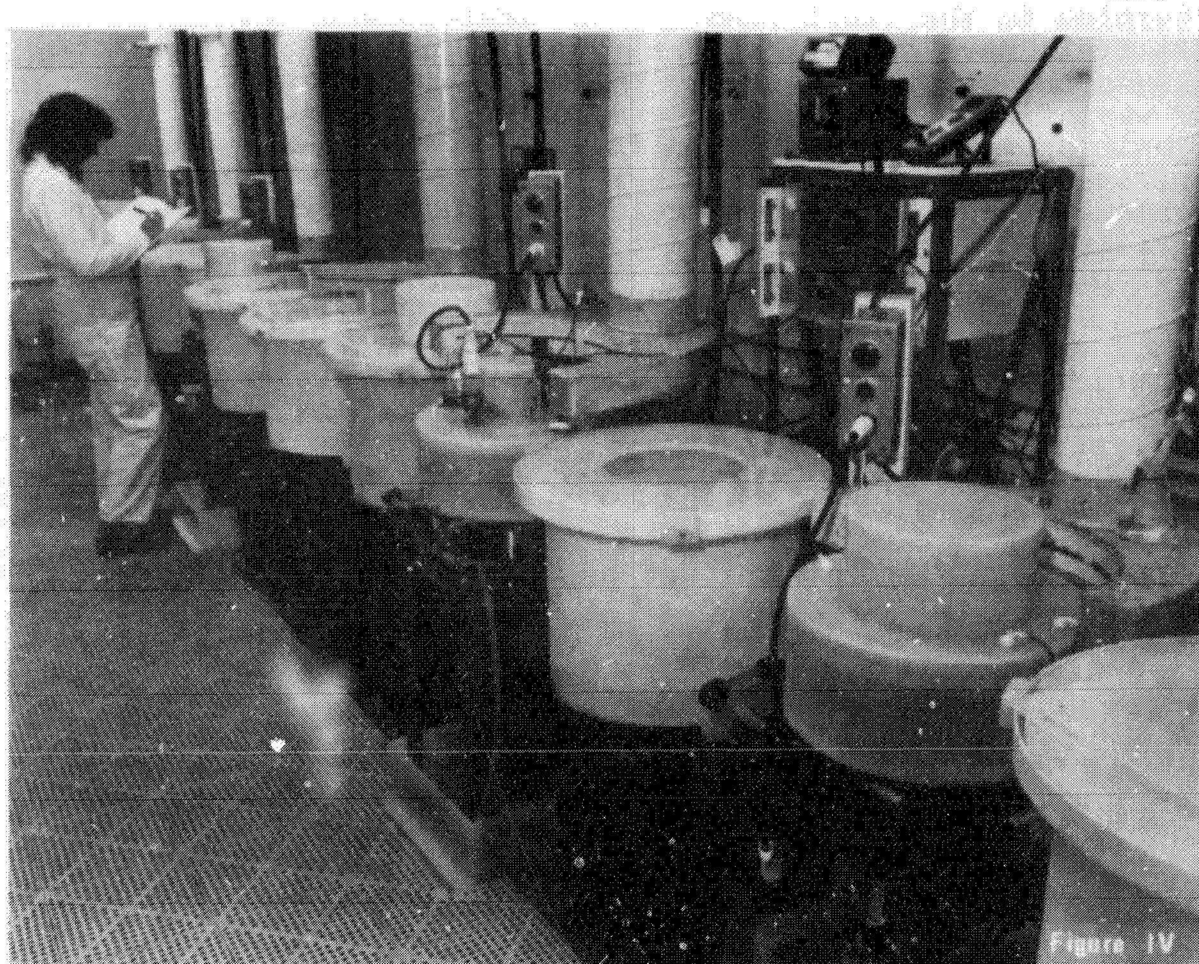

Returning to the first item, we and perhaps most working in this field have found that the investigation of relationships between the properties of the thin film photovoltaic device and variations of the parameters controlling the thin film deposition or formation are difficult to take much beyond empirical observations. A clear understanding of the mechanisms underlying these relationships are difficult to establish but could be of great value in advancing the development.

In our opinion, the availability of a variety of specialized analytical apparatus capable of the accurate evaluation, analysis and examination of thin film material -- such as the latest in SEM's or advanced surface analysis and high sensitivity elemental analysis instruments -- would be of great help in understanding these mechanisms.

Unfortunately for most companies, especially the smaller ones, such an array of equipment is far beyond their financial reach. This leaves such groups with the choice of sporadic testing using the services of an independent test laboratory or continued groping in a microscopic dark.

We would suggest the consideration of the establishment of one or more laboratories, fully equipped with all the latest in this type of equipment, and staffed with experienced personnel with whom the thin film development group could work with in a close, continuing and confidential relationship to advance their progress.

Such a service need not be free but should be reasonable in cost. Undoubtedly some method of identifying reputable groups entitled to the use of the service would be required but this should present no major problem.

With regard to the second characteristic noted -- the junction -- we should like to propose the establishment of a project to investigate the junction forming techniques used in the principal thin film device processes with the aim of defining more accurately the mechanisms by which the electrostatic fields are established and developing more generally applicable models for use in device analysis and design.

Our last comment with regard to the spectral response of thin film devices may be more of a caveat than a recommendation for a project. In our R & D and engineering laboratories, we use a number of different size and type commercial solar simulators. A calibrated silicon cell based reference is used to measure the integrated spectral output and this measure is used to adjust the power setting for the lamp.

Although all simulators were routinely checked against this reference and found to be set to an intensity of 100 mW/cm^2 cross checking with cadmium telluride cells yielded variable reading especially with regard to the short circuit current.

Our efforts to eliminate these variations led us to measure the spectral outputs of the lamps which were found to be in reasonable conformance with the AM-1 spectra on an overall basis but with the spectrum skewed so that the shorter wave lengths are more intense and the longer wave lengths less intense than the standard spectrum.

The entire spectral output of these simulators varies more or less linearly with the power supply setting. The use of a silicon based calibration reference which is more responsive in the longer wave lengths to adjust the overall power intensity can result in the shorter wave length intensities being considerable in excess of AM-1 levels and can therefore result in erroneous reading for thin film devices which are more responsive in this range of wave lengths.

These errors are not insignificant -- we have found it necessary to reduce the integrated power measurement of some of our commercial simulators by as much as 30 percent below AM-1 values when using a silicon based calibration reference cell in order to obtain the correct spectral intensity in the wave lengths to which cadmium telluride is responsive. We have found this type of error to some degree in all our simulators although in most cases the simulators are quite suitable for the evaluation of silicon devices with their greater responsivity in the longer wave lengths without correction.

We would therefore, propose a project to better define the unique aspects of testing thin film devices and reporting photovoltaic properties not only to establish more meaningful comparisons of the effect of material, processing and degradation studies but to also permit more effect utilization of the technical studies and reports of other investigators, both of which should help advance progress in the thin film development effort.

o

On behalf of AMETEK, I should like to express our appreciation for the opportunity to describe our activities in photovoltaic development and offer our suggestions for advancing the progress of the researchers in this important field.

$CdZnS/CuInSe_2$ THIN-FILM CELL R&D PRIORITIES

BOEING ENGINEERING & CONSTRUCTION

Development Plan

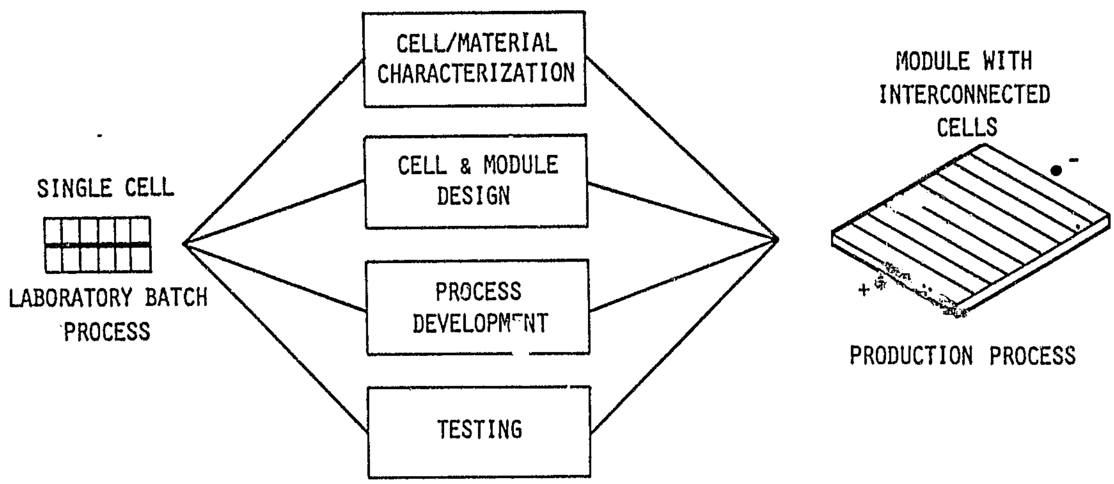

Cell/Material Characterization

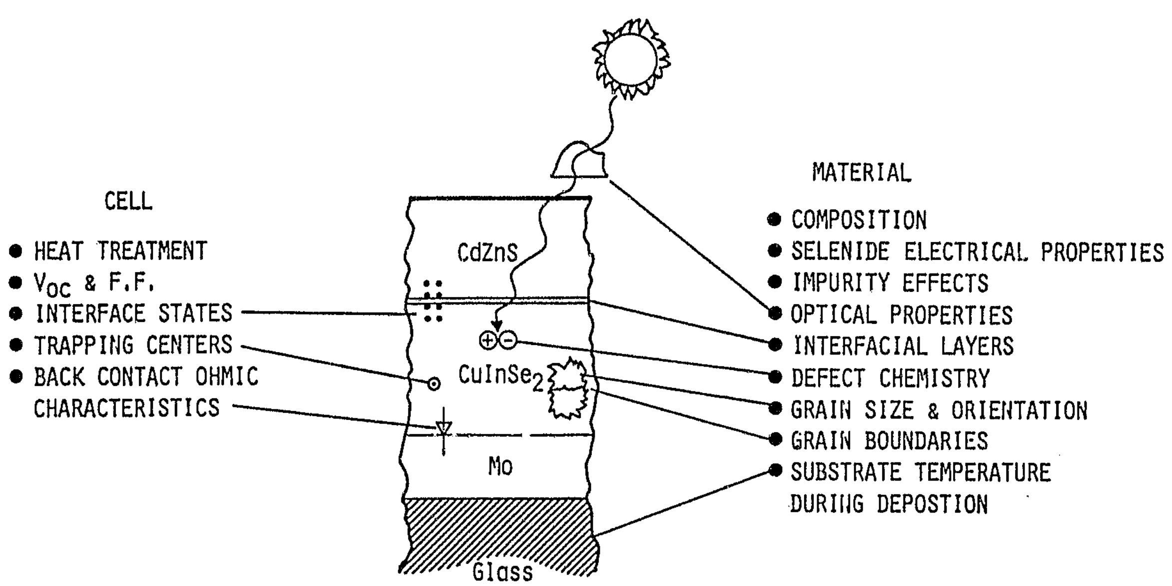

PAGE 94 INTENTIONALLY BLANK

PRECEDING PAGE BLANK NOT FILMED

THIN-FILM SOLAR CELL AND MODULE DEVELOPMENT

Cell & Module Design

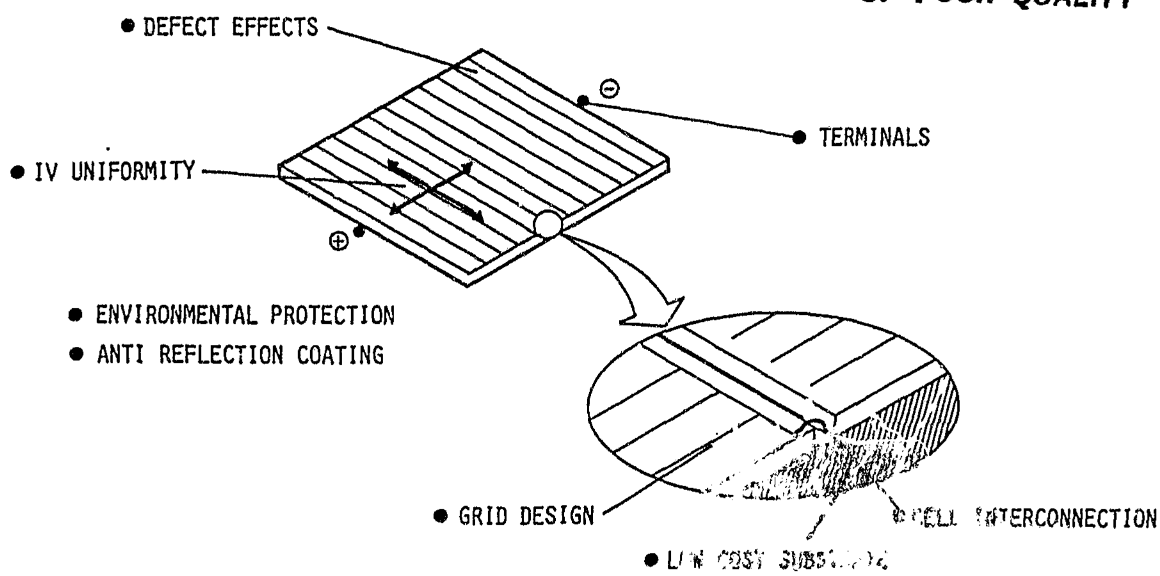

Key Process Development

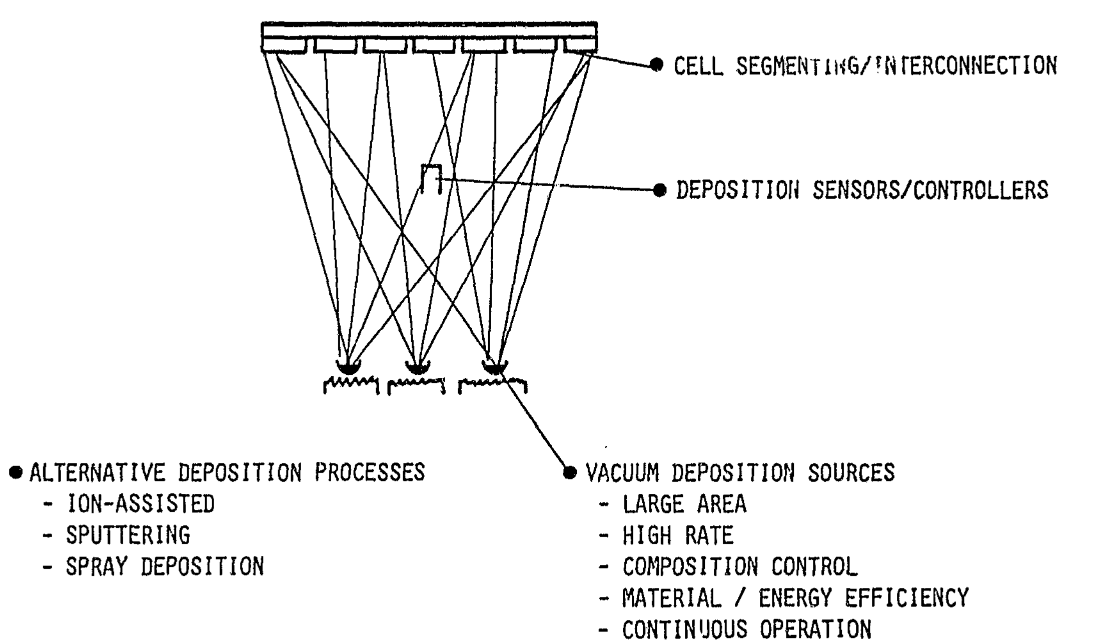

CHEMICAL REACTOR DESIGN FOR PHOTOVOLTAICS

UNIVERSITY OF DELAWARE

T.W.F. Russell

Chemical Reaction Engineering

LABORATORY
EXPERIMENTS

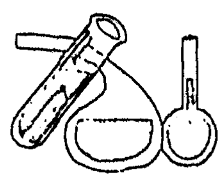

ANALYSIS OF
RESULTS

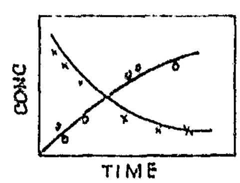

REACTOR
DESIGN AND
PROCESS ANALYSIS

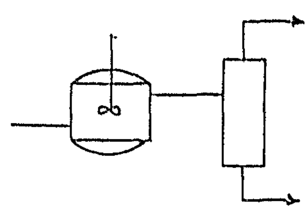

Thin-Film Technology (Profitable Operations, 1982)

SUBSTRATE	COATING MATERIALS	TYPICAL PROCESSING PLANT SIZE (10^6 m^2/year)
Glass	Metals (Ag, Al, Au, Cr, Cu) Metal Oxides	0.1 - 1.0
Paper Plastic	Metal (Al)	1.0 - 50
Steel	Metal (Al, Zn)	10 - 50

Thin-Film Technology (Mechanical)

SUBSTRATE	TYPICAL FILM THICKNESS (nm)	RATE OF DEPOSITION (μm/sec)	SPEED (m/sec)
GLASS	50 – 300	.001 - .01	0.01 — 0.05 (panes)
PAPER PLASTIC	30 — 50	30 — 120	1 — 10
STEEL	1,000 — 5,000	20 — 50	1 — 5

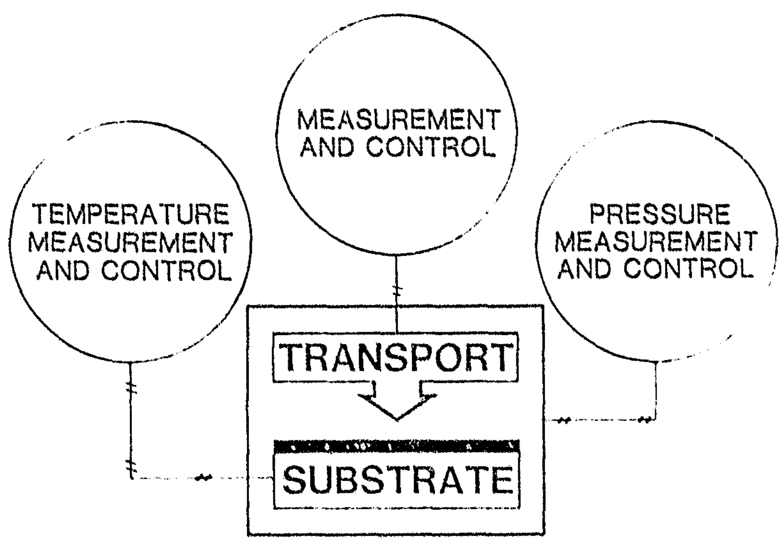

ORIGINAL PAGE IS
OF POOR QUALITY

THIN-FILM SOLAR CELL AND MODULE DEVELOPMENT

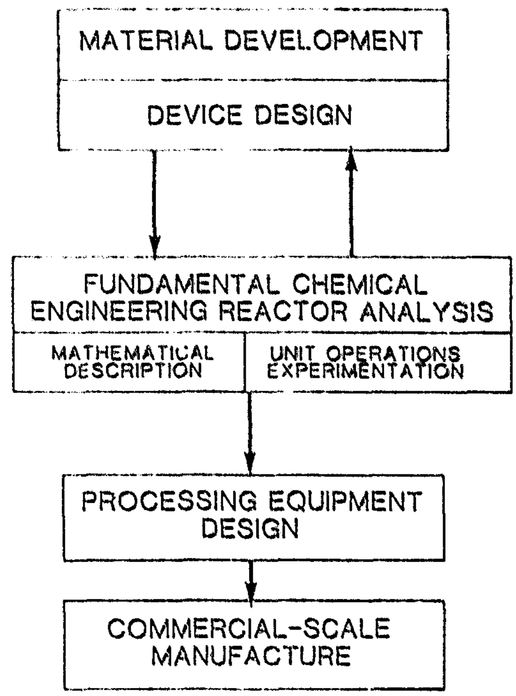

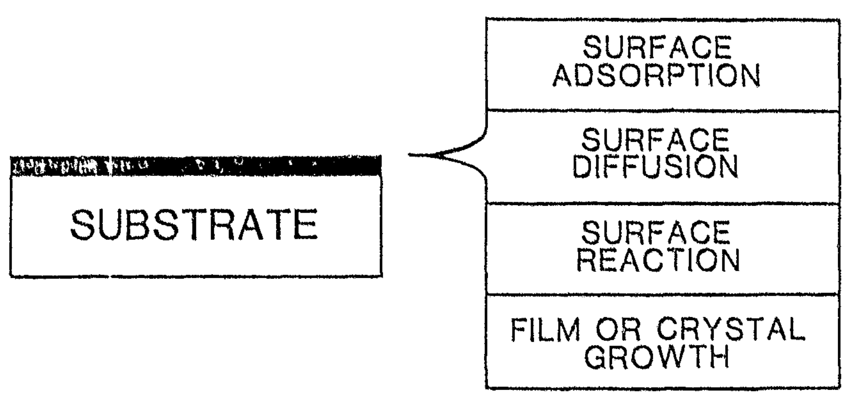

Chemical Vapor Deposition

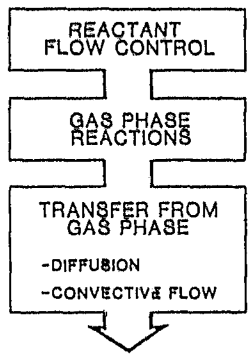

$$\text{Rate} = K_G A\,(P^* - P)$$

$$\text{Rate} = \frac{1 + K_1 P_A}{1 + K_2 P_B + K_3 P_A}$$

Physical Vapor Deposition (Evaporation)

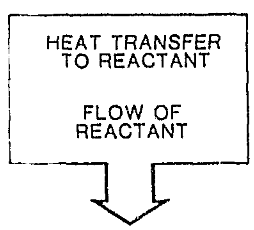

$$\text{Rate} = K\,(T)^{-\frac{1}{2}}\,(P_1 - P_2) = \frac{K}{T}\,(P_1^2 - P_2^2)$$

L
D
λ

Chemical Reactions

VAPOR PHASE
SUBSTRATE

Transport Phenomena

FLUID MECHANICS
MASS TRANSFER
HEAT TRANSFER

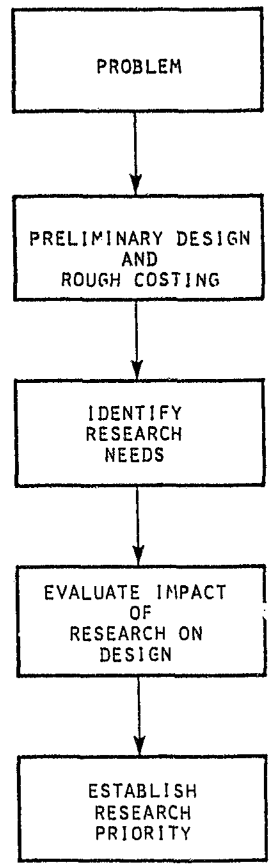

Cell Efficiencies

Material System CdS/Cu_2S	Laboratory Scale (Batch)	Unit Operations Scale (Continuous)
Wet Process CdS	9%	8%
Dry Process CdS/Cu_2S	7%	7%

QUANTIFYING DEGRADATION RESEARCH FORUM

December 6 to 8 at Williamsburg, Virginia

SUMMARY

JET PROPULSION LABORATORY

E.F. Cuddihy

Research Forum Objectives

- Review the state of the art in quantifying degradation, and in assessing the life potential of materials and products
  - (1) Where are we today?
  - (2) What can be adopted or modified for photovoltaics?
- Evaluate the technical approach and quality of the FSA Life-Assessment Program
  - (1) Analytical methods
  - (2) Experimental methods

Six Degradation Concerns for PV Modules

- Corrosion
- Cyclic fatigue
- Photothermal aging
- Soiling
- Debonding
- Electric stress breakdown

Forum Sessions

Session I: Industrial Approaches to Quantifying Degradation
Ron Ross, Chairman

Session II: Analytical Modeling of Degradation
Ami Gupta, Chairman

Session III: Accelerated Testing Criteria and Constraints
Ed Royal, Chairman

Session IV: Experimental Testing for Quantifying and Validating Degradation
Dan Runkle, Chairman

Session V: Experimental Testing for Identifying Degradation Behavior and for Product Qualification
Cliff Coulbert, Chairman

Audience and Speaker Mix

	Audience	Speakers	Non-Speakers
Industrial	39 (59%)	13 (52%)	26 (63%)
Government	21 (32%)	8 (32%)	13 (32%)
University	6 (9%)	4 (16%)	2 (5%)
Totals	66	25	41

QUANTIFYING DEGRADATION RESEARCH FORUM

Session I: Industrial Approaches to Quantifying Degradation

- Experiences at Quantifying Degradation and Assessing Life Potential of Paints and Coatings

  N.H. Frick, PPG Industries, Inc.

- Quantifying the Image Degradation of Photographic Materials

  T.J. Hutteman, Eastman Kodak Co.

- Testing of Power Cables for Electrical Applications

  B.S. Berstein, Electric Power Research Institute

- Environmental Testing to Study Circuit Failure Mechanisms and Accelerated Factors

  N.L. Sbar, Bell Telephone Laboratories, Inc.

- Quantifying Degradation and Assessing Durability of Materials in the Automotive Industry

  S.S. Labana, Ford Motor Co.

Other Industrial Presentations

- 3M Co.
- Intermedics, Inc.
- Hoffman and Feige, Inc.
- Underwriters Laboratories, Inc.
- LaQue Center for Corrosion Technology, Inc.
- Springborn Groups, Inc.
- Spectrolab, Inc.
- Electric Power Research Institute (EPRI)
- Chronar Corp.

Thermal Aging of a Chicken Egg
(A Problem of Prediction)

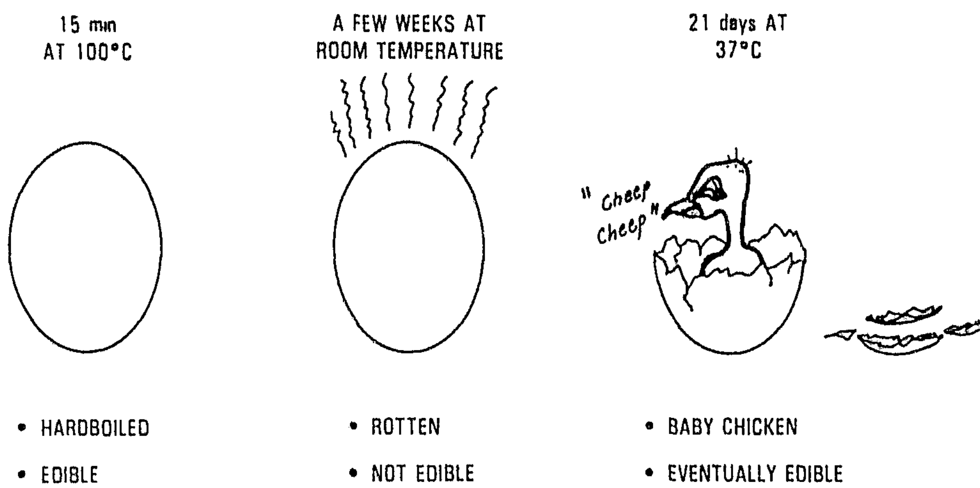

Relative Corrosivities of Various Atmospheric Environments

Location	Type of Atmosphere	Average Weight Loss of Iron Specimens in 1 yr, mg/cm^2	Relative Corrosivity
Khartoum, Sudan	Dry inland	0.08	1
Singapore	Tropical marine	0.69	9
State College, PA	Rural	1.90	25
Panama Canal Zone	Tropical marine	2.28	31
Kure Beach, NC (250-m lot)	Marine	2.93	38
Kearny, NJ	Industrial	3.92	52
Pittsburgh, PA	Industrial	4.88	65
Frodingham, UK	Industrial	7.50	100
Daytona Beach, FL	Marine	10.34	138
Kure Beach, NC (25-m lot)	Marine	35.68	475

ORIGINAL PAGE IS
OF POOR QUALITY

Effect of Elevation on Corrosion Rates at Kure Beach, NC

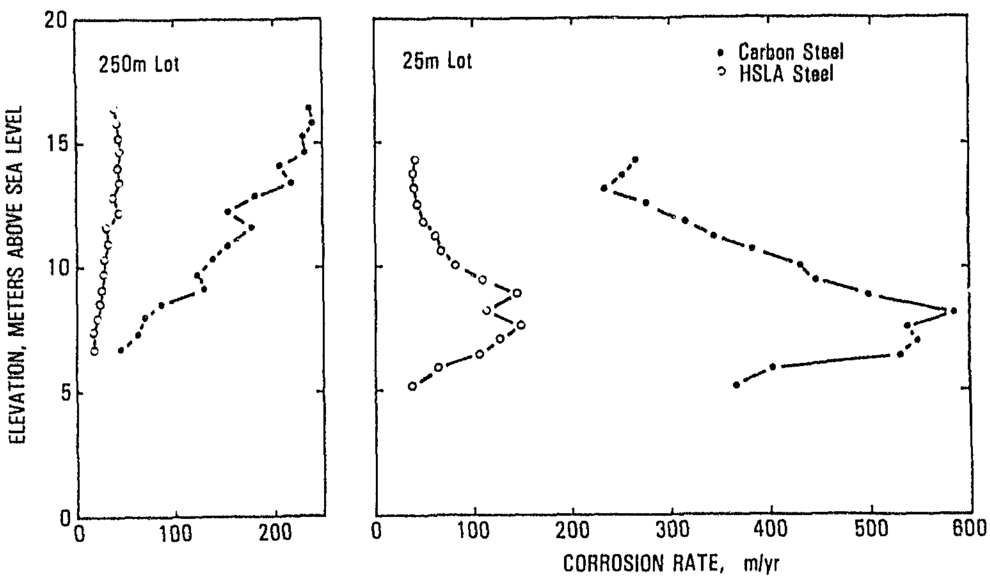

ORIGINAL PAGE IS
OF POOR QUALITY

A Quotation on Prediction

It is a divine plan of God, for His eternal amusement, that He made the behavior of both man and his environment unpredictable.

Anonymous

Use Condition -- Accelerated Test Condition

- Definitions / control of use and environment
  - Use
  - Test
- Correlation
- Accelerating factors
  - Type
  - Magnitude
  - Duration
- Sensitivity vs accelerated test efficacy

QUANTIFYING DEGRADATION RESEARCH FORUM

Conclusions

- Prediction of durability possible only if:
  - Failure mechanisms are identified
  - Kinetics of degradative reactions are studied
  - Computer models are developed to relate major degradative reactions to failure criteria
- Environmental acceleration chambers should not be viewed as life-prediction tools, but as research equipment to identify degradation mechanisms, and to establish degradation kinetics

Research Activities

- Establish and quantify fundamental degradation reactions and mechanisms of photovoltaic components
- Advance analytical modeling techniques for integrating the various degradation reactions and mechanisms of photovoltaic components, to be able to assess module performance and life potential
- Improve existing techniques or develop new techniques to achieve a better laboratory simulation of the natural environment
- Develop general rules for specifying acceleration limits for environmental stresses (i.e., UV, temperature, moisture, etc.)
- Investigate the long-term combined effects of outdoor weathering and low-voltage dc ($\leq$3000 Vdc) on the electrical insulation properties of encapsulation materials

Central-Station Activities

ORIGINAL PAGE IS
OF POOR QUALITY

S. Leonard, Chairman

100-MWe PHOTOVOLTAIC POWER PLANT: SMUD PV

SACRAMENTO MUNICIPAL UTILITY DISTRICT

First Megawatt of SMUD 100-MW Photovoltaic System

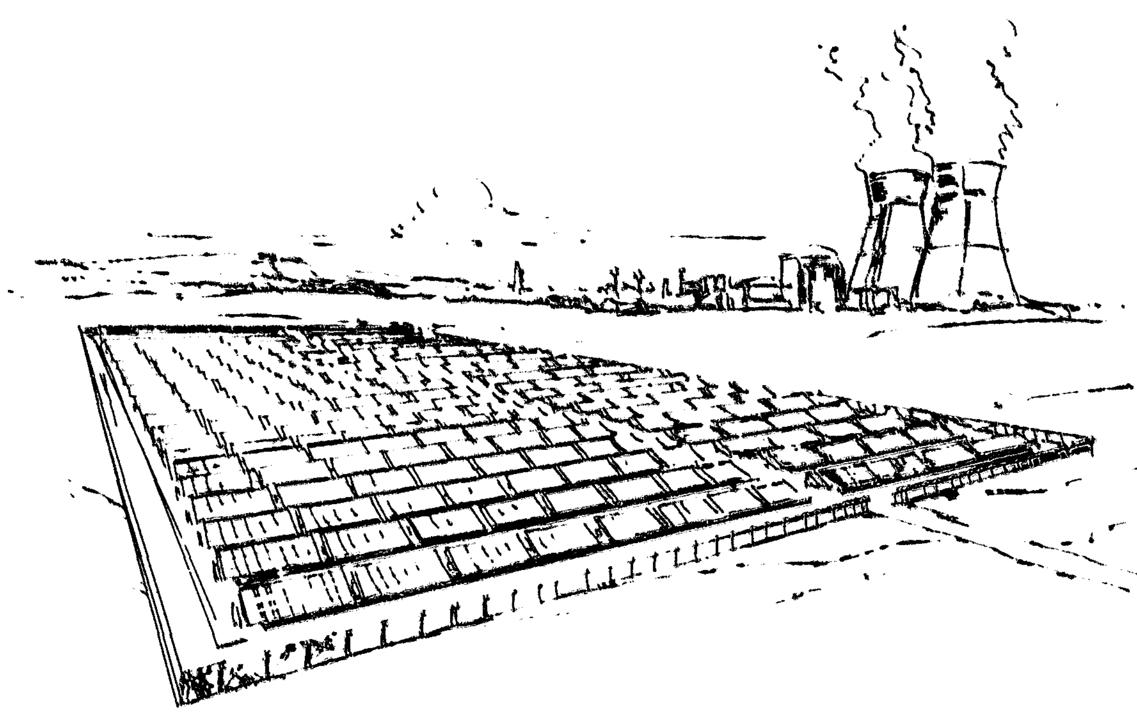

SMUD PV Project Overview

- 100-MWe photovoltaic powerplant on SMUD land near Rancho Seco nuclear generating station
- Will be built in 10 phases over 12 years
- Projected cost \$320 million (\$3,200/installed kW) in 1982 dollars
- Federal and state funds will offset the high cost of early phases
- First phase (1 MWe) operational in 1984

SMUD PV Installation Schedule

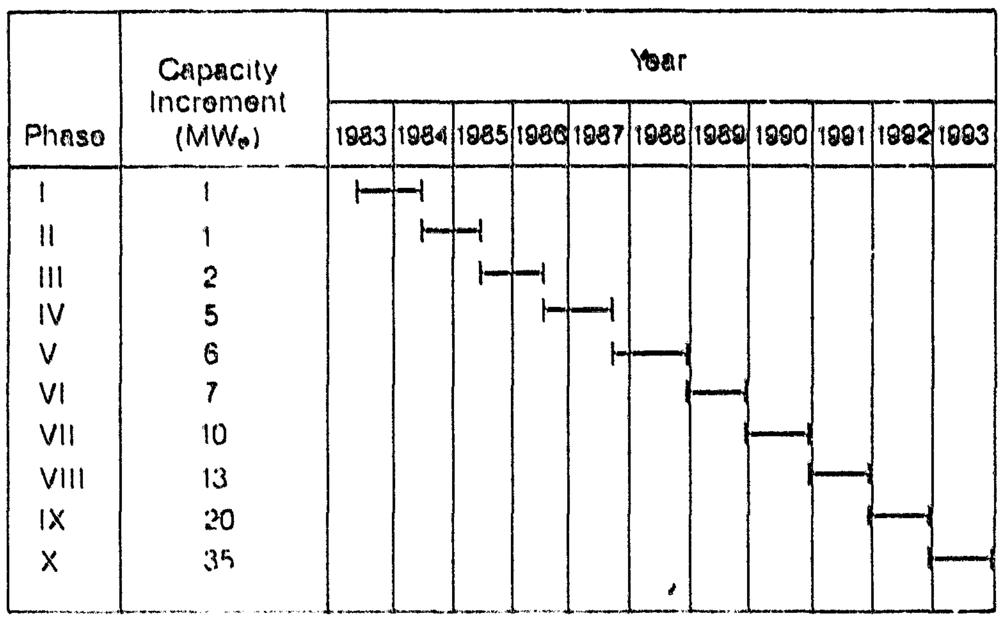

Project Cost Estimate (1982 $)

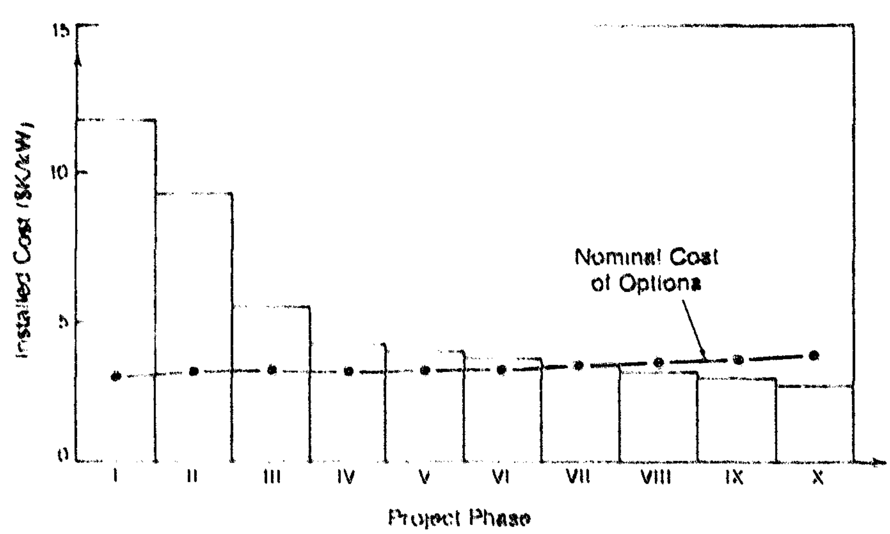

CENTRAL-STATION ACTIVITIES

Status of Phase I

- Conceptual Design Selection -- Complete
    - Flat panel PV
    - Single-axis tracking
- PV Equipment Procurement -- Ongoing
    - Purchase modules assembled in panels
    - Bid opening December 14, 1982
- Array Design and Test -- Ongoing
    - Design complete
    - Test array being procured
- Power Conditioning Unit -- Bid request in preparation

Strategic Approach

- Phase I
    - Benchmark of current PV module technology
    - Design and construction of central station system
- Phase II
    - Standardized central station equipment (voltage, size, cost)
    - Structure refinements (weight, cost)
- Subsequent Phases
    - Lower cost PV devices
    - Power conditioning
    - Automated installation
    - Structure mass production

SMUD PV1 Tracking Array Design

- 1 kW_{DC} per panel
- Eight panels per array drive
- 124 arrays for 1-MW_e field

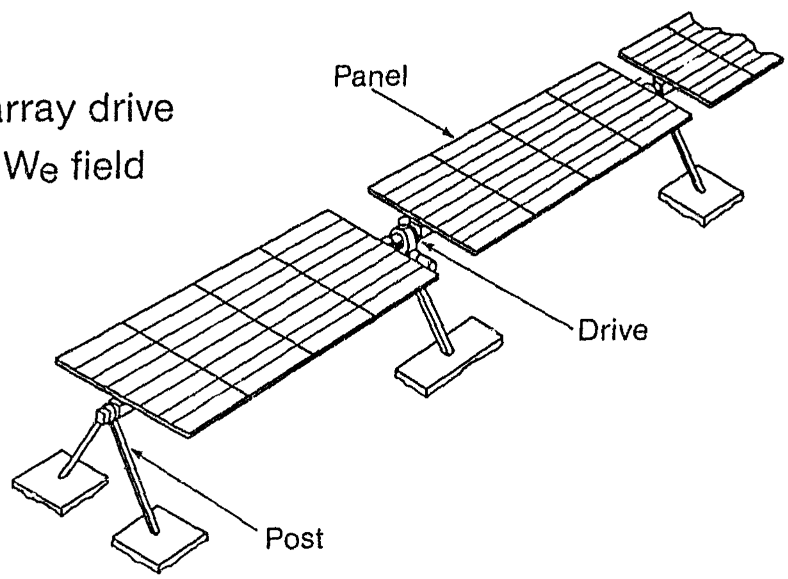

SMUD PV1 Panel Design

- Torque tube and rib structure supports PV modules
- PV modules slide into adjacent ribs

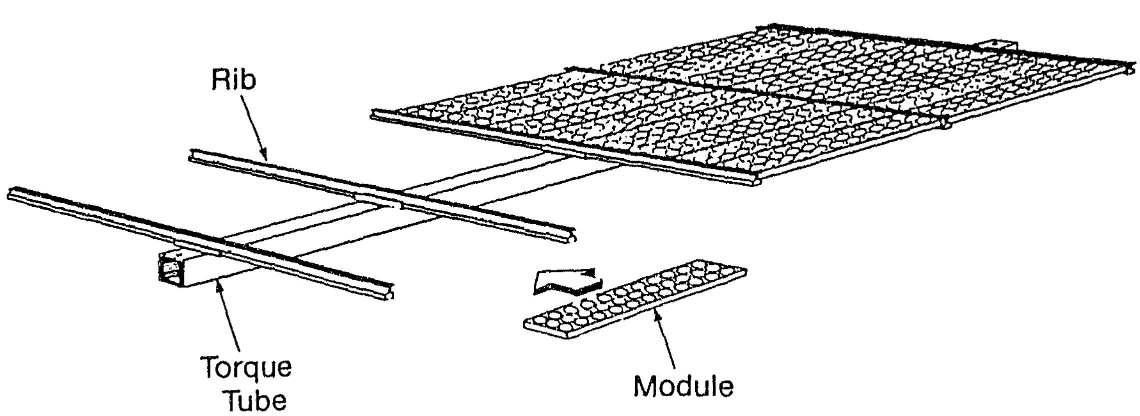

ORIGINAL PAGE IS
OF POOR QUALITY

Summary of PV Panel Bids

BIDDER	ARCO Solar	Solarex	Solar Power
Total price, $M	7.17	8.78	13.80
Dimension, ft	1.0 × 4.0	2.1 × 4.1	1.0 × 4.4
Power at STC, W	41	73.8	40
Efficiency, %	11.07	9.13	9.95

Phase II Summary

- Objectives
  - Add 1 MW generating capability
  - Standardize panel/module design specification
  - Achieve unit cost reduction
- Funds
  - FY 1983 federal $ 6.8M
  - SMUD share 3.6
  - Total $10.4M
- Status
  - Federal funds are appropriated
  - Change to SMUD-DOE contract by March

SMUD PV Schedule

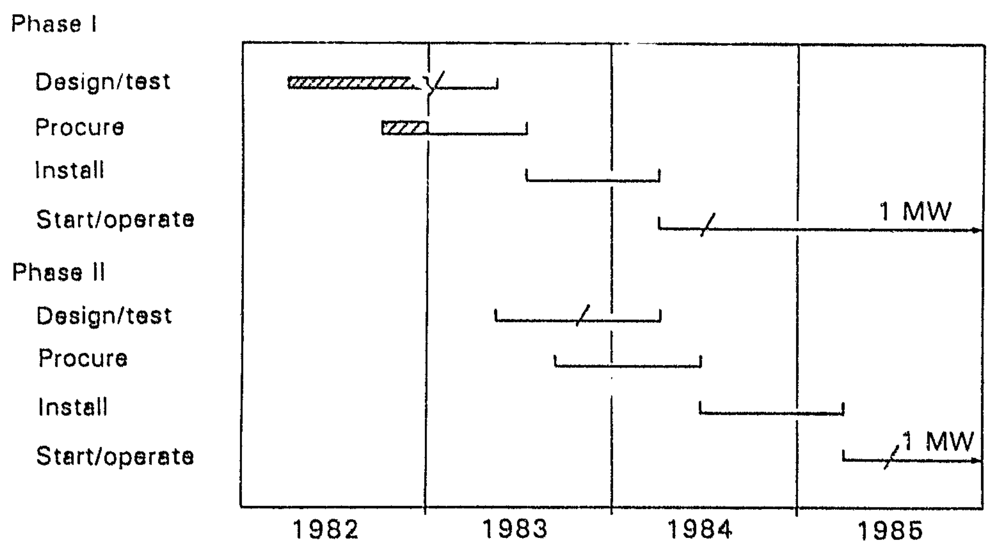

THE ARCO SOLAR 1-MW PV PLANT

ARCO SOLAR, INC.

R.E.L. Tolbert

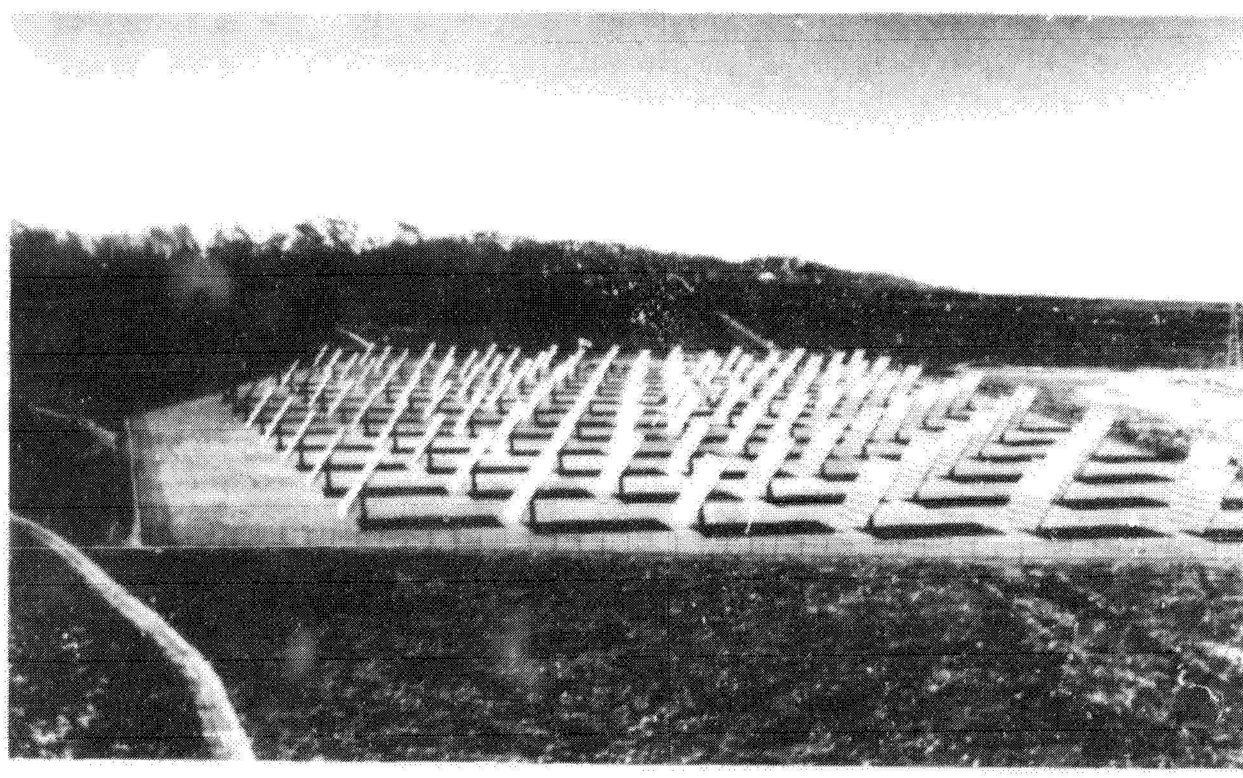

From April to December

This 1-MW ARCO Solar photovoltaic power plant was completed in 38 weeks. A small crew operated a minimal number of pieces of heavy equipment to prepare the site and install the equipment.

The subcontractor on the ARCO Solar Photovoltaic Power Plant project was the BDM Corp., which in turn subcontracted the construction operation to Townsend and Bottum.

April 1, 1982: Agreement with Southern California Edison (SCE) signed and announced.

April 29, 1982: San Bernardino County Planning department approved site for construction.

May 10, 1982: Site cleared and graded.

June 21, 1982: Installation of tracker pedestals begun.

August 27, 1982: Control building constructed.

September 9, 1982: Tracker installation complete.

October 18, 1982: Underground conduit installed; trenches refilled.

October 25, 1982: Inverters installed in control building.

October 29, 1982: Electrical switch gear installed in control building; 40 miles of wire installed in buried conduit.

November 18, 1982: Test run, successful in all respects; half the field began operation and was synchronized to the SCE line.

December 15, 1982: Remainder of field synchronized to the utility line; full daily operation begun.

Site Before Groundbreaking

Site Grading

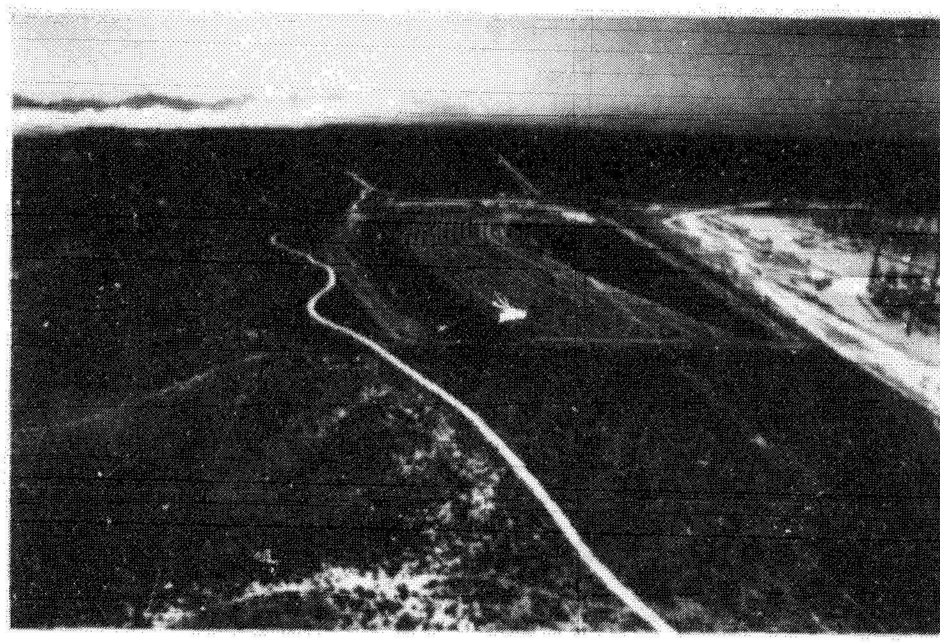

Drilling Holes for Tracker Pedestals

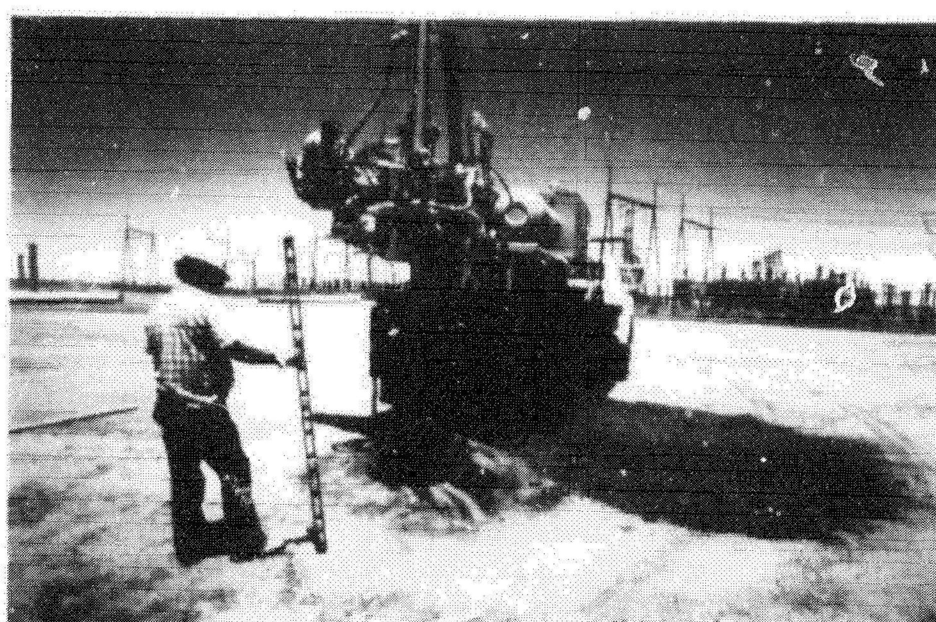

Positioning Tracker Pedestal

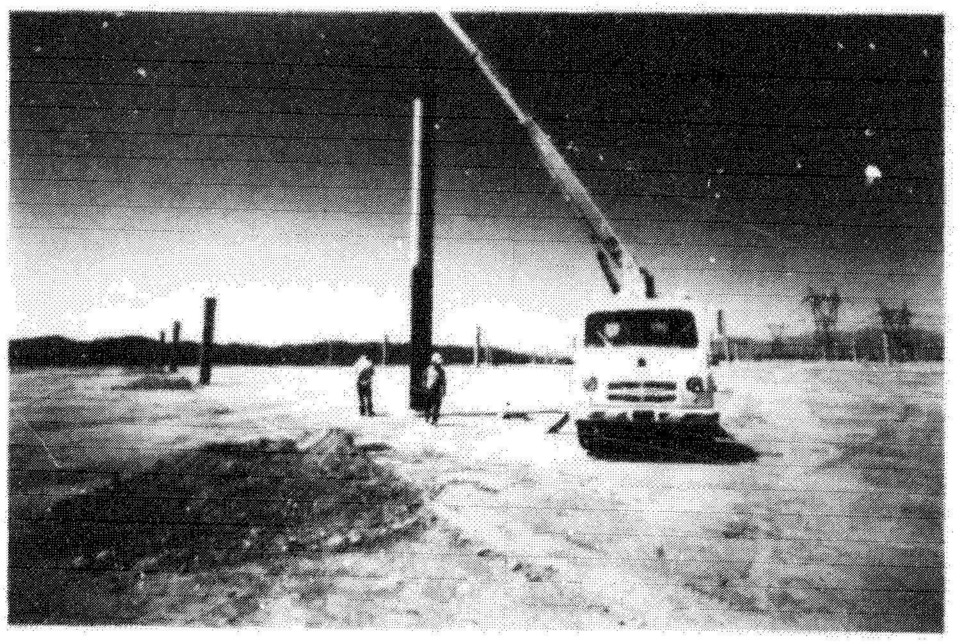

Gearboxes Attached to Pedestals

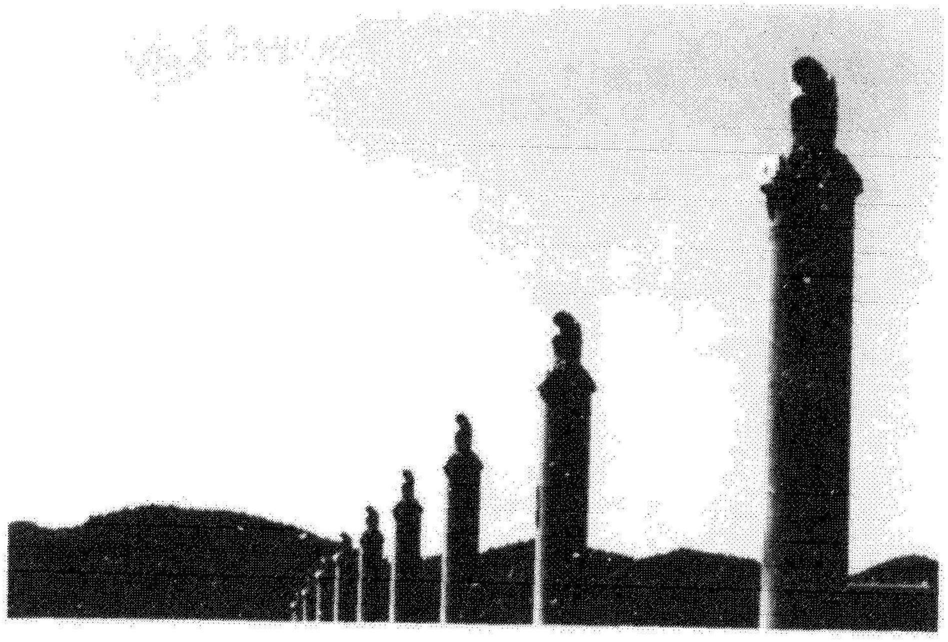

Panel Ready to Be Mounted

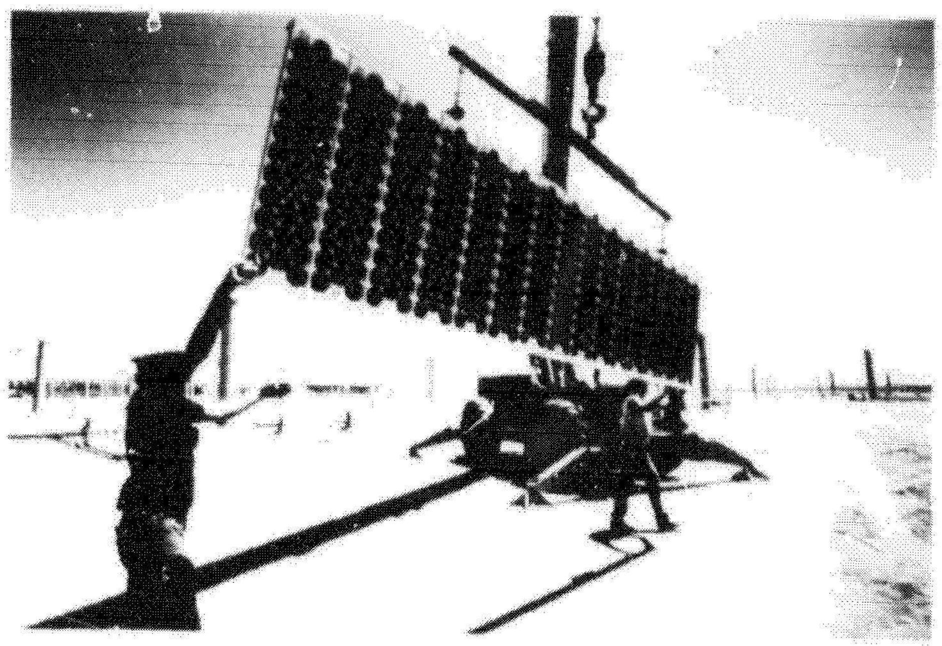

PV Panels Assembled

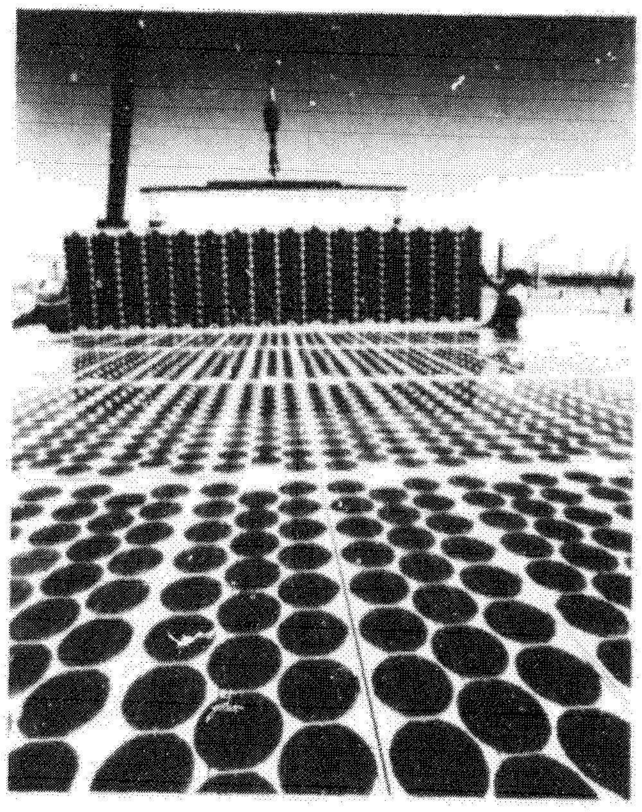

PV Panels Attached to Support Units at Ground Level

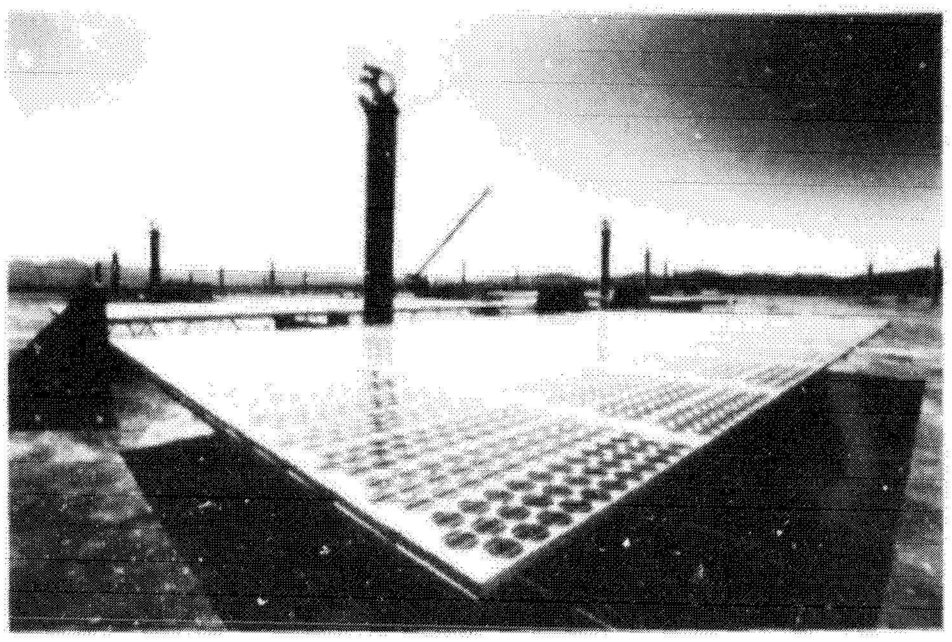

Support Unit With PV Modules Bolted
to Gearbox on Pedestal

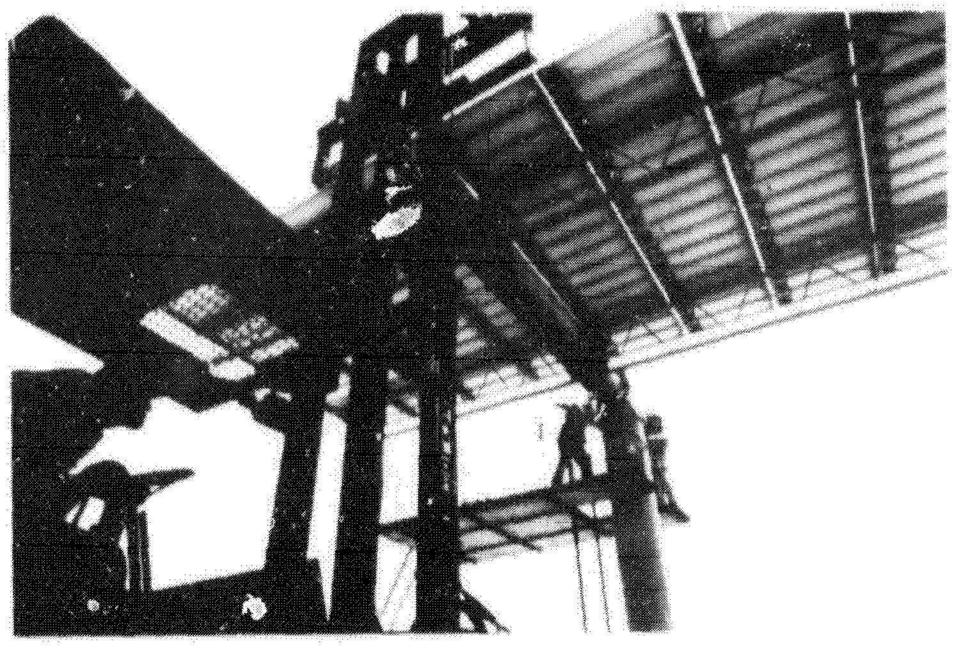

Double-Axis Tracker

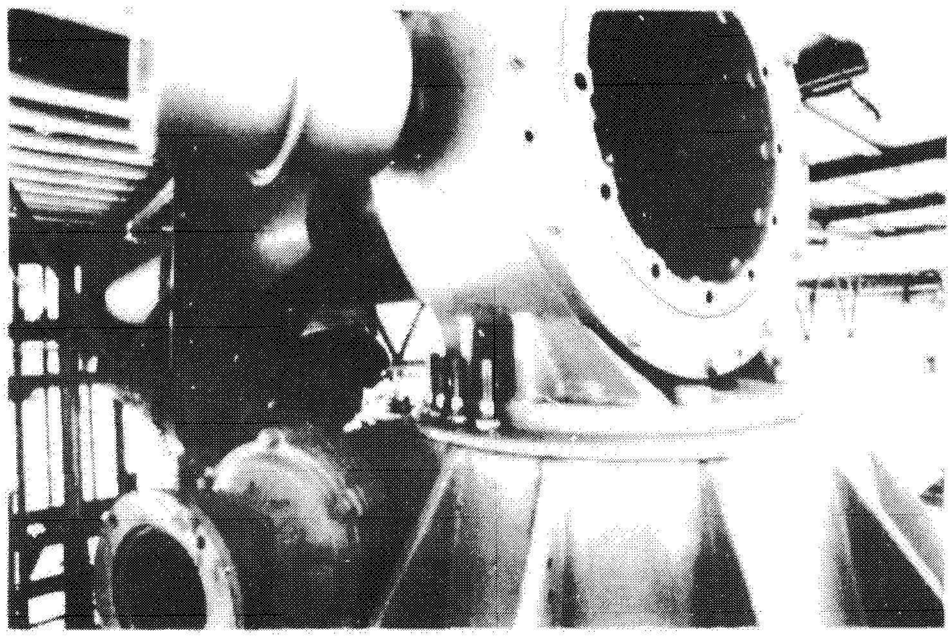

Both Support Units Bolted in Place on Pedestal

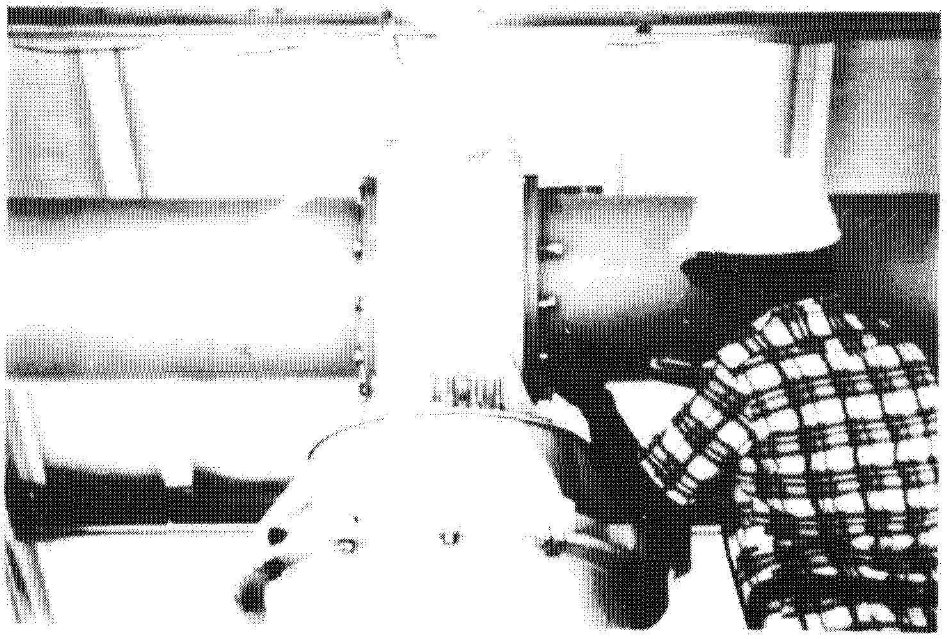

PV Support Units Await Attachment to Pedestals

Trenches Dug to Accommodate Wiring

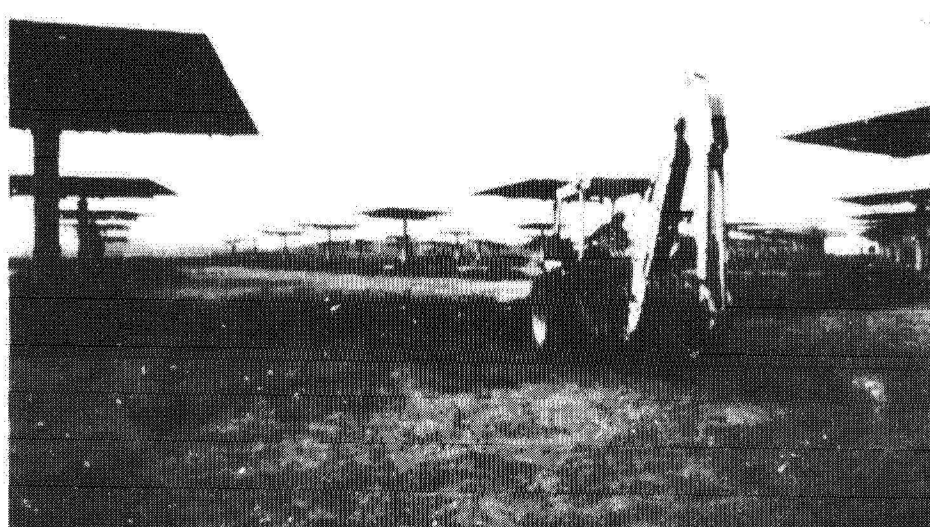

The Completed Installation

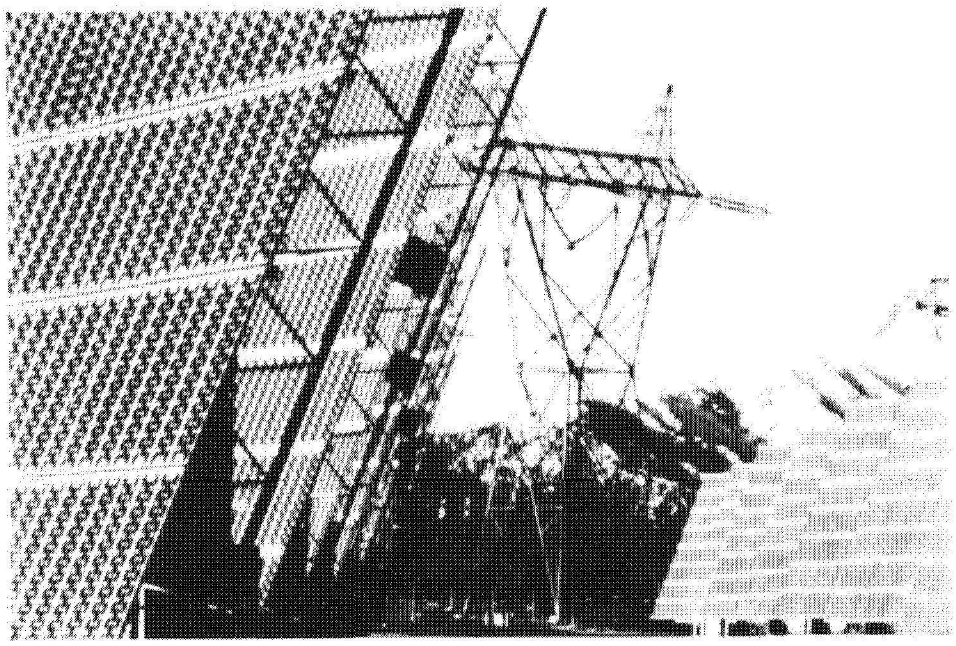

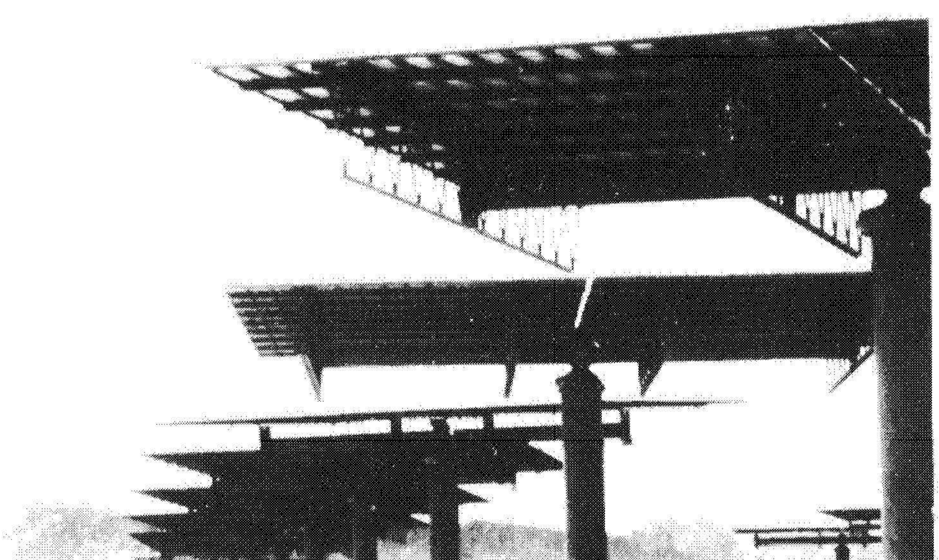

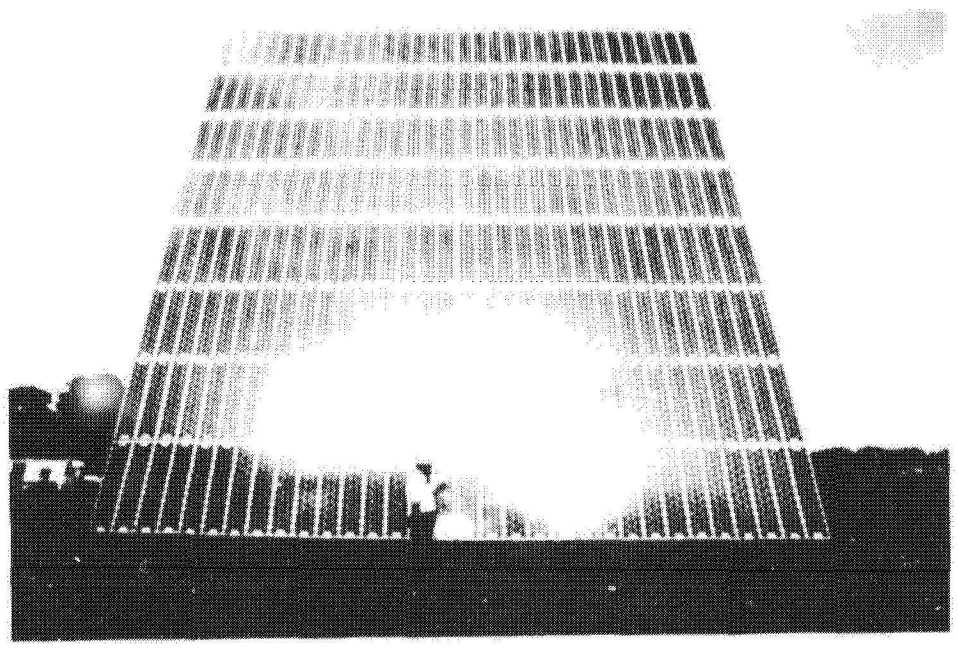

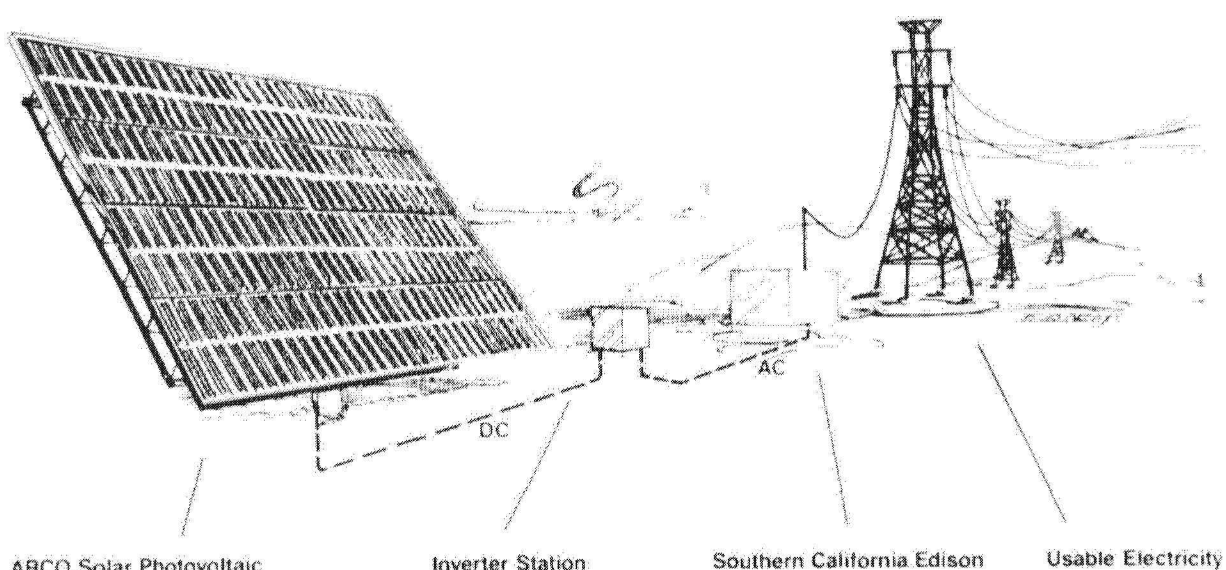

ORIGINAL PAGE
BLACK AND WHITE PHOTOGRAPH

THE ECONOMIC VIABILITY OF TRACKING FOR FLAT-PLATE COLLECTORS

SANDIA NATIONAL LABORATORIES

G.J. Jones

Extended Abstract

It has been generally known for several years that the use of two-axis tracking structures in flat panel array fields would greatly increase annual system energy output. However, the perceived complexity of the tracking array field and the current market of small remote applications has led to the present emphasis on simple, fixed-structure concepts.

The recent decision by ARCO Solar, Inc. to use a two-axis tracking flat-panel array in their one-megawatt (1-MW) power station has renewed interest in this system option. At today's module prices the ARCO design is definitely more cost effective than a fixed flat-panel, with the increased annual energy production per m^2 more than compensating for the increased array field cost. The question is whether this is still a cost effective option when module prices have dropped by a factor of ten to the level necessary for economic viability of grid-connected photovoltaic systems.

We have approached this question by comparing the various photovoltaic (PV) system design options under the constraint that they must produce energy for the same per unit cost ($/kWh). The individual cost elements can then vary within this constraint, so that equivalent array field and module costs for two competing options can be obtained as a function of annual energy production per m^2 and array efficiency.

As stated, a tracking flat-panel collector receives substantially more solar input than a fixed flat-panel. Since the modules are the same in both designs, the annual efficiencies are almost identical (excluding any temperature effects of mounting techniques). The major cost impact for tracking comes from increased land, field preparation, wiring, and structure costs, due to the reduced land utilization in tracking (~20% versus ~43% for fixed flat-panel). Therefore, for tracking to be cost effective, the increased energy must cover the increased array field costs if energy costs are to remain unchanged.

System energy costs were compared using recent data for array field costs and projections of other subsystem costs and collector efficiency. The field costs for two-axis trackers were obtained from cost estimates for concentrating arrays. Results indicate that two-axis tracking results in lower energy costs than fixed collectors for all sites considered, even at a deliverable module price of $\$1/W_{AP}$. For single axis tracking to be more cost effective than two-axis tracking, savings on the order of 20% in array field costs are needed to offset the lower annual energy. Unfortunately this is still an open question since no detailed cost analyses currently exist for a single axis flat-panel tracking structure.

Premise

BASED ON ARRAY FIELD COST ESTIMATES FOR FIXED AND TRACKING COLLECTOR CONCEPTS, TRACKING OFFERS AN ECONOMIC ADVANTAGE EVEN AT DELIVERED MODULE PRICES OF LESS THAN $\$1/W_{AP}$.

Determining Break-Even Tracking Field Costs: Approach

- TWO DESIGN CONCEPTS ARE EQUIVALENT IF THEY PRODUCE ENERGY AT THE SAME ANNUAL COST, OR

$$\left.\frac{\text{CAPITAL COST}}{\text{ANNUAL OUTPUT}}\right|_{\substack{\text{TRACKING}\\ \text{SYSTEM}}} = \left.\frac{\text{CAPITAL COST}}{\text{ANNUAL OUTPUT}}\right|_{\substack{\text{FIXED}\\ \text{SYSTEM}}}$$

- CAPITAL COST = $(C_{MOD} + C_{PCS})\ S_P \cdot \eta_A + C_{AF}$ $(\$/M^2)$
- ANNUAL OUTPUT = $S \cdot \eta_A$ (KWH/M^2)

Determining Break-Even Tracking Field Costs: Assumptions

- ALL COSTS ARE FOR DELIVERED HARDWARE
- AVERAGE ANNUAL EFFICIENTY (η_A) OF SYSTEM IS UNCHANGED BY TRACKING
- C_{PCS} IS UNCHANGED BY TRACKING
- O&M COSTS ARE NOT INCLUDED
- LAND COSTS OF ~$10,000/ACRE.

ORIGINAL PAGE IS
OF POOR QUALITY

Break-Even Tracking Field Costs

THE TRACKING ARRAY FIELD COSTS RESULTING IN EQUIVALENT ENERGY COST AS THE FLAT PANEL SYSTEM IS

$$C_{AF/T} = C_{AF/F} + \frac{S_T - S_F}{S_F}\left[C_{AF/F} + 1000\eta_A\ (C_{MOD} + C_{PCS})\right].$$

THE INCREASE FOR TRACKING = (INCREASED ENERGY OUTPUT)

x (CAPITAL COST OF FIXED SYSTEM)

Increased Annual Solar Availability* Due to Tracking

$S_T - S_F/S_F$

SITE \ CONCEPT	2-AXIS	1-AXIS (N-S) LAT. TILT	1-AXIS (N-S) HORIZONTAL
ALBUQUERQUE	.30	.22	.16
BOSTON	.22	.13	.09
FRESNO	.30	.21	.19
MIAMI	.17	.13	.09
PHOENIX	.28	.21	.15
SANTA MARIA	.23	.16	.11

*BASED ON TMY DATA. ASSUMES UNIFORMLY BRIGHT DIFFUSE SKY AND MAY UNDERESTIMATE SOLAR AVAILABILITY TO TRACKER.

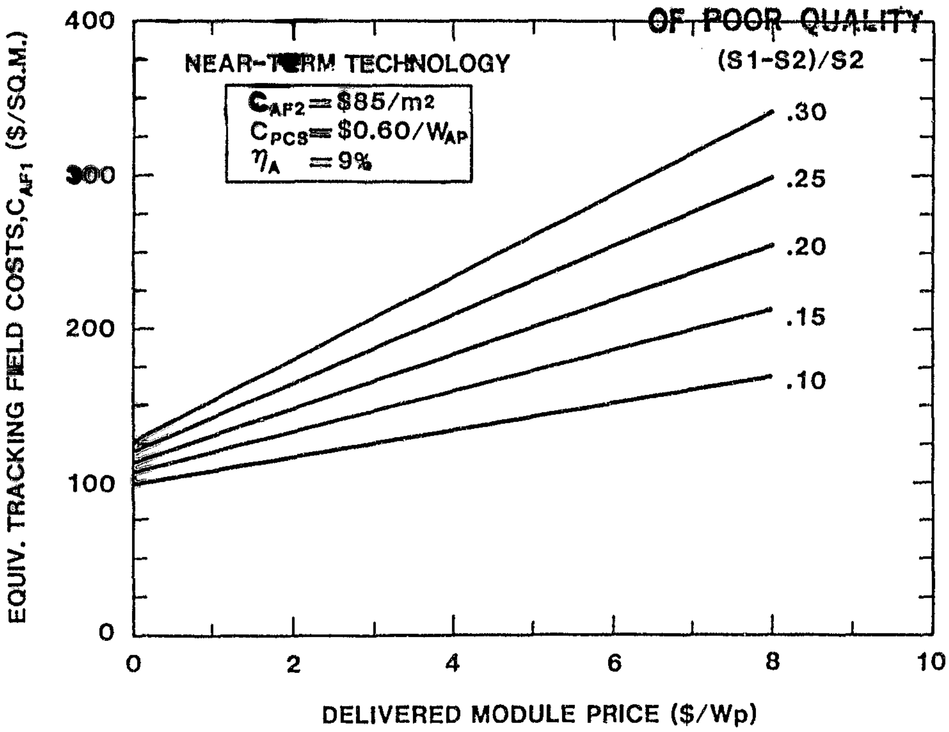
NEAR-TERM TECHNOLOGY
C_{AF2} = \$85/m2
C_{PCS} = \$0.60/W_{AP}
η_A = 9%
(S1-S2)/S2
.30
.25
.20
.15
.10
400
300
200
100
0
0
2
4
6
8
10
DELIVERED MODULE PRICE (\$/Wp)
EQUIV. TRACKING FIELD COSTS, C_{AF1} (\$/SQ.M.)

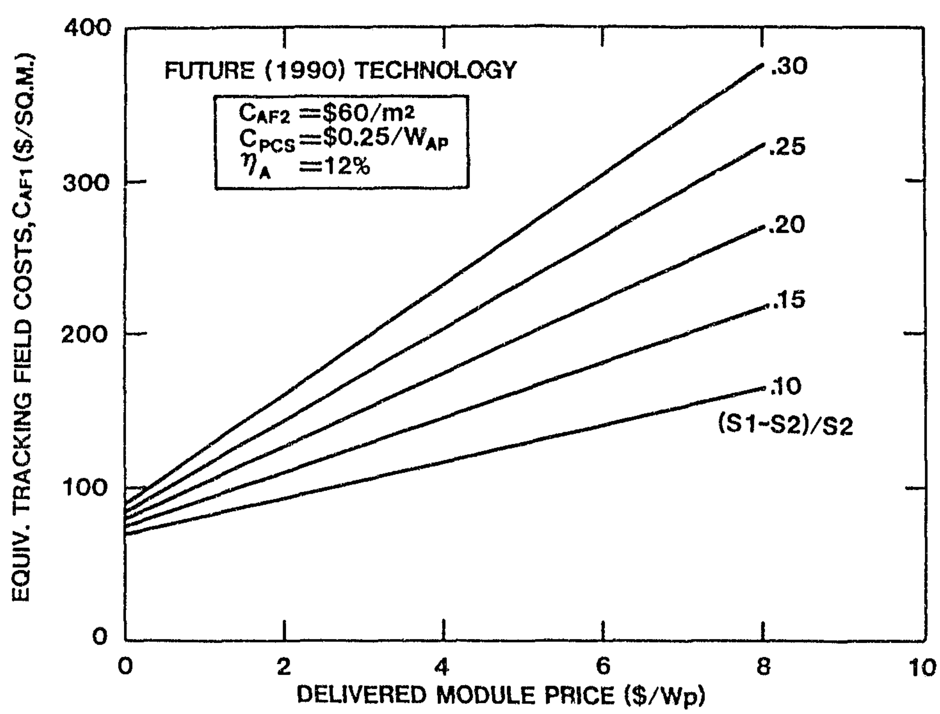
FUTURE (1990) TECHNOLOGY
C_{AF2} = \$60/m2
C_{PCS} = \$0.25/W_{AP}
η_A = 12%
.30
.25
.20
.15
.10
(S1-S2)/S2
400
300
200
100
0
0
2
4
6
8
10
DELIVERED MODULE PRICE (\$/Wp)
EQUIV. TRACKING FIELD COSTS, C_{AF1} (\$/SQ.M.)

Equivalent Array Field Costs for Tracking Flat-Panel Collectors

(ASSUMES $\$1/W_{AP}$ PANELS)

PERIOD \ CONCEPT	ONE-AXIS 0° TILT	ONE-AXIS LATITUDE TILT	TWO AXIS
	(1980 $\$/M^2$)		
NEAR TERM ($C_{AF/F} = \$85/M^2$)	105-128*	115-135	135-155
FUTURE TECHNOLOGY ($C_{AF/F} = \$60/M^2$)	80-100	90-106	106-123

*RANGE = OVERCAST - SOUTHWEST

Conclusion

- IF THE ARRAY FIELD COSTS OF TWO-AXIS TRACKING CONCENTRATORS ARE ASSUMED TO REPRESENTATIVE OF A TWO-AXIS FLAT PANEL, $C_{AF/T} \sim \$95/M^2$ ARE PROJECTED.

- THIS IS LESS THAN THE ALLOWABLE ARRAY FIELD COSTS FOR ALL SITES CONSIDERED, AT $\$1/W_{AP}$ PANELS.

∴ TWO-AXIS TRACKING IS A COST EFFECTIVE OPTION FOR FLAT PANEL COLLECTORS EVEN AT MODULE PRICES LOWER THAN $\$1/W_{AP}$.

Technology Sessions

SILICON-SHEET GROWTH AND CHARACTERISTICS

A.H. Kachare, Chairman

Reports of progress in silicon-sheet growth and characteristics were presented by four contractors and JPL.

Westinghouse Electric Corp., conducting research on advanced dendritic-web growth methods of making Si ribbons, reported that a first-generation computer model of silicon-web growth has been developed and verified and a temperature model has been expanded. The first computer-defined web growth configuration has been verified in actual operation. The experimental web machine is operational and has been verified in steady-state growth. The coordinated program using the computer models and experimental web growth data has been proven as a mechanism for attaining increased area growth rate.

Mobil Tyco Energy Corp. is conducting research to develop an understanding of the mechanism of stress generation in silicon sheet growth. It reported that computer code for stress calculations for a two-dimensional moving silicon sheet is fully operational. Calculations using the stress program have identified areas where experimental data are required to test and to apply the model.

Applied Solar Energy Corp., conducting research in solar-cell fabrication and analysis, reported on studies made on cast silicon: UCP (Semix, Inc.), HEM (Crystal Systems, Inc.) and Silso (Wacker Siltronic Corp.) a comparison of the three cast materials shown very similar performances (UCP 10.4%, HEM 11.1%, and Silso 10.2%).

Cornell University, conducting research on characterization of silicon sheet properties, reported that melt-spun ribbons, low-angle grain boundaries, $\langle 110 \rangle$ tilt boundaries to 109°, and hydrogenation of HEM silicon.

In the JPL in-house program, a summary of the Stress/Strain in High-Speed Ribbon Growth Miniworkshop was presented.

PRECEDING PAGE BLANK NOT FILMED

STRESS/STRAIN IN HIGH-SPEED RIBBON GROWTH MINIWORKSHOP

November 8 and 9, 1982, at Waltham, Massachusetts

SUMMARY

JET PROPULSION LABORATORY

J.K. Liu

Objective

- SUMMARIZE PRESENT EXPERIENCE WITH STRESS/STRAIN EFFECTS IN SILICON RIBBON GROWTH
- DEFINE AND DISCUSS THE PROBLEM
- INCLUDE EXPERTS IN THE FIELD OUTSIDE FSA PROGRAM
- PROMOTE INTERCHANGE OF INFORMATION
- FORMULATE DIRECTION OF FUTURE RESEARCH

Program

- DESCRIPTION OF FOUR RIBBON GROWTH PROCESSES (WEB, EFG, ESP, LASS) AND DISCUSSION OF STRESS/STRAIN EFFECTS ON THE PRODUCT
- PRESENTATION OF CURRENT ACTIVITIES IN STRESS MODELING
- TOUR OF MOBIL SOLAR'S FACILITY (EFG GROWTH PROCESS)
- OPEN DISCUSSION

Discussion

- DESCRIPTION OF THERMAL STRESS MODELS FROM CALCULATED AND MEASURED TEMPERATURE FIELDS IN SILICON SHEET IN THE REGION JUST BEYOND GROWTH INTERFACE
- REFINEMENTS TO MODEL INCLUDING:
  - ACCOMODATION OF MULTI PATH HEAT CONDUCTION AND RADIATION EFFECTS IN THE GROWTH REGION
  - ACCOMODATION OF CREEP EFFECTS TO TAKE INTO ACCOUNT PLASTIC DEFORMATION
  - STRESS DEPENDENCE ON GROWTH SPEED AND RIBBON WIDTH
- DESCRIPTION OF DISLOCATION DENSITY DISTRIBUTIONS VERSUS RESIDUAL STRESS IN RIBBON
- GENERAL REVIEW OF FOUR DIFFERENT SILICON RIBBON GROWTH PROCESSES (WEB, EFG, ESP, LASS)

Future Work

- A GENERAL THERMAL STRESS MODEL INTEGRATING CREEP BEHAVIOUR, GROWTH SPEED AND RIBBON WIDTH SHOULD BE COMPLETED AND APPLIED TO ALL RIBBON GROWTH PROCESSES
- CORRELATION OF OBSERVED BUCKLING PHENOMENA AND STRESS MODEL
- DATA ON BASIC SILICON MATERIAL PROPERTIES (i.e. CREEP BEHAVIOUR, STRESS MODULII) AT TEMPERATURE RANGE OF INTEREST (1300-1400°C)
- CORRELATION OF "STRUCTURE" (i.e. DISLOCATIONS, GRAIN BOUNDARIES) EFFECTS WITH GENERATED STRESS
- IMPURITY EFFECTS ON STRESS GENERATION
- VERIFICATION OF STRESS MODEL WITH EXPERIMENTAL GROWTH SYSTEM(S) IN INDUSTRY
- CONSTRUCTION OF A GROWTH SYSTEM THAT INTEGRATES ALL INFORMATION GENERATED TO PRODUCE OPTIMUM SILICON RIBBONS AT HIGH SPEED

ADVANCED DENDRITIC WEB GROWTH DEVELOPMENT

WESTINGHOUSE ELECTRIC CORP.

Long-Range Goals of Program

- Continuously-Melt-Replenished Growth Period Of 65 Hours With Area Rate Of Growth Greater Than 25 cm^2/minute*
- Length Of Web Crystal Greater Than 10 Meters
- Dislocation Density Below $10^4/cm^2$
- Terrestrial Solar Cell Efficiency Greater Than 15%

* Current Program Concentrates On Area Growth Rate Aspect Of This Goal. Other Goals Essentially Achieved Or Surpassed

Program Logic for Increased Area Growth Rate

- Deformation Is Major Limitation Of Ribbon Width And Area Growth Rate
- Deformation Is Correlated To Thermally Generated Stress
- Computer Models Provide Understanding Of Web Growth, Thermal Requirements For Stress Reduction, And Optimized Area Growth Rate
- Coordinated Program Of Models And Experimental Web Growth Achieves Major Improvement Of Area Growth Rate

Status at Start of Reporting Period

- First-Generation Computer Models Of Silicon Web Growth Developed And Verified. Temperature Model Expanded
- First Computer-Defined Web Growth Configuration Verified In Actual Web Growth
- Experimental Web Growth Machine Operational And Verified In Steady-State Web Growth

Principal Activity In Reporting Period

Computer Models

- Define Growth Configurations For Increased Area Rate Of Growth
- Continued Development Of Models
- Evaluation Of Conceptual Configurations For Dynamic Thermal Trimming

Experimental Web Growth

- Evaluate Computer-Defined Growth Configuration
- Measure Growth System Parameters To Obtain Model Input And To Optimize Configuration For Growth
- Demonstrate Improved Growth

Application of Computer Models

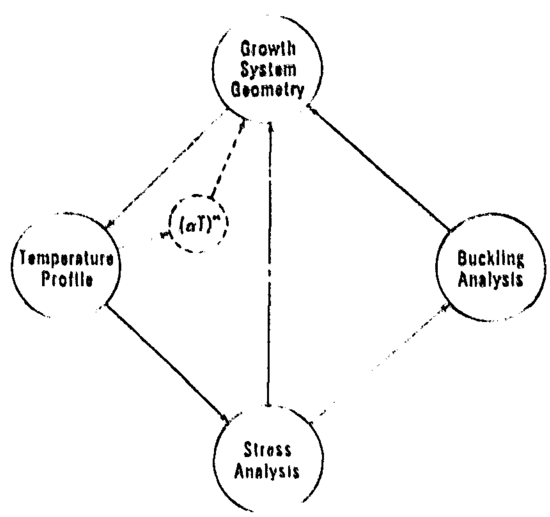

- Improved Temperature Model Verified By Comparing Model Predictions With Known Growth Behavior Of Experimentally-Derived Growth Configurations
- Conceptual Configurations Evaluated And Modified To Determine New-Generation Model-Derived Configuration: J460
- J460 Configuration Verified By Experimental Web Growth. Measured Data From Experimental Growth Fed Back To Models
- New Conceptual Configurations Evaluated And Modified For Next-Generation Of Experimental Web Growth And Increased Area Rate Of Growth

Performance of J460 Configuration

- Maximum Low-Stress Growth Width: 5.5 cm (Up 12%)
- Growth Width At Standard Thickness: 4.9 cm (Up 30%)
- Quasi-Steady-State Area Growth Rate: 13 cm^2/min (Up 60%)

Development of Models

- Graphics Output Added To Temperature Model To Provide Capability Of Evaluating Larger Number Of Conceptual Cases At Less Cost Per Case
- Buckling Model Evaluated And Verified For Application To Wider Web Growth

Dynamic Thermal Trimming of Web Growth

- Evaluation Of Conceptual Configurations Initiated
- First-Generation Configuration For Experimental Web Growth Will Likely Include Trimming Of Top Shields And/Or Melt Level

Sequence of Experimental Web Growth for Model-Defined Growth Configurations

- Fabricate Configuration And Subsequent Variations
- Determine Growth Equipment Operating Settings
- Measure Web And Growth System Parameters
- Demonstrate Improved Growth

Combined Use of Models and Experimental Web Growth

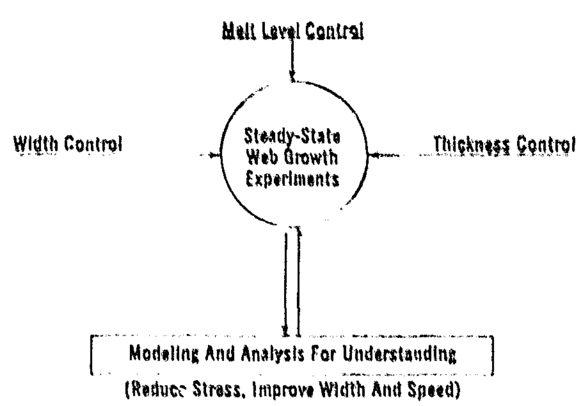

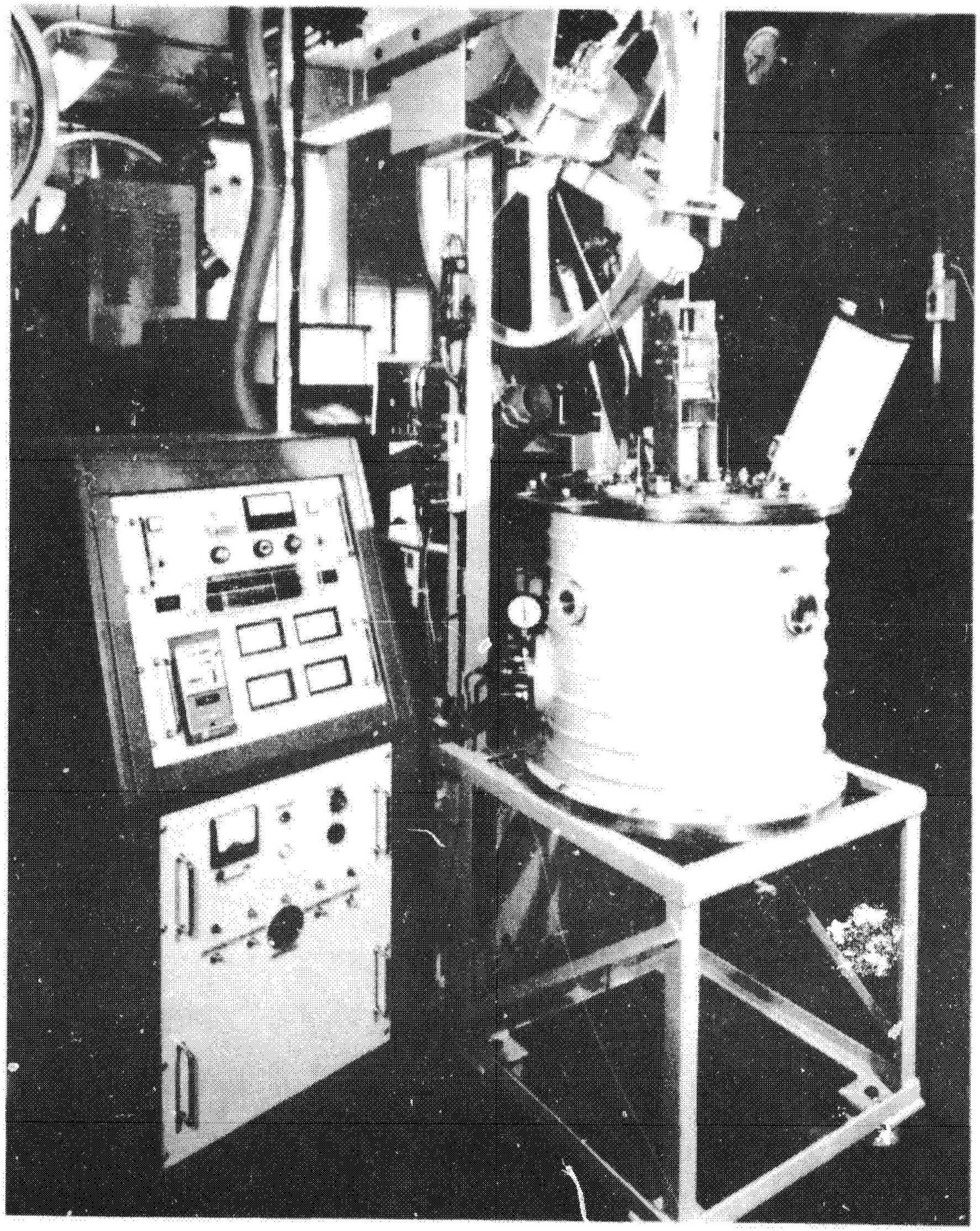

ORIGINAL PAGE
BLACK AND WHITE PHOTOGRAPH

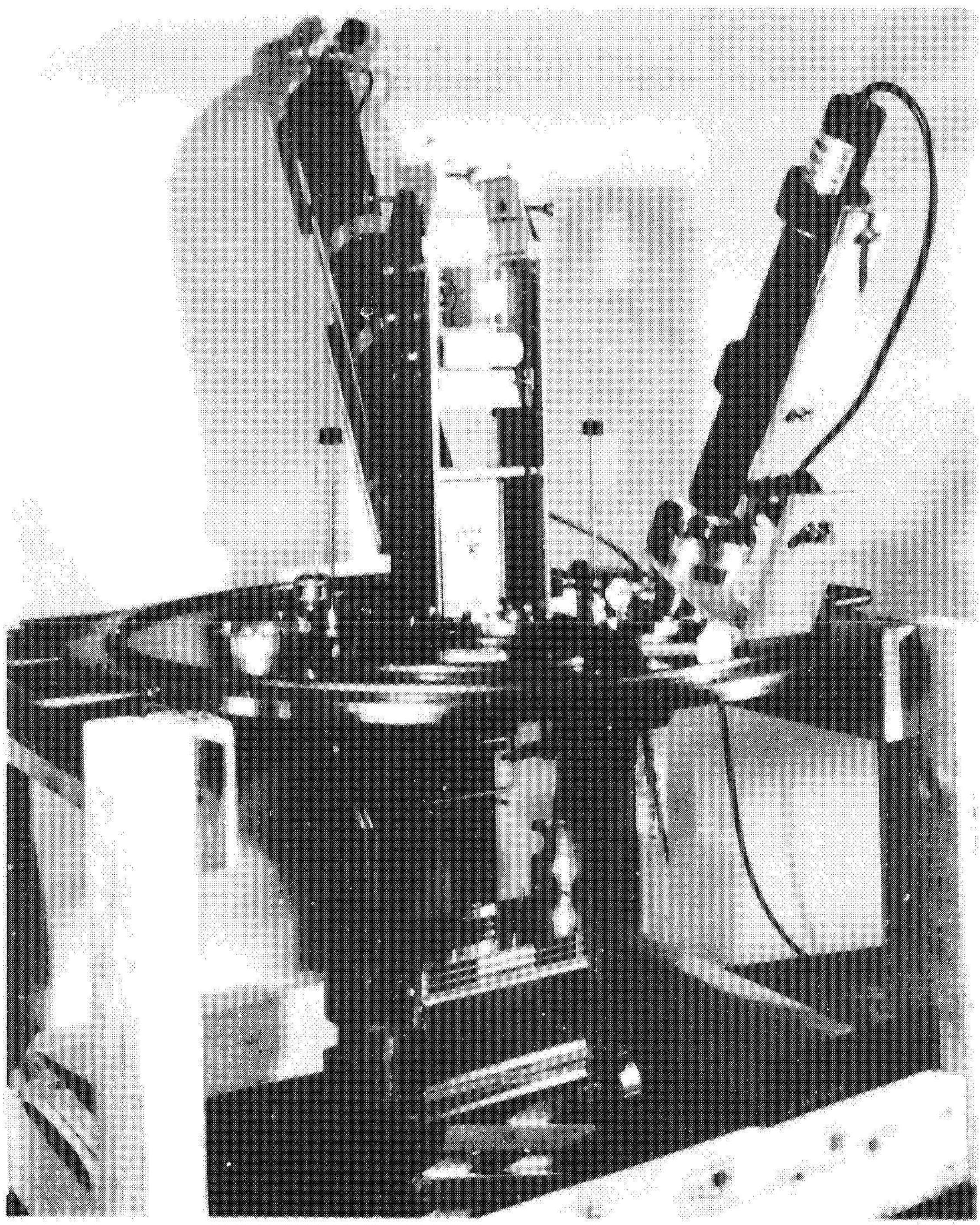

ORIGINAL PAGE IS
OF POOR QUALITY

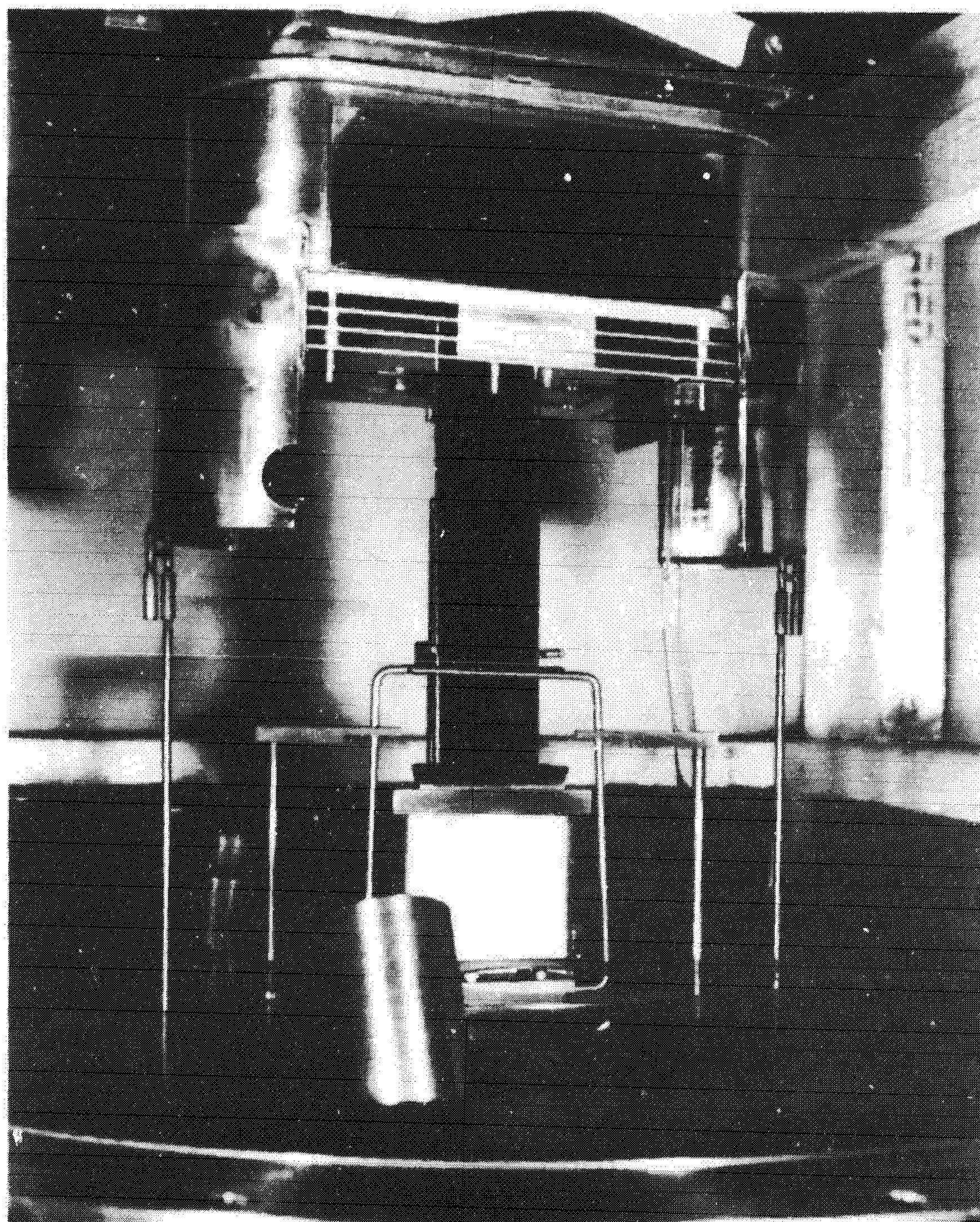

ORIGINAL PAGE
BLACK AND WHITE PHOTOGRAPH

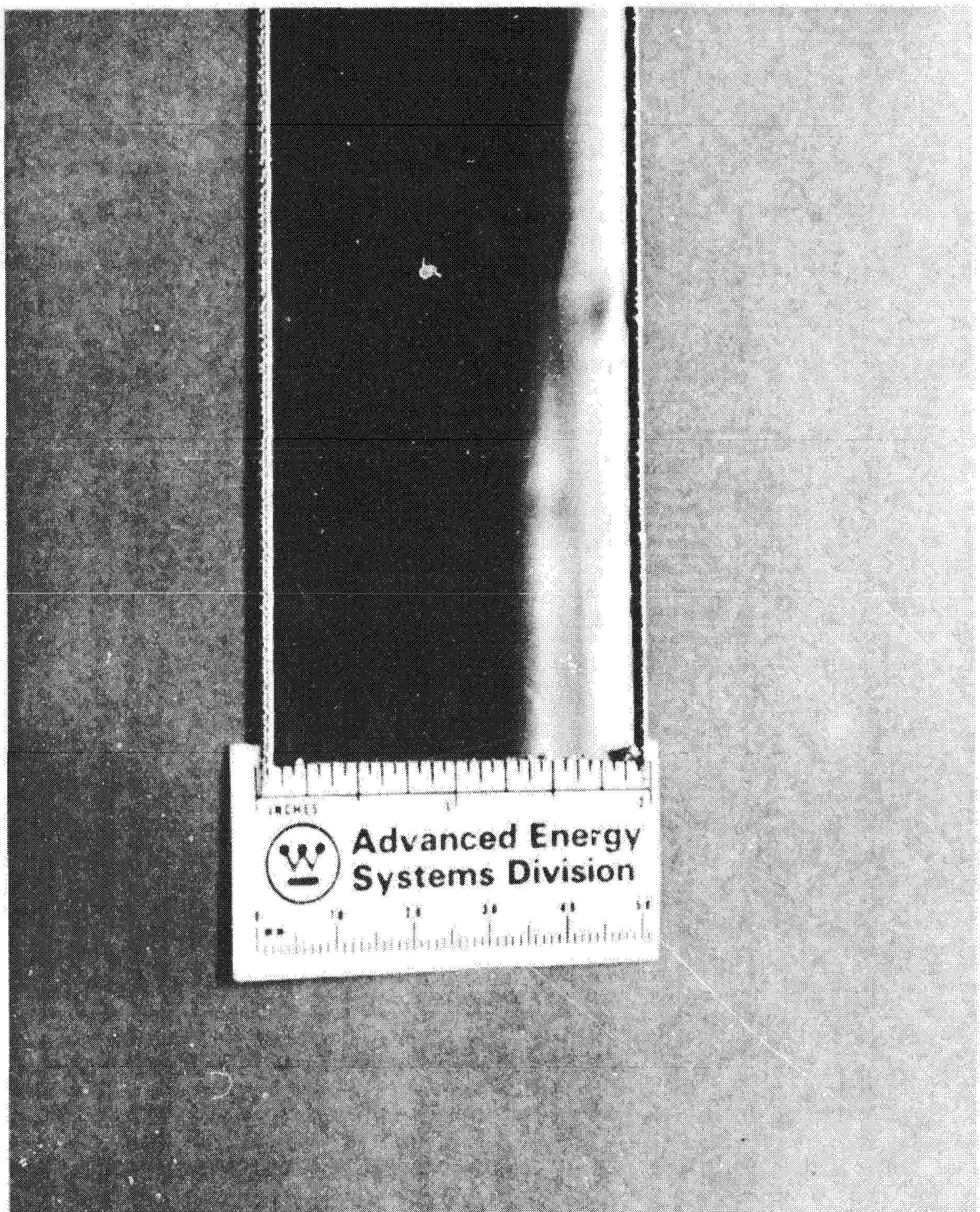

ORIGINAL PAGE
BLACK AND WHITE PHOTOGRAPH

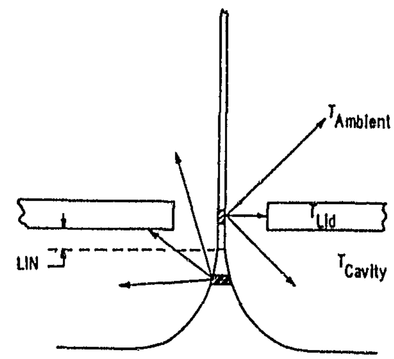

Development Progress

Development	1977	1978	1979	1980	1981	1982 Early	1982 Late	1983 Plan
Area Growth Rate, cm^2/min								
1) Transient (Lengths Of Several Centimeters)	2.3	8	23	27				30-35
2) Quasi-Steady-State (Lengths Of 30 To 100 cm)					7	8	13	18-20
3) Steady-State (Meters Of Length, Hours Of Growth)					4	6	8	12-15
Maximum Undeformed Width, Centimeters	2.4	3.5	4.0	4.4	4.4	4.9	5.5	6-7
W_{150}-Undeformed Width At 150 μm Thickness (An Inverse Measure Of Buckling Stress)		2.0	2.7	3.2	3.2	3.8	4.9	6
Maximum Demonstrated Solar Cell Efficiency, AM1	13	14	15	15.5	15.5		~17	17-18

Problems and Concerns

No Unworkable Problems Or Concerns At This Time

Summary

- Coordinated Program Using Computer Models And Experimental Web Growth Proven As A Mechanism For Attaining Increased Area Growth Rate
- Substantial Increase In Area Growth Achieved

ORIGINAL PAGE IS
OF POOR QUALITY

STUDIES OF STRESS IN EFG

MOBIL SOLAR ENERGY CORP.

TECHNOLOGY ADVANCED MATERIALS RESEARCH TASK	REPORT DATE JANUARY 12, 1983
APPROACH STRESS STUDIES IN EFG CONTRACTOR MOBIL SOLAR ENERGY CORPORATION, CONTRACT NUMBER 956312 GOALS • DEVELOP UNDERSTANDING OF MECHANISM OF STRESS GENERATION IN SILICON SHEET GROWTH AND DEFINE MINIMUM STRESS GROWTH CONFIGURATIONS FOR 200 μM THICK 10 CM WIDE EFG RIBBON GROWING AT 4 CM/MIN.	STATUS • COMPUTER CODE FOR CALCULATION OF STRESSES FOR A TWO-DIMENSIONAL MOVING SILICON SHEET IS FULLY OPERATIONAL. • MODELING AND EXPERIMENTAL TASKS ARE IN PROGRESS TO: - OBTAIN TEMPERATURE DISTRIBUTIONS IN RIBBON. - DEVELOP UNDERSTANDING OF PLASTIC DEFORMATION (CREEP) PROCESS. - EVALUATE RESIDUAL STRESS.

Stress Analysis Program

- DEVELOPMENT OF COMPUTER CODE FOR STRESS CALCULATIONS (J.W. HUTCHINSON AND J.C. LAMBROPOLOUS, HARVARD UNIVERSITY):
  - TWO-DIMENSIONAL CALCULATION (ZERO SHEET THICKNESS).
  - PLASTIC DEFORMATION IS INCLUDED THROUGH CREEP LAW.
  - STEADY-STATE CONDITIONS ARE ASSUMED.

- CALCULATIONS HAVE IDENTIFIED AREAS WHERE EXPERIMENTAL DATA IS REQUIRED TO TEST AND TO APPLY MODEL:
  - SHEET TEMPERATURE FIELD.
  - INTERFACE STRESS STATE.
  - CREEP PROCESSES ABOVE 1000°C.
  - RESIDUAL STRESS STATE OF SHEET.

Stress Analysis Parameters

- INPUT PARAMETERS:
  - TEMPERATURE FIELD T(X,Y),
  - INTERFACE STRESS BOUNDARY CONDITIONS

    $\sigma_{XX} = \sigma_{XY} = \sigma_{YY} = 0$
  - CREEP LAW

    $\dot{\epsilon} = \frac{C\sigma^5}{T} \text{EXP}(-Q/KT)$
  - GROWTH SPEED V
- OUTPUT PARAMETERS:
  - STRAIN RATE COMPONENTS $\dot{\epsilon}_{XX}$, $\dot{\epsilon}_{YY}$
  - STRESS COMPONENTS σ_{XX}, σ_{YY}

Idealized Temperature Profile Used for Computer Code Testing

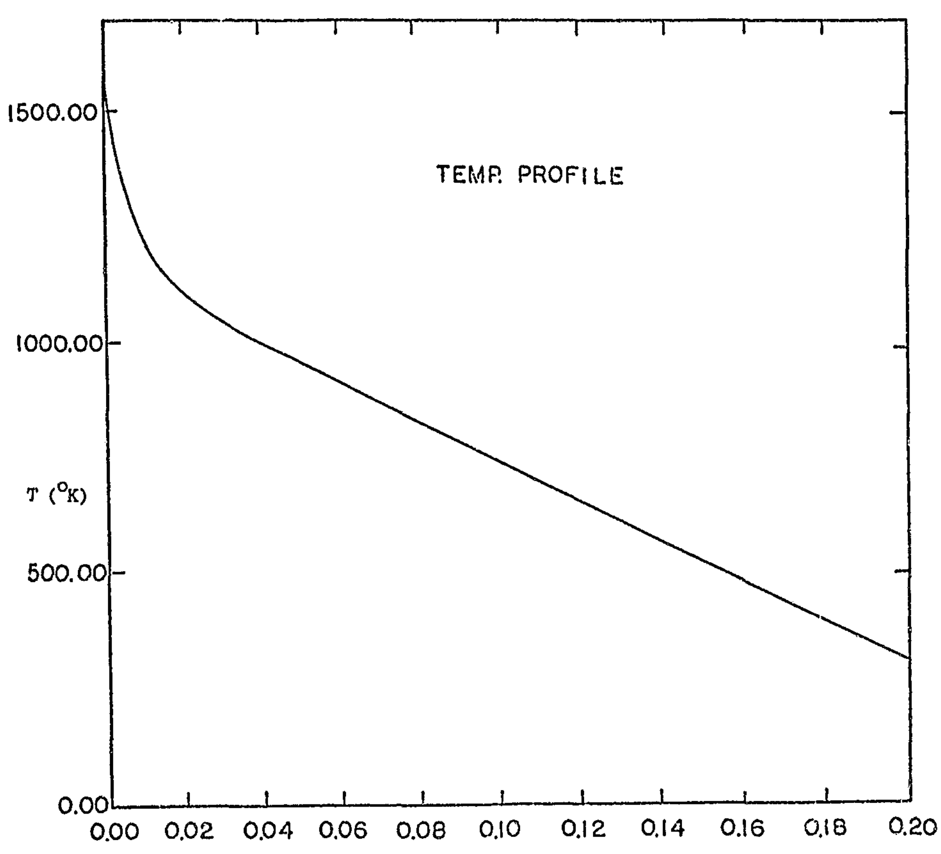

Grid Pattern for Calculation Domain

ULTRA FINE GRID

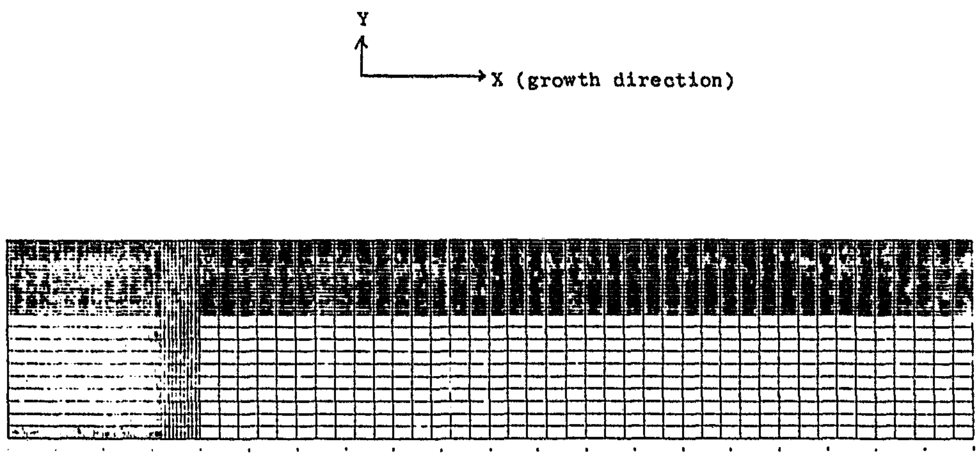

ORIGINAL PAGE IS OF POOR QUALITY

σ_{xx} Component of Stress Variation Across Ribbon Width at Room Temperature

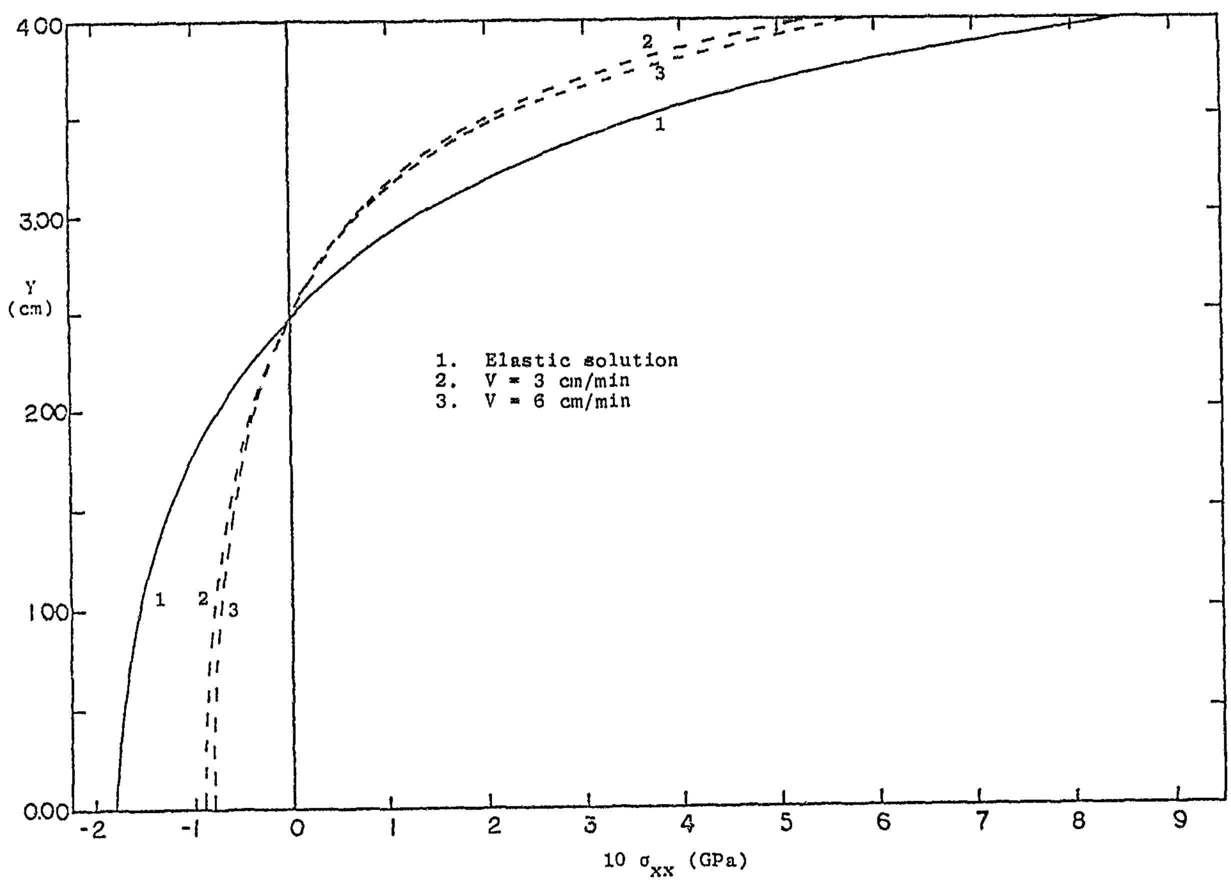

Creep Strain Rate Variations Along Growth Direction at y / H = 0.031

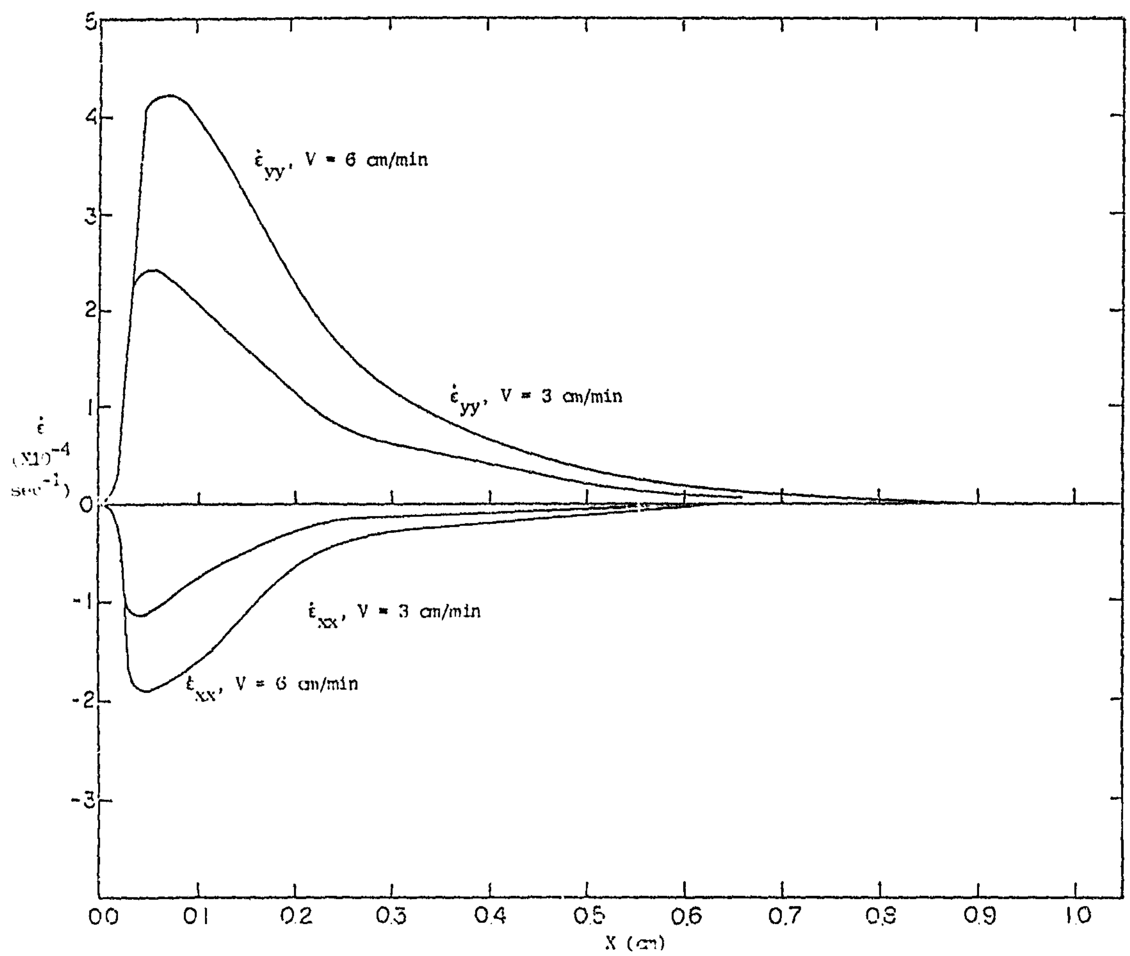

Experimental Program

- MODEL AND MEASURE TEMPERATURE FIELD FOR GROWING EFG RIBBON (R.O. BELL AND J.P. KALEJS, MSEC).
  - CALCULATION SCHEME TO ACCOUNT FOR RADIATION FLUXES ON GROWING SHEET HAS BEEN DEVELOPED AND EVALUATED EXPERIMENTALLY.
  - TEMPERATURE PROFILES FOR THE COLD SHOE SYSTEM FOR 10 CM WIDE RIBBON HAVE BEEN OBTAINED.

- EXPERIMENTAL WORK AND ADDITIONAL MODELING ARE IN PROGRESS TO
  - DEVELOP TEMPERATURE MEASUREMENT CAPABILITY USING FIBER OPTICS.
  - REFINE CALCULATIONS FOR TEMPERATURE FIELD IN MOVING RIBBON (V-t DATA, INTERFACE SHAPE).

Cold-Shoe Geometry Used to Calculate Temperature Distribution in Ribbon

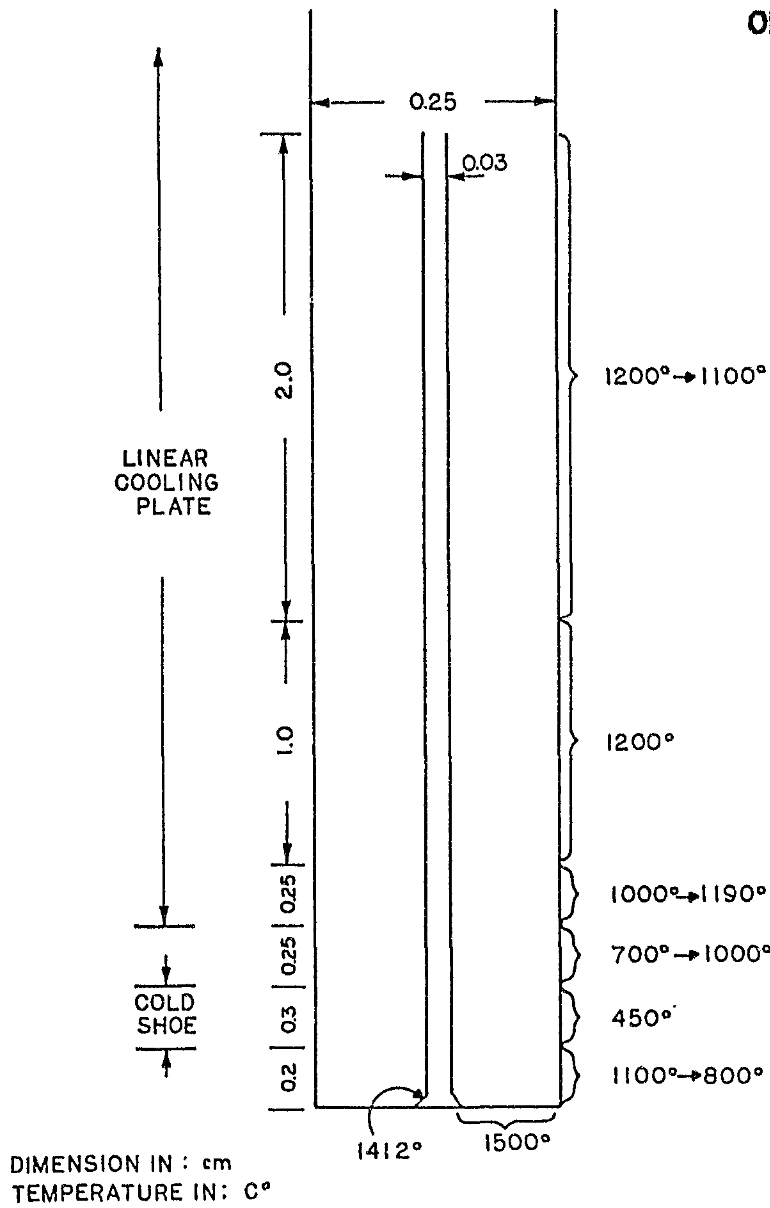

Temperature Distribution of Environment
and in a 300-μm-Thick Ribbon

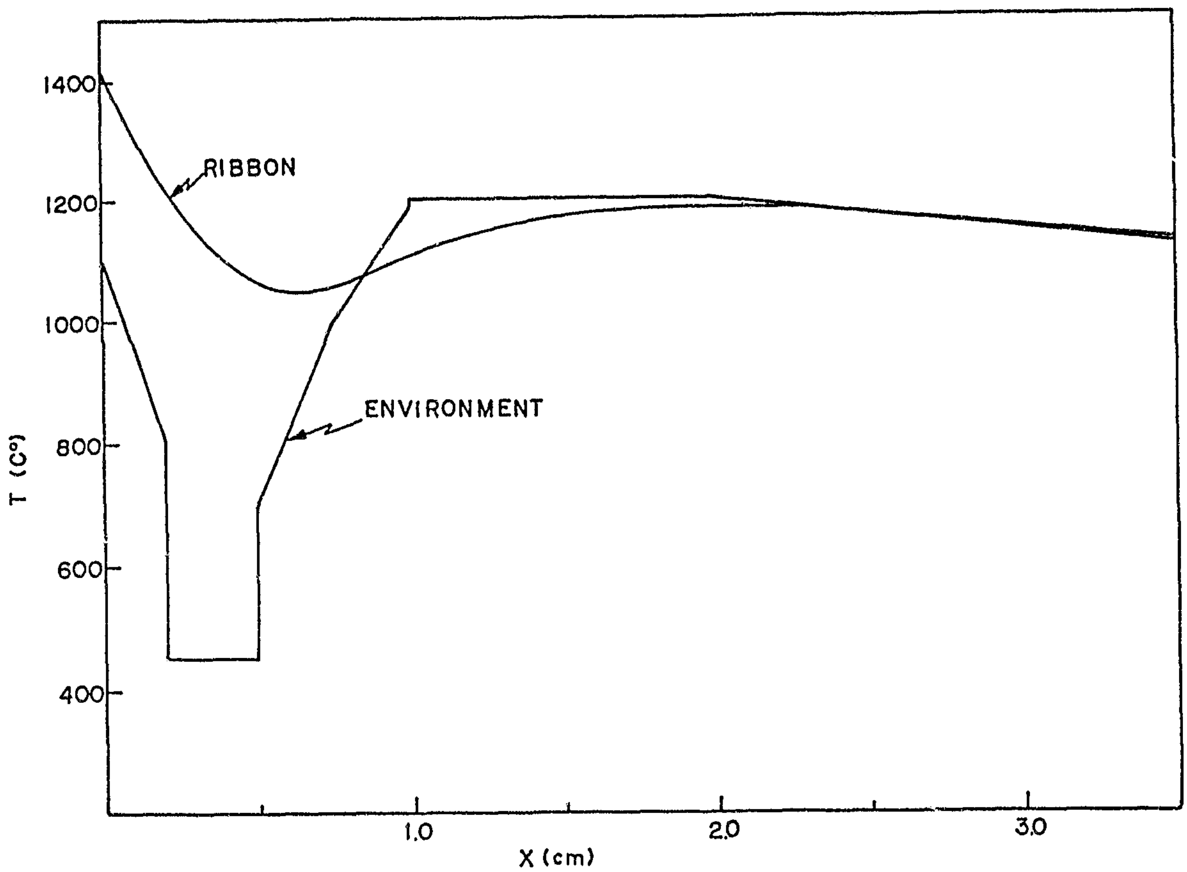

ORIGINAL PAGE IS
OF POOR QUALITY

V-t Curves for 10-cm Ribbon

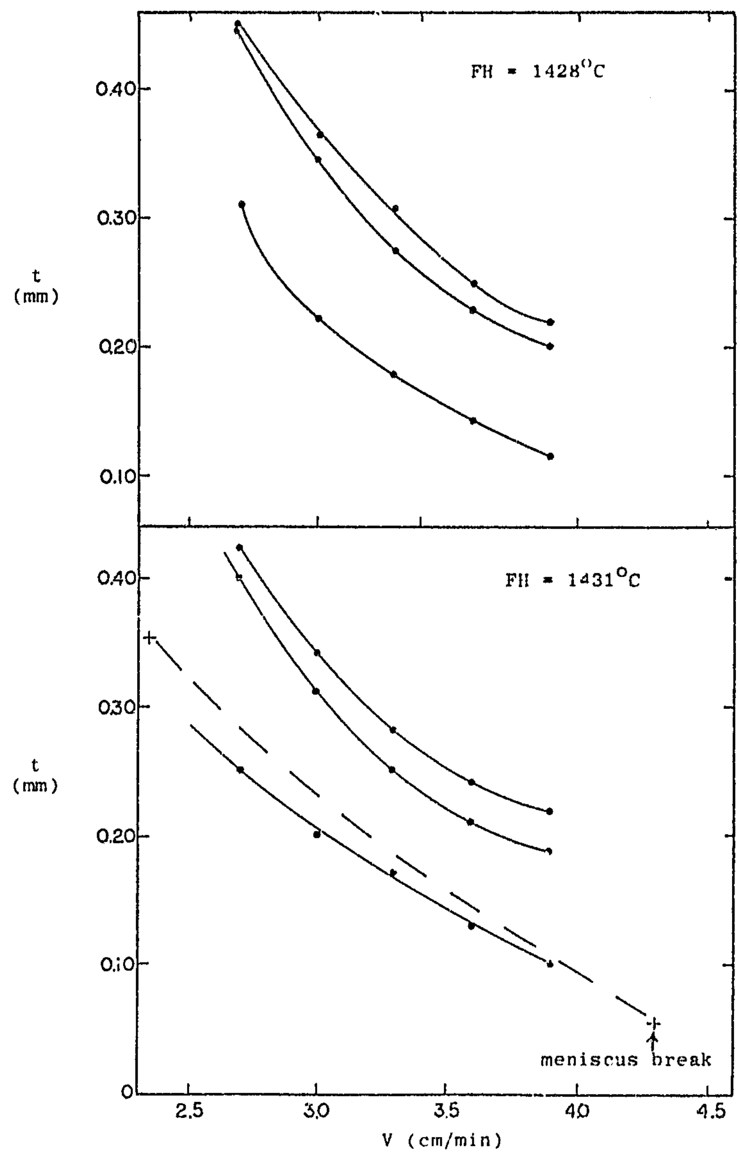

Temperature Profile for 10-cm-Wide Ribbon System Calculated From Heat-Transfer Model

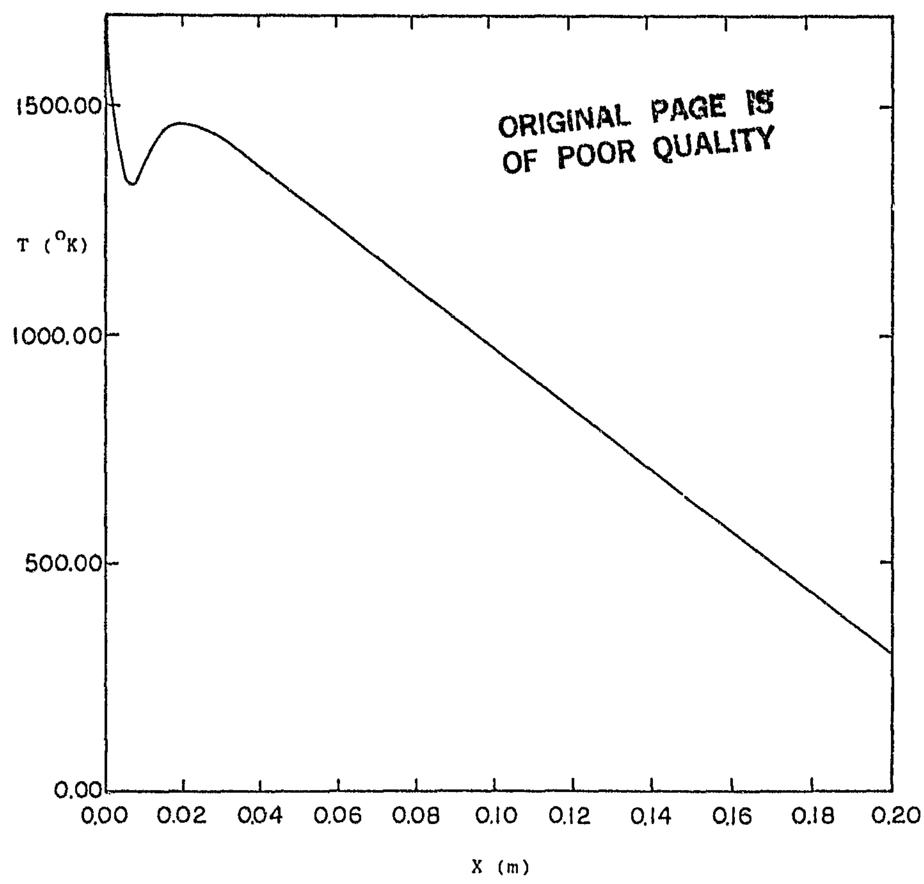

Room-Temperature σ_{xx} Component of Stress Variation Across Ribbon Width for Cold-Shoe System

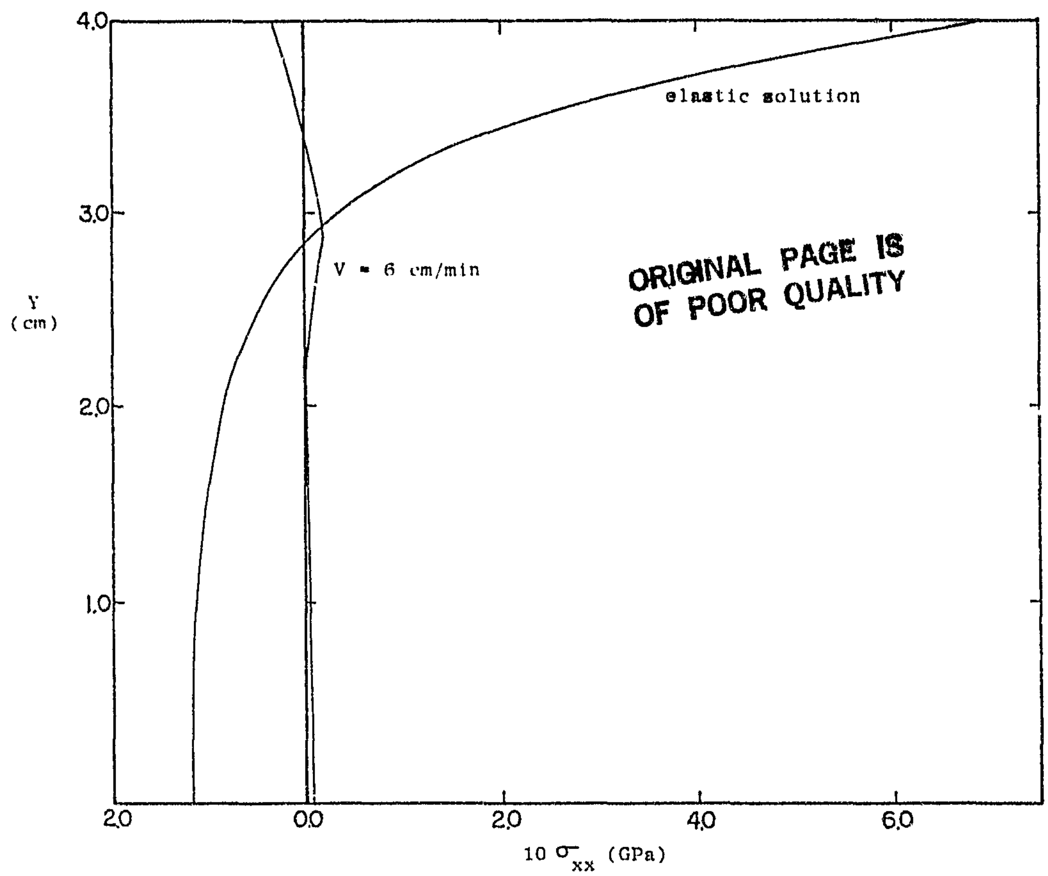

Strain Rate $\dot{\epsilon}_{xx}$ Along Growth Direction at Y = 0

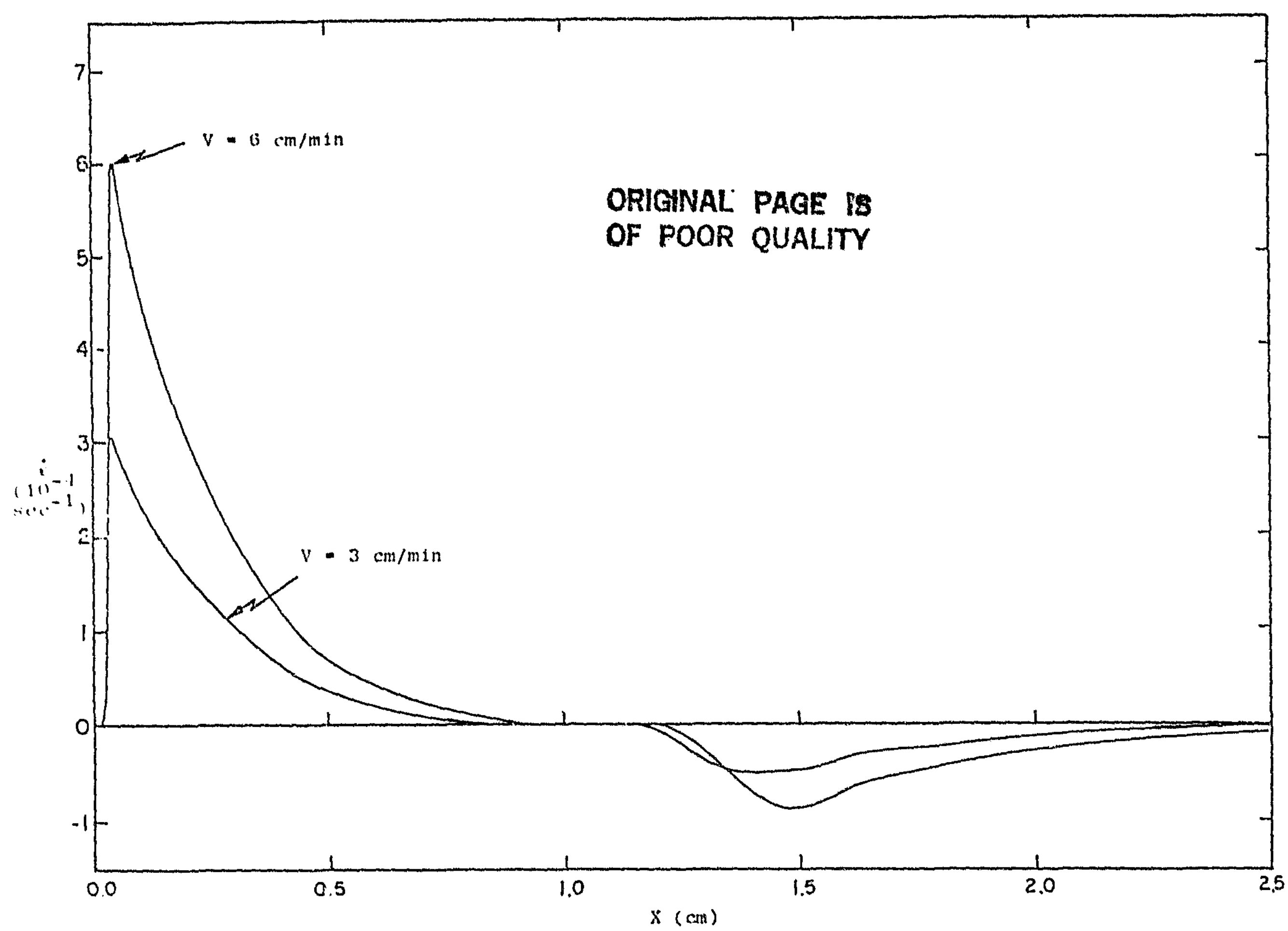

Stress Component Variation Along Growth Direction at y / H = 0.025

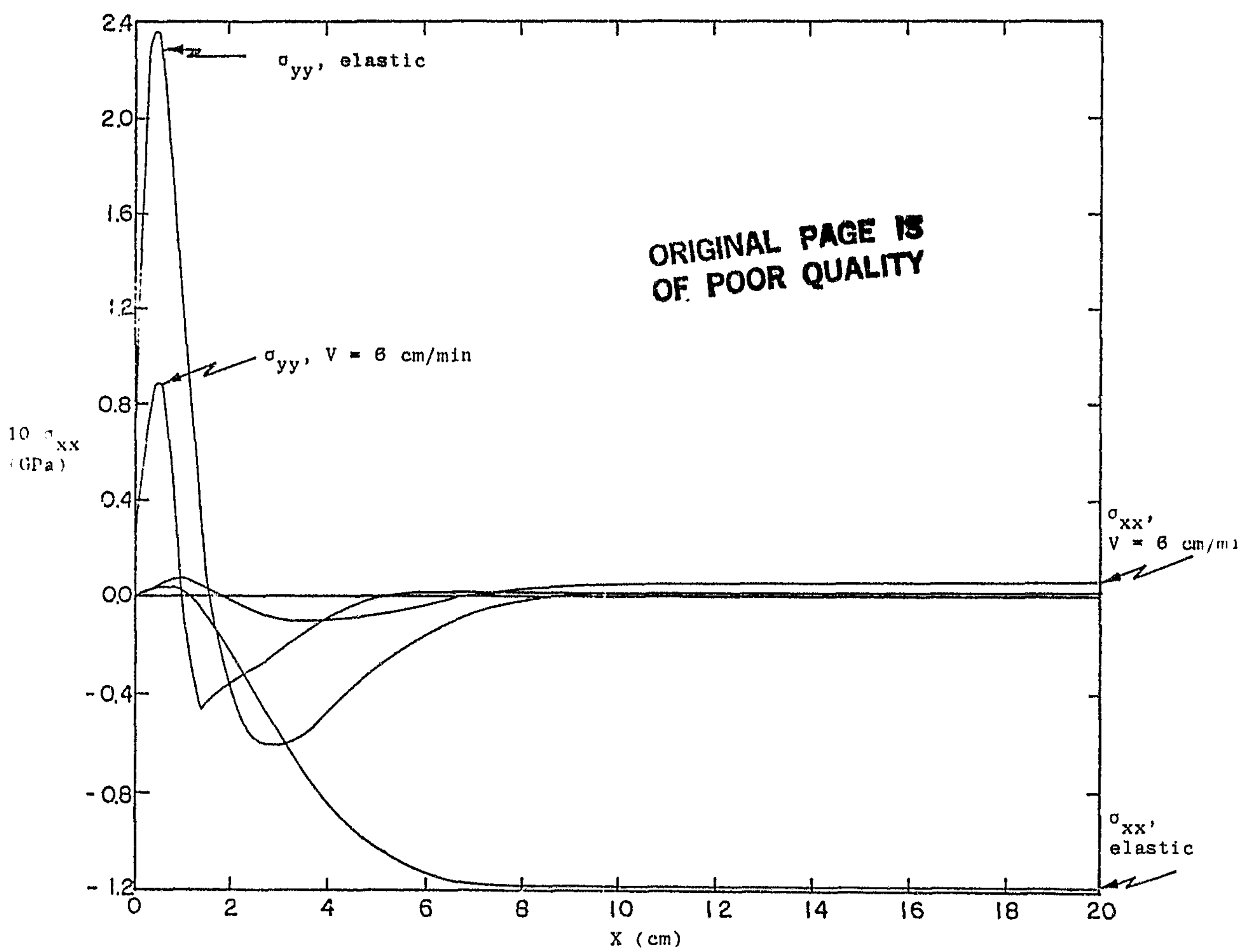

Concerns

- DATA ON HIGH TEMPERATURE PROPERTIES OF SILICON ARE REQUIRED TO GUIDE MODELING.
- TEMPERATURE FIELD, RESIDUAL STRESS MEASUREMENT CAPABILITIES NEED TO BE DEVELOPED.

Plans

- CARRY OUT SENSITIVITY ANALYSIS FOR STRESS DEPENDENCE ON:
  (1) TEMPERATURE FIELD, (2) CREEP BEHAVIOR, (3) INTERFACE STRESS σ_{YY}.

- DEVELOP MEASUREMENT CAPABILITIES FOR
  (1) RIBBON TEMPERATURE FIELD (FIBER OPTICS),
  (2) CREEP LAW STUDIES (FOUR-POINT BENDING),
  (3) RESIDUAL STRESS DETERMINATION (LASER INTERFEROMETRY).

SOLAR CELL FABRICATION & ANALYSIS

APPLIED SOLAR ENERGY CORP.

<table>
<tr><td>TECHNOLOGY
SOLAR CELL FABRICATION & ANALYSIS</td><td>REPORT DATE</td></tr>
<tr><td>APPROACH
1) FABRICATION OF SOLAR CELLS BY BASELINE & ADVANCED PROCESSES POSSIBLY INCLUDING GETTERING AND ANNEALING.
2) ANALYSIS USING DARK AND LIGHT I-V, DIFFUSION LENGTH MEASUREMENTS, SPECTRAL RESPONSE.
CONTRACTOR
APPLIED SOLAR ENERGY CORPORATION</td><td rowspan="2">STATUS</td></tr>
<tr><td>GOALS
1) AN UNDERSTANDING OF THE MECHANISMS THAT LIMIT THE DEFICIENCIES OF SOLAR CELLS MADE FROM VARIOUS SILICON SHEETS.
2) AN UNDERSTANDING OF THE EFFECT ON SOLAR CELL EFFICIENCY OF VARIATIONS IN GROWTH PARAMETERS.</td></tr>
</table>

Ingot C-4-21A

1) UCP INGOT C-4-21A (SEMIX)
   RESULTS OF BASELINE PROCESS AND GETTERED PROCESS.
2) COMPARISON OF UCP, (SEMIX) SILSO (WACKER) AND HEM (CRYSTAL SYSTEM)
   RESULTS OF BASELINE, GETTERED AND HIGH EFFICIENCY PROCESSES ARE COMPARED.
3) SMALL DIODE STUDY (UCP)
   DARK DIODE I-V
   DIFFUSION LENGTHS

ORIGINAL PAGE IS OF POOR QUALITY

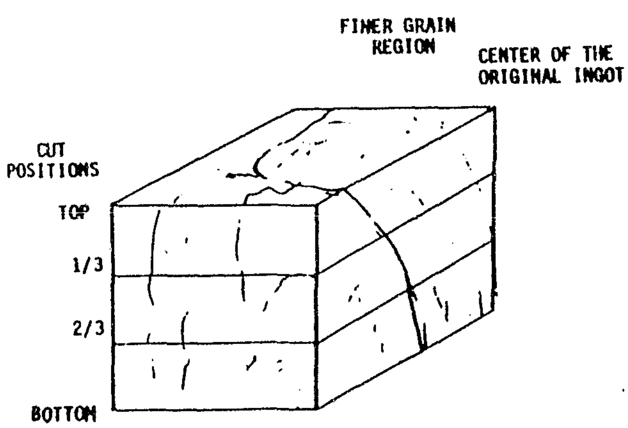

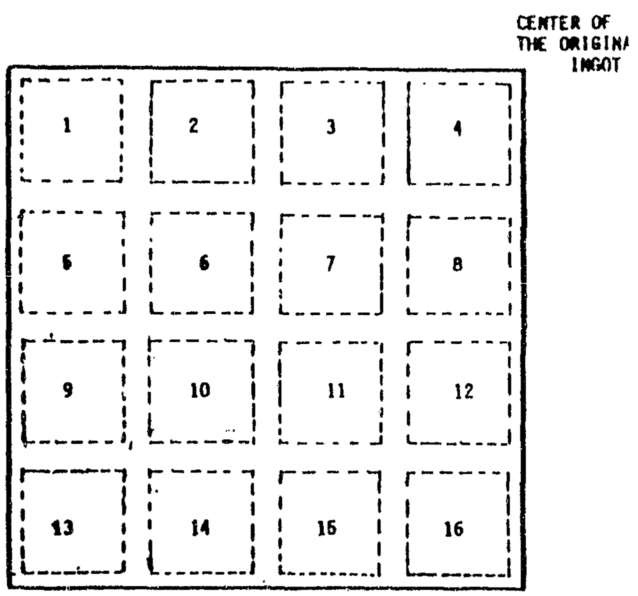

Summary of Baseline Results From Ingot C-4-21A

		Voc(mV)	Jsc (mA/cm^2)	CFF(%)	η(%)	(#1,5,9,13-16 Large Grain Area) Jsc (mA/cm^2)
TOP	AVE.	553	26.3	75	11.0	
	S.D.	± 7	± 0.8	± 1	± 0.4	
	RANGE	542-570	25.1-28.0	72-78	10.2-11.9	
1/3	AVE.	557	26.9	75	11.2	26.7
	S.D.	± 7	± .6	± 2	± .5	± .7
	RANGE	548-568	25.6-28.3	71-77	10.3-12.2	25.6-27.8
2/3	AVE.	556	26.4	73	10.7	26.3
	S.D.	10	± .6	± 14	± 1.4	± 1.5
	RANGE	530-572	25.4-27.5	45-78	6.0-11.7	25.4-26.9
BOTTOM	AVE.	549	25.7	72	10.2	25.9
	S.D.	29	± .8	± 12	± 2.0	± .6
	RANGE	422-566	24.4-26.9	26-77	28-11.4	25.3-26.9
CZ CONTROL	AVE.	584	29.1	77	13.0	
	S.D.	± 2	± 0.28	± 1	± 0.2	
	RANGE	580-586	28.8-29.4	75-77	12.6-13.1	

ORIGINAL PAGE IS
OF POOR QUALITY

875°C 1/2-hour Gettered and Then Baseline Results From Ingot C-4-21A

		Voc(mV)	Jsc (mA/cm^2)	CFF(%)	η (%)	(#1,5,9,13-16 Large Grain Area) Jsc (mA/cm^2)
TOP	AVE.	556	27.0	76	11.4	
	S.D.	± 11	± 0.8	± 1	± 0.6	
	RANGE	530-572	24.8-28.5	74-78	9.9-12.4	
1/3	AVE.	560	26.8	76	11.4	26.7
	S.D.	± 5	± 0.6	± 1	± 0.3	± 0.6
	RANGE	552-570	25.8-27.9	73-78	10.9-11.8	
2/3	AVE.	563	26.9	76	11.4	26.7
	S.D.	± 6	± 0.5	± 2	± 0.4	± .4
	RANGE	548-574	26.0-27.5	68-78	10.5-12.1	26.1-27.4
BOTTOM	AVE.	561	26.5	76	11.3	26.8
	S.D.	± 8	±0.6	± 1	± 0.6	± 0.2
	RANGE	542-572	25.5-27.0	73-77	10.3-11.9	26.5-27.0

Summary of Results From Baseline Cells for Comparing Three Cast Si Materials

		Voc(mV)	Jsc(mA/cm^2)	CFF(%)	η(%)
<u>UCP</u>					
A	AVE.	514	25.6	74	10.1
	RANGE	20-550	24.4-26.1	25-78	0.1-11.2
B	AVE.	555	25.8	76	10.9
	RANGE	534-568	24.1-27.0	68-79	8.8-12.1
C	AVE.	550	25.3	72	10.1
	RANGE	512-564	24.4-26.5	38-79	4.8.11.8
UCP OVERALL	AVE.	539	25.6	74	10.4
	RANGE	20-568	24.1-27.0	25-79	0.1-12.1
<u>SILSO</u>					
D(Long Grain)	AVE.	552	24.4	72	9.8
	RANGE	526-564	21.6-26.6	46-79	6.1-11.3
E (Medium Grain)	AVE.	556	26.2	76	11.1
	RANGE	552-564	25.4-27.0	72-78	10.1-11.6
F(Fine Grain)	AVE.	547	23.7	75	9.7
	RANGE	536-552	22.6-24.4	61-78	7.9-10.5
SILSO OVERALL	AVE.	552	24.7	74	10.2
	RANGE	526-564	21.6-27.0	46-79	6.1-11.6
<u>HEM</u>					
G(Single Crystal)	AVE.	579	27.7	73	11.7
	RANGE	574-588	26.9-28.5	66-79	10.1-13.2
H(Poly)	AVE.	566	26.7	76	11.5
	RANGE	552-576	25.4-27.5	70-78	10.3-12.2
I(Poly)	AVE.	564	26.6	74	11.1
	RANGE	550-574	25.0-27.6	67-78	9.7-12.1
J(Poly)	AVE.	551	24.8	74	10.1
	RANGE	538-560	23.6-25.5	65-78	8.5-11.0
HEM OVERALL	AVE.	565	26.5	74	11.1
	RANGE	538-588	23.6-28.5	65-79	8.5-13.2
CZ CONTROL	AVE.	586	29.0	77	13.1
	RANGE	586-586	28.8-29.3	76-77	12.9-13.3

Comparison of Average J_{sc} of Gettered (1-hour 950°C) Cells With Corresponding Baseline Cells

		AVERAGE Jsc (mA/cm^2) Baseline	AVERAGE Jsc (mA/cm^2) Gettered
SILSO	Long Grain	24.4	24.9
	Medium Grain	26.2	25.9
	Fine Grain	23.7	24.8
UCP	(4-21A)	25.7	26.7
	Random	25.6	26.4
HEM		25.9	26.1

High-η Cells (With SJ P^+ Back and MLAR) UCP, Silso and HEM

			Voc (mV)	Jsc (mA/cm^2)	CFF (%)	(%)
UCP	(C4-21A)	AVE.	553	29.9	77	12.7
		S.D.	19	0.8	5	1.2
		RANGE	508-576	28.8-31.3	64-80	9.9-13.9
	RANDOM	AVE.	554	29.7	78	12.9
		S.D.	7	0.6	1	0.3
		RANGE	542-558	28.8-30.4	76-80	12.3-13.3
SILSO	(MEDIUM GRAIN)	AVE.	564	29.9	78	13.1
		S.D.	7	0.5	1.3	0.4
		RANGE	554-574	29.4-30.8	76-80	12.6-13.6
HEM	(SINGLE CRYSTAL)	AVE.	555	31.4	54	9.6
		S.D.	39	0.5	18	4.0
		RANGE	478-594	30.9-32.3	31-77	4.6-14.4
CZ CONTROL		AVE.	597	32.5	77	14.7
		S.D.	3	0.9	3	0.7
		RANGE	588-596	31.4-33.7	73-80	13.7-15.5

Dark I-V of a Group of Grain-Boundary Diodes
on a Wafer on the Top of Ingot C-4-21A

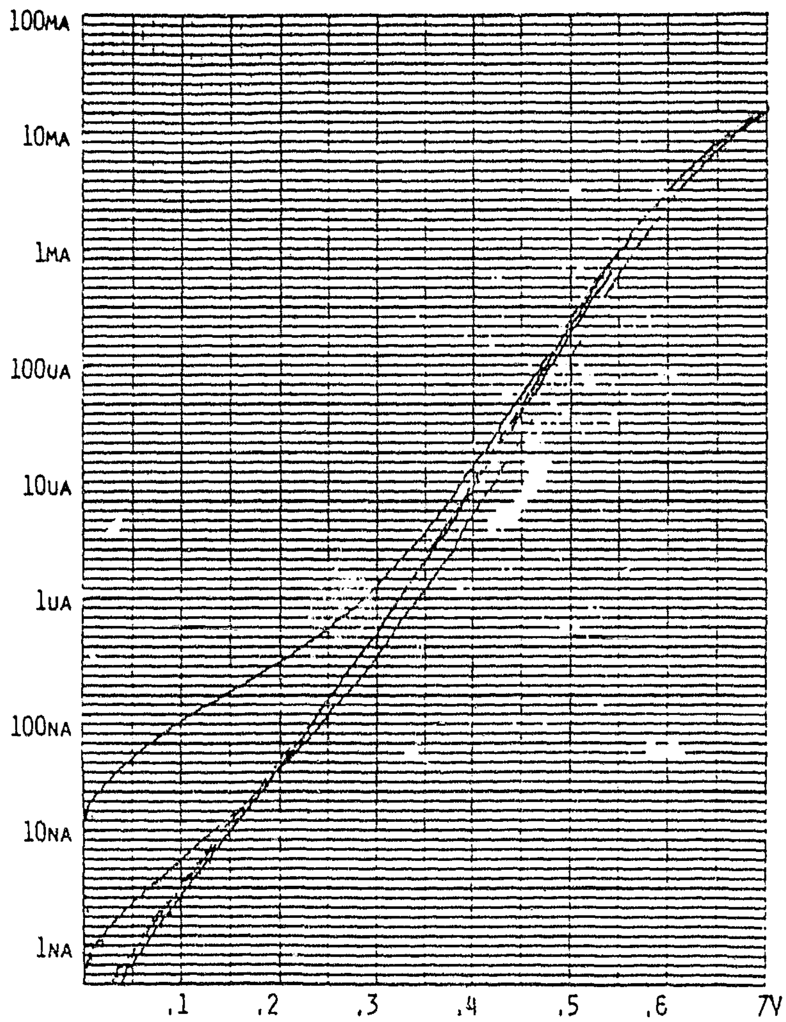

Dark I-V of a Group of Single-Crystal Diodes
on a Wafer on the Top of Ingot C-4-21A

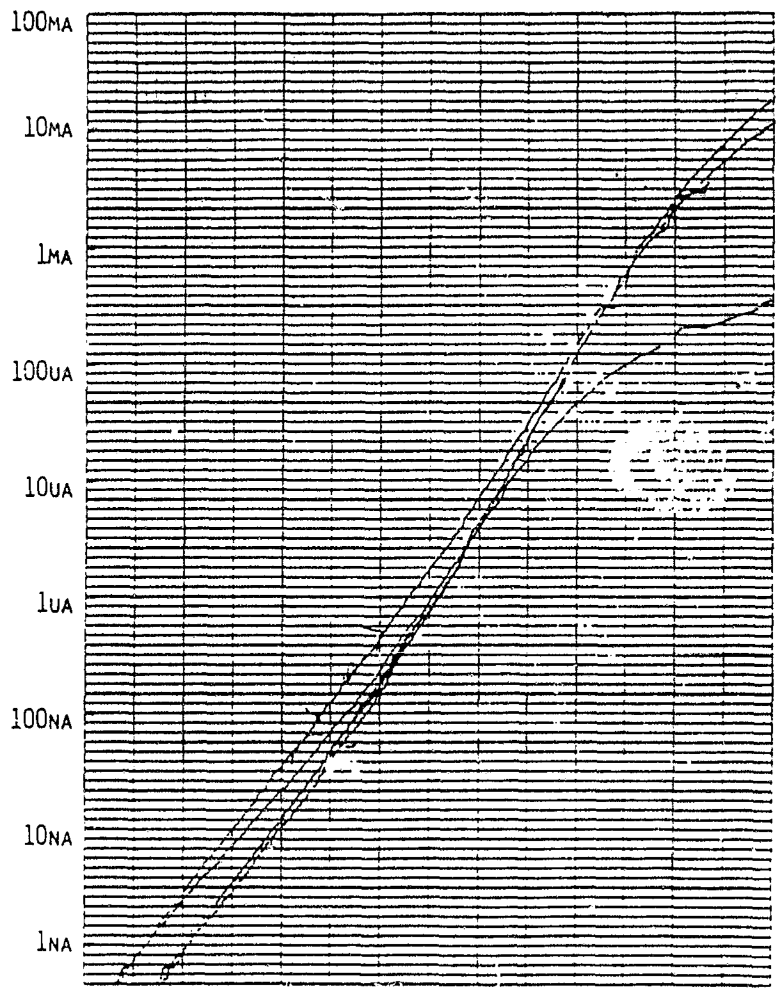

ORIGINAL PAGE IS
OF POOR QUALITY

Dark I-V of a Group of Cz Control Diodes

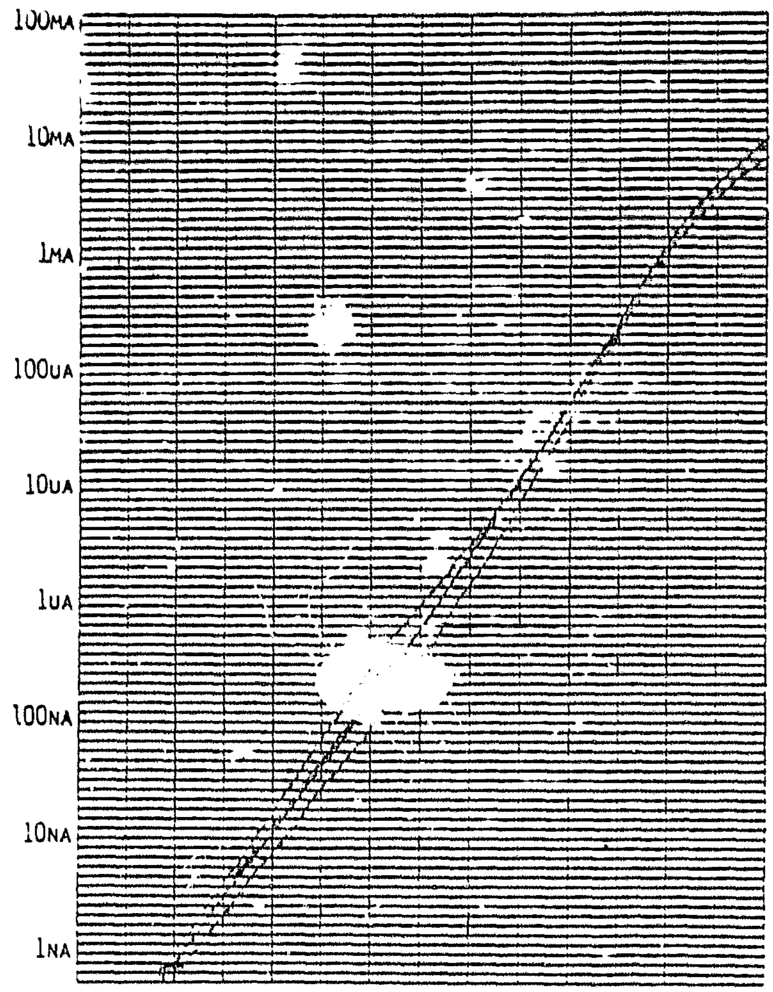

Minority Carrier Diffusion Lengths of Diodes Made from UCP Silicon

WAFER	DIODE #	L_D (um)	CHARACTER
A	1	141	Single Crystal
	2	162	Single Crystal
(Top Of	3	44	Grain Boundary
C4-21A)	4	48	Grain Boundary
B	1	69	Single Crystal
	2	26	Single Crystal
(Bottom Of	3	22	Grain Boundary
C4-21A)	4	28	Grain Boundary
C	1	71	Single Crystal
	2	126	Single Crystal
(Random	3	42	Grain Boundary
Source)	4	118	Grain Boundary
Cz Control	1	204	Single Crystal

SILICON SHEET GROWTH AND CHARACTERISTICS

CORNELL UNIVERSITY

D. Ast

Subjects

- MELT-SPUN Si-RIBBONS
- LOW ANGLE GRAIN BOUNDARIES
- <110> TILT BOUNDARIES TO 109°
- HYDROGENATION OF HEM

Melt-Spun Ribbon

ADVANTAGES:

- HIGH SPEED
- RIBBON SHAPED

DISADVANTAGE:

- POLYCRYSTALLINE
  (POSSIBLE FURTHER PROCESSING BY LASER, H^+...)

$\eta \approx 5\%$

OUR INTEREST IS GRAIN BOUNDARY STRUCTURE, ESPECIALLY IF HIGH QUENCHING SPEED (10^5 ~ 10^6 °C/SEC) LEADS TO UNUSUAL BOUNDARIES

Principle of Melt-Spun Ribbon Technique

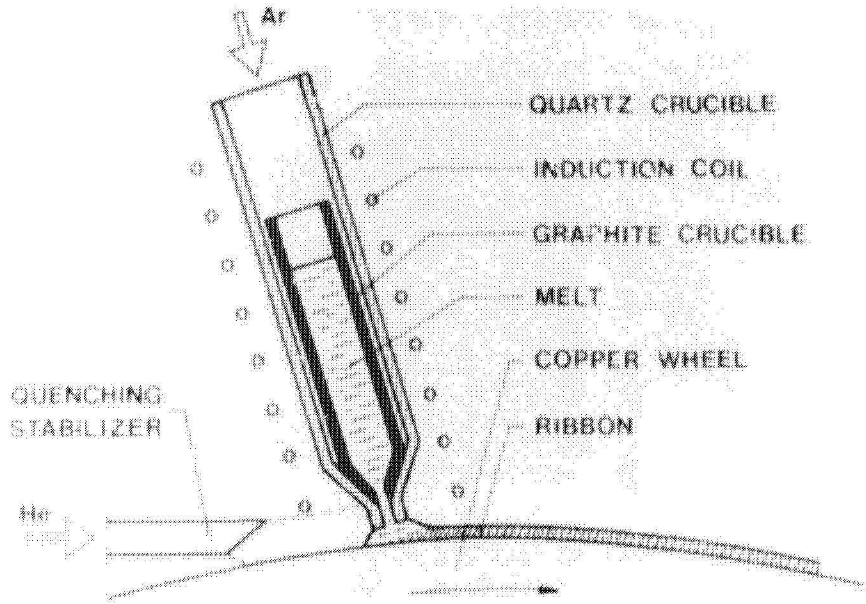

Melt-Spun Ribbon Segment

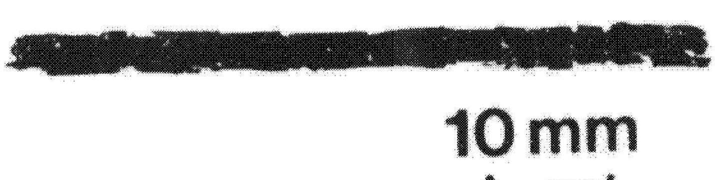

Etched Melt-Spun Si Ribbon Under Optical Microscope

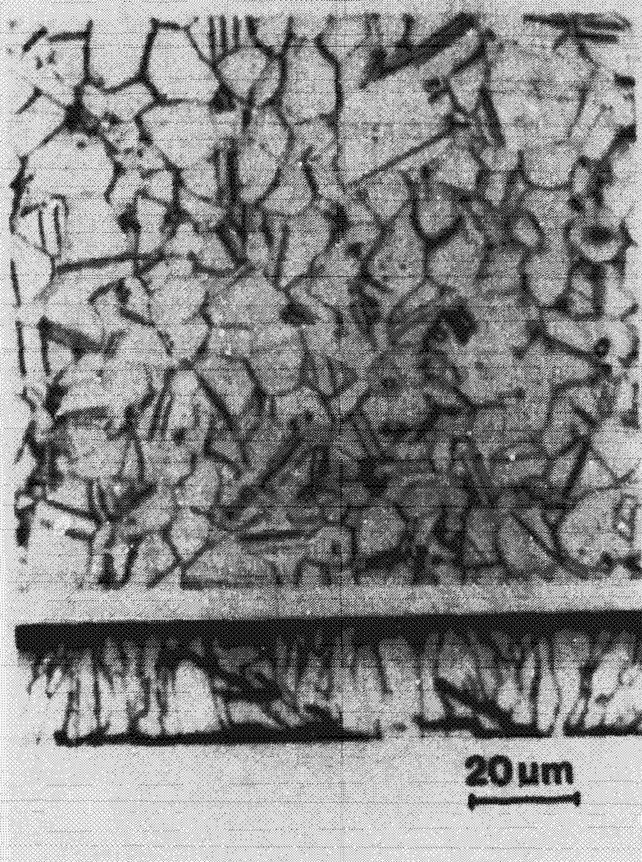

Summary

GRAIN SIZE: ~ 20...30 µm

BOUNDARIES: MOSTLY TWIN RELATED AND PERPENDICULAR TO RIBBON (SUITABLE FOR PASSIVATION)

ELECTRICAL PROPERTIES NOT CHARACTERIZED

POSSIBLE USE: SEED MATERIAL
(F.B.R.)

ORIGINAL PAGE IS
OF POOR QUALITY

Low-Angle Grain Boundaries

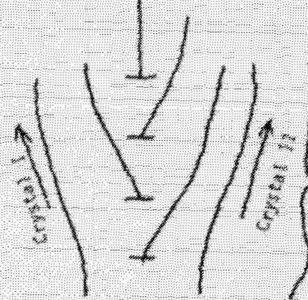

INDIVIDUALLY
RESOLVABLE
DISLOCATION
ARRAY ~ 16°

ALSO, E(θ) FOLLOWS CLASSICAL SHOCKELY-READ FORMULA

HIGH RESOLUTION (LATTICE OR STRUCTURAL) IMAGING ALLOWS

DIRECT DETERMINATION OF BOUNDARY STRUCTURE OF ⟨110⟩

BOUNDARIES BY IMAGING OPEN CHANNELS

TEM Photo Showing That Low-Angle Grain Boundaries Consist of Various Types of Dislocations

Summary of Low-Angle Grain Boundaries

▶ BOUNDARY STRUCTURE HIGHLY COMPLEX:

→ DISSOCIATED AND UNDISSOCIATED DISLOCATIONS

→ CLEAN AND DECORATED DISLOCATIONS

→ UNUSUAL BURGERS VECTORS, NOT FOUND FOR LATTICE DISLOCATIONS

▶ MOVING BOUNDARY (COOL DOWN) INDUCES LONG TRAILING STACKING FAULTS

<110> Tilt Boundaries to 109 deg

INCLUDES 2ND, 3RD ORDER TWIN BOUNDARIES

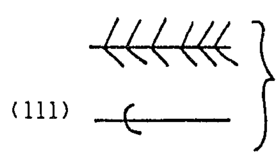

1ST ORDER TWIN BOUNDARY

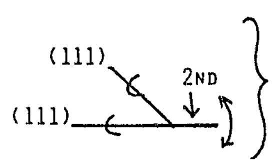

2ND ORDER TWIN BOUNDARY RESULTS FROM TWO CONSECUTIVE TWINNING OPERATIONS ON NON PARALLEL (111) PLANES

3RD ORDER TWINS HIGHEST TWINS EXPERIMENTALLY OBSERVED

UNSYMMETRIC BOUNDARIES VERY COMPLEX → MAY DISSOCIATE WITH INT. PHASE

High-Order Tilt Boundaries Dissociated Into Low-Order Tilt Boundaries

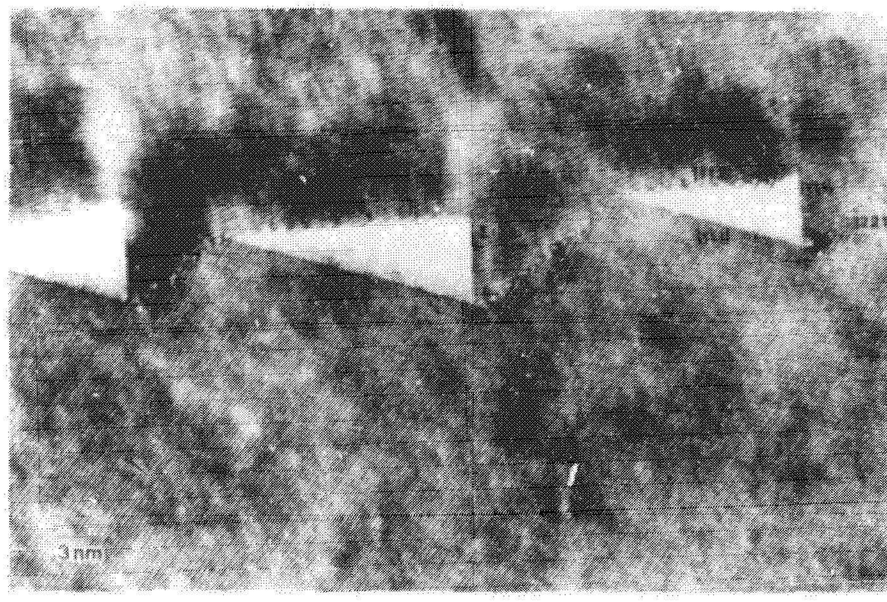

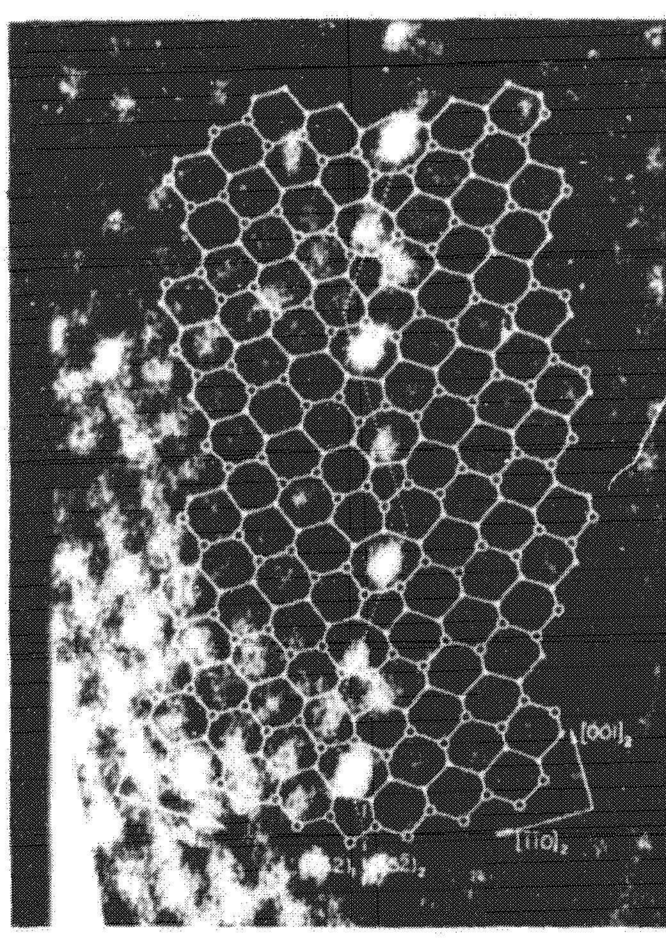

Structural Model of (221) / (221) Tilt Boundaries Showing No Dangling Bonds

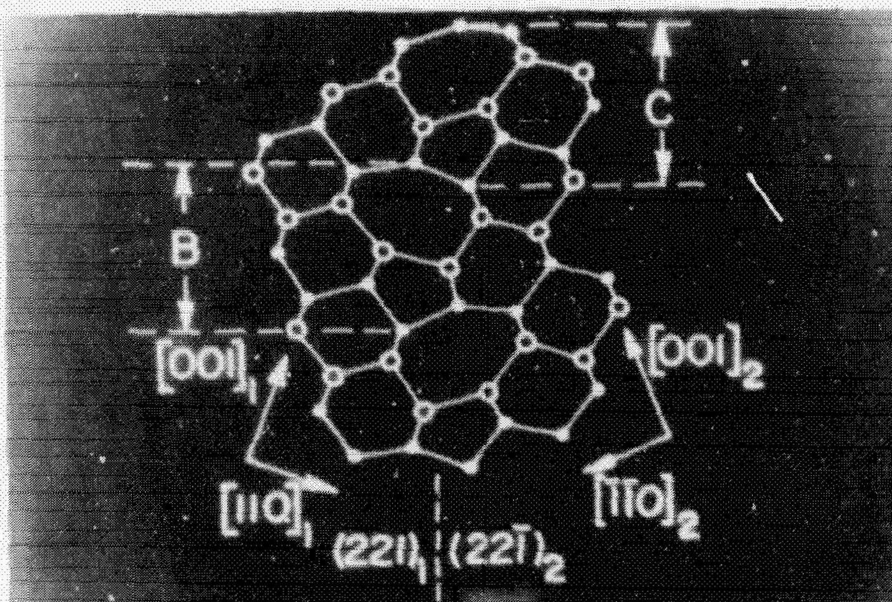

Summary of <110> Tilt Boundaries

- UN-SYMMETRIC TILT BOUNDARIES FREQUENTLY DISSOCIATED ON A MICROSCOPIC SCALE, TYPICALLY BY FORMING A $\Sigma = 3$ (COHERENT TWIN BOUNDARY)
- SYMMETRIC BOUNDARIES TO 109° CAN BE BUILT WITHOUT BROKEN BONDS WITH REPEATING GROUPS, A, B, C, T, G, H AND F.S.
- THIS DESCRIPTION CAN BE FORMALLY LINKED TO BOLLMANN THEORY (AS FIRST SHOWN BY VITEK FOR METALS)

ORIGINAL PAGE IS
OF POOR QUALITY

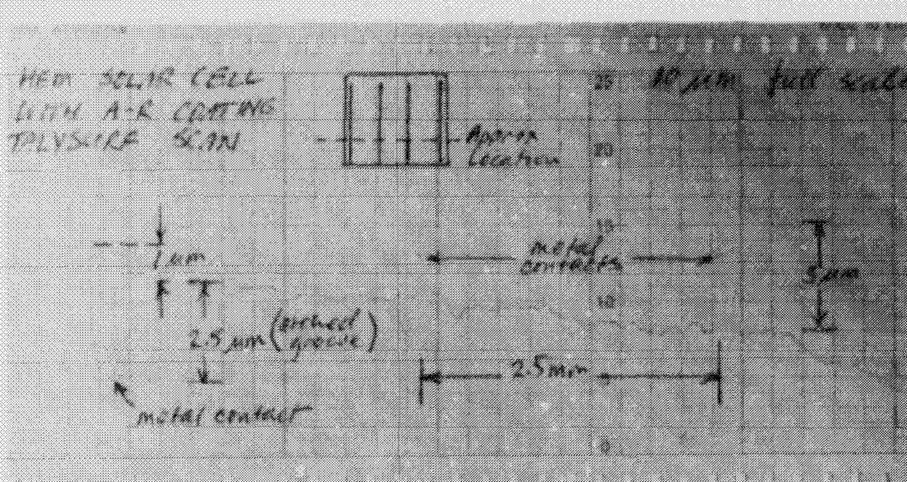

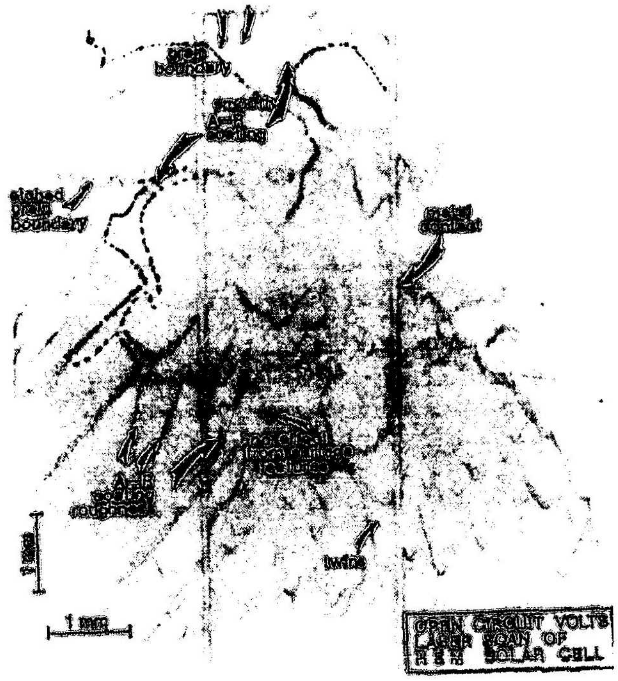

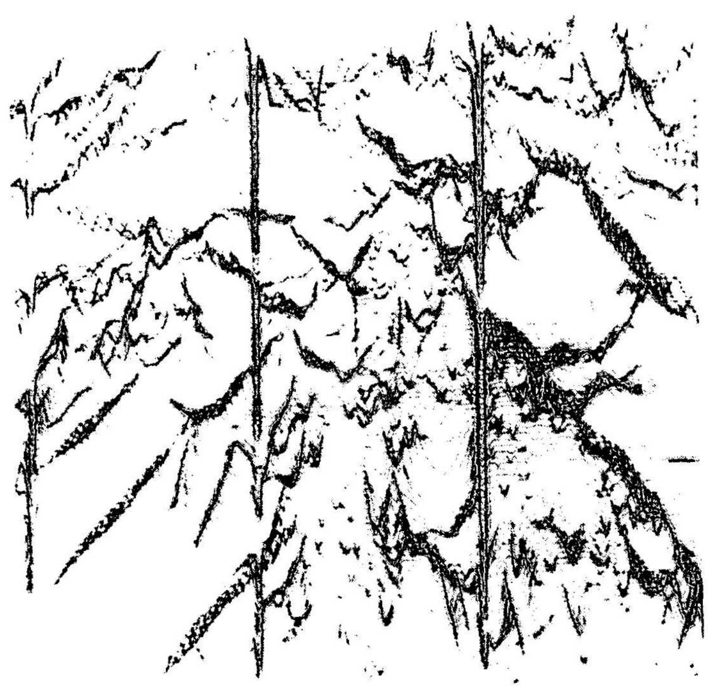

OPEN CIRCUIT VOLTS
LASER SCAN OF
HEM SOLAR CELL

12 HRS
HYDROGENATION

Summary of HEM

- SYMMETRIC BOUNDARIES NOT, OR ONLY WEAKLY ELECTRICALLY EFFECTIVE
- {111}/{115} FIRST OBSERVED IN EFG ALSO FOUND IN HEM
- IN PROCESSED CELL, NO OBVIOUS CORRELATION BETWEEN G-B AND AREAS OF LOW V_{OC}
- FURTHER INVESTIGATION BY TEM REQUIRED
- HYDROGENATION INEFFECTIVE ⟶ CHEMICAL DEFECTS?

ORIGINAL PAGE IS
OF POOR QUALITY

MODULE TECHNOLOGY

C.D. Coulbert, Chairman

Encapsulation material systems that have been developed and evaluated as having the best potential for achieving the FSA goals for PV module performance, cost, and durability are currently undergoing extensive testing for assessment of life limiting degradation mechanisms. Testing is being conducted at JPL as well as at various contractor sites under both accelerated and real-time field conditions.

Results of testing of thermally aged and UV-aged specimens of pottants and cover materials exposed at temperatures up to 130°C were reported by Springborn. Property changes reported included tensile strength and elongation plus optical and electrical characteristics. Clear stabilized EVA (A-9918) has been exposed for more than 35,000 hours without a cover film (equivalent to solar UV for 27 years) with excellant retention of optical and mechanical properties. Data from ongoing tests of other materials out to 10,000 hours were reported.

Results of outdoor exposure of Tedlar, glass and Acrylar (PMMA film) for 18 months have demonstrated the effectiveness and durability of antisoiling surface treatments. Soiling losses on treated but unwashed Tedlar were reduced from 6% to 2%. Transmission losses on treated Acrylar film during the 18 months were reduced from 8% to less than 2%.

Spectrolab is continuing development of analytical tools to facilitate the selection and design of optimum encapsulation systems and to evaluate the sensitivity of PV module performance to encapsulation aging effects. Results of an analysis of the possible effects of solar-cell thickness and edge radius on local electric fields and voltage isolation were presented.

An outline prepared by JPL of a PV module failure-anlaysis matrix approach to organizing and classifying the many potential and observed module degradation mechanisms was reviewed. The objective of the outline is to provide a rational basis for quantifying and differentiating encapsulant aging characteristics and their effects on actual PV array performance and reliability. Examples were presented of the use of the failure analysis matrix in four ways:

(1) As a checklist of failure-causing stresses, failure sequences and potential interactions.

(2) As an outline or framework for developing a test plan, assuring its completeness and defining its limitations.

(3) As a framework for assessing available test results in scope, sequence and applicability.

(4) As a framework for compiling and integrating general material-property data and any related technology information.

ACCELERATED TESTING OF ENCAPSULATION SYSTEMS

SPRINGBORN LABORATORIES, INC.

Candidate Polymer Encapsulation Materials

POTTANTS: MECHANICAL STRESS RELIEF, ELECTRICAL ISOLATION, CELL POSITIONING, ENVIRONMENTAL ISOLATION, CORROSION BARRIER

- LAMINATION TYPES:
  - ETHYLENE/VINYL ACETATE (EVA)
  - ETHYLENE/METHYL ACRYLATE (EMA)
- CASTING TYPES:
  - ALIPHATIC POLYURETHANE (PU)
  - POLY(BUTYL ACRYLATE) (BA)

OUTER COVERS: PROVIDES HARD SOIL RESISTANT SURFACE, UV SCREENING, MECHANICAL BARRIER

TEDLAR 100BG30UT , TEDLAR 4462
ACRYLAR 22417

BACK COVERS: MECHANICAL BARRIER, ELECTRICAL ISOLATION EMMISIVITY FOR COOLING MODULE

KORAD 63000, TEDLAR 150BS30WH
SCOTCHPAR 20CP - WHITE (POLYESTER)

SUBSTRATES: MILD STEEL, HARDBORAD/WOOD PRODUCTS

GASKETS: EPDM RUBBER

ORIGINAL PAGE IS
OF POOR QUALITY

Thermal Aging: EVA A-9918, 130°C

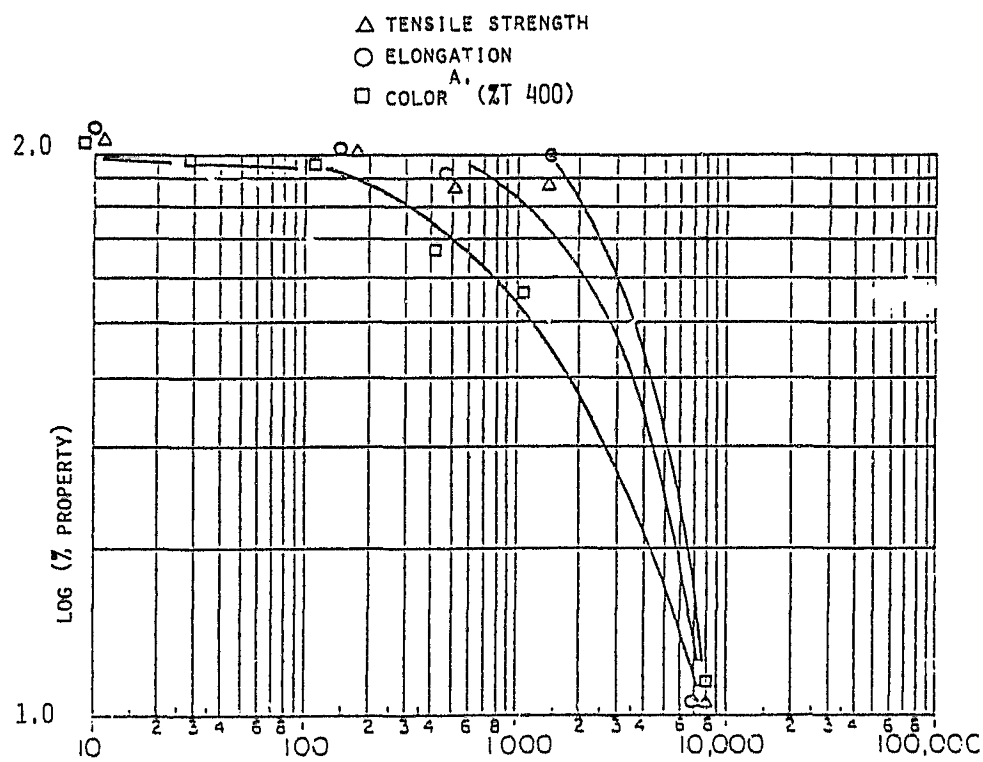

- PROPERTIES ALMOST GONE AFTER 7200 HOURS (STILL HAS 74% T OPTICAL)
- NO CHANGE IN OPTICAL, MECHANICAL OR ELECTRICAL PROPERTIES AFTER:

  7200 HRS - 90°C
  1000 HRS - 105°C

A. AIR AND NITROGEN VALUES APPROXIMATELY THE SAME.

Thermal Aging: EMA 13439, 130°C

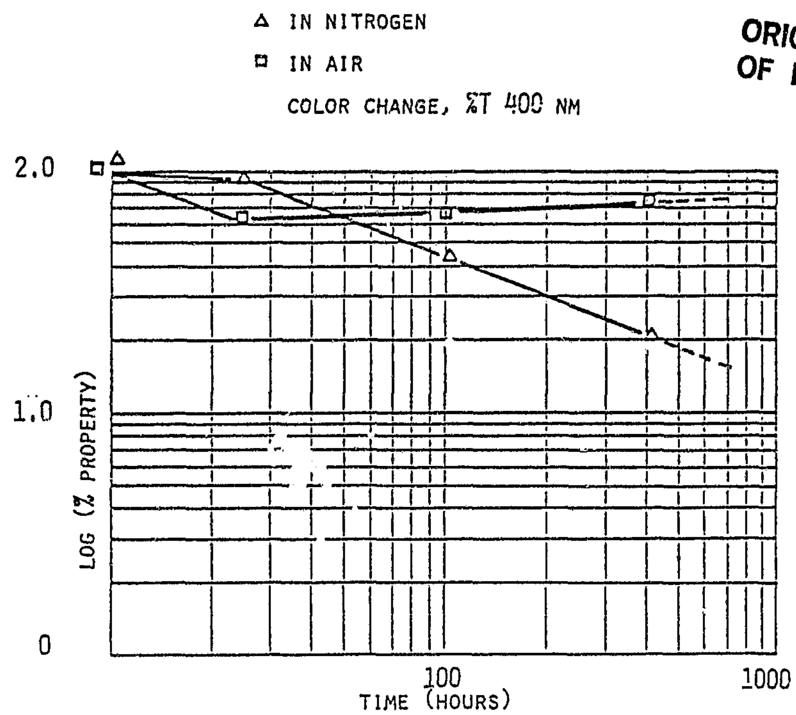

- AT 80°C AND 105°C, NO CHANGES IN OPTICAL MECHANICAL OR ELECTRICAL PROPERTIES AFTER 400 HRS.
- AT 130°C, ONLY COLOR CHANGE
- LESS COLOR FORMATION IN AIR THAN NITROGEN

Thermal Aging: Polyurethane Z-2591

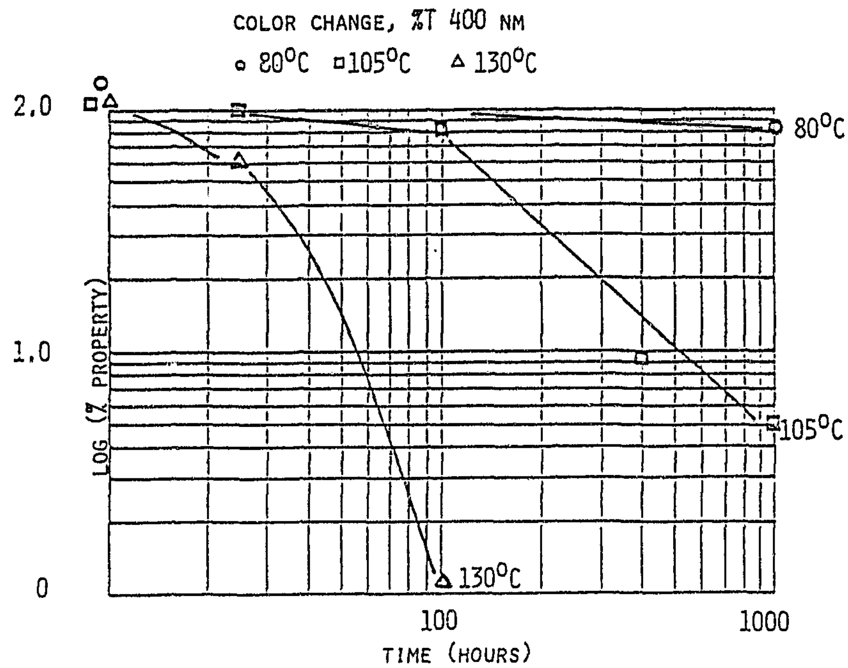

- NO CHANGE IN OPTICAL, MECHANICAL OR ELECTRICAL PROPERTIES AFTER 1000 HRS AT 80°C AND 105°C
- AT 130°C ALL PROPERTIES LOST AFTER 250 HOURS
- COLOR CHANGE APPX. SAME IN AIR AND NITROGEN

ORIGINAL PAGE IS
OF POOR QUALITY

RS/4 Sunlamp Exposure: EVA Pottant, No Cover Film

- CLEAR STABILIZED EVA EXPOSED 35,000 HOURS, SOLAR UV EQUIVALENT, 27 YEARS

	TOTAL INTEGRATED TRANSMISSION (%)	ULTIMATE ELONGATION (%)	TENSILE STRENGTH (PSI)	COLOR (%T 400)
CONTROL	91	510	1890	75
EXPOSED 35,000 HRS.	90	480	1450	24
% CONTROL	99%	94%	77%	31%

- SPECIMEN NOW SHOWING SMALL SURFACE CRACKS
- UNSTABILIZED ELVAX 150 (EVA) BECOMES SOFT, TACKY, - LOSES PHYSICAL PROPERTIES IN LESS THAN 1,000 HOURS.

RS/4 Sunlamp Exposure: Outer-Cover Candidates

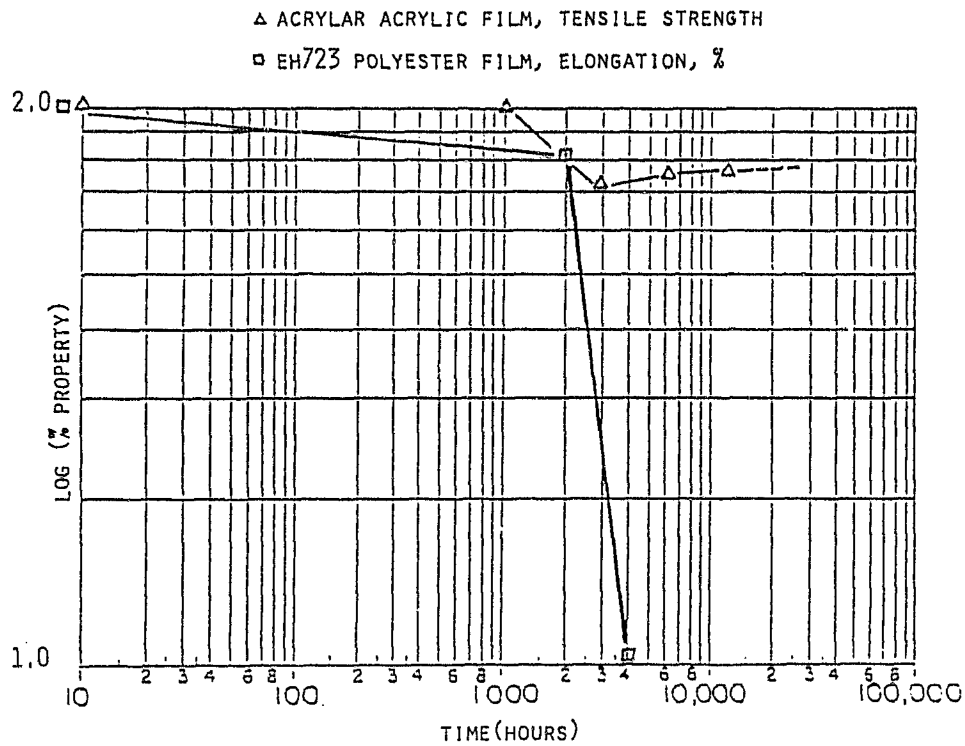

- NO CHANGE IN PROPERTIES FOR:
  - TEDLAR 100BG30UT, 15,000 HRS[A.]
  - TEDLAR 4462 , 11,000 HRS
- EH723 POLYESTER DEGRADES TO ~1% ELONGATION IN 4,000 HRS.
- ACRYLAR LOSES 40% TENSILE IN 3000 HRS. THEN STABILIZES. (STRESS RELAXATION AND SOME LOSS OF $\bar{M}v$)

A. EQUIVALENT SOLAR UV, 11 YEARS

ORIGINAL PAGE IS
OF POOR QUALITY

RS/4 Sunlamp Exposure: Back-Cover Candidates

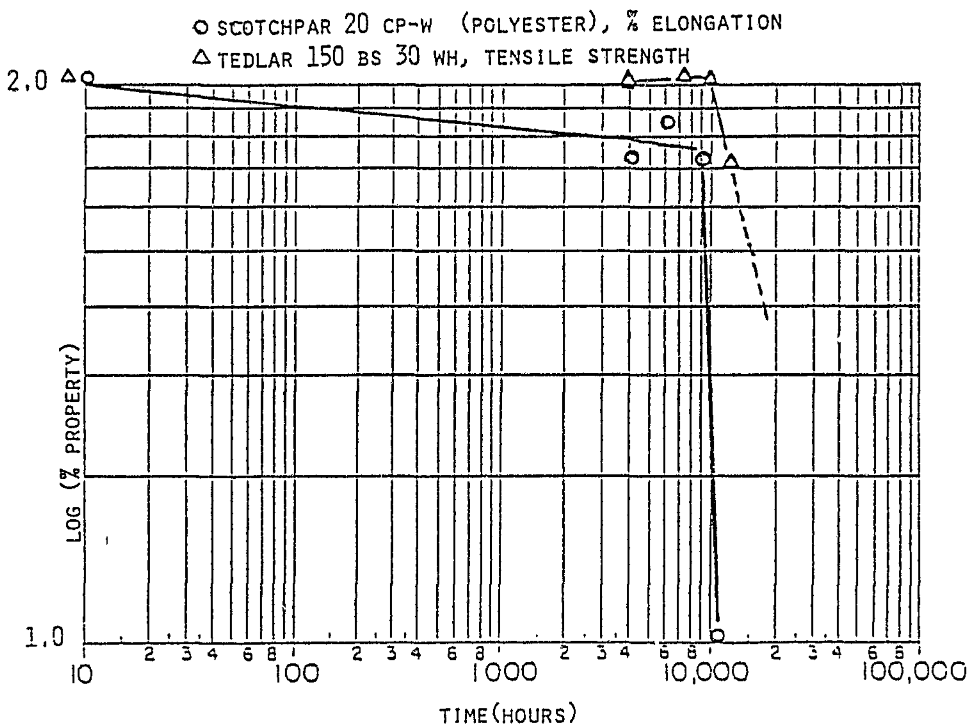

- END OF INDUCTION PERIOD FOR SCOTCHPAR; RETAINS 3% ELONGATION, 40% OF TENSILE AT 10,000 HOURS[A]
- END OF INDUCTION PERIOD FOR TEDLAR?
- KORAD 6300 WHITE ACRYLIC FILM NO CHANGE AT 8,000 HOURS

A. EQUIVALENT SOLAR UV, 8 YEARS

Soiling Experiments: 18 mo Exposure, Enfield CT

% LOSS IN I_{SC} WITH STANDARD CELL TREATED TEDLAR 1000BG300UT
(SUPPORTED ON GLASS)

ORIGINAL PAGE IS OF POOR QUALITY

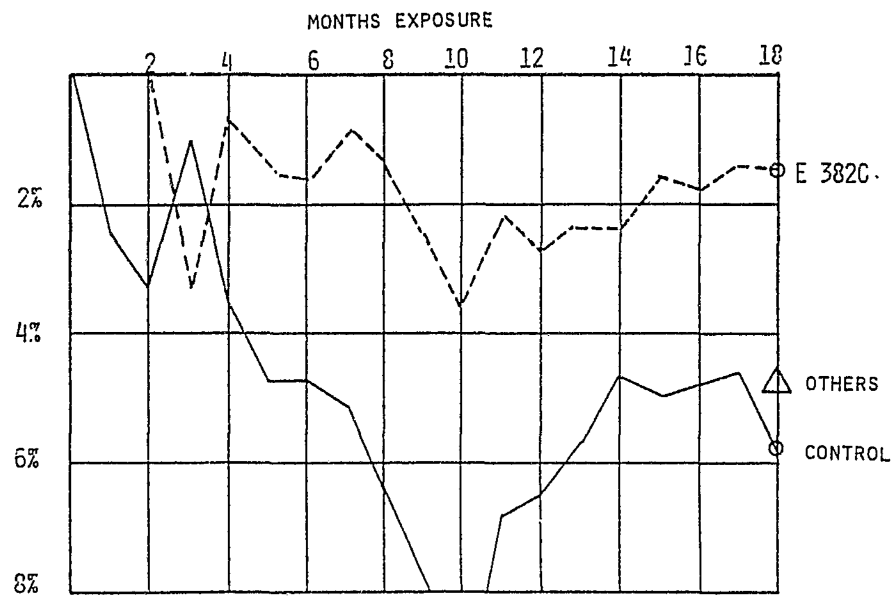

BEST TREATMENT, E3820

% LOSS IN I_{SC} WITH STANDARD CELL TREATED ACRYLAR
(SUPPORTED ON GLASS)

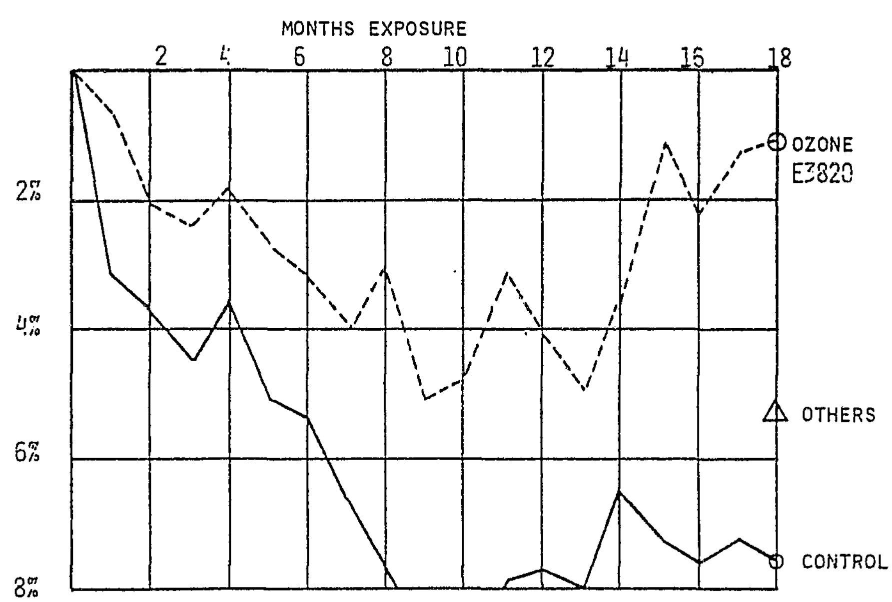

BEST TREATMENT: E3820
WITH OZONE ACTIVATION

ENCAPSULATION DESIGN ANALYSIS

SPECTROLAB, INC.

Master Curve for Pressure Stress Analysis

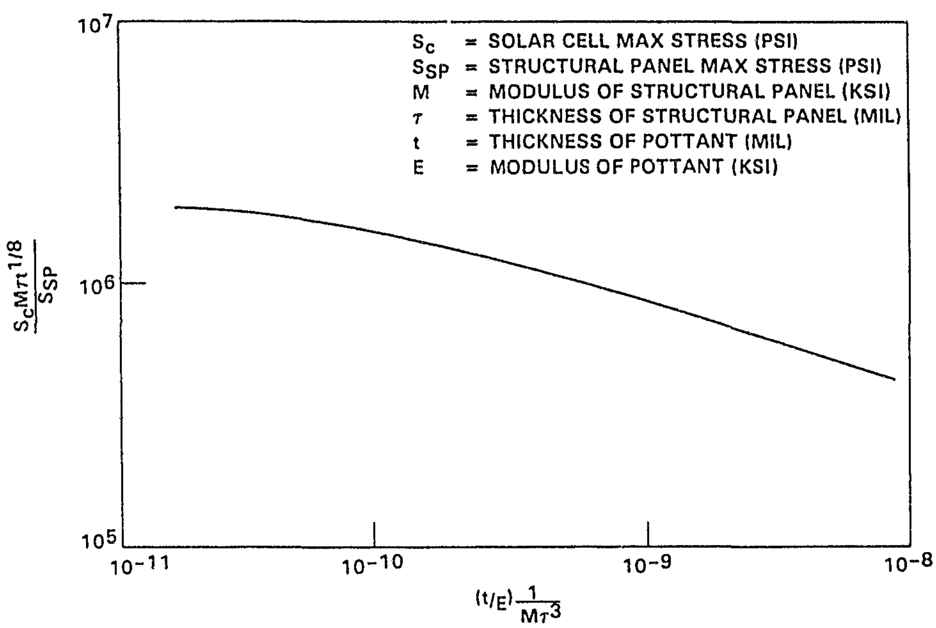

Usage Guide for the Pressure Stress Master Curve

1. DETERMINE MAX. STRESS IN THE STRUCTURAL PANEL (NOTE: USE JPL CURVES OR OTHER ANALYSIS).
2. COMPUTE $\left(T/E\right)\frac{1}{M\tau^3}$
3. USE MASTER CURVE TO DETERMINE VALUE OF $\frac{S_C M\tau^{1/8}}{S_{SP}}$ WHERE

   S_{SP} = MAX. STRESS IN STRUCTURAL PANEL.
4. CALCULATE CELL STRESS, S_C.

Electric Field Distribution in Module

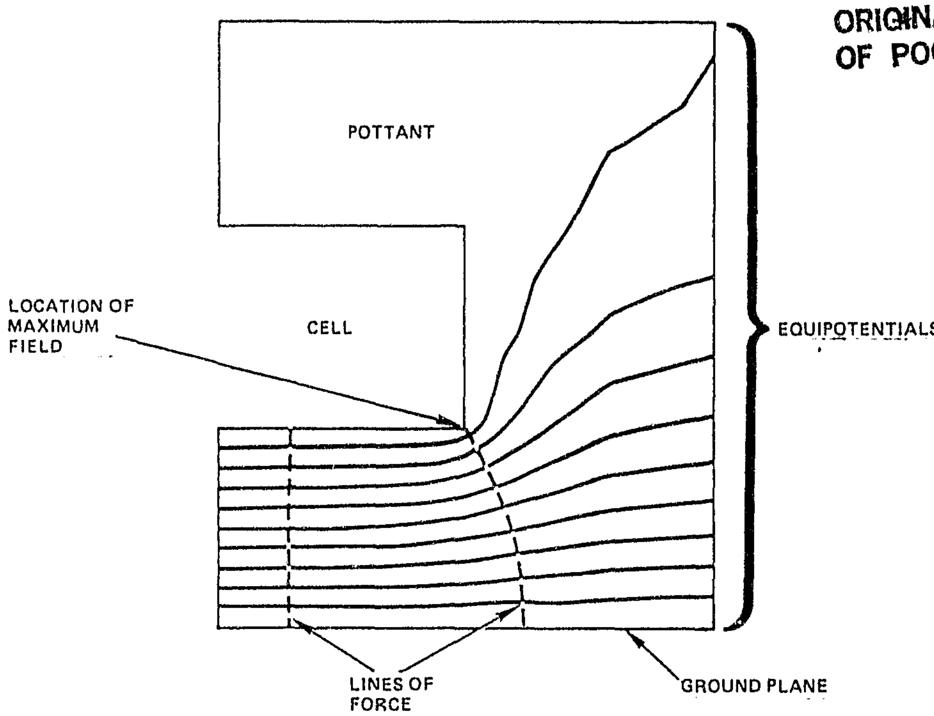

Electrical Field on Disc-Shaped Cell: Effect of Cell Thickness

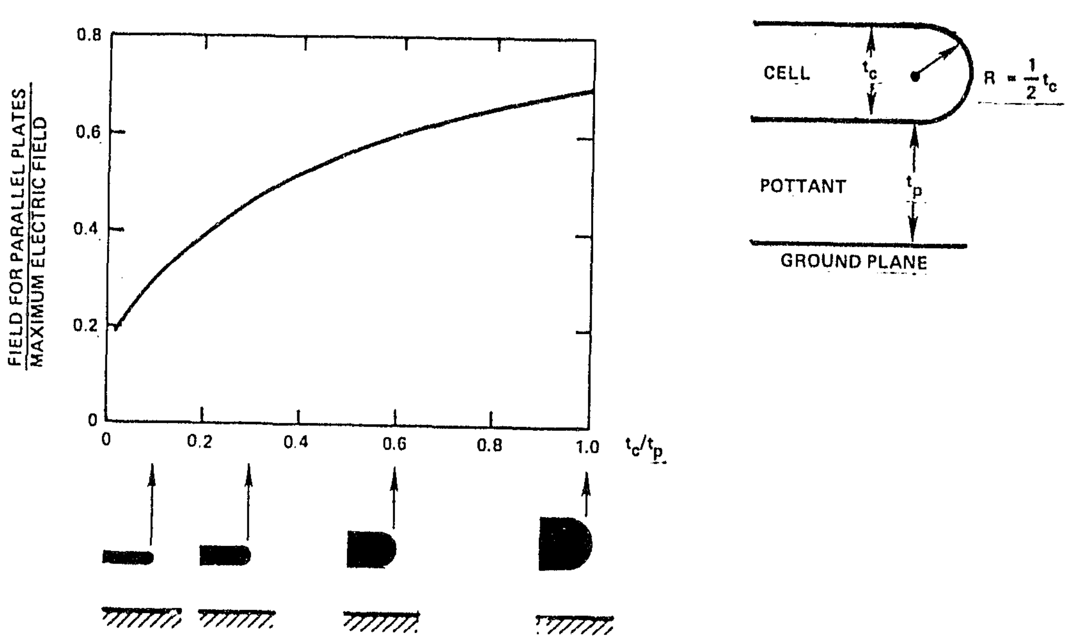

Electric Field on Disc-Shaped Cell: Effect of Cell-Edge Radius of Curvature

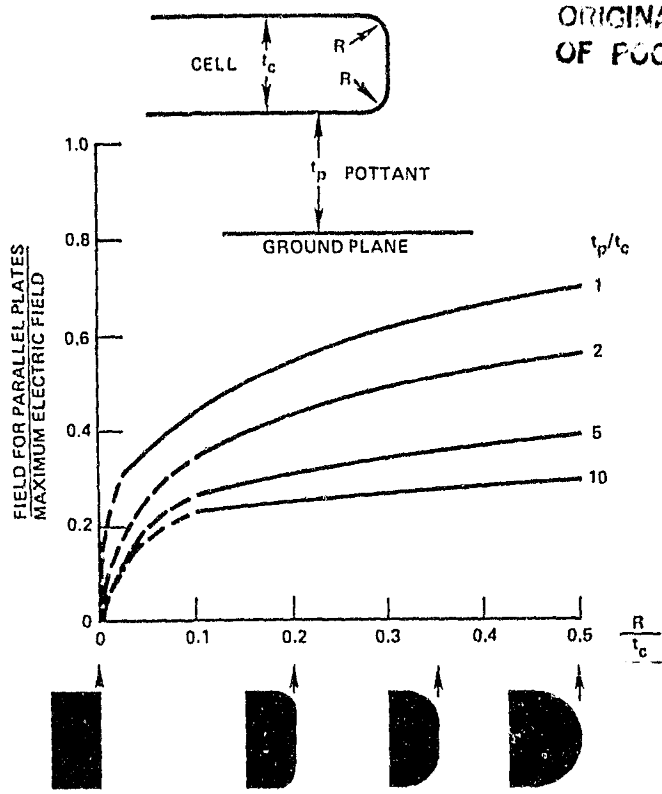

USING ENCAPSULATION MATERIAL TESTING TO ASSESS MODULE LIFE

JET PROPULSION LABORATORY

C.D. Coulbert

PV Module Failure-Analysis Matrix

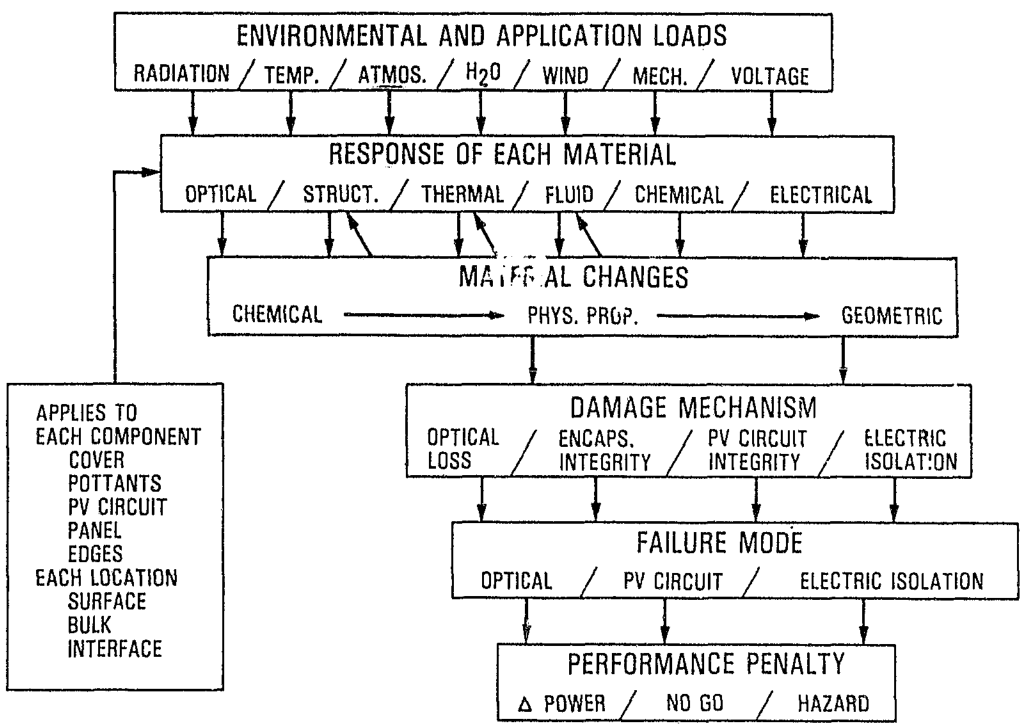

Optical Durability Test Plans

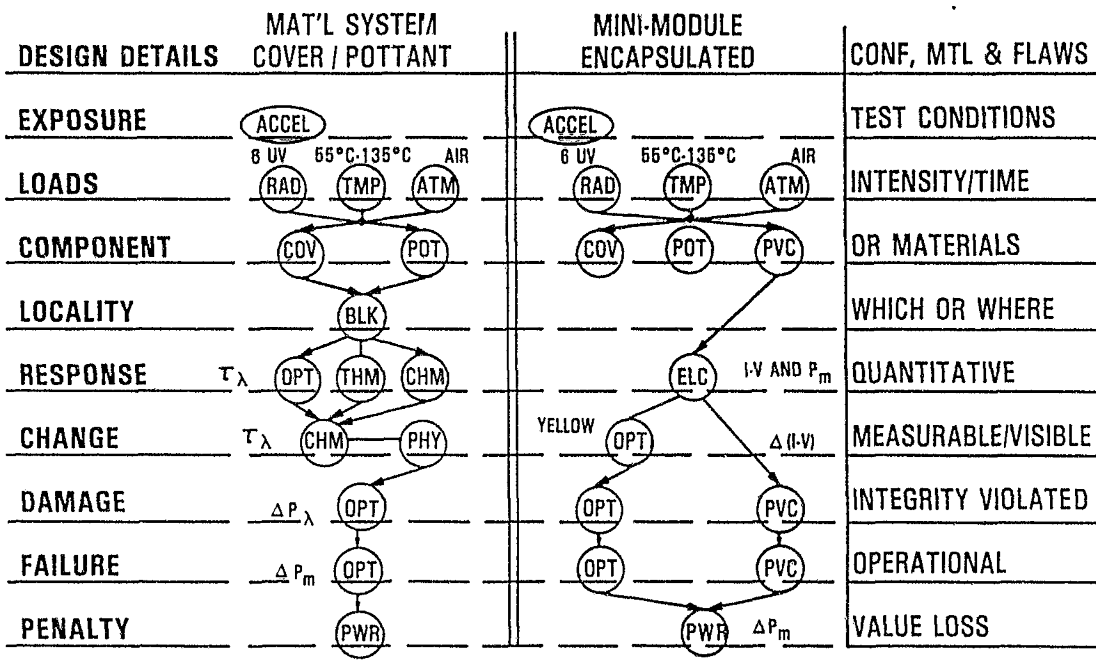

Predicting PV Power Loss Due to Optical Degradation

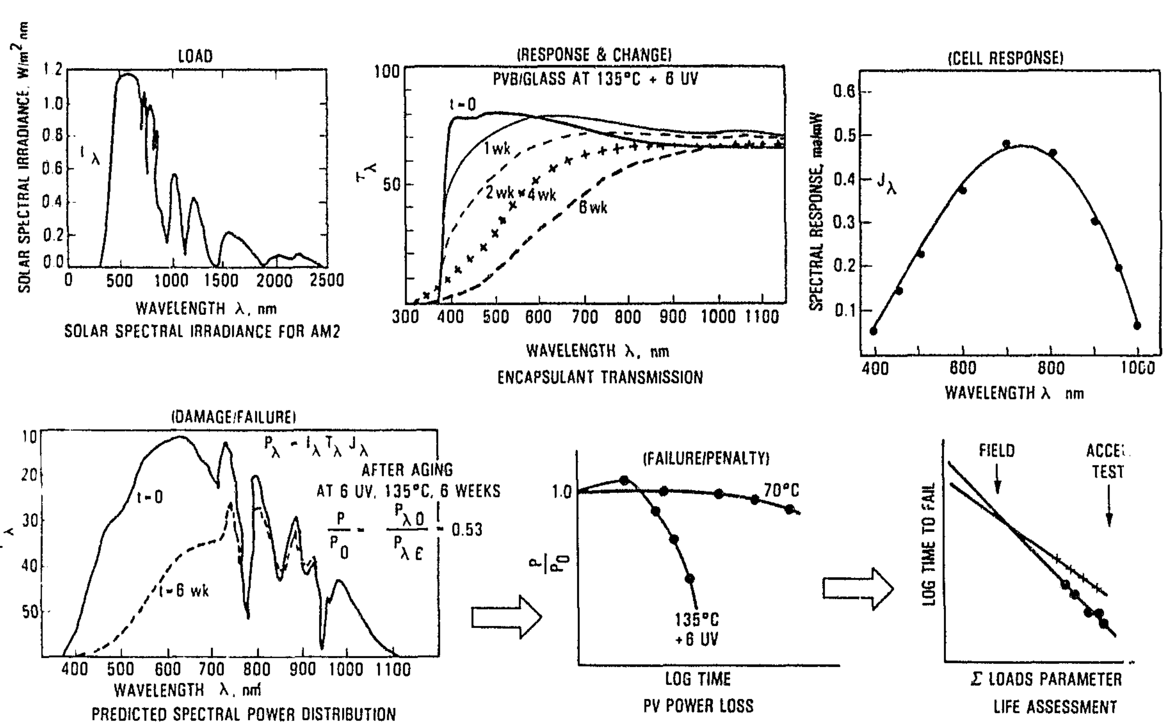

THIN-FILM ENCAPSULATING COSTS

JET PROPULSION LABORATORY

R.W. Aster

Approach

- Focus is on glass-superstrate encapsulating material and process costs
- Cell and metal deposition costs are not included
- Minimum-cost materials and minimal process steps at very low costs are used to establish lower-bound preliminary cost estimates
- R&D is expected to:
  (1) Validate feasibility
  (2) Reduce process costs from current levels
  (3) Possibly establish that higher costs are necessary

Materials

INCLUDES	REMARKS	COST, $/m^2
Glass	High optical quality, meets environmental loads, large panels	5.5 to 9.1
Pottant	20 mils EVA, EMA, or PnBA	1.0 to 3.0
Back cover	Korad (4 mils) or Tedlar (4 mils)	0.5 to 3.1
Edge seal & gasket	Tape and EPDM gasket	1.9 to 5.2
Module connectors		0.5 to 2.0
Material overhead	(20% of above)	1.9 to 4.1
Total	Excluding frame, primers, spacers	11.4 to 26.5

Process Steps

1. Glass preparation: (a) cleaning, (b) AR coat,* (c) priming*
2. Cell and metal deposition* and processing*
3. Cell interconnection* and wiring*
4. Module assembly
5. Lamination
6. Edge process: (a) trim, (b) seal, (c) gasket, (d) frame*
7. Module test
8. Package for shipping

*Not included in this study

Lower-Bound Processing Value Added*, $/m²

STEP	LARGE MODULE 8 ft²	SMALL MODULE 1 ft²
1a. Glass cleaning	0.1	0.3
4. Assembly	1.0	1.8
5. Lamination 6. Edge trim, seal, gasket	2.0	3.3
7. Module test	0.1	1.0
8. Package	0.1	0.4
Total	3.3	6.8

*No materials

Efficiency Sensitivity

LOWER-BOUND MODULE ENCAPSULATING COSTS ($\$/W_p$)

	MODULE EFFICIENCY					
	4	6	8	10	12	14
Large modules, $14.7/m²	0.37	0.25	0.19	0.15	0.12	0.11
Small modules,* $24/m²	0.60	0.40	0.30	0.24	0.20	0.17
Small modules,** $31/m²	0.78	0.52	0.39	0.31	0.26	0.22

*Lower-bound glass and back-cover costs
**Larger glass and back-cover costs

Observations

- Encapsulation is a universal PV requirement
- Encapsulant requirements and module lifetime have been significant areas of research in FSA and need to be applied to thin-film modules
- Thin-film cost projections should properly account for encapsulation costs that are consistent with long-life, high-performance systems
- Lower-bound encapsulating costs are comparable in magnitude to projected cell deposition costs found in recent projections of extremely low-cost PV modules (e.g., 15¢/W)
- R&D may show that reliability and long life require more expensive encapsulation

C-3

ADVANCED MATERIALS

A.D. Morrison, Chairman

Presentations covering research on advanced processes for depositing silicon (Si), and on Si shaped-sheet technology, were made by contractors, the California Institute of Technology (Caltech), and JPL.

Hemlock Semiconductor Corp. presented a resume of the entire effort on the dichlorosilane (DCS) Si process since its inception in October 1979. The conversion of trichlorosilane (TCS) to DCS was successfully demonstrated. In the step whereby Si is deposited from the DCS in Siemens-type reactors, Hemlock came very close to simultaneous achievement of the goals for Si deposition rate and conversion efficiency of DCS to Si. However, reactor power consumption was about 50% higher than the goal, and excessive amounts of Si deposited on the reactor bell-jar walls caused breakage and loss of product. In a program recently undertaken on cold-wall reactors, early tests gave promising results in that wall deposition was reduced by as much as two orders of magnitude.

In the study of a process for making TCS by the hydrochlorination of metallurgical-grade Si and silicon tetrachloride, Solarelectronics reported that the program had been aimed toward obtaining more basic-research-oriented information on the reaction. The equilibrium constants and rate constants were measured over ranges of temperature, pressure, and hydrogen/silicon tetrachloride feed ratios. Also, the heat of reaction and activation energy were calculated from experimental data. A number of reaction kinetic models for the hydrochlorination reaction were tested, and preliminary results showed that the rate of formation of TCS fits reasonably well in a pseudo-first-order rate equation.

A study of the hydrochlorination reaction mechanism by use of the deuterium isotope was started.

Union Carbide Corp. reported on its research program on converting silane to semiconductor-grade Si in a fluidized-bed reactor (FBR). The experimental program at Tonawanda, New York, which had the objectives of demonstrating process feasibility, determining a suitable operating window, and conducting steady-state runs, was successfully completed. Silane feed concentrations as high as about 24% in hydrogen were employed, and the longest test was 13 hours. Product withdrawal and seed introduction were successfully demonstrated.

The FBR process development unit was moved to Washougal, Washington, where UCC's silane-to-silicon EPSDU (Experimental Process System Development Unit) is situated, and it is being reinstalled for additional research, including an investigation of product purity.

JPL research on converting silane to Si in an FBR was described. It has the objectives of of establishing a fundamental understanding of FBR Si deposition in terms of particle-growth mechanisms and deposition kinetics and defining key design features such as the gas distributor. An experimental program was conducted with a 6-in.-dia FBR and with high silane feed concentrations (ranging from 20 to 100 mole %). The results of these preliminary

experiments confirmed the feasibility of using the FBR to achieve production of low-cost Si. Complete conversion of silane to Si was achieved, no bed agglomeration and no wall deposition occurred, and the effluent dust was ≤11% of the total amount of Si in all cases.

Oregon State University reviewed its effort on an internally heated fluidized-bed reactor, the work having started in May 1982. Such a configuration presents an attractive alternative to wall heating. A reactor was designed and built, and it is being tested to obtain information on fluidization and heat-transfer characteristics.

Caltech reported on an investigation, undertaken in this period, of silane pyrolysis in a free-space reactor (FSR). This work is important not only for the exploration of the use of this reactor for making semiconductor-grade Si but also as a means of studying gas-phase homogeneous decomposition and nucleation of silane. Promising results have already been achieved in this effort. Theoretical work led to a reactor of novel design that has produced Si particles of unusually large size (35-μm mean particle dia) compared with the typical FBR product consisting of particles in the 0.1 to 1-μm-dia range that are difficult to handle. Work is continuing with the additional objective of producing particles that will be large enough to use as FBR seed material.

A stochastic approach to silicon cost analysis using the SIMRAND (SIMulation of Research ANd Development) model and the IPEG costing method was presented by L.J. Reiter of JPL. The IPEG approach was validated for the Si manufacturing process. Then, using the capabilities of SIMRAND, stochastic inputs to a step-by-step analysis of the actual manufacturing process of Union Carbide and Hemlock were combined to yield cost probability distributions. The implications of the final results as well as some of the intermediate results and original, encoded distributions were discussed.

Semix Inc. reviewed progress in development and verification of a semi-crystalline Si casting process. This work covered fundamental studies of the material, measurement of electrical properties, and fabrication and test of high-efficiency solar cells. Fifty 10 x 10-cm cells with average and maximum efficiency of 13.4% and 14.1%, respectively, were made from the material.

A presentation was given by JPL on a study of characteristics of cast Si made by three processes: Silso (Wacker Siltronic Corp.), the heat exchanger method (Crystal Systems, Inc.), and the Ubiquitous Crystallization Process (Semix Inc.). The study showed that these three casting methods have produced solar cells with comparable levels of efficiency, that the expected maximum cell efficiencies for the three materials are comparable, and that the cell efficiencies are limited by dislocations, precipitates, and dislocation cellular structure. Also, results from a study of Si grown by a new method using an oscillating crucible were presented by JPL. Silicon from preliminary growth runs, processed using no growth-process optimization and employing base-line cell-fabrication methods, produced devices up to 12.9% efficiency AM1. These studies were conducted by JPL, IBM, and Applied Solar Energy Corp.

ADVANCED MATERIALS

Materials Research, Inc., reviewed results of an analysis of defect structure in Si made by the Ubiquitous Crystallization Process (Semix). Trends were identified between quantitative structural imperfection measurements, cell efficiency, and diffusion length. Grain boundary substructure appears to have an important effect on efficiency of solar cells made from Semix material.

Progress at the University of Illinois at Chicago on a study of Si surface-property modification by fluid absorption was reviewed. Correlations were obtained for abrasion rate when the surface is brittle or ductile, this surface condition being dictated by the properties of the fluid being used. The fluids were found to affect microhardness as well as fracture strength.

CVD OF POLYSILICON FROM DCS

HEMLOCK SEMICONDUCTOR CORP.

TECHNOLOGY

POLYCRYSTALLINE SILICON

APPROACH

CHEMICAL VAPOR DEPOSITION OF POLYSILICON FROM DICHLOROSILANE (DCS)

CONTRACTOR

HEMLOCK SEMICONDUCTOR CORPORATION

GOALS

ESTABLISH PROCESS FEASIBILITY THROUGH LABORATORY EXPERIMENTS AND COMPONENT TESTING

INVESTIGATE CRITICAL ELEMENTS OF PROCESS VIA OPERATION OF PROCESS DEVELOPMENT UNIT

POLYSILICON PRICE OF LESS THAN $21/KG (1980 $, 1000-MT/YR, 20% ROI) AND PURITY APPROACHING OR EQUALLING SEMICONDUCTOR-GRADE POLYSILICON

REPORT DATE

JANUARY, 1983

STATUS

▲ PHASE 2 OF PROJECT COMPLETE

- PDU OPERATED SUCCESSFULLY
- $15.60/KG MANUFACTURING COST PROJECTED FOR 1000 TN/YR PLANT
- PURITY OF DEPOSITED SILICON IS SEMICONDUCTOR GRADE

▲ COOLED WALL REACTOR

- HAS AMORPHOUS SILICON DEPOSITION ON WALL
- HAS SAME DEPOSITION RATE AND CONVERSION EFFICIENCY AS HOT WALL REACTOR, BUT HAS 10% HIGHER POWER CONSUMPTION, FOR IDENTICAL FEED CONDITIONS

Reasons for Considering Chlorosilane Technology

- ONLY MAJOR PRODUCTION PROCESS
- PROVEN MATERIAL QUALITY
- IN-PLACE CAPACITY FORMS BASE FOR MEETING EXPANDED DEMAND
- SIGNIFICENT COST REDUCTION POSSIBLE TO MEET INTERMEDIATE AND LONG RANGE PHOTOVOLTAIC OBJECTIVES

Limitations of Conventional Polysilicon Process

- LOW CONVERSION EFFICIENCY AT THE DECOMPOSITION REACTOR
- HIGH POWER CONSUMPTION AT THE DECOMPOSITION REACTOR
- LABOR INTENSIVE
- POOR SILICON AND CHLORINE EFFICIENCY

Reasons for Considering DCS as Decomposition Reactor Feedstock

- THERMODYNAMICALLY MORE FAVORABLE
- PRODUCTION TECHNOLOGY AVAILABLE FOR PROCESSING CHLOROSILANES
- UCC WORK INDICATES FAVORABLE ECONOMICS FOR HYDROGENATION OF $SiCl_4$

Performance Characteristics of DCS Decomposition Reactors

	Deposition Rate $gh^{-1}cm^{-1}$	Conversion Efficiency %	Power Consumption kWh/kg
JPL Goal (1000 T/Y Plant)	2.0	40.0	60
Experimental Reactor	1.6	35.2	96
Intermediate Reactor	2.0	35.1	82
Advanced Reactor	2.0	38.7	90

Base Conditions for Economic Analysis of Hemlock DCS-to-Si Process

ORIGINAL PAGE IS OF POOR QUALITY

1. General

Plant size: 1000 metric tonne of silicon
Product: High purity silicon
Process: Production of DCS (SiH_2Cl_2); generation of silicon from reductive chemical vapor deposition (CVD) of DCS

2. Production of TCS ($SiHCl_3$)

From hydrogenation of STC ($SiCl_4$)
Fluidized bed reactor, containing metallurgical grade silicon
Reactor operates at 500°C and 500 psig
Equimolar feed of STC and H_2
Product composition approximately

STC	70%
TCS	29%
DCS	1%

3. Removal/recycle of STC

Distillation (TCS still)
Separation of TCS + DCS from STC
Overhead stream to DCS still
Bottoms stream to hydrogenation reactor

4. Boron Removal

Removal of BCl_3 via complexation with nitrogen or oxygen based on non-volatile support
Fixed bed reactor
Feed from TCS still
Effluent to DCS still
No chlorosilane material loss

5. DCS Production

Redistribution of TCS with Dowex[R] ion exchange resin
Pure TCS feed
Liquid phase operation @ 70°C, 80 psig
Products to TCS still
Product composition as follows

DCS	10.5% (includes <1% SiH_3Cl (MCS))
TCS	78.5%
STC	11.0%

6. DCS purification

Distillation (DCS still)
Feed from TCS still
Separate DCS (+MCS) from TCS
Overhead stream to CVD reactors
Bottoms steam to redistribution reactor

7. Silicon production

45 Siemens CVD reactors (modified as appropriate)
DCS/H_2 feed
Molar conversion to silicon of 40%
Deposition ate of 3000 g/hr
Vent composition (per mole of DCS fed)

HCl	.14
DCS	.10
TCS	.34
STC	.16

ORIGINAL PAGE IS
OF POOR QUALITY

8. Operating ratio

85% utilization (on line time) of CVD reactors
7445 production hours/yr

9. Waste treatment

Waste gas streams to water scrubber. Resultant HCl neutralized with $Ca(OH)_2$.

Waste liquid streams process with current Dow Corning technology. Chlorosilanes neutralized with $Ca(OH_2$; silica generate sold or disposed of depending on quality.

10. Storage requirements

TCS	3 days
STC	3 weeks
Silicon	14 days
$Ca(OH)_2$	14 days

11. Recycle streams

Hydrogen from CVD reactors returned to same reactors
Chlorosilanes, HCl from CVD reactor vent to recovery system
Recovery system condenses, separates HCl, chlorosilanes; HCl sold for credit ($.12/lb), chlorosilanes returned to TCS still
Recovery system modified Siemens technology

12. Slim rod pullers

Pull rate average of 470 cm/hr (for each of five machines)
Thin rod diameter of 6 mm

Hemlock Low-Cost Si Process Manufacturing Capital

		1980 Dollars
1.	Direct Plant Investment (battery limit)	
	a. Major Process Equipment (except CVD rxs)	$2653.1 M
	b. Installation/Instrumentation/Buildings (not including the reactor building) (100% of 1a.)	2653.1
	Subtotal	5306.2
	c. CVD Reactors (installed)/Reactor Building	5401.0
	d. Total Battery Limit Investment	10707.2
2.	Other Direct Plant Investment Costs	
	a. Utilities, installed	2300.0
	b. Other direct (general offices, shops etc.) (55% of 1a.)	1266.0
3.	Total of Direct Plant Investment	14273.2
4.	Indirect Plant Investment Costs	
	a. Engineering overhead (10% of 3.)	1427.3
	b. Normal contingency (18% of 3.)	2569.2
	Total of Indirect Plant Investment	3996.5
5.	Total Direct & Indirect Investment	18269.7
6.	Overall Conntingency (20% of 5.)	3653.9
7.	Fixed Capital Plant Investment (5 + 6)	21923.6

1000 MT / yr Raw Materials Summary

		lb/kg poly	$/lb	$/kg poly
1.	MG silicon	2.53	.636	1.62
2.	Copper	.053	1.29	.068
[illegible]	STC	2.57	.189	.49
4.	[illegible] (ft^3/kg)	50.2	.0075	.37
	[illegible] me	1.50	.021	.032
[illegible]	[illegible] Cl (credit)	1.00	.140	(.14)
[illegible]	N_2 (ft^3/kg)	1.00	0.0034	0.34
		Total Raw Materials		2.78

1000 MT / yr Utilities Summary

		kwh/kg (BTU/kg)	$/unit /kwh	$/kg
1.	Electricity		.036	
	CVD rxs	60.0		
	Recovery system	7.0		
	Pumps	0.6		
	Refrigeration	0.4		
		68.0		2.45
			/MM BTU	
2.	Steam/hot oil	126.7 M	1.89	.24
3.	Cooling water	133.1 M	1.51	.20
			/M gal	
4.	Process water	2.4 gal.	.567	.001
			/M BTU	
5.	Natural gas	32.3 BTU	1.96	.06
6.	Refrigerant	1.32 M BTU	0.1047	.02
		Total Utilities		2.97

1000 MT / yr Labor Summary

Skilled labor @ $9.66/hr

Semiskilled labor @ $6.86/hr

114 kg/hr; 913 kg/shift

Unit Operation	Operators/Shift	$/kg Silicon
DCS production (includes hydrog., rearr., distillation)	1.5	.127
Silicon production	4	.339
Recovery System	1	.085
Thin rod production	1	.085
Waste treatment	1	.085
Total Labor	8.5	.721

Manufacturing Cost (1980 $)

		$/kg Silicon
1.	Direct Manufacturing Cost	
	1.1 Raw Materials	2.78
	1.2 Direct Operating Labor	.72
	1.3 Utilities	2.97
	1.4 Supervision/Clerical	.18
	1.5 Maintenance and Repair	2.00
	1.6 Operating Supplies	.40
	1.7 Laboratory Charge	.18
2.	Indirect Manufacturing Cost	
	2.1 Depreciation (10% of manf. cap.)	2.19
	2.2 Local Taxes (2% of manf. cap.)	.44
	2.3 Insurance (1% of manf. cap.)	.22
3.	Plant Overhead (12.3% of 1 + 2)	1.49
4.	Total Manufacturing Cost	13.57
5.	General Expenses	
	5.1 Administration (6% of 4)	.81
	5.2 Distribution and Sales (6% of 4)	.81
	5.3 R&D (3% of 4)	.41
6.	Product Cost without Profit	15.60

Cost and Profitability Summary of DCS Process (1980 $)

1. Process Type — CVD Reactors
2. Plant Size — 1000 Metric Tonnes
3. Plant Product — Solid Silicon
4. Product Form — Czochralski or chunk
5. Plant Investment — $\$25.21 \times 10^6$

Fixed Capital	$\$21.92 \times 10^6$
Working Capital (15%)	$\$3.29 \times 10^6$
Total	$\$25.21 \times 10^6$

6. Return on Original Investment (% ROI after Tax)

	Sales Price of Polycrystalline Silicon ($/kg)
0% ROI	15.60
5% ROI	17.93
10% ROI	20.27
15% ROI	22.60
20% ROI	24.94

7. Federal tax rate — 46%

Decomposition Reactor

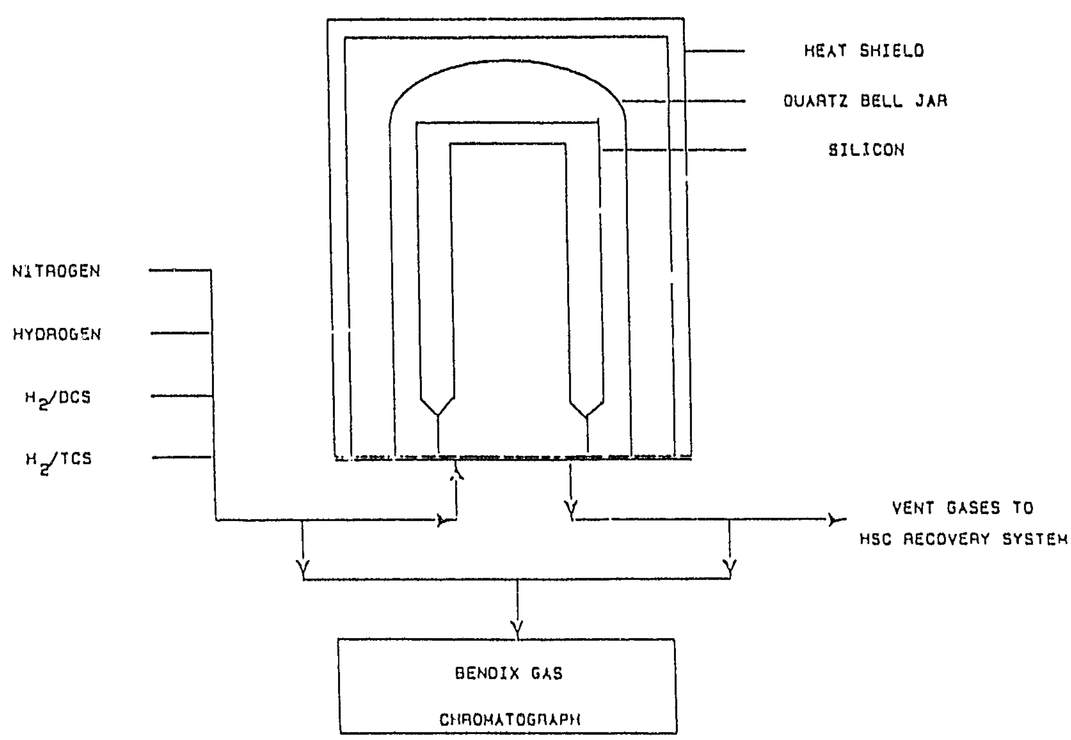

ORIGINAL PAGE IS
OF POOR QUALITY

Quartz Tube Deposition Results

FEED SPECIES	MOLE %	TEMPERATURE OF DEPOSITION INITIATION
DCS	5.	760°C
TCS	5.	860°C
STC	5.	960°C

Si Deposition on Bell Jar

FEED CONDITION	$\frac{\text{Si ON WALL}}{\text{Si ON RODS}}$ FOR INSIDE JAR TEMP. < 500°C	>800°C
A	0.00081	0.077
B		0.077
C		0.016
D	0.0032	0.010

For >800°C inside jar temperature silicon on bell jar wall was polycrystalline. For inside jar temperature <500°C silicon on bell jar was amorphous.

Decomposition Performance Summary for Wall Temperature < 500°C

FEED CONDITION	FINAL DIAMETER	SI FED GM/HR/CM	SI DEPOSITED GM/HR/CM	CONVERSION %	POWER CONSUMPTION KWH/KG
A	34	4.46	1.24	28.1	86
A	55	4.47	1.58	35.2	103
B	48	5.28	1.48	28.1	108
C	39	6.09	1.43	23.5	94
D	40	4.06	1.32	32.6	104
D	54	4.06	1.49	36.7	118
GOAL	100	5.0	2.0	40.	60

CONCLUSION: THE FEED CONDITIONS USED TO DATE WILL NOT ALLOW SIMULTANEOUS ACHIEVEMENT OF PERFORMANCE GOALS.

FUTURE ACTIVITIY: INVESTIGATE NEW FEED CONDITIONS THAT WILL INCREASE DEPOSITION RATE AND REDUCE POWER CONSUMPTION.

Problems and Concerns

ACHIEVING 40 PERCENT CONVERSION EFFICIENCY

ACHIEVING A POWER CONSUMPTION AT THE REACTOR OF 60 KWH/KG

ECONOMICS AND FEASIBILITY OF HYDROGENATION PROCESS

HYDROCHLORINATION PROCESS

SOLARELECTRONICS, INC.

TECHNOLOGY	REPORT DATE
POLYCRYSTALLINE SILICON METAL	JANUARY 12, 1983. 21ST PIM

APPROACH

HYDROCHLORINATION OF METALLURGICAL GRADE SILICON TOGETHER WITH SILICON TETRACHLORIDE AND HYDROGEN TO FORM TRICHLOROSILANE FOR PRODUCING SILICON METAL

CONTRACTOR

SOLARELECTRONICS, INC.

GOALS

TO PROVIDE A BASIC UNDERSTANDING ON THIS NEW METHOD OF MAKING TRICHLOROSILANE.

A. REACTION KINETIC MEASUREMENTS: UNDER A WIDE RANGE OF REACTION CONDITIONS

B. REACTION MECHANISM STUDIES:
- EQUILIBRIUM CONSTANT MEASUREMENTS
- DEVELOPMENT OF A RATE EQUATION, REACTION ORDER
- THERMODYNAMIC FUNCTION: $\Delta H, \Delta E$, ETC.
- DEUTERIUM KINETIC ISOTOPE EFFECTS

STATUS JPL CONTRACT NO. 956061 (JULY 9, 1981 - APRIL 30, 1983.)

$$3\ SiCl_4 + 2\ H_2 + Si = 4\ SiHCl_3$$

I. REACTION KINETIC MEASUREMENTS:
- TEMPERATURE: 350°C TO 650°C
- PRESSURE: ATMOSPHERIC TO 500 PSIG
- $H_2/SiCl_4$ FEED RATIO: 1.0 TO 5.0

II. EQUILIBRIUM CONSTANT MEASUREMENTS:
- FUNCTION OF T,P,C; $\Delta H = 10.6$ KCAL/MOLE

III. DEVELOPMENT OF A RATE EQUATION:
- PSUEDO-FIRST ORDER KINETICS
- FUNCTION OF T,P,C; $\Delta E = 13.2$ KCAL/MOLE

IV. REACTION MECHANISM STUDIES:
- QUARTZ HYDROCHLORINATION REACTOR SYSTEM COMPLETED
- EXPERIMENTS ON DEUTERIUM KINETIC ISOTOPE EFFECTS IN PROGRESS.

Hydrochlorination of $SiCl_4$ and mgSi at 450°C, H_2 : $SiCl_4$ Ratio of 2.0 and at Various Pressures

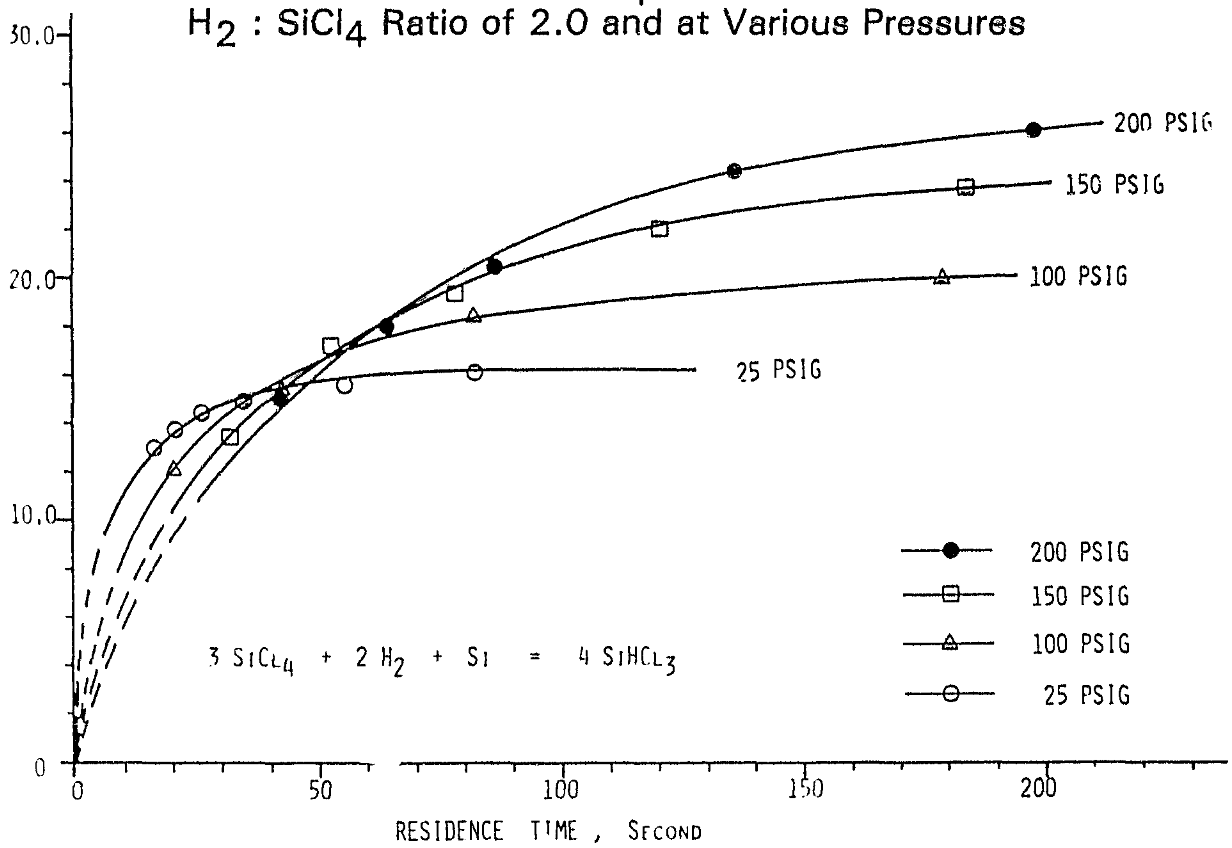

ORIGINAL PAGE IS OF POOR QUALITY

Effect of Temperature on Hydrochlorination of $SiCl_4$ and mgSi at 100 psig and H_2 : $SiCl_4$ Molar ratio of 2.0

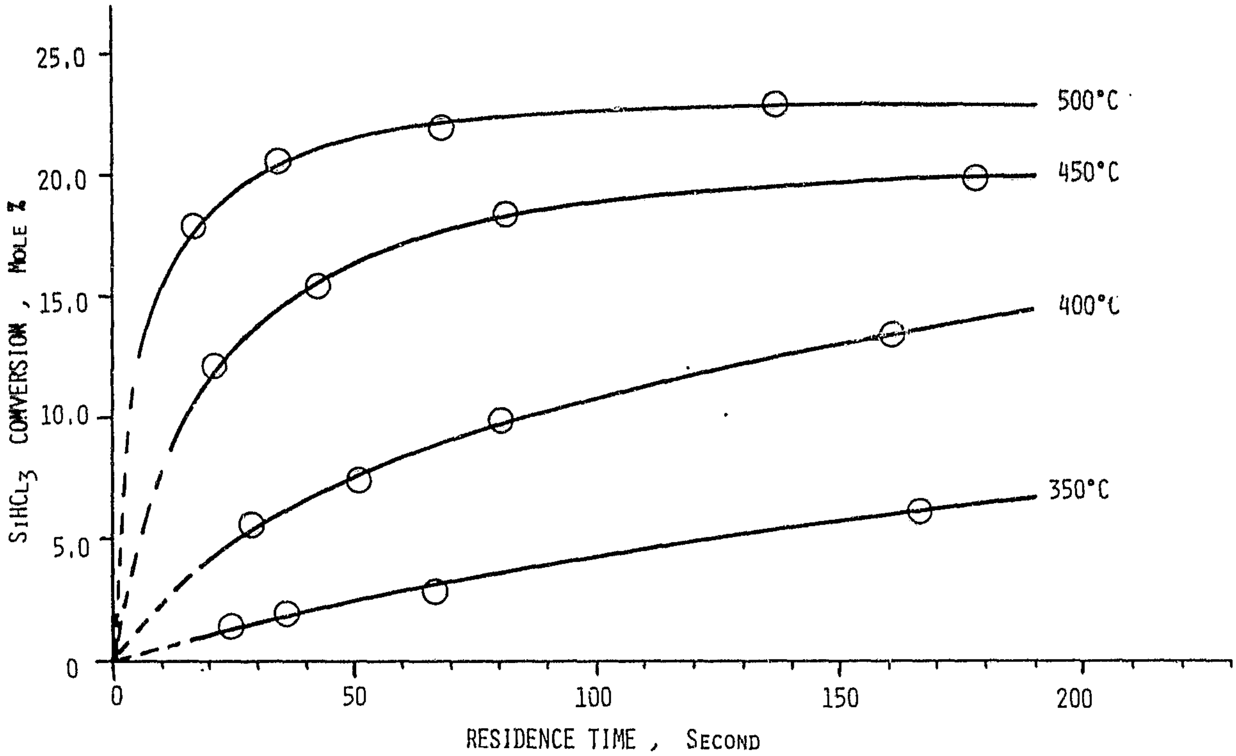

ORIGINAL PAGE IS OF POOR QUALITY

Hydrochlorination of $SiCl_4$ at 100 psig, 500°C and at Various Ratios of $H_2 : SiCl_4$

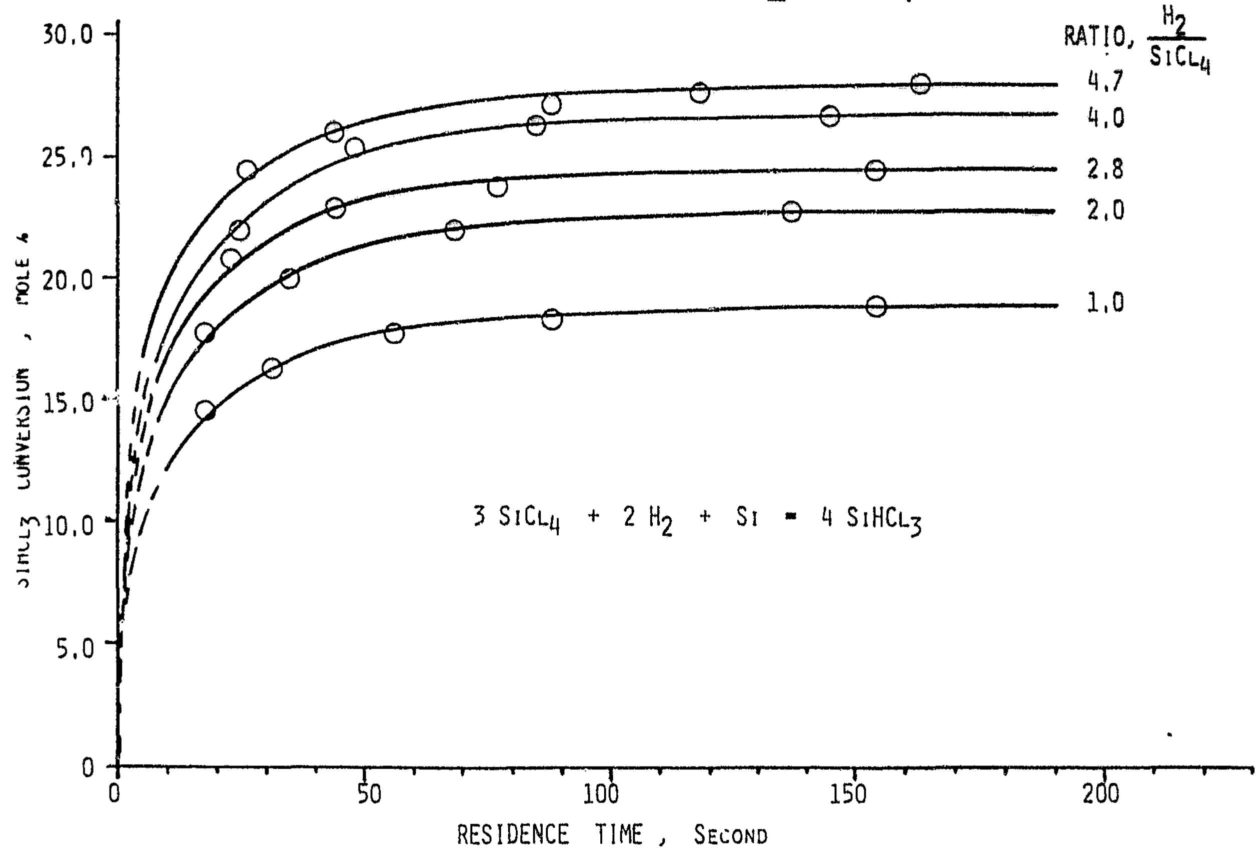

ORIGINAL PAGE IS
OF POOR QUALITY

Kinetic Modeling of a Typical Equilibrium Reaction

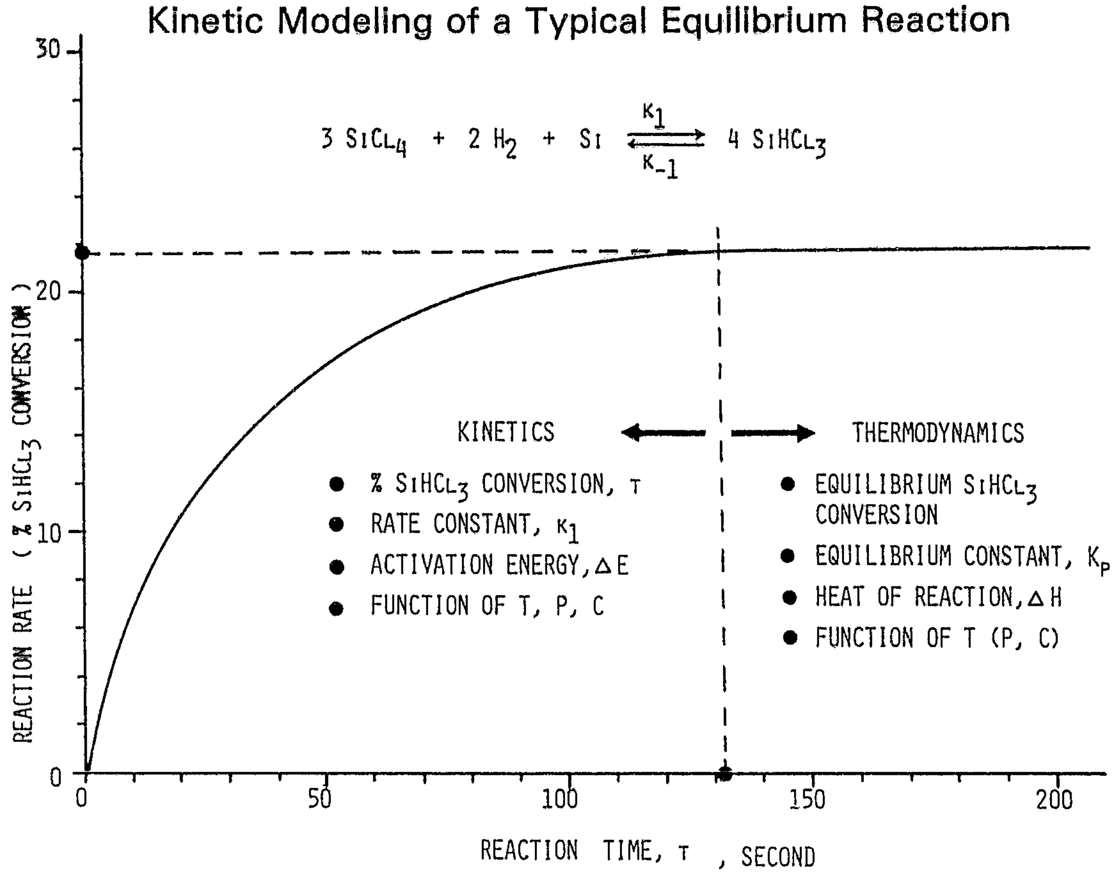

ORIGINAL PAGE IS
OF POOR QUALITY

Equilibrium Compositions

EQUILIBRIUM COMPOSITIONS OF CHLOROSILANE PRODUCTS FOR THE HYDROCHLORINATION OF $SiCl_4$ AND M.G. SILICON METAL AT 100 PSIG, $H_2/SiCl_4$ = 2.0 AND AT VARIOUS TEMPERATURES

Sample No.	Reaction Temperature °C	Residence Time Second	Product Composition, Mole % SiH_2Cl_2	$SiHCl_3$	$SiCl_4$
I	500	148	0.3726	22.29	77.33
I	500	148	0.3596	21.98	77.66
I	500	148	0.3779	22.15	77.47
I	500	148	0.3600	22.11	77.53
		Average =	0.3675	22.13	77.50
II	525	138	0.4781	23.25	76.27
II	525	138	0.3651	22.98	76.66
II	525	138	0.4141	22.92	76.66
II	525	138	0.4359	22.93	76.64
		Average =	0.4233	23.02	76.56
III	550	101	0.5750	24.05	75.38
III	550	101	0.5125	23.98	75.51
III	550	101	0.5099	24.21	75.28
III	550	101	0.5650	23.98	75.45
		Average =	0.5406	24.06	75.40
IV	575	98	0.5857	24.89	74.53
IV	575	98	0.5294	24.84	74.63
IV	575	98	0.5070	24.85	74.64
IV	575	98	0.4828	24.92	74.60
		Average =	0.5262	24.88	74.60

Equilibrium Constants

EQUILIBRIUM CONSTANTS FOR THE HYDROCHLORINATION OF $SiCl_4$ AND M.G. SILICON AT 100 PSIG, $H_2/SiCl_4 = 2.0$ AS A FUNCTION OF TEMPERATURE

EXPT'L No.	REACTION TEMP. °C	MOLE FRACTIONS AT EQUILIBRIUM SiH_2Cl_2	$SiHCl_3$	$SiCl_4$	H_2	EQUILIBRIUM CONSTANT K $\times 10^{-3}$	K_P $\times 10^{-3}$ ATM.$^{-1}$
I	500	0.001326	0.079855	0.27965	0.63916	4.55	0.583
II	525	0.001533	0.083363	0.27725	0.63786	5.57	0.714
III	550	0.001967	0.087535	0.27432	0.63618	7.03	0.901
IV	575	0.001920	0.090774	0.27218	0.63513	8.35	1.07

$$3\,SiCl_4 + 2\,H_2 + Si = 4\,SiHCl_3 \qquad K = \frac{(SiHCl_3)^4}{(SiCl_4)^3\,(H_2)^2} = \frac{K_P}{P}$$

ORIGINAL PAGE IS OF POOR QUALITY

Plot of the Van't Hoff Equation

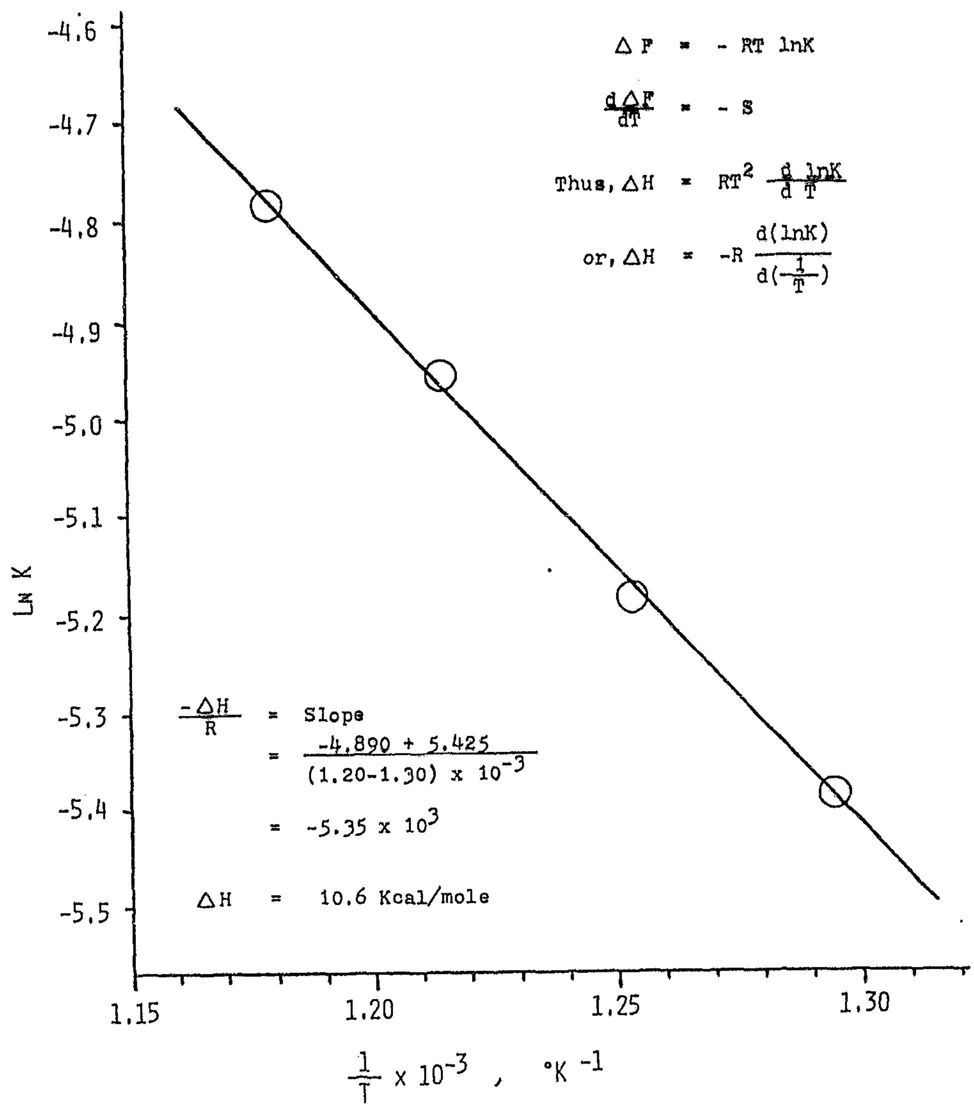

Equilibrium Constants

EQUILIBRIUM CONSTANTS FOR THE HYDROCHLORINATION OF $SiCl_4$ AND M. G. SILICON AT 100 PSIG, 500°C AS A FUNCTION OF $H_2/SiCl_4$ RATIOS

$H_2/SiCl_4$ RATIO	EQUILIBRIUM COMPOSITION MOLE % $SiHCl_3$	$SiCl_4$	EQUILIBRIUM CONSTANT K $\times 10^{-3}$	$K_P \times 10^{-3}$ ATM.$^{-1}$
4.7	28.0	72.0	4.81	0.617
4.0	26.7	73.3	4.58	0.587
2.8	24.5	75.5	4.67	0.599
2.0	22.8	77.2	5.19	0.665
1.0	18.5	81.5	5.43	0.696

EQUILIBRIUM CONSTANTS FOR THE HYDROCHLORINATION OF $SiCl_4$ AND M.G. SILICON AT 500°C AND AT VARIOUS PRESSURES AND $H_2/SiCl_4$ FEED RATIOS

REACTOR PRESSURE PSIG	ATM.	$H_2/SiCl_4$ RATIO	EQUILIBRIUM COMPOSITION MOLE % $SiHCl_3$	$SiCl_4$	EQUILIBRIUM CONSTANT K $\times 10^{-3}$	$K_P \times 10^{-3}$ ATM.$^{-1}$
25	2.70	2.0	18.5	81.5	1.85	0.685
73	5.97	2.8	23.7	76.3	3.95	0.661
100	7.80	1.0	18.5	81.5	5.43	0.696
100	7.80	2.0	22.8	77.2	5.19	0.665
150	11.2	2.0	27.9	72.1	14.9	1.33
200	14.6	2.0	30.5	69.5	24.2	1.65
300	21.4	2.8	35.0	65.0	32.6	1.52
500	35.0	2.8	37.0	63.0	45.3	1.29
(500)	(35.0)	(2.8)	(33.1)*	(66.9)	(23.5)	(0.67)

* CALCULATED EQUILIBRIUM % $SiHCl_3$ CONVERSION BASED ON $K_P = 0.67 \times 10^{-3}$ ATM.$^{-1}$

EQUILIBRIUM CONSTANTS FOR THE HYDROCHLORINATION OF $SiCl_4$ AND M.G. SILICON AT 450°C AND AT VARIOUS PRESSURES AND $H_2/SiCl_4$ FEED RATIOS

REACTOR PRESSURE PSIG	ATM.	$H_2/SiCl_4$ RATIO	EQUILIBRIUM COMPOSITION MOLE % $SiHCl_3$	$SiCl_4$	EQUILIBRIUM CONSTANT K $\times 10^{-3}$	K_p $\times 10^{-3}$ ATM.$^{-1}$
25	2.70	2.0	16.2	83.8	0.983	0.364
73	5.96	2.8	20.8	79.2	2.06	0.345
100	7.80	2.0	20.4	79.6	2.98	0.382
150	11.2	2.0	24.0	76.0	6.73	0.601
200	14.6	2.0	27.0	73.0	12.5	0.854
300	21.4	2.8	31 0	69.0	16.3	0.764
500	35.0	2.8	33.0	67.0	23.2	0.664

Development of a Rate Equation

DEVELOPMENT OF A RATE EQUATION FOR THE HYDROCHLORINATION OF $SiCl_4$ AND M.G. SILICON METAL TO FORM $SiHCl_3$

PSUEDO-FIRST ORDER KINETICS

$$R \underset{k_{-1}}{\overset{k_1}{\rightleftharpoons}} P \qquad SiCl_4 \underset{k_{-1}}{\overset{k_1}{\rightleftharpoons}} SiHCl_3$$

$$\ln \frac{X_E}{X_E - X} = \frac{k_1 A}{X_E} t$$

WHERE: X = CONCENTRATION OF $SiHCl_3$ AT TIME t

X_E = CONCENTRATION OF $SiHCl_3$ AT EQUILIBRIUM

A = INITIAL CONCENTRATION OF $SiCl_4$

A PLOT OF $\ln X_E/X_E - X$ VERSUS TIME t GIVES A STRAIGHT LINE WITH SLOPE EQUALS TO $k_1 A/X_E$.

Hydrochlorination of $SiCl_4$ at 100 psig and H_2 : $SiCl_4$ Ratio of 2.0

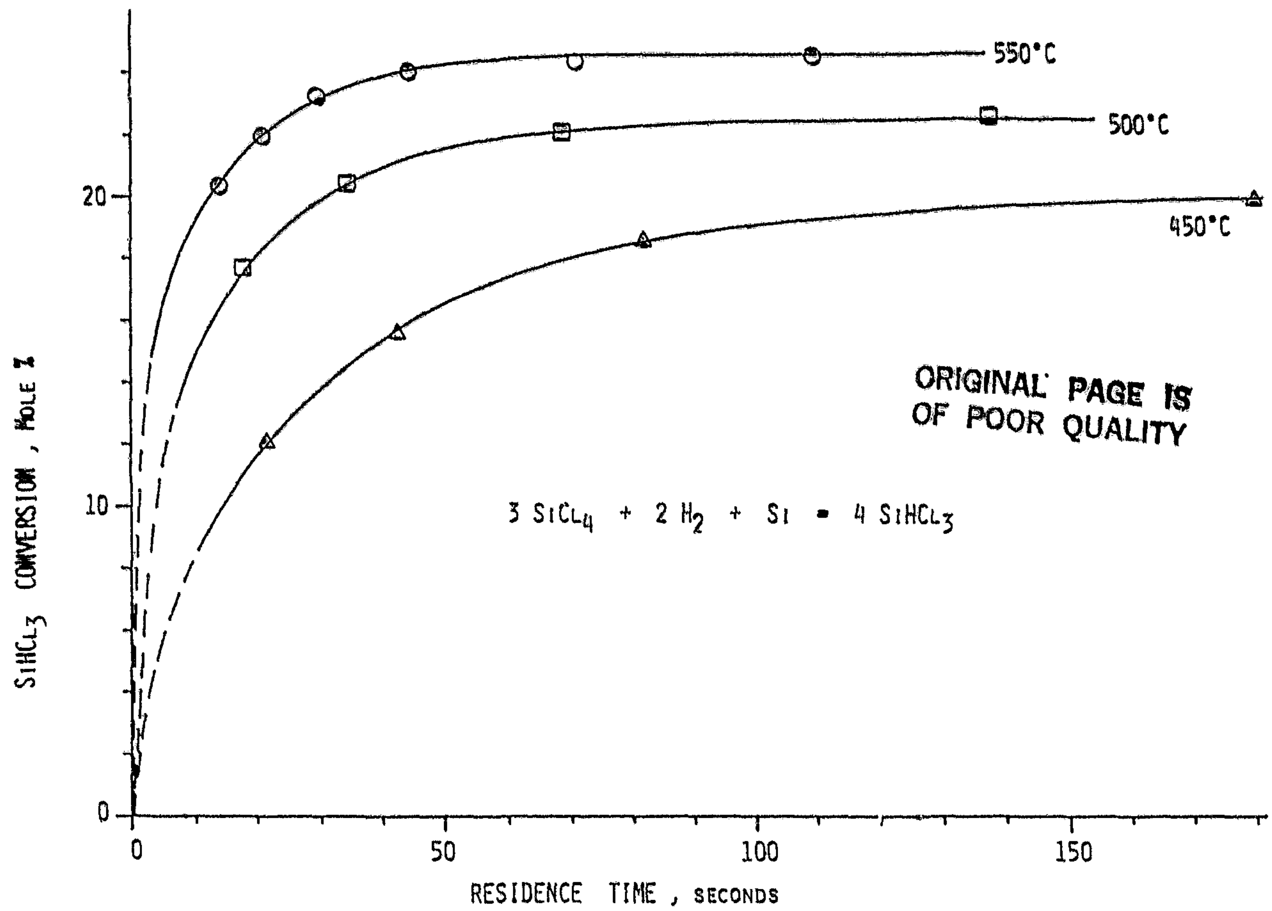

Hydrochlorination of $SiCl_4$ and mgSi to $SiHCl_3$

Pressure 114.7 psia, Temperature 500 °C, $H_2/SiCl_4$ Feed Ratio 2.0.

Time t sec.	Composition Mole % SiHCl$_3$	SiCl$_4$	Composition at Time t (psia)/Mole Fraction H_2	SiHCl$_3$	SiCl$_4$	Initial Partial Press. SiCl$_4$ a	Equil. Partial Press. SiHCl$_3$ x_e	$\ln \frac{x_e}{x_e - x}$	Rate Constant k_1 x 10^{-3} sec.$^{-1}$
10	15.1	84.9	(74.44) 0.6490	(6.079) 0.05300	(34.18) 0.2980	38.23	-	1.034	
20	18.0	82.0	(74.03) 0.6454	(7.321) 0.06383	(33.35) 0.2908	38.23	-	1.496	
30	19.6	80.4	(73.79) 0.6433	(8.018) 0.06990	(32.89) 0.2867	38.23	-	1.896	
40	20.6	79.4	(73.65) 0.6421	(8.457) 0.07373	(32.60) 0.2842	38.23	-	2.268	
60	21.9	78.1	(73.46) 0.6404	(9.032) 0.07875	(32.21) 0.2808	38.23	-	3.156	
Eq.	22.8	77.2	(73.32) 0.6393	(9.434) 0.08225	(31.94) 0.2785	38.23	9.434	-	10.9

Reference To: Figure V, fourth Quarterly Report, April 9 -July 8, 1982.

ORIGINAL PAGE IS OF POOR QUALITY

Plot of Pseudo-First-Order Rate Equation

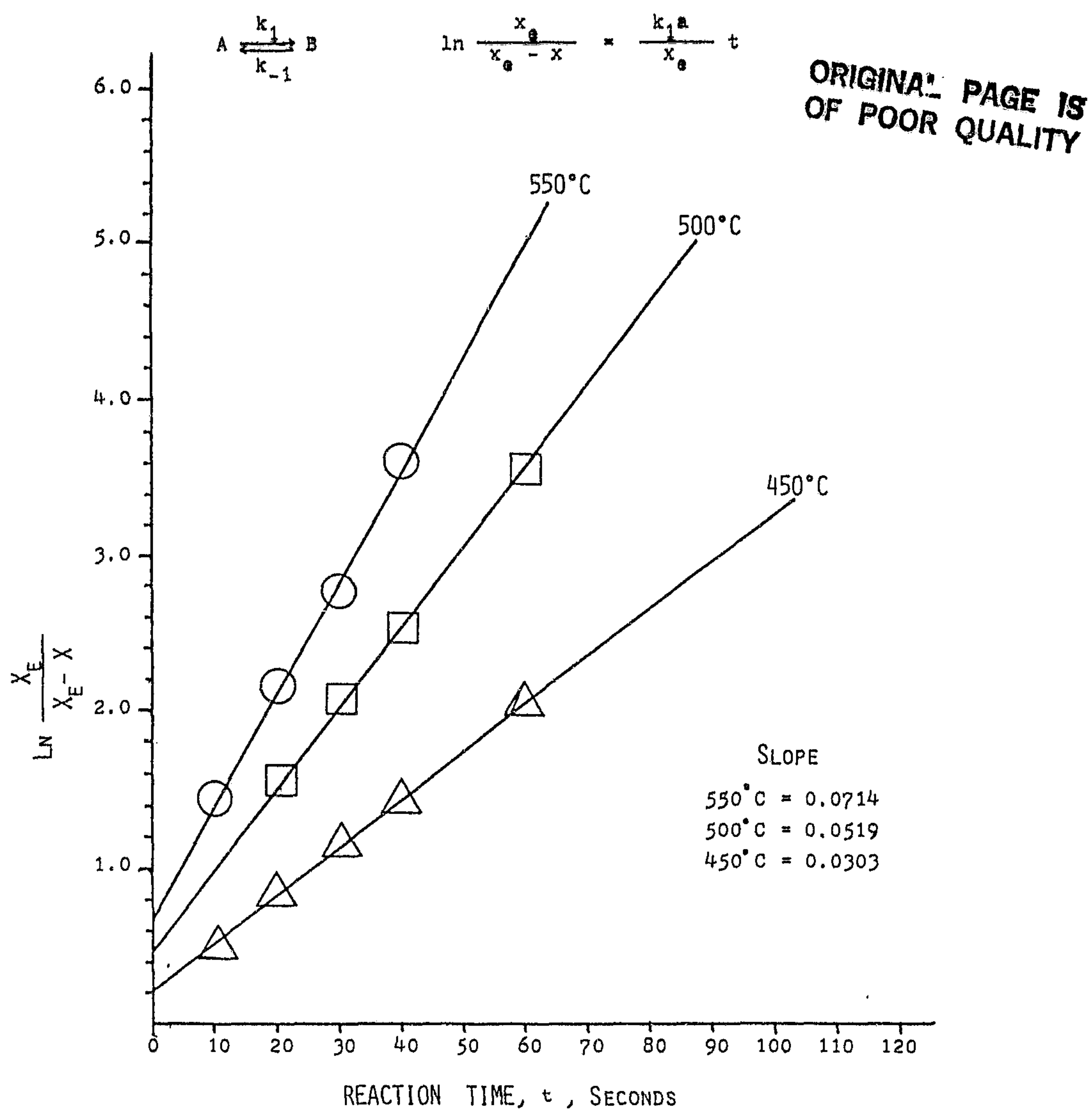

Effect of Temperature

EFFECT OF TEM-ERATURE ON THE RATE CONSTNAT FOR THE HYDROCHLORINATION OF $SiCl_4$ AND M.G. SILICON AT 100 PSIG AND $H_2/SiCl_4$ FEED RATIO OF 2.0

REACTION TEMPERATURE °C	EQUILIBRIUM COMPOSITION MOLE % $SiHCl_3$	$SiCl_4$	RATE CONSTANT K_1 x 10^{-3} SEC.$^{-1}$
450	20.4	79.6	6.50
500	22.8	77.2	12.7
550	24.7	75.3	19.2

ORIGINAL PAGE IS
OF POOR QUALITY

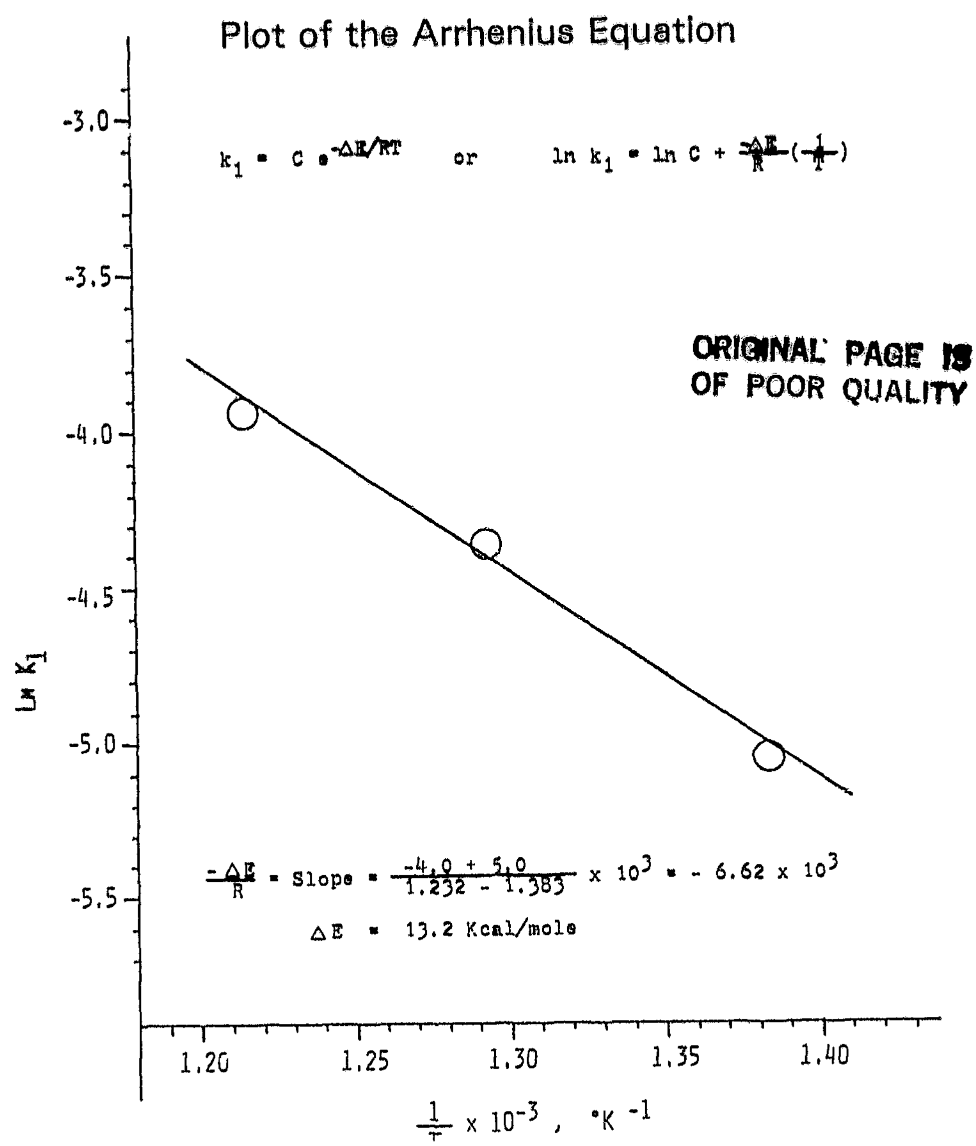
Plot of the Arrhenius Equation
-3.0
-3.5
-4.0
-4.5
-5.0
-5.5
Ln k1
k1 = C e-ΔE/RT or ln k1 = ln C + -ΔE/R (1/T)
ORIGINAL PAGE IS
OF POOR QUALITY
-ΔE/R = Slope = (-4.0 + 5.0)/(1.232 - 1.383) x 10^3 = - 6.62 x 10^3
ΔE = 13.2 Kcal/mole
1.20
1.25
1.30
1.35
1.40
1/T x 10^-3 , °K -1

Effect of Concentration

EFFECT OF CONCENTRATION ON THE RATE CONSTANT FOR THE HYDROCHLORINATION OF $SiCl_4$ AT 100 PSIG, 500 °C AS A FUNCTION OF $H_2/SiCl_4$ FEED RATIOS

$H_2/SiCl_4$ RATIO	EQUILIBRIUM COMPOSITION MOLE %		RATE CONSTANT K_1 $\times 10^{-3}$ SEC.$^{-1}$
	$SiHCl_3$	$SiCl_4$	
4.7	28.0	72.0	12.7
4.0	26.8	73.2	12.2
2.8	24.5	75.5	11.4
2.0	22.8	77.2	10.9
1.0	18.8	81.2	9.30

Hydrochlorination at Various Pressures

FIGURE VII HYDROCHLORINATION OF $SiCl_4$ AND M.G. SILICON AT 500°C, $H_2/SiCl_4$ RATIO OF 2.0 AND AT VARIOUS PRESSURES

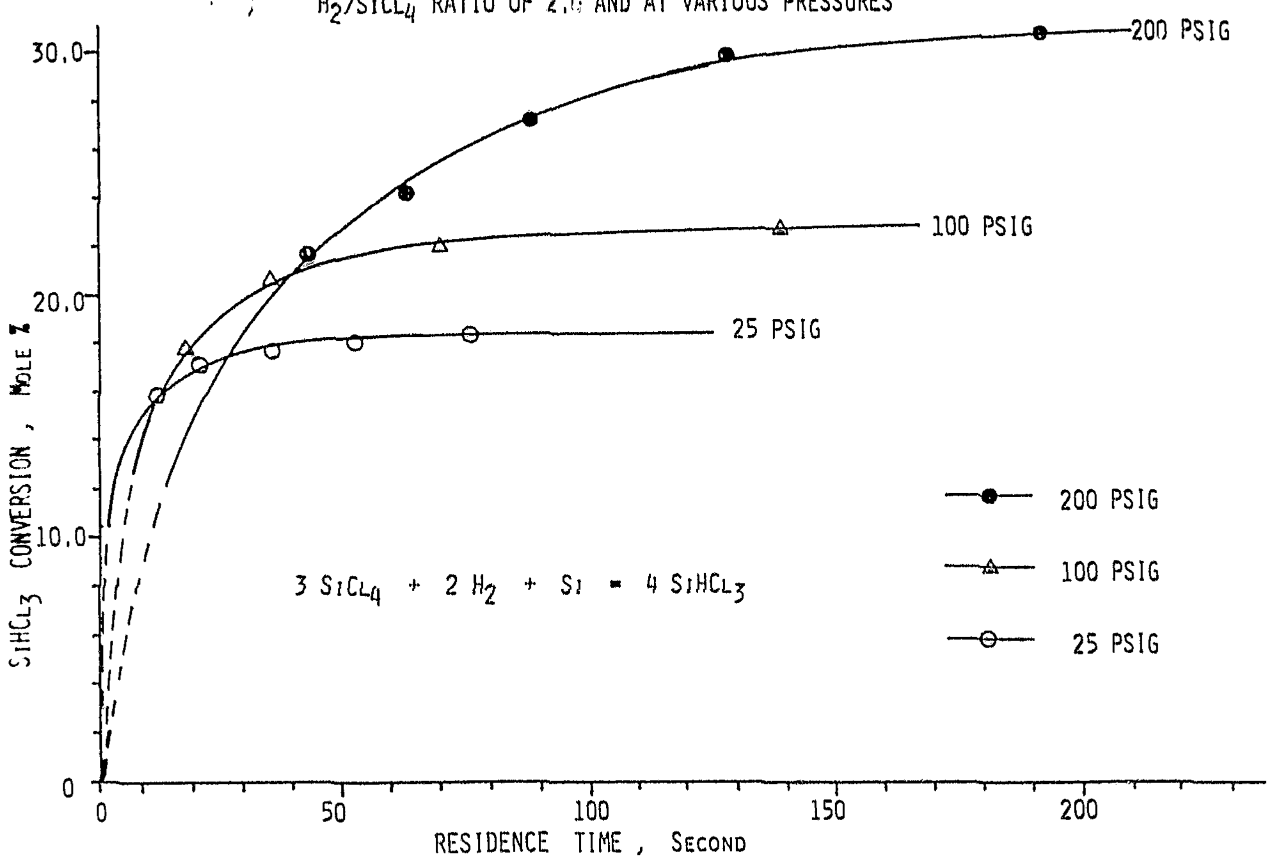

Effect of Pressure

EFFECT OF PRESSURE ON THE RATE CONSTANT FOR THE HYDROCHLORINATION OF $SiCl_4$ AT 500 °C AND AT VARIOUS $H_2/SiCl_4$ FEED RATIOS

REACTOR PRESSURE		$\frac{H_2}{SiCl_4}$	EQUILIBRIUM COMPOSITION MOLE %		RATE CONSTANT k_1
PSIG	ATM.	RATIO	$SiHCl_3$	$SiCl_4$	$\times 10^{-3}$ SEC.$^{-1}$
25	2.70	2.0	18.4	81.6	14.5
73	5.97	2.8	23.4	76.6	13.0
100	7.80	2.0	22.9	77.1	12.2
200	14.6	2.0	31.0	69.0	8.33
500	35.0	2.8	37.0	63.0	7.06

Plausible Reaction Mechanism

A. INTERPRETATION OF THE PSUEDO-FIRST ORDER KINETICS

$$SiCl_4 \longrightarrow [\text{INTERMEDIATE}] \longrightarrow SiHCl_3$$

$$\begin{array}{c} Cl_3Si \cdots Cl \\ \vdots \quad\;\; \vdots \\ -\,Si - Si - Si\,- \end{array} + H_2 \longrightarrow SiHCl_3 + HCl$$

$$\begin{array}{c} H \cdots H \\ \vdots \quad\; \vdots \\ -\,Si - Si - Si\,- \end{array} + SiCl_4 \longrightarrow SiHCl_3 + HCl$$

B. DEUTERIUM KINETIC ISOTOPE EFFECT

- IF HYDROGEN IS INVOLVE IN THE RATE-DETERMINING STEP, SIGNIFICANT KINETIC ISOTOPE EFFECT WILL BE EVIDENT.
- EXPERIMENTS ARE IN PROGRESS.

SILANE DECOMPOSITION IN FBR TO MAKE SEMICONDUCTOR-GRADE SILICON

UNION CARBIDE CORP.

TECHNOLOGY POLYCRYSTALLINE SILICON R&D	REPORT DATE JANUARY 13, 1983
APPROACH SILANE DECOMPOSITION IN A FLUID BED REACTOR TO MAKE SEMICONDUCTOR GRADE SILICON CONTRACTOR UNION CARBIDE CORPORATION	STATUS • PDU WAS OPERATED WITH SILANE FEED CONCENTRATIONS UP TO 25% • PDU AT TONAWANDA, N. Y. UCC LAB WAS DISMANTLED AND SHIPPED TO WASHOUGAL, WA. • THE UNIT IS CURRENTLY BEING REINSTALLED FOR FURTHER R&D WORK
GOALS • DEMONSTRATE PROCESS FEASABILITY • DETERMINE OPERATING WINDOW • CONDUCT STEADY STATE RUNS • INVESTIGATE SILICON PURITY	

Fluid-Bed Silane Decomposition: R&D

- 6-INCH DIAMETER FLUID BED PDU WAS OPERATED WITH SILANE FEED CONCENTRATIONS UP TO 25 PERCENT
- SUITABLE OPERATING WINDOW WAS IDENTIFIED
- PDU WAS OPERATED CONSECUTIVELY FOR 33 HOURS WITH COMPLETE SILANE CONVERSION WITHIN THE FLUID BED
- PRODUCT WITHDRAWAL AND SEED INTRODUCTION WERE SUCCESSFULLY DEMONSTRATED
- PDU WAS TRANSFERRED FROM TONAWANDA, N. Y. TO WASHOUGAL, WA., WHERE IT IS BEING REINSTALLED
- FBR EXPERIMENTS TO DATE HAVE BEEN VERY PROMISING

Consecutive Experiments: Run Summary

RUN NO.	SILANE FEED DURATION HRS.	MAX. SILANE IN FEED %	BED TEMP.	SILANE CONVERSION %	POWDER FORMATION, % OF SILICON FED
B-2	6.5	21.6	520°C-780°C	100	4.5
B-3	6.5	23.5	580°C-790°C	100	7.9
B-4	7.0	21.0	520°C-750°C	100	7.8
B-5	13.0	20.5	550°C-750°C	100	12.8

DISTRIBUTOR TEMPERATURE = 300°C
U/Umf AT BOTTOM OF BED = 4

Consecutive Experiments: Mass Balance

Si FROM SILANE → FBR → Si PRODUCT
= 28.70 kg → = 23.55 kg

Si SEED → FBR → Si POWDER
= 0.76 kg → = 2.62 kg

INITIAL BED WEIGHT	= 41.73 kg
ESTIMATED INCREASE IN BED WEIGHT	= Silicon IN-Silicon OUT
	= 3.29 kg
ESTIMATED FINAL BED WEIGHT	= 45.02 kg
ACTUAL FINAL BED WEIGHT	= 46.32 kg

MASS BALANCE AGREEMENT WITHIN 3% MARGIN OF ERROR

Technical Assessment

- FLUID BED PROCESS IS TECHNICALLY FEASIBLE AND ECONOMICALLY ATTRACTIVE
- COMPLETE SILANE CONVERSION CAN BE OBTAINED IN A COMPACT, HIGH-THROUGHPUT REACTOR
- POWDER FORMATION CAN BE CONTROLLED
- FBR PRODUCT WITH GOOD MORPHOLOGY CAN BE OBTAINED
- FURTHER WORK IS NECESSARY TO:
  - MAXIMIZE THROUGHPUT
  - OPTIMIZE PARAMETERS
  - CONDUCT LONG RUNS
  - DEMONSTRATE PRODUCT PURITY BY EVALUATING SINGLE CRYSTAL RESISTIVITY; C, O_2, B & DONOR LEVELS; & SOLAR CELL PERFORMANCE

FY83 R&D Plans

- COMPLETE THE REINSTALLATION OF PDU AT WASHOUGAL
- RESTART EXPERIMENTS WITH HIGH-PURITY SILANE
- CONDUCT LONG RUNS TO DETERMINE PRODUCT PURITY
- PERFORM ANALYSES TO ESTABLISH SILANE AND SILICON PURITY

JPL FBR Si-DEPOSITION RESEARCH

JET PROPULSION LABORATORY

G. Hsu

1982 Objectives

- ESTABLISH FUNDAMENTAL UNDERSTANDING OF FLUIDIZED BED SILICON DEPOSITION IN TERMS OF GROWTH MECHANISM AND DEPOSITION KINETICS.
- DEFINE KEY DESIGN FEATURES FOR 6-INCH FLUIDIZED BED REACTOR (FBR) SYSTEM, E.G. DISTRIBUTOR, HEATER, COOLING DEVICES.
- CONSTRUCT AND OPERATE 6-INCH FBR; PARAMETRIC EXPERIMENTS TO CHARACTERIZE REACTOR PERFORMANCE IN TERMS OF DESIGN PARAMETERS.

232

FBR With Instrumentation and Heaters

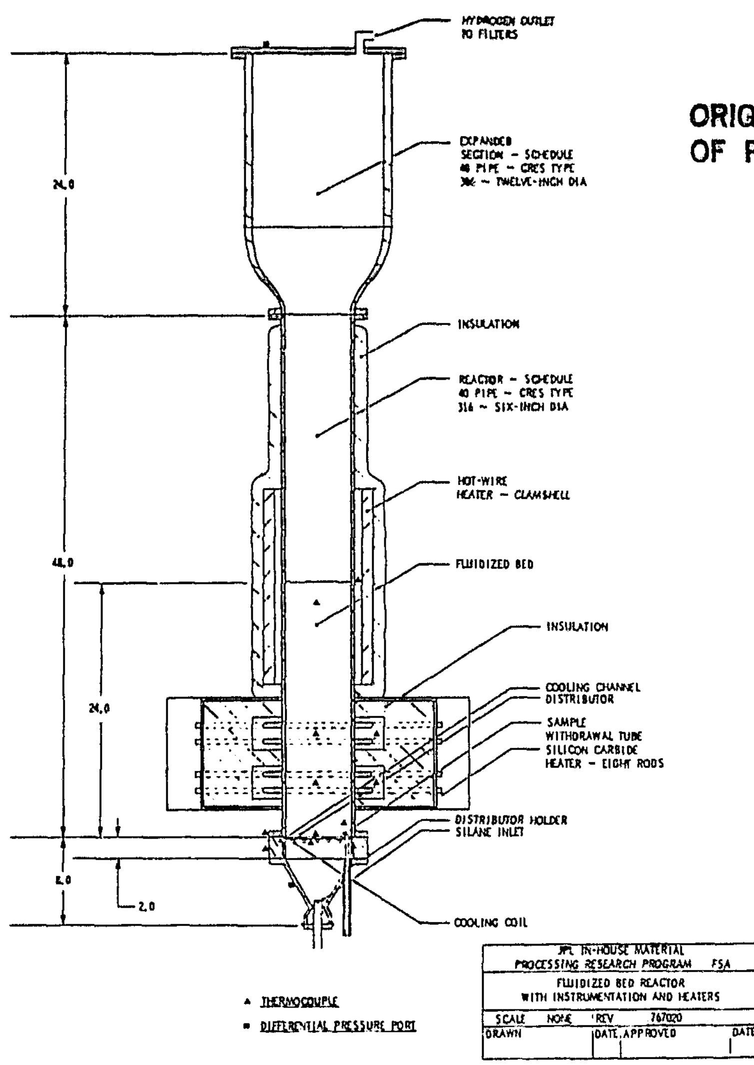

ORIGINAL PAGE IS
OF POOR QUALITY

Progress

CONSTRUCTED, CHECKED OUT AND OPERATED A 6-INCH DIAMETER FBR.

- HEATER: (3 ZONES)
  TWO SECTIONS OF 5.5-INCH SiC HIGH-DENSITY ROD HEATER
  ONE 18-INCH WIRE/CERAMIC HEATER

- DISTRIBUTOR:
  MULTILAYER SCREEN
  POROUS CARBON WITH 9 SPOUTS, FLAT POROUS CARBON
  325 (OR 200) MESH SCREEN, SUPPORTED ON 1/20" S.S. PLATE WITH 1/8" HOLES
  NOZZLE DISTRIBUTOR

- COOLING DEVICES:
  A WATER OR STEAM COOLING AROUND DISTRIBUTOR HOLDER.
  A WATER OR STEAM COOLING RING ABOVE DISTRIBUTOR.
  MULTIPLE COOLING TUBES JUST ABOVE DISTRIBUTOR (INTERNALLY IN THE REACTOR)
  A COOLING COIL WELDED AT THE BOTTOM OF DISTRIBUTOR.

Temperature Profile in 6-in. FBR

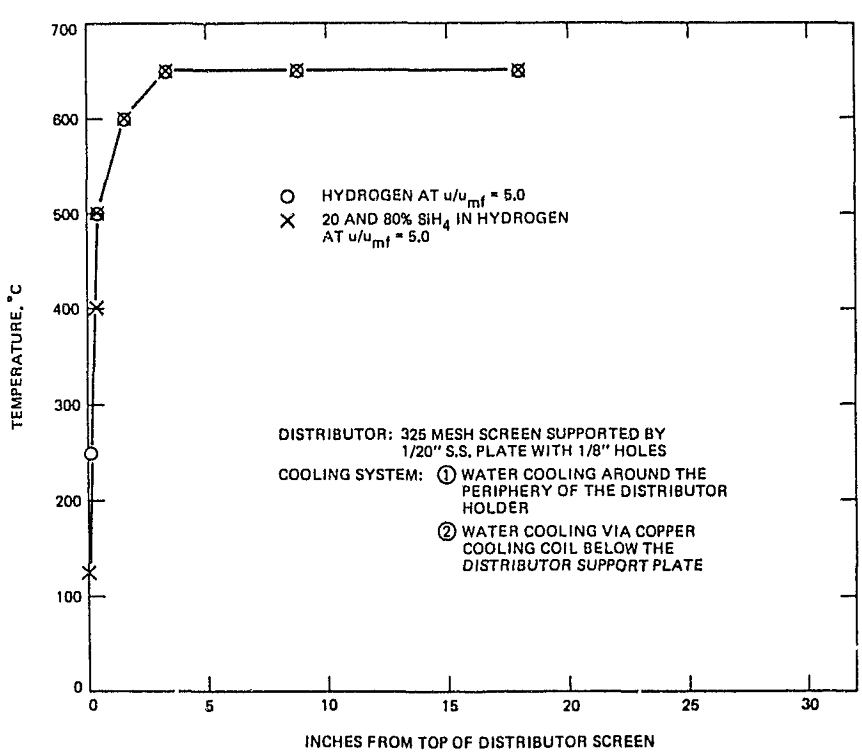

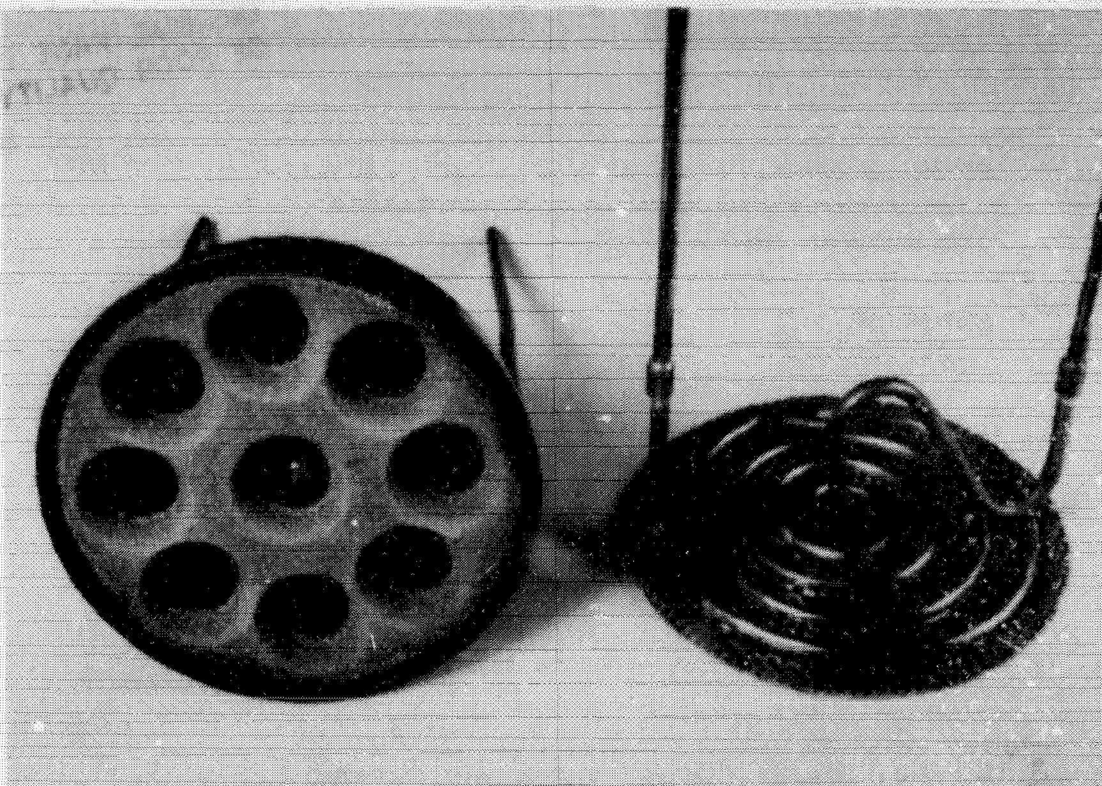

Progress

PERFORMED TEN KEY PARAMETRIC EXPERIMENTS IN 6-INCH FBR
(200 μM FEED PARTICLES, 650°C, U/U_{MF} = 5, 2-FT BED HEIGHT)

- 20% SILANE-IN-HYDROGEN FEED FOR 90 MINUTES -- DEPOSITION RATE 1 KG/HR.
- HIGH SILANE FEED CONCENTRATION (20% - 100%) FOR 2 HRS -- DEPOSITION RATE 3 KG/HR (AVE. SILANE CONCENTRATION 57%)
- 80% SILANE-IN-HYDROGEN FEED FOR 3 HRS -- DEPOSITION RATE 3.5 KG/HR.

Summary of Key 6-in. FBR Experiments (Data Analysis)

RUN # & DATE	DISTRIBUTOR & COOLING SYSTEM	SILICON SEED: WEIGHT (kg) & BED HEIGHT (inches)	SILICON SEED: $\bar{d}_p$ (μm)	SILICON SEED: LEACHING (10% HF)	EXPERIMENTAL CONDITIONS: TEMP (°C)	EXPERIMENTAL CONDITIONS: SILANE CONCENTRATION (%)	EXPERIMENTAL CONDITIONS: DURATION (min)	EXPERIMENTAL CONDITIONS: u/u_{mf}	EXPERIMENTAL CONDITIONS: SILANE FLOW RATE (SLPM)	EXPERIMENTAL CONDITIONS: SUPERFICIAL VELOCITY (cm/sec)	PRODUCT: PRODUCTION RATE (kg/hr)	PRODUCT: $\bar{d}_p$ (μm)	PRODUCT: PARTICLE GROWTH RATE (μm/(min) (kg of seed))	OVERALL MASS-BALANCE: % IN BED	OVERALL MASS-BALANCE: % IN DUST	OVERALL MASS-BALANCE: % SILANE CONVERSION
4 9/17/82	MULTILAYER SCREEN INTERNAL COOLING	11.48 (24")	92	NO	650	20	30	5.0*	14.4	14.5	0.96	–	–	96.2	2.8	[illegible]
8 9/28/82	MULTILAYER SCREEN INTERNAL COOLING	11.34 (24")	92	NO	650	20	60	5.0*	14.4	13.0	0.15	–	–	93.5	5.4	–
9 10/1/82	MULTILAYER SCREEN INTERNAL COOLING	11.34 (24")	92	NO	650	20	90	5.0*	14.4	14.5	1.05	98.9	0.43	104(2)	2.1	100
10 10/5/82	MULTILAYER SCREEN INTERNAL COOLING	5.9 (12")	194	NO	650	20	30	5.0*	14.4	14.5	0.97	198.5	0.21	96.9	1.23	100
11 10/12/82	200 MESH SCREEN SUPPORTED BY 1/8" PLATE WITH MULTIPLE HOLES. EXTERNAL COOLING	11.34 (24")	194	NO	650	20	30	5.0*	14.4	14.5	0.96	191	–	96.6	1.3	100
15 11/2/82	325 MESH SCREEN SUPPORTED BY 1/8" PLATE WITH MULTIPLE HOLES. EXTERNAL COOLING	10.5 (24")	227	YES	650	20	90	5.0*	14.4	14.5	0.87	235.5	0.61	91.1	3.75	100
16 11/4/82	325 MESH SCREEN SUPPORTED BY 1/8" PLATE WITH MULTIPLE HOLES. EXTERNAL COOLING	11.3 (24")	236	PRODUCT OF RUN # 15	650	20 35 50 65 80 100	20.3 18.3 21.1 21.2 21.0 18.0	5.0**	18.7 30.2 40.24 50.3 58.9 69.7	20.1 18.6 17.4 16.7 15.9 15.0	2.9(1)	251.9	0.75	99(2)	9.5	100
17 11/10/82	325 MESH SCREEN SUPPORTED BY 1/8" PLATE WITH MULTIPLE HOLES. EXTERNAL COOLING	11.34 (24")	212	YES	650	80	173	5.0**	47.5	12.7	3.6	241.5	0.96	98.1(2)	11.1	100
18 11/12/82	POROUS CARBON WITH SPOUTS. EXTERNAL COOLING	10.9 (24")	148	NO	650	20	30	5.0*	14.4	14.5	1.0	153.5	1.0	97.6	6.7	100

* u/u_{mf} IS CALCULATED BASED ON AVERAGE 200 μm PARTICLE SIZE

** u/u_{mf} IS CALCULATED BASED ON ACTUAL PARTICLE SIZE

(1) PRODUCTION RATE IS FOR AN AVERAGE 56.9% SILANE CONCENTRATION

(2) THIS ERROR IN MASS BALANCE IS EITHER DUE TO ROUGH CALIBRATION OF SILANE FLOWMETER OR DUE TO OXIDATION OF SILICON FINES

Dust Formation Data

RUN # & DATE	TEMP (°C)	SILANE CONCENTRATION (v%)	DUST IN THE FILTERS COLLECTED DURING STEADY-STATE: DURATION (min)	DUST IN THE FILTERS COLLECTED DURING STEADY-STATE: AMOUNT (grams)	DUST IN THE FILTERS COLLECTED DURING STEADY-STATE: WT. %	TOTAL DUST COLLECTED IN THE FILTERS: AMOUNT (grams)	TOTAL DUST COLLECTED IN THE FILTERS: WT. %	DUST IN THE EXPANDED HEAD OF THE REACTOR: AMOUNT (grams)	DUST IN THE EXPANDED HEAD OF THE REACTOR: WT. %	OVER ALL DUST: AMOUNT (grams)	OVER ALL DUST: WT. %
4 9/17/82	650	20	30	18.1	2.9	18.1	2.9	–	–	18.1	2.9
8 9/28/82	550	20	60	54.9	5.7	63.0	5.4	–	–	63.0	5.4
9 10/1/82	650	20	90	20.5	1.36	32.2	2.1	–	–	32.2	2.1
10 10/5/82	650	20	30	2.4	0.48	7.2	1.23	–	–	7.2	1.23
11 10/12/82	650	20	30	6	1.2	6.8	1.3	–	–	6.8	1.3
15 11/2/82	650	20	90	58	3.75	58	3.75	–	–	58	3.75
16 11/4/82	650	20 35 50 65 80 100 OVERALL	16.2 13 14.8 15.0 14.8 15 123.7	3.0 5.9 22.4 46.4 57.9 73.2	0.85 1.3 3.2 5.3 5.7 6.0	341.6	5.5	255	4.1	596.6	9.5
17 11/10/82	650	80	163.4	701.6	7.3	733.6	7.0	436.6	4.2	1170.2	11.1
18 11/12/82	650	20	30	3.9	0.76	3.9	0.67	35.3	6.1	39.2	6.7

- NO BED AGGLOMERATION AND NO WALL DEPOSIT
- EFFLUENT DUST BELOW 11% IN ALL CASES
- COMPLETE CONVERSION
- MASS BALANCE: GENERALLY MORE THAN 90% DEPOSITION IN THE BED
- COLOR OF DEPOSIT WAS DULL GRAY -- COHERENT AND DENSE DEPOSITION
- MORPHOLOGY, DEPOSITION AND GROWTH PATTERNS ARE BEING ANALYZED BY SEM.

Conclusions

- THE SCAVENGING CAPABILITY OF FLUIDIZED BED PARTICLES TO INCORPORATE HOMOGENEOUS FINES APPEARS INCREASING THE SILANE FEED CONCENTRATION LIMIT.
- PRELIMINARY EXPERIMENTS HAVE IDENTIFIED A NEW RESEARCH AREA FOR SILICON PRODUCTION, NAMELY HIGH SILANE FEED CONCENTRATION.
- FURTHER RESEARCH IS NEEDED TO CHARACTERIZE GROWTH MECHANISM AND EXPLORE THIS NEW RESEARCH AREA

1983 Objectives

- REACTOR CHARACTERIZATION
  EMPHASIS WILL BE ON DISTRIBUTOR AND DEPOSITION KINETICS.
- PRODUCT CHARACTERIZATION -- SEM, SELECTIVE IMPURITY ANALYSIS.
  EMPHASIS WILL BE ON INITIAL PURITY IDENTIFICATION OF FLUIDIZED BED PARTICLES.
- (OPTIONAL, DEPENDING ON FUNDING SCOPE) DEPOSITION MECHANISM CHARACTERIZATION.
- (OPTIONAL) FEED GENERATION RESEARCH FOR FLUIDIZED BED

AN AEROSOL REACTOR FOR SILICON PRODUCTION

CALIFORNIA INSTITUTE OF TECHNOLOGY

R.C. Flagan
M.K. Alam

ORIGINAL PAGE IS
OF POOR QUALITY

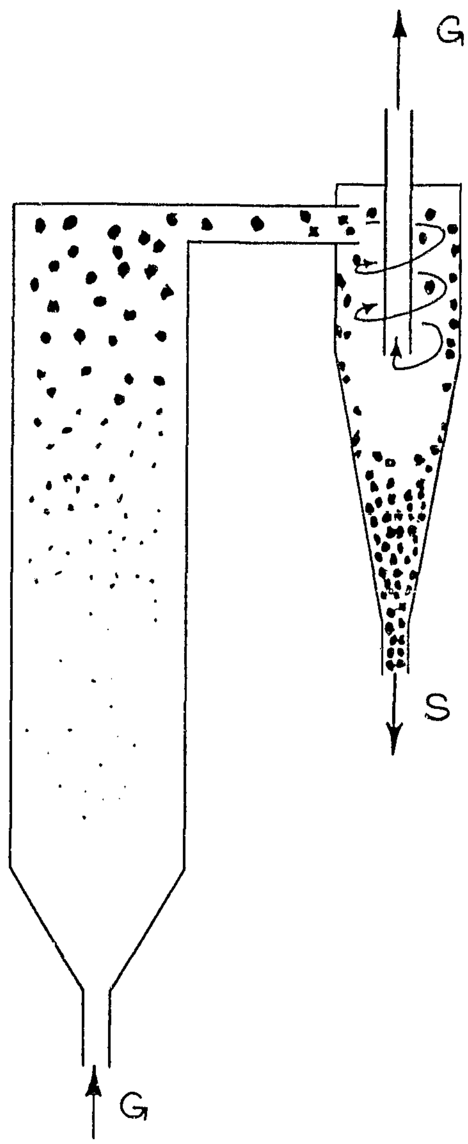

Free-Space Reactors

ANTICIPATED ADVANTAGES:

- HIGH REACTION RATE
- SMALL REACTOR SIZE
- REDUCED ENERGY CONSUMPTION
- CONTINUOUS OPERATION
- COMPLETE REACTION OF SILANE
- DIRECT CONVERSION OF SILANE-TO-MOLTEN-SILICON

PERFORMANCE (UNION CARBIDE, JPL):

- CONVERSION OF SILANE TO SILICON AT GREATER THAN 99%
- OPERATION UP TO 24 HOURS AT 2.5 - 4.3 KG/HR SILANE THROUGHPUT
- 55 Ω-CM POLYCRYSTALLINE SILICON PRODUCED

PROBLEMS

- SMALL SIZE OF PRODUCT PARTICLES -0.1 - 0.9 MICRON (DIFFICULT TO COLLECT AND PROCESS)

Processes in Free-Space Reactor

- HOMOGENEOUS PYROLYSIS OF SILANE
- HOMOGENEOUS NUCLEATION
- HETEROGENEOUS CONDENSATION
- HETEROGENEOUS REACTION
- COAGULATION

Silane Pyrolysis

$$SiH_4 \xrightarrow{k_1} SiH_2 + H$$

$$SiH_2 + SiH_4 \rightleftharpoons Si_2H_6$$

$$SiH_2 + Si_2H_6 \rightleftharpoons Si_3H_8$$

. . . . .

$$k_1 = 10^{15.5}\ \mathrm{EXP}(-59600/RT)\ \mathrm{SEC}^{-1}$$

Objectives

- ELUCIDATE FACTORS GOVERNING PARTICLE SIZE
- IDENTIFY SOURCE OF PROBLEM WITH PREVIOUS DESIGNS
- DEVELOP METHOD FOR GROWTH OF LARGE (>10 MICRON DIAMETER) DIRECTLY FROM SILANE PYROLYSIS

Approach

THEORETICAL INVESTIGATION OF:

- MECHANISMS OF PARTICLE GROWTH
- MAXIMUM PARTICLE SIZE
- INHIBITION OF NUCLEATION

Particle Growth

CONSIDER THE UNION CARBIDE SYSTEM

- -- 0.2 TO 1.0 MICRON PARTICLES ARE PRODUCED, ACCOUNTING FOR 82.5% OF THE MASS AT REACTOR OUTLET ($\sim 10^{-4}$ GM/CM^3).
- -- CORRESPONDS TO $10^8 - 10^{10}$ PARTICLES/CM^3.
- -- GROWTH OF THESE PARTICLES TO 10 MICRON SIZE REQUIRES INCREASE MASS OF EACH PARTICLE BY FACTOR OF $10^3 - 10^5$.
- -- THUS NEED $10^{-1} - 10^{+1}$GM/CM^3 SiH_4, i.e., $10^3 - 10^5$ ATMOSPHERES PRESSURE.
- -- GROWTH OF LARGE PARTICLES REQUIRES THAT NUMBER CONCENTRATION BE LIMITED TO ORDER 10^5/CM^3.
- -- CAN ADDITIONAL NEW PARTICLE FORMATION BE PREVENTED AT SUCH LOW PARTICLE CONCENTRATIONS?

Homogeneous Nucleation

ORIGINAL PAGE IS
OF POOR QUALITY

$$A_{\nu-1} + A_1 \rightleftharpoons A_\nu$$

CRITICAL NUCLEUS

$$d_p^* = \frac{4\sigma V_m}{kT \ln S} \simeq 8\ \text{Å} \quad \text{FOR } S_1$$

NUCLEATION RATE (CLASSICAL THEORY)

$$J\left(\frac{\text{PARTICLES}}{\text{CM}^3\ \text{SEC}}\right) = 2n_1^2 \left(\frac{kT}{2\pi m}\right)^{1/2} V_m^{2/3} \left[\frac{\sigma V_m^{2/3}}{kT}\right]^{1/2} \text{EXP} - \left\{\frac{16\pi\sigma^3 V_m^2}{3(kT)^3(\ln S)^2}\right\}$$

Particle Growth

- COAGULATION IS TOO SLOW TO GENERATE PARTICLES APPRECIABLY LARGER THAN 1 MICRON WITHIN REASONABLE RESIDENCE TIMES
- PARTICLE GROWTH MUST, THEREFORE, BE ACCOMPLISHED BY CONDENSATION OR HETEROGENEOUS REACTIONS
- THESE MECHANISMS CONSERVE THE TOTAL NUMBER CONCENTRATION OF PARTICLES

Nucleation in Presence of Growing Aerosol

- CLASSICAL THEORY OF HOMOGENEOUS NUCLEATION ASSUMES VAPOR CONCENTRATION IN GAS IS UNIFORM.
- PESTHY, FLAGAN AND SEINFELD (1981) SHOWED THAT VAPOR CONCENTRATION DEPRESSION DUE TO PARTICLE GROWTH CAN SUBSTANTIALLY REDUCE MEAN NUCLEATION RATES - ANALYSIS LIMITED TO CONTINUUM SIZED PARTICLES.

∴ WE NEED TO EXTEND THEORY INTO THE FREE MOLECULAR AND TRANSITION SIZE RANGES.

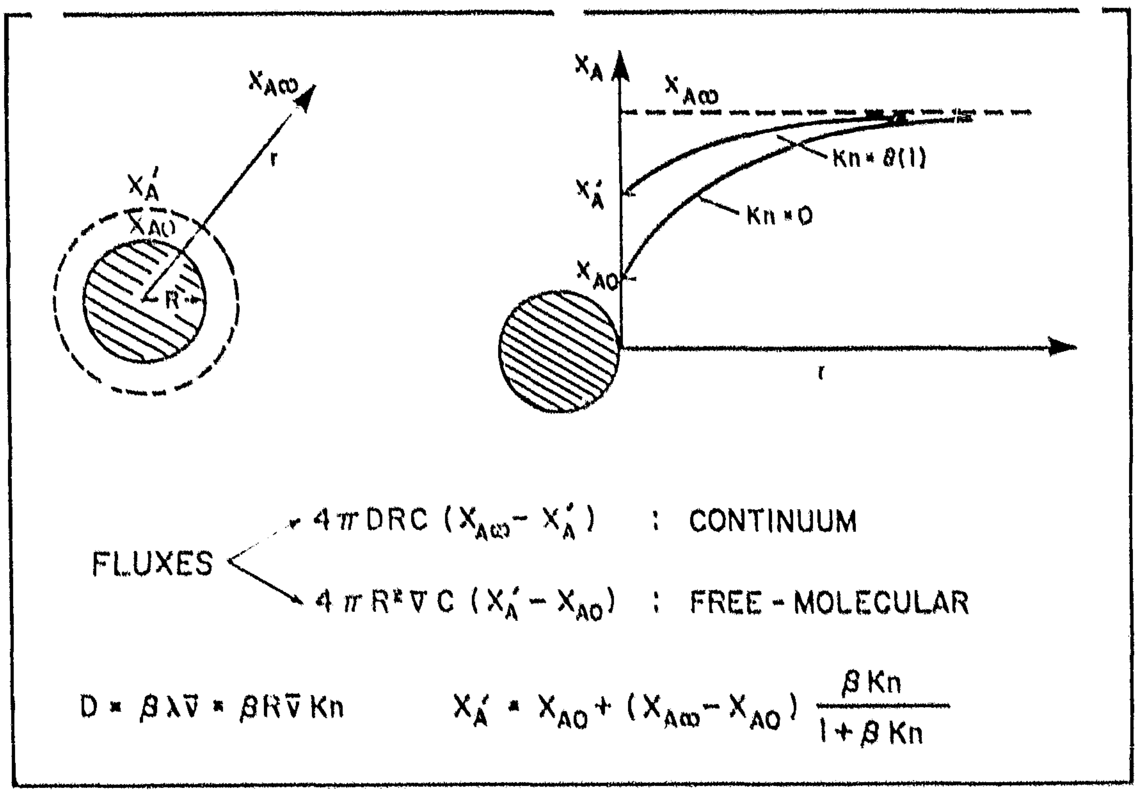
$X_{A\infty}$
X_A'
X_{A0}
R
r
X_A
$Kn = \theta(1)$
$Kn = 0$
FLUXES
$4\pi DRC\,(X_{A\infty} - X_A')$: CONTINUUM
$4\pi R^2 \bar{v} C\,(X_A' - X_{A0})$: FREE - MOLECULAR
$D = \beta\lambda\bar{v} = \beta R\bar{v}\,Kn$
$X_A' = X_{A0} + (X_{A\infty} - X_{A0})\,\dfrac{\beta\,Kn}{1+\beta\,Kn}$

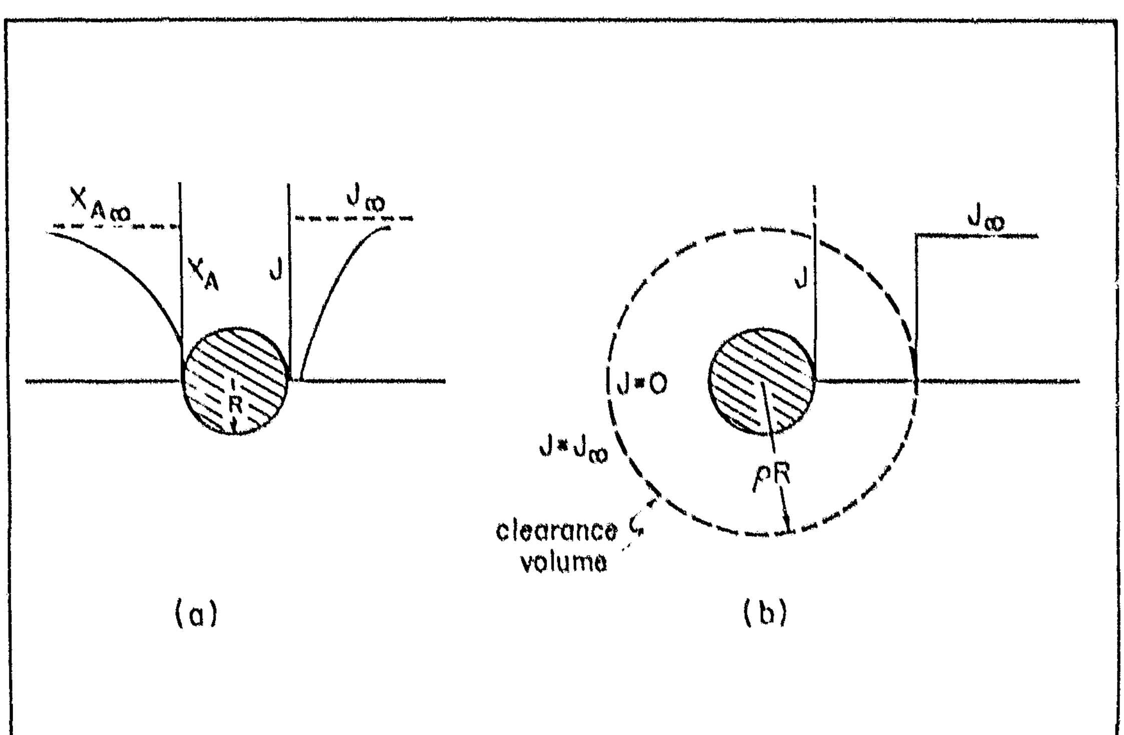
$X_{A\infty}$
X_A
J
J_∞
R
$J = 0$
$J = J_\infty$
ρR
clearance volume
(a)
(b)

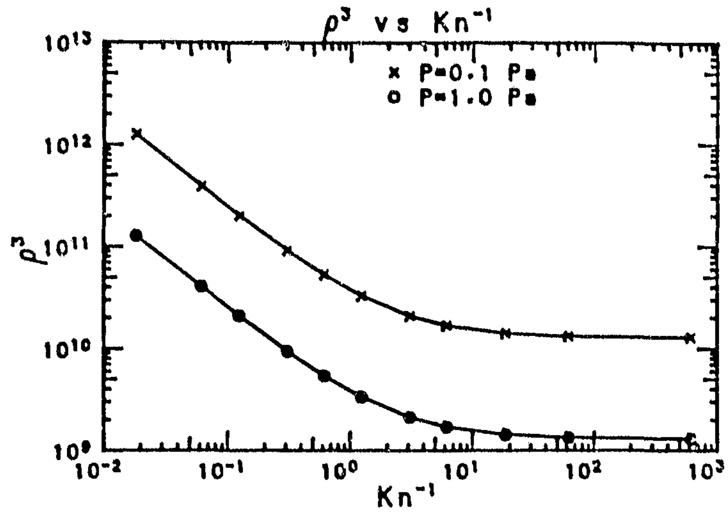

Aerosol Reactor for Growth of Large Silicon Particles by Homogeneous Pyrolysis of Silane

1. GENERATE SEED PARTICLES BY PYROLYSIS OF A SMALL AMOUNT OF SILANE.

2. MIX SEED AEROSOL WITH PRIMARY SILANE FLOW, LIMITING NUMBER CONCENTRATION SUCH THAT THE AMOUNT OF SILANE IS SUFFICIENT TO GROW THE DESIRED SIZE OF PARTICLES FROM THE SEED.

3. REACT THE SILANE AT A RATE WHICH IS CONTROLLED SUCH THAT THE SEED PARTICLES SCAVENGE VAPOR RAPIDLY ENOUGH TO INHIBIT FURTHER NUCLEATION.

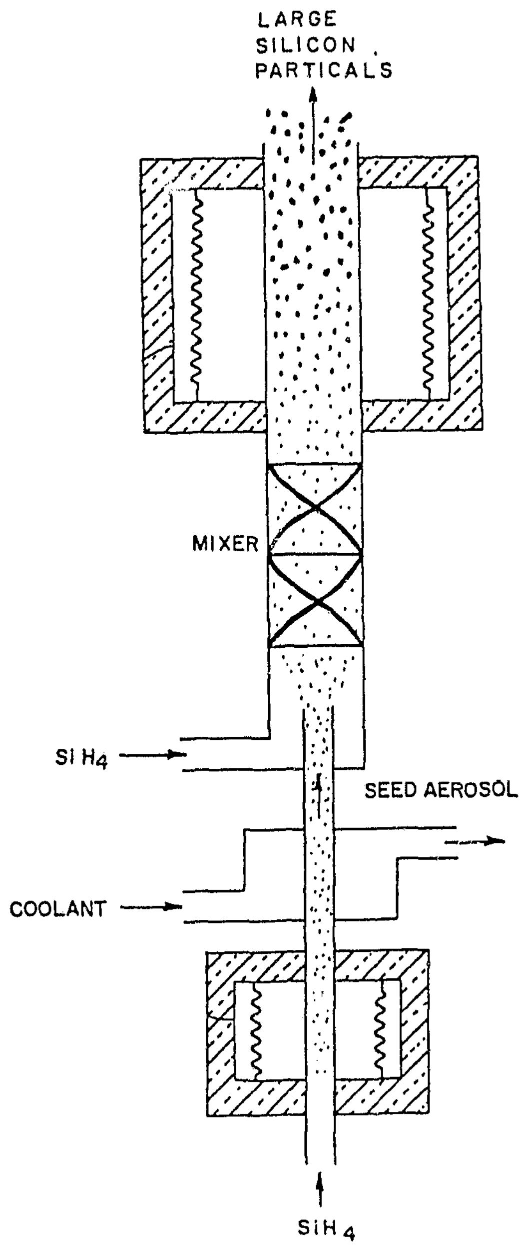
LARGE
SILICON
PARTICALS
MIXER
SI H4
SEED AEROSOL
COOLANT
SiH 4

Aerosol Reactor Results

1. PRIMARY REACTOR ALONE

   $T = 800°C$

   $P = 1$ ATMOSPHERE

   $N > 2 \times 10^8/cm^3$

   $d \approx 0.1 - 0.5\ \mu m$

2. FULL AEROSOL REACTOR

   (a) SEED GENERATOR

   $T = 700°C$

   $P_{SiH_4} = 10^{-3}$ ATMOS.

   $d \approx 0.1 - 1.0\ \mu m$

   $N \sim 10^8/cm^3$

   (b) PRIMARY REACTOR

   $T = 500 - 700°C$ (ACCELERATING RAMP)

   INLET $N \approx 3 \times 10^4/cm^3$

   OUTLET $N = 6 \times 10^4/cm^3$

   $d \approx 1 - 10\ \mu m$

ORIGINAL PAGE IS
OF POOR QUALITY

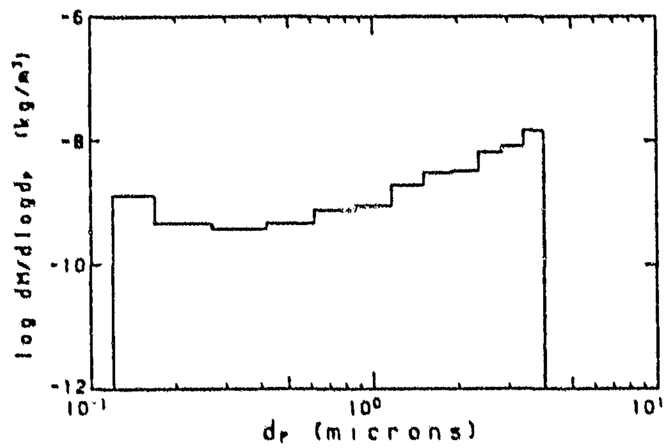

Size distribution of seed aerosol

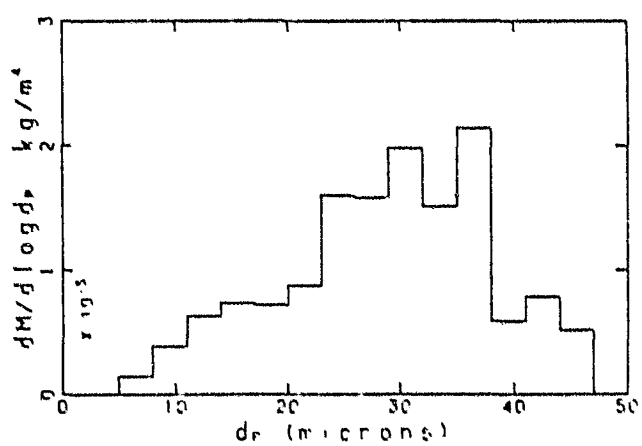

Size distribution of aerosol from two stage reactor

ADVANCED MATERIALS

SILICON COST SENSITIVITY STUDY

JET PROPULSION LABORATORY

J. Glyman and L. Reiter

Introduction

- Two-phase study performed

  (1) Verify IPEG2 for silicon manufacturing processes. Compare with Lamar/TREI study using their inputs

  (2) Probabilistic cost analysis of Union Carbide and Hemlock Semiconductor processes, using inputs encoded from JPL contract managers. Inputs are preliminary and were based on Lamar/TREI and other data sources

Phase I: Cost Comparison of Silicon Manufacturing Processes

- Lamar/TREI study economic analysis
- Processes included: Conventional Siemens, SiI_4, UCC Silane, Battelle A&B, and Hemlock A&B
- JPL used Lamar/TREI data as input to IPEG cost estimation methodology
- Result: IPEG price was within an average of 2.6% of Lamar/TREI price. Therefore, IPEG is verified for silicon manufacturing processes.

IPEG/Lamar Price Comparison

PROCESS	LAMAR PRICE $/kg AT 20% DCF	IPEG PRICE $/kg AT 20% ROE	% DIFFERENCE FROM LAMAR
Polysilicon (conventional)	N/A	107.98*	–
SiI_4	106.47	102.47	3.3
Silane UCC	13.65	13.59	0.5
Battelle BCL-A	17.53	17.39	0.8
Battelle BCL-B	15.55	15.46	0.6
Hemlock HSC-A	33.80	32.06	5.2
Hemlock HSC-B	33.73	32.00	5.1

*IPEG for new plant

Phase II: Probabilistic Cost Analysis

- Uncertainty in silicon cost is as important as the cost itself
- Single-cost estimate leads to unwarranted confidence in that number
- Level of detail of analysis affects the amount of information in the result
- Results and input data will be useful information to support future R&D decisions. Indicate risk and payoff

Methodology

- Using IPEG equation and SIMRAND model
- Based upon preliminary inputs encoded from contract managers (25 distributions)
- IPEG inputs: Plant investment, materials, utilities, and labor
  - Partial inputs encoded for each process step (Plant INV, MATS) or utility type (UTIL) or for total process (DLAB)
- SIMRAND totals partial inputs; then uses totals in IPEG equation

ORIGINAL PAGE IS
OF POOR QUALITY

SIMRAND

(SIMulation of Research ANd Development Model)

- **Originally designed for the allocation of limited R&D funds under uncertainty**
- **Is able to perform arithmetic operations with random variables (probabilistic inputs) using a Monte Carlo simulation technique**
- **Performs probabilistic analysis on systems too complex for practical application of probability theory**
- **Can incorporate equations supplied by the user. In this case, the IPEG equations were used**

Sample Encoded Distribution

Modified Siemens Electricity Usage

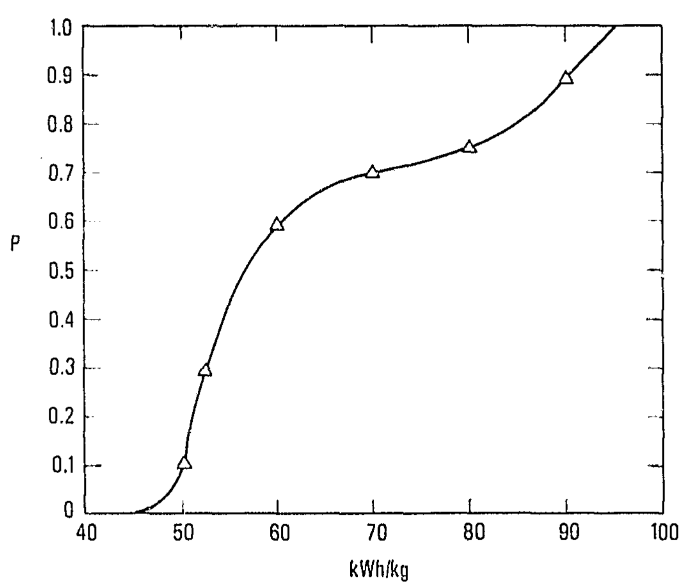

Insights from Input Data

Items With High Uncertainty and Payoff

Hemlock

- **Modified Siemens reactor equipment cost**
- **Solarelectronics equipment cost**
- **Modified Siemens reactor electricity use costs**

Union Carbide

- **Fluidized-bed reactor system equipment cost**
- **Silane production equipment costs**
- **Modified Siemens reactor system equipment cost**
- **Fluidized-bed reactor electricity use costs**
- **Modified Siemens electricity use costs**

Comparison of Results

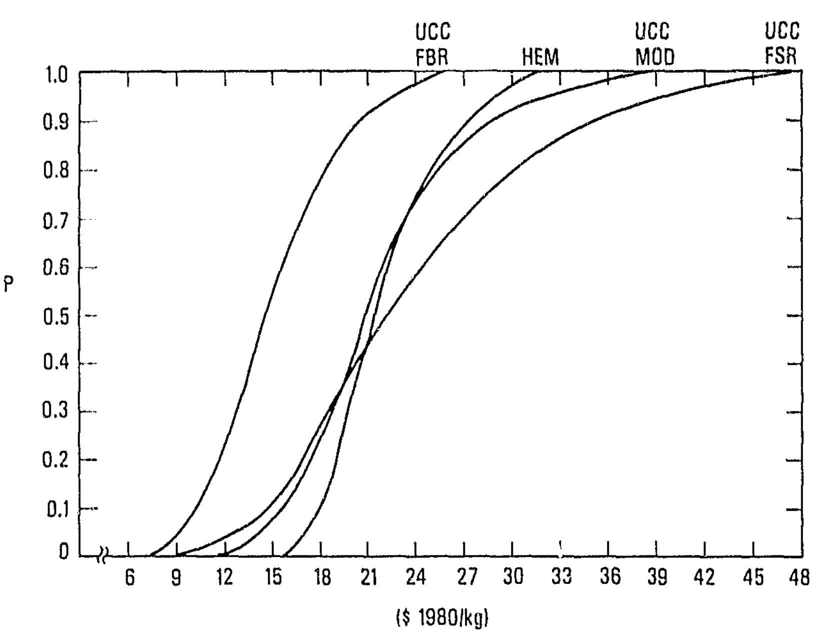

ORIGINAL PAGE IS
OF POOR QUALITY

Cost Drivers

HEMLOCK		UNION CARBIDE	
		Modified Siemens	
(1) Plant investment	(57-67%)	(1) Plant investment	(59-68%)
(2) Utilities	(13-24%)	(2) Utilities	(12-31%)
(3) Materials and supplies	(11-16%)	(3) Materials and supplies	(10-14%)
(4) Labor	(8-9%)	(4) Labor	(6-7%)
		Fluidized-Bed Reactor	
		(1) Plant investment	(53-74%)
		(2) Materials and supplies	(15-22%)
		(3) Utilities	(7-15%)
		(4) Labor	(8-10%)

Conclusions

- IPEG method is valid for silicon manufacturing processes
- Probabilistic inputs and outputs give more insight and information than point estimates
- Prospects for lower-cost silicon in the near- and mid-term future are promising
- Results are preliminary. Further analysis is scheduled

UBIQUITOUS CRYSTALLIZATION PROCESS

SEMIX INC.

W.F. Regnault

Principal Areas of Research

A. FUNDAMENTAL STUDIES OF SEMICRYSTALLINE MATERIAL

B. ELECTRICAL PROPERTY MEASUREMENTS

C. HIGH EFFICIENCY SEMICRYSTALLINE SOLAR CELLS

Areas of Fundamental Study

THE INTERFACE STRUCTURE OF GRAIN BOUNDARIES IN SEMICRYSTALLINE SILICON

THE STRUCTURAL EVALUATION OF LARGE GRAIN SEMICRYSTALLINE SILICON

The Interface Structure of Grain Boundaries in Semicrystalline Silicon

PURPOSE: TO ANALYZE THE STRUCTURAL AND ELECTRICAL PROPERTIES OF A BOUNDARY BETWEEN TWO GRAINS

APPROACH: DETERMINE THE RELATIVE ORIENTATION OF THE NEIGHBORING GRAINS

DETERMINE THE BOUNDARY INTERFACE POSITIONS

MEASURE THE ELECTRICAL ACTIVITY ALONG THE GRAIN BOUNDARY

Results

1. Grain Orientations In Polysilicon Material Are Related By Single Or Multiple Twinning Steps Which Results In Grain Boundaries Having A Varying Degree Of Electrical Activity.

   1. {221} / {221} Symmetric Coherent Second Order Twin Interface Has An Extremely Weak Electrical Response Due To The Relatively Few Dislocations Being Required To Account For The Misorientation Between The Grains.

   2. {115} / {111} and {326} / {735} Asymmetric Interface Structures Have A Larger Degree Of Electrical Activity Which Can Be Accounted For By Misfit Dislocations In The Interface.

   3. The Electrical Activity Of Grain Boundaries In Polysilicon Material Is Associated With The (Low Angle) Subgrain Boundary Component Of The Total Misorientation Between The Grains.

Structural Characterization of Large-Grain Semicrystalline Silicon

PURPOSE

INVESTIGATION OF THE DEVELOPMENT AND PROGRESSION OF A DISLOCATION SUBGRAIN STRUCTURE FOUND IN SEMICRYSTALLINE SILICON.

DETERMINATION OF THE CAUSATIVE FACTORS IN THE NUCLEATION OF THIS DEFECT STRUCTURE.

COMPARISON OF THE PHOTOVOLTAIC PROPERTIES ASSOCIATED WITH THE DEFECT AREA TO MORE TYPICAL REGIONS.

Approach

SELECT WAFERS AT REGULAR INTERVALS THROUGH UCP INGOT

TEXTURE AND DEFECT ETCH ADJACENT WAFERS TO SELECT REGIONS OF INTEREST

ANALYZE WAFERS BY MEANS OF:

OPTICAL MICROSCOPY;
LAUE ORIENTATION STUDIES;
X-RAY TOPOGRAPHY;
PHOTORESPONSE MEASUREMENTS

Orientation Studies

TO DETERMINE THE CRYSTALLOGRAPHIC RELATIONSHIP BETWEEN NEIGHBORING GRAINS

TO DETERMINE REFLECTING PLANES FOR TOPOGRAPHIC WORK

Results

AS IN PREVIOUS STUDIES NEIGHBORING GRAINS IN SILICON PRODUCED VIA THE UCP ARE CRYSTALLOGRAPHICALLY RELATED THROUGH TWINNING MECHANISMS:

- GRAINS A&B ARE RELATED THROUGH A 2ND ORDER TWINNING PROCESS CONTAINING A COHERENT {221}/{221} INTERFACE

- GRAINS A&C ARE 1ST ORDER TWINS WITH A {111}/{111} INTERFACE

BOTH ARE SYMMETRIC ABOUT THESE INTERFACES

Development of Subgrain Structure

PURPOSE: TO DETERMINE THE NUCLEATING MECHANISM FOR THE SUBGRAIN STRUCTURE

APPROACH: SUBJECT SEQUENTIAL WAFERS TO A DEFECT ETCH EXAMINE REGION WHERE SUBGRAIN STRUCTURE NUCLEATING BY X-RAY TOPOGRAPHY AND OPTICAL MICROSCOPY

Results

LANG X-RAY TRANSMISSION TOPOGRAPHY REVEALS A HIGH DENSITY OF DISLOCATION ASSOCIATED WITH SUBGRAIN STRUCTURE AT THE SUBGRAIN BOUNDARIES

BERG-BARRETT SURFACE TOPOGRAPHY SHOWS SUBGRAINS ROTATED OUT OF REFLECTING POSITION

OPTICAL MICROSCOPY REVEALS GRAIN BOUNDARY FACETING BETWEEN GRAINS A&C

DEFECT ETCH SHOWS DISLOCATION DENSITY ON THE ORDER OF $10^5/CM^2$ IN REGION OF SUBGRAIN ROTATIONS WITH A DENSITY OF $10^3/CM^2$ OUTSIDE THESE REGIONS

ETCH PIT PATTERN INDICATES DISLOCATIONS DUE TO SLIP ON (111) TYPE PLANES

BERG-BARRETT SURFACE TOPOGRAPH AND DEFECT ETCH SHOW CONTINUED WORSENING OF SUBGRAIN STRUCTURE AS GRAIN GROWTH PROCEEDS.

Photovoltaic Properties

PURPOSE: TO ESTABLISH THE EFFECT OF THE SUBGRAIN STRUCTURE ON THE PHOTORESPONSE OF A CELL

APPROACH: DIFFUSED JUNCTION N ON P DEVICES WERE MADE ON THE AREAS STUDIED BY X-RAY TOPOGRAPHY

HIGH RESOLUTION LIGHT SPOT SCANS AT 1.0μM AND 0.65μM WERE MADE OVER THE AFFECTED AREAS

Results

AM1 SHORT CIRCUIT CURRENT DENSITY OF 22.5 MA/CM^2 OBTAINED ON NON AR COATED CELL CONTAINING DEFECT REGION

AS EXPECTED THE DISLOCATION SUBGRAIN BOUNDARIES SHOWED THE MOST ELECTRICAL ACTIVITY

THE LONG WAVELENGTH SCAN DID NOT SHOW ANY APPRECIABLE EFFECT DUE TO THE DISLOCATION STRAIN FIELD.

Conclusions

DURING GRAIN GROWTH AND SUBSEQUENT COOL DOWN, STRESS BUILDS UP ALONG THE FACETED GRAIN BOUNDARY BETWEEN THE GRAINS LABELED A&C

THE GRAIN BOUNDARY CONTAINS NUMEROUS DISLOCATIONS ALONG THE STEPS

STRESS BUILDS UP IN GRAIN A DUE TO INTERACTION OF THE DISLOCATION STRAIN FIELDS

GRAIN A DEFORMS BY SLIP DUE TO THE STRESS CONCENTRATION

THE TWIN STRUCTURE OF GRAIN C IS PROBABLY CAUSED BY THE SAME MECHANISM

Electrical Property Measurements

MEASUREMENTS OF VARIATIONS IN MINORITY CARRIER LIFETIME DUE TO MICROSTRUCTURAL DEFECTS IN LARGE AREA SEMICRYSTALLINE SILICON WAFERS

PURPOSE: DEVELOP A TECHNIQUE TO DISTINGUISH BETWEEN STRUCTURAL AND IMPURITY RELATED MINORITY CARRIER LIFETIME DEGRADATION MECHANISMS

EVALUATE THE MINORITY CARRIER LIFETIME HOMOGENEITY OF LARGE AREA POLYSILICON WAFERS

Approach

ORIGINAL PAGE IS OF POOR QUALITY

SELECT FOUR SERIAL 10cm x 10cm SECTIONS FROM TWO DIFFERENT UCP INGOTS DENOTED A AND B

TEXTURE ETCH ONE WAFER FOR VISUAL EXAMINATION

DEFECT ETCH (SECCO) ONE WAFER

FABRICATE SIXTEEN 2cm x 2cm CELLS ON ONE WAFER

DETERMINE MINORITY CARRIER DECAY TIME USING A CONTACTLESS MICROWAVE REFLECTION TECHNIQUE ON THE FOURTH WAFER

9.2 5.4	4.2 6.7	9.4 7.6	9.4 7.2
9.2 3.7	7.5 10.6	3.8 6.8	6.6 4.0
9.6 4.7	3.4 2.1	8.6 9.2	10.0 12.8
5.9 9.2	5.2 10.2	11.4 13.4	9.6 11.2

Ingot A, microwave decay time, in μsec.

100 (54)	100 (55)	101 (55)	101 (55)
96 (54)	98 (53)	96 (51)	93 (49)
99 (53)	93 (49)	97 (52)	97 (52)
99 (54)	94 (50)	99 (54)	97 (52)

Ingot A, AM0 and (red) short-circuit current in mA.

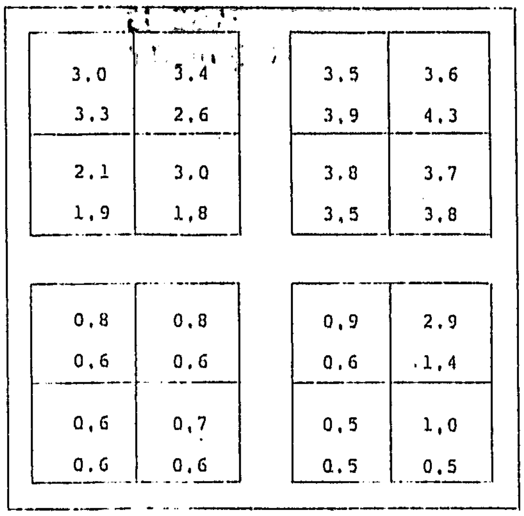

Ingot B, microwave decay time, in μsec.

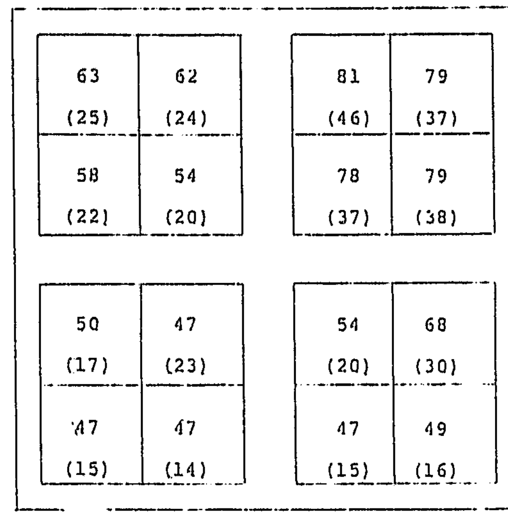

Ingot B, AMO and (red) short-circuit current, in mA.

AMO and Red I_{sc} of Solar Cells From Ingots A and B as a Function of Microwave Decay

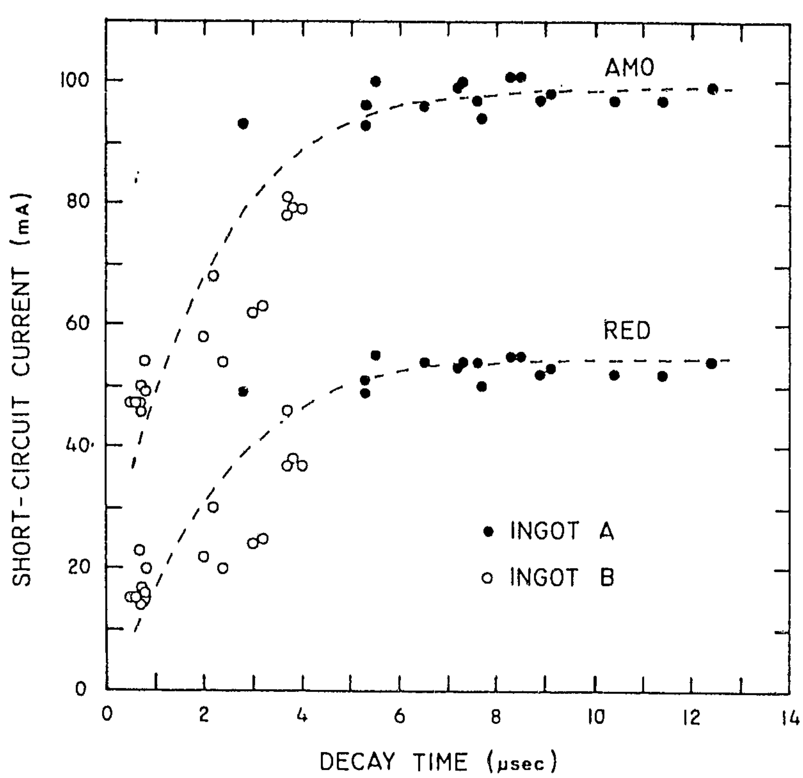

ORIGINAL PAGE IS
OF POOR QUALITY

Results

GOOD CORRELATION IS OBTAINED BETWEEN THE MEASURED MICROWAVE DECAY TIME AND THE SHORT-CIRCUIT CURRENT

AREAS OF LOW LIFETIME WERE FOUND TO BE CAUSED BY:

- SUBGRAIN BOUNDARIES AND DISLOCATION DENSITIES EXCEEDING 10^5 IN INGOT A

- IMPURITY EFFECTS IN INGOT B

Conclusion

THE CONTACTLESS MICROWAVE REFLECTION TECHNIQUE IN COMBINATION WITH A DEFECT ETCH HAS SHOWN TO BE AN EFFECTIVE WAY OF DISTINGUISHING MINORITY CARRIER LOSS MECHANISMS

High-Efficiency Semicrystalline Solar Cells

PURPOSE: DEMONSTRATION OF MATERIAL QUALITY

APPROACH: FABRICATE 2cm x 2cm AND 10cm x 10cm CELLS USING STATE-OF-THE-ART PROCESSING SEQUENCES

ORIGINAL PAGE IS
OF POOR QUALITY

UCP Solar Cells

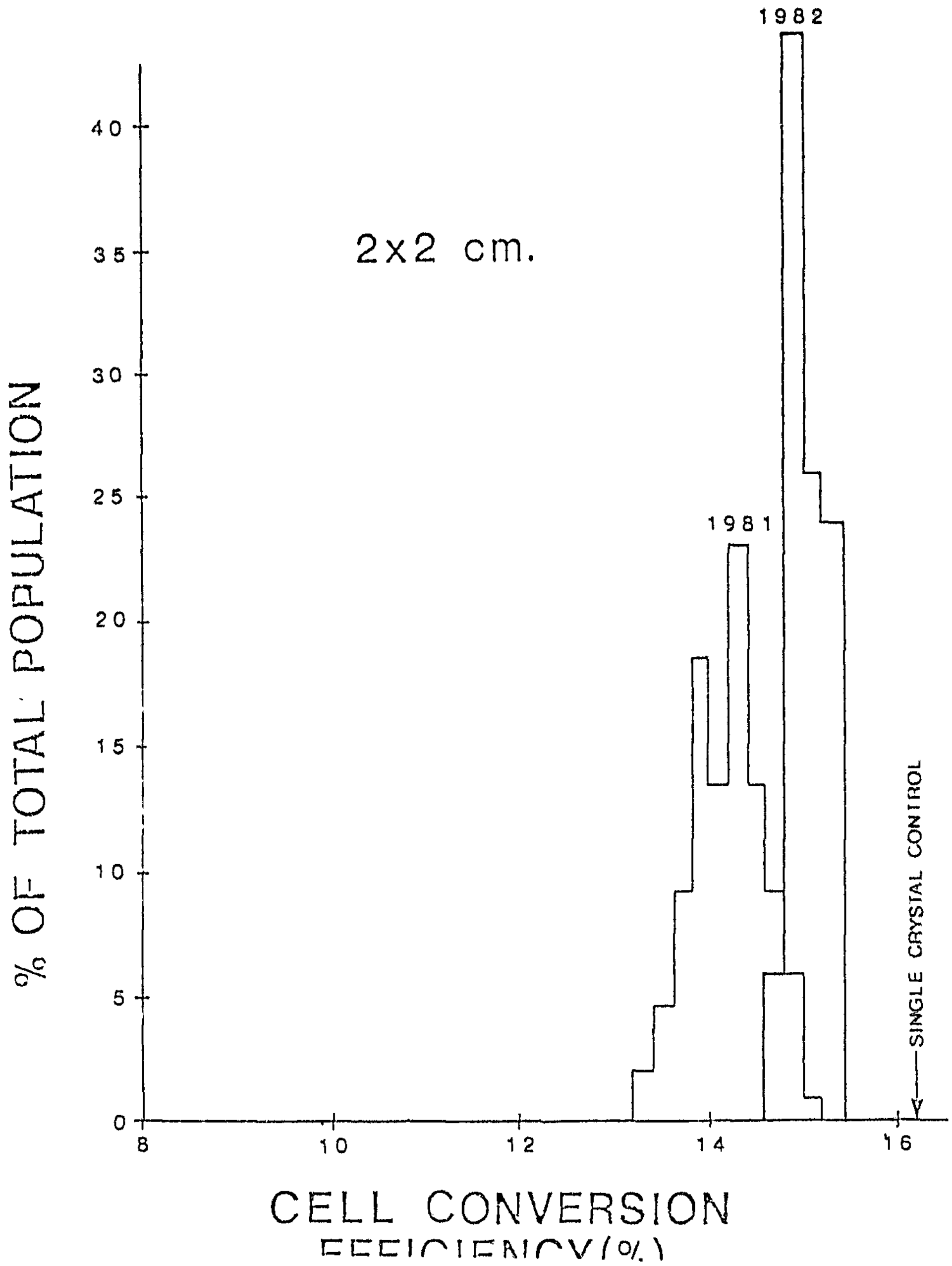

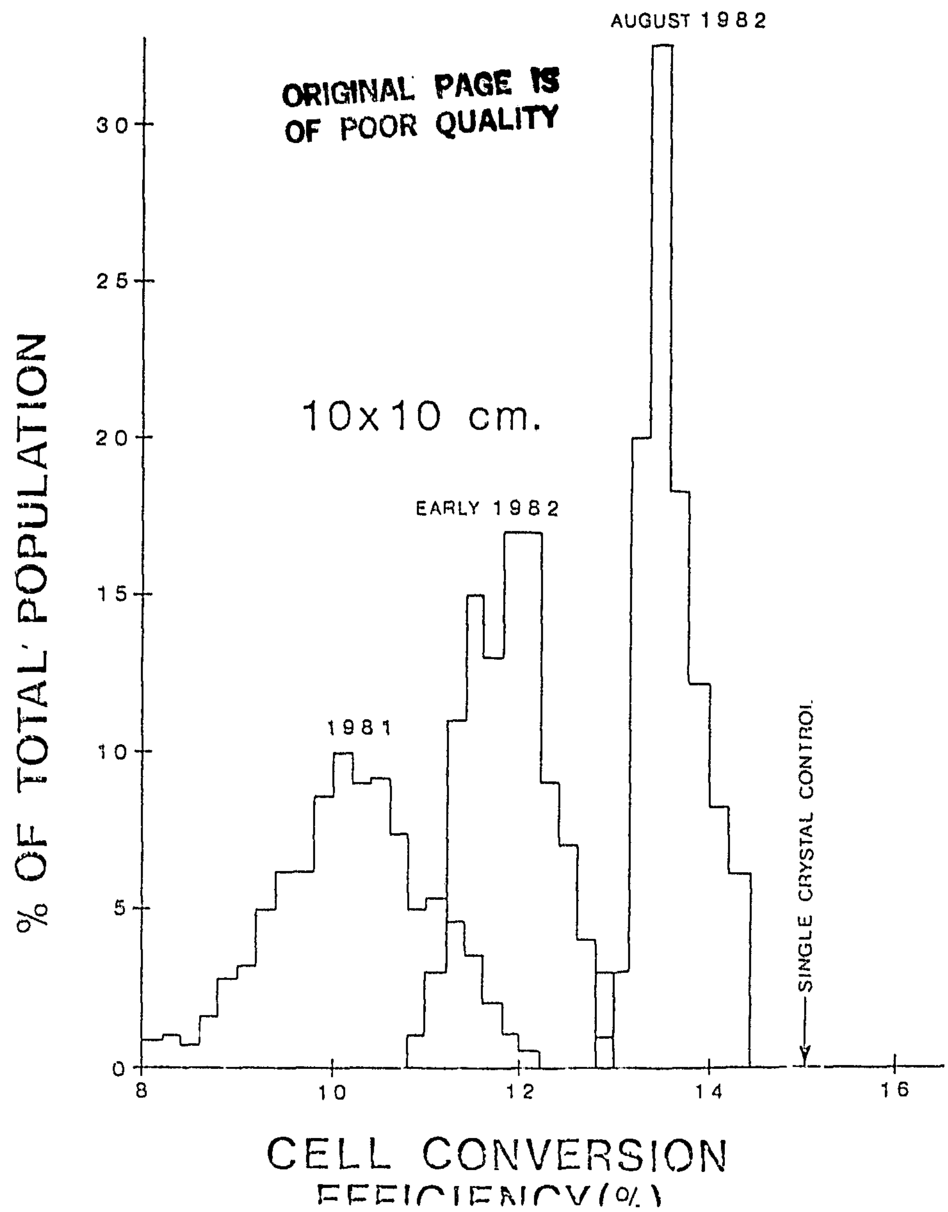

AUGUST 1982
ORIGINAL PAGE IS
OF POOR QUALITY
10x10 cm.
EARLY 1982
1981
SINGLE CRYSTAL CONTROL
% OF TOTAL POPULATION
0
5
10
15
20
25
30
8
10
12
14
16
CELL CONVERSION
EFFICIENCY(%)

AN OVERVIEW OF CAST SILICON MATERIALS

JET PROPULSION LABORATORY

S. Hyland
K. Dumas
T. Daud

IBM

G.H. Schwuttke
P. Smetana
K.A. Kim
J.A.A. Engelbrecht

APPLIED SOLAR ENERGY CORP.

D. Leung
P. Iles

STUDY OF SILICON CAST BY THREE MATURE TECHNIQUES

Types of Cast Silicon Studied

SILSO (WACKER CHEMITRONIC)

- DIRECTIONALLY SOLIDIFIED INGOT
- COLUMNAR, SMALL GRAINS (0.15 cm) IN CENTER
- LONG, NARROW GRAINS AT THE EDGES, NUCLEATING FROM THE SIDES OF THE CRUCIBLE

HEAT-EXCHANGER METHOD (CRYSTAL SYSTEMS)

- DIRECTIONALLY SOLIDIFIED INGOT FROM SEED AT BOTTOM OF CRUCIBLE
- SINGLE CRYSTAL CENTER "CONE"
- LARGE GRAIN POLYCRYSTALLINE AROUND EDGES (0.3 cm)

UBIQUITOUS CRYSTALLIZATION PROCESS (SEMIX)

- DIRECTIONALLY SOLIDIFIED INGOT*
- MEDIUM GRAIN (0.2 cm) CENTRAL CORE
- VERY LARGE GRAIN (> 2 cm) EDGES

*BASED ON PREVIOUS WORK

Optical Photographs of Cast Si Wafers

a)

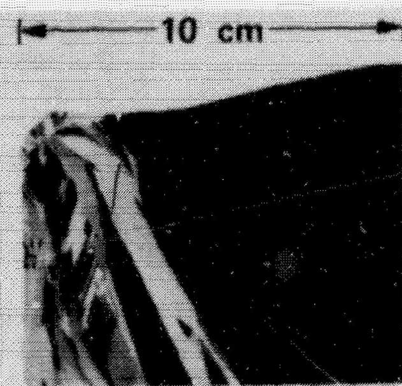

b)

c)

a) SILSO

b) HEM

c) UCP

Optical Photographs of Dislocations
Caused by Stress in UCP

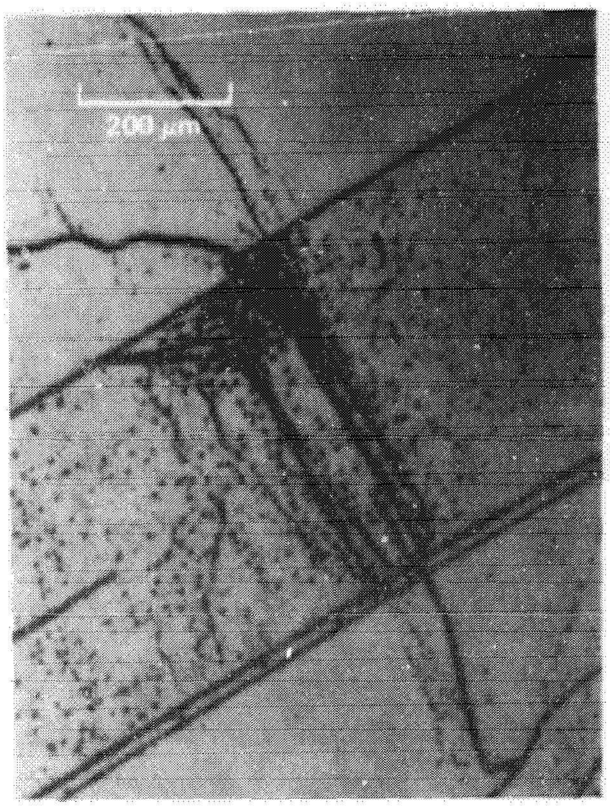

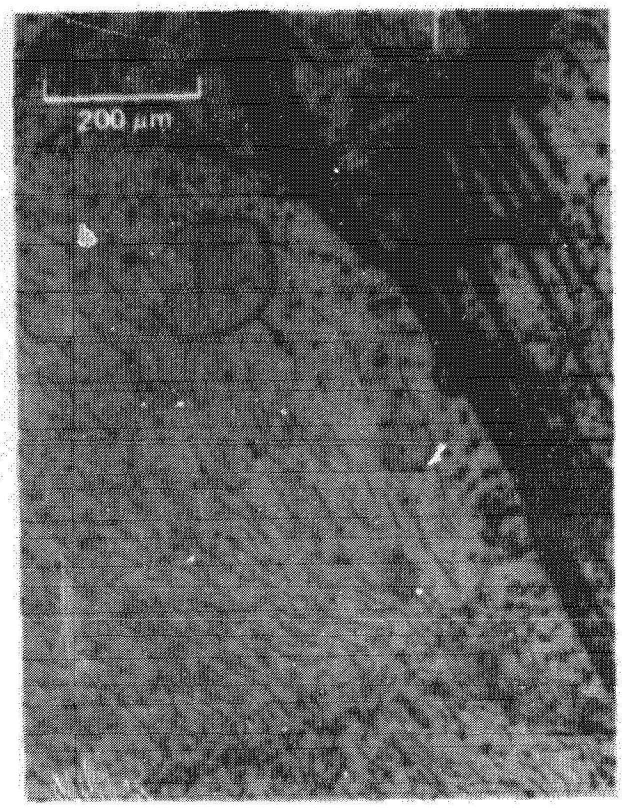

Optical Photograph of Silicon Carbide
Precipitate in HEM

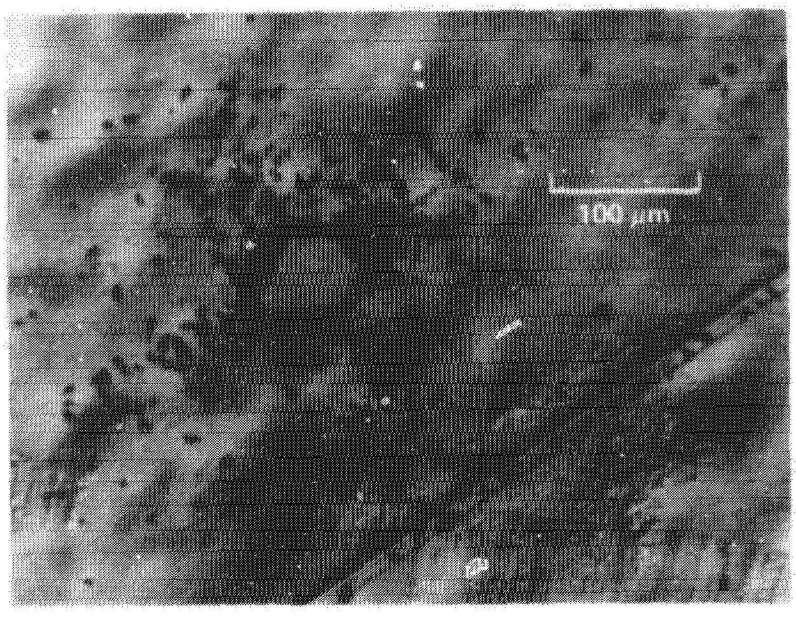

TEM Micrograph of Cellular Structure in HEM

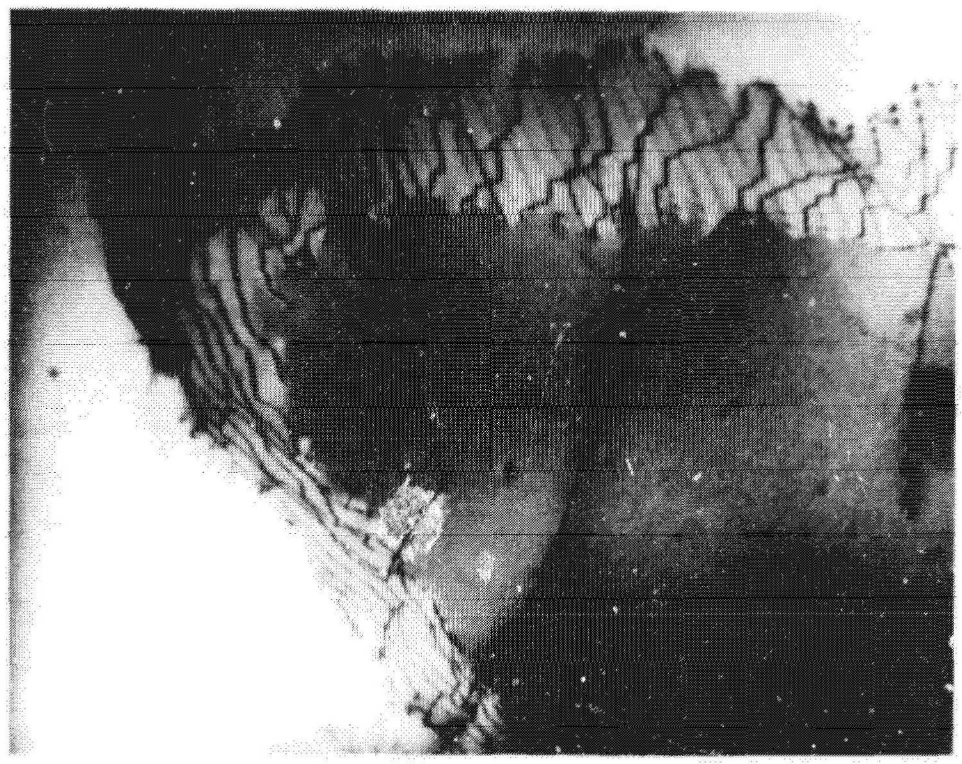

AM1 Solar-Cell Performance

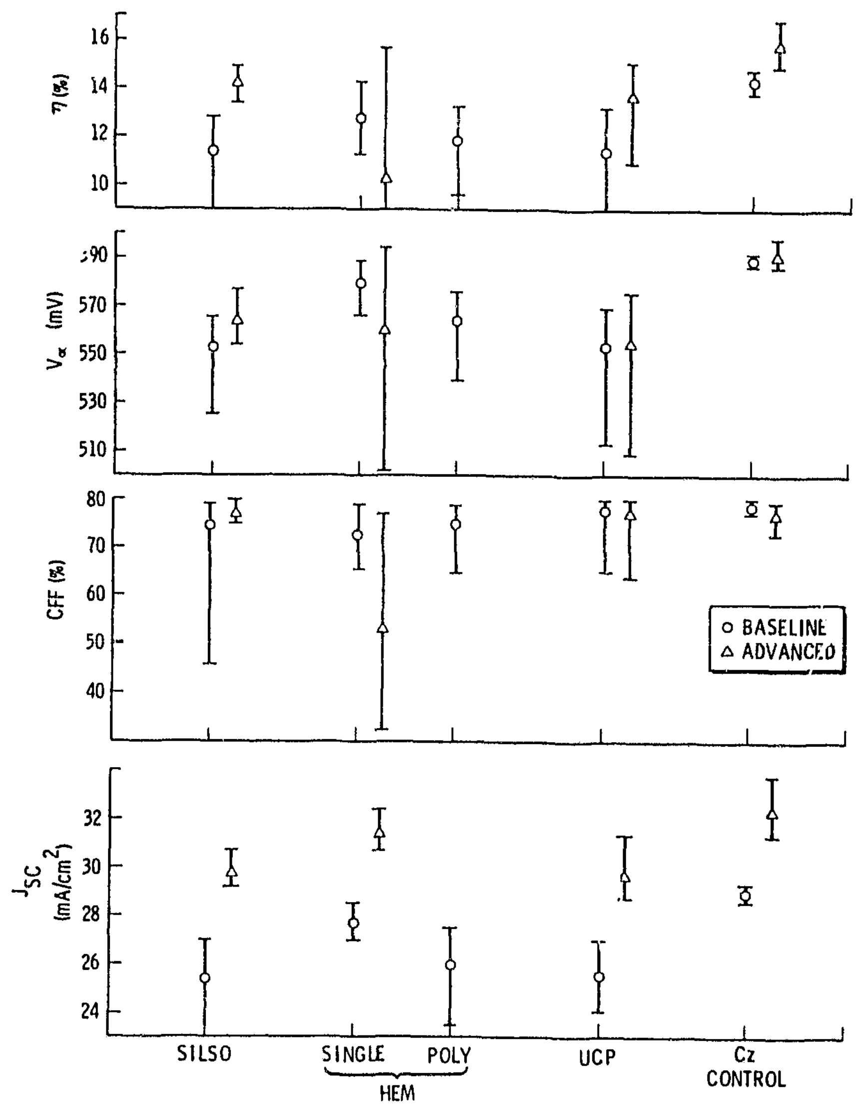

Conclusions

- THESE THREE CASTING METHODS HAVE PRODUCED SOLAR CELLS WITH COMPARABLE LEVELS OF EFFICIENCY
- EFFICIENCIES OF SOLAR CELLS MADE BY ADVANCED PROCESSES SHOW THAT THE EXPECTED MAXIMUM EFFICIENCIES OF THE THREE MATERIALS ARE COMPARABLE
- CELL EFFICIENCIES ARE LIMITED BY:
  - DISLOCATIONS
  - PRECIPITATES
  - DISLOCATION CELLULAR STRUCTURE

STUDY OF SILICON SOLIDIFICATION BY THE OSCILLATING CRUCIBLE TECHNIQUE

Introduction

1. NECESSARY CONDITIONS FOR SEEDED SINGLE CRYSTAL GROWTH (SCHEEL AND SCHULZ-DUBOIS)
   A. CONTROL OF NUCLEATION
   B. FAST LIQUID FLOW AT LIQUID-SOLID INTERFACE
   C. PREVENTION OF CONSTITUTIONAL SUPERCOOLING
   D. PREVENTION OF DENDRITIC GROWTH AFTER NUCLEATION

2. PRESENT TECHNIQUES OF DIRECTIONAL SOLIDIFICATION
   - UNSEEDED GROWTH GIVES GRAIN BOUNDARIES AND DISLOCATIONS IN SILICON
   - SEEDED GROWTH GIVES CELLULAR DISLOCATION NETWORKS IN SILICON

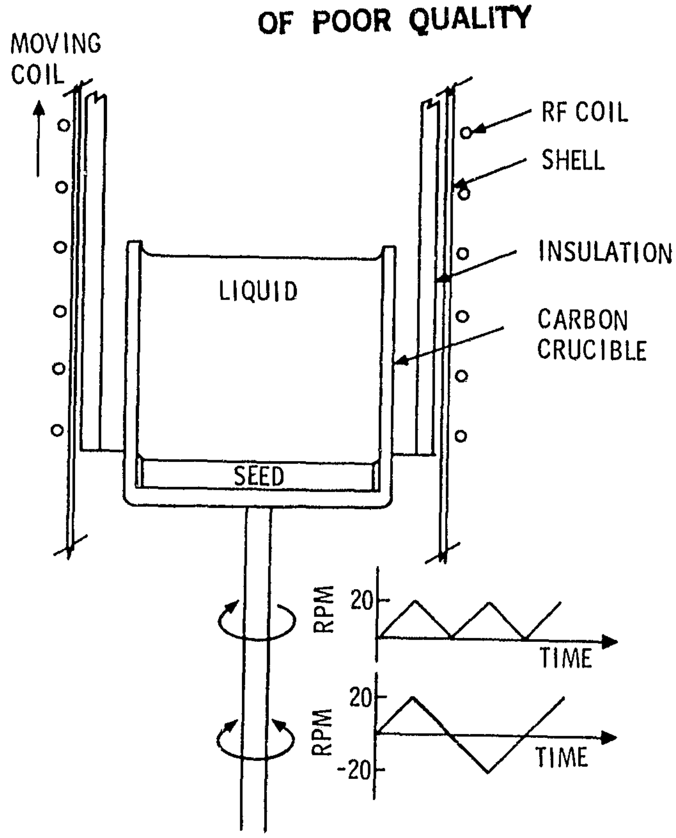
MOVING COIL
RF COIL
SHELL
INSULATION
CARBON CRUCIBLE
LIQUID
SEED
RPM
20
TIME
20
-20
TIME

Vertical Section Micrographs

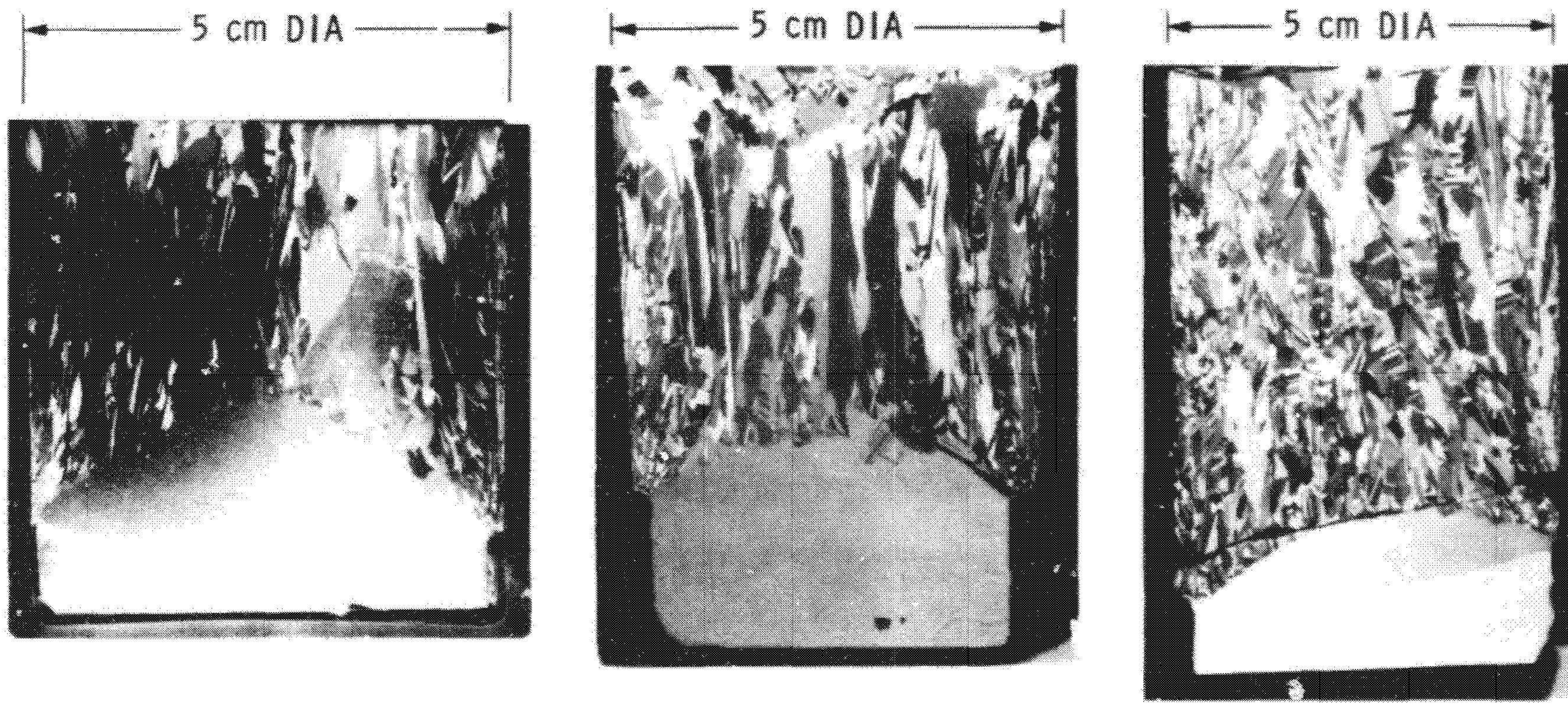

a) INGOT 7
(CRUCIBLE RPM 0:20:0
SOLIDIFICATION RATE
4.2 cm/hr)

b) INGOT 9
(CRUCIBLE RPM 0:20:0:-20:0
SOLIDIFICATION RATE
4.2 cm/hr)

c) INGOT 11
(STATIONARY CRUCIBLE
SOLIDIFICATION RATE
15.0 cm/hr)

ORIGINAL PAGE IS
OF POOR QUALITY

Characterization Summary

- SEEDED SINGLE CRYSTAL GROWTH
- LARGE AREA STACKING FAULTS IN SINGLE CRYSTAL REGIONS
- OSCILLATING CRUCIBLE
  - GRAINS ALONG CRUCIBLE WALLS SAME ORIENTATION AS SEED
  - COLUMNAR GRAINS NUCLEATING FROM SINGLE CRYSTAL GROWTH
- STATIONARY CRUCIBLE
  - RANDOMLY ORIENTED GRAINS

Solar Cell Efficiency Distribution, Ingots 7 Through 10

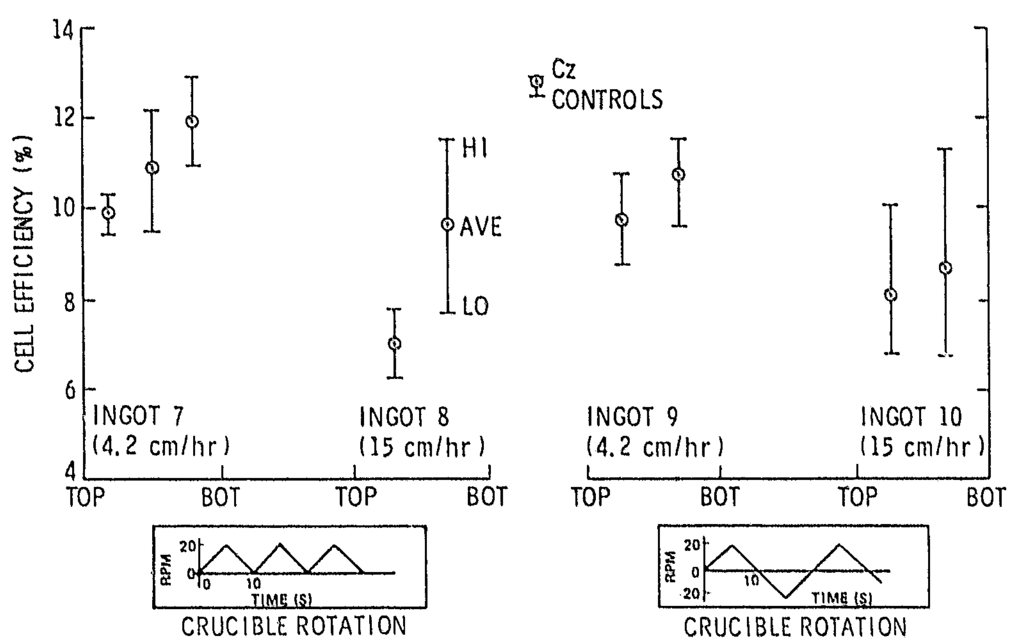

Conclusions

1. NEW TECHNIQUE FOR SEEDED SILICON INGOT GROWTH (APPLICABLE TO OTHER GROWTH TECHNIQUES)

2. CAPABLE OF GIVING GOOD QUALITY SEEDED GROWTH

3. COLUMNAR GRAINS WITH SAME ORIENTATION

4. 12.9% AM1 EFFICIENCY DEMONSTRATED

5. MINORITY CARRIER DIFFUSION LENGTHS
   - SINGLE CRYSTAL REGIONS $\sim 200\ \mu m$
   - POLYCRYSTALLINE REGIONS $\sim 100\ \mu m$

Future Work

1. BETTER THERMAL PROFILE CONTROL

2. USE OF LARGER CRUCIBLES

3. USE OF NONCARBON CRUCIBLES

4. OPTIMIZE CRUCIBLE ROTATION AND GROWTH SPEED

ANALYSIS OF DEFECT STRUCTURE IN SILICON

MATERIALS RESEARCH, INC.

Position of Wafers From UCP Ingot 5848-13C

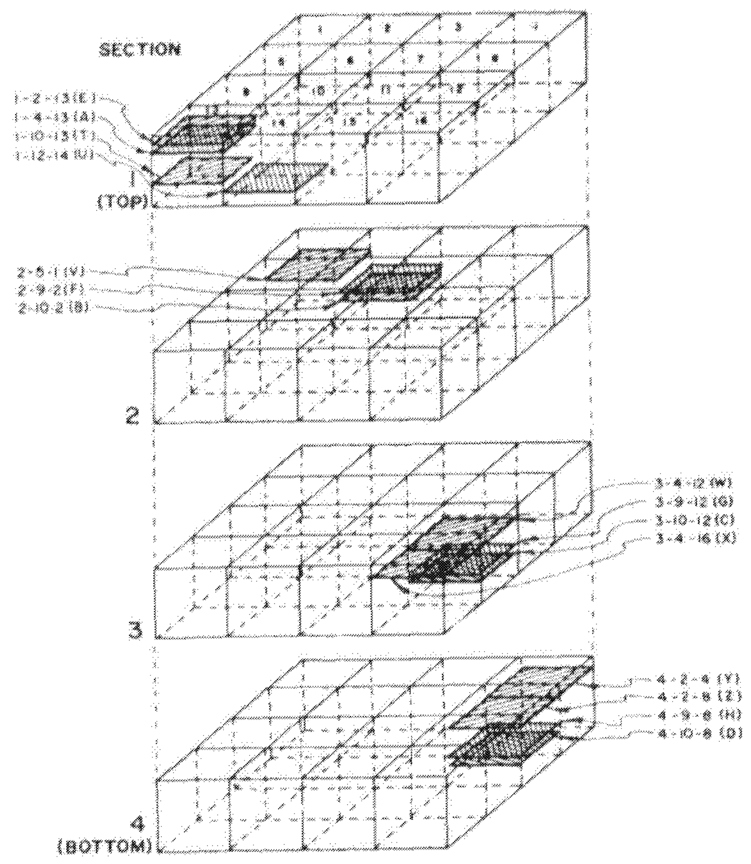

Relative Positions of the Measured Fields on the Semix Wafers

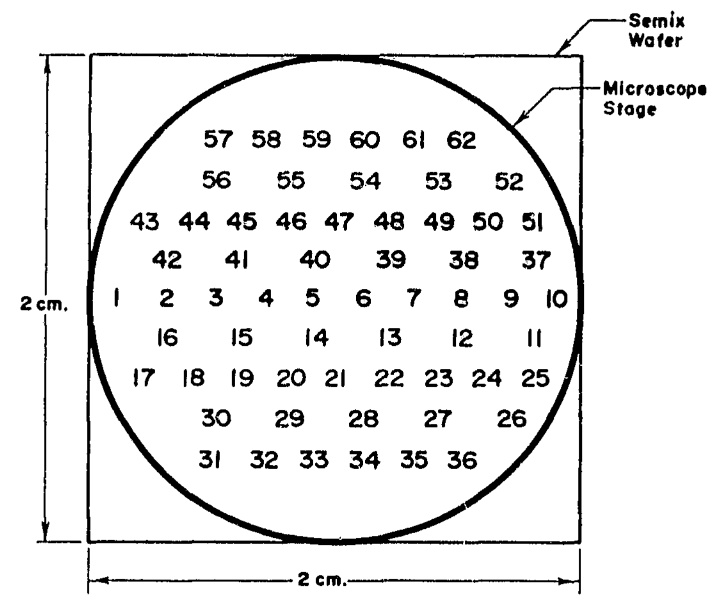

ORIGINAL PAGE IS
OF POOR QUALITY

Grain Boundary and Twin Boundary Length per Unit Area in the Semix Samples

SEMIX Sample Number	Grain Boundary Length per unit area (cm/cm^2)	Twin Boundary Length per unit area (cm/cm^2)
A - 13	8.2 $\bar{x}$ = 2.9 σ = 2.0	99.0 $\bar{x}$ = 34.6 σ = 56.5
B - 2	4.5 $\bar{x}$ = 1.6 σ = 2.2	15.8 $\bar{x}$ = 5.6 σ = 9.3
C - 12	13.4 $\bar{x}$ = 4.7 σ = 2.7	31.9 $\bar{x}$ = 11.2 σ = 11.1
D - 8	13.8 $\bar{x}$ = 4.8 σ = 3.2	44.5 $\bar{x}$ = 15.6 σ = 17.1
E - 13	7.1 $\bar{x}$ = 2.5 σ = 2.1	68.5 $\bar{x}$ = 24 σ = 38
F - 2	5.4 $\bar{x}$ = 1.9 σ = 2.6	12.2 $\bar{x}$ = 4.3 σ = 6.8
G - 12	12.1 $\bar{x}$ = 4.2 σ = 2.6	40.7 $\bar{x}$ = 14.3 σ = 15.5
H - 8	9.4 $\bar{x}$ = 3.3 σ = 1.9	35.9 $\bar{x}$ = 12.6 σ = 13.3
Average for all samples	9.2	43.6

$\bar{x}$ = arithmetic mean = $\dfrac{\sum \text{features in all fields}}{\text{Total number of fields}}$

σ standard deviation = $\left[\dfrac{1}{n-1} \sum_{i=1}^{n} (x_i - \bar{x})^2\right]^{1/2}$

32

Precipitate Particle and Dislocation Density in Semix Samples

SEMIX Sample Number	Precipitate Particle Density (particles/cm^2)			Dislocation Density (pits/cm^2)
	small	large	total	
A - 13	22×10^3 $\bar{x} = 33$ $\sigma = 36.5$	745 $\bar{x} = 1.1$ $\sigma = 1.5$	23×10^3	4.9×10^4 $\bar{x} = 12$ $\sigma = 23$
B - 2	19.5×10^3 $\bar{x} = 29.1$ $\sigma = 18.1$	444 $\bar{x} = 0.66$ $\sigma = 0.95$	20×10^3	9.5×10^4 $\bar{x} = 23$ $\sigma = 45$
C - 12	6.2×10^3 $\bar{x} = 9.2$ $\sigma = 7.7$	65 $\bar{x} = 0.1$ $\sigma = 0.4$	6.3×10^3	37×10^4 $\bar{x} = 89$ $\sigma = 62$
D - 8	2.5×10^3 $\bar{x} = 3.8$ $\sigma = 4.0$	152 $\bar{x} = 0.23$ $\sigma = 0.46$	2.7×10^3	10×10^4 $\bar{x} = 24$ $\sigma = 51$
E - 13	9.1×10^3 $\bar{x} = 13.5$ $\sigma = 10.6$	400 $\bar{x} = 0.6$ $\sigma = 0.7$	9.5×10^3	37×10^4 $\bar{x} = 89$ $\sigma = 96$
F - 2	4.8×10^3 $\bar{x} = 7.2$ $\sigma = 10.5$	740 $\bar{x} = 1.1$ $\sigma = 2.1$	5.6×10^3	17×10^4 $\bar{x} = 40$ $\sigma = 111$
G - 12	6.4×10^3 $\bar{x} = 9.6$ $\sigma = 8.0$	140 $\bar{x} = 0.21$ $\sigma = 0.41$	6.6×10^3	45×10^4 $\bar{x} = 108$ $\sigma = 161$
H - 8	9.5×10^3 $\bar{x} = 14.1$ $\sigma = 10.9$	250 $\bar{x} = 0.4$ $\sigma = 0.8$	9.7×10^3	86×10^4 $\bar{x} = 204$ $\sigma = 235$
Avg. for all samples	10.0×10^3	367	10×10^3	31×10^4

For precipitate particle density, 2.3% of the total area was measured.

For dislocation pit density, 0.37% of the total area was measured.

ORIGINAL PAGE IS
OF POOR QUALITY

Defect Density, Conversion Efficiency, and Diffusion Length of Semix Samples

SEMIX Sample number	Large precipitate density (cm^{-2})	Dislocation density (cm^{-2})	Grain boundary length per unit area (cm^{-1})	Twin boundary length per unit area (cm^{-1})	Cell efficiency* (%)	Diffusion length* (μm)
A - 13	745	4.9×10^4	8.2	99.0	7.2	53
B - 2	444	9.5×10^4	4.5	15.8	10.0	51
C - 12	65	37×10^4	13.4	31.9	9.7	41
D - 8	152	10×10^4	13.8	44.5	10.8	47
E - 13	400	37×10^4	7.1	68.5	6.2	35
F - 2	740	17×10^4	5.4	12.2	9.6	22
G - 12	140	45×10^4	12.1	40.7	9.5	19
H - 8	250	86×10^4	9.4	35.9	10.7	31

Twin Boundary Length per Unit Area vs Relative Position of Wafer From Top of Solidified Ingot

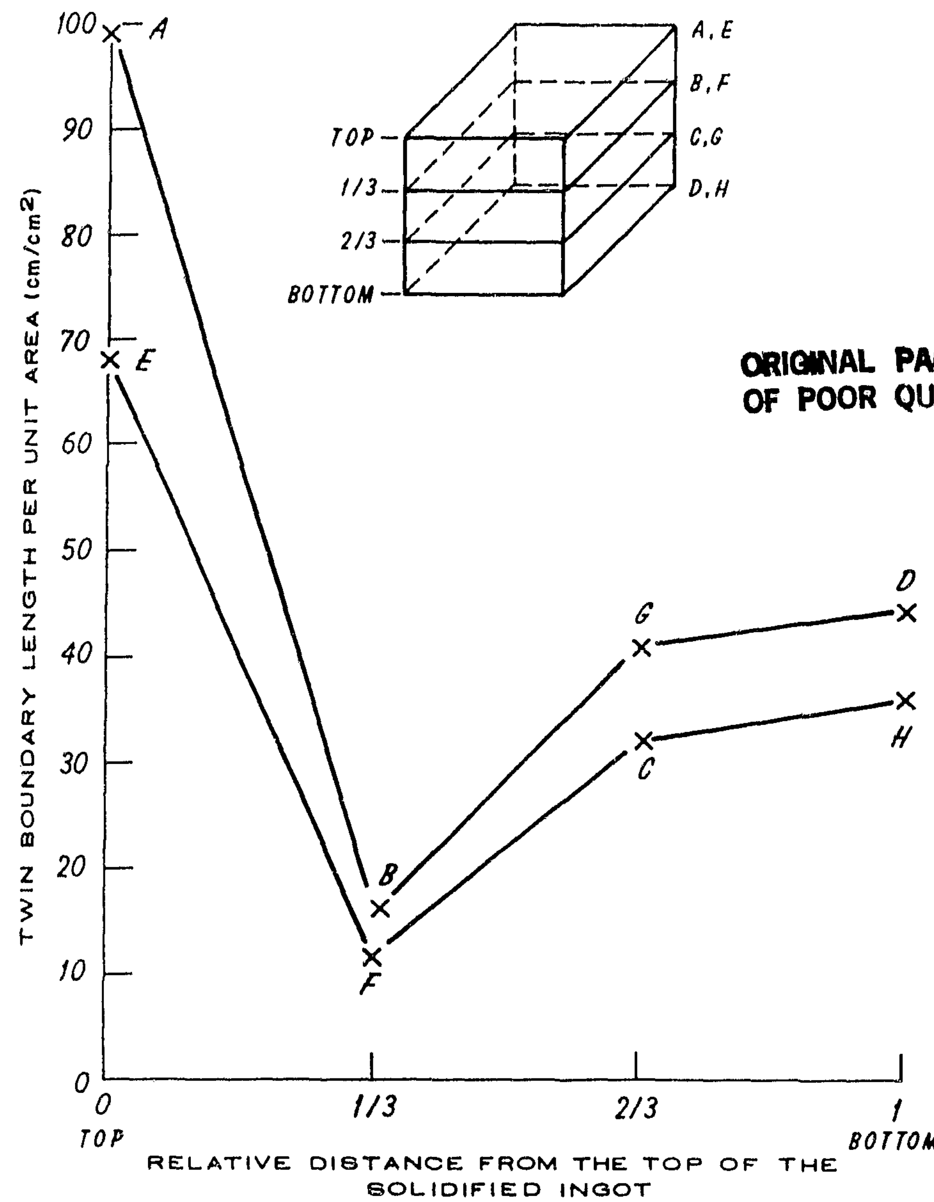

Twin Boundary Length per Unit Area
vs Grain Boundary Length per Unit Area

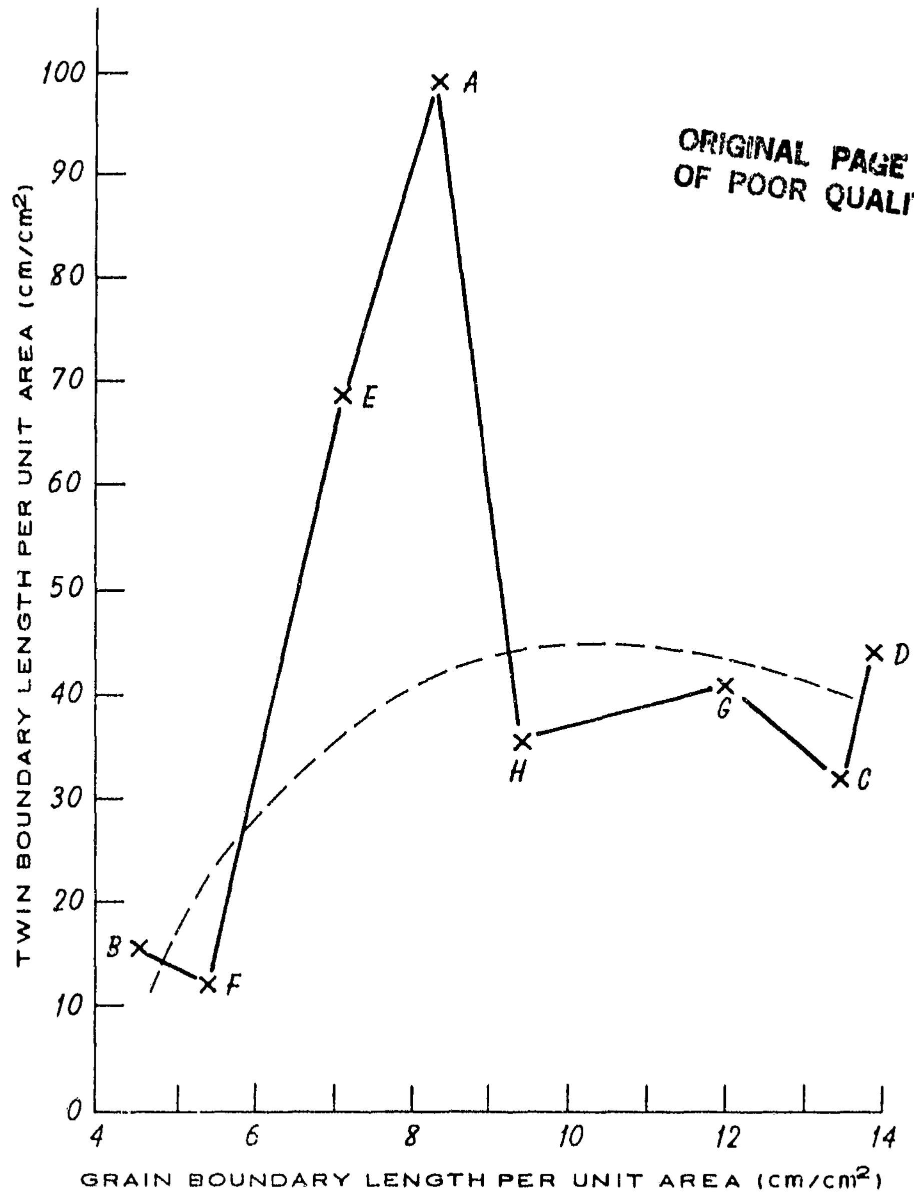

Dislocation Pit Density vs Large Precipitate Particle Density

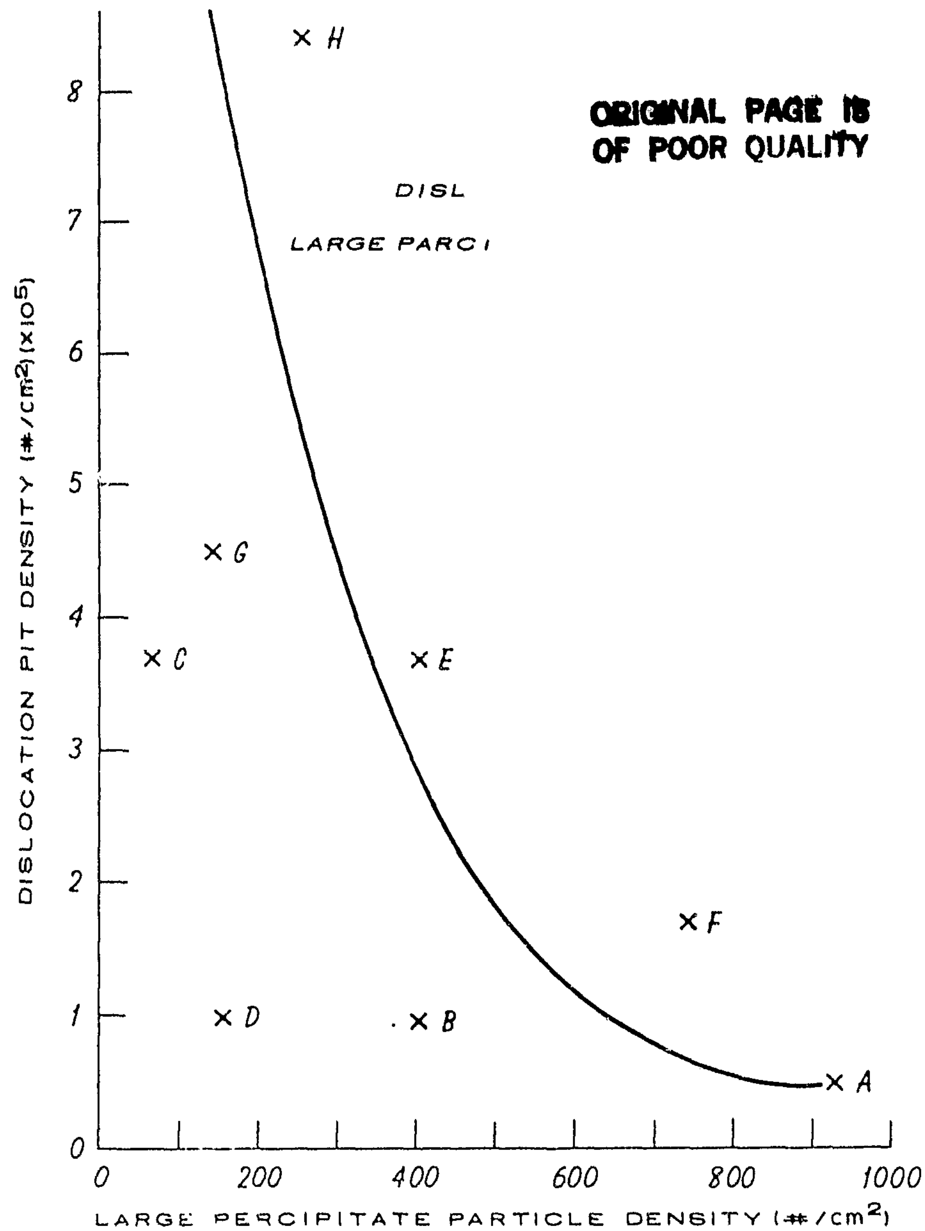

Solar Cell Efficiency vs Twin Boundary Density (cm / cm^2)

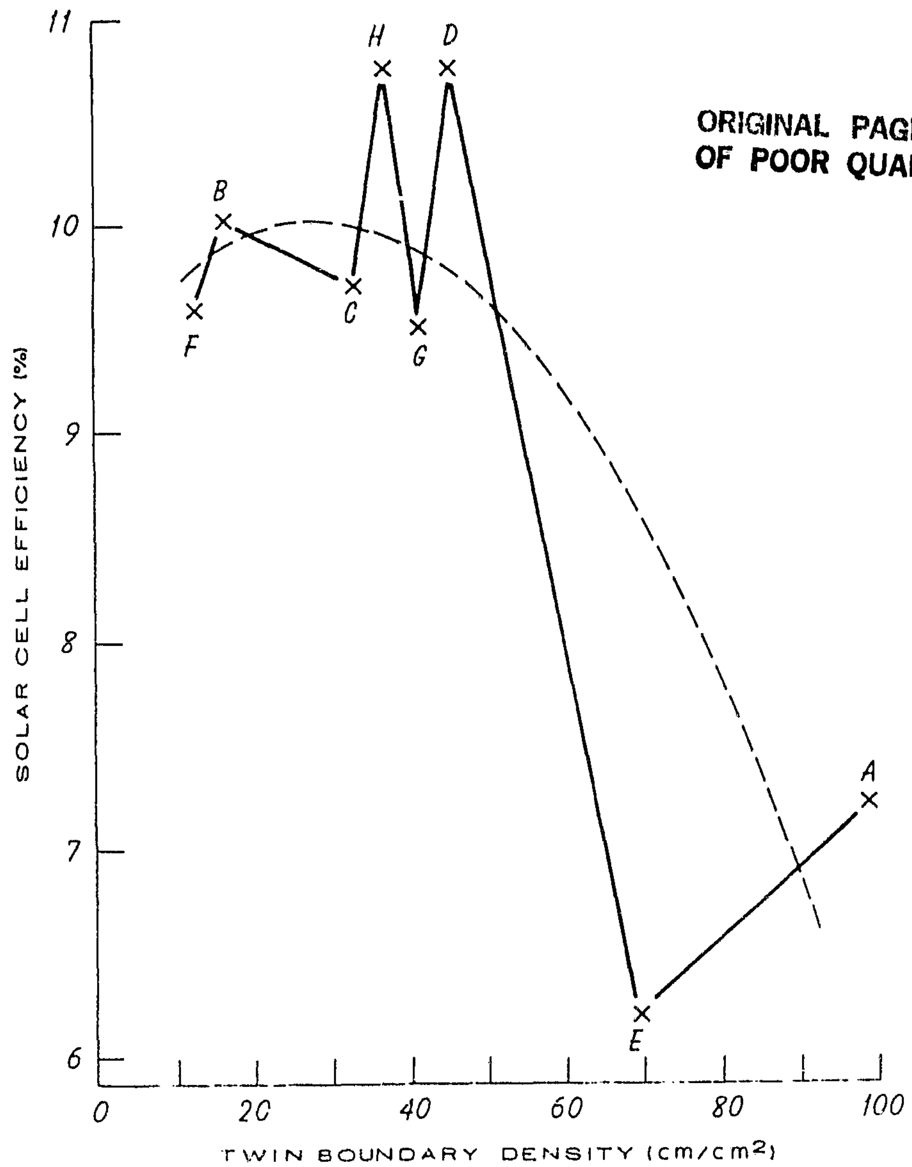

Diffusion Length vs Dislocation Pit Density

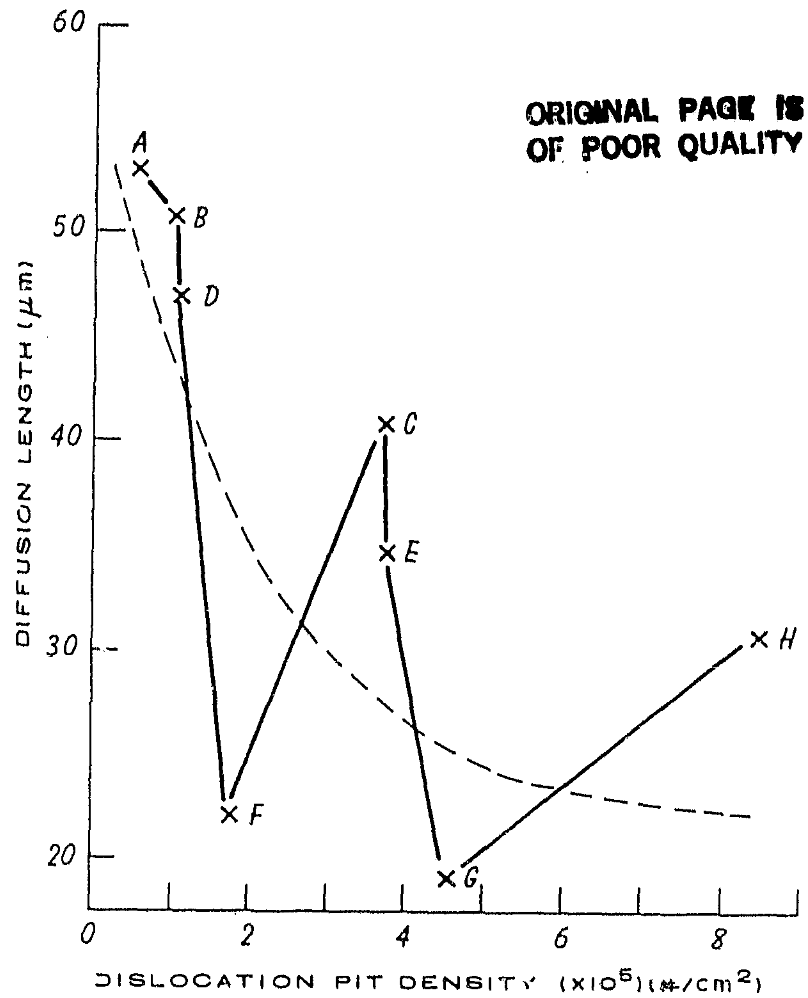

ORIGINAL PAGE IS
OF POOR QUALITY

Precipitate Density vs Relative Position in the Ingot

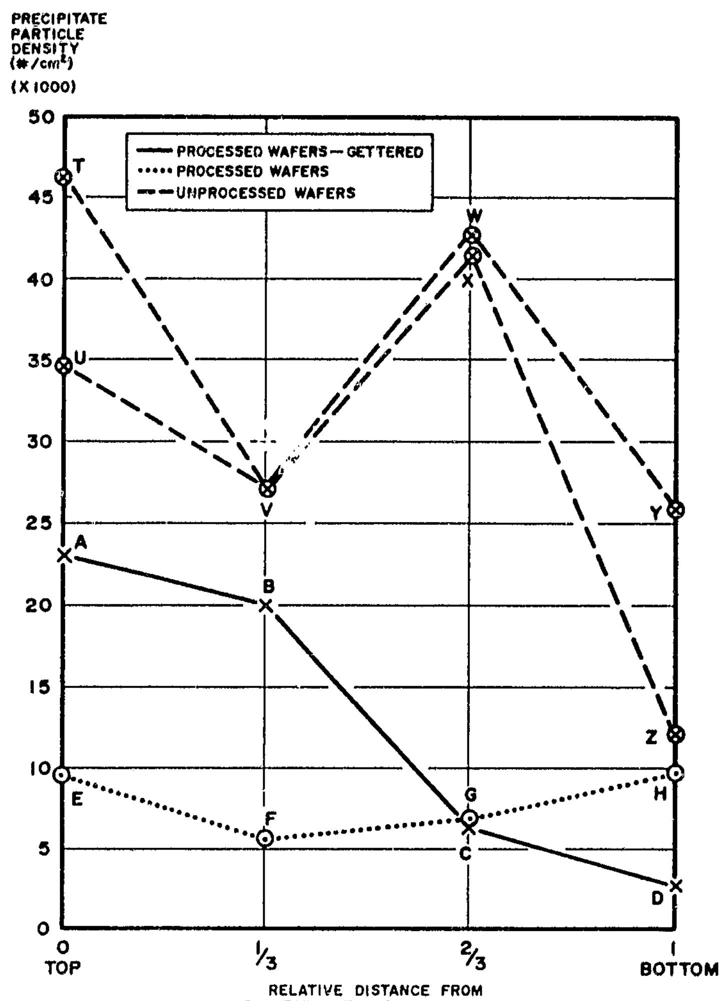

Large Precipitate Density vs Relative Position in the Ingot

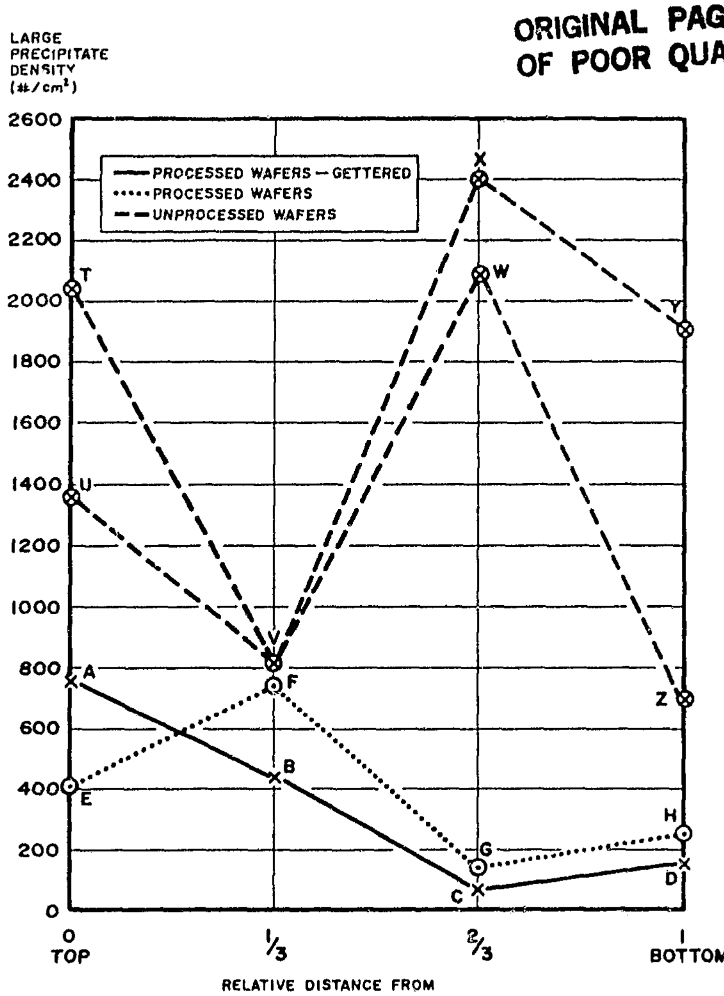

Dislocation Pit Density vs Relative Position in the Ingot

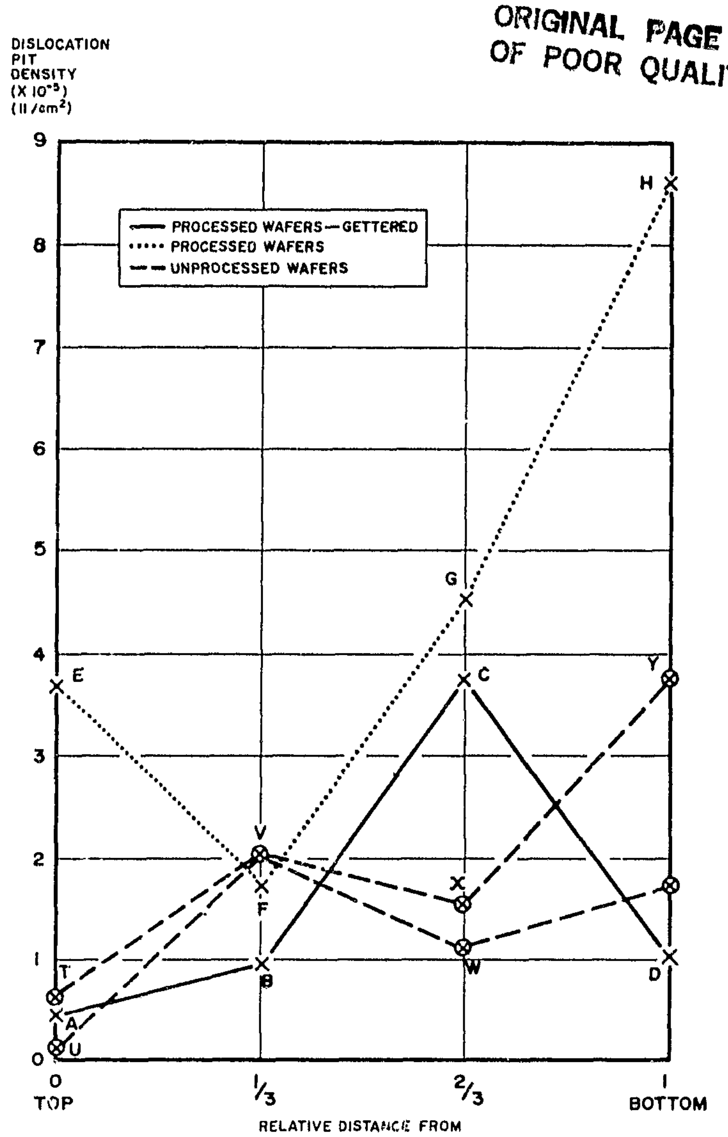

Twin Boundary Length per Unit Area vs Relative Distance From Top of Ingot

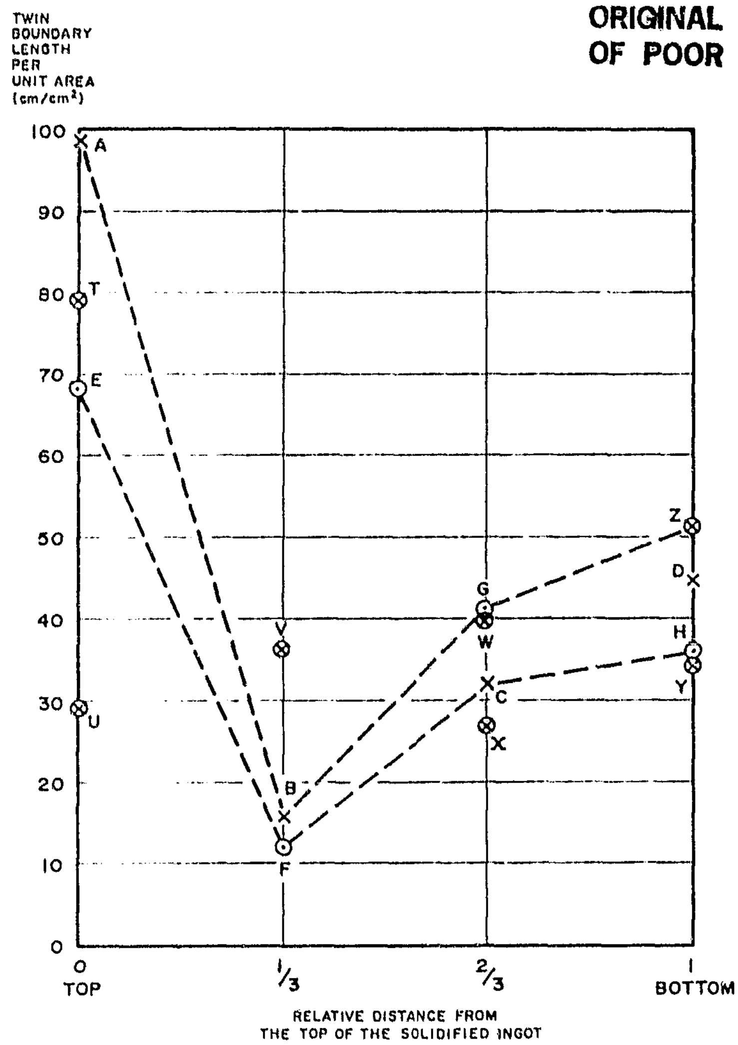

ORIGINAL PAGE IS
OF POOR QUALITY

Grain Boundary Length per Unit Area vs Relative Distance From Top of Ingot

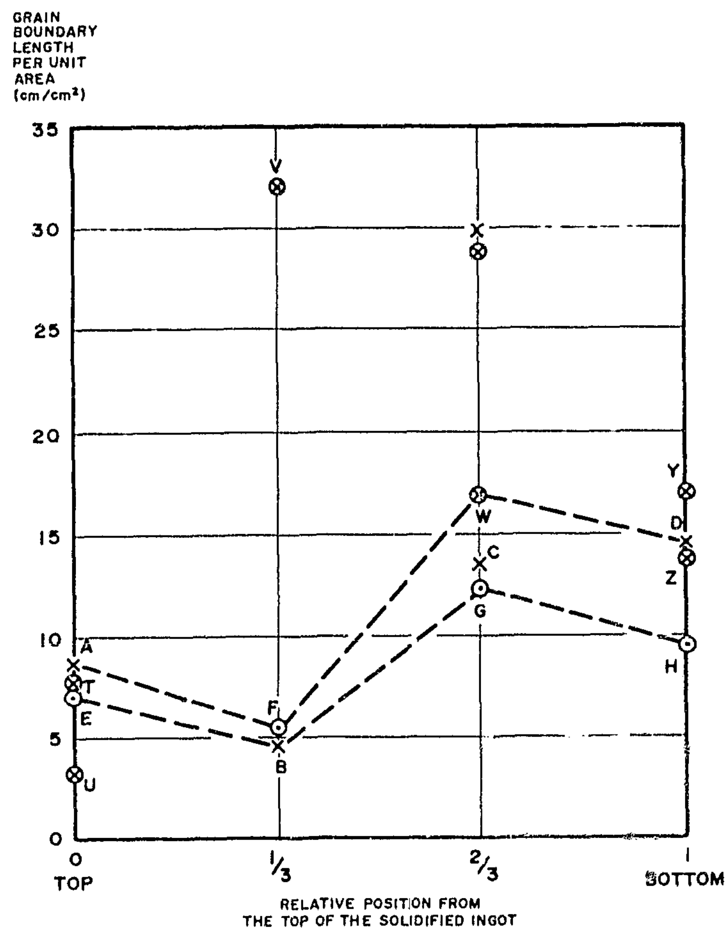

Region Showing High Twin Density in Semix A-13 (50 X)

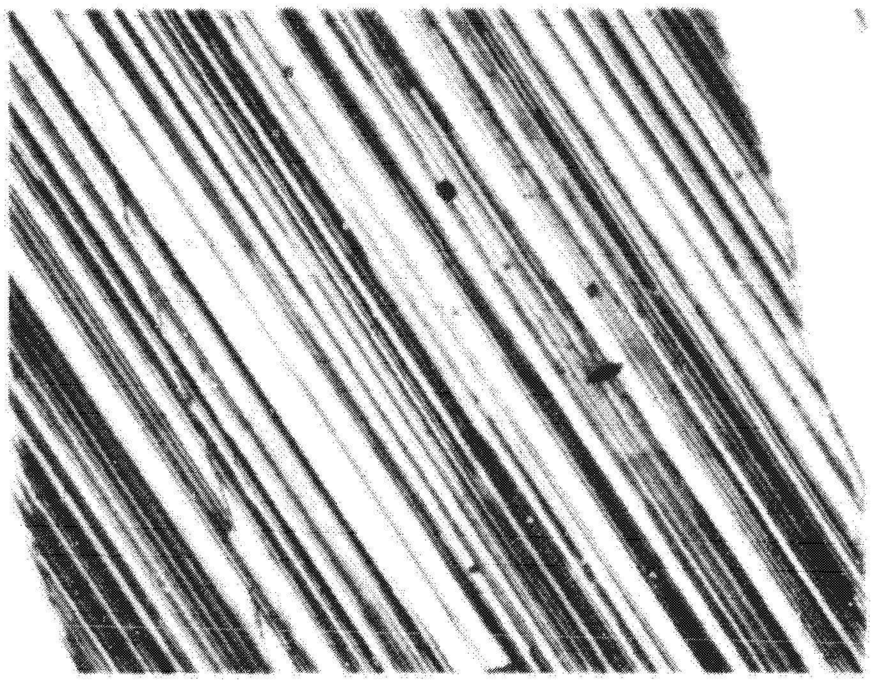

Region Showing Large Number of Precipitates in Semix A-13 (50 X)

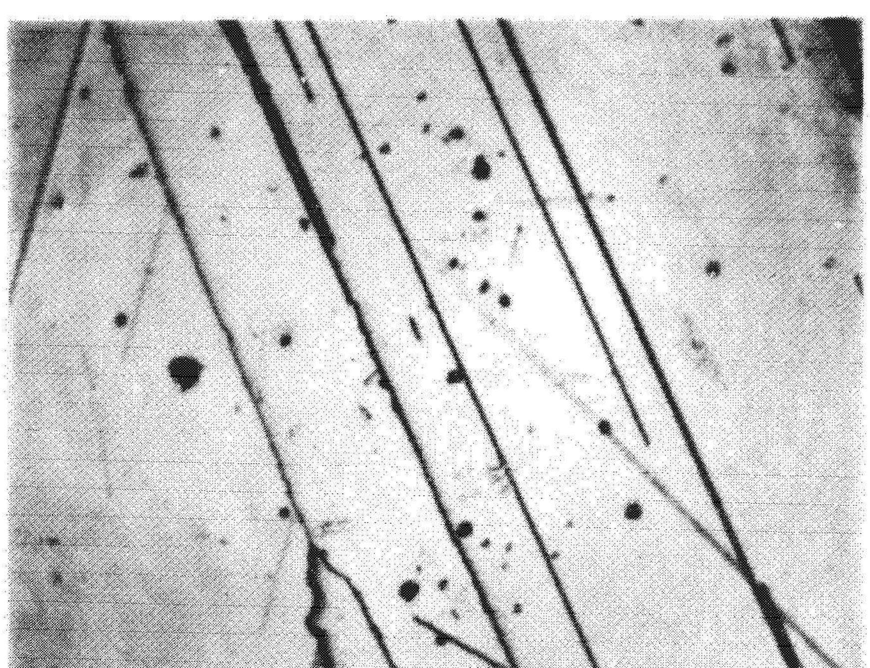

Large and Small Precipitates in Semix B-2 (1330 X)

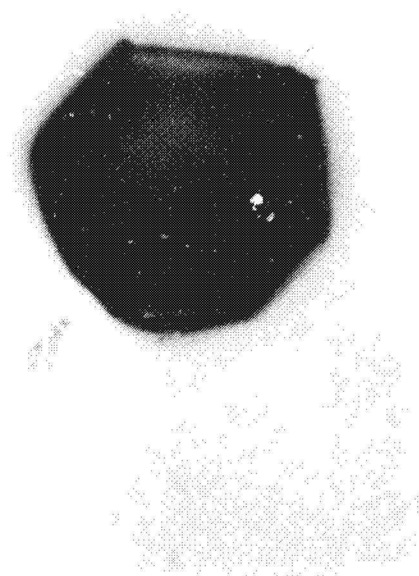

Precipitates in Semix B-2 (530 X)

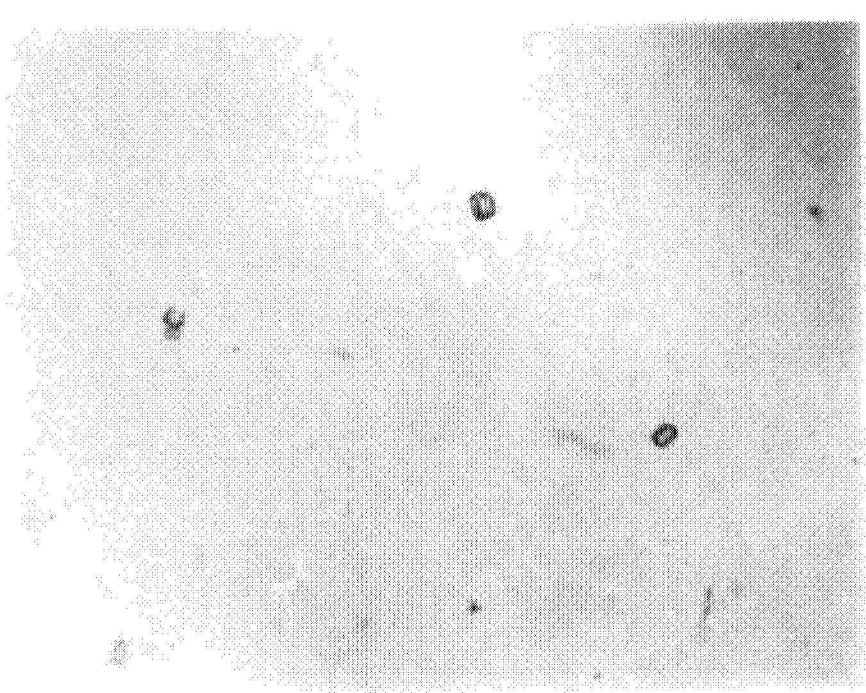

Dislocation Pileups in Semix H-8 (1330 X)

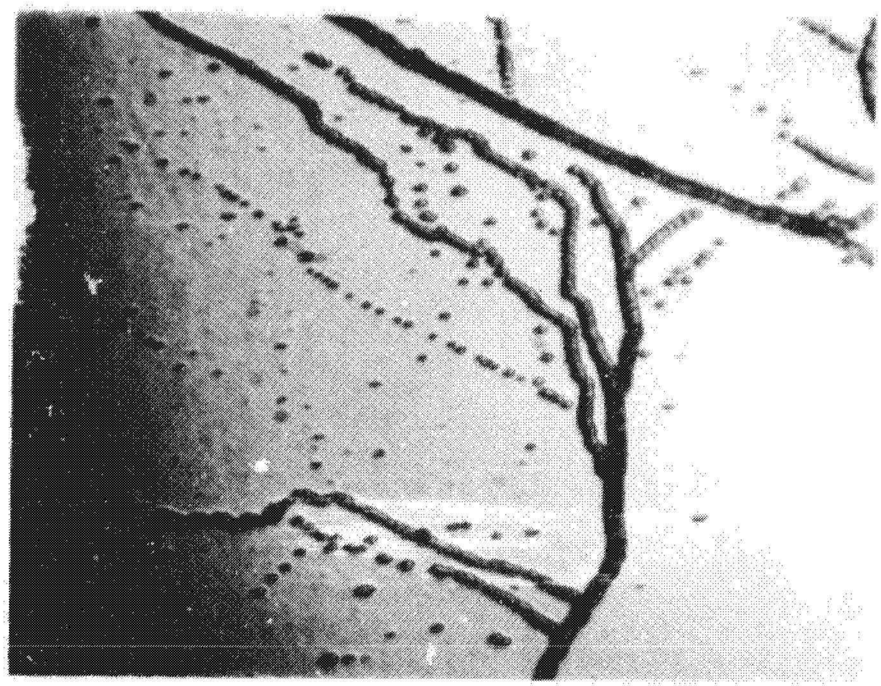

High Dislocation Density Between Twins in Semix H-8 (1330 X)

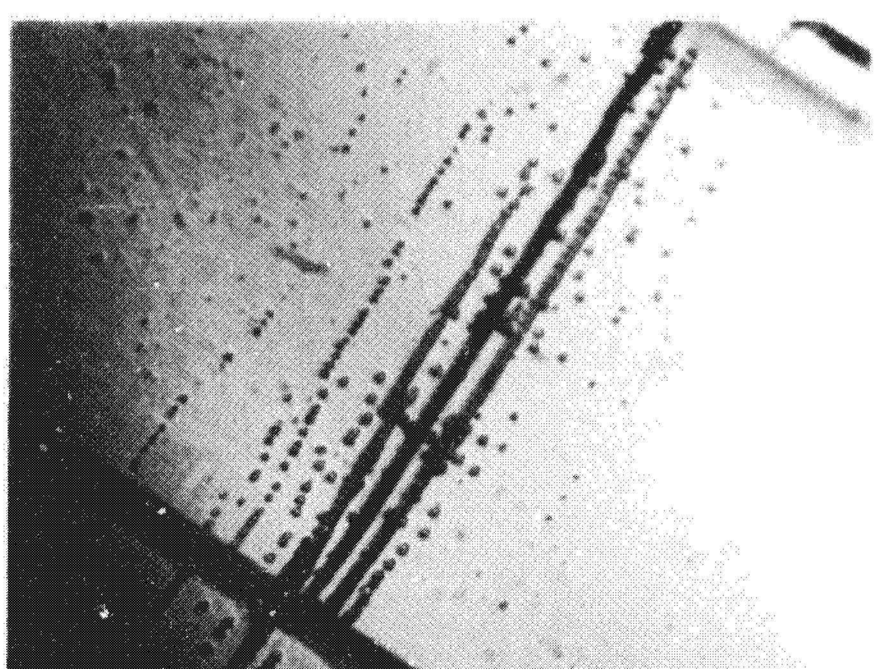

SURFACE PROPERTY MODIFICATION IN SILICON BY FLUID ADSORPTION

UNIVERSITY OF ILLINOIS AT CHICAGO

S. Danyluk

1. Multiple-Scratch Diamond Abrasion Test
2. Microhardness Test in Fluids
3. Fracture Strength after Abrasion in Fluids

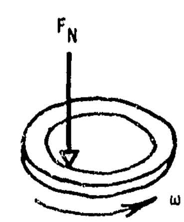

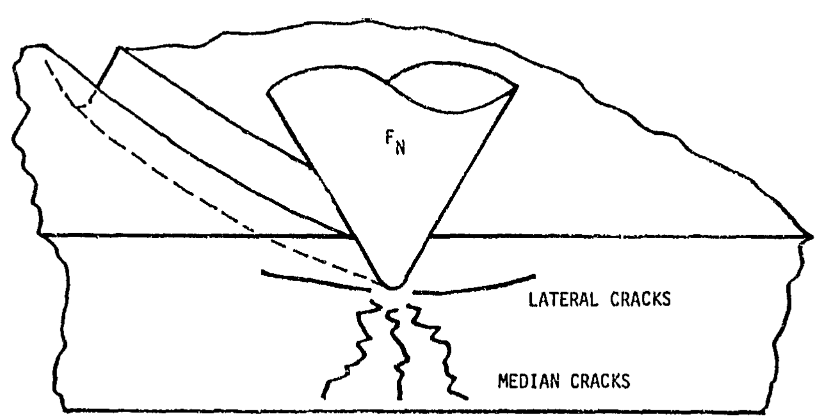

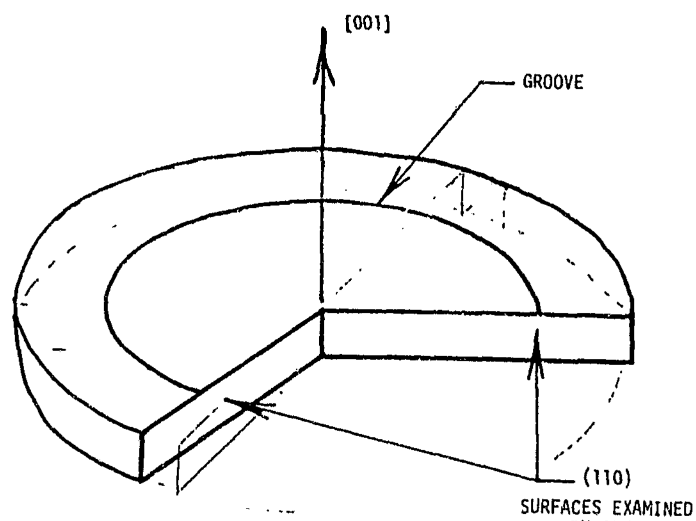

0.3, 0.6 and 1.3×10^2 s
grooves; $F_N = 0.2$ N;
Ethanol

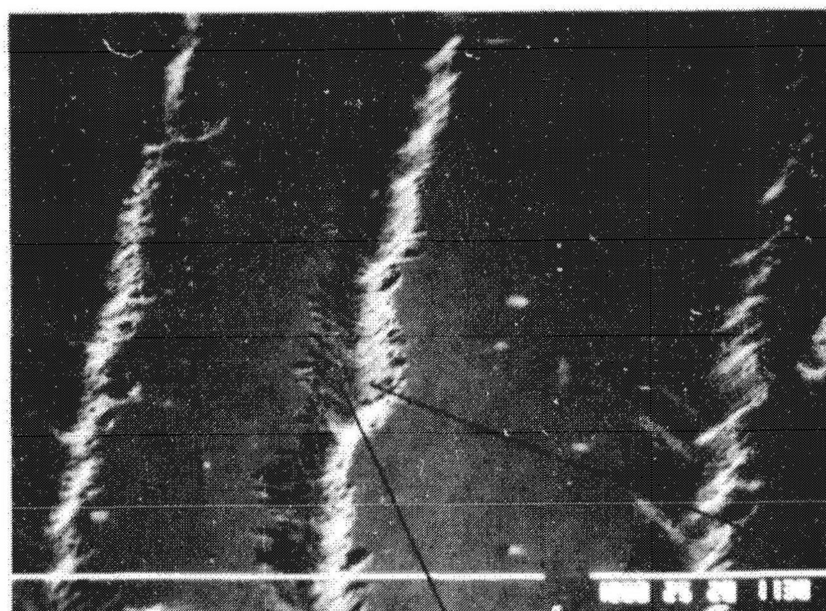

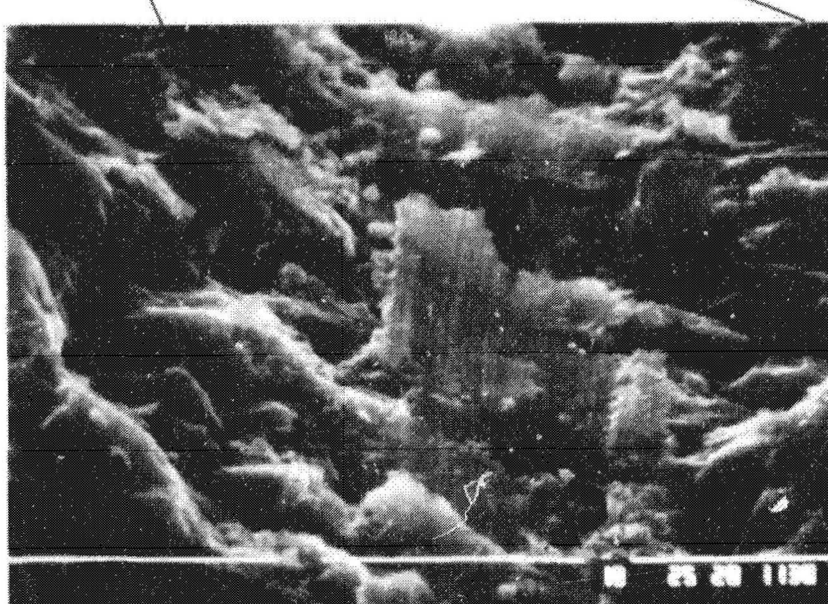

Bottom of Groove;
Plastic Deformation
of Protrusions
$t = 0.6 \times 10^2$ s

0.3, 0.6 and 1.2 x 10^2 s
grooves; F_N = 0.2 N;
deionized water

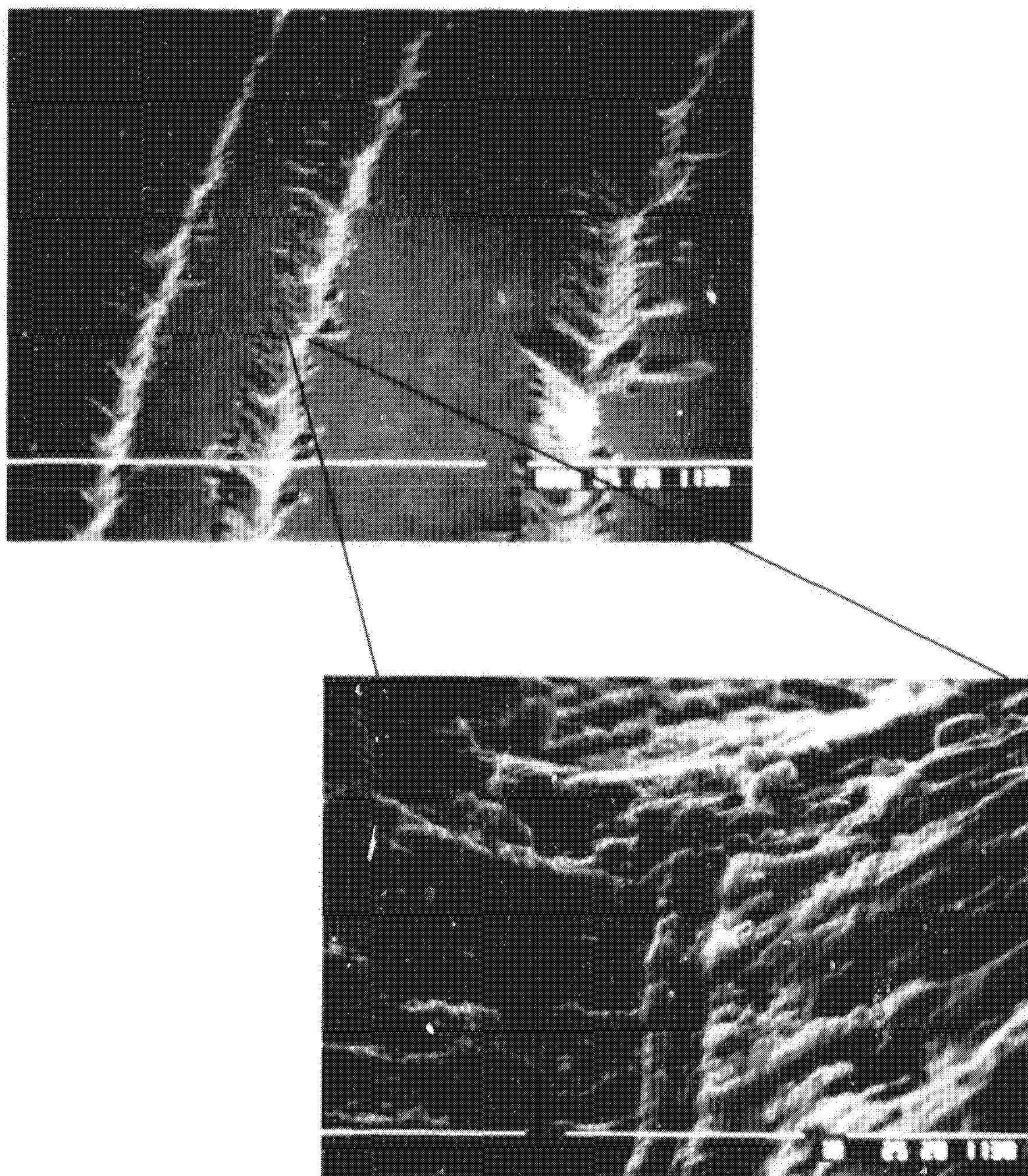

Bottom of groove
t = 0.6 x 10^2 s

ORIGINAL PAGE IS
OF POOR QUALITY

Deionized
Water

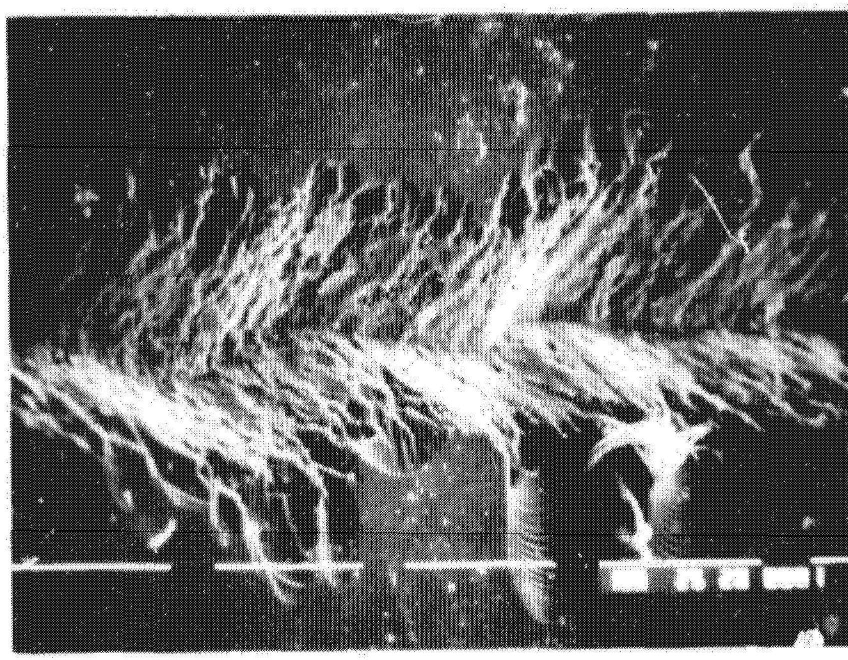

Ethanol

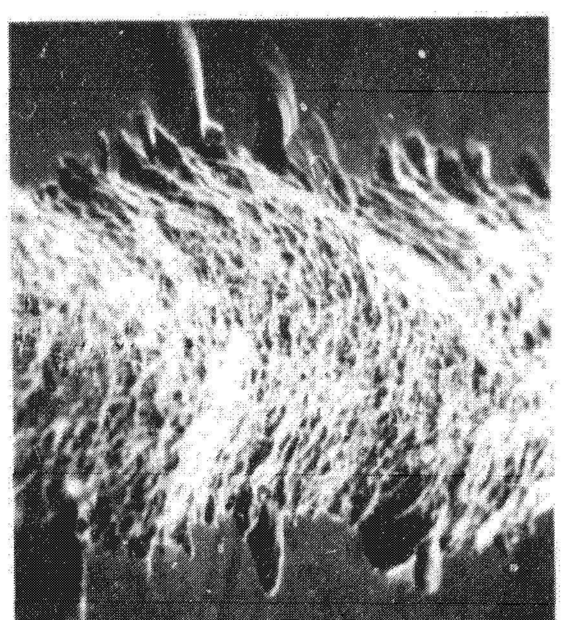

Top view of two grooves; $F_N = 0.5$ N; $t = 0.6 \times 10^2$ s; areas are different when fluid is changed.

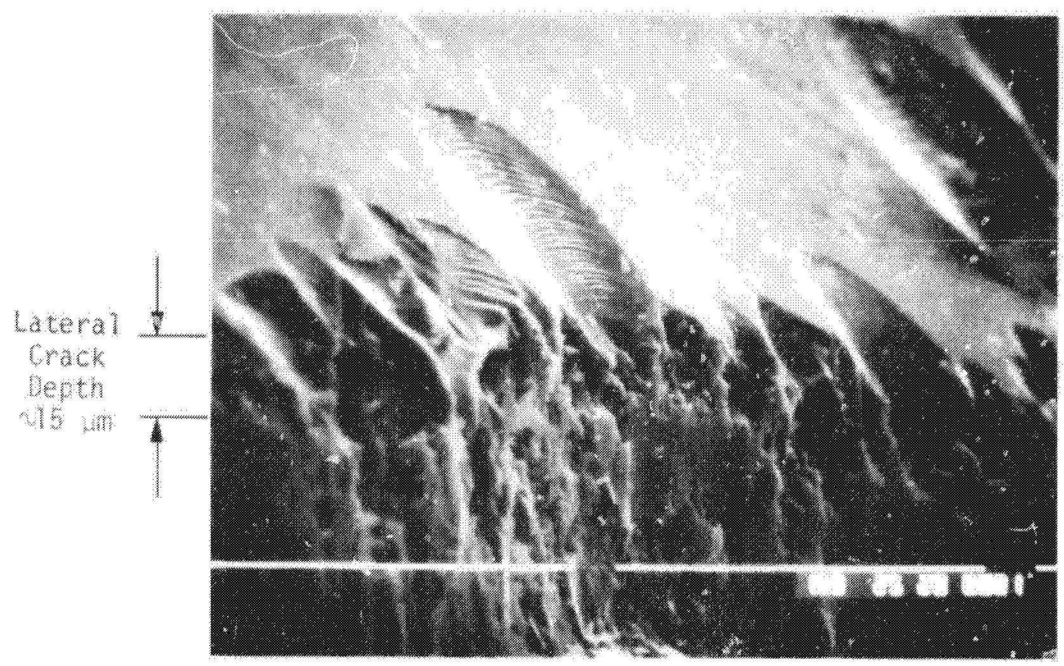

Shallow lateral cracks that lead to conchoidal fracture.
(H_2O; F_N = 0.5 N)

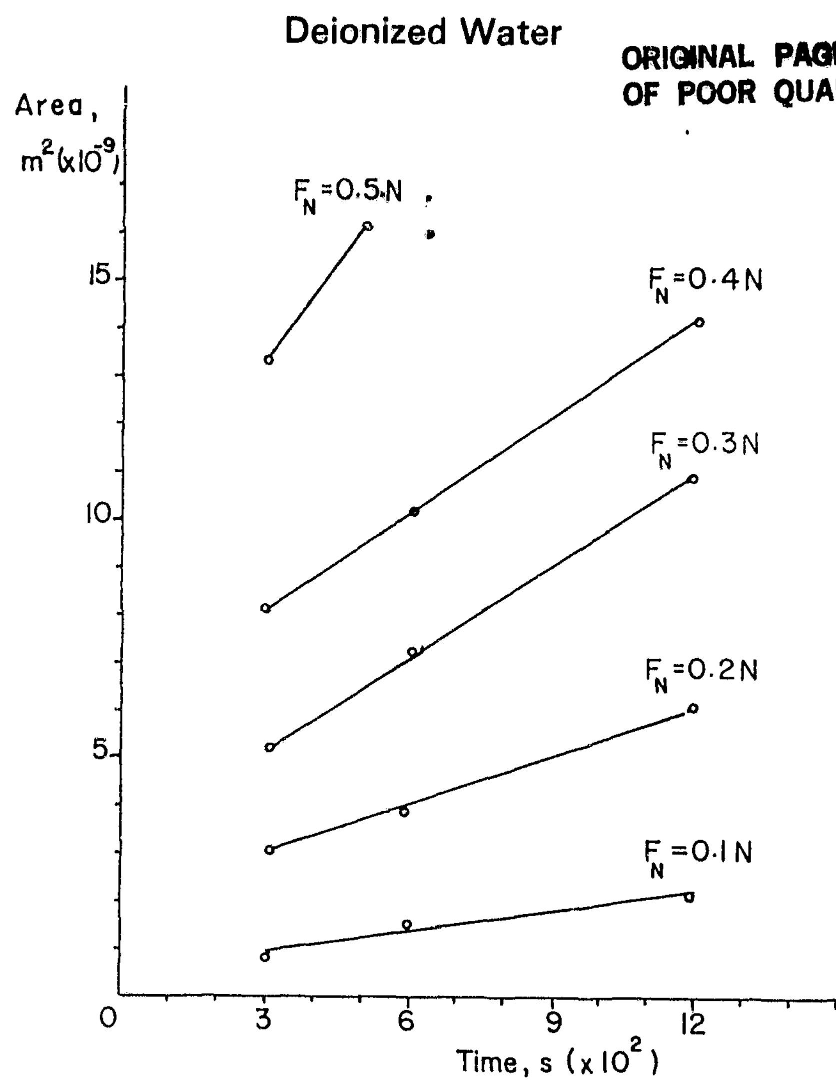
Deionized Water
Area, $m^2 (x10^{-9})$
F_N=0.5N
F_N=0.4N
F_N=0.3N
F_N=0.2N
F_N=0.1N
15
10
5
0
3
6
9
12
Time, s (x 10^2)

C-4

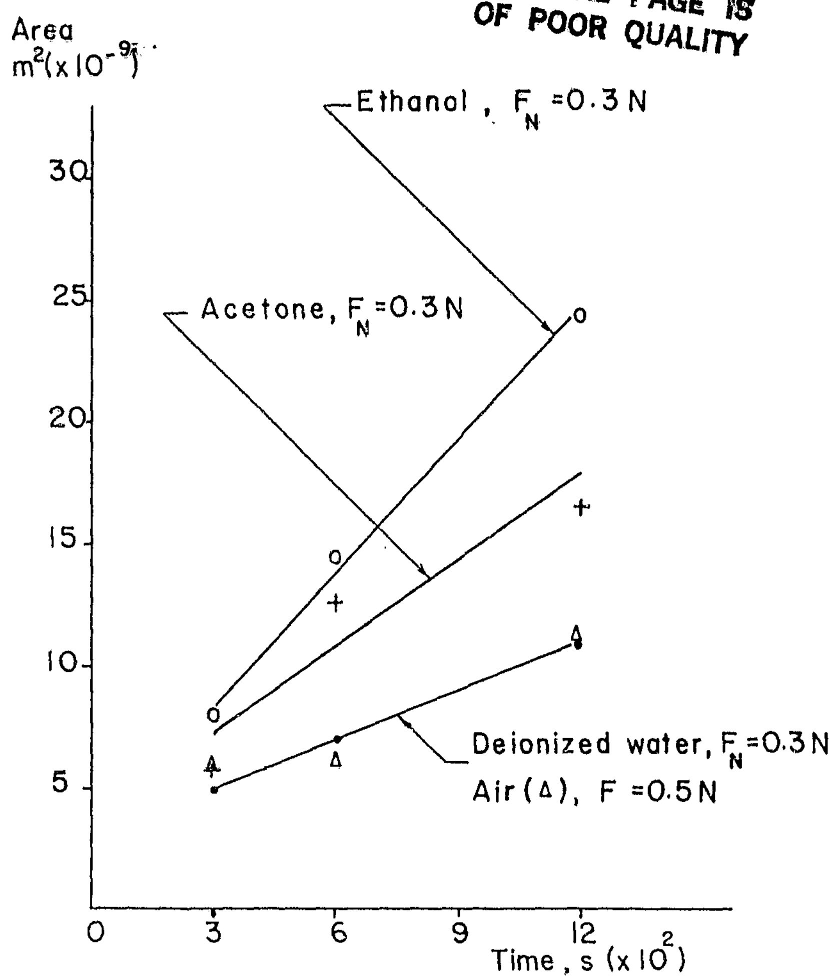
Area
m²(x 10⁻⁹)
Ethanol, F_N = 0.3 N
Acetone, F_N = 0.3 N
Deionized water, F_N = 0.3 N
Air (Δ), F = 0.5 N
Time, s (x 10²)
0
3
6
9
12
5
10
15
20
25
30

Model of Deformation

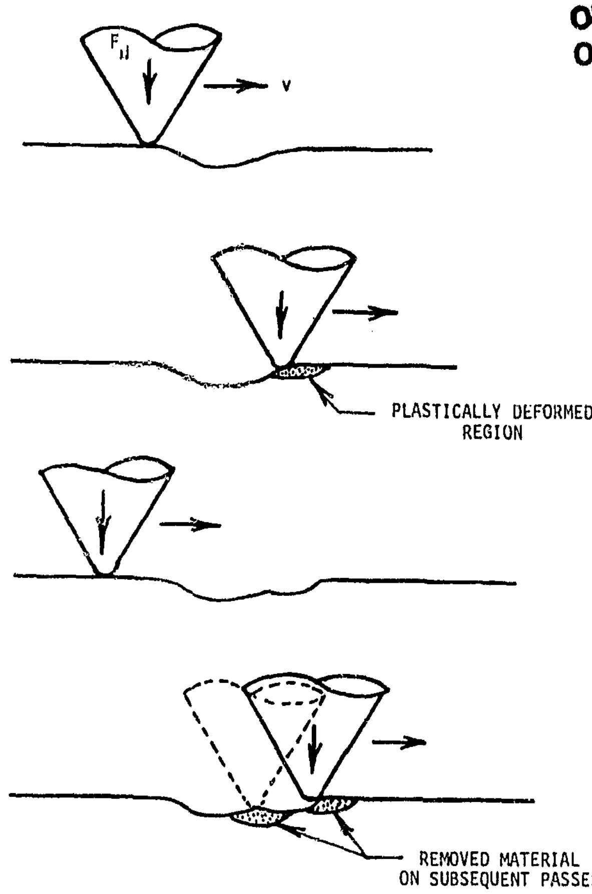

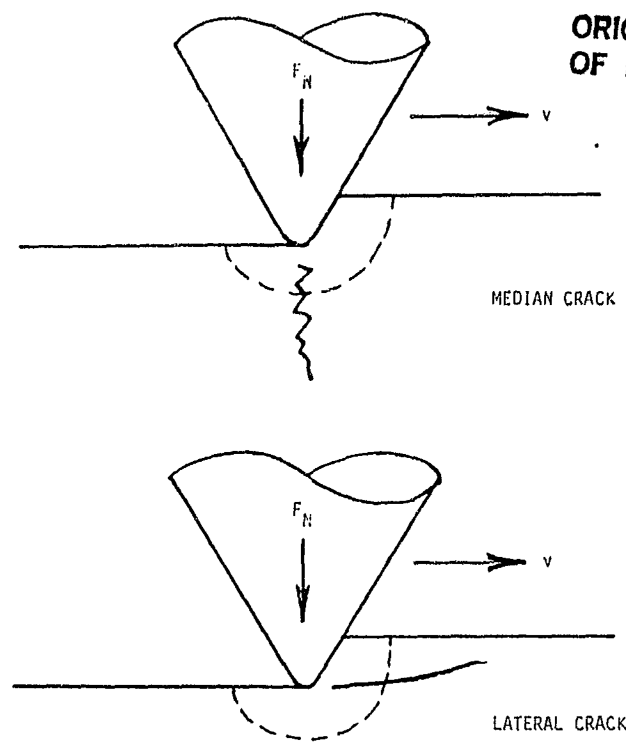
F_N
v
MEDIAN CRACK
F_N
v
LATERAL CRACK

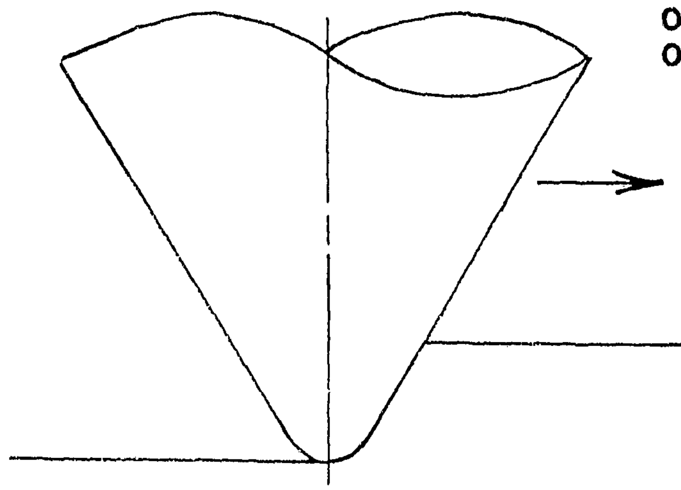

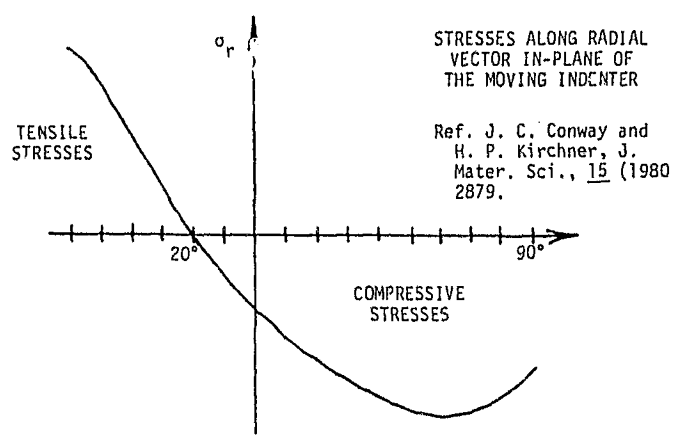

Theoretical Analysis of Wear

$$A = \frac{\tan\theta\, \omega\, F_N}{\pi H} \cdot t \quad \text{(Rabinowicz)}$$

$$A = \frac{0.58\psi\, \omega\, F_N^{7/6}}{(\pi B)^{7/6}\, K_{I_c}^{2/3}\, H^{1/2}} \cdot t \quad \text{(Evans)}$$

$$A = \frac{c\omega F_N}{\sigma_y} \cdot t \quad \text{(Shaw)}$$

Three-Point Bend Test

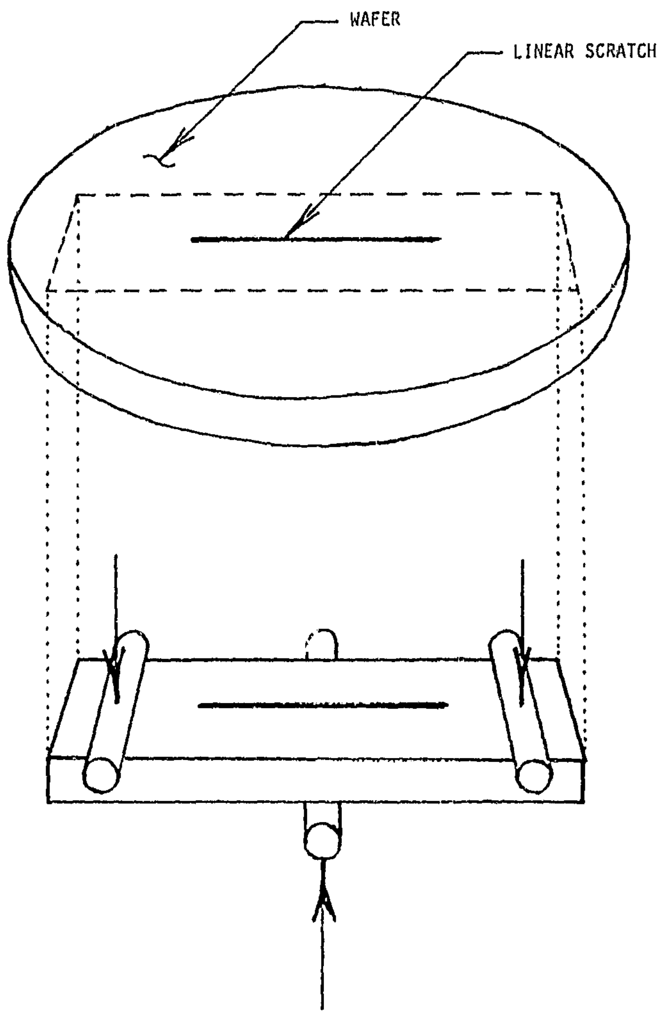

ORIGINAL PAGE IS
OF POOR QUALITY

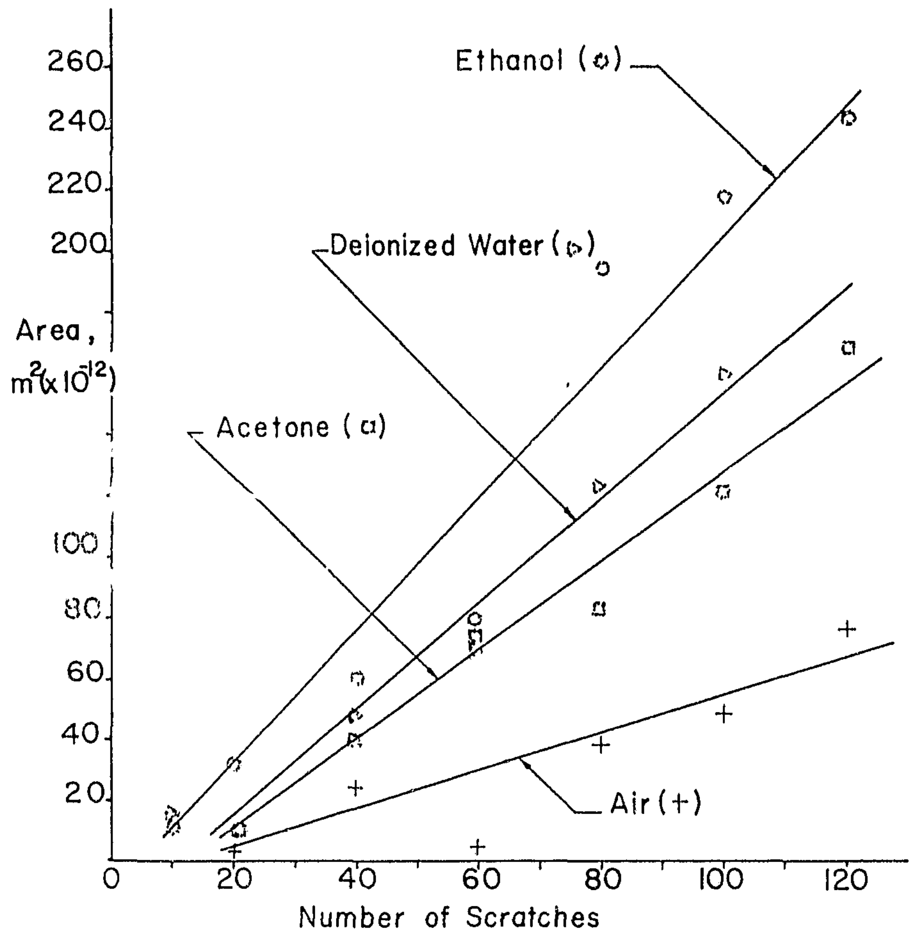

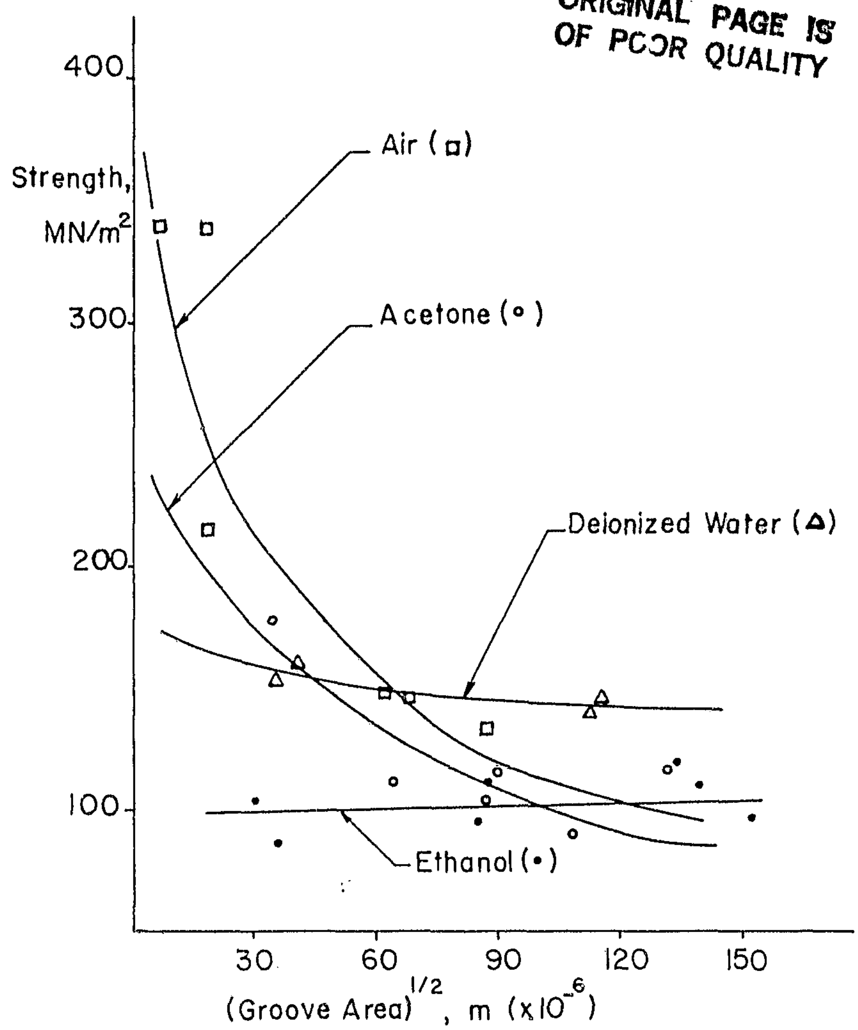
Strength, MN/m²
400
300
200
100
Air (□)
Acetone (∘)
Deionized Water (△)
Ethanol (•)
30
60
90
120
150
(Groove Area)^1/2, m (x10^-6)

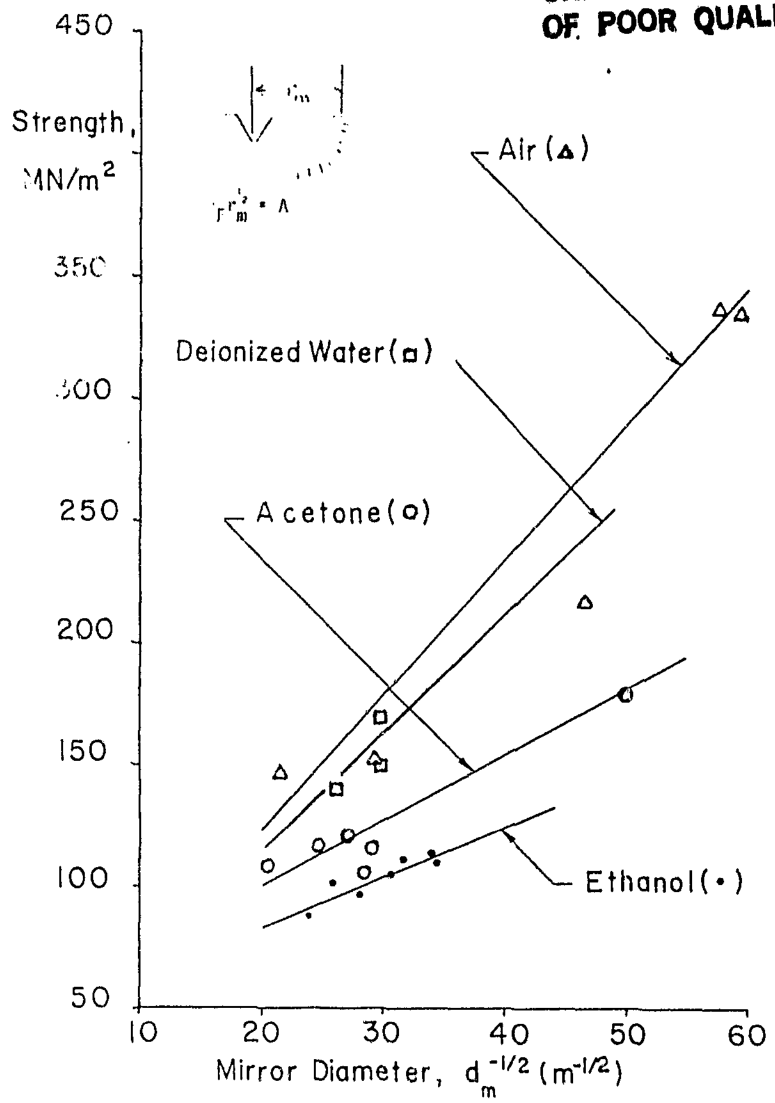

Mechanisms of Deformation

1. Material removal by lateral cracks (initiation of groove; apparent high wear rate)
2. Material removal by medial cracks (propagation of groove; lower wear rate than (1))
3. Adsorption of fluid to dislocation core that intersects the surface
4. Adsorption affects double kink formation by which dislocation moves

Conclusions

Deformation changes from lateral to median crack mode

Abrasion rate depends on fluid

Microhardness depends on fluid

Chemo-mechanical effect influences fracture strength

CELLS AND PROCESSES

D.R. Burger and A.H. Kachare, Chairmen

Reports of progress in research on solar cells and processes were presented by 12 contractors and JPL.

C.T. Sah Associates are conducting research on material limitations on high-efficiency solar-cell performance. They reported that a computer-aided analysis (CAA) using the exact transmission line model has been performed for 34 $n^+/p/p^+$ and $p^+/n/n^+$ cells. The CAA includes: exponential gradient drift-field model, 50 μm optimum cell thickness with 0.25 μm emitter layer, drift-field thickness from 1 to 48 μm, back-surface concentrations of $5 \times 10^{18}/cm^3$ and $2.5 \times 10^{20}/cm^3$, base concentrations of $5 \times 10^{15}/cm^3$ and $10^{17}/cm^3$, constant and exponential profiles of recombinations impurity (Z_n model), and interband Auger recombination.

University of California at Los Angeles, conducting research on high-efficiency silicon solar-cell structures by molecular beam epitaxy (MBE), reported results on silicon MBE solar cells. First results were that using heat treatment alone to clean in ultra-high vacuum does not degrade lifetime in substrate ($L \approx 100\ \mu m$) and the cleaning plus growth of 0.7 μm SB-doped epitaxy layer produced a measureable cell, but of poor quality.

University of Pennsylvania, conducting research on the development and analysis of silicon solar cells of near 20% efficiency, reported on the status of this contract, which started in September, 1982. Currently substrates have been received from Wacker Chemie with $0.2 \rightarrow 0.4\ \Omega$-cm, $\tau > 500\ \mu s$, p-type, boron doped, which have been multiple-float-zoned. A multivariable experiment has been designed to study the process parameters including type of source gas and dopants that yield the highest minority carrier lifetimes in CVD-deposited epitaxially grown silicon layers.

Applied Solar Energy Corp., conducting research on microcrystalline silicon growth for heterojunction solar cells, reported on the approach and goals of this contract. The approach will include studies of predeposition cleaning of substrate, deposition temperature, film thickness, deposition rate, and cell fabrication parameters. The goals are to investigate the possibility of low-cost solar cells manufactured from micro-crystalline silicon.

The JPL in-house program reported on multi-junction (cascade) silicon solar-cell modeling calculations for use with solar-cell structures made by MBE.

The nine Process Research presentations reflected the continuing change in emphasis of process research. During the eight months since the 20th Project Integration Meeting a number of contracts have been redirected to meet new DOE guidelines. More emphasis has been placed on high-risk, research-oriented efforts. This change in emphasis was reflected in the presentations and the inclusion of the advanced cell-design presentations in the same technology session.

CELLS AND PROCESSES

In the past, process-related presentations were grouped into four major categories: surface preparation, junction formation, metallization and assembly. It was notable that of the nine such presentations made at this meeting, four were on metallization and five were on junction formation. A void in PV research has been noted in microcrystalline or thin-film-device surface preparation and assembly processes. These items may be addressed in the future, depending upon new research priorities.

Metallization presentations started with a discussion by Spectrolab, Inc., on advanced metallization and conductive coatings. This investigation has successfully demonstrated screen-printed cell coatings using a fritless paste of molybdenum, tin and titanium hydride. All cell characteristics were identical with those of silver thick-film contacts, except for a higher series resistance and some concern with adhesion. The next step in this program is the use of a transparent conductive oxide coating to reduce series resistance and to provide higher cell efficiencies and a test of possible reactions with the molybdenum-tin metallization.

Bernd Ross Associates presented a summary of their work on metal thick-film systems using copper. Sintering copper at low temperatures is difficult; high temperatures tend to degrade cell performance. Another problem area related to copper was the reduction of copper oxide. It was found that carbon monoxide was superior to hydrogen as a reducing agent. Fritless silver pastes were sucessfully demonstrated and could provide superior field performance compared with that of present silver-glass frit formulations. During an earlier discussion period, glass frits were identified as causative agents in some encapsulation discoloration.

Application of metal thick-film contacts through a silicon nitride anti-reflection coating was addressed by Photowatt International, Inc. This effort was undertaken to obtain contacts on a surface that had been passivated to reduce recombination losses. Initial efforts to plate up a nickel-glass frit system were unsuccessful because of the corrosive nature of plating solutions. Fritless nickel paste systems did not succeed because they required high sintering temperatures, which caused junction shunting. Fritless tin pastes with 1% silver fluoride added produced ohmic contacts.

R.W. Aster of JPL presented a comparison of metallization system costs using data provided by FSA contractors and some projections made by the FSA Project Analysis and Integration Area. Twelve different systems were covered to illustrate the range of metallization costs and resultant cell power-collection efficiency. Since different metallization approaches create different series resistance and shadowing losses, this factor was addressed by use of a cell grid-line optimization computer program developed at JPL. This study can assist in defining worthwhile future metallization research efforts.

Junction formation and back-surface fields on dendritic web were discussed by Westinghouse Electric Corp.'s Advanced Energy Systems Division. Liquid dopant sources have been shown to produce cell efficiencies at least equal to those of gaseous-diffusion cells and to have a much better potential for process automation and control. Similarly, liquid oxide-mask formulations provide as good protection as chemical-vapor-deposited masks. These liquid preparations were successfully applied by meniscus coating, a new process

under investigation. Also being examined is a shot tower developed at Kayex Corp. and transferred to Westinghouse for verification that the silicon material produced by this tower can be used as feedstock for the dendritic-web growth machines.

Spire Corp. presented development data on non-mass-analyzed ion implantation. By deleting the large mass analyzer, significant equipment-cost savings can be made. Much higher available beam currents allow another cost saving by providing higher process throughput. Experiments have shown that solar-cell efficiency is only weakly dependent upon implant energy, so a large process window seems to be available. Further research is planned after the equipment is completely operational.

Another Spire effort was the demonstration of implantation and pulsed electron-beam annealing of silicon-sheet materials other than Cz. Successful operation of the pulse annealer has already been demonstrated and some ion implantation experiments have been made.

Processing of cast silicon was discussed by Solarex Corp. After studying grain-boundary effects and bulk-material properties, it was shown that the bulk diffusion length is the limiting factor in improving cell efficiency. A 400 minicell test program that will increase the information available on cast silicon cell performance is in progress. During these studies it was found that a two-layer (TiO_x/Al_2O_3) antireflection coating can be applied inexpensively by hot spraying rather than by evaporation.

D.J. Fitzgerald of FSA made a short presentation on a new processing option-pulsed plasma. This process holds some promise of usefulness in sintering metals or in ion implantation.

ANALYSIS OF EFFECTS OF DRIFT FIELD ON THIN-BASE SOLAR CELL PERFORMANCE

C.T. SAH ASSOCIATES

TECHNOLOGY	REPORT DATE
MATERIAL LIMITATIONS ON HIGH EFFICIENCY SOLAR CELL PERFORMANCE	01/12/1983
APPROACH ANALYSIS OF EFFECTS OF DRIFT FIELD ON THIN-BASE SILICON CELL PERFORMANCE **CONTRACTOR** C. T. SAH ASSOCIATES **GOALS** • DETERMINE THE IMPROVEMENT OF THE TOLERANCE TO RESIDUAL RECOMBINATION IMPURITIES AND PHYSICAL DEFECTS BY INCLUSION OF DOPANT IMPURITY DENSITY GRADIENT IN THE BASE OF THIN-BASE SILICON SOLAR CELLS; EXTENDED BACK-SURFACE FIELD CELLS (EXBSF).	**STATUS** • COMPUTER-AIDED ANALYSIS (CAA) USING THE EXACT TRANSMISSION LINE MODEL. • EXPONENTIAL GRADIENT DRIFT FIELD MODEL. • 50 uM OPTIMUM CELL THICKNESS WITH 0.25uM EMITTER LAYER. • DRIFT FIELD THICKNESS FROM 1 TO 48 uM. • BS CONCENTRATIONS OF 5E18 and 2.5E20 cm^{-3} • BASE CONCENTRATIONS; 5E15 and 1E17 cm^{-3} • CONSTANT AND EXPONENTIAL PROFILES OF RECOMBINATION IMPURITY (Zn model). • INTERBAND AUGER RECOMBINATION INCLUDED. • CAA PERFORMED FOR 34 N+/P/P+ and P+/N/N+ CELLS.

ORIGINAL PAGE IS OF POOR QUALITY

PRECEDING PAGE BLANK NOT FILMED

PAGE 314 INTENTIONALLY BLANK

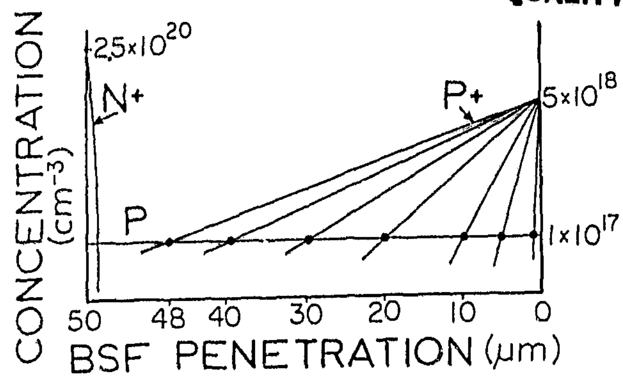
CONCENTRATION (cm^{-3})
2.5x10^{20}
N+
P+
5x10^{18}
P
1x10^{17}
50
48
40
30
20
10
0
BSF PENETRATION (μm)

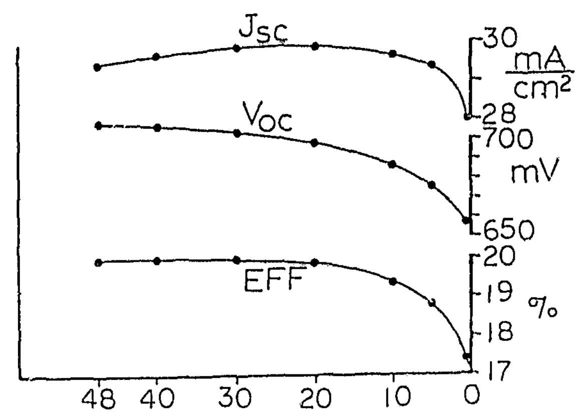
Jsc
30
mA/cm^2
28
Voc
700
mV
650
EFF
20
19
%
18
17
48
40
30
20
10
0

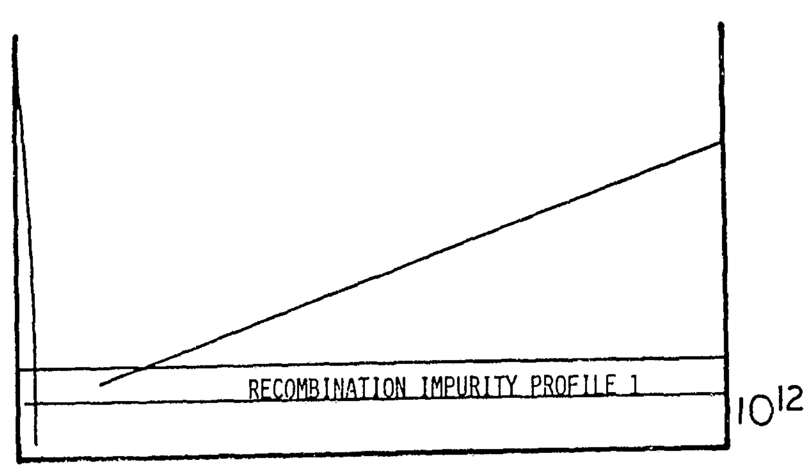
RECOMBINATION IMPURITY PROFILE 1
10^{12}

HIGH-EFFICIENCY SILICON SOLAR-CELL STRUCTURES BY MBE

UNIVERSITY OF CALIFORNIA AT LOS ANGELES

F.G. Allen

GOAL: TO APPLY THE NEW CAPABILITIES OF MBE FOR PRECISE CONTROL OF ARBITRARY DOPING PROFILES TO PRODUCE OPTIMUM SILICON SOLAR CELLS.

Outline

1. SILICON MBE:
   - THE GROWTH PROCESS
   - ITS POTENTIAL ADVANTAGES FOR SI SOLAR CELLS
2. UCLA MBE SYSTEM :
   - STATION DESIGN
   - PROFILES GROWN
3. ACTIVITY TO DATE ON THIS TASK:
   - SILICON QUALITY DETERMINATION
   - RESULTS FIRST CELL
4. PLANS FOR FUTURE WORK.

Silicon MBE: New Method of Fabricating Silicon Devices

- GROWS SILICON SINGLE CRYSTALS IN U.H.V.
- SIMULTANEOUS BEAMS DEPOSITED AND CONTROLLED:
  - SILICON
  - n-DOPANT (ANTIMONY)
  - p-DOPANT (GALLIUM)
- OFFERS ULTIMATE CONTROL IN
  - SHARP DOPING PROFILES
  - ARBITRARY DOPING SEQUENCE
  - THIN LAYERS (A FEW ATOMS)
- LOW GROWTH TEMPEPATURES (350-750° C)
  - NEGLIGEABLE DOPANT DIFFUSION

Process Schematic of Silicon MBE Growth

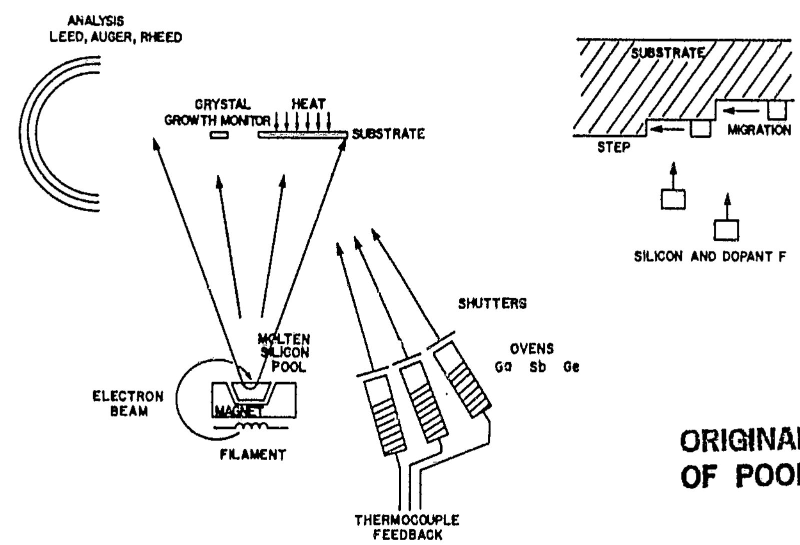

Pure Silicon Source

- BY EVAPORATING FROM A POOL OF MOLTEN SILICON ENTIRELY SURROUNDED BY PURE SOLID SILICON IN HEARTH OF e-GUN, ACHIEVES "SILICON CRUCIBLE"

Dopant Control: Two Methods

1. EFFUSION CELL METHOD

   - SIMPLE TO IMPLEMENT, BUT
   - STICKING COEFFICIENT EXTREMELY TEMP. SENSITIVE (SEE Fig.)
   - REQUIRES "PRE-BUILD-UP" AND "FLASH-OFF" TECHNIQUES TO AVOID TRANSIENT EFFECTS

   MAX DOPING LEVELS THUS FAR LIMITED TO $< 10^{19}$ cm^{-3}

2. LOW ENERGY (200 eV) ION IMBEDDING

   - COMPLEX EQUIPMENT
   - IDEAL DOPANT CONTROL - CLOSED LOOP COMPUTER CONTROL POSSIBLE
   - ANNEALS DAMAGE AS IT GROWS AT $T_s > 700°C$
   - COULD LEAD TO BEAM WRITING OF PATTERN IN FUTURE

Advantages of MBE for Silicon Device Fabrication

- LOW SUBSTRATE TEMPERATURE - 600–700°C - RESULTS IN NEGLIGEABLE DIFFUSION - SEE TABLE.
- DEPTH CONTROL TO WITHIN A FEW ATOMIC LAYERS
- ARBITRARY SEQUENCE p-i-n
- ARBITRARY PROFILE BY COMPUTER CONTROL OF BEAMS
- ENTIRE PROFILE ONE STEP PROCESS IN U H V

  (MAY LATER INCLUDE LAYERS OF INSULATORS AND METALLIZATION)
- HIGH QUALITY MATERIAL NOW DEMONSTRATED

  (LIFETIME, MOBILITY, DISLOCATION COUNT)

Diffusion Distance, $\sqrt{Dt}$, of Dopants in Silicon

	p-TYPE		n-TYPE	
	Ga	B	Sb	As
Conventional Diffusion T= 1200°C t = 20 MINS	5000Å	3800Å	2000Å	5800Å
MBE Growth T = 700°C t = 5 HRS	7Å	22Å	4.5Å	1.8Å

ORIGINAL PAGE IS OF POOR QUALITY

Current Silicon MBE Systems

- U H V, ~1 x 10^{-10} TORR
- HEATED SILICON SUBSTRATE, ATOMICALLY CLEAN
  LEED, RHEED, AUGER, MASS SPECTROMETER
- e-GUN SILICON EVAPORATOR
- THICKNESS MONITOR; GROWTH RATES OF 1 TO 50Å/SEC
- n AND p TYPE DOPANT BEAMS, EITHER

  EFFUSION CELLS, (GALLIUM AND ANTIMONY)
  OR
  ION BEAM DOPANTS, (BORON AND ARSENIC)
- LIQUID NITROGEN COOLED SHROUD AROUND HEATED PARTS
- LOAD-LOCK

UCLA Silicon MBE System

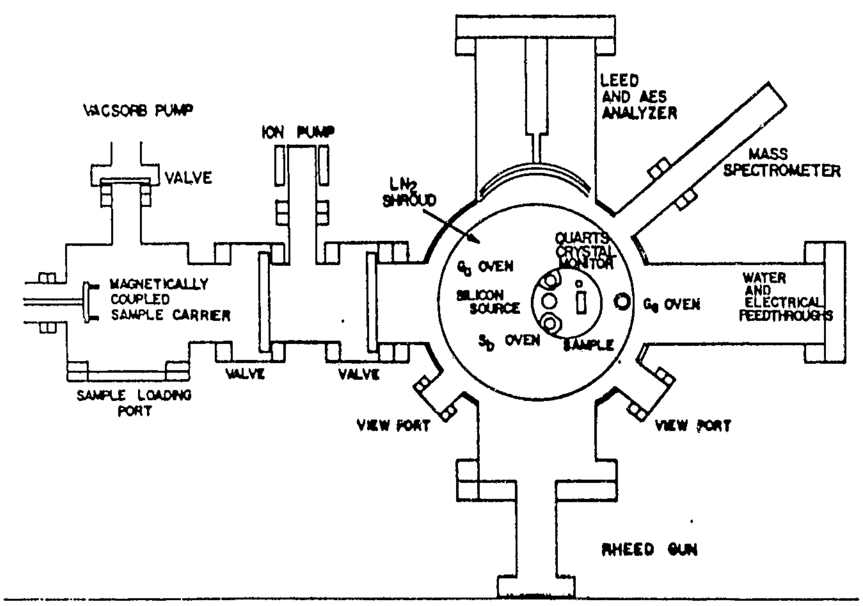

Hole Mobility vs Acceptor Concentration
for All G_a-Doped Silicon MBE Films Grown at UCLA

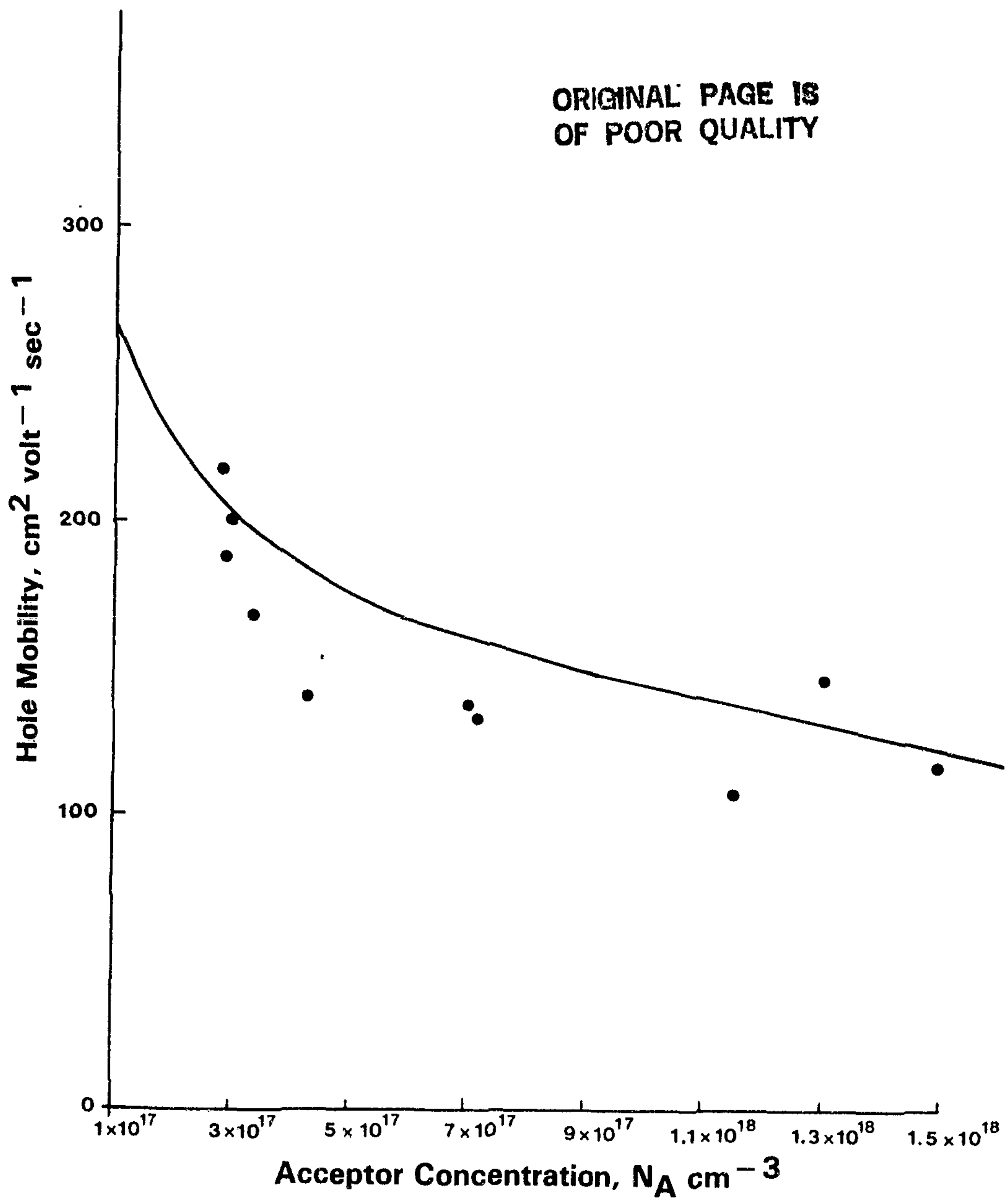

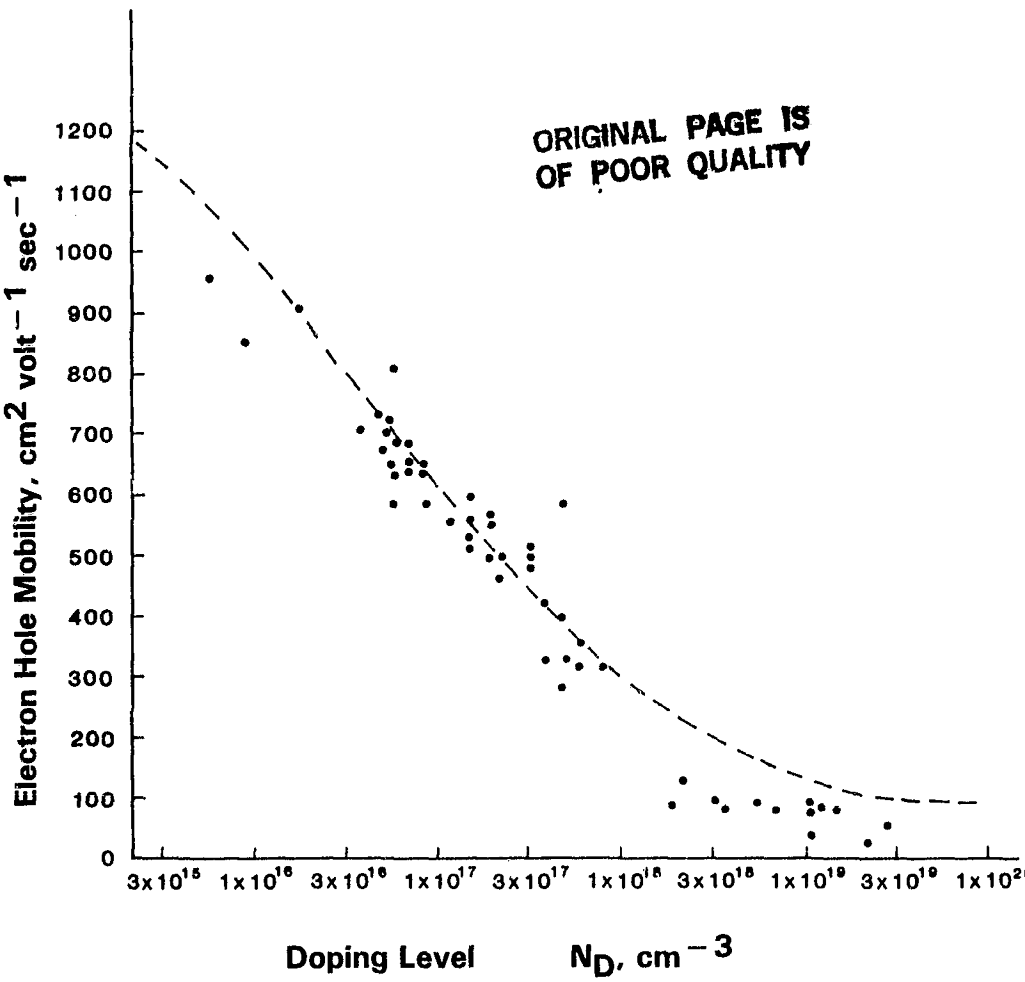

Examples of Usefulness of MBE for Si Solar Cells

(FOR DEVELOPMENT STAGE ONLY)

- SPECIAL OR CRITICAL DOPING PROFILES

  FRONT FIELD
  BACK FIELD
  DRIFT FIELD
  MULTI-LAYER (TANDEM)

- REPRODUCIBILITY OF PROFILES

  CONFIRM CALCULATIONS
  OPTIMIZE DESIGN

Front-Field Solar-Cell Profiles by MBE in Si for JPL

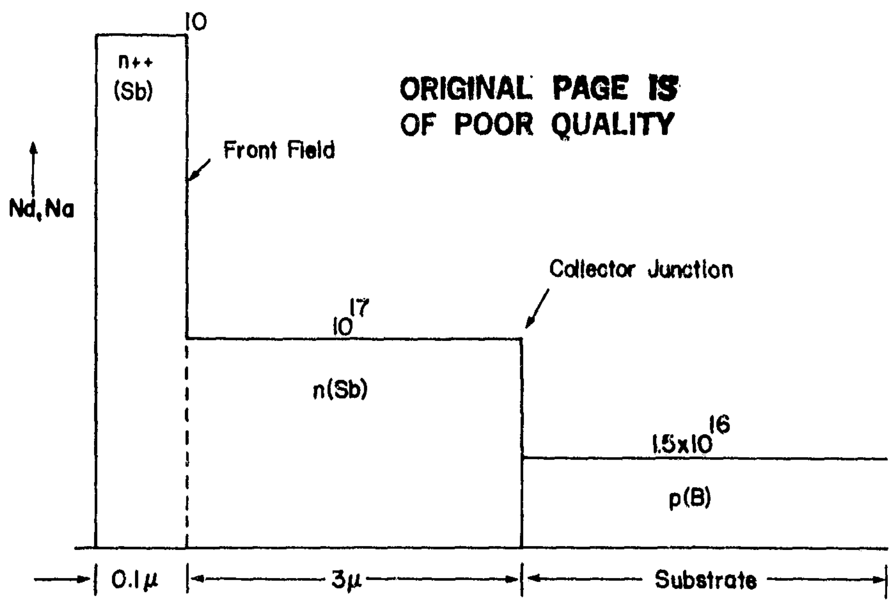

a) Junction Near Surface

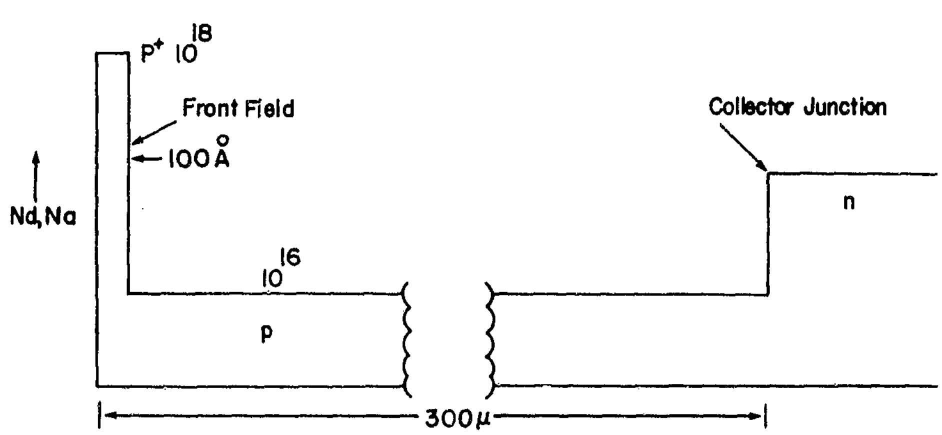

b) Junction at Rear

Front Field With Drift Field Shallow-Base Si Solid Cell

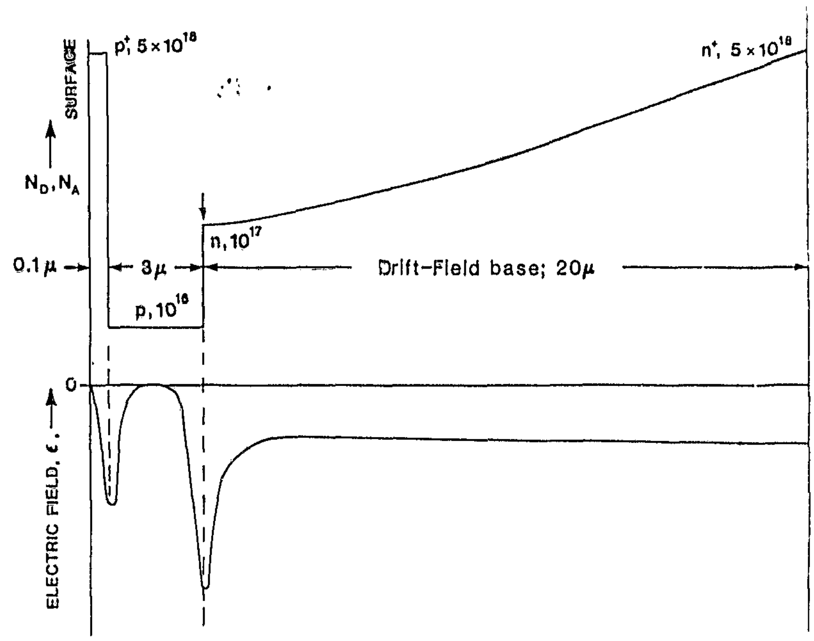

Two-Layer Tandem Si Solar Cell

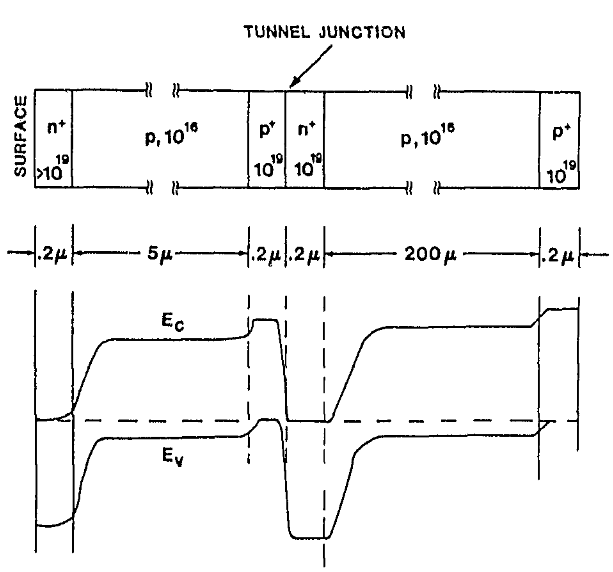

First Results on Si MBE Solar Cell for JPL

1. HEAT TREATMENT ALONE TO CLEAN IN UHV (1250°C 1 MIN) DOES NOT DEGRADE LIFETIME IN SUBSTRATE (L ~ 100 MICRONS)
2. ABOVE CLEANING PLUS GROWTH OF 0.7μ SB-DOPED EPI LAYER PRODUCED A MEASURABLE CELL, BUT POOR QUALITY.

   - LONG WAVELENGTH RESPONSE GOOD - BETTER THAN CONTROL
   - SHORT WAVELENGTH RESPONSE POOR
   - VERY HIGH REVERSE CURRENT GIVING POOR

     EFFIENCY, FILLING FACTOR, V_{oc}, I_{sc}
     (~3%) (.58) (.38V) (30 ma)

<u>CONCLUDE THUS FAR:</u> QUALITY OF EPI JUNCTION AND/OR EPI LAYER GROWN BY MBE STILL POOR.

SIMS Results on Si MBE Films

DONE BY K.M. STIKA AT JPL

<u>TO DATE</u>

1. VERY USEFUL - SHOWS PROFILES OF DOPANTS AND IMPURITIES AT $> 10^{14}$ cm^{-3} LEVEL
2. DISCLOSES CARBON PEAKS AT INTERFACE AND SURFACE
3. MONITORS OXYGEN LEVEL
4. SHOWS ANTIMONY (n-type) DOPING PROFILE
   SHOWS GALLIUM (p-type) DOPING PROFILE
5. DISCOVERED UNEXPECTED BORON COMING FROM BORON-NITRIDE CRUCIBLE IN GE/SI WORK

<u>FUTURE</u>

1. WILL GIVE QUANTITATIVE CONFIRMATION OF DOPING PROFILES (BUT RESOLUTION IN DEPTH LIMITED TO ~ 50Å)

ORIGINAL PAGE IS
OF POOR QUALITY

Future Work

1. IMPROVE MBE – GROWN p–n JUNCTIONS

   REDUCE DISLOCATIONS, CARBON AT INTERFACE

   DEMONSTRATE LOW REVERSE CURRENT

   MEASURE τ, L_D, WITHIN MBE FILM

2. ACHIEVE COMPARABLE RESULT WITH DIFFUSED CONTROL CELL.

3. GROW FRONT-FIELD, DRIFT-FIELD CELLS AND COMPARE WITH CALCULATED RESULTS.

MULTIJUNCTION (CASCADE) SILICON SOLAR CELL

JET PROPULSION LABORATORY

T. Daud

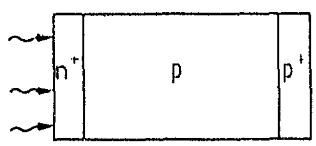

a) CONVENTIONAL

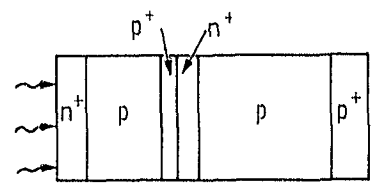

b) MULTI-JUNCTION

MULTIJUNCTION CELL: -

1. VOLTAGES OF INDIVIDUAL CELLS ADD UP
2. BETTER COLLECTION DUE TO VICINITY OF JUNCTIONS
3. EFFICIENT FIRST JUNCTION BSF, AND HIGH V_{OC}
4. LOWER CURRENTS REDUCE LOSSES
5. IT IS REQUIRED THAT CURRENTS OF CELLS ARE EQUAL

Multijunction Solar Cell

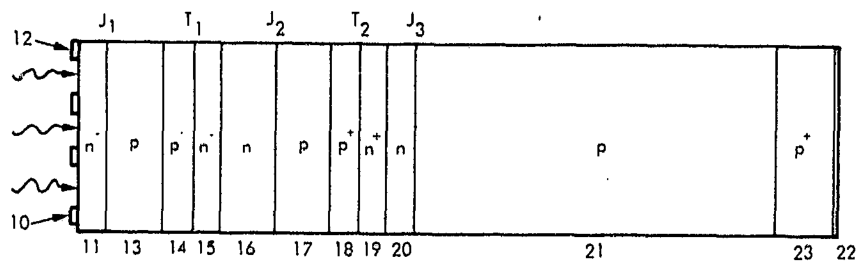

FIG. 1

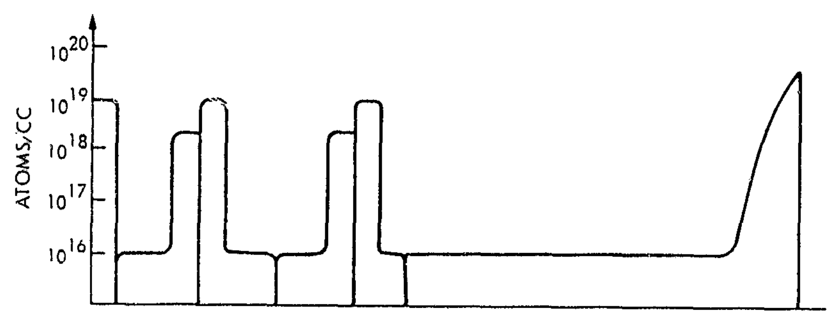

FIG. 2

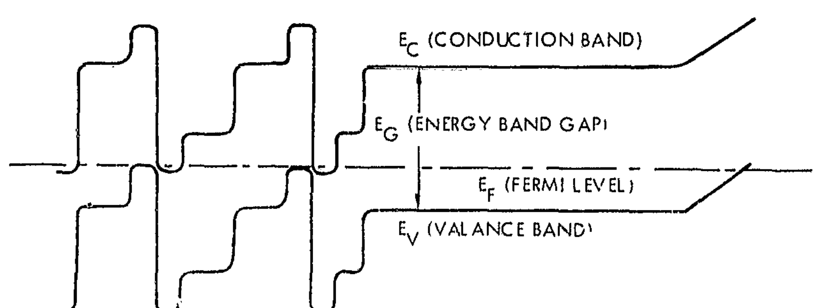

ORIGINAL PAGE IS
OF POOR QUALITY

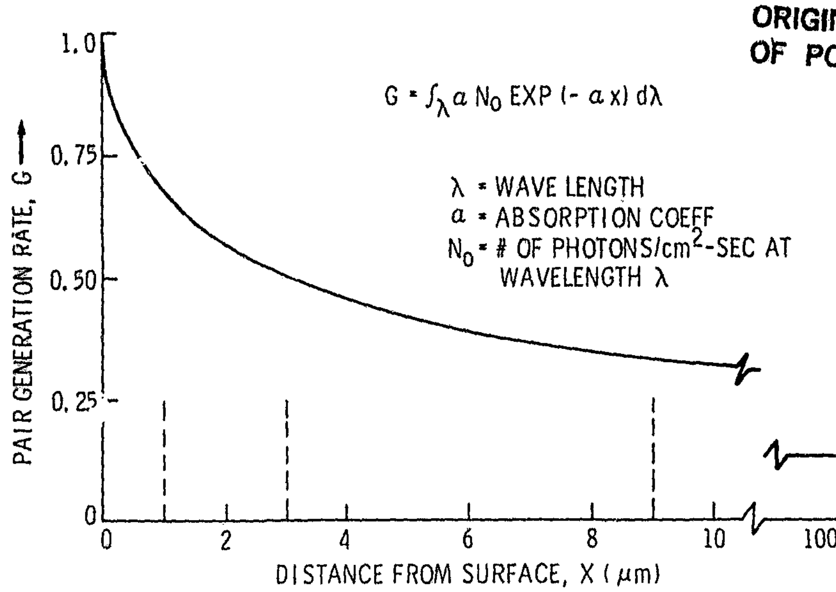

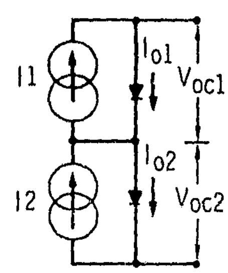

MODELING: -

a) $I1 (I_{p1} + I_{n1} + I_{sc1}) = I2 (I_{p2} + I_{n2} + I_{sc2})$
THICKNESSES OF CELLS OBTAINED BY ITERATIONS

b) $I_{o1} = I_{o2}$
THE OPERATING POINT IS DETERMINED GIVING $V_{oc1} + V_{oc2}$ AS TOTAL V_{oc}

SUCH TAILORED STRUCTURES ARE POSSIBLE WITH
MOLECULAR BEAM EPITAXY

Modeling Calculations

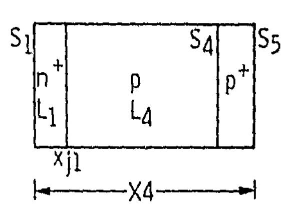

a) CONVENTIONAL

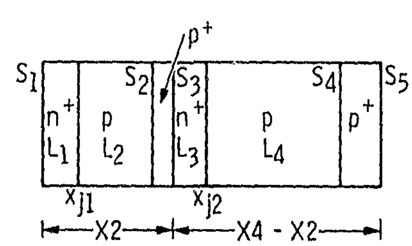

b) TWO-JUNCTION

1 cm^2 AREA, AM-0

$x_j = 0.1\ \mu m$, $S_1 = S_3 = S_5 = 10^5$ cm/sec
$L_1 = 5\ \mu m\ (= L_3)$, $L_4 = X_4 = 200\ \mu m$, $L_2 = 100\ \mu m$

$I_{sc} = 38.7$ mA, $V_{oc} = 580$ mV
EFF. = 13.7%

X2 = 1.0 μm, $I_{sc1} = 28.1$ mA, $V_{oc1} = 680$ mV
$I_{sc2} = 28.1$ mA, $V_{oc2} = 580$ mV
EFF. = 20.5%

DEVELOPMENT AND ANALYSIS OF SILICON SOLAR CELLS OF NEAR 20% EFFICIENCY

UNIVERSITY OF PENNSYLVANIA

M. Wolf

ORIGINAL PAGE IS OF POOR QUALITY

Purpose

TO DETERMINE:

A. THROUGH A MULTIVARIABLE EXPERIMENT, THE PROCESS PARAMETERS, INCLUDING TYPE OF SOURCE GAS AND DOPANTS WHICH YIELD THE HIGHEST MINORITY CARRIER LIFETIMES IN CVD DEPOSITED EPITAXIALLY GROWN SILICON LAYERS;

B. WHETHER HIGH MINORITY CARRIER LIFETIMES CAN BE MAINTAINED IN THE SUBSTRATE WITH APPLICATION OF THE CVD-EPI PROCESS.

C. WHETHER THE DEFECT DENSITY AT THE EPI-LAYER/SUBSTRATE INTERFACE CAN BE KEPT LOW ENOUGH TO YIELD ACCEPTABLE IV-CHARACTERISTICS FOR PN-JUNCTIONS FORMED AT THIS INTERFACE.

D. WHETHER THE RECOMBINATION CENTER DENSITY IN THESE LAYERS IS SMALL ENOUGH SO THAT AUGER RECOMBINATION CAN PREVAIL IN THE DOPANT CONCENTRATION RANGE OF $5 \cdot 10^{16}$ TO $2 \cdot 10^{18}$ cm^{-3};

E. WHETHER CVD-EPITAXY CAN BE CONSIDERED AS A SUITABLE PROCESS IN THE PREPARATION OF MULTILAYER, HIGH EFFICIENCY SILICON SOLAR CELLS.

Status

1. SUBSTRATE WAFERS ORDERED FROM WACKER CHEMIE AND RECEIVED. 0.2-0.4 Ωcm, $\tau > 500$ μs, P-TYPE, B-DOPED, MULTIPLY FLOAT ZONED.

2. MULTIVARIABLE EXPERIMENT DESIGNED.

3. 20 WAFERS SENT TO M/A-COM FOR CVD-EPITAXY DEPOSITIONS.

4. EXPERIMENTAL EQUIPMENT BEING READIED, MODELING COMPLETE.

PRECEDING PAGE BLANK NOT FILMED

PAGE 330 INTENTIONALLY BLANK

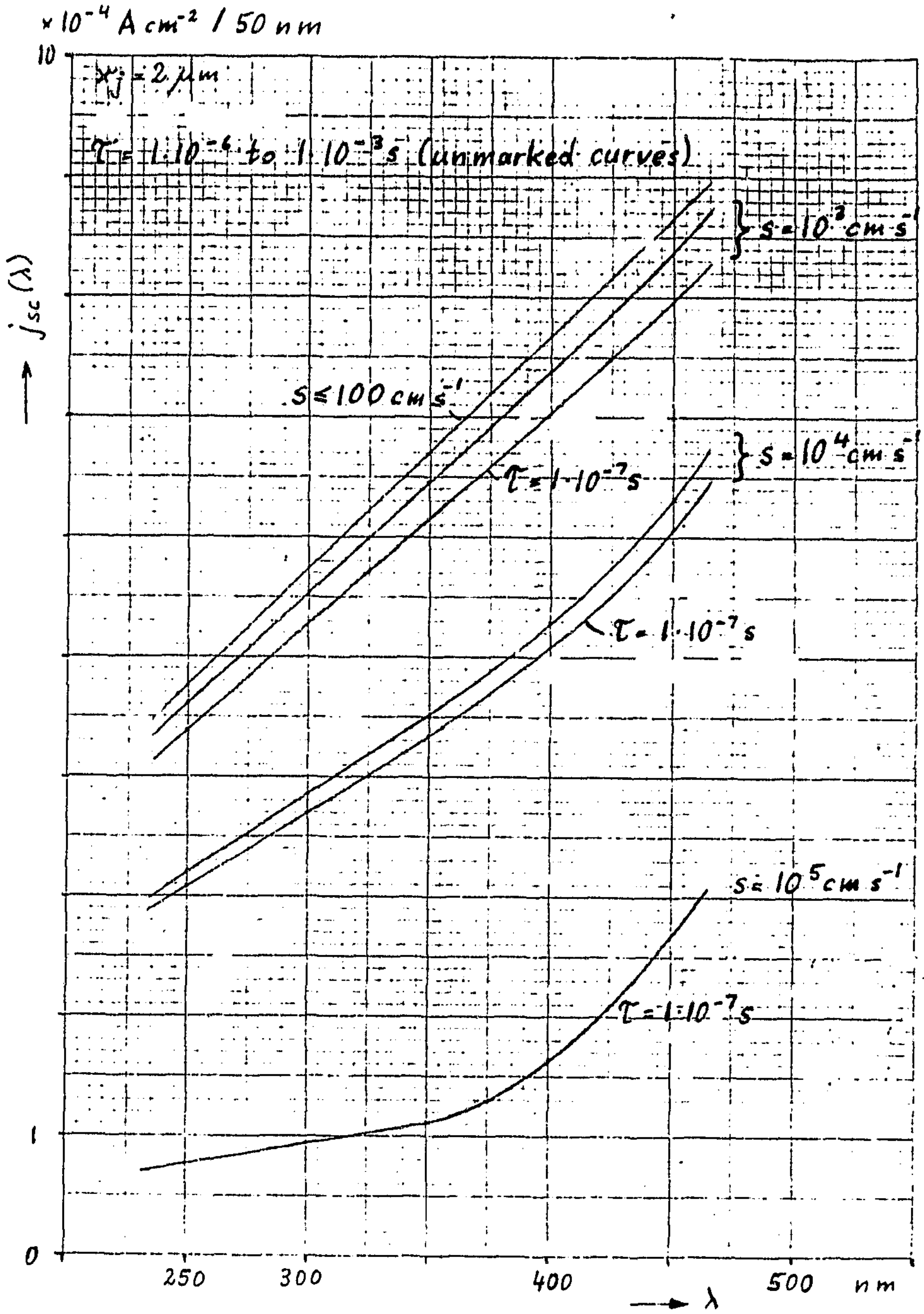
× 10^-4 A cm^-2 / 50 nm
10
1
0
$x_j = 2\,\mu m$
τ = 1·10^-6 to 1·10^-3 s (unmarked curves)
s = 10^3 cm s^-1
s ≤ 100 cm s^-1
τ = 1·10^-7 s
s = 10^4 cm s^-1
τ = 1·10^-7 s
s = 10^5 cm s^-1
τ = 1·10^-7 s
j_sc (λ)
250
300
400
500
nm
λ

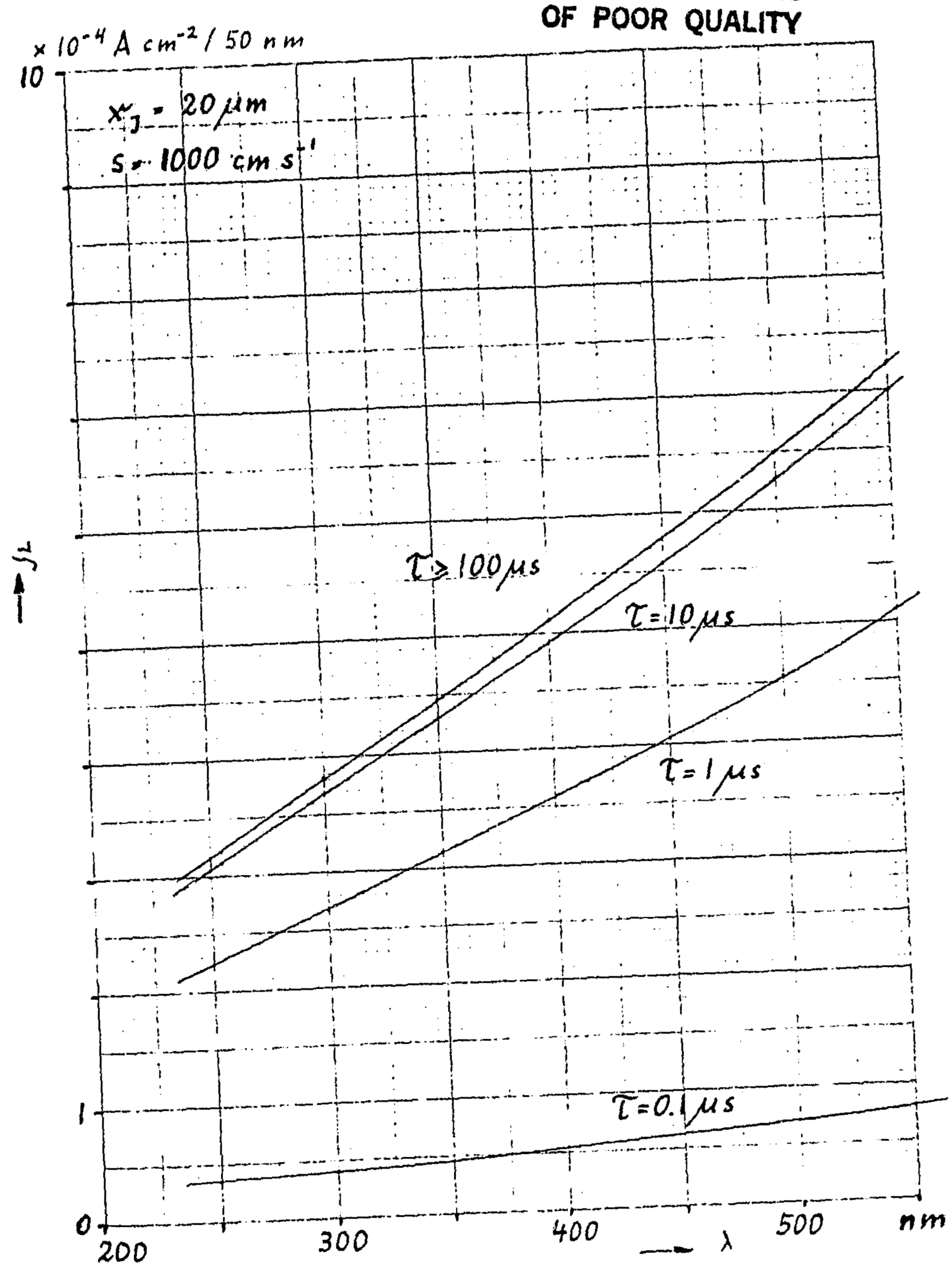
x 10⁻⁴ A cm⁻² / 50 nm
10
1
0
x_J = 20 μm
s = 1000 cm s⁻¹
τ ≥ 100 μs
τ = 10 μs
τ = 1 μs
τ = 0.1 μs
200
300
400
500
nm
λ
j_L

MICROCRYSTAL HETEROJUNCTION SILICON SOLAR CELLS

APPLIED SOLAR ENERGY CORP.

D. Leung

TECHNOLOGY MICROCRYSTALLINE SILICON GROWTH FOR HETEROJUNCTION SOLAR CELLS	REPORT DATE
APPROACH 1) DEPOSIT P-TYPE MICROCRYSTALLINE Si (m-Si) ON N-TYPE SINGLE CRYSTALLINE Si(C-Si) TO FORM HETEROJUNCTION 2) DEPOSIT P-TYPE M-Si ON P-n JUNCTION FORMED IN C-Si TO FORM A WINDOW LAYER CONTRACTOR APPLIED SOLAR ENERGY CORPORATION BOSTON COLLEGE	STATUS
GOALS 1) TO STUDY THE POTENTIAL OF M-Si AS A Voc ENHANCER IN BOTH HETEROJUNCTION AND HETEROFACE SYSTEMS. 2) INVESTIGATE THE POSSIBILITY OF LOW COST SOLAR CELL MANUFACTURE BY USING M-Si.	

Properties of Microcrystalline Si

1)	CRYSTALLINE DIMENSION:	HUNDREDS OF ANGSTROMS
2)	ENERGY BANDGAP:	1.7eV
3)	GROWTH METHOD:	E-GUN EVAPORATION
4)	HYDROGENATED IN HYDROGEN PLASMA	
5)	CONDUCTIVITY:	MUCH HIGHER THAN α-Si

Heterojunction

P-TYPE M-Si

N-TYPE C-Si

Heteroface

P-TYPE M-Si
P-TYPE C-Si

N-TYPE C-Si

Parameters of Interest

1) PRE-DEP CLEAN OF SUBSTRATE.
2) DEPOSITION TEMPERATURE
3) FILM THICKNESS
4) DEPOSITION RATE
5) CELL FABRICATION PARAMETERS

DEVELOPMENT OF METALLIZATION PROCESS

SPECTROLAB, INC.

Alexander Garcia III

Program Personnel

JPL TECHNICAL MONITOR - BRIAN GALLAGHER

PROGRAM MANAGER - NICK MARDESICH

PRINCIPAL INVESTIGATOR - ALEC GARCIA

Objectives

- OPTIMIZATION, EVALUATION AND DEMONSTRATION OF A NOVEL METALLIZATION SYSTEM
- BOTH CZ AND NON CZ WAFERS
- Mo/Sn/TiH SYSTEM

Work Flow Diagram

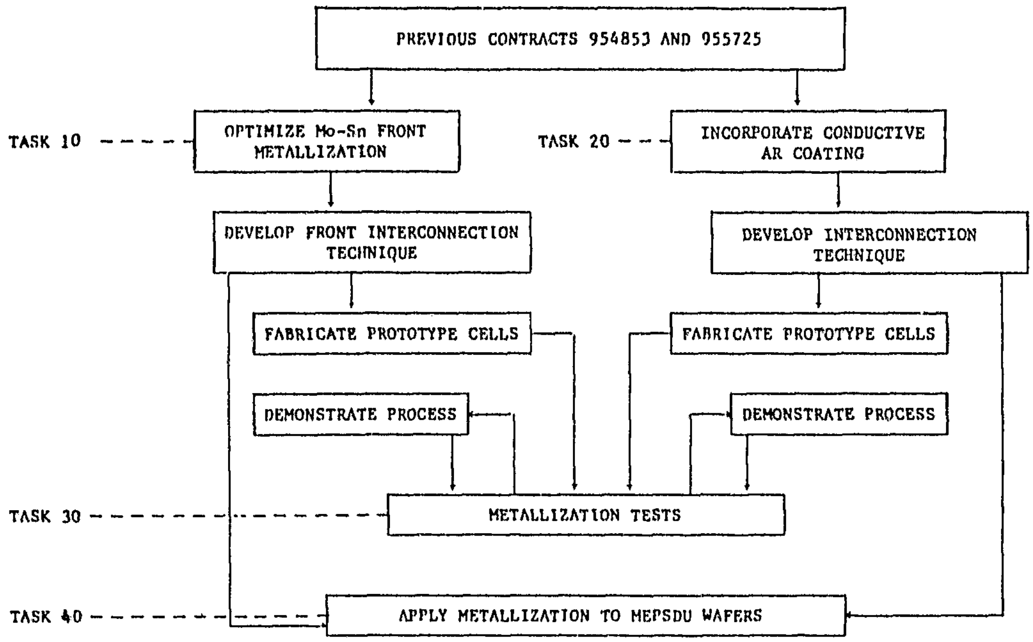

Approach

ORIGINAL PAGE IS OF POOR QUALITY

- Screen Printing
- Air Firing
- Reducing Atmosphere Firing
- Conductive AR Coating (ITO)

Metallization Paste Formulations

	A (RH 3659)	B	C	D	E
MOLYBDENUM (SYLVANIA 280-325)	19.5	50.0	70.0	49.0	48.0
TIN (ATLANTIC EQUIPMENT ENGINEERS SN 266)	80.0	49.5	29.5	49.0	48.0
TITANIUM HYDRIDE (FERRO PLANT FX-41)	0.5	0.5	0.5	2.0	4.0

ORIGINAL PAGE IS
OF POOR QUALITY

Initial Effort I

PREFIRE

	500°C			550°C		
BELT SPEED	18"/MIN.	24	36	18	24	36

FIRE   600°C 30 MIN. IN 5% H_2/95% N_2

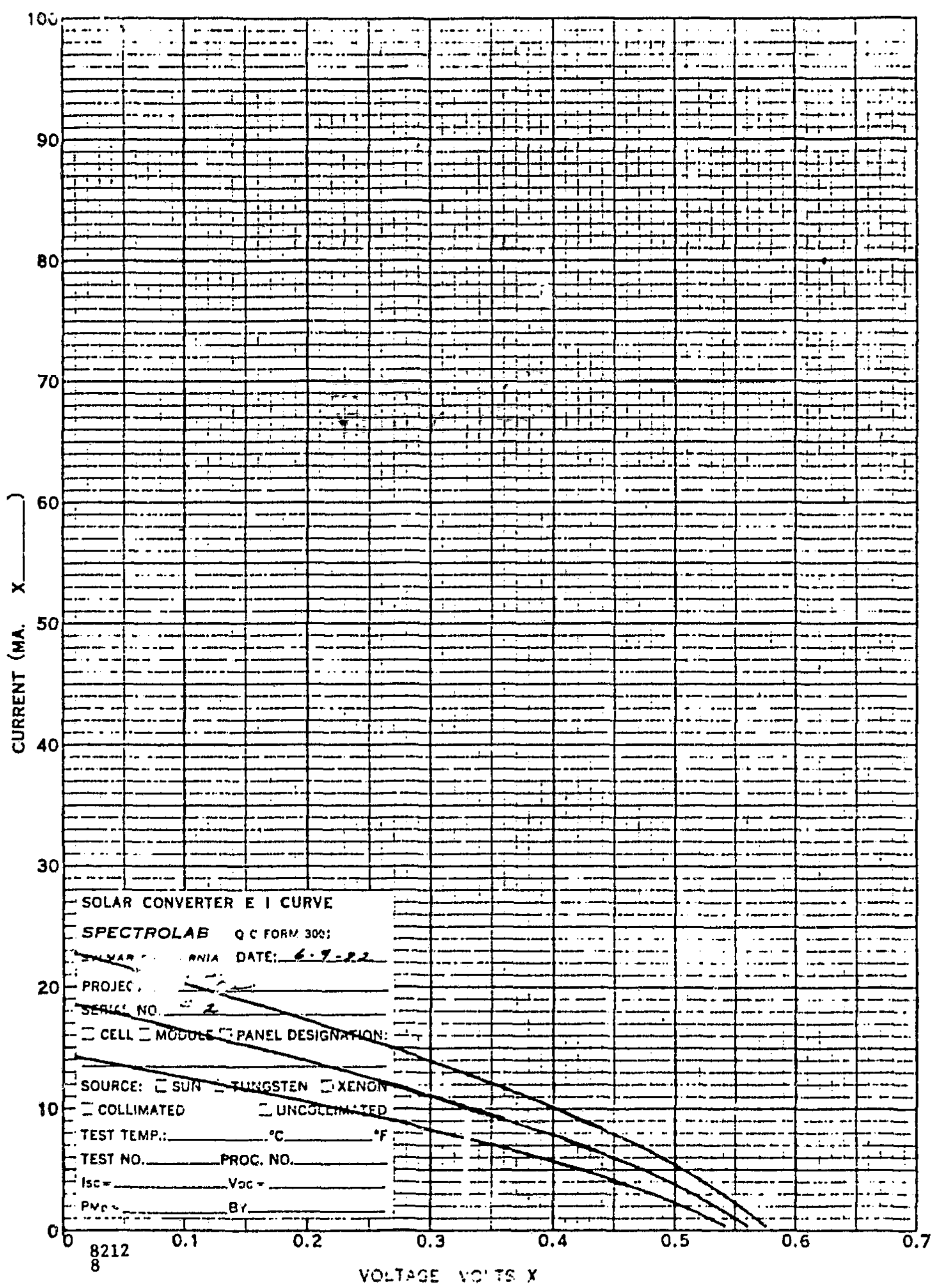

ORIGINAL PAGE IS
OF POOR QUALITY

Initial Effort II

PREFIRE	450°			500°	
	9	18	24	9	18

FIRE AT 650°C $5\%\ H_2/95\%\ N_2$

5, 10, AND 15 MIN.

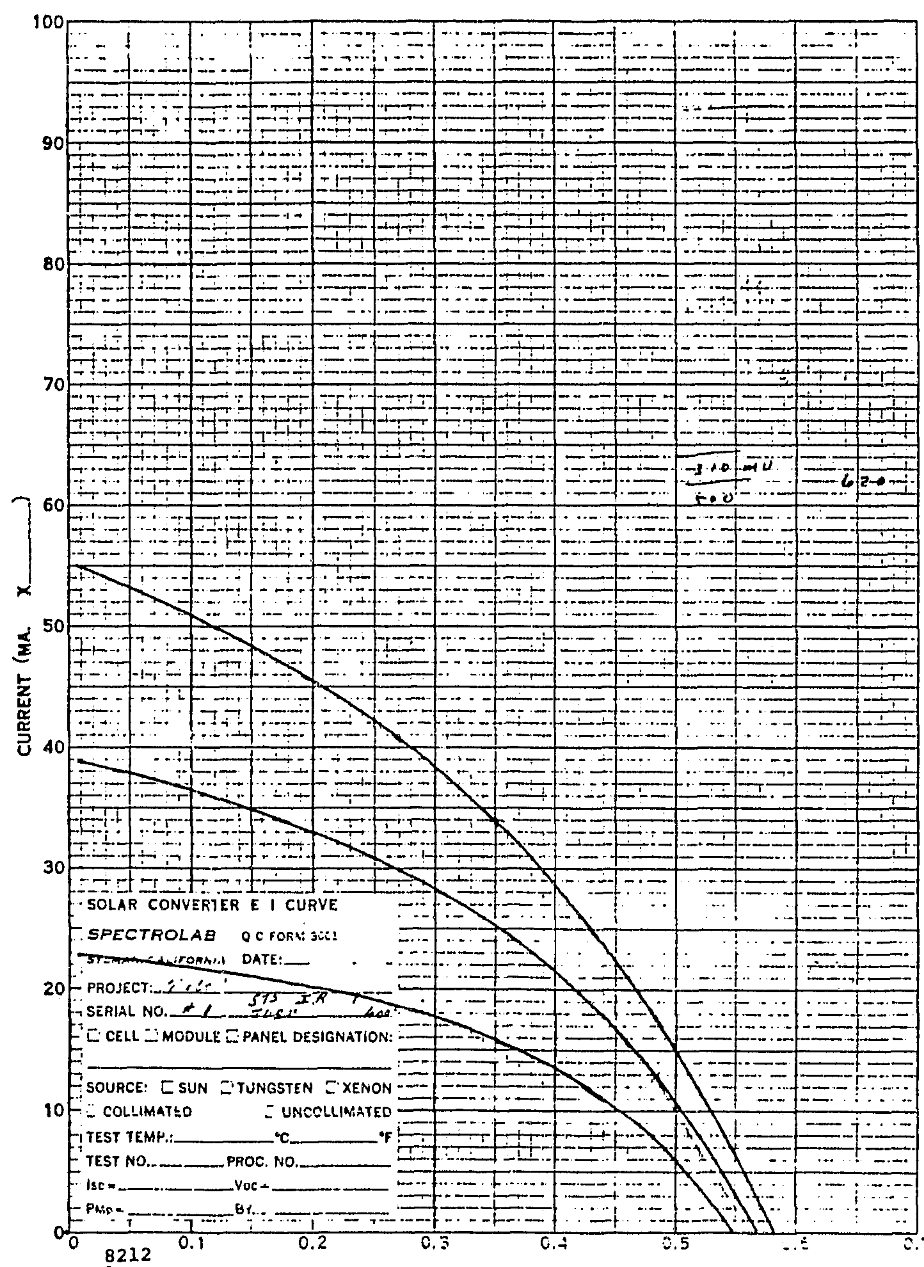

Initial Effort III

PREFIRE

400^{0}, 450^{0}, 550^{0}
AT 24"/MIN.

FIRE

550^{0}, 600^{0}
30 MIN., 200% H_2

CELLS SHOWED METALLIC-LIKE CONTACTS

Initial Optimization for Paste A

PREFIRE	18"/MIN.	500^{0}C
FIRE	1 MIN.	575^{0}C

COMPARABLE TO SILVER PASTE CELLS

Front Metallization Pattern

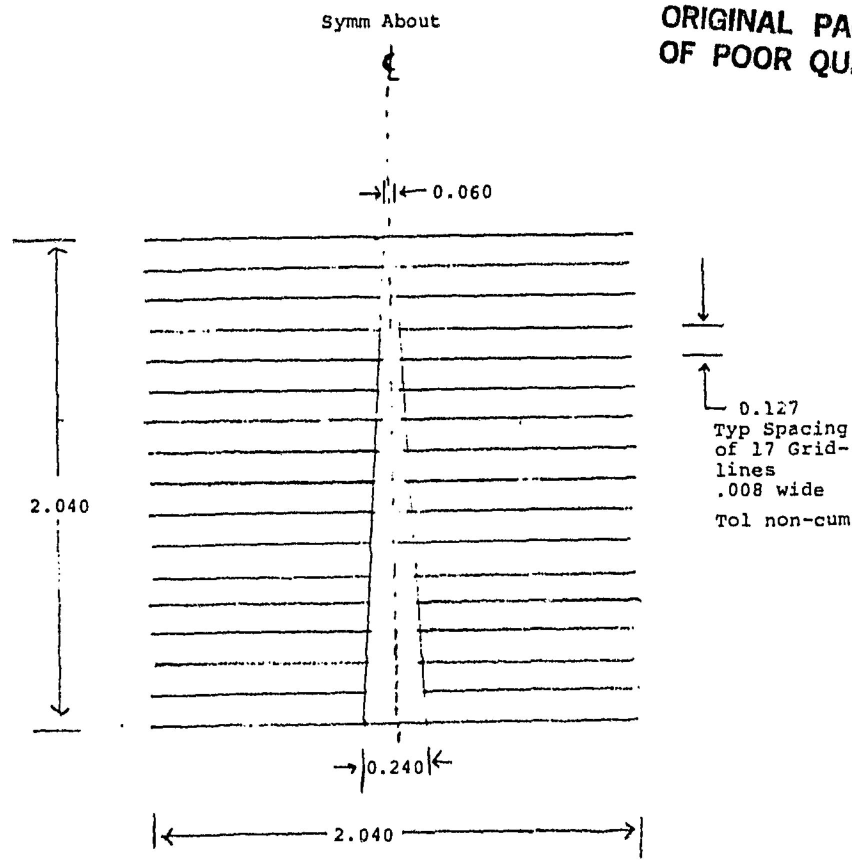

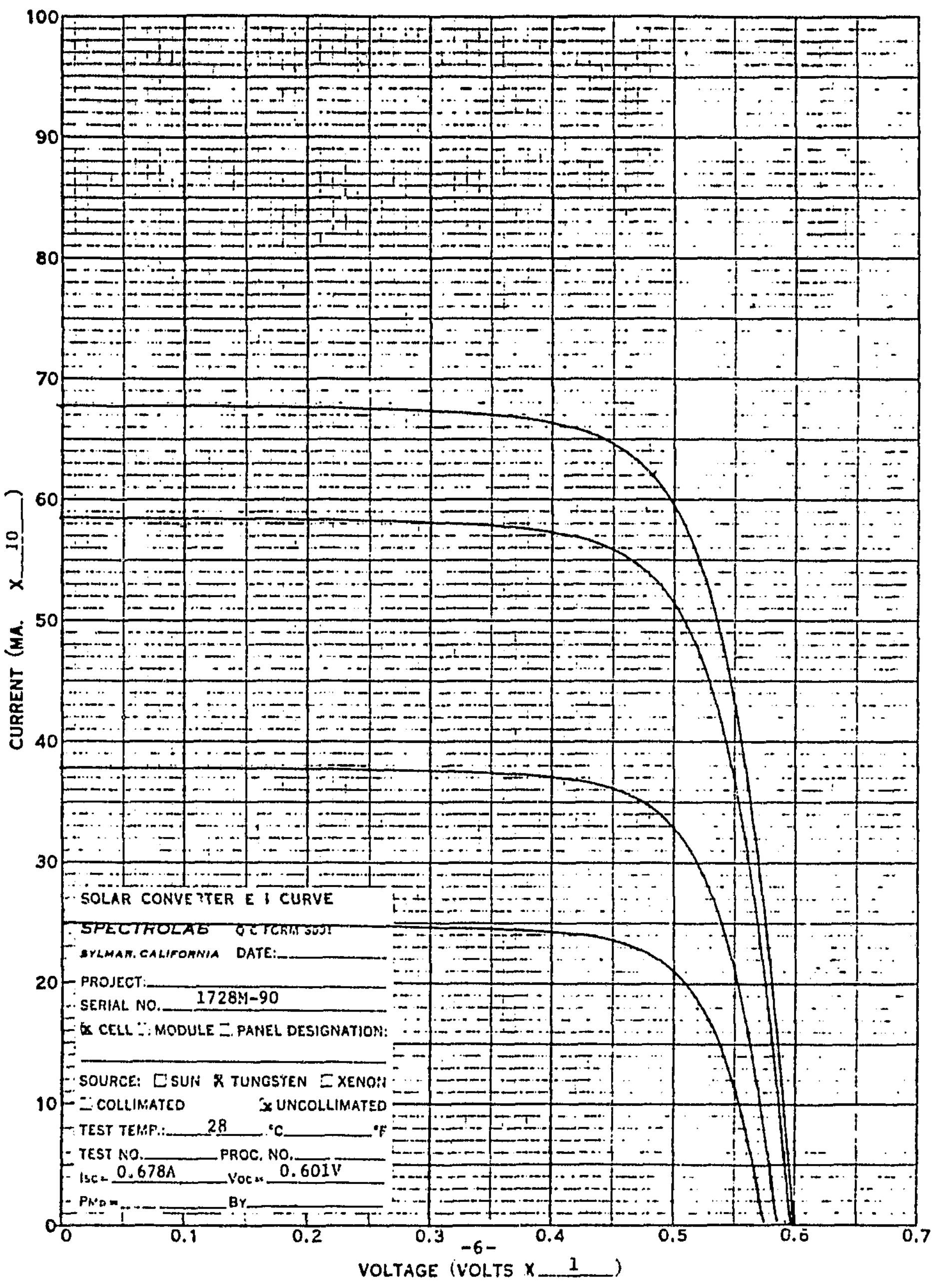

-6-

ORIGINAL PAGE IS
OF POOR QUALITY

ORIGINAL PAGE IS
OF POOR QUALITY

Figure 3

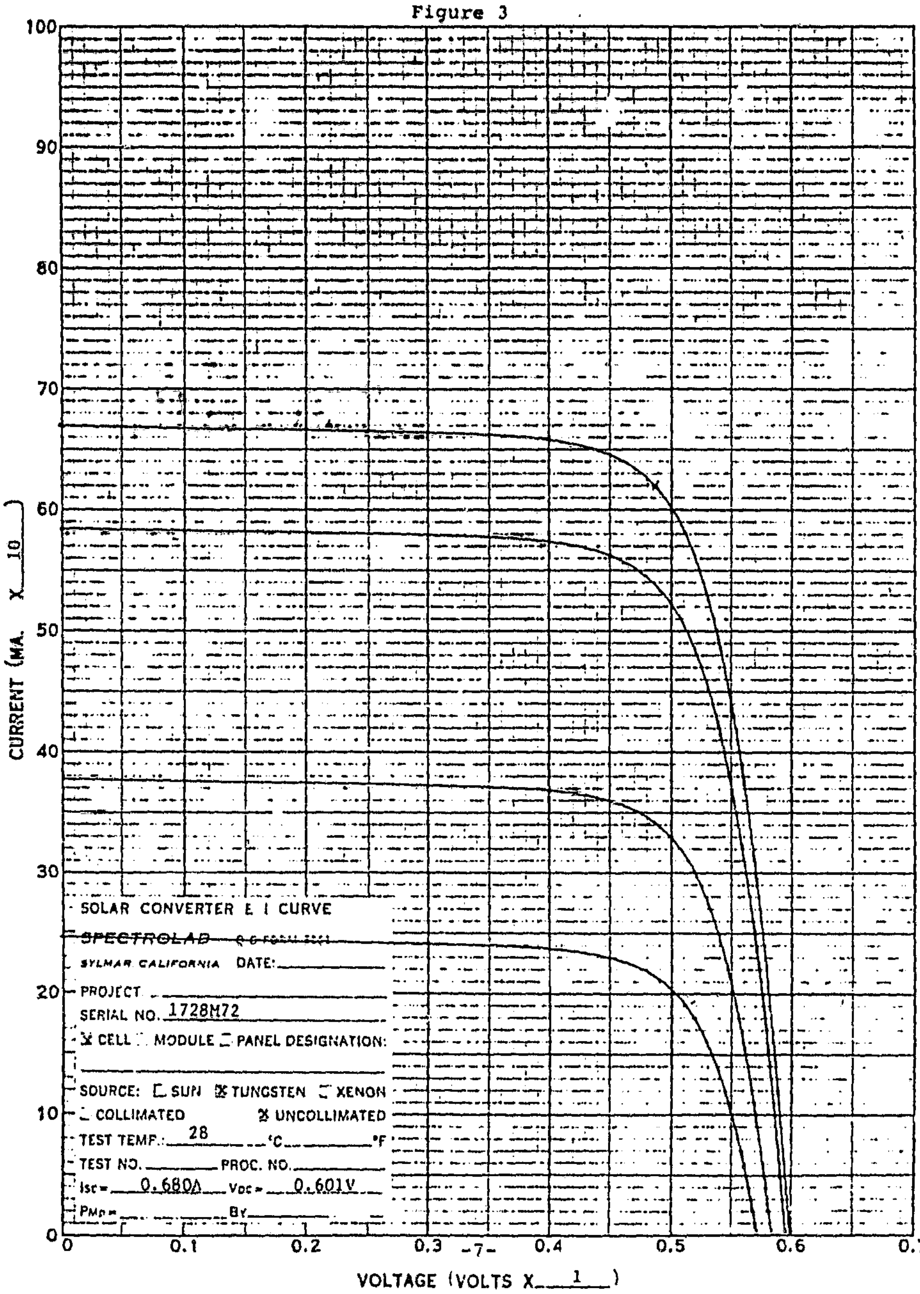

-7-

Cell	V_{oc}	I_{sc}	I_{500}	P_{max}	FF	E
1728M-90 (Mo/Sn)	.601	.678	.596	.229	.73	10.5%
1728M-72 (Ag)	.601	.680	.600	.302	.74	10.6%

Firing Sequences

1) 18"/1 min. 500°C prefire, 1 min. 575°C H_2 fire
2) 18"/min. 500°C prefire, 1 min. 600°C H_2 fire
3) 9"/min. 500°C prefire, 1 min. 575°C H_2 fire
4) 9"/min. 500°C prefire, 1 min. 600°C H_2 fire

Paste Type	Pre-Fire Speed @ 500°	Fire Temp. @ 1 min.	Cell #	V_{oc}	I_{sc}	I_{500}	I_{450}
A	9"	575	1	600	701	482	569
A	9"	575	2	598	677	390	490
A	9"	600	3	601	700	469	553
A	9"	600	4	597	696	458	548
A	18"	575	5	603	702	450	543
A	18"	575	7	599	560	286	359
A	18"	600	6	598	701	440	530
A	18"	600	8	602	70[illegible]	461	550
B	9	575	9	600	687	377	488
B	9	575	11	598	676	297	398
B	9	600	10	600	689	369	478
B	9	600	12	597	644	282	371
B	18	575	13	602	681	345	451
B	18	575	14	602	681	331	438
B	18	600*	15	598	686	409	515
B	18	600*	16	596	692	389	497
C	9	575	20	594	617	194	266
C	9	575	17	589	369	109	150
C	9	600	19	592	668	246	345
C	9	600	18	587	300	90	123
C	18	575	21	597	684	305	415
C	18	575	23	598	667	285	388
C	18	600	22	600	687	350	463
C	18	600	24	596	680	347	458
D	9	575	26	598	684	330	447
D	9	575	25	599	681	320	429
D	9	600	28	598	676	328	435
D	9	600	27	599	678	351	455
D	18	575	31	596	686	346	464
D	18	575	29	598	682	336	448
D	18	600	32	601	691	378	441
D	18	600	30	600	694	393	502
E	9	575	33	596	668	260	356
E	9	575	34	596	639	229	312
E	9	600	35	596	674	265	363
E	9	600	36	598	677	262	417
E	18	575	37	597	672	295	396
E	18	575	38	598	669	286	385
E	18	600	39	597	690	333	440
E	18	600	40	600	685	318	420

Problems

- Poor Adhesion
- Frit Does Not Appreciably Work
- Si-Powder Bond a Problem

Summary and Conclusions

- Comparable to Ag Electrically
- High Shunt Resistances
- Contact Adhesion a Problem
- Future Work with ITO

ALL-METAL THICK-FILM METALLIZATION SYSTEM

BERND ROSS ASSOCIATES

B. Ross

ORIGINAL PAGE IS OF POOR QUALITY

Progress

PROGRESS TO DATE

1. THE SOLAR CELL TEST BEGUN DURING THE PREVIOUS PERIOD WAS ANALYZED.
2. EXPERIMENTATION WAS DONE WITH ALUMINUM PASTES ON SILICON AS WELL AS COPPER AND SILVER PASTES ON ALUMINUM BACK ELECTRODES.
3. AN ANALYSIS OF SILICON SURFACES BY RESONANCE NUCLEAR REACTION PROFILING FOR HYDROGEN WAS BEGUN. SAMPLES PREPARED IN DIFFERENT AMBIENTS WERE EXAMINED TO DETERMINE POTENTIAL GROUNDS FOR LOSS OF ADHESION.
4. SOLAR CELLS PREPARED WITH AIRFIRED ALUMINUM PASTE ELECTRODES WERE SCREENED WITH FRITTED AND UNFRITTED COPPER AND SILVER ELECTRODES. TESTS ARE IN PROGRESS.

Results of Solar-Cell Experiment

PASTES: F31 Cu, 10 WT% Pb, 0 WT% AlSi, 1 WT% AgF
F32 Cu, 10 WT% Pb, 5 WT% AlSi, 1 WT% AgF

PASTE	FIRING TEMP °C	AMBIENT GAS	EFFICIENCY %	FILL FACTOR	SERIES RESIST	SHUNT RESIST
F31	550	N_2	5.9	.48	7.2	239
F31	550	CO	7.7	.63	3.2	330
F31	600	CO	6.5	.55	5.9	375
F31	650	CO	8.1	.68	0.66	237
F32	550	CO	7.1	.66	0.56	475
F32	600	CO	8.0	.72	0.64	181
F32	650	CO	7.5	.74	0.47	400
CONTROLS	Ti-Pd-Ag		8.0	.73	.43	356

PRECEDING PAGE BLANK NOT FILMED

PAGE 348 INTENTIONALLY BLANK

Hydrogen Profiling of Silicon Surfaces by Resonant Nuclear Reactions

$${}_{1}H^{1} + {}_{7}N^{15} \rightarrow {}_{2}He^{4} + {}_{6}C^{12} + 4.45\gamma \quad E_R = 6.385\,\text{Mev}$$

$\sigma_{H-N} = 200$ mb $\quad \sigma_{E \neq E_R} = 10^{-3}\,\sigma_R$

6.385Mev

Detection Window ± 0.005 Mev

Background $\approx 5 \cdot 10^{19}$ cm^{-3}

Depth Resolution 50 - 100 Å

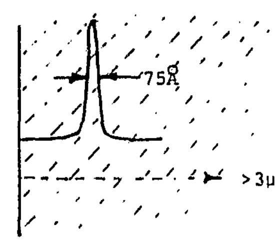

Hydrogen Concentration:

$$H_{\text{cm}^{-3}} = 0.75 \cdot 10^{19}\,\frac{dE}{dx}\frac{\text{Mev}}{\mu m} \cdot \frac{\#\ \text{counts}}{2\mu\text{coul}}\ (N^{15++})$$

Exptl const. $(1.5\frac{\text{Mev}}{\mu m})$
(Detector η, σ,
Geometry etc.)

Example of Method: Hydrogen Implant

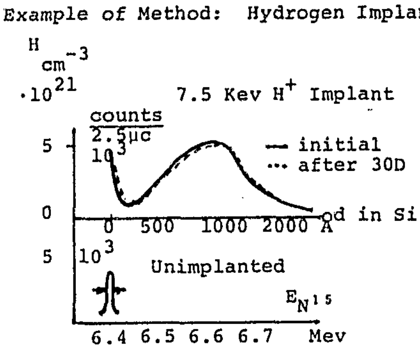

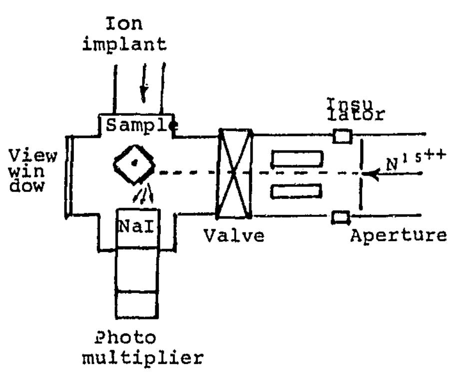

After W. A. Lanford, S.U.N.Y., Albany, N.Y.

ORIGINAL PAGE IS OF POOR QUALITY

ORIGINAL PAGE IS
OF POOR QUALITY

Preliminary Hydrogen Profiling Data

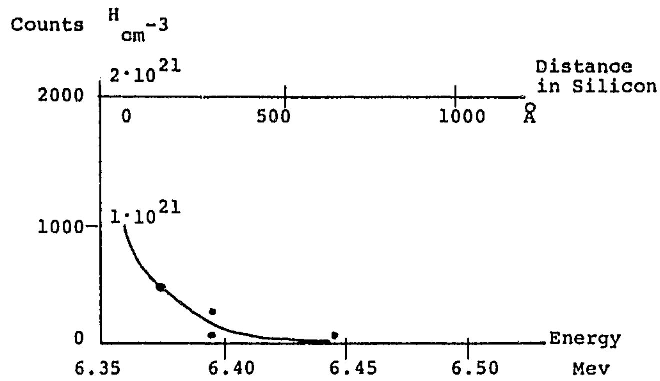

Control sample (untreated)

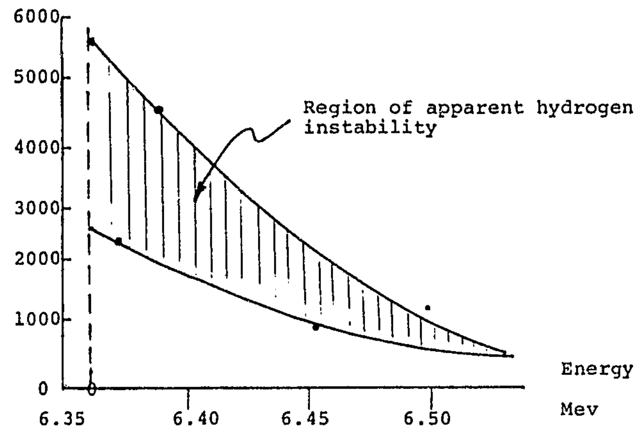

Sample #10, Carbon monoxide fired at 600°C with F31 copper print (removed by scraping)

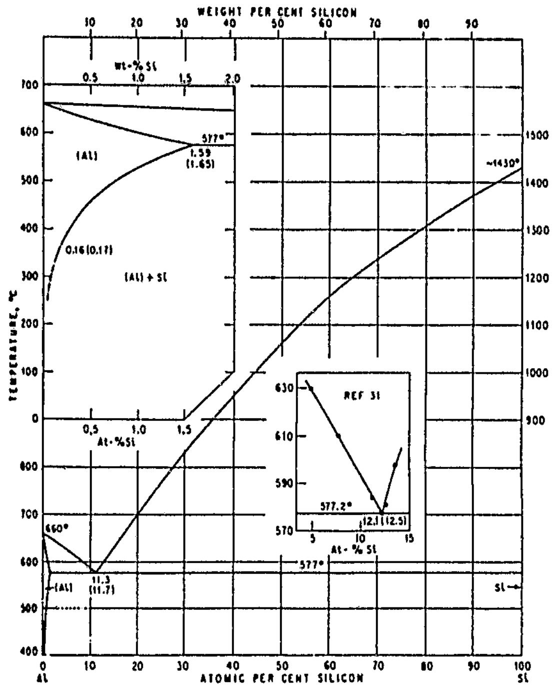

Fig. 77. Al-Si

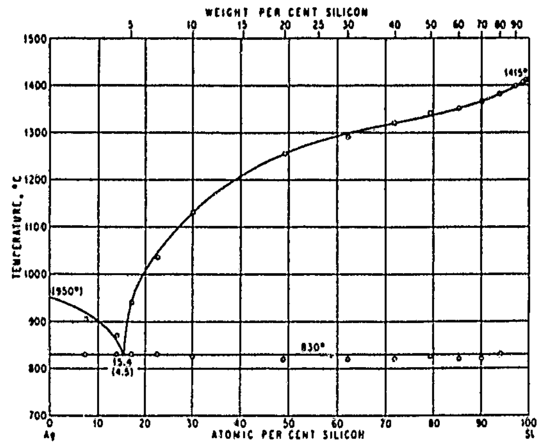

Fig. 32. Ag-Si

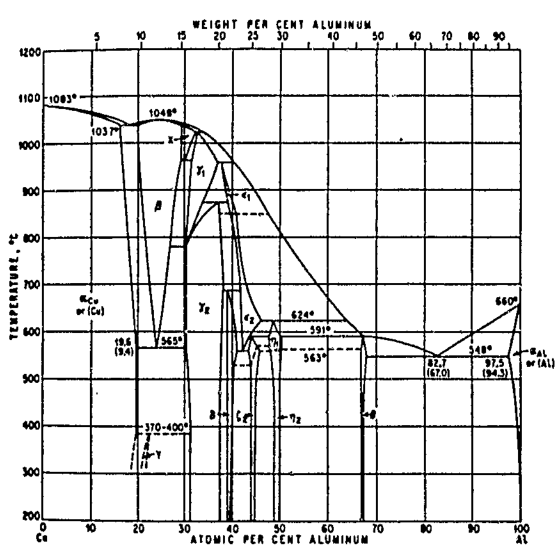

Fig. 52. Al-Cu. (See also Fig. 53.)

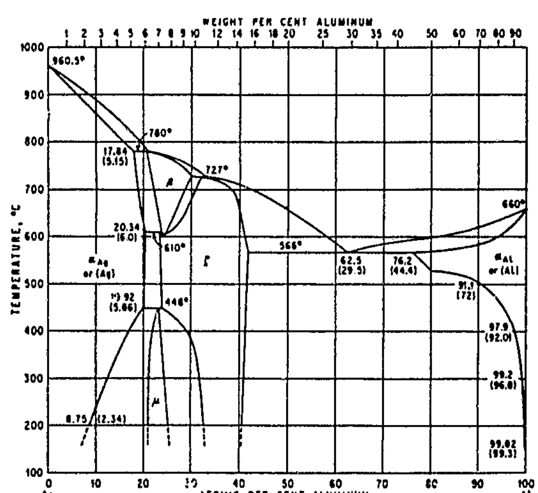

Fig. 1. Ag-Al

PHASE DIAGRAMS RELATED TO THE APPLICATION OF SILVER AND COPPER TO ALUMINUM SILICON CONTACTS (FROM "CONSTITUTION OF BINARY ALLOYS" BY M. HANSEN, 2ND ED., MCGRAW HILL, N.Y., 1958)

Screen-Printed Contacts on Aluminum

Low-Thermal-Mass Quartz Boat for Aluminum Firing (2 x 2-cm Wafers)

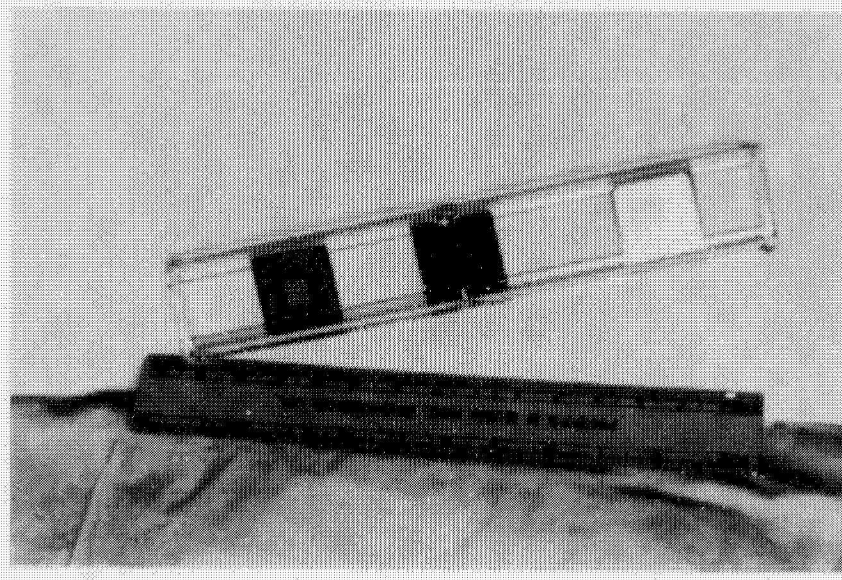

Fritted Silver Paste on As-Fired Aluminum (650°C)

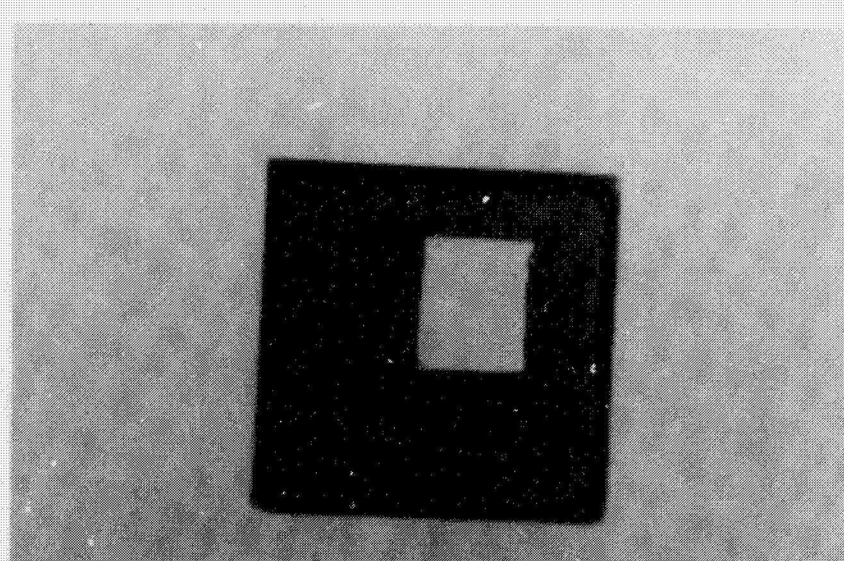

All-Metal Silver on Cleaned Aluminum (650°C)

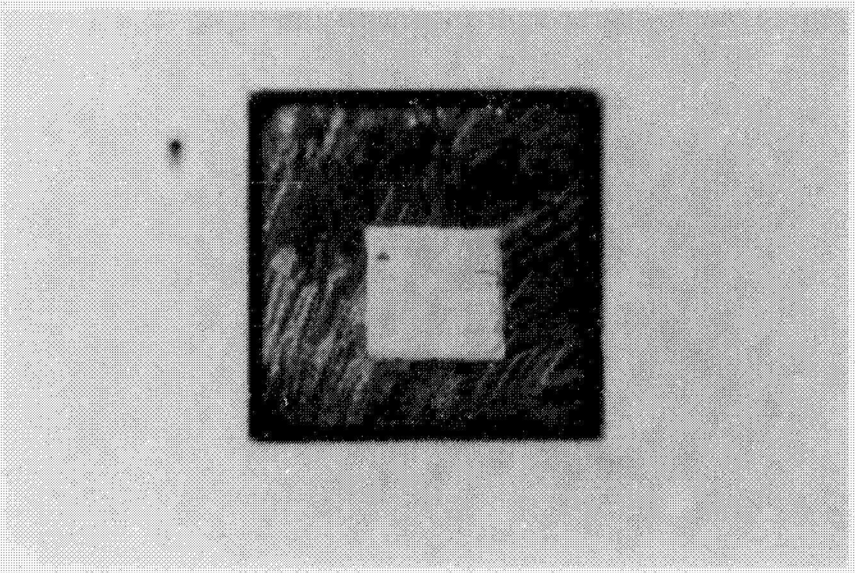

All Metal Silver on As-Fired Aluminum (650°C)

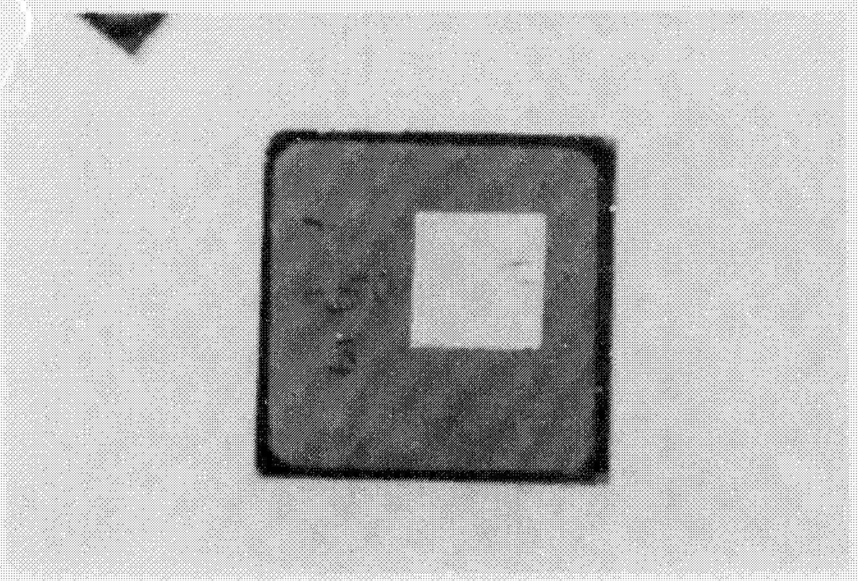

All-Metal Copper on As-Fired Aluminum (600°C)

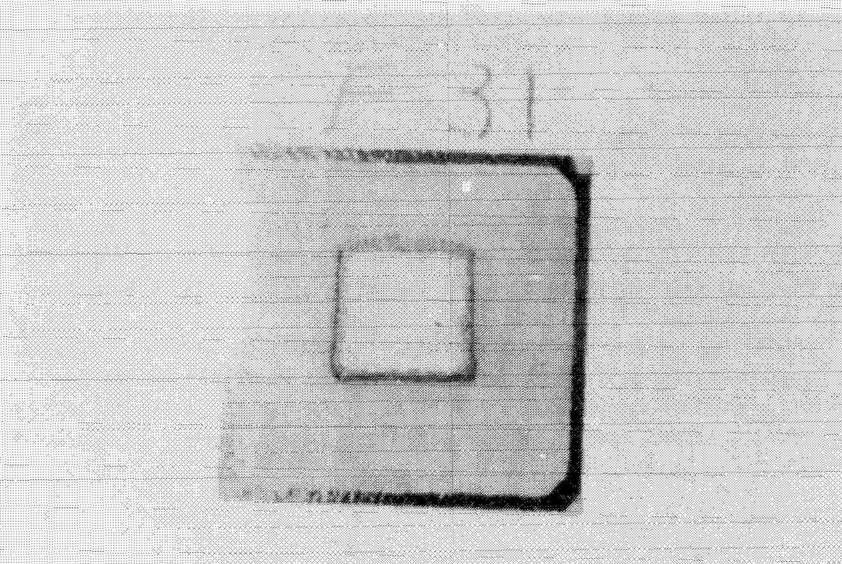

Photomicrograph (100X) of All-Metal Copper on Cleaned Aluminum

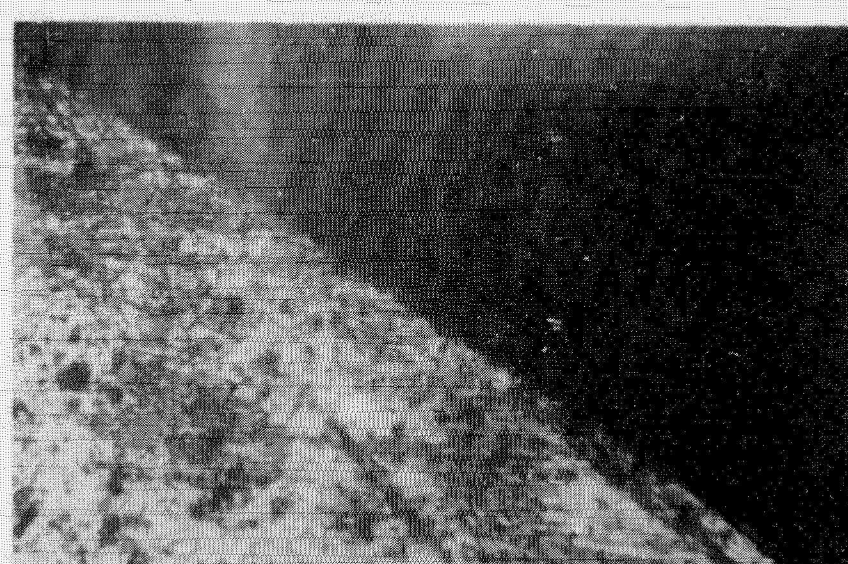

Conclusions and Problems

1. ANALYSIS OF DATA FROM A SOLAR CELL EXPERIMENT SHOWED THAT AL-SI EUTECTIC ADDITIONS TO COPPER PASTES GAVE CONSISTENTLY LOWER SERIES RESISTANCE.

2. ADHESION OF COPPER ELECTRODES FIRED IN CARBON MONOXIDE, WHILE BETTER THAN HYDROGEN FIRED CONTACTS, IS STILL MARGINAL.

3. CELLS WERE PREPARED WITH FRITTED AND UNFRITTED COPPER AND SILVER PASTES ON CLEANED AND UNCLEANED AIR FIRED ALUMINUM BACK CONTACTS. ADHESION APPEARS TO BE GOOD AND ELECTRICAL TESTS ARE IN PROGRESS.

4. PRELIMINARY RESULTS OF NUCLEAR REACTION PROFILING OF THE HYDROGEN CONCENTRATION ON SILICON SURFACES, EXPOSED TO FIRING PROCESSES IN AIR, HYDROGEN AND CARBON MONOXIDE WERE AMBIGUOUS. A SECOND EXPERIMENT IS IN PROGRESS WITH MORE OPTIMIZED SAMPLE SIZES. (W.A.LANFORD, S.U.N.Y., ALBANY, N.Y.)

NICKEL-COPPER METALLIZATION

PHOTOWATT INTERNATIONAL, INC.

Objective

STUDY AND DEVELOP BASE METAL CONTACTS TO BE APPLIED OVER SILICON NITRIDE AR COATING

- FRITTED NICKEL PRINTING INKS
- FRITLESS PRINTING INKS
  - NICKEL BASE
  - TIN BASE

Fritless Nickel Printing Inks

90Ni 10Sn + $ZnCl_2$
TFS 5522 Ni
98 TFS 5522 2 AgF
95 TFS 5522 5 AgF
TFS 5522 + 0.5 Teflon Powder
98 TFS 5522 2 $AgPO_3$
98 TFS 5522 5 $AgPO_3$

Current-Voltage Curves for TFS 5522 Nickel Fired at 850°C on Si_3N_4, Not Plated

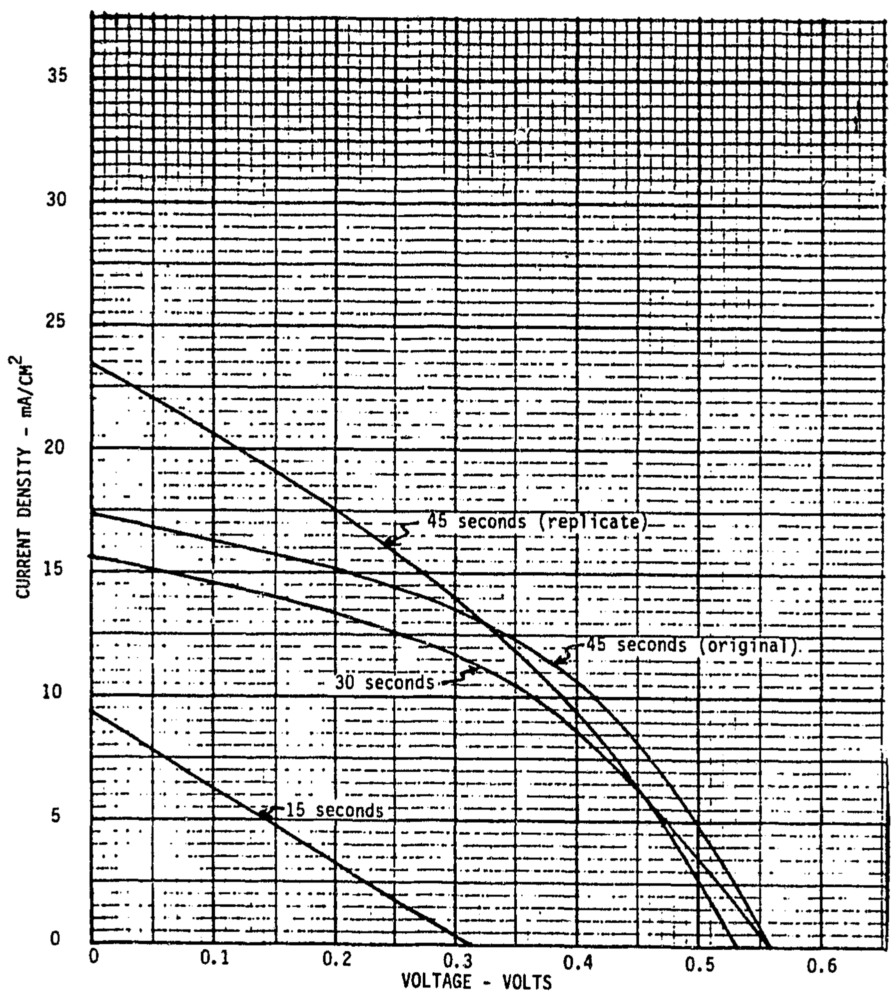

ORIGINAL PAGE IS
OF POOR QUALITY

Current-Voltage Curves for TFS 5522 Nickel + 5% AgF Fired at 850°C on Si_3N_4, Not Plated

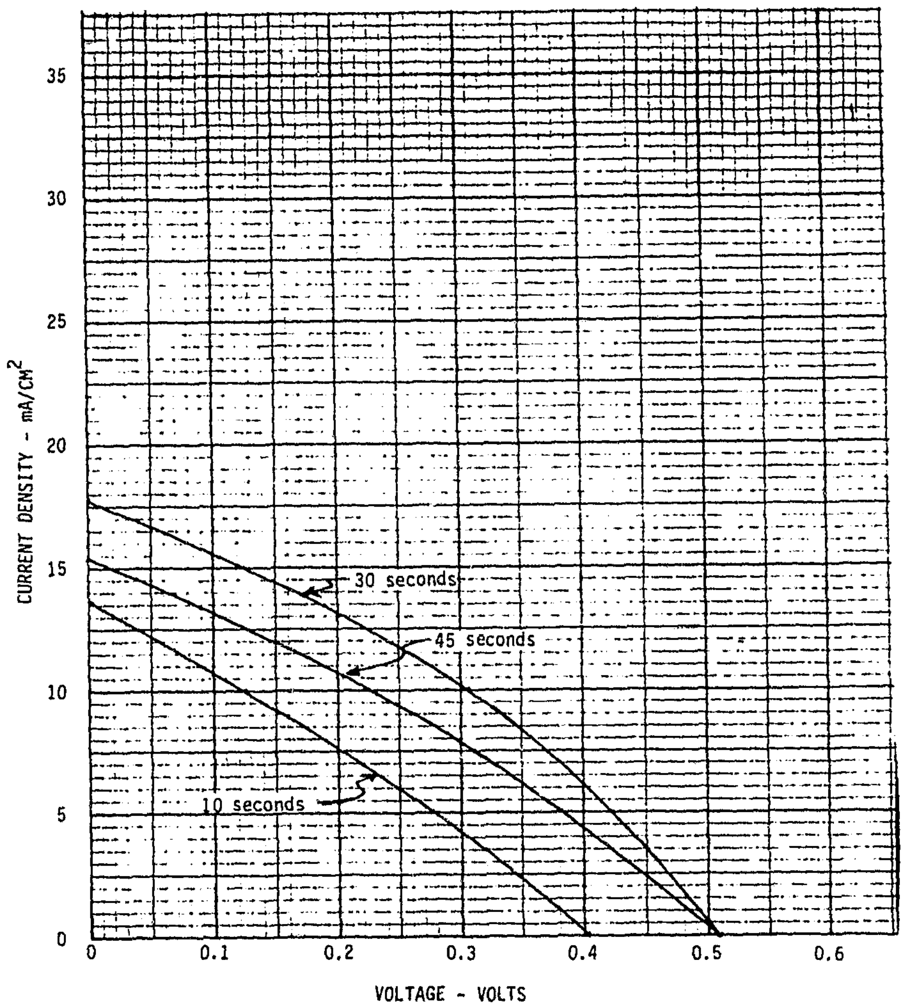

Fritless Tin-Base Printing Inks

98 Sn 2 TiH_3
99 Sn 1 AgF
Sn + 0.05 Teflon Powder
90 Sn 10 Ag
89 Sn 10 Ag 1 AgF
80 Sn 18 Mo 2 TiH_3
98 (Sn/Mo/TiH_3) 2 AgF
90 (Sn/Mo/TiH_3) 10 Ag
80 (Sn/Mo/TiH_3) 20 Ag

Current-Voltage Curve for Sn + 1% AgF Fired for 5 min at 800°C in N_2 + CO Atmosphere; Silver Plated

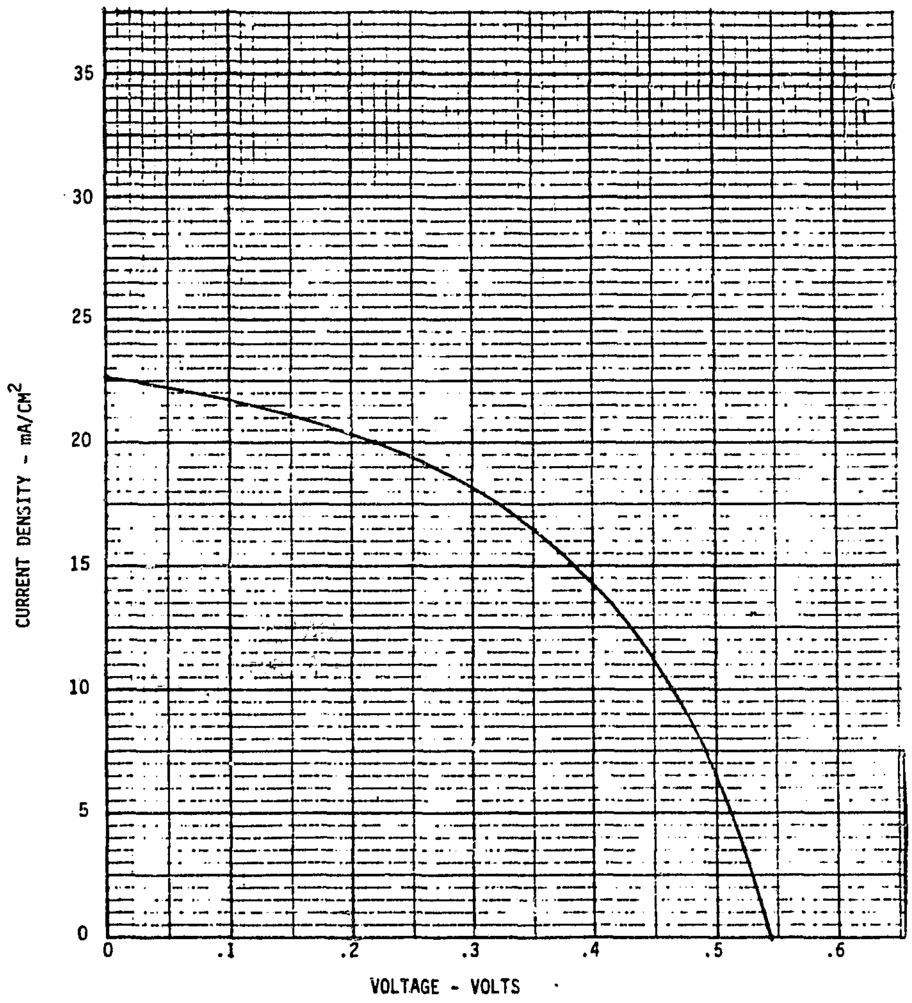

METALLIZATION COST COMPARISON

JET PROPULSION LABORATORY

R.W. Aster
H. Awaya
R. Daniel
D. Burger

Introduction

Purpose of this analysis:

- **Compare costs and effectiveness of SOA metallization and projected metallization approaches**
- **Estimate the potential impact of R&D in this area**

Approach:

- **Use data from FSA contractors and other sources with IPEG2 to establish costs**
- **Use R. Daniel's Grid Optimization Model to establish electrical performance ratios**

Study Limitations

- **There are many metallization processes, only 12 have been analyzed so far**
- **SOA metallization costs are typically based on commercial experience of industry**
- **Advanced metallization costs are typically based on laboratory-scale experiments and extrapolations**
- **Reliability is not yet addressed. There are two basic reliability issues:**
  - **Immediate mechanical and subsequent electrical test yields**
  - **Lifetime (e.g., 20-year) performance**
- **Compatibility with other process steps and with unusual sheet specifications will not be addressed**

Candidate Processes/Systems

PROCESS/SYSTEM	COST/m^2	DATA SOURCE
Evaporation		
• SOA (Ti/Pd/Ag)	\$90	ASEC
• Advanced (Ti/Ni + Cu plating*)	\$14	Westinghouse
Screen print		
• SOA (Ag paste)	\$8 to \$35	2.80/W, Block IV
• 1990 (Ag paste*)	\$7 to \$34	JPL BPU
• SOA (Al paste)	\$2.4	2.80/W, Block IV
• 1990 (Al paste*)	\$1.4	JPL BPU
• 1990 (Mo/Sn*)	\$2.0	JPL BPU, Dr. Macha
Electroless plating		
• SOA (Print resist, Ni-plate, Sinter, Wave solder)	\$8	Solarex, Motorola
• Advanced (PR, Ni plate, Sinter, Cu plating*)	\$9.4	Motorola
Midfilm* (Ag)	\$5 to \$16	Spectrolab
Midfilm* (Mo/Sn)	\$2	Spectrolab, Dr. Macha
Ion plating* (Ti/Ni/Cu)	\$6	Illinois Tool Works

*Advancement of PV SOA

ORIGINAL PAGE IS
OF POOR QUALITY

Electrical Performance Methodology

- Optimum spacing and dimensions (within process constraints) are calculated by R. Daniel's Grid Optimization Model
- Cell efficiency is strongly influenced by sheet characteristics, junction quality, AR coating, and test conditions as well as by metallization process/system
- Therefore, *relative* electrical performance is derived in this study
- Input data that influence relative electrical performance are:
  - Metallization material resistivity, ρ_M (Ω-cm)
  - Metal-to-silicon contact resistivity, ρ_C (Ω-cm^2)
  - Metallization thickness, T (cm)
  - Fine grid line width, B (cm)
  - Resistivity of busbar strapping material, ρ_{MB} (Ω-cm)
  - Strapping material thickness, T_B (cm)

Electrical Performance Optimization Model Inputs

PROCESS/SYSTEM	ρ_M (Ω-cm)	ρ_C (Ω-cm^2)	T (μm)	B (μm)	ρ_{MB} (Ω-cm)	T_B (μm)	RATIO
Lossless*	0	0	–	0	0	–	1.000
EVAP SOA	1.6×10^{-6}	1×10^{-4}	4	38	1.76×10^{-6}	63.5	0.919
EVAP Advanced	2.03×10^{-6}	1×10^{-4}	4	38			0.914
Print Ag SOA	4.77×10^{-6}	1×10^{-3}	8	127			0.892
Print Ag Advanced	4.77×10^{-6}	1×10^{-3}	12.7	127			0.898
Print Al SOA	2.00×10^{-5}	1×10^{-6}	10	127			0.854
Print Al Advanced	2.00×10^{-5}	1×10^{-6}	12.7	127			0.871
Print Mo/Sn	2.95×10^{-5}	1×10^{-3}	12.7	127			0.856
Electroless Ni/Solder SOA	2.00×10^{-5}	1×10^{-3}	50.8	457.2			0.833
Electroless Ni/Cu Advanced	2.03×10^{-6}	1×10^{-4}	4	38			0.914
Midfilm Ag	4.77×10^{-6}	1×10^{-3}	10	45.7			0.913
Midfilm Mo/Tin	2.95×10^{-5}	1×10^{-3}	15	45.7			0.871
Ion Plating, Ti/Ni/Cu	1.76×10^{-6}	1×10^{-4}	4	38			0.917

*Baseline values are 40 $\Omega/\square$ sheet resistance, 0.45V max power voltage, 30 mA/cm^2 max power current density

Efficient Frontier: State of the Art

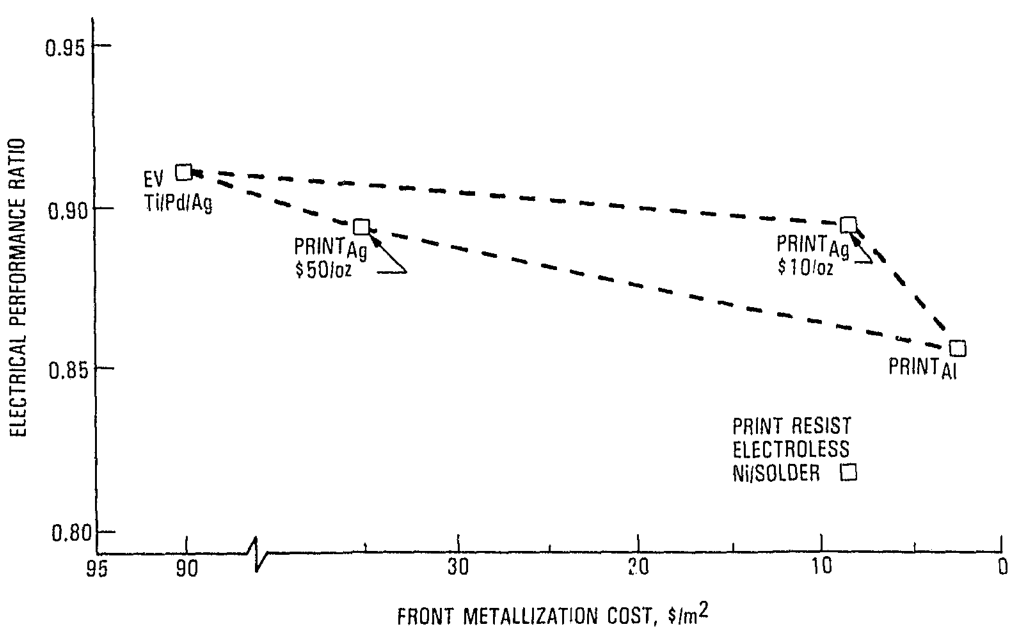

Efficient Frontier: State of the Art Plus Advanced Technology

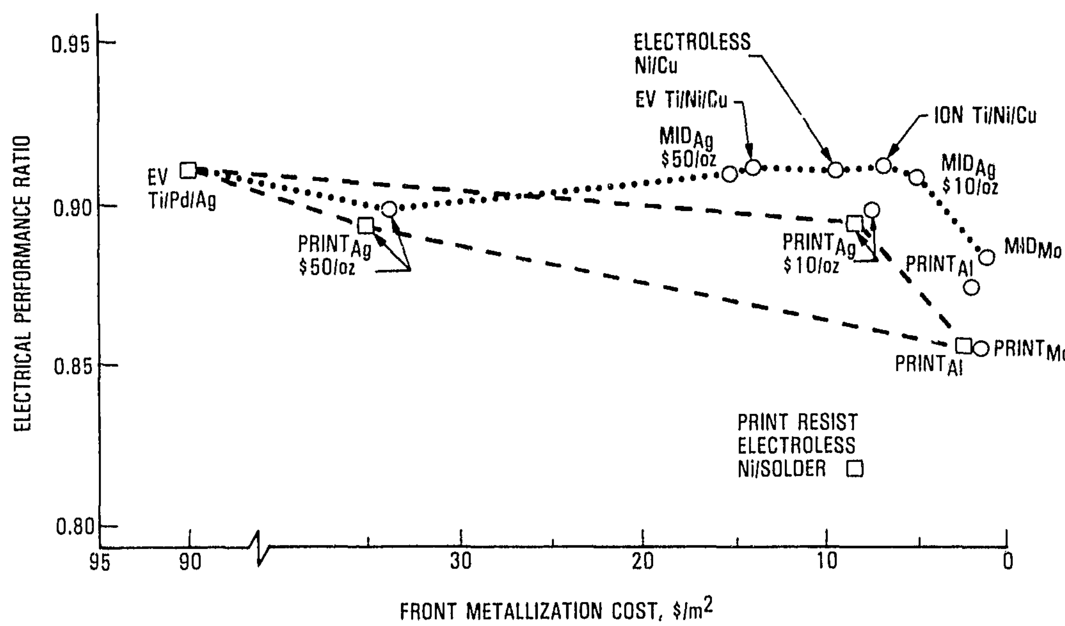

Optimization

- The optimal metallization process/system will be on the efficient frontier
- However, the best point on the frontier is dependent on the total system cost (this determines the value of enhanced electrical performance)
- A SOA PV system has a tradeoff slope of 0.00076 (based on SMUD data)
- An advanced PV system could have a tradeoff slope of 0.00624 (based on PV Lead Center advanced system goals)
- These slopes are used on the next figure to identify preferred metallization processes/systems

Efficient Frontier: State of the Art Plus Advanced Technology and Optimization

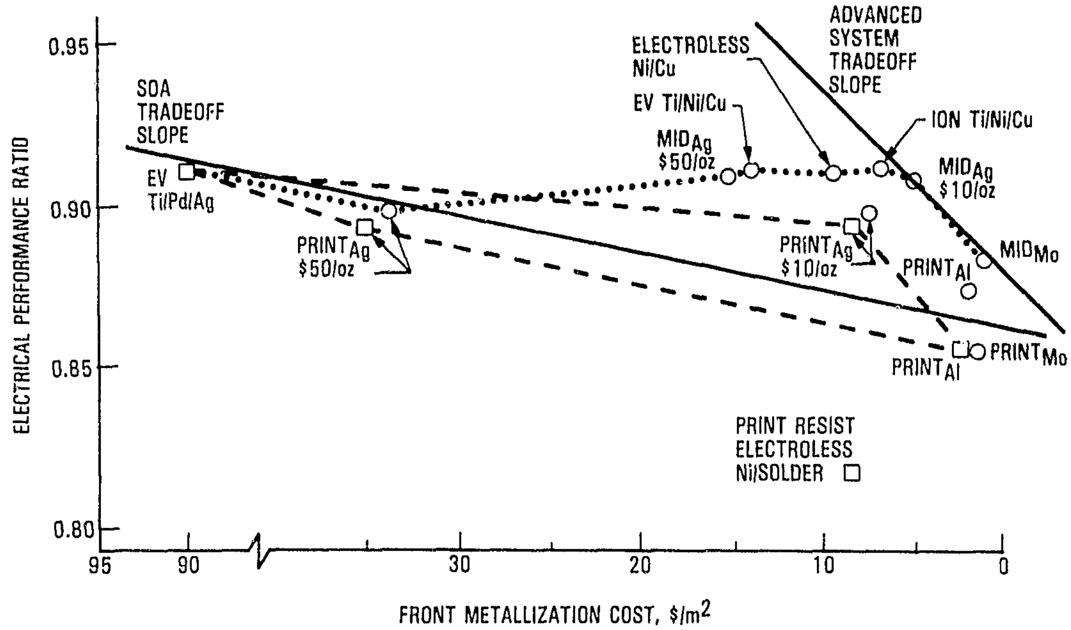

Status

- **The efficient frontier study for metallization is not yet complete. Necessary steps toward completion include:**
  - **Analysis of a larger number of SOA processes/systems**
  - **Incorporating reliability into the study**
- **Completion should occur in time for the next FSA PIM. A full report should be prepared by the end of this year**

PROCESS RESEARCH ON NON-Cz SILICON MATERIAL

WESTINGHOUSE ELECTRIC CORP.

C.M. Rose

- Westinghouse originally planned to meet a commercial window of '87-'88, based largely on a U.S. market.

- Our scale-up sequence and schedule (semi-automated line, 25 MW fully automated line) was predicated on the '87-'88 commercialization target.

- The worldwide recession and softening oil price indicate that a significant commercial market will not develop until the mid '90s.

- Because of the delay in market development, Westinghouse has decided to delay scale-up to permit further technology development. (Note: Technical performance of Westinghouse solar photovoltaic technology is demonstrated. Development is focused on steps to provide the lowest cost product and thus lower commercial risk.)

- Market will develop sooner in overseas locations, such as India. Westinghouse is willing to support nearer term scale-up schedule to meet objectives of Indian Government. This involves some modest, additional risk with respect to meeting product cost projections.

Contract Information

Objective:	Investigate High-Risk; High-Payoff Improvements to Ⓦ Baseline Process Sequence
Time Period:	February 1982 through September 1983
Funding:	JPL Funds Used for Engineering Effort Only; Technician and Material Costs Borne By Ⓦ

Contract Tasks

- Liquid Application
- Liquid Dopant Junction Formation
- Liquid Diffusion Mask
- Ion Implantation
- Silicon Pellet Formation
- Cost Implications

Advantages of Liquid Dopants

- Fewer Cleaning Operations
- Fewer Chemicals Required
- Simplified Process Controls
- Less Expensive Equipment Required
- More Automatable Process
- Improved Cell Property Uniformity
- Baseline Sequence Compatibility

Junction Formation Process Steps

PROCESS	BASELINE PROCESS	LIQUID BORON ONLY	LIQUID BORON + LIQUID MASK	LIQUID BORON + LIQUID PHOSPHOROUS	LIQUID BORON + LIQUID PHOSPHOROUS + LIQUID MASK	SIMULTANEOUS DRIVE OF BORON AND PHOSPHOROUS
CVD SiO_2 N+ SIDE	•	•		•		
HF ETCH	•	•		•		
APPLY LIQUID BORON AND BAKE		•	•	•	•	•
APPLY LIQUID MASK AND BAKE			•		•	
PRE-DIFFUSION CLEAN	•					
DIFFUSE P+	•	•	•	•	•	
OXIDE ETCH	•	•	•	•	•	
APPLY LIQUID PHOSPHOROUS AND BAKE				•	•	•
CVD SiO_2 P+ SIDE	•	•		•		
APPLY LIQUID MASK AND BAKE			•		•	
HF ETCH	•	•				
PRE-DIFFUSION CLEAN	•	•	•			
DIFFUSE N+	•	•	•	•	•	
DRIVE BORON AND PHOSPHOROUS						•
OXIDE ETCH	•	•	•	•	•	•

Liquid-Dopant/Liquid-Mask Application Studies

- Manual Application
  - Squeegee Applicator Acceptable
  - Liquid Boron/Liquid Mask Satisfactory
  - Initial Liquid Phosphorus Applications Unsuccessful
- Spray-On Application Unsuccessful
- Spin-On Application Impractical
- Meniscus Applicator
  - Successful Tests Completed For All Liquids
  - Cavex Unit On Order

Meniscus Coater

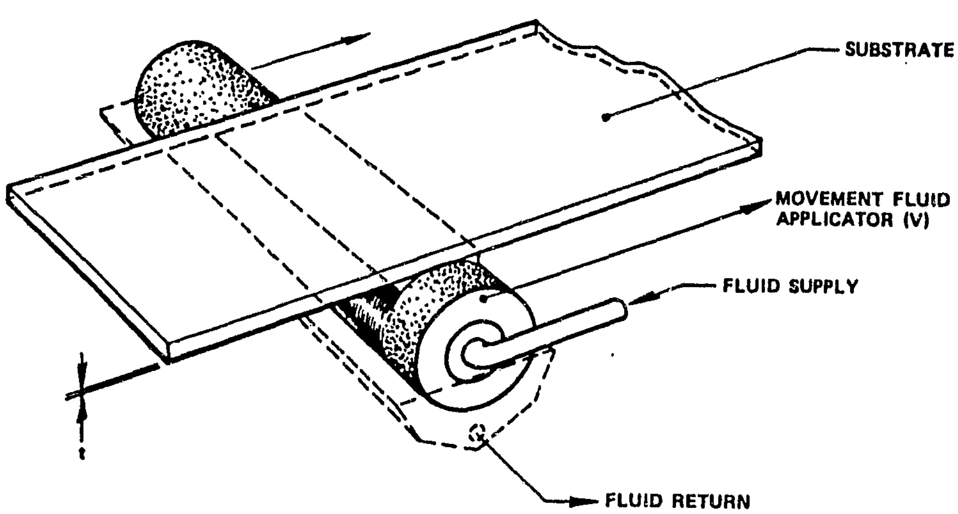

Liquid Diffusion-Mask Studies

- Time/Temperature Parameters for Bake
- Film Thickness Investigations
- Effects of Furnace Atmospheres
- Post-Diffusion Mask Removal

Liquid Junction-Formation Studies

- Optimum Time/Temperature for Boron Drive
- Optimum Time/Temperature for Phosphorus Drive
- Vendor Survey
- Belt Furnace Drive Investigations

Liquid-Dopant Evaluation Techniques

- Sheet Resistivity
- Junction Profiles — Spreading Resistance
- Cell Fabrication — Light & Dark IV Parameters

Liquid vs Gaseous P^+P Junction Profiles

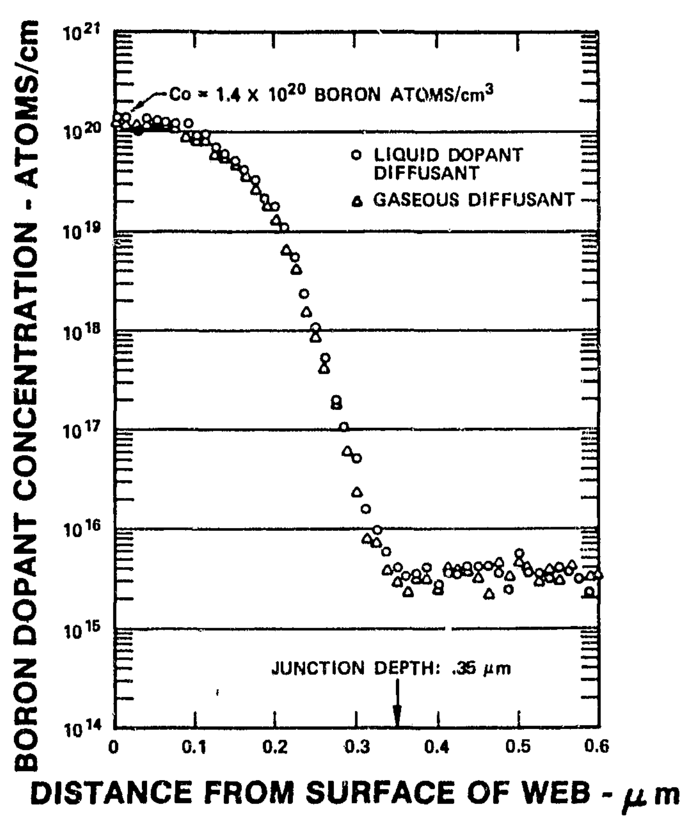

Overall Comparison of Baseline and Liquid Boron/Liquid Mask Processes

- Cells Processed In AESD Pre-Pilot Line
- Experiment Period: July 1, 1982 Through Nov. 24, 1982
- Cell Sizes: 15.7 cm^2 ; 19.6 cm^2 ; and 24.5 cm^2
- Various Vendors' Liquid Dopants/Masks Used
- Results

	No. of Cells	Avg. Efficiency
Baseline (Gaseous) Process	6161	12.6%
Liquid Boron/Mask Process	9265	12.7%

Baseline Process

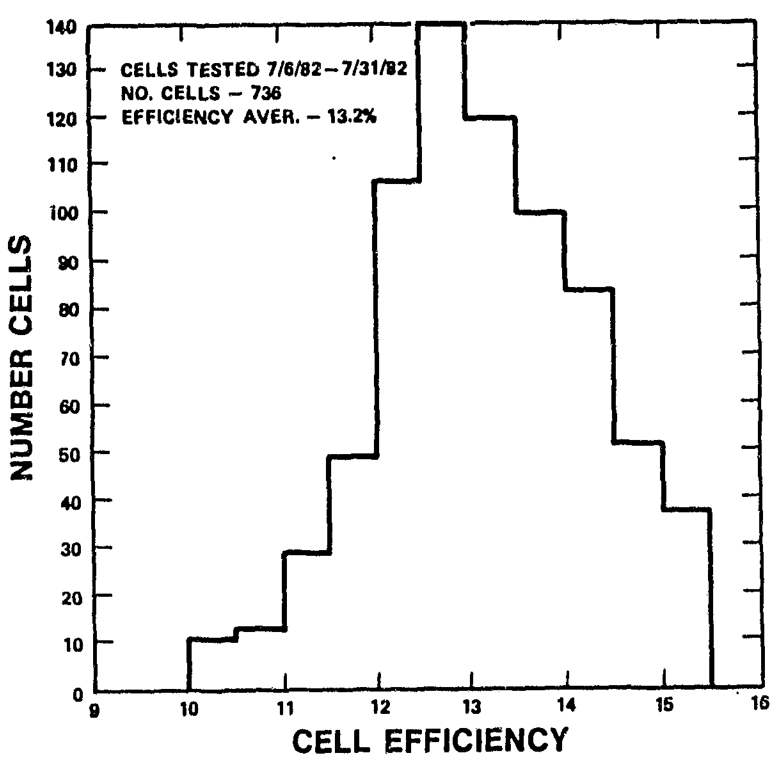

ORIGINAL PAGE IS
OF POOR QUALITY

Low-Cost Process

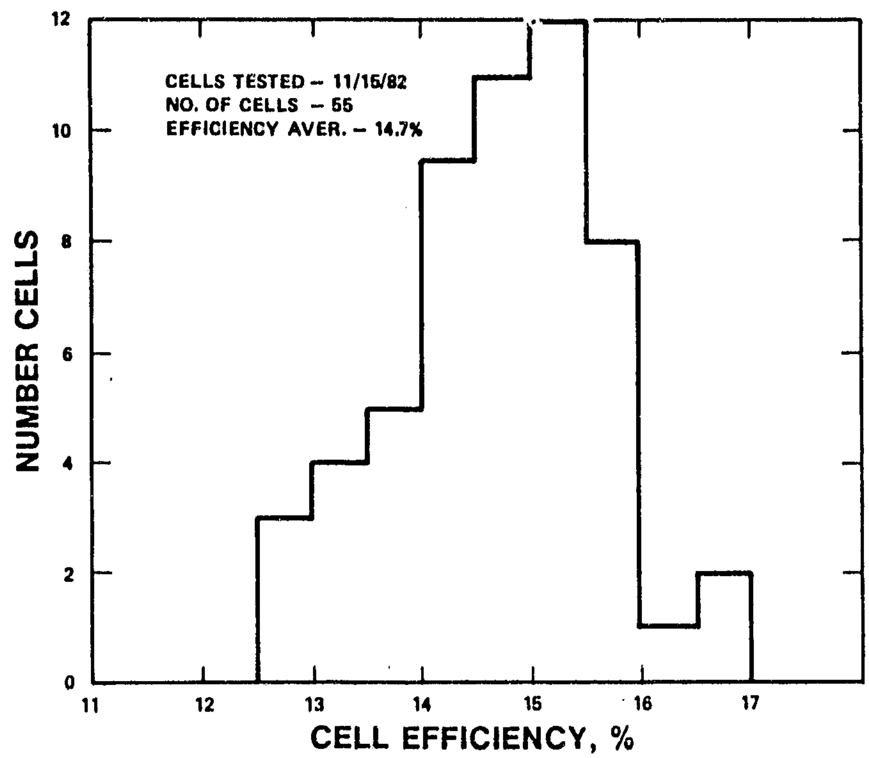

Belt Furnace Junction Drive Experiment

- Conducted Sept. 30, 1982 At Radiant Technologies Inc.
- Ambients Investigated
- Diffusion Temperatures Investigated
- Strip Orientation Investigated
- Crystal Pairs Processed In Diffusion Furnace

Belt Furnace Feasibility Data

	Belt Furnace Run	Diff. Furnace Run
No. of Cells	96	86
Voc. (Volts)	.544 + .010	.542 + .008
Isc. (Amps)	.578 + .027	.578 + .028
Fill Factor	.780 + .023	.778 + .029
Avg. Eff. (Pct.)	12.7	12.5

Ion Implantation Anticipated Advantages

- Higher Cell Efficiency
- Improved Cell Property Uniformity
- Dry, Environmentally Benign, Processing
- Baseline Sequence Compatibility

Status of Ion Implantation Study

- 2.1 cm x 2.5 cm Dendritic Web Blanks Delivered to JPL
- Junctions To Be Formed In Blanks By Spire *
  To Study Effects Of:
  - Ion Species
  - Energy Dose For Front And Back Junctions
  - Implantation Angle
  - Annealing Method/Time/Temperature
  - Surface Treatment Of Input Web
- Cell Processing/Evaluation To Be Completed By Westinghouse

* Under Separate Contract

Silicon Shot Tower Investigation

- Equipment Transferred From Kayex-Hamco, July, 1982
- Purpose: Evaluate Dendritic Web Grown From Small Silicon Shot
- Cost: No Cost To JPL
- Status
  - Shot Tower Reinstalled At AESD
  - Shake Down/Check Out Tests Completed
  - Numerous Shotting Runs Completed
  - Web Growth From Pellets Initiated
  - Evaluation Of Cell Quality To Be Initiated

Conclusions

- All Program Tasks Within Budget
- Liquid Boron/Liquid Diffusion Masks Incorporated Into Westinghouse Baseline Process Sequence
- Delay Encountered In Meniscus Coater Delivery
- Junction Drive Using Belt Furnace Successful
- Ion Implantion Material Delivered To JPL
- Silicon Shot Tower Installed And Operational

EVALUATION OF THE ION IMPLANTATION PROCESS FOR PRODUCTION OF SOLAR CELLS FROM Si SHEET MATERIALS

SPIRE CORP.

PROGRAM STARTED: 15 DECEMBER 1982

OBJECTIVE: EVALUATE ION IMPLANTATION WITH EITHER THERMAL ANNEAL OR PULSED ELECTRON BEAM ANNEAL (PEBA) AND SPACE CELL PROCESSING TECHNIQUES.

TASK I: DENDRITIC WEB ION IMPLANTATION STUDY

TASK II: SILICON SHEET MATERIAL ION IMPLANTATION STUDY

STATUS: PROGRAM INITIATED
STARTING MATERIAL IN PREPARATION

Task I: Dendritic Web Ion Implantation Study

MATERIALS: DENDRITIC WEB AND CZ CONTROLS

APPROACH: UTILIZE ION IMPLANTATION AND THERMAL ANNEALING; IMPLEMENT BSF AND BSR PROCESSING

SUBTASKS

- ESTABLISH BASELINE
- INVESTIGATE JUNCTION FORMATION PARAMETERS
  - IMPLANT ENERGY
  - ANNEAL CYCLE
- INVESTIGATE BSF FORMATION PARAMETERS
  - IMPLANT ENERGY
  - ANNEAL CYCLE
- EVALUATE SURFACE PASSIVATION
- EVALUATE ALUMINUM BSR

Task II: Silicon Sheet Material Ion Implantation Study

MATERIALS: SILSO, SEMIX, EFG, HEM AND CZ CONTROLS

APPROACH: INVESTIGATE ION IMPLANTATION AND ANNEAL PARAMETERS FOR EACH MATERIAL; STUDY PEBA AND THERMAL ANNEALS (SEPARATELY); NO BSF.

SUBTASKS

- ESTABLISH THERMAL ANNEAL BASELINE
- EVALUATE ION IMPLANTATION AND THERMAL ANNEAL PROCESS PARAMETERS
- EVALUATE ION IMPLANTATION AND PEBA PROCESS PARAMETERS

ORIGINAL PAGE IS OF POOR QUALITY

DEVELOPMENT OF ION IMPLANTATION AND PULSE ANNEALING SOLAR-CELL PROCESSING TECHNIQUES

SPIRE CORP.

Program Description

OBJECTIVES

1. To develop junction formation processes using Ion Implantation and pulsed annealing using equipment designed especially for solar cells.

PROGRAM PLAN

1. Develop 4" Capability Pulse Annealer
2. Develop 4" Capability N M A Ion Implanter
3. Use this equipment to develop junctions on Advanced Sheet Materials

Cross Section of SPI-ION 1000 Ion Implanter

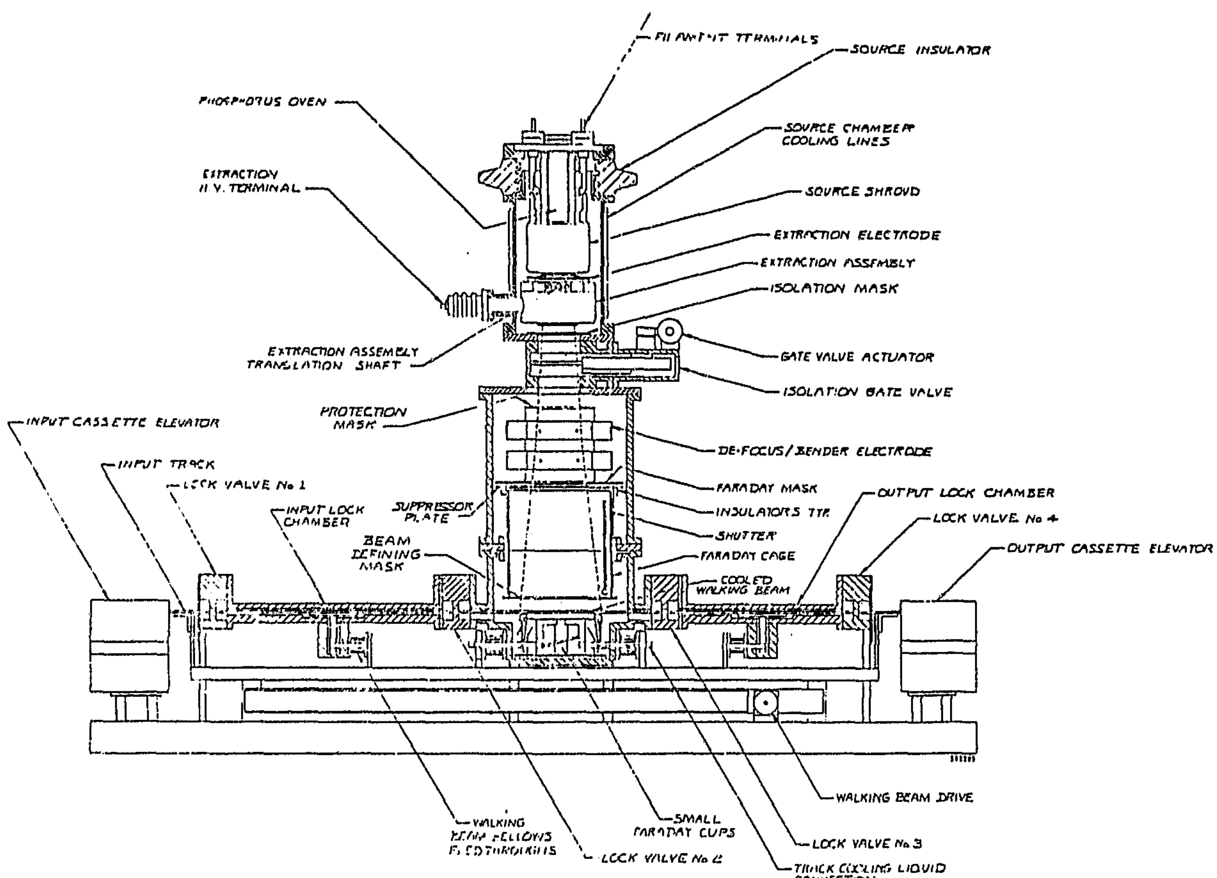

Measured AMO Performance of Phosphorus-Implanted Furnace-Annealed Solar Cells

Implant Energy (keV)	Open Circuit Voltage (mV)	Short Circuit Current (mA/cm^2)	FF (%)	AMO Eff. (%)
2.5	556	29.43	63.6	7.69
5.0	600	29.91	75.9	10.07
7.5	596	29.23	75.2	9.68
10.0	593	28.66	76.3	9.58
10.0 (controls)	593	29.2	77.1	9.87

Notes: T = 25°C, no AR coatings

Performance of AR-Coated Cells

Group	V_{oc} (mV)	J_{sc} (mA/cm^2)	FF (%)	Eff. (%)
10 keV controls	605	39.87	77.2	13.8
5 keV	609	41.0	75.7	14.0

Note: $T = 25^{\circ}C$

AM1 Performance of Two Cells as Measured by SERI

Cell	V_{oc} (mV)	J_{sc} (mA/cm^2)	FF (%)	Eff. (%)
5C	597.7	34.20	74.97	15.33
5D	597.8	34.17	76.15	15.55

Note: $T = 28^{\circ}C$

Si PN 5D

SAMPLE: SD1769 Voc =0.5978 VOLTS

DATE: JUN 30 1982 16:09 Jsc =34.17 mA/cm^2

TEMP = 28.0 Deg C FILL FACTOR = 0.7615

AREA = 4.0460 cm^2 EFFICIENCY = 15.55 %

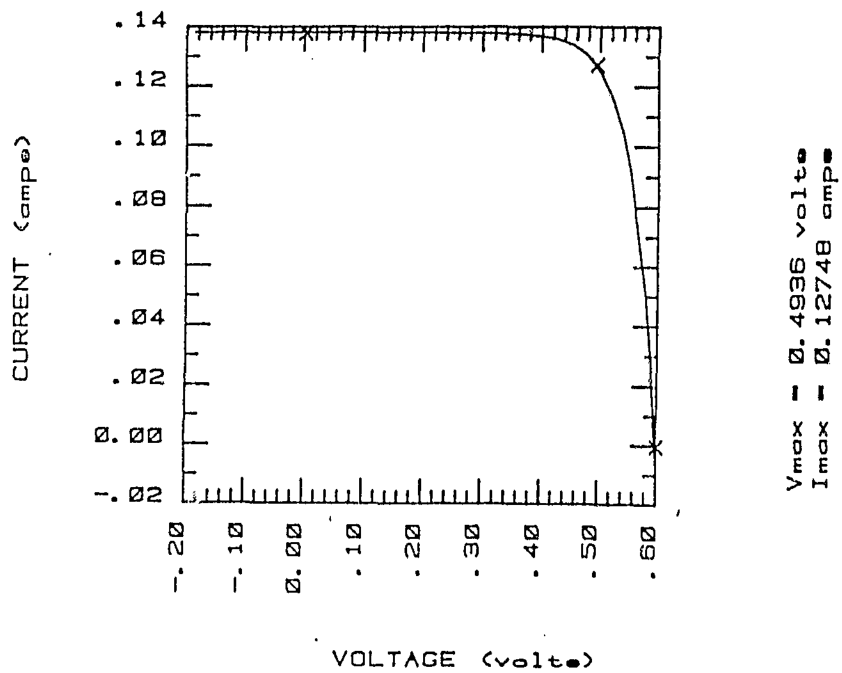

ORIGINAL PAGE IS
OF POOR QUALITY

Spreading Resistance Analysis of NMA-Implanted Junctions

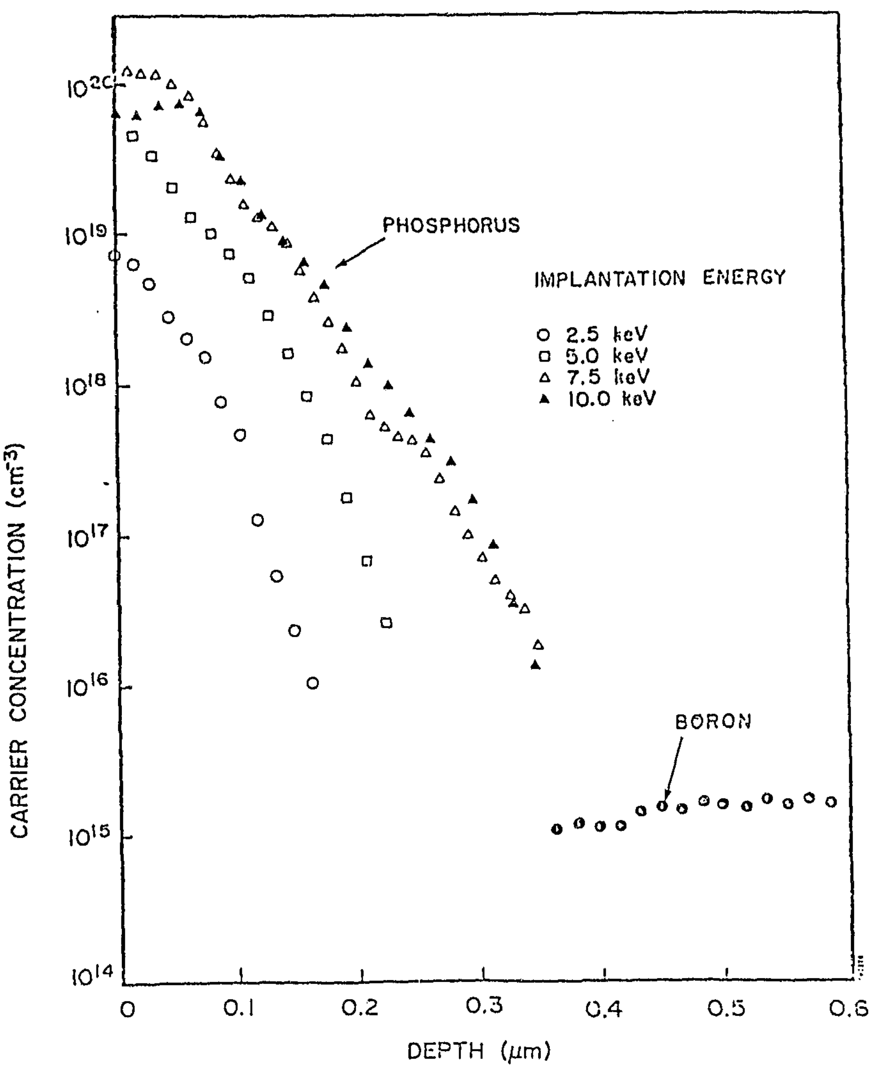

ORIGINAL PAGE IS
OF POOR QUALITY

Spreading Resistance Analysis of PEBA Junctions

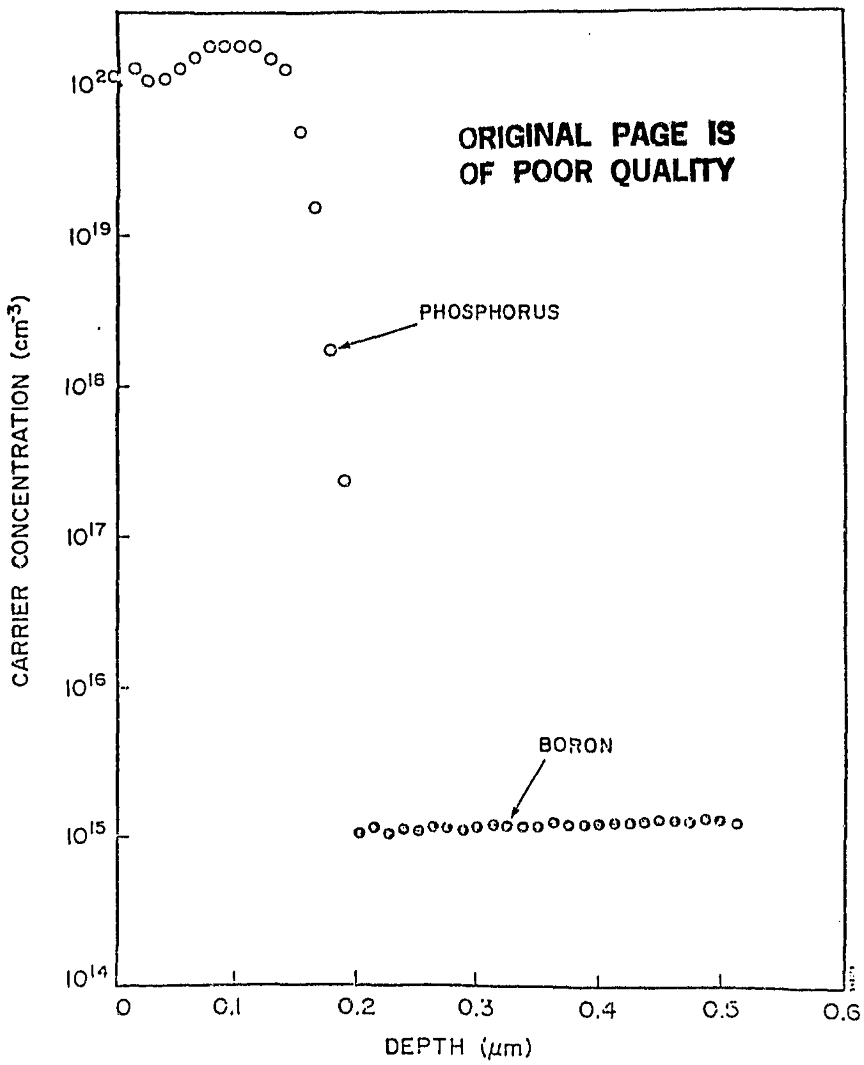

Spectral Response of the 5-keV Implanted Cell

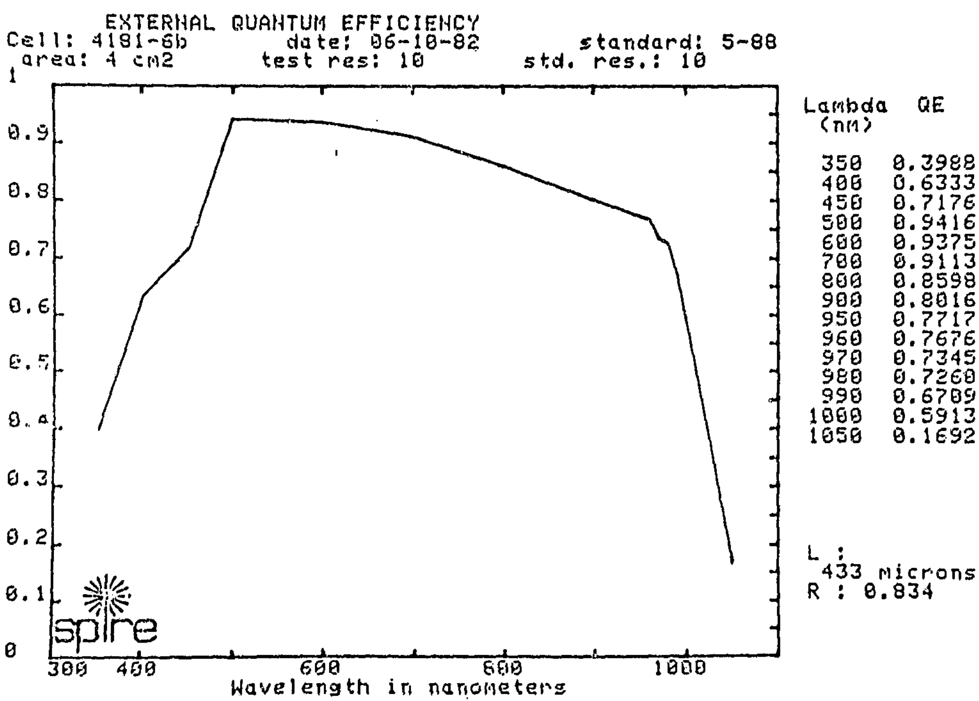

Program Status

- Pulse Annealer
  - completed and demonstrated October 1981
- NMA Ion Implanter
  - experimentation complete
  - solar cell evaluation complete
  - detail design completed
  - 90% of parts fabricated
  - assembly in progress

ORIGINAL PAGE IS OF POOR QUALITY

Automated Solar-Cell Ion Implanter

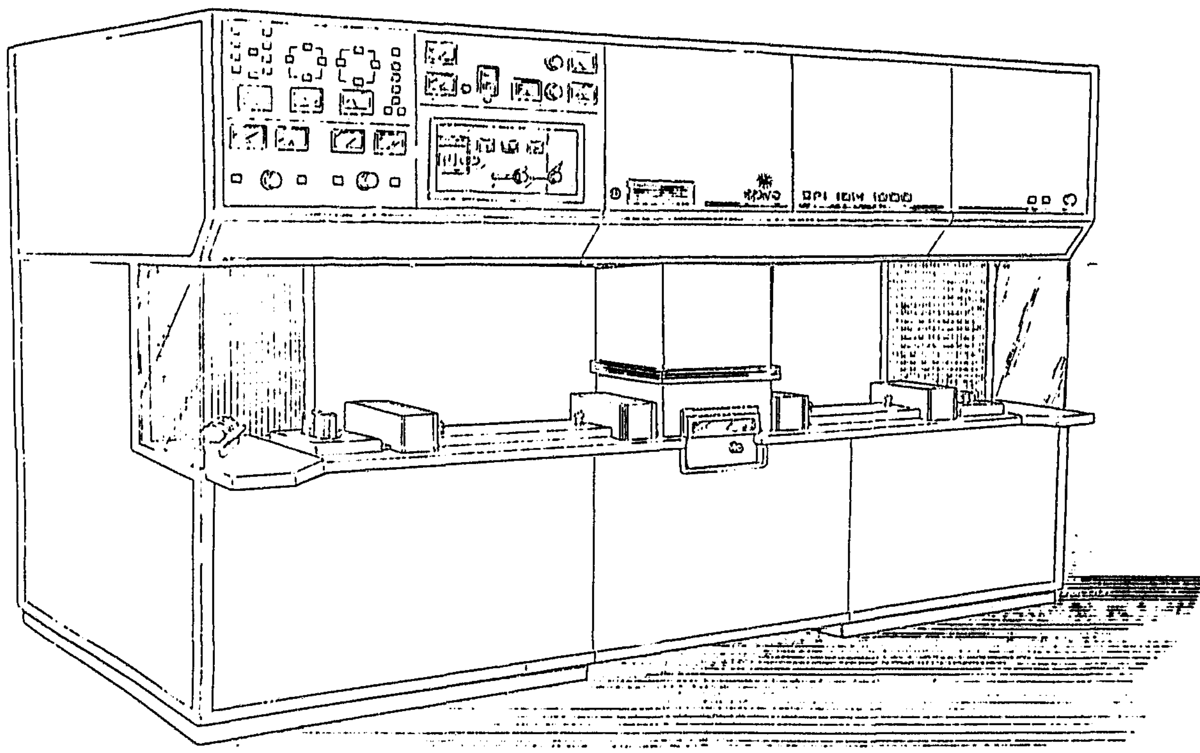

ORIGINAL PAGE IS
OF POOR QUALITY

PROCESS RESEARCH ON POLYCRYSTALLINE SILICON MATERIAL (PROPSM)

SOLAREX CORP.

Jerry Culik and John Wohlgemuth

PROPSM Program

- IDENTIFY MECHANISMS LIMITING CELL PERFORMANCE (SHORT-CIRCUIT CURRENT, OPEN-CIRCUIT VOLTAGE, FILL FACTOR, PEAK POWER).
- DEVELOP CELL FABRICATION PROCESSES TO IMPROVE PERFORMANCE WHICH ARE COMPATIBLE WITH LIMITING MECHANISMS.

Summary

LIMITING MECHANISMS: THICKNESS-BULK RESISTIVITY MATRIX

- SHORT-CIRCUIT CURRENT IS NOT SENSITIVE TO THICKNESS GREATER THAN 150 μM AND TENDS TO DECREASE AS RESISTIVITY DECREASES.
- OPEN-CIRCUIT VOLTAGE TENDS TO INCREASE AS THICKNESS AND BULK RESISTIVITY DECREASE , BUT APPEARS TO BE MORE SENSITIVE TO OTHER BULK PROPERTIES.
- FILL-FACTOR IS NOT SIGNIFICANTLY DIFFERENT FROM SINGLE CRYSTAL CONTROLS IN MOST CASES.

PROCESSES: HOT-SPRAYED AR COATING

- POWER INCREASE ON TEXTURED SURFACE CELL EQUIVALENT TO EVAPORATED TiO_x.
- POSSIBLE ADDITIONAL INCREASE IN OPEN-CIRCUIT VOLTAGE.
- LOW COST, HIGH THROUGHPUT.

Limiting Mechanisms: Thickness – Bulk Resistivity Matrix

J. Wohlgemuth
G. Johnson
K. Lenk

- FABRICATE 4 cm^2 CELLS ON POLYCRYSTALLINE MATERIAL OF VARIOUS THICKNESSES AND BULK RESISTIVITIES.
- THICKNESS: 100, 150, 200, 250, 300 μM.
- BULK RESISTIVITY: ~0.5, ~1.5, ~5.0 OHM-CM.
- HIGH EFFICIENCY PROCESS:
  - 70-80 OHM/□ DIFFUSION
  - ALUMINUM PASTE BSF
  - Ti/Pd/Ag METALLIZATION
  - Ta_2O_5 AR COATING

Thickness-Bulk Resistivity Matrix: Sample Size

	Lot No.	Thickness (μM) 100	150	200	250	300	Bulk Resistivity (ohm-cm)
Low Resistivity	6		20	26	20		0.4 - 0.6
Medium Resistivity	1		6	20	19		1.3 - 1.7
	2		5	12	13	19	1.0 - 1.9
	7	9	14	11	8		1.2 - 1.8
High Resistivity	3	5	9	19			5.5 - 6.5
	5		10	18	22		4.2 - 6.2

Number of 4cm^2, AR-coated polycrystalline cells in each thickness - bulk resistivity category, by lot.

Thickness-Bulk Resistivity Matrix: Short-Circuit Current

		Thickness (μm)				
	Lot No.	100	150	200	250	300
Low Resistivity	6		126 (4)	127 (4)	127 (4)	
Medium Resistivity	1		132 (6)	128(16)	126(15)	
	2		132 (2)	127 (3)	135 (7)	131 (5)
	7	143 (2)	146 (2)	140 (3)	142 (2)	
High Resistivity	3	141 (3)	141 (2)	143 (2)		
	5		145 (4)	147 (5)	146 (6)	

Mean (in mA), (standard deviation about mean (in mA))

Measured at AM0, 135 mW/cm^2, 25°C

RESULTS

- o I_{sc} DECREASES AS BULK RESISTIVITY DECREASES, SAME AS CZ SINGLE CRYSTAL SILICON.
- o I_{sc} DOES NOT APPEAR TO BE SENSITIVE TO BASE THICKNESS GREATER THAN 150 μM.
- o I_{sc} FOR POLYCRYSTALLINE SILICON IS 5-10 % LESS THAN CZ SINGLE CRYSTAL CONTROLS; DIFFERENCE APPEARS TO INCREASE AS RESISTIVITY DECREASES.

CONCLUSIONS

- o MINORITY CARRIER DIFFUSION LENGTH IS ON THE ORDER OF 150-200 μM.
- o LIGHT-GENERATED CURRENT IN LARGE GRAIN (> 1-2 MM DIAMETER) POLYCRYSTALLINE SILICON IS DOMINATED BY MINORITY CARRIER LIFETIME WITHIN THE BULK OF THE GRAINS.
- o MECHANISMS LIMITING LIGHT-GENERATED CURRENT IN LARGE GRAIN POLYCRYSTALLINE SILICON ARE THE SAME AS THOSE IN SINGLE CRYSTAL SILICON, NAMELY, INCORPORATION OF THOSE IMPURITIES AND DISLOCATIONS WHICH ACT TO REDUCE THE MINORITY CARRIER LIFETIME.

ORIGINAL PAGE IS OF POOR QUALITY

Thickness-Bulk Resistivity Matrix: Open-Circuit Voltage

	Lot No.	Thickness (μm) 100	150	200	250	300
Low Resistivity	6		577(24)	583 (8)	580 (8)	
Medium Resistivity	1		559 (5)	559(19)	559(14)	
	2		539(36)	538(67)	555(16)	553(11)
	7	587 (4)	586 (3)	573(10)	582 (4)	
High Resistivity	3	573 (8)	570 (4)	570 (5)		
	5		570(13)	552(30)	566(16)	

Mean (in mV), (standard deviation about mean (in mV))

Measured at AM0, 135 mW/cm^2, 25°C

- V_{oc} tends to decrease slightly as the thickness increases.
- V_{oc} tends to increase as the bulk resistivity decreases.
- V_{oc} has substantial scatter which does not appear to be due to thickness or bulk resistivity variations, i.e., not macroscopic phenomena.

Thickness-Bulk Resistivity Matrix: Fill Factor

	Lot No.	Thickness (μm) 100	150	200	250	300
Low Resistivity	6		68(11)*	73 (3)	71 (5)*	
			80 (1)	77 (6)	79 (1)	
Medium Resistivity	1		76 (2)	75 (2)	75 (4)	
			75 (1)	76 (1)	76 (1)	
	2		70(10)	70(14)	68(13)	74 (3)
			80 (1)	80 (1)	78 (2)	78 (1)
	7	76 (1)	75 (1)	75 (1)	76 (2)	
		76 (1)	77 (2)	78 (2)	79 (1)	
High Resistivity	3	70 (7)	64 (4)*	64 (4)*		
		75 (5)	78 (1)	77 (1)		
	5		75 (2)	64(15)	75 (1)	
			77 (1)	77 (3)	77 (3)	

Polycrystalline mean (in %), (standard deviation about mean (in %))
Single crystal mean (in %), (standard deviation about mean (in %))

- IN GENERAL, FILL-FACTOR OF POLYCRYSTALLINE CELLS IS NOT SIGNIFICANTLY DIFFERENT FROM THAT OF SINGLE CRYSTAL CONTROL CELLS; HOWEVER, THERE IS NEARLY ALWAYS MORE SCATTER FOR THE POLYCRYSTALLINE MATERIAL.
- FILL-FACTOR IS REDUCED FOR LOW (~ 0.5 OHM-CM) AND HIGH (~ 6.0 OHM-CM) BULK RESISTIVITY POLYCRYSTALLINE CELLS.

Thickness-Bulk Resistivity Matrix: Peak Power

	Lot No.	Thickness (μm) 100	150	200	250	300
Low Resistivity	6		49.9(10.0)	54.0 (3.6)	52.2 (4.0)	
Medium Resistivity	1		55.8 (2.4)	53.6 (8.8)	52.9 (ε	
	2		50.0 (9.5)	49.7(12.9)	51.9(11.8)	53.8(4.7)
	7	64.5 (1.4)	65.4 (1.6)	60.1 (2.7)	63.6 (2.4)	
High Resistivity	3	56.9 (5.7)	52.0 (3.4)	52.0 (3.6)		
	5		62.5 (3.4)	52.5(14.6)	62.5 (4.3)	

Mean (in mW), (standard deviation about mean (in mW))
Measured at AMO, 135 mW/cm^2, 25^{o}C

- o FOR THE PRESENT SAMPLES, MAXIMUM POWER WAS ACHIEVED WITH 1.5 OHM-CM BULK RESISTIVITY AT A THICKNESS OF 150 μM.
- o TREND IS FOR MAXIMUM POWER FROM MEDIUM TO HIGH BULK RESISTIVITY (1.0-6.0 OHM-CM) AT 150-250 μM THICKNESS.

Thickness-Bulk Resistivity Matrix: Conclusions

- MECHANISMS LIMITING LIGHT-GENERATED CURRENT IN LARGE GRAIN POLYCRYSTALLINE SILICON ARE THE SAME AS THOSE IN SINGLE CRYSTAL SILICON; I_{sc} IS DOMINATED BY MINORITY CARRIER LIFETIME WITHIN THE BULK OF THE GRAINS.
- V_{oc} TENDS TO DECREASE SLIGHTLY AS THE BASE THICKNESS INCREASES, AND TO INCREASE AS THE BULK RESISTIVITY DECREASES, SIMILAR TO SINGLE CRYSTAL SILICON.
- IN GENERAL, THE FILL-FACTOR OF POLYCRYSTALLINE CELLS IS NOT SIGNIFICANTLY DIFFERENT FROM THAT OF SINGLE CRYSTAL CONTROLS.
- HOWEVER, BOTH V_{oc} AND FILL-FACTOR OF POLYCRYSTALLINE CELLS HAVE SUBSTANTIAL SCATTER WHICH DOES NOT APPEAR TO BE DUE TO THICKNESS OR BULK RESISTIVITY VARIATIONS.
- THIS INDICATES THAT THERE ARE ADDITIONAL MECHANISMS CAUSING VARIATIONS IN FILL-FACTOR AND LOSSES IN V_{oc}.
- NEED FOR FINER-SCALE EVALUATION TO DETERMINE MECHANISM(S): MINI-CELL.

Limiting Mechanisms: Minicell Evaluation

1. FABRICATE 400 - 0.5CM X 0.5CM (0.25 CM^2) CELLS ACROSS 10CM X 10CM POLY-CRYSTALLINE WAFER USING MESA STRUCTURE FOR ISOLATION.
2. MEASURE I-V CHARACTERISTICS ACROSS WAFER.
3. LOCATE AREAS WHICH SUFFER FROM REDUCED V_{oc} AND/OR FILL-FACTOR.
4. DETERMINE CAUSE:
   - DARK I-V ANALYSIS FOR I_{QNO}, I_{SCO}, AND N-FACTOR
   - DEFECT ETCH OF SERIAL SECTION FOR DISLOCATION CONTENT
   - LIGHT-SPOT SCANNING TO LOCATE ELECTRICALLY ACTIVE GRAIN BOUNDARIES
   - DLTS FOR IMPURITY CONTENT

Processes to Improve Performance

- GETTERING TO REMOVE IMPURITIES FROM BULK
- OPTIMIZE DIFFUSION FOR POLYCRYSTALLINE SILICON
- OPTIMIZE BSF FOR POLYCRYSTALLINE
- SURFACE PASSIVATION
- HYDROGEN PASSIVATION OF GRAIN BOUNDARIES

Low-Cost AR Coating

PROBLEM:

PREVIOUS LOW COST SPRAY AR COATINGS WERE NOT EFFECTIVE ON SEMICRYSTALLINE SILICON SURFACES.

SOLUTION:

- REMOVE SOLVENTS FROM SPRAY.
- SPRAY TITANIUM ISOPROPOXIDE DIRECTLY.
- SPRAY ONTO HEATED WAFERS AT TEMPERATURE ABOVE WHICH TITANIUM ISOPROPOXIDE DECOMPOSES (410°C)

RESULT:

- BETTER AR COATING
- LOWER COST

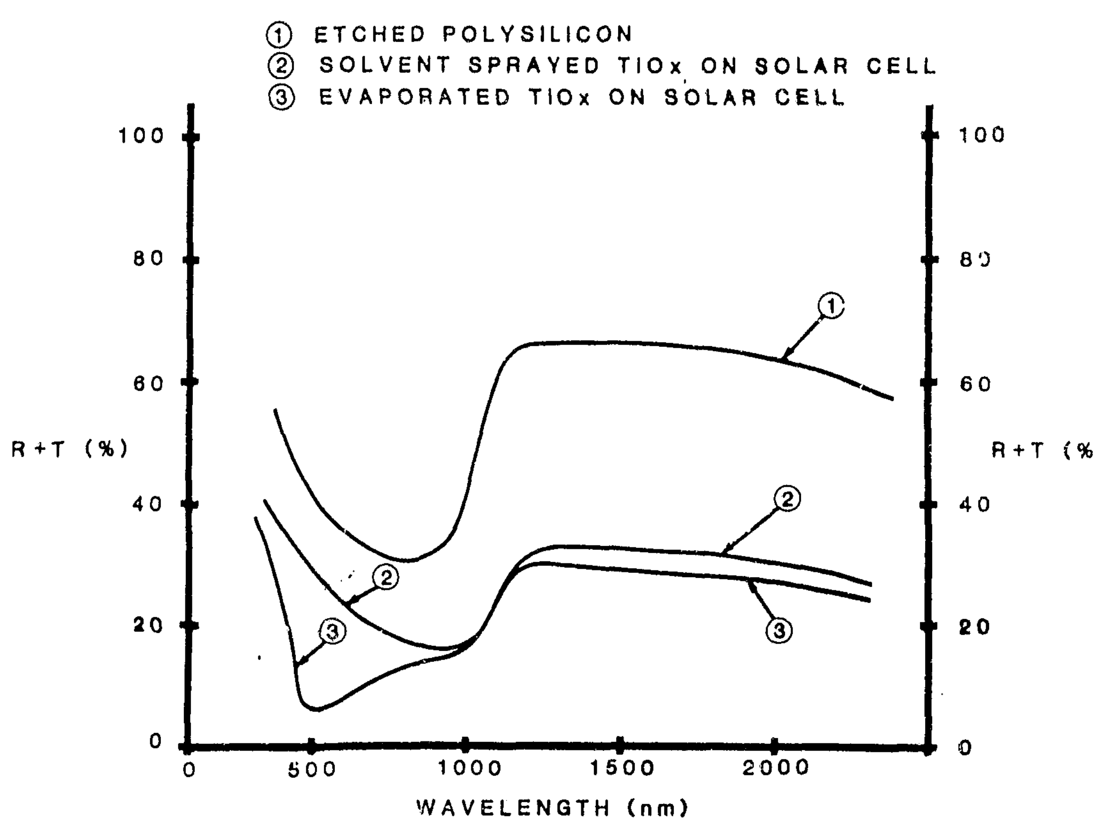

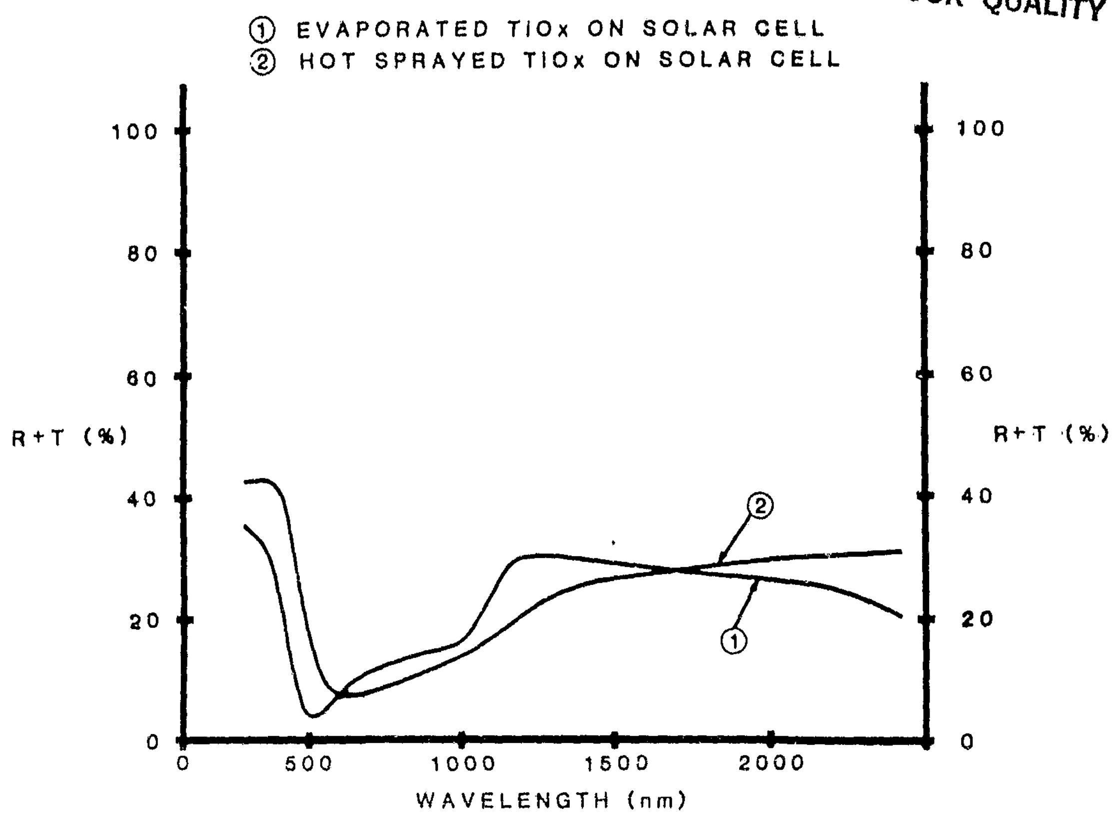

Comparison of Sprayed vs Evaporated TiO_X AR Coating on Solar-Cell Performance

	COATING TYPE	IMPROVEMENT AFTER AR COATING* ΔV_{OC}	ΔI_{SC}	ΔP_{MAX}	INDEX OF REFRACTION
SEMICRYSTALLINE	SPRAY TiO_X	+ 5.4	+29.9	+12.0	2.4
	EVAPORATED TiO_X	+ 3.2	+30.0	+12.2	2.1
SINGLE CRYSTAL	SPRAY TiO_X	10.3	39.5	20.2	
	EVAPORATED	5.4	40.9	20.5	

*FOR 2CM X 2CM CELLS WITH TiPdAg METALLIZATION, AT AM0, 135.3 mW/cm^2 AND 25°C

CELLS AND PROCESSES

PULSED PLASMA DEPOSITION

JET PROPULSION LABORATORY

D.J. Fitzgerald

OBJECTIVE: INVESTIGATE FEASIBILITY OF PULSED PLASMA SOURCE FOR SURFACE PROCESSING

APPLICATIONS:

- ENERGY DEPOSITION - SURFACE HEATING/MELTING
  - CHEMICAL REACTIONS (SILICON NITRIDE/CARBIDE FORMATION, SINTER OF METAL CONTACTS)
  - ENHANCED DIFFUSION (LIQUID DOPANT "DRIVE IN")
  - ANNEAL OF ION IMPLANT DAMAGE

- MATERIAL DEPOSITION - PLASMA ACCELERATION
  - ION IMPLANTATION

Experimental Pulsed Plasma Source

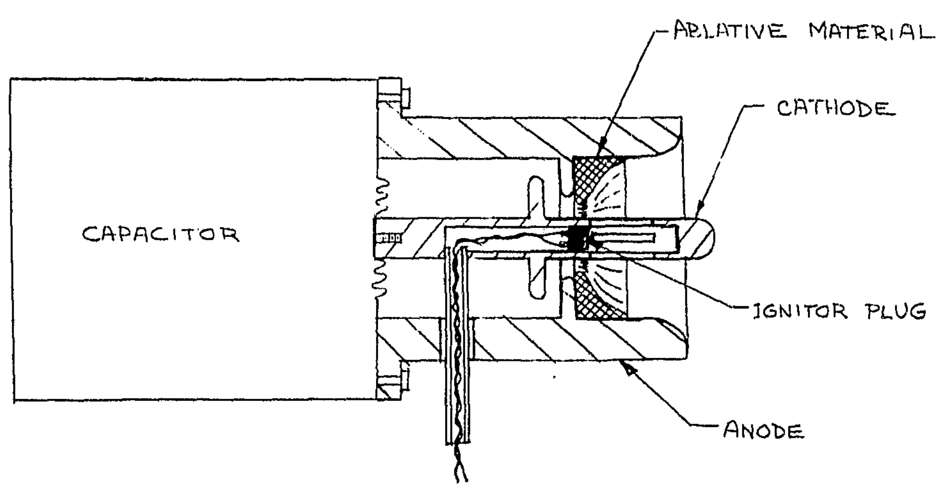

Status

- PRELIMINARY EXPERIMENTS TO FORM SILICON NITRIDE LAYER ARE IN PROGRESS.
- DESIGNING PULSE FORMING NETWORK FOR PULSED PLASMA SOURCE TO PERMIT FLEXIBILITY IN PULSE ENERGY AND DURATION.
- BUILDING UP SURFACE DEPOSITION CHAMBER CAPABLE OF:
  - ION BEAM SPUTTERING (SURFACE CLEANING)
  - N-M-A ION IMPLANTATION
  - PULSED PLASMA PROCESSING
  - CLUSTER ION DEPOSITION

MODULE TECHNOLOGY

R.G. Ross Jr., Chairman

D. H. Otth of JPL presented the latest results of long-term module testing at Wyle Laboratories. A variety of Block IV module types were presented that appeared consistent with 20-year life with regard to typical temperature-humidity site stress.

D. Hawkins, Clemson University, presented an outline of FSA cell-reliability research activities. This report included latest interim results from accelerated testing of different cell types packaged using various types of encapsulation systems, and testing of individual unencapsulated cell types in a real-time outdoor environment. In addition to the cell-testing activities, Clemson reported interim progress on a laboratory study to develop testing methods appropriate for reliability investigation of thin-film cells.

D. M. Moore of JPL presented his updated method for the thickness sizing of rectangular glass plates subject to pressure loads. The method uses design nomographs to obtain an estimate of the stress in the plate as a function of the pressure load and the dimensions of the plate. This stress is compared with an allowable glass strength, also obtained from design curves.

R. G. Ross Jr. of JPL presented the results of a recent study that measured the effects of steep angles of incidence on PV power output of modules when considering cell background reflectance, configuration of the glass cover surface (smooth versus stippled) and various levels of soiling. The results were used to compute prediction error in annual energy performance due to commonly assumed pure cosine dependence and improved alogrithms.

C. C. Gonzales of JPL reviewed a recent investigation into the translation characteristics of different types of current-voltage curves under conditions of varying irradiance level and temperature. Specific examples presented included modules with single point failures (e.g., cracked or shadowed cells) and the dramatic results that occured in I-V curve shape changes.

LONG-TERM MODULE TEST RESULTS AT WYLE LABORATORIES

JET PROPULSION LABORATORY

D.H. Otth

Long-Term Module Testing Schedule

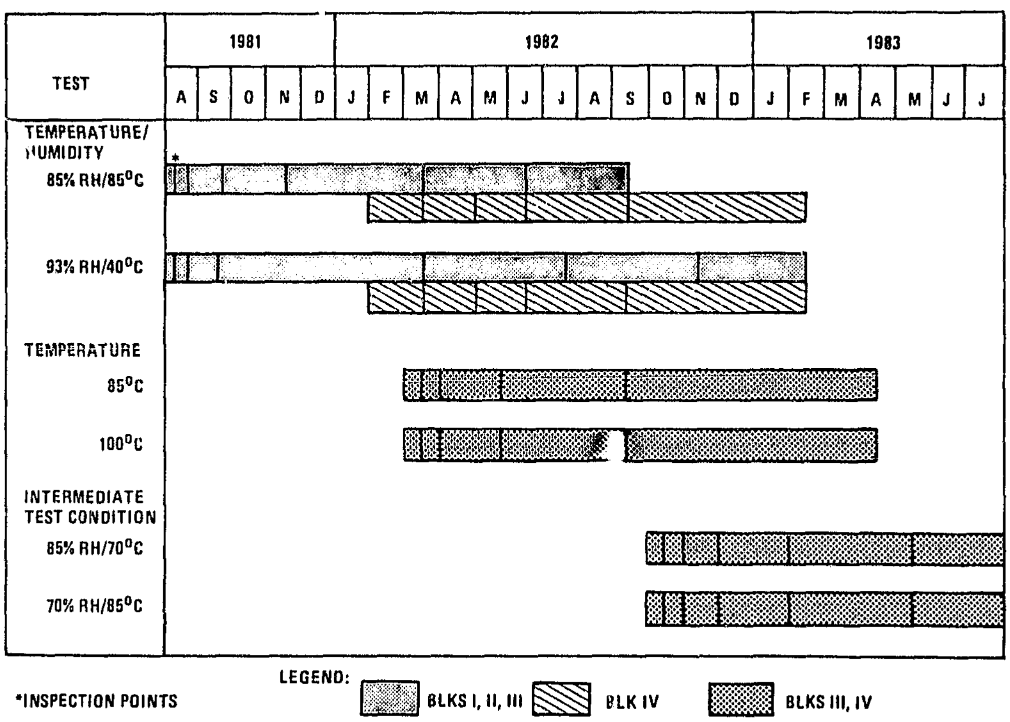

Module Design Comparisons at Day 180

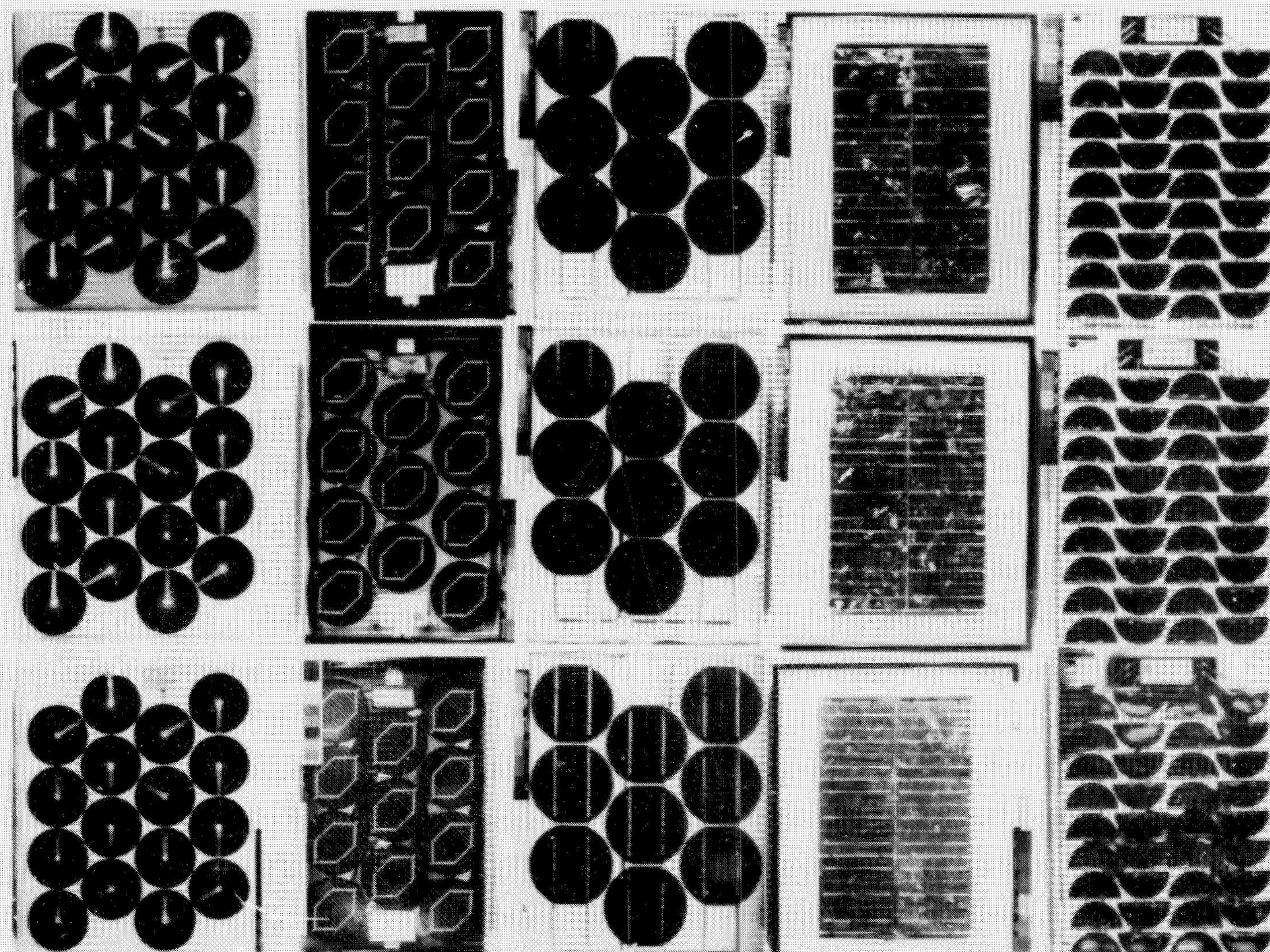

85°C/85% RH, 149 days

85°C, 180 days

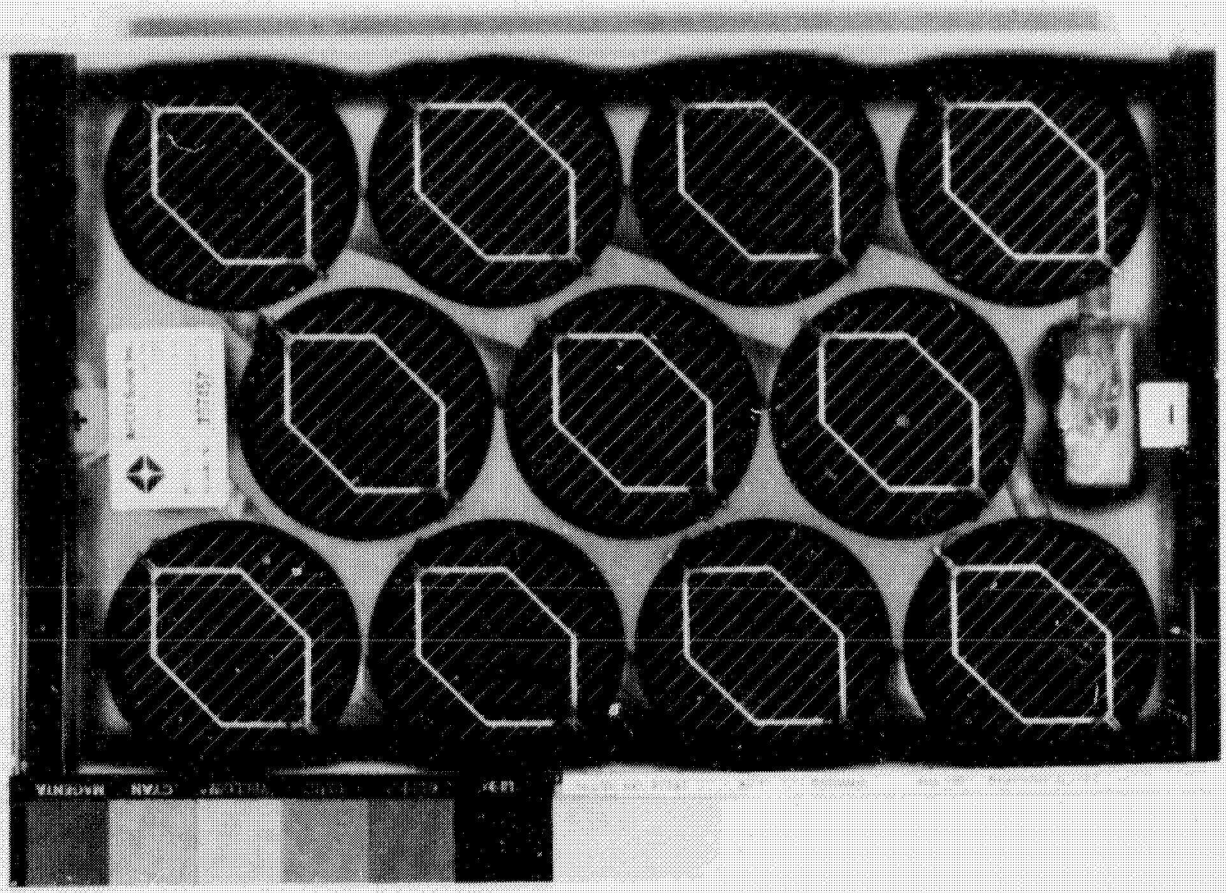

85°C/85% RH, 20 days, Biased

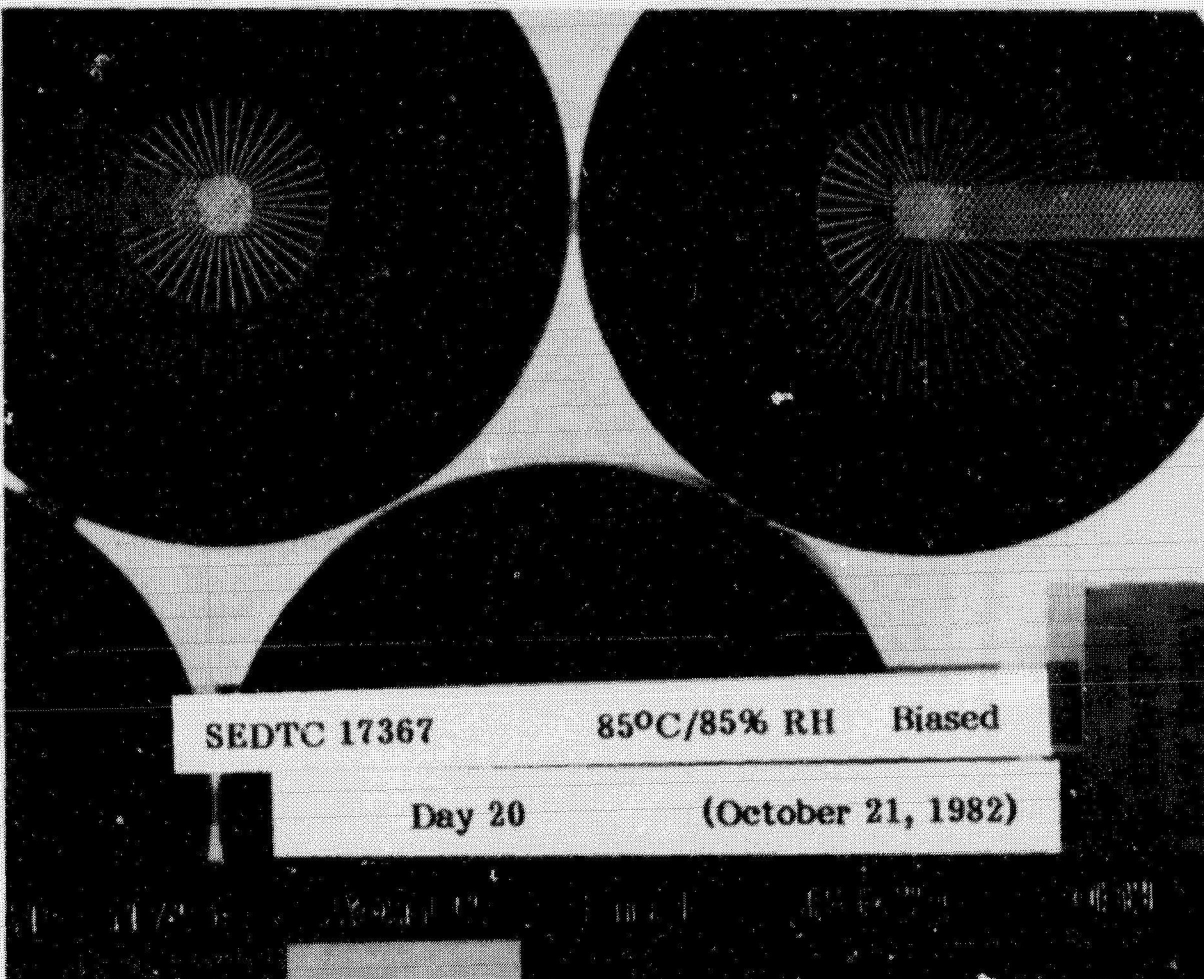

Electrochemical Corrosion

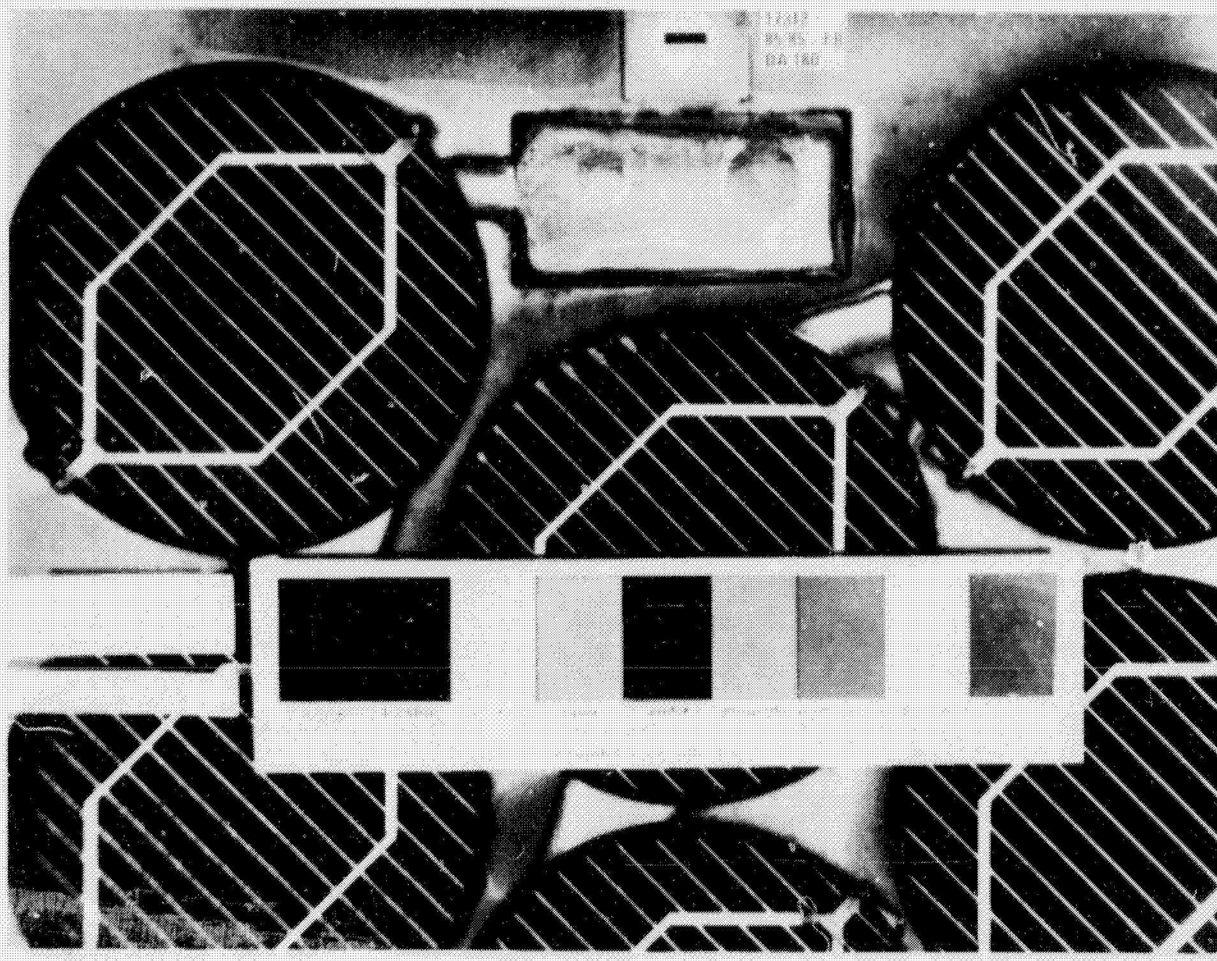

Electrochemical Corrosion, Field SW RES

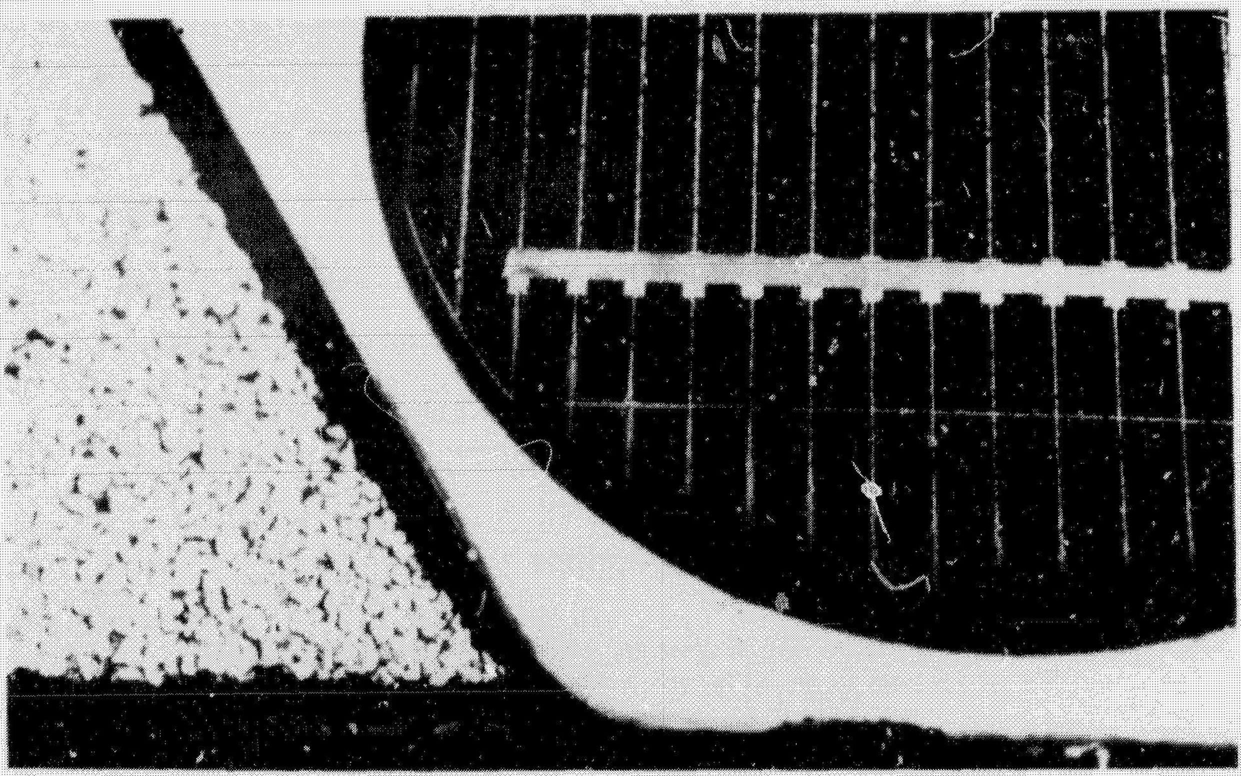

Arrhenius Plot for Time to Degradation vs Cell Temperature

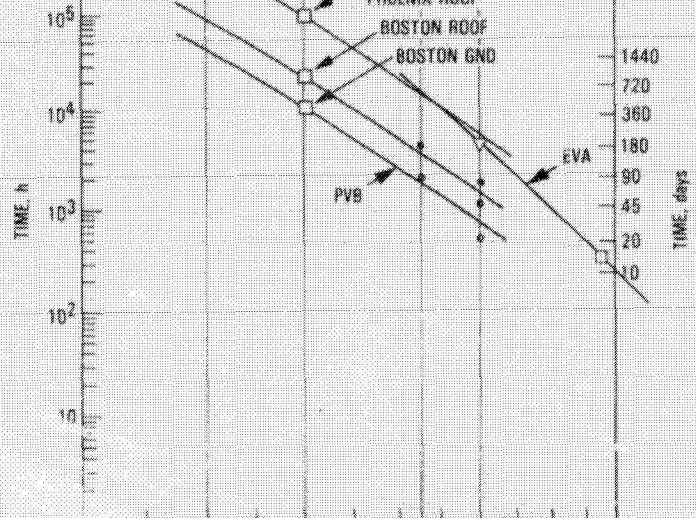

Module P_{max} Degradation From Electrochemical Corrosion in 85°C/85% RH

MODULE DESIGN	CELL METALLIZATION	FWD BIAS	P_{max} DAYS 0	10	20	45	90	180
Glass/PVB/Tedlar	Print-Ag	4.6 V	1	0.97	0.94	0.88	0.78	0.60
	Ti-Pd-Ag	9.4 V	1	0.94	0.90	0.86	-	-

Conclusions

- **A variety of present module types appears to be consistent with 20-year life with respect to typical temperature/humidity site stress**
- **Results to date indicate the following encapsulant ranking:**
  - **Glass/silicon rubber**
  - **Glass/EVA or glass/PVB/foil**
  - **Glass/PVB**
- **Degradation mechanisms identified include:**
  - **Discoloration of encapsulants**
  - **Electrochemical corrosion of cell metallization**
  - **Material diffusion from edge seals**
  - **Delamination (foil), and embrittlement of back covers**
- **Important to have forward voltage bias in qualification tests**
- **Additional data are needed to establish functional relationships between observed failure mechanisms and module lifetimes**

C-5

DEGRADATION OF SOLAR CELLS

CLEMSON UNIVERSITY

Jay W. Lathrop and Dexter C. Hawkins

Accelerated Testing Methodology

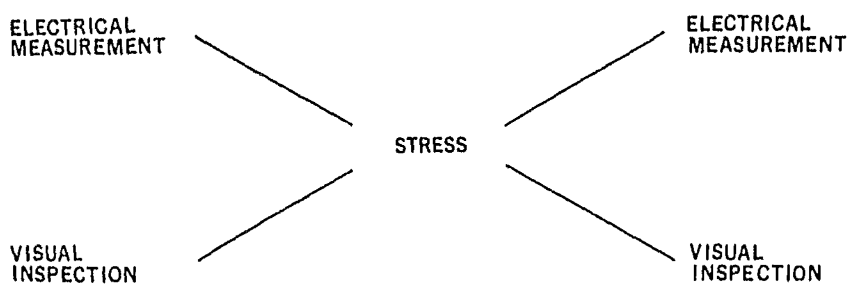

Typical B-T Test Results

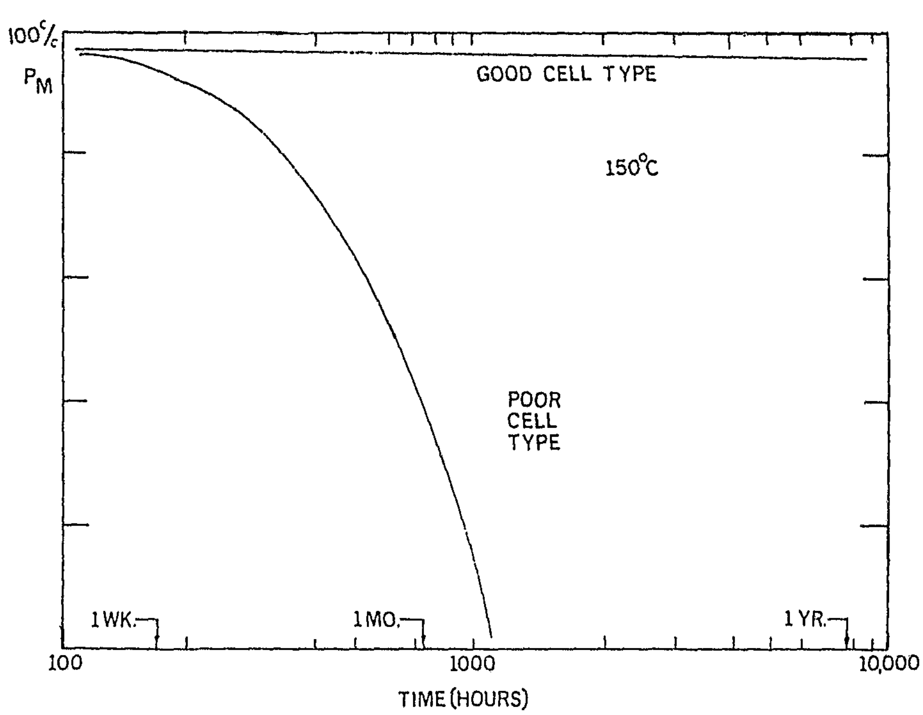

Cumulative Stress Hours

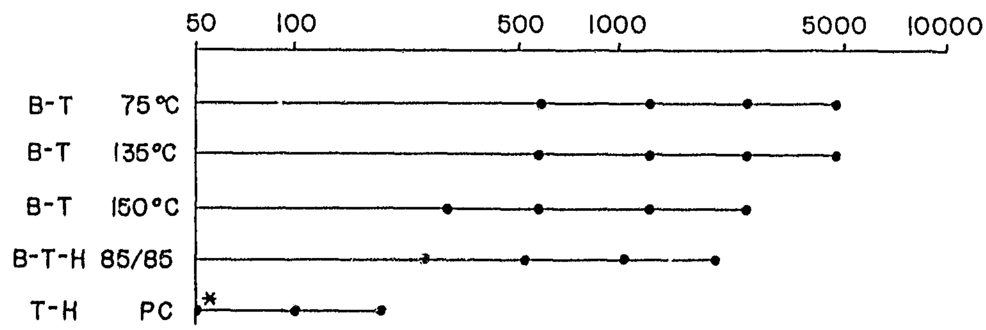

Cumulative Cycles

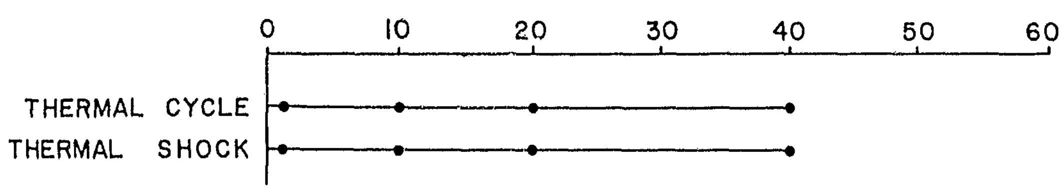

* 25 AND 50 HOURS

Encapsulated Cell Test Matrix

CELL METALLIZATION	G/EVA	G/EVA/T	G/EMA/T	G/EVA/F	G/EVA/G	T/EVA/S	G/SR/G
	ENCAPSULATION SYSTEM						
Ni/SOLDER		X	X	X	X		
Ni/SOLDER		X	X			X	
Ni/SOLDER		X	X	X		X	
Ni/SOLDER		X	X	X	X	X	X
Ni/SOLDER		X	X	X	X	X	
Ni/SOLDER		X	X	X	X	X	
Ag FRIT		X	X	X	X		
Cu PLATED				X			
PLATED	X	X	X	X	X	X	

G = GLASS T = TEDLAR F = FOIL S = STEEL SR = SILICONE RUBBER

Encapsulation Systems Under Test

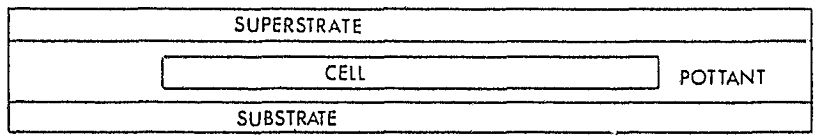

SUPERSTRATE	POTTANT	SUBSTRATE	CODE
GLASS	EVA	NONE	G/EVA
GLASS	EVA	TEDLAR	G/EVA/T
GLASS	EMA	TEDLAR	G/EMA/T
GLASS	EVA	FOIL	G/EVA/F
GLASS	EVA	GLASS	G/EVA/G
TEDLAR	EVA	STEEL	T/EVA/S
GLASS	SIL. RUBBER	GLASS	G/SR/G

Avg. Pct. Decrease in P_M Observed for "Indicator" Cell Type After 85/85 Testing

ENCAPSULATION SYSTEM	TEST TIME (HOURS)			
	250	500	1000	2000
NONE	7	8	11	
G/EVA/T	18	28	41	
G/EMA/T	26	38	54	
G/EVA/G	-7	-5	20	
G/EVA/F	23	41	56	
T/EVA/S	1	0	6	

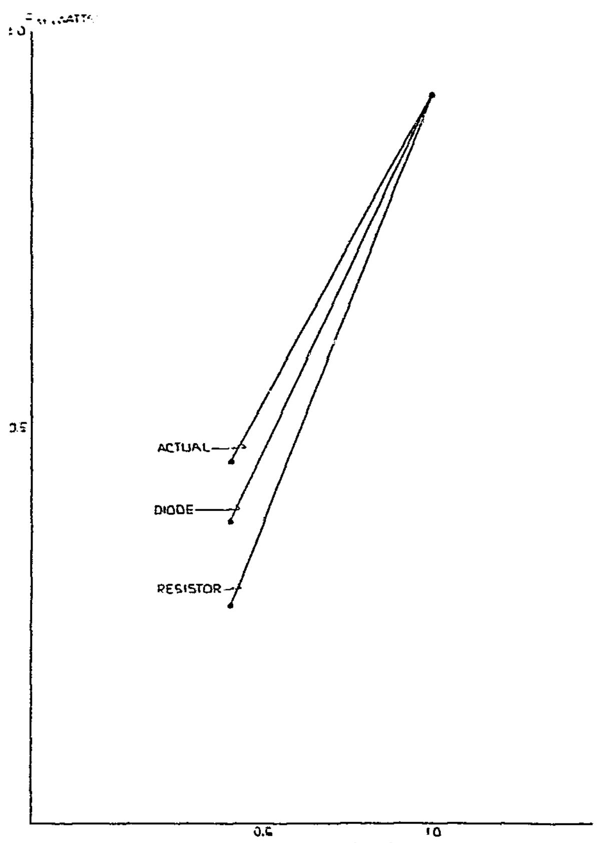

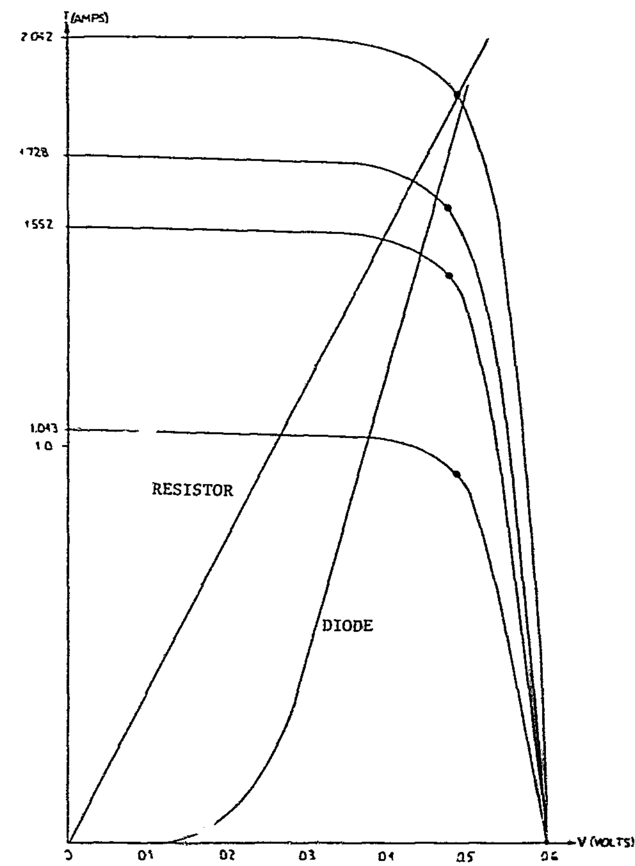

REAL TIME LOAL

Type A I-V Characteristics for 150°C Bias-Temperature Stress, Typical Case

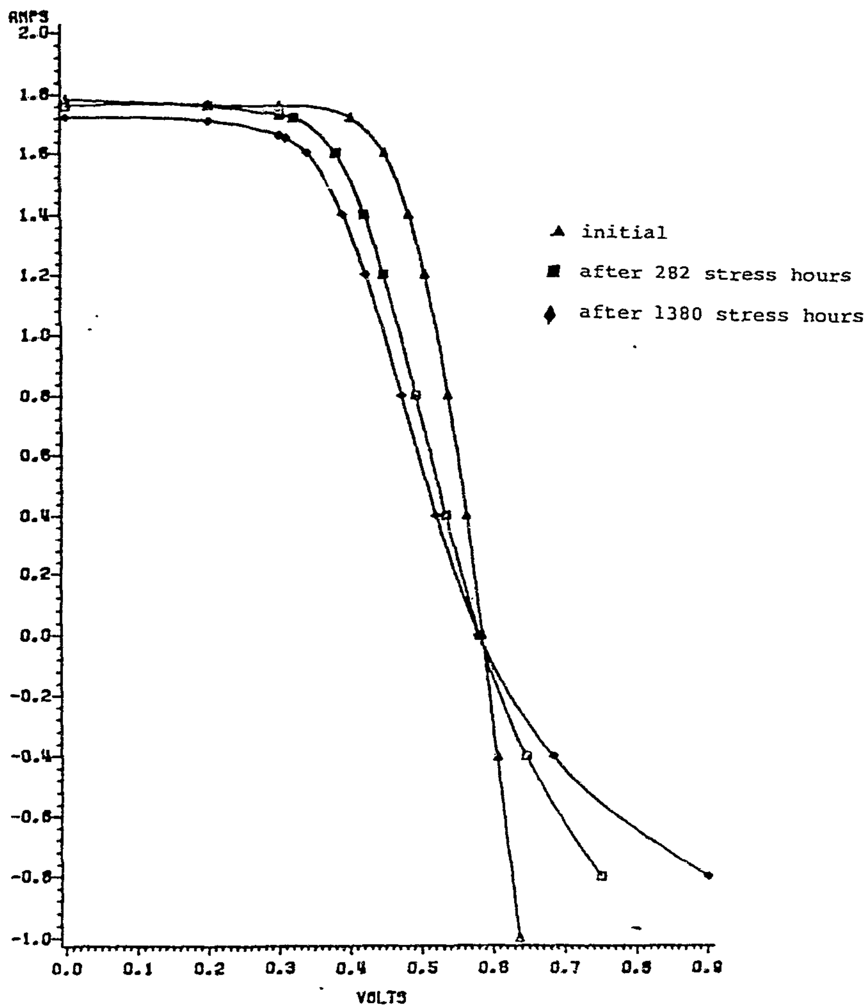

Type A I-V Characteristics for 75°C Bias-Temperature Stress, Typical Case

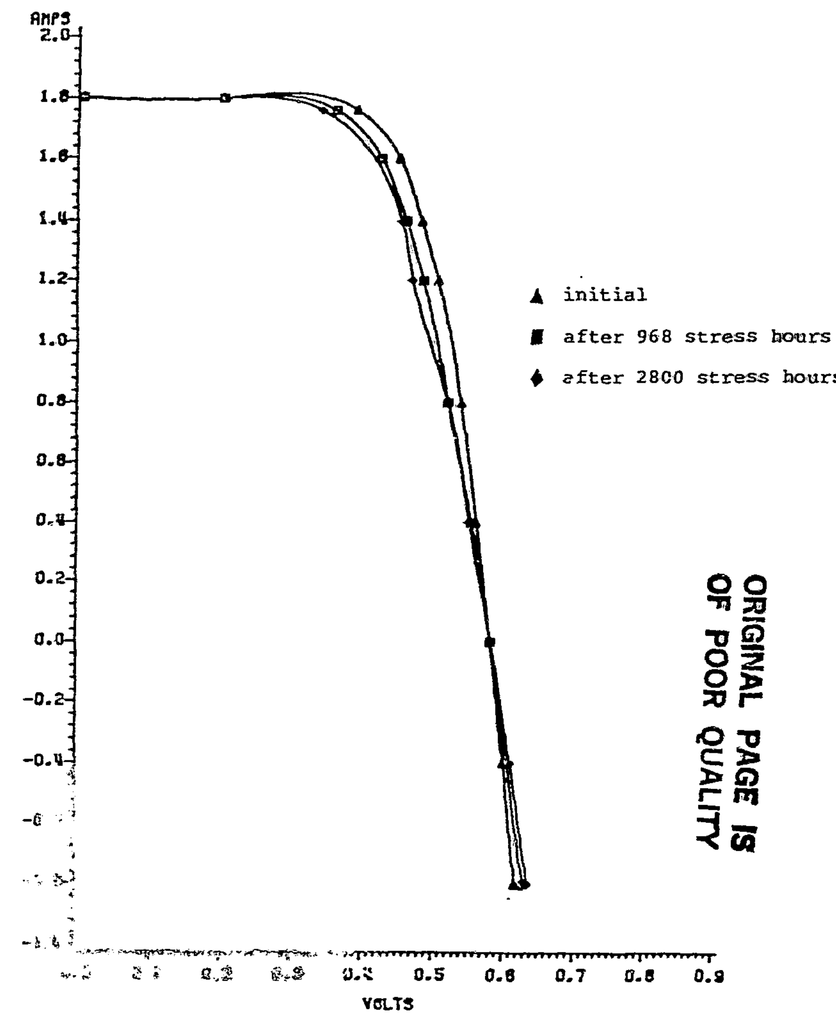

Type A I-V Characteristics for 135°C Bias-Temperature Stress, Typical Case

ORIGINAL PAGE IS OF POOR QUALITY

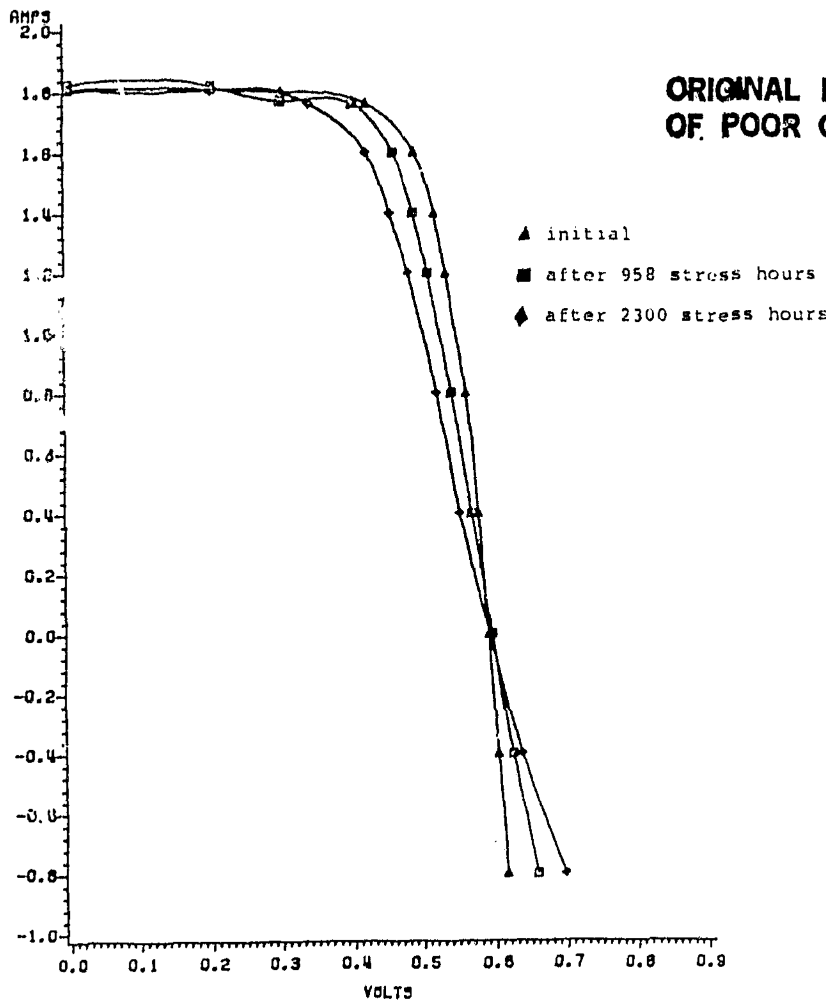

GLASS STRENGTH REVISITED

JET PROPULSION LABORATORY

D.M. Moore

Overview

Objective:

- Thickness sizing of rectangular glass panels subject to pressure loads

Background:

- Non-linear behavior of pressure-loaded plates
  - Tensile membrane stresses at mid-thickness
  - Less deflection and stress than linear theory
- Statistical nature of glass breakage

Current Window Design Practice:

- Empirical curves for glass thickness and area vs load for 8 per 1000 failure rate

Recent Developments:

- PPG, TTU, JPL – 1980
- Good estimate of stress obtained by non-linear FEM
- Statistical methods applied to glass breakage strength

ORIGINAL PAGE IS OF POOR QUALITY

Glass Thickness Sizing Method

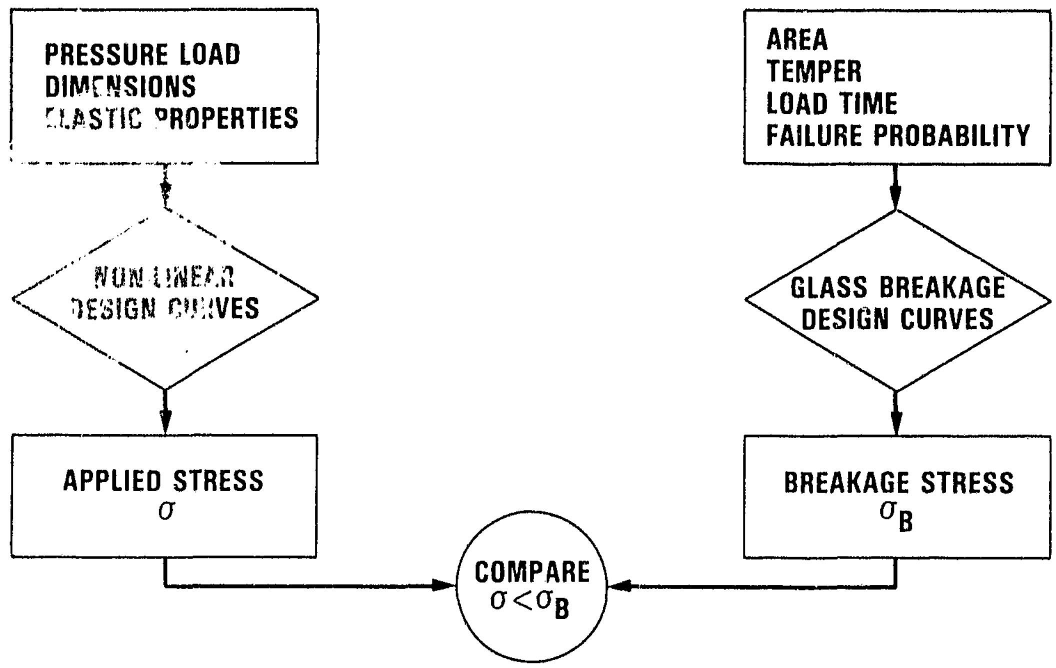

Uniformly Loaded, Simply Supported Rectangular Plate

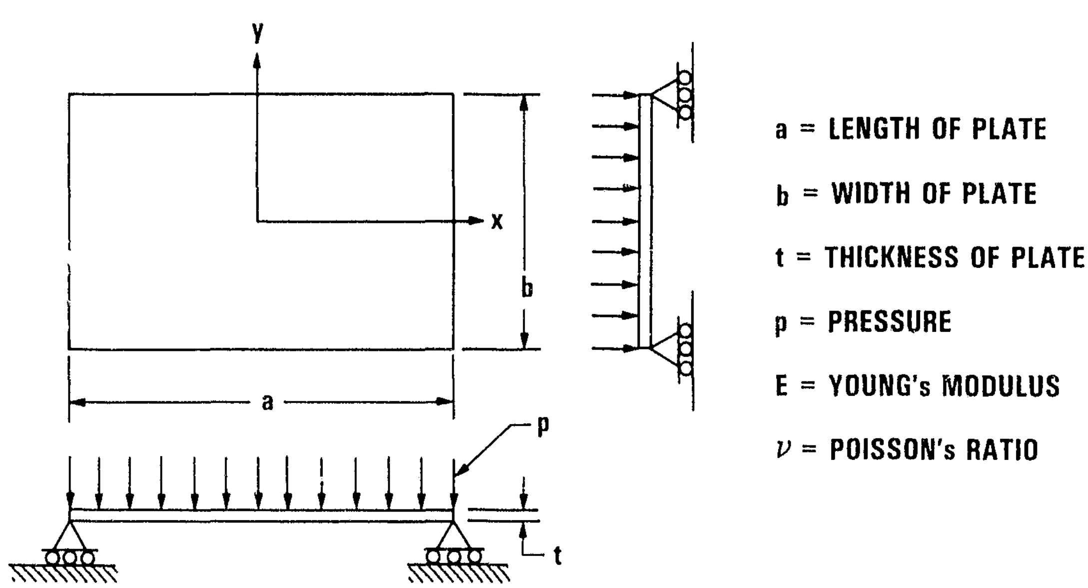

Maximum Principal Stress Contours

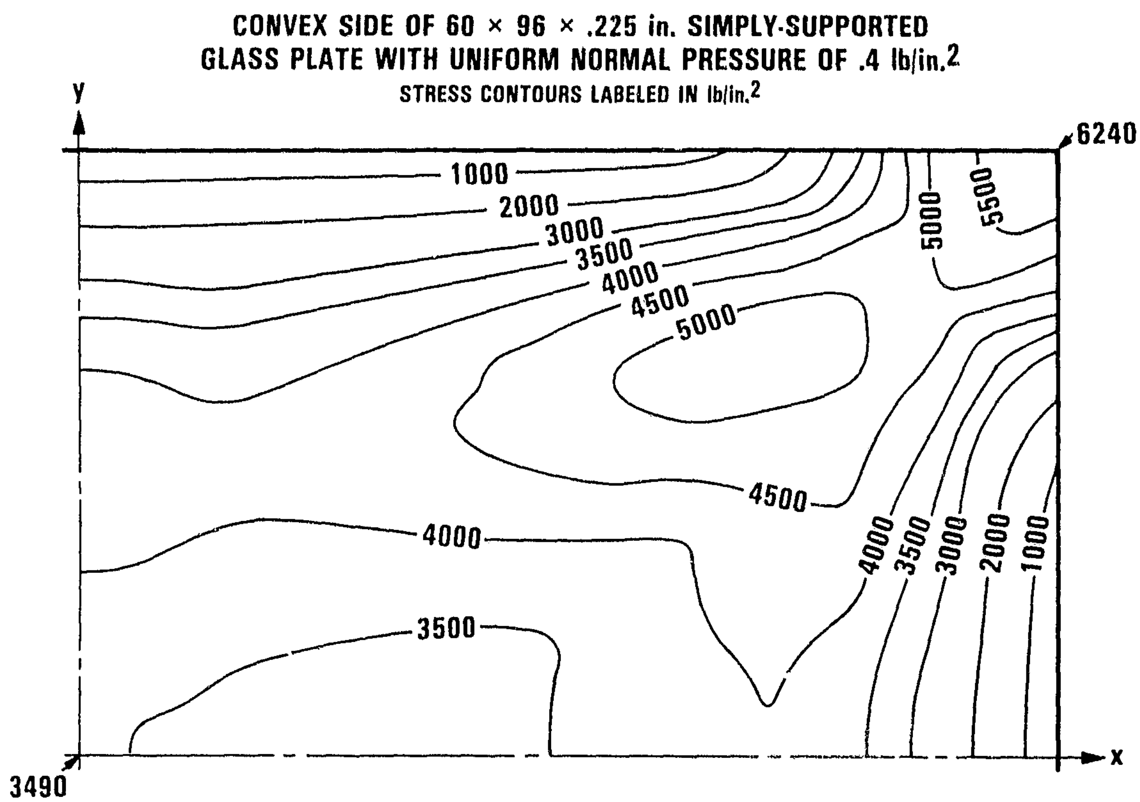

Deflection vs Load

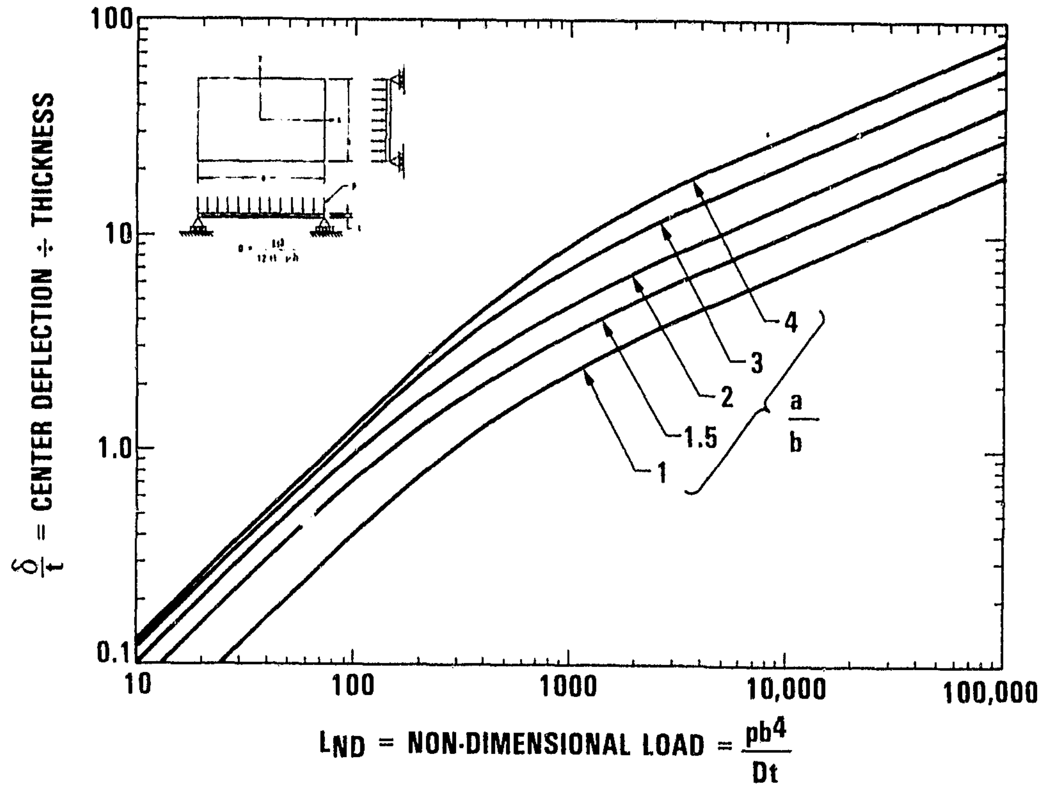

ORIGINAL PAGE IS
OF POOR QUALITY

Stress vs Load

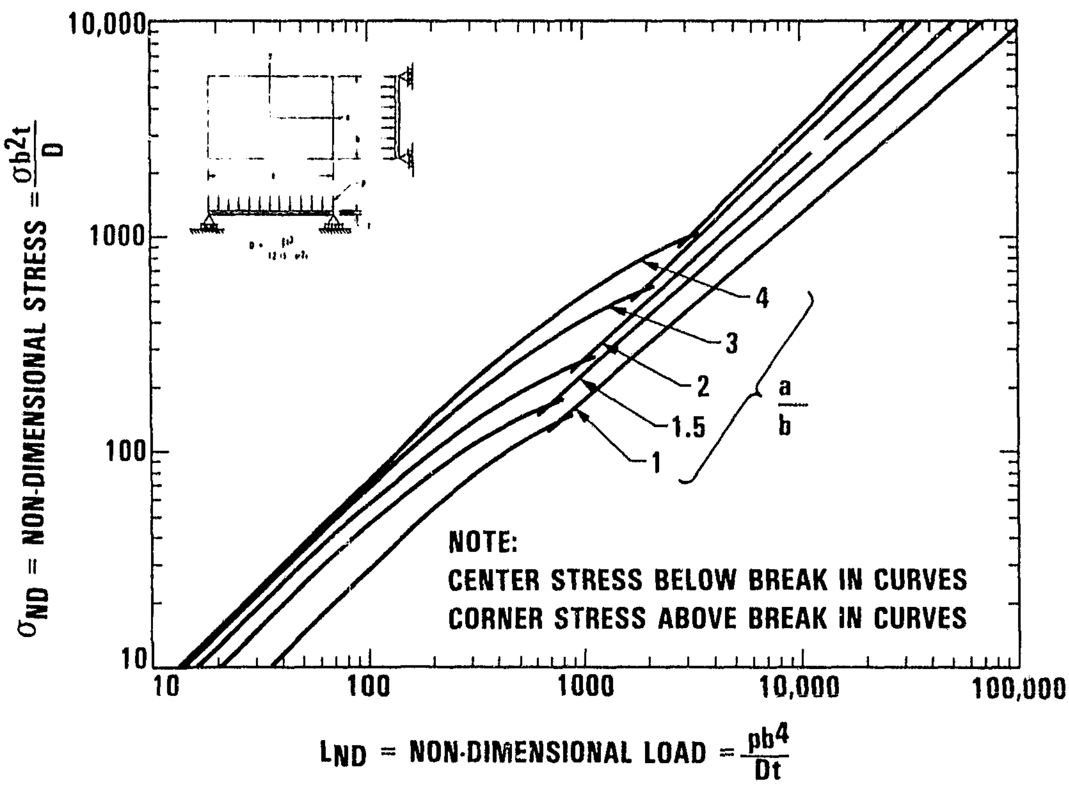

Glass Breakage Strength

Brittle failure mechanism
- Fails in tension at flaws
- Inherent strength $\approx$ 1,000,000 lb/in.^{2}
- Apparent strength $\approx$ 10,000 lb/in.^{2}

Depends On:
- Load duration time
- Surface area of plate
- Length/width ratio of plate
- Probability of failure

Approach:
- Analyze existing glass breakage data
- Least-squares curve fitting:
  $\sigma_B = f(\tau, A, P_f)$
- Weibull statistical analysis:
  $\sigma_B = f(P_f)$

Glass Breakage Data

SOURCE	SIZE	TOTAL NO. ANALYZED
Bowles and Sugarman	41 × 41 × .110 TO .373 in.	220
Texas Tech (TTU)	16.3 × 19.8 × .125 in. 28.5 × 60.5 × .219 in.	50 10
Ontario Research Foundation (ORF)	60 × 96 × .225 in.	120
Libbey Owens Ford	30 × 48 × .090 in. TO 120 × 168 × .312 in.	1300
Swedish Data	39.4 × 39.4 × .118 in. TO 66.9 × 66.9 × .236 in.	600
		2300

Glass Breakage Stress vs Time to Break: Ontario Research Foundation Phase II Data, Manufacturer B

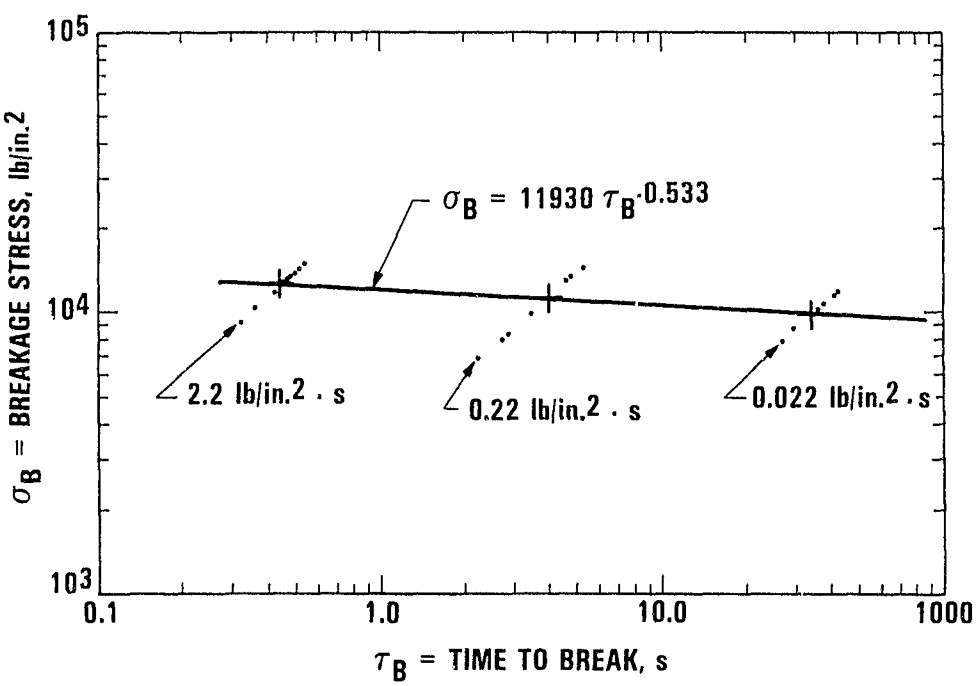

ORIGINAL PAGE IS OF POOR QUALITY

Fraction of One-Minute Strength vs Load Duration

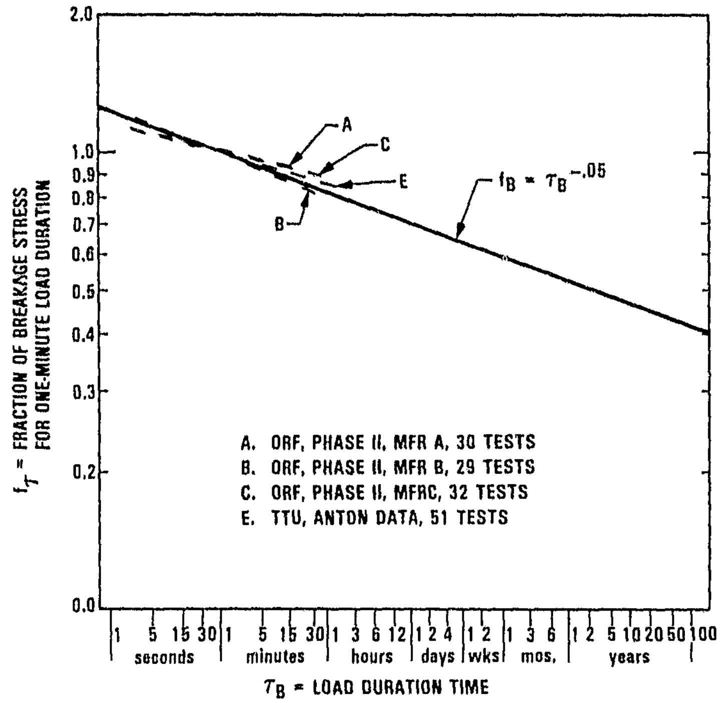

Average One-Minute Breakage Stress vs Area of Plate

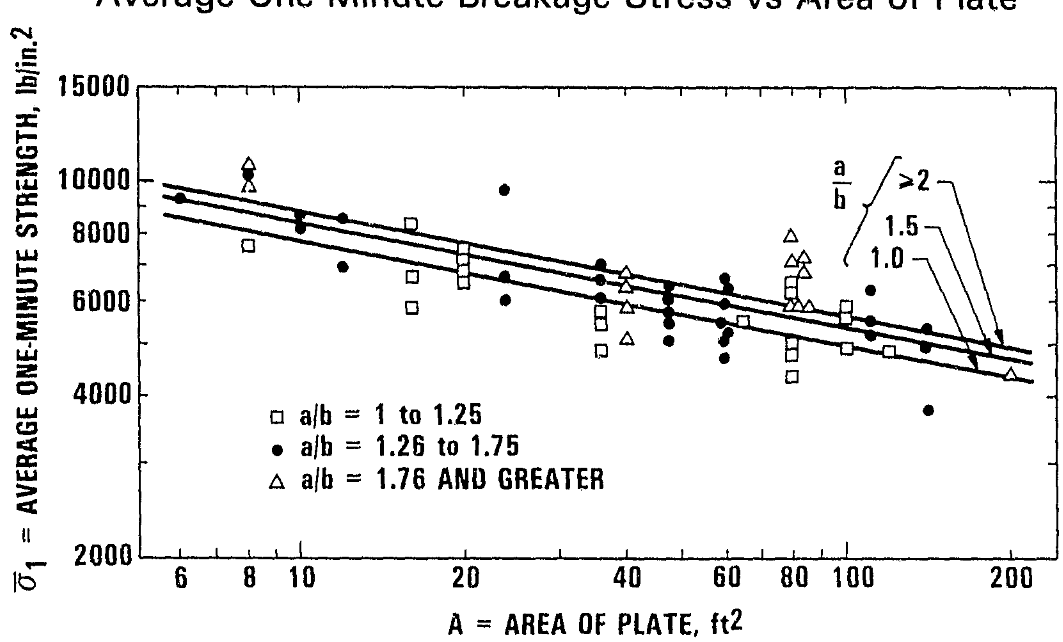

Fraction of Strength of 1 x 1 m Plate vs Area of Plate

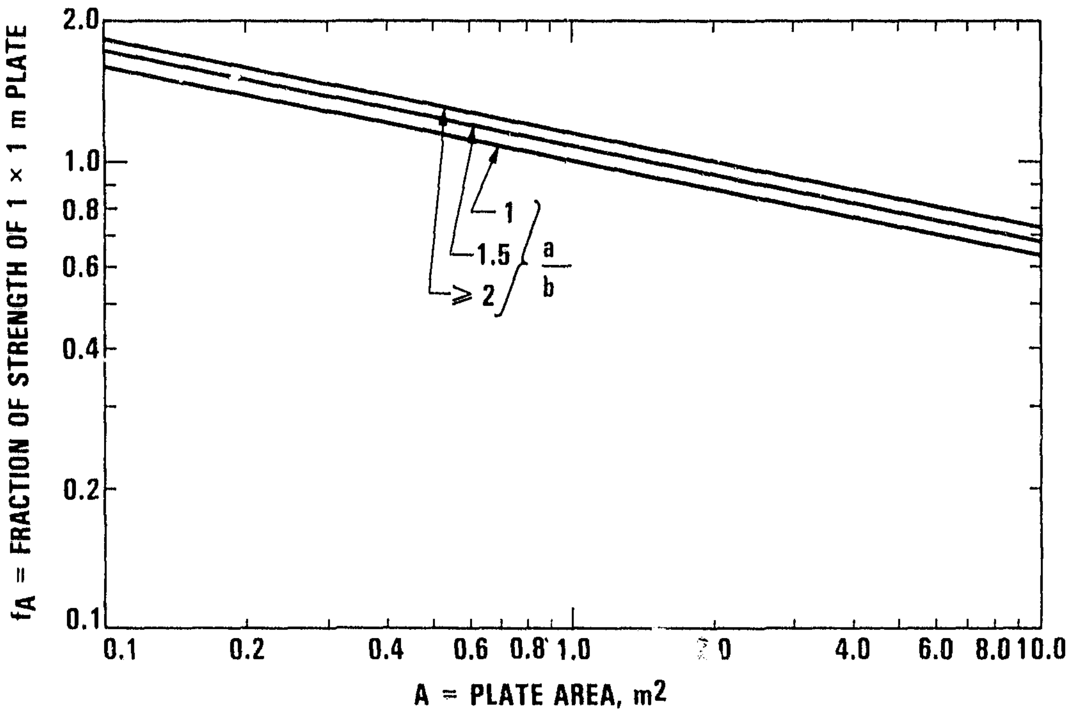

Glass Strength vs P_f

ORIGINAL PAGE IS OF POOR QUALITY

$$P_f = 1 - e^{-\left(\frac{\sigma_{11} \cdot \sigma_u}{\sigma_o}\right)^m}$$

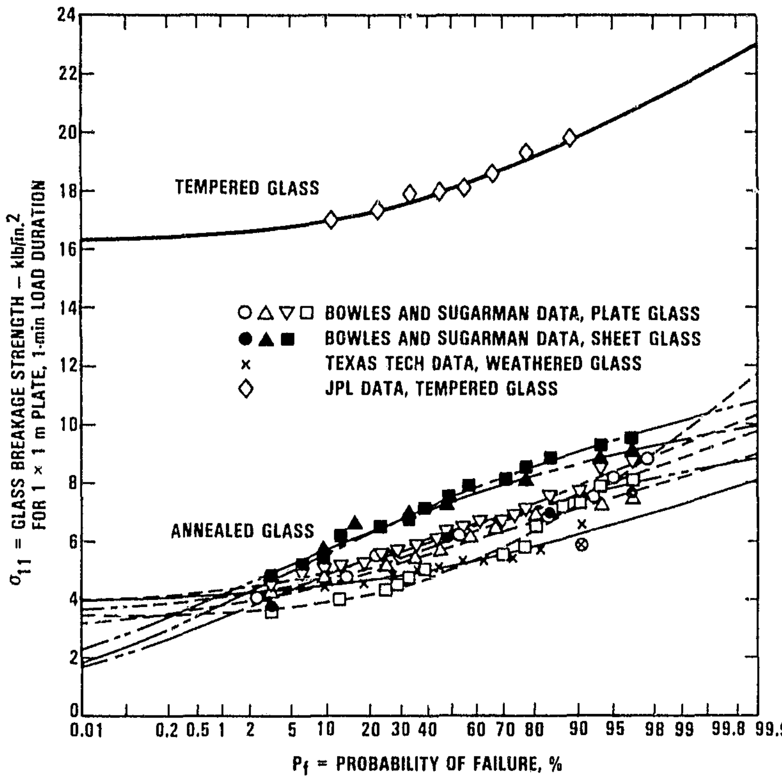

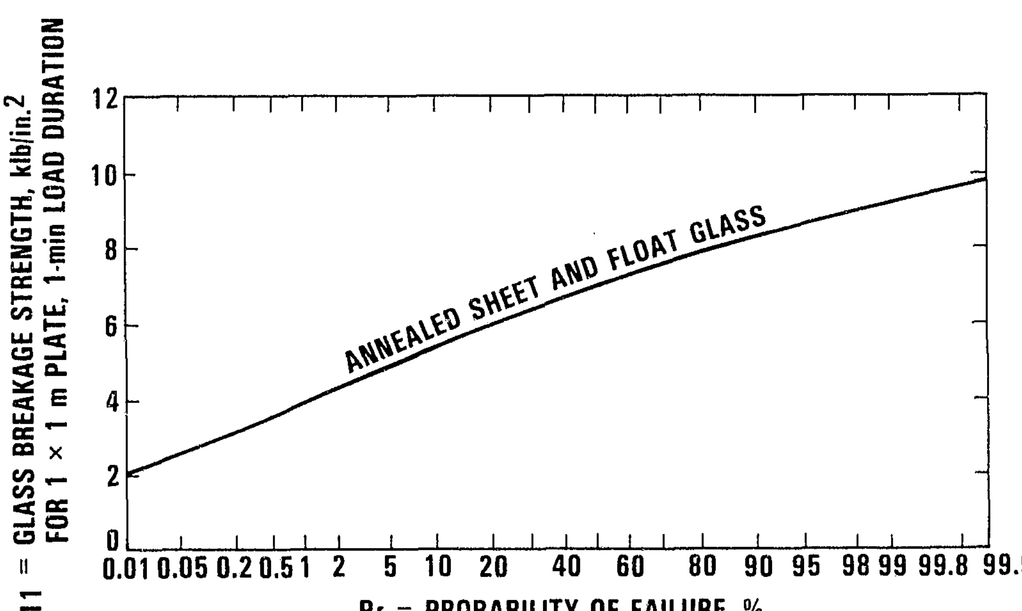

Conclusions

Stress prediction

- In excellent agreement with other researchers

Glass strength prediction

- Much additional glass breakage data included
- 2300 vs 230 failed plates

Stress-and-strength prediction internally consistent

- Glass strength is obtained from pressure load at failure using stress prediction method

ANGLE-OF-INCIDENCE EFFECTS ON MODULE POWER AND ENERGY PERFORMANCE

JET PROPULSION LABORATORY

A. Wilson and R. Ross

Study Objective

- **Measure effects of steep angles of incidence on photovoltaic (PV) power output including:**
  - **Cell background reflectance**
  - **Glass surface (smooth vs stippled)**
  - **Soiling level**
- **Develop analytical expressions for predicting power output vs angle of incidence and optical surface parameters**
- **Compute prediction error in annual energy performance due to commonly assumed pure cosine dependence and improved algorithms**

Test Configuration

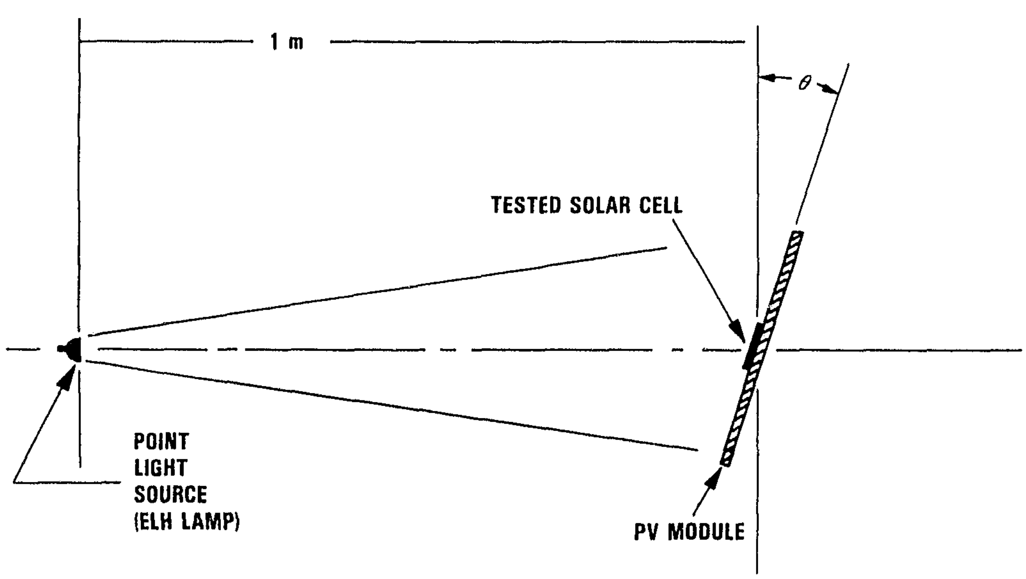

Measured Angle-of-Incidence Dependence vs Cosine Model

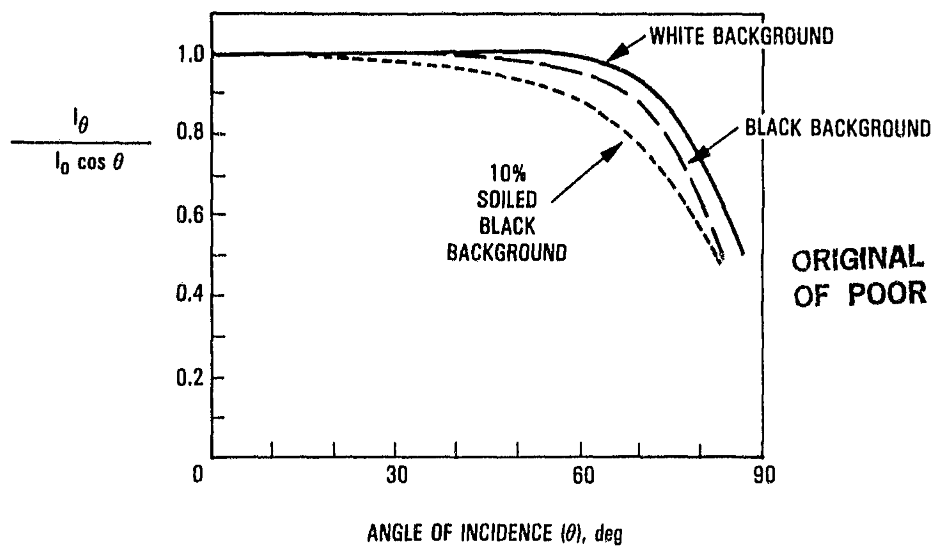

ORIGINAL PAGE IS OF POOR QUALITY

Reflection Loss Dependence on Angle of Incidence

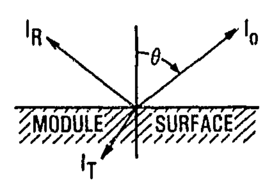

From Fresnel's Law: $\rho(\theta) = \frac{I_R}{I_0} = \frac{1}{2}\left[\frac{\tan^2(\theta - \theta')}{\tan^2(\theta - \theta')} + \frac{\sin^2(\theta - \theta')}{\sin^2(\theta - \theta')}\right]$

where $\theta' = \text{arc sin}\left(\frac{(\sin\theta)}{n}\right)$

n = index of refraction of optical surface

Define $F_R = \frac{I_T(\theta)}{I_T(o)} = \frac{I_0 - I_R(\theta)}{I_0 - I_R(o)}$

or $\boxed{F_R = \frac{1 - \rho(\theta)}{1 - \rho(o)}}$

where $\rho(o) = \left(\frac{n-1}{n+1}\right)^2$

Soiling Loss Dependence on Angle of Incidence

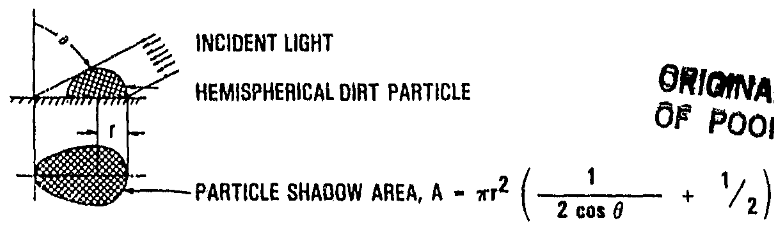

ORIGINAL PAGE IS OF POOR QUALITY

Define

$$F_S = \frac{\text{current with actual enlarged shadowing}}{\text{current with } \pi r^2 \text{ shadowing}}$$

Given fraction soiling loss at normal incidence = f

$$f = \frac{I_0 - I_{s0}}{I_0}$$

where I_0 = current when $\theta = 0°$ for clean surface

I_{s0} = current when $\theta = 0°$ for soiled surface

Then

$$\boxed{F_S = \frac{1 - f\left(\frac{1}{2\cos\theta} + \frac{1}{2}\right)}{1 - f}}$$

Angle-of-Incidence Correction Factors

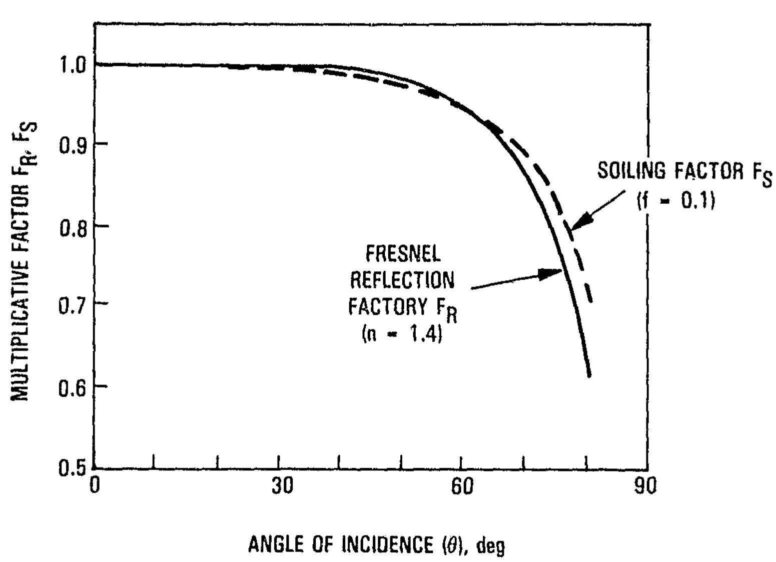

Measured Angle-of-Incidence Dependence vs Improved Models

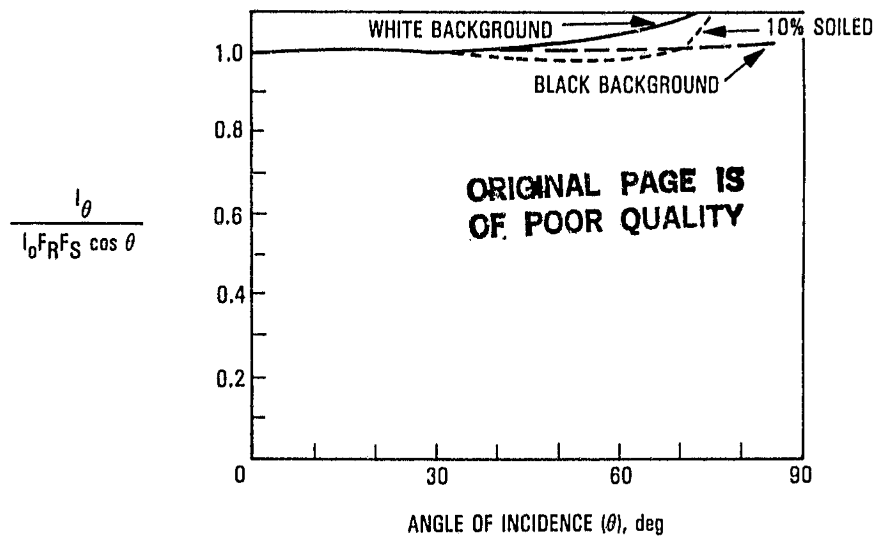

ORIGINAL PAGE IS OF POOR QUALITY

Conclusions

- **Angle-of-incidence effects are influenced by:**
  - **Surface index of refraction**
  - **Soiling level**
  - **Surface texture (smooth vs stippled)**
  - **Cell background reflectance**
- **Fresnel reflection and soil shadowing models provide good prediction for these effects**
- **Conventional cosine model provides acceptable accuracy for energy prediction calculations when soiling is low**

MODULE POWER AND ENERGY PERFORMANCE VS IRRADIANCE LEVEL

JET PROPULSION LABORATORY

C.C. Gonzalez

Objective

To investigate the translation of current-voltage (I-V) curves with changes in irradiance level and temperature

- Effect of module used in translation of I-V curves on results obtained in analytical studies
- Selection of optimum operating voltage for photovoltaic array/power conditioner system

Approach

Analytical:

- Determination of annual array energy using hour-by-hour simulation based on SOLMET data
  - Determination of total annual array energy based on ideal maximum power tracking
  - Determination of fraction of annual array energy produced at given cell temperature and irradiance level intervals
- Use of this analytical approach with I-V curves representing degraded arrays

Experimental:

- Observation of translation of I-V curves with changes in irradiance level

Topics

- Consideration of rate of degradation of annual array energy output with array power degradation
- Consideration of translation characteristics of different types of I-V curves
- Experimental translation of module I-V curves
- Comparison of power-conditioner fixed-voltage operation vs voltage/temperature tracking

Annual Array Energy Loss vs Power Degradation as a Function of PCS Voltage Operation Mode

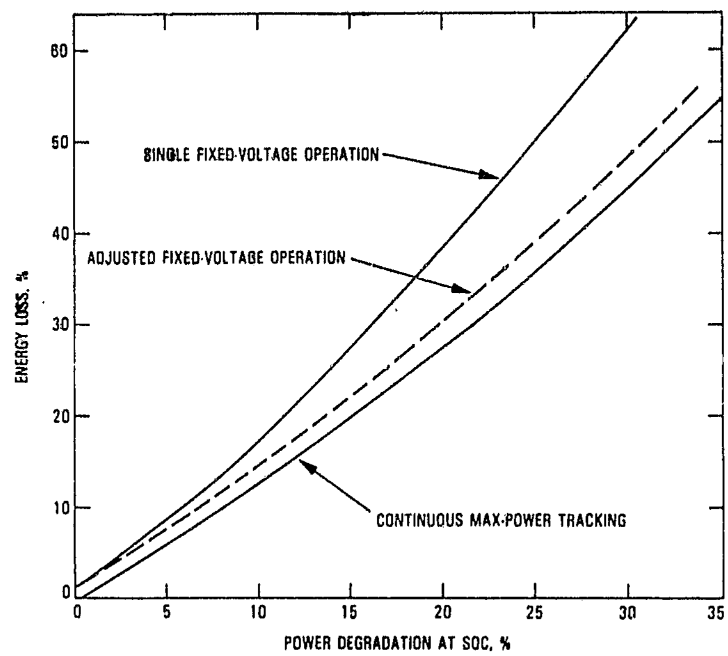

Annual Array Energy Loss vs Power Degradation

As array ages and I-V curve degrades, energy performance decreases 1.4 times faster than power performance referenced to 100 mW/cm^2

- **Has significant economic implications relative to:**
  - **Heavily degraded array systems**
  - **Arrays with poor fill factor such as those with thin-film cells**
- **Additional work required to determine those reference conditions which will indicate a level of array power degradation closer to the level of expected energy performance degradation**

Comparison of Translation of I-V Curves With Changes in Irradiance Level

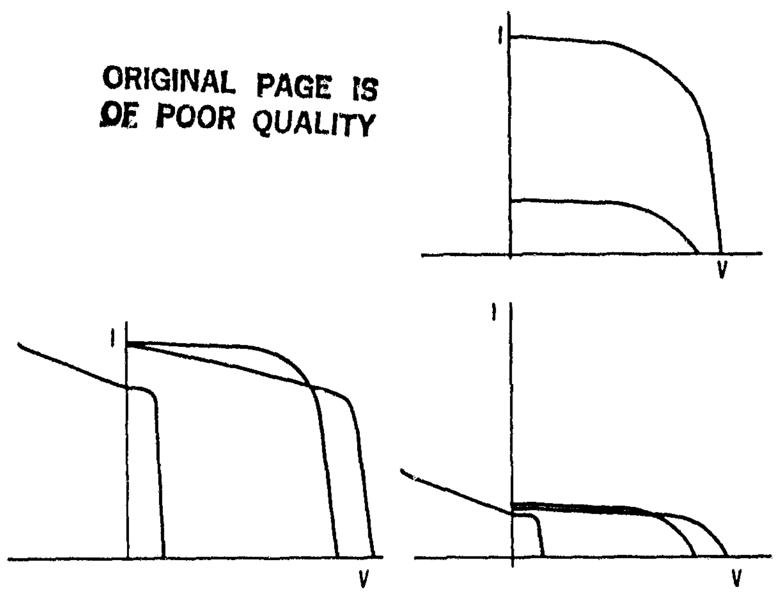

Selection of Array Operating Voltage Based on Array Cell Temperature

- **Power tracking based on temperature alone would provide increased stability over conventional maximum power tracking**
- **Optimum operating voltage varies with both temperature and irradiance**
- **Significant reduction of energy loss may require irradiance measurement and sophisticated algorithms similar to those used in maximum power tracking**

Translation of Single-Point-Failure Module I-V Curves With Change in Irradiance Level Under Sunlight

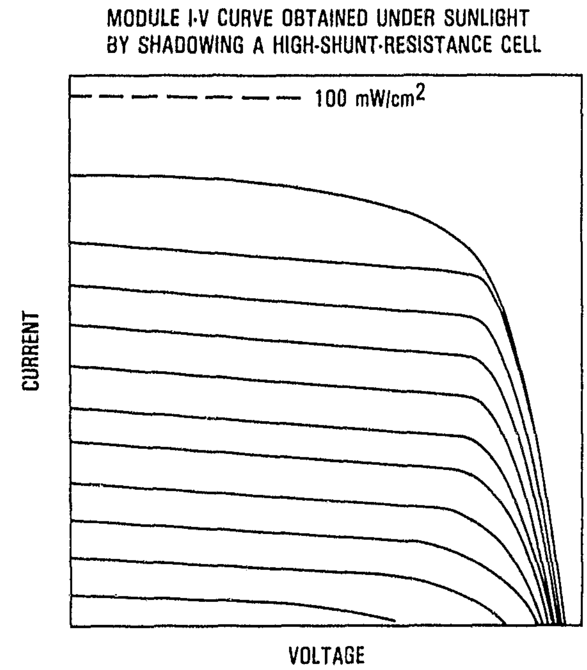

Translation of Single-Point-Failure Module I-V Curves With Change in Irradiance Level With a Simulator

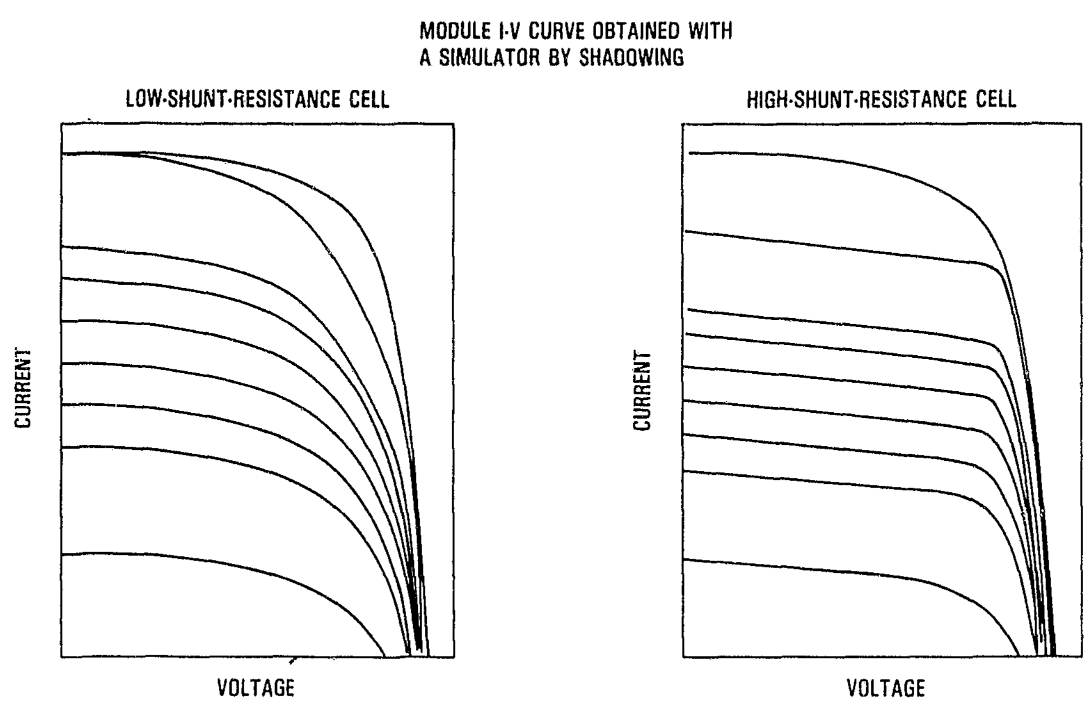

Optimum Operating Voltage vs Cell Temperature and Irradiance Level

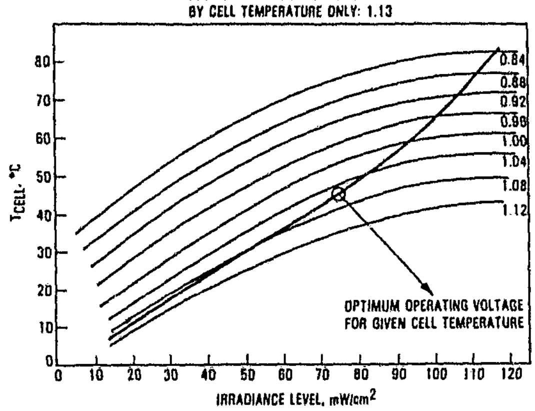

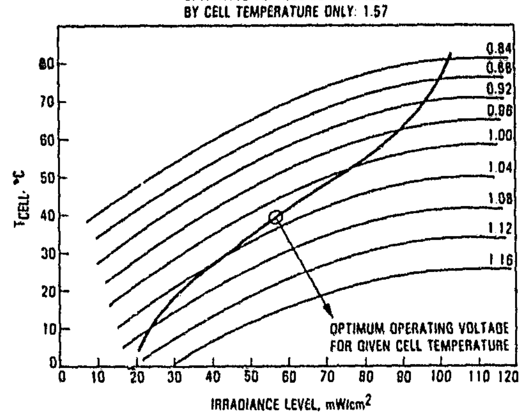

Summary

Model for translation of module (array) I-V curves with temperature and irradiance must reflect the intrinsic structure of the curves and account for shape changes

- **I-V curves for modules containing single-point failures such as cracked or shadowed cells will dramatically change shape with changes in temperature and irradiance**
- **Use of temperature to determine array/power-conditioner operating voltage will result in minimal gain in annual energy unless irradiance level is taken into account**
- **Predictions of relative energy output of modules with I-V curves of different shapes based on peak power ratings at 100 mW/cm^2 may prove erroneous unless the model used to translate I-V curves is selected in conformity with the basic structure of the I-V curve**

Future Work

Determination of preferred module rating conditions for predicting relative energy output based on computer optimization program using various:

- **Sites**
- **Cell temperatures**
- **Irradiance levels**
- **Module thermal characteristics**

ENVIRONMENTAL ISOLATION

C.D. Coulbert, Chairman

Rockwell Science Center presented and showed examples of an experimental technique for evaluating the statistical distribution of localized interface bond strengths. The analysis of these data for evaluating the failure probability of bonded interfaces was also described. This technique, which uses miniature shear-test coupons cut from a bonded interface component, will be evaluated as a method for gathering data on interface aging effects in encapsulated PV modules.

A computer model developed by the University of Toronto has been used to simulate the mechanism and kinetics of the photooxidation of ethylene vinyl acetate (EVA). It was found that the results, relative to the chemical species evolved and the time scale, compared favorably with the limited experimental knowledge of such systems. In particular, a better understanding has been gained of the degradation induction period and factors that control it. Results with added stabilizers also suggest that criteria for optimizing stabilization systems can be developed.

Outdoor weatherability tests by JPL of PV minimodules using new and developing encapsulation materials have completed two years of outdoor exposure at sites in Southern California (JPL, Pasadena; JPL, Goldstone, and U.S. Coast Guard Station, Pt. Vicente). The minimodules (12 x 16 in.) included 12 different material configurations using top covers of glass, Tedlar, and Korad with pottants of EVA, silicone, and polyurethane and with back covers or substrates of wood hardboard, galvanized steel, glass-fiber-reinforced concrete, foil laminates, or Mylar.

The only significant performance losses measured during the two-year period outdoors were due to cells cracking in modules with wood hardboard substrates. Performance losses due to surface soiling were recovered by washing the modules. Visible yellowing of the polyurethane pottant had not yet resulted in significant power loss.

Solutions to the problems of cover soiling, pottant yellowing, and cell cracking due to hardboard expansion are being developed and evaluated and the results are encouraging.

One of the experimental activities at JPL in assessing and demonstrating life potential of low-cost encapsulation designs is photothermal characterization of encapsulation materials. This involves measurements of chemical and physical properties and performance parameters (e.g., electrical, optical, mechanical, and thermal properties) as a function of aging in an accelerated stress environment. Photothermal characterization of all candidate encapsulant materials is being carried out to achieve this goal. Field-test validation with a 2-cell minimodule is also being carried out.

ENVIRONMENTAL ISOLATION

Materials tested include ethylene vinyl acetate (Springborn A-9918 EVA), ethylene methyl acrylate (A-13404 EMA, Springborn), polyvinyl butyral (PVB Saflex, Monsanto), silicone rubber (RTV 615, GE), aliphatic polyurethane (Quinn), Acrylar (X22416/17, 3M) and other encapsulation materials developed at JPL. Results of these tests have been used to develop a photothermal ranking scheme for encapsulation materials. Critical experimental parameters have been identified for monitoring of degradation. They are weight loss, change in transmission, tensile modulus, crosslinking density, formation of carbonyl and hydroxyl functional groups, and electrical resistivity.

BOND DURABILITY RESEARCH

ROCKWELL INTERNATIONAL SCIENCE CENTER

From Science 82, May 1982, p. 6:

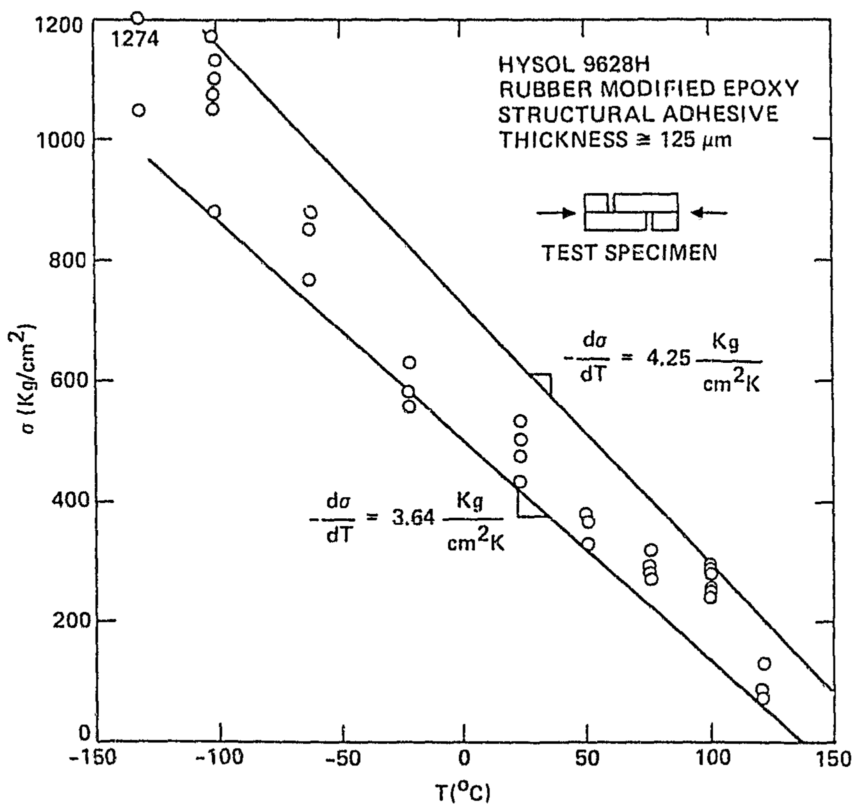

MODELING OF POLYMER PHOTOOXIDATION

UNIVERSITY OF TORONTO

Professor James Guillet and Allan Somersall

Photooxidation of Unstabilized PE
Time to Failure as a Function of Initiator Type and Concentration

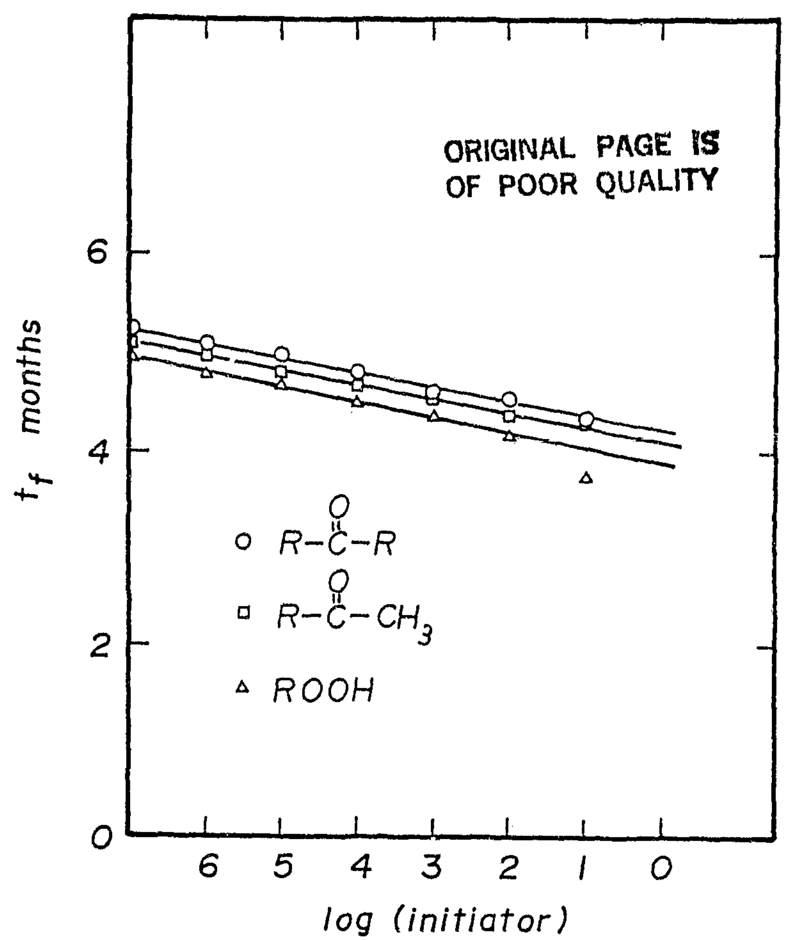

Time to Failure Varies With Light Intensity

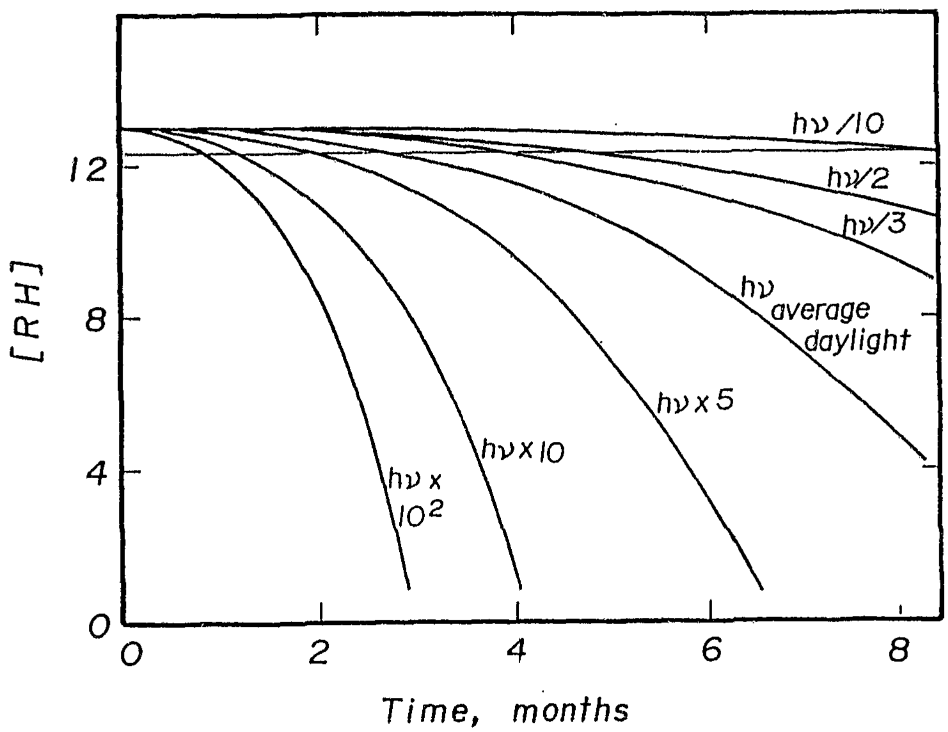

Stabilization Mechanisms

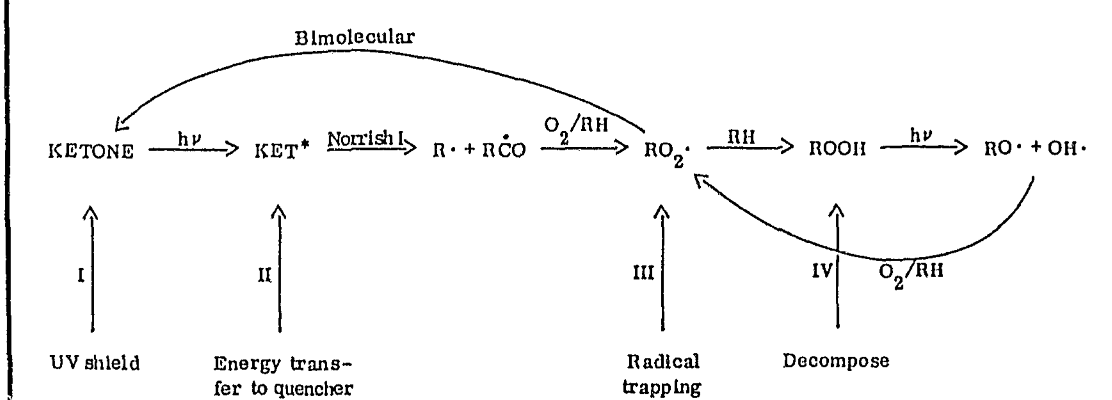

Stabilisation mechanisms

MINIMODULE TEST STATUS

JET PROPULSION LABORATORY

J.A. Amy

Typical Minimodules

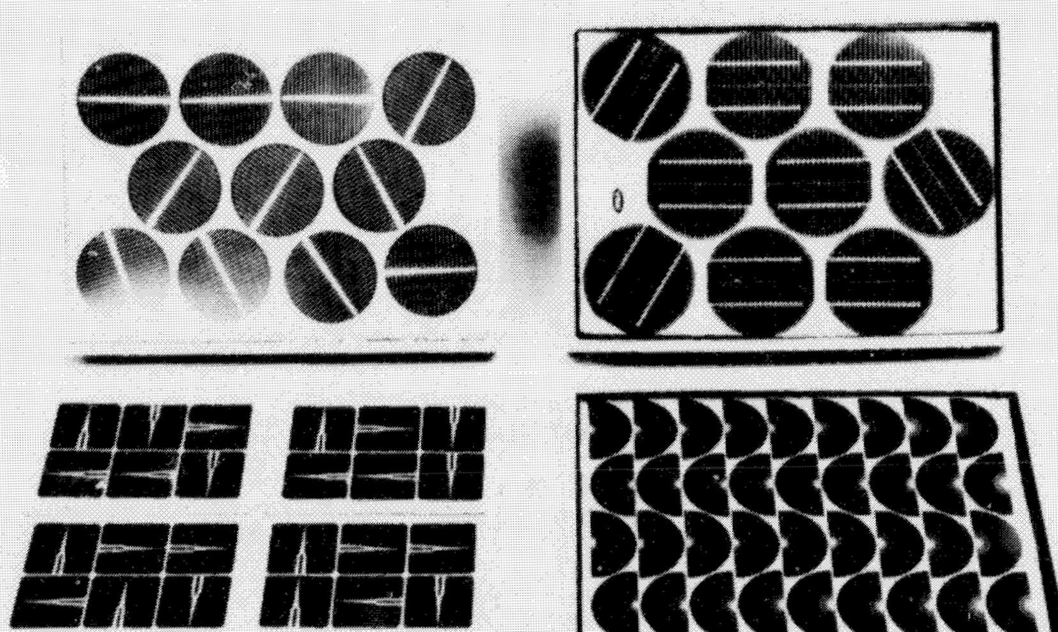

ORIGINAL PAGE IS
OF POOR QUALITY

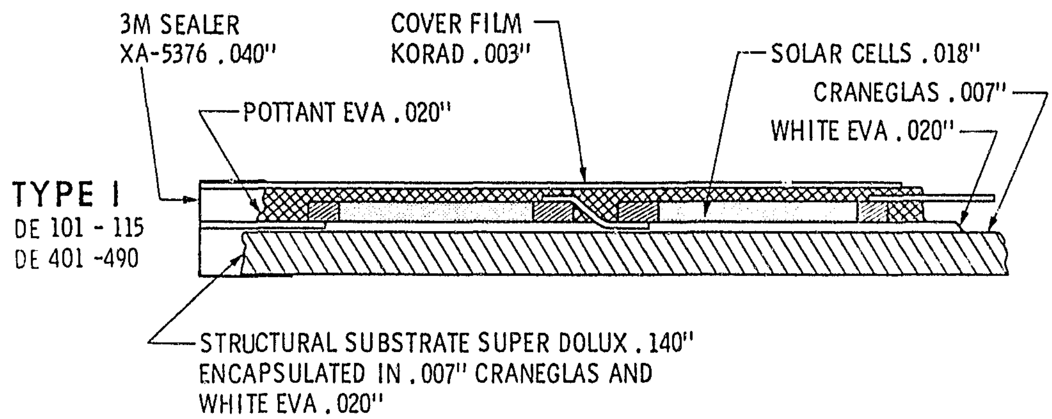

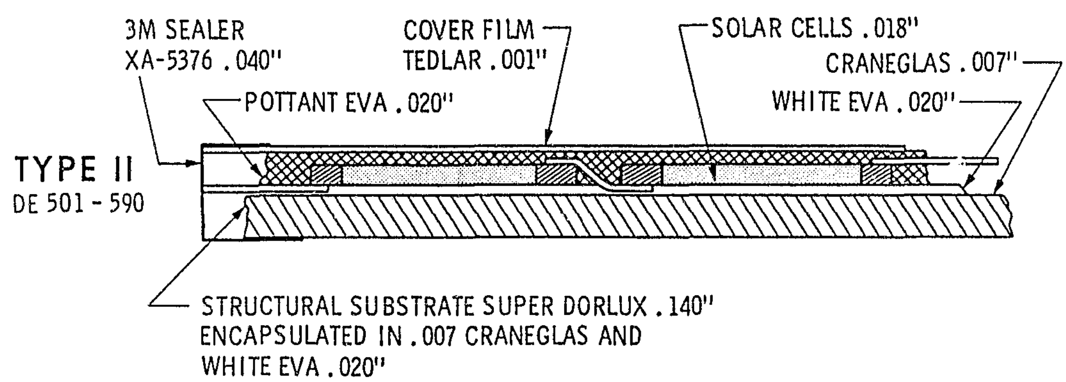

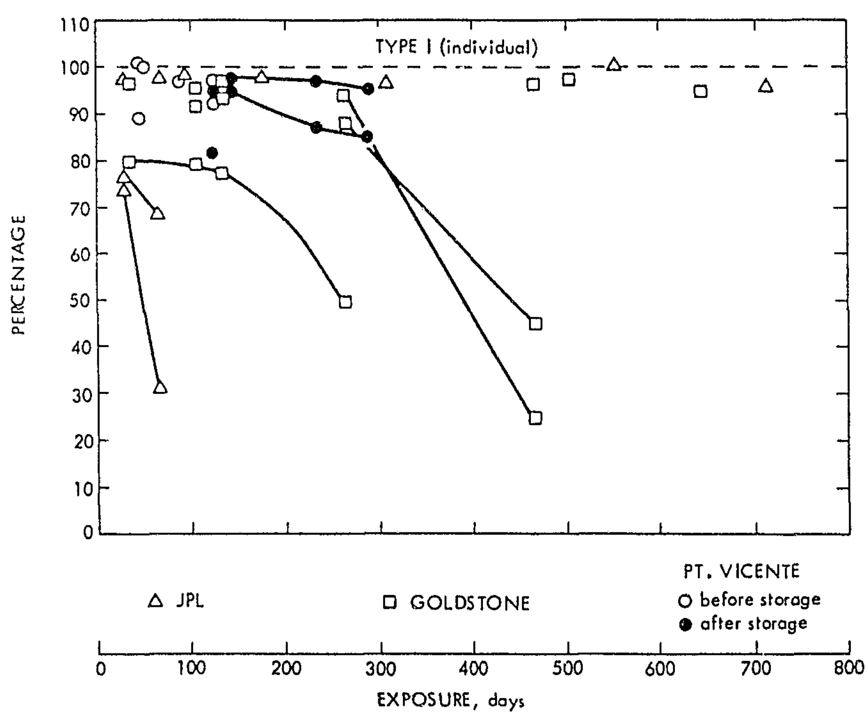

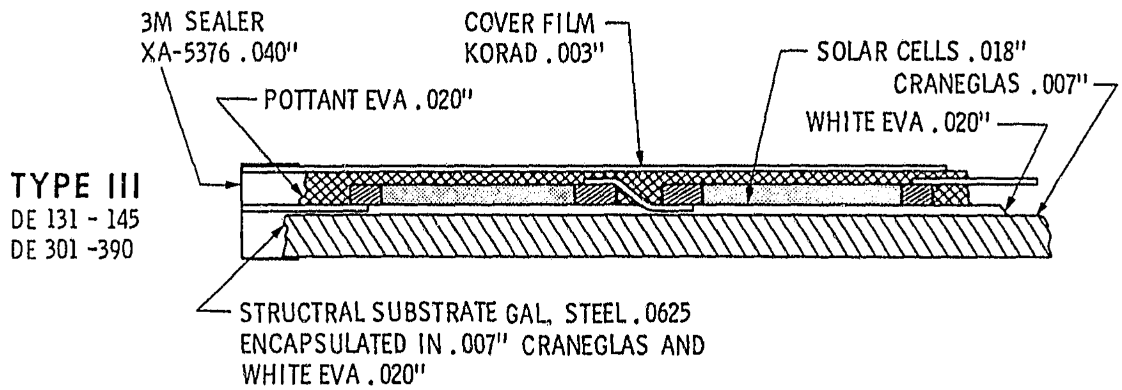
3M SEALER
XA-5376 .040"
COVER FILM
KORAD .003"
SOLAR CELLS .018"
CRANEGLAS .007"
POTTANT EVA .020"
WHITE EVA .020"
TYPE III
DE 131 - 145
DE 301 -390
STRUCTRAL SUBSTRATE GAL. STEEL .0625
ENCAPSULATED IN .007" CRANEGLAS AND
WHITE EVA .020"

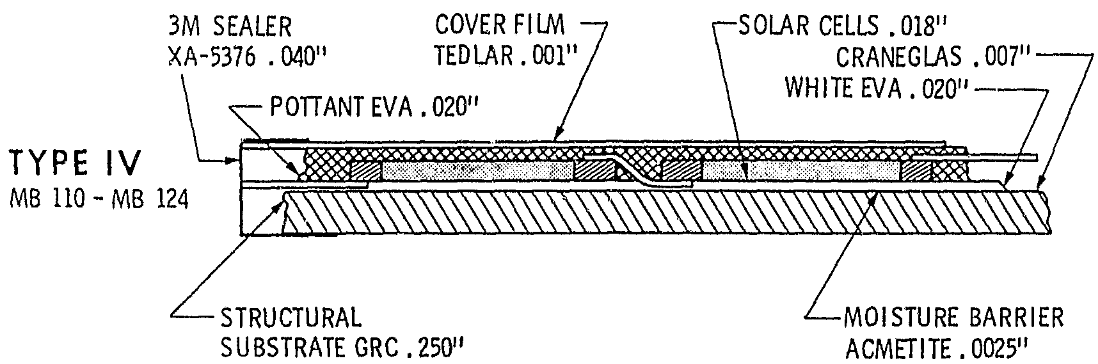
3M SEALER
XA-5376 .040"
COVER FILM
TEDLAR .001"
SOLAR CELLS .018"
CRANEGLAS .007"
WHITE EVA .020"
POTTANT EVA .020"
TYPE IV
MB 110 - MB 124
STRUCTURAL
SUBSTRATE GRC .250"
MOISTURE BARRIER
ACMETITE .0025"

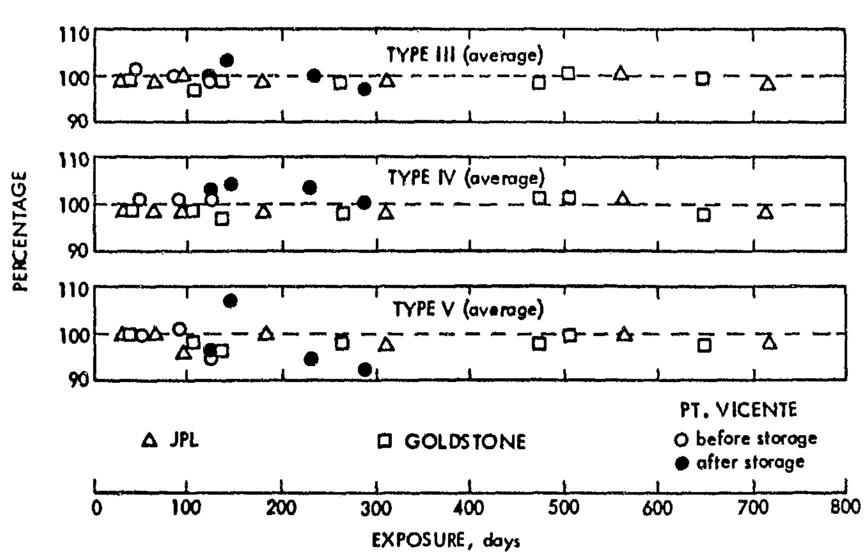
TYPE III (average)
TYPE IV (average)
TYPE V (average)
PERCENTAGE
110
100
90
JPL
GOLDSTONE
PT. VICENTE
before storage
after storage
0
100
200
300
400
500
600
700
800
EXPOSURE, days

Weight Loss of EVA at 135°C

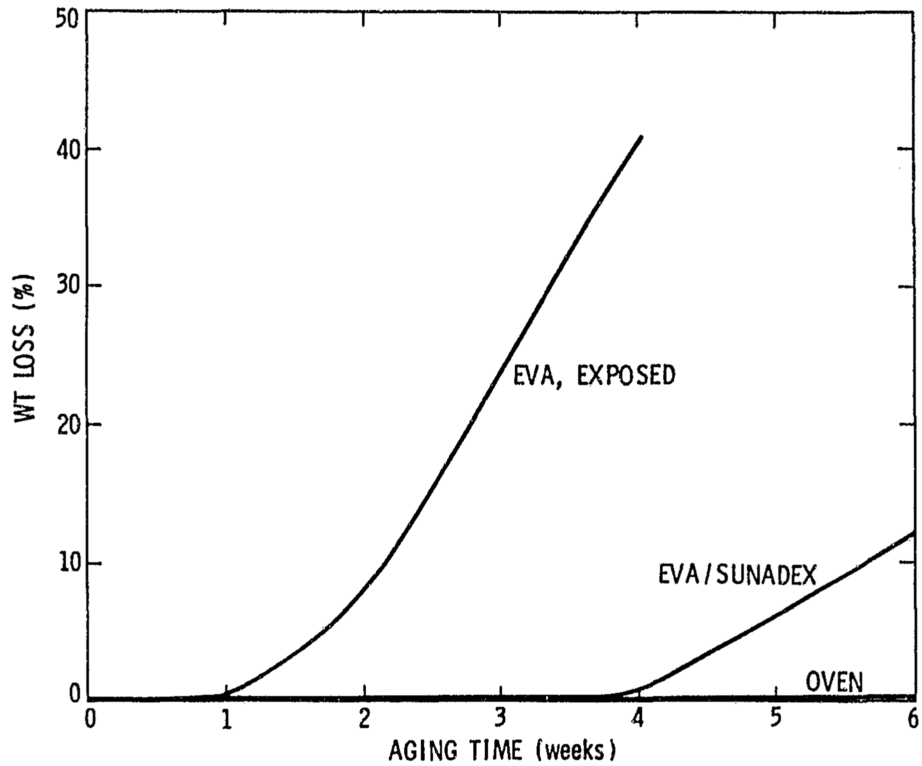

Transmission Spectra of EVA-Sunadex, 135°C
(Dark Oven)

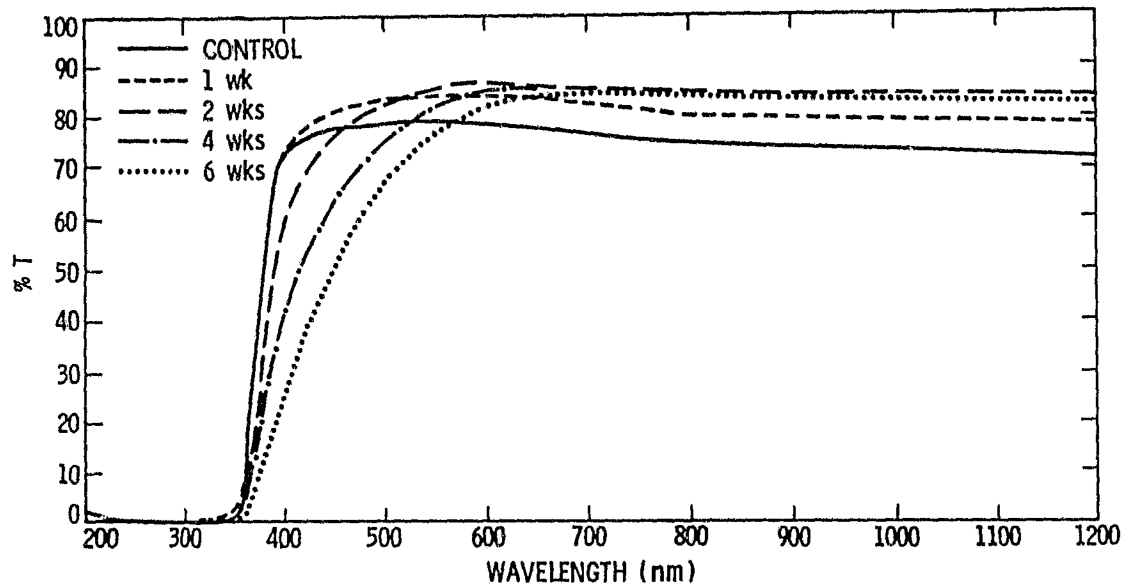

(6 suns)

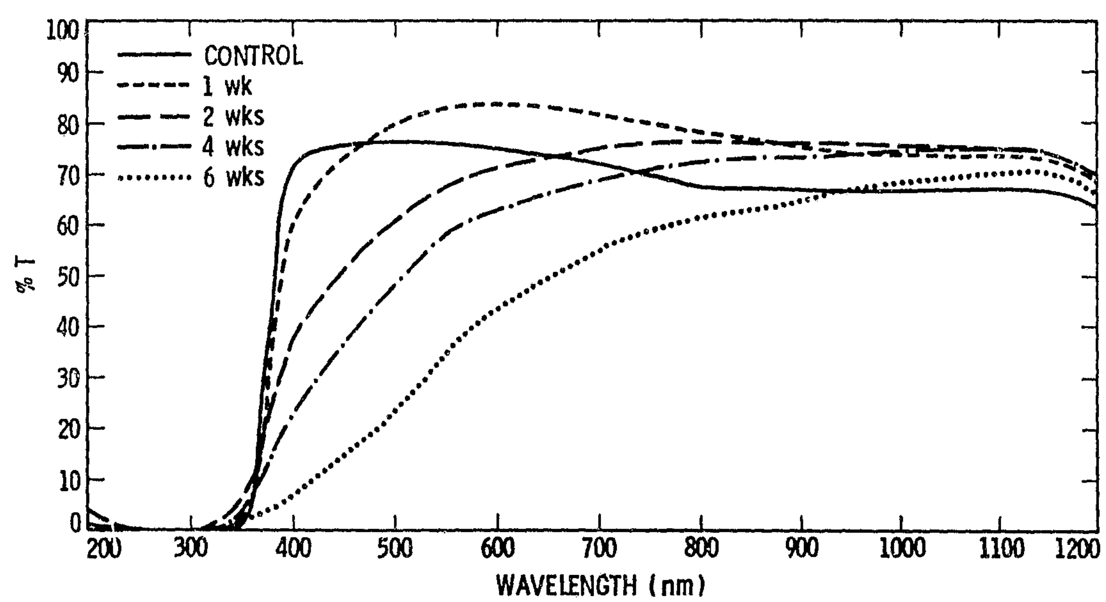

Leakage Current of EVA in 0.1 M NaCl
as a Function of Soaking Time

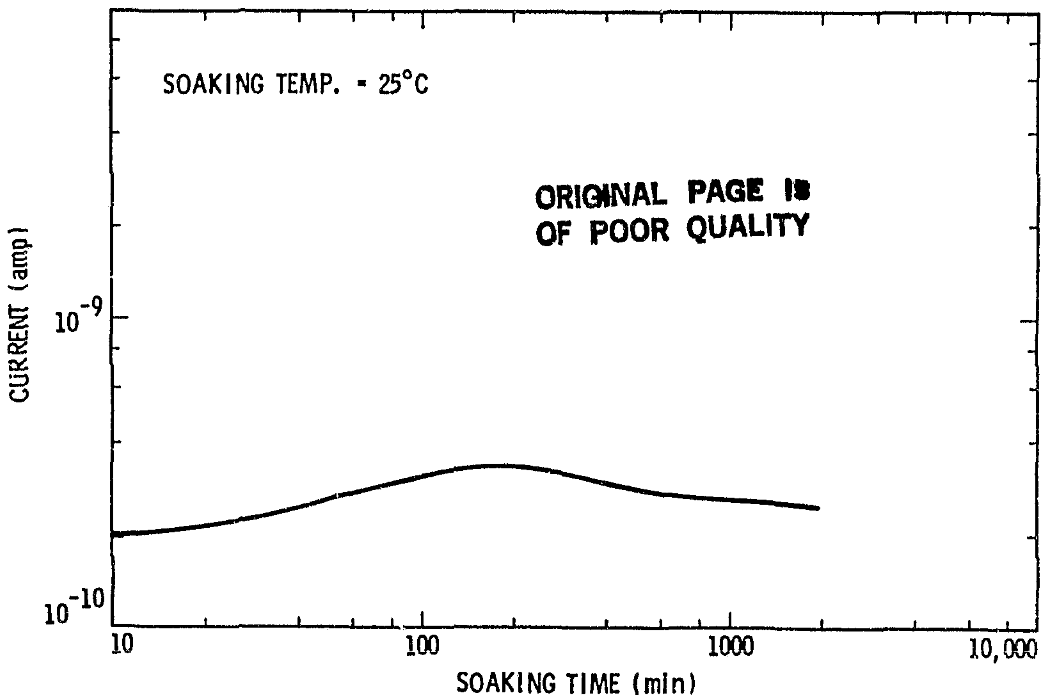

Leakage Current of EVA at 50 Volts

TEMPERATURE	CURRENT (AMP)
25°C	8×10^{-12}
50°C	6×10^{-11}
75°C	4.5×10^{-10}
90°C	1.3×10^{-9}

ENGINEERING AND MODULE PERFORMANCE

R.G. Ross Jr., Chairman

G. R. Mon of JPL presented the current status of interconnect performance investigations. Included was a recently developed solution algorithm that uses least life-cycle costing economics as a rational approach to creative module design. As an example, the algorithm was used to select an optimal interconnect material, considering tradeoffs among fatigue performance, ohmic losses in interconnects, and fabrication costs. The algorithm is available for use by manufacturers.

Neal Shepard discussed recent research activity at General Electric Co. on encapsulation of bypass diodes that was conducted in PV modules. Discussions included installation and configuration, method of thermal heat-sinking, electrical isolation and environmental protection relative to integral PV junction diodes.

Allen Levins of Underwriters Laboratories (UL) reported on research on candidate safety-system concepts including discussions of hazards and solutions relative to array subsystem safety considerations. The safety features of the proposed National Electrical Code (NEC) Article 690 for Solar PV Systems and the proposed Safety Standard (UL 1703) for Flat-Plate PV Modules and Panels were also discussed.

Tom Lundveit of UL discussed research supporting the development of PV array wiring concepts for residentail applications. Proposed NEC Article 690 permits wiring methods specific to PV systems that are currently accepted within allowed conditions. Wiring and termination requirements were identified for PV arrays and several existing wire assemblies were supplied as examples of wiring candidates that appeared capable of passing the UL tests.

R. L. Mueller presented an update on developments involving improvements of the LAPSS source to simulate an AM1.5 source. The improvement consists of installing a Schott GG-4 filter to reduce the excess radiant intensity at the blue end of the spectrum. Experiments using four sunlight-calibrated reference cells of different spectral responses have indicated that with the filtered source, a silicon cell module may be measured using a spectrally non-matched calibrated reference cell with an expected error of less than 1% due to mismatch. The installed filter has exhibited no detectable temporal instability after 1500 LAPSS flashes in a two-month period.

R. W. Weaver reported on experience with the portable array data logger, which had been developed at JPL to enable measurement and evaluation of field performance of high power arrays. This instrument can obtain, display and store I-V curve data for arrays of power output up to 16 kW, producing up to 400 volts and up to 40 amperes. The logger has been operational since July, 1982. It has been used to assess performance of eight arrays at four field sites. Deficiencies revealed by this assessment have been corroborated by other techniques.

FATIGUE OF SOLAR-CELL INTERCONNECTS

JET PROPULSION LABORATORY

G.R. Mon

Interconnect Fatigue Failure Mechanism

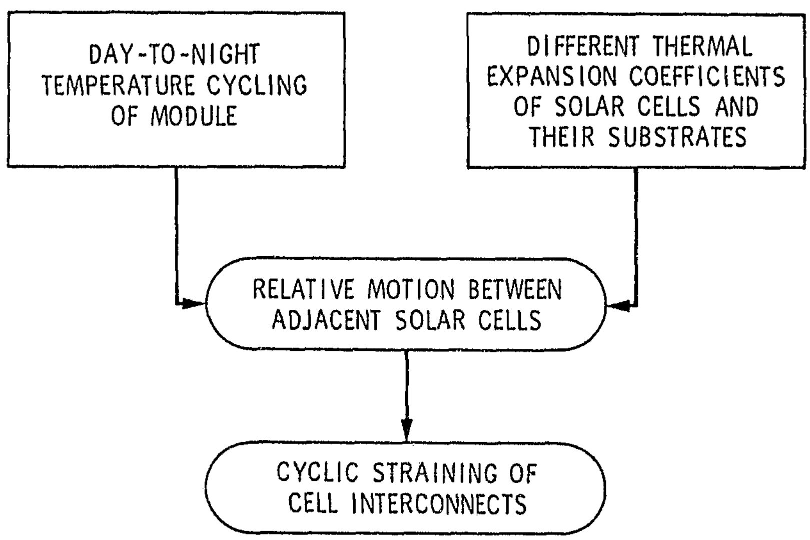

Interconnect Failure Prediction Algorithm

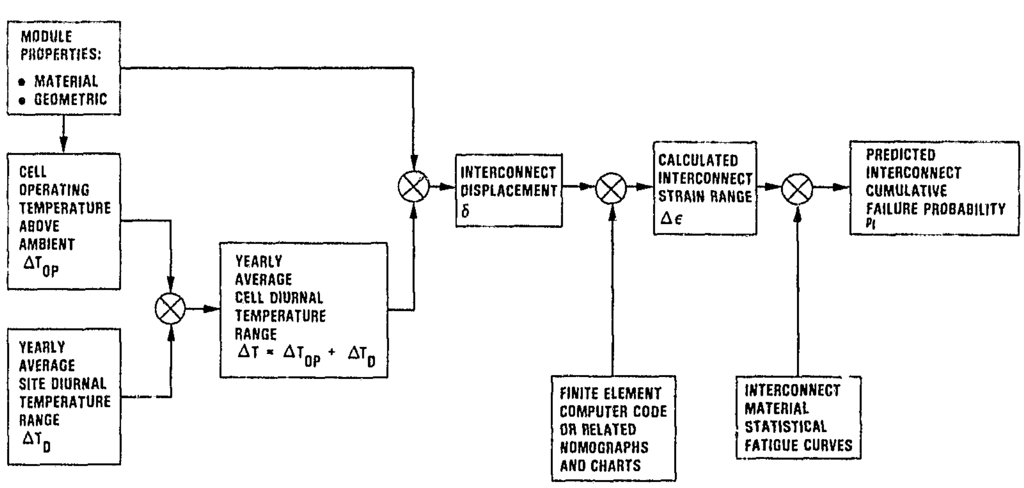

PRECEDING PAGE BLANK NOT FILMED

Candidate Interconnect Materials

- **Homogeneous Materials**
  - **1100 aluminum**
  - **OFHC 1/4-hard copper**
- **Clad Materials**
  - **33.3 Cu/33.3 INV/33.3 Cu**
  - **12.5 Cu/75.0 INV/12.5 Cu**
  - **16 Cu/68 SS/16 Cu**

Statistical Fatigue Curves for Tinned, Annealed 1100 Aluminum

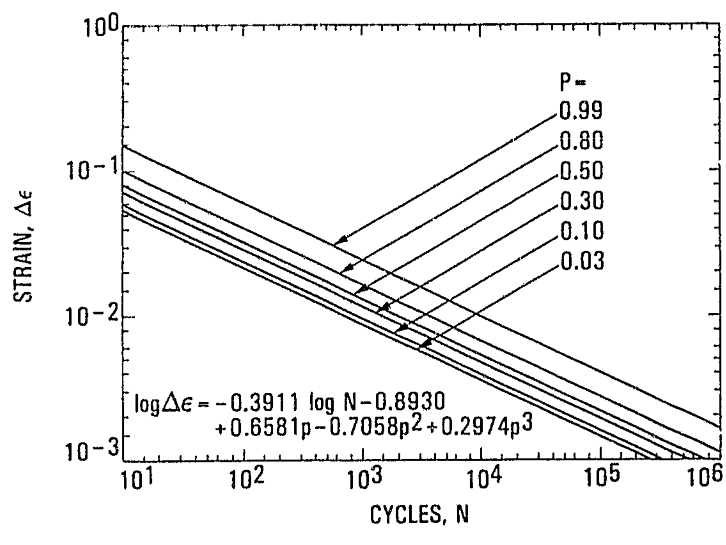

ORIGINAL PAGE IS OF POOR QUALITY

Statistical Fatigue Curves for OFHC ¼-Hard Copper

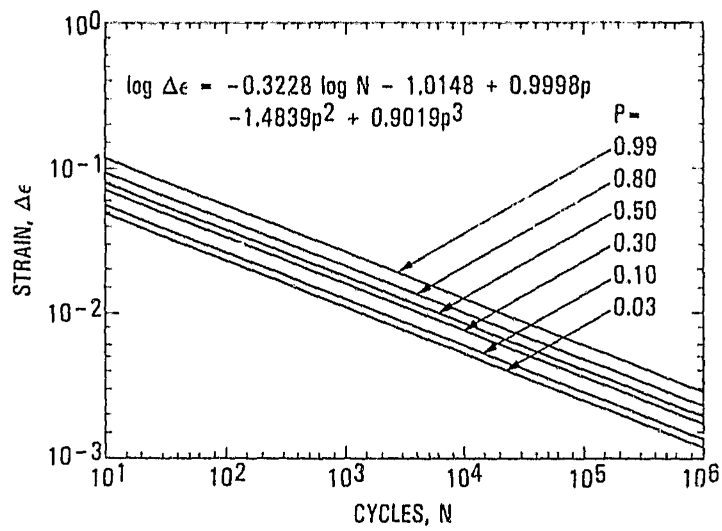

Statistical Fatigue Curves for 33 Cu/33 Inv/33 Cu

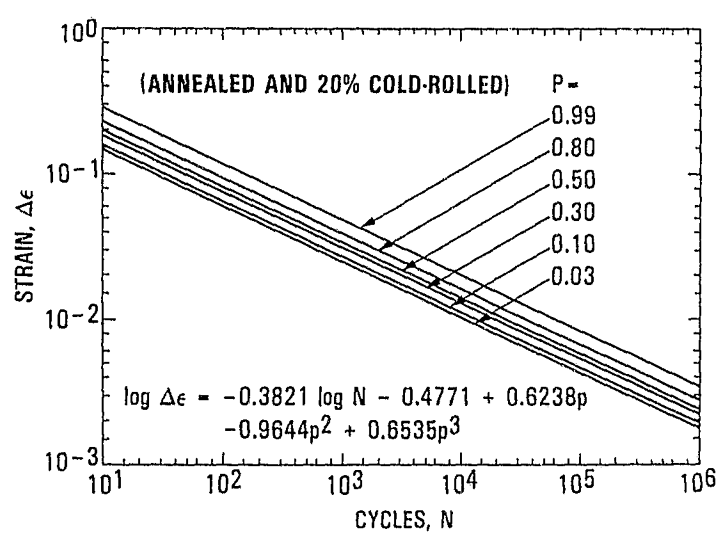

Statistical Fatigue Curves for Cladding,
12.5 Cu/75 Inv/12.5 Cu

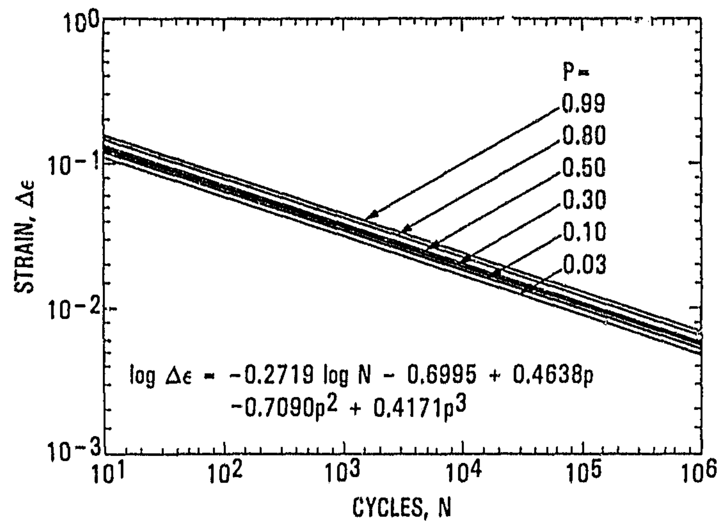

Statistical Fatigue Curves for Cladding,
16 Cu/68 SS/16 Cu

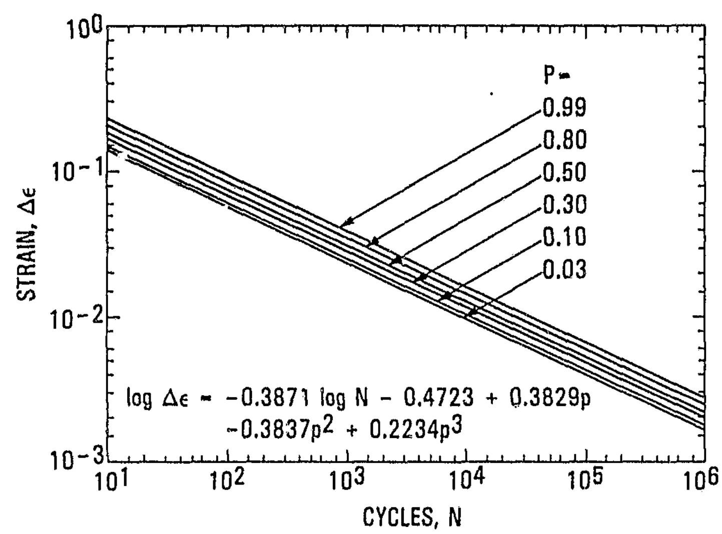

ORIGINAL PAGE IS
OF POOR QUALITY

Experimental Fatigue Testing Results

- **Comparison at same strain level for which 10% of copper interconnects fail in 20 years**

Material	Years to 10% failures
Aluminum	7
Copper	20
33 Cu/33 INV/33 Cu	106
12.5 Cu/75.0 INV/12.5 Cu	1030
16 Cu/68 SS/16 Cu	85

Array Degradation Analysis Algorithm

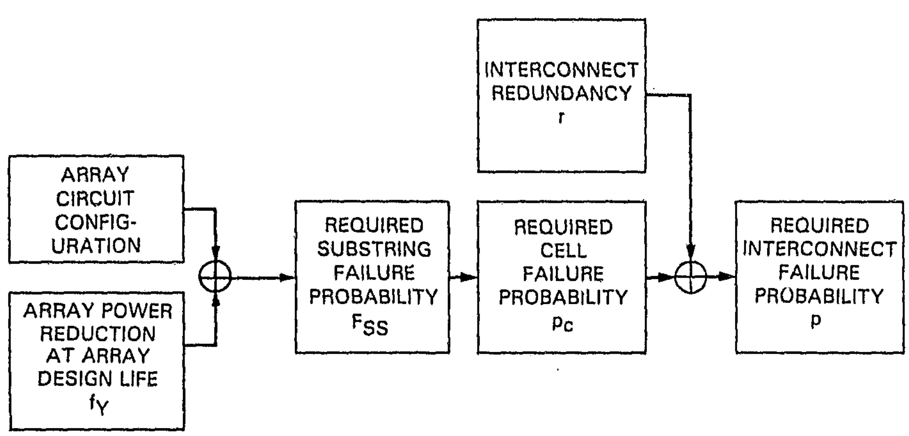

Example Design Parameters

Array Configuration:

- 8 parallel by 11 series cells per series block
- 57 series blocks per branch circuit
- One series block per diode
- V_{ARRAY} = 250 volts

Array Power Reduction at 20 Years

20-YEAR INTERCONNECT FAILURE PROBABILITY P_I	ARRAY POWER REDUCTION AT 20 YEARS f_Y					
	r = 1	2	3	4	5	6
0.005	0.125	0.0018	0	0	0	0
0.010	0.240	0.0059	0	0	0	0
0.050	0.71	0.05	0.0070	0.0004	0	0
0.100	0.96	0.24	0.029	0.0055	0.0007	0
0.150	1.00	0.31	0.054	0.019	0.005	0.0013
0.200	1.00	0.57	0.19	0.038	0.013	0.003
0.300	1.00	0.90	0.46	0.20	0.048	0.023
0.400	1.00	1.00	0.90	0.45	0.26	0.085
0.500	1.00	1.00	1.00	0.80	0.53	0.32

Effect of Material Properties on Life-Cycle Energy Costs

BALANCE OF PLANT COSTS

INITIAL PLANT COST

COST OF INTERCONNECTS

LIFE-CYCLE OPERATION AND MAINTENANCE COSTS

LIFE-CYCLE ENERGY COST

$$R = \frac{C_B + \dfrac{C_A + C_I + C_M}{\eta}}{I_0 \quad \epsilon_{LC}}$$

PLANT EFFICIENCY (RESISTIVITY AND SHADOWING)

ANNUAL SOLAR INSOLATION

RELATIVE ENERGY OUTPUT (FATIGUE)

Module Interconnect Assessment Algorithm

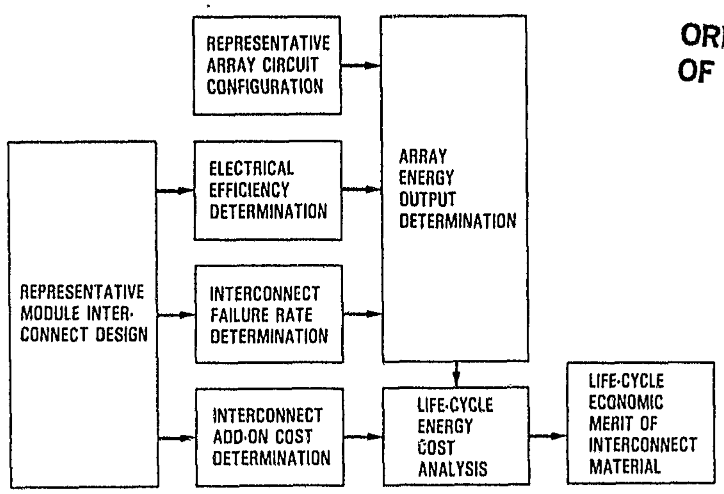

Life-Cycle Energy Fractions

20-Year Cumulative Interconnect Failure Probability	Life-Cycle Energy Fraction ϵ_{LC}					
P_I	r = 1	2	3	4	5	6
0.005	17.8	19.95	20	20	20	20
0.010	16.6	19.90	19.96	20	20	20
0.050	11.7	19.45	19.89	19.98	20	20
0.100	7.7	18.2	19.76	19.92	19.98	20
0.150	4.4	16.5	19.55	19.88	19.96	20
0.200	2.25	13.2	18.47	19.55	19.88	20
0.300	1.74	11.2	17.1	18.65	19.66	19.91
0.400	1.60	9.9	15.17	17.1	18.7	19.15
0.500	1.5	8.9	13.2	15.6	17.4	17.9

Parameters Used in Life-Cycle Cost Analysis

$C_B = 250$ \$/kW	$\eta_0(1 - \frac{LW}{A}) = 0.092$
$C_A = 113$ \$/m^2	$I = 2.0$ amps
$C_M = 0$	$P_0 = 1.2$ watts
$I_0 = 2000$ kWh/m^2/yr	$\ell = 3.0$ in.
	$W = 0.2$ in.

Fractional Increment in Life-Cycle Energy Cost Due to Interconnects vs Thickness, with Interconnect Redundancy as Parameter

ORIGINAL PAGE IS OF POOR QUALITY

Tinned, Annealed Aluminum

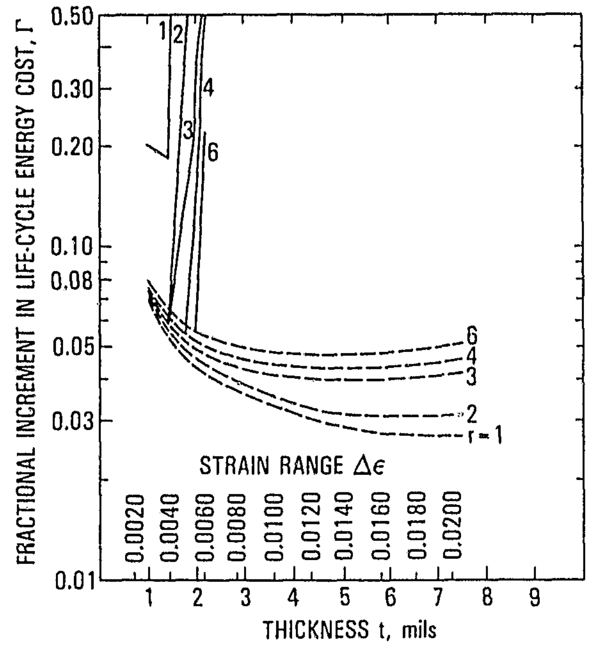

OFHC ¼-Hard Copper

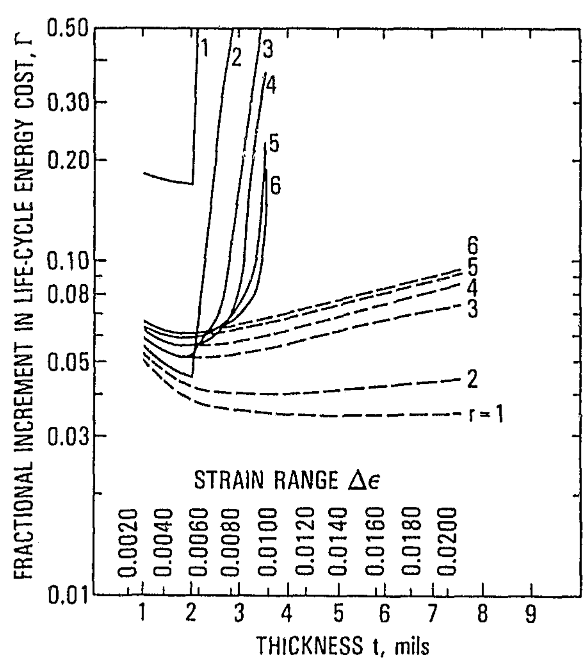

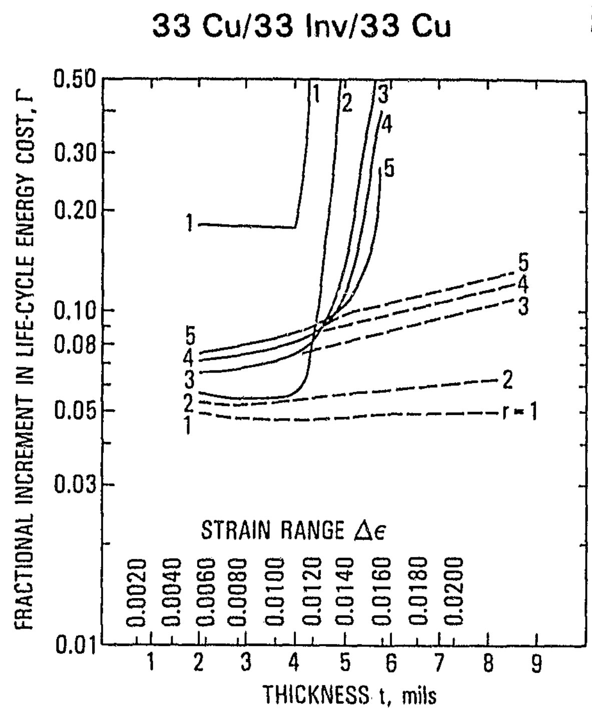
33 Cu/33 Inv/33 Cu
FRACTIONAL INCREMENT IN LIFE-CYCLE ENERGY COST, Γ
0.50
0.30
0.20
0.10
0.08
0.05
0.03
0.01
STRAIN RANGE Δε
0.0020
0.0040
0.0060
0.0080
0.0100
0.0120
0.0140
0.0160
0.0180
0.0200
r = 1
THICKNESS t, mils

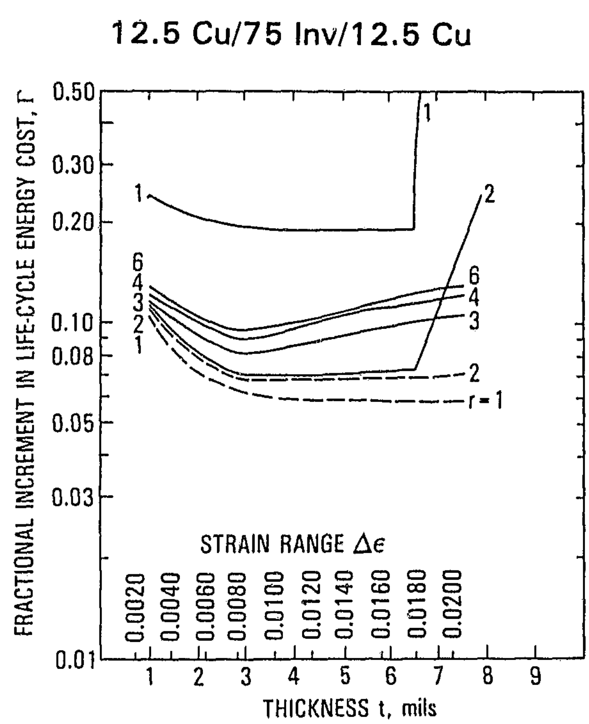
12.5 Cu/75 Inv/12.5 Cu
FRACTIONAL INCREMENT IN LIFE-CYCLE ENERGY COST, Γ
0.50
0.30
0.20
0.10
0.08
0.05
0.03
0.01
STRAIN RANGE Δε
0.0020
0.0040
0.0060
0.0080
0.0100
0.0120
0.0140
0.0160
0.0180
0.0200
r = 1
THICKNESS t, mils

16 Cu/68 SS/16 Cu

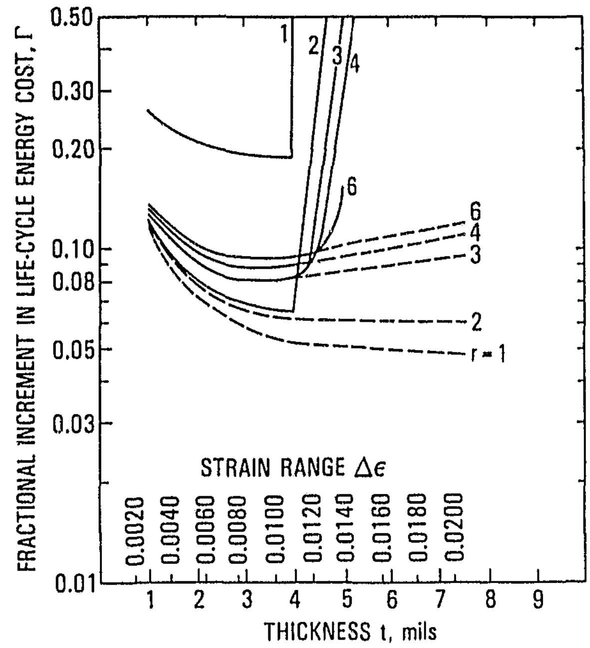

Percentage Life-Cycle Energy Cost Increment
Due to Doubly Redundant Interconnects

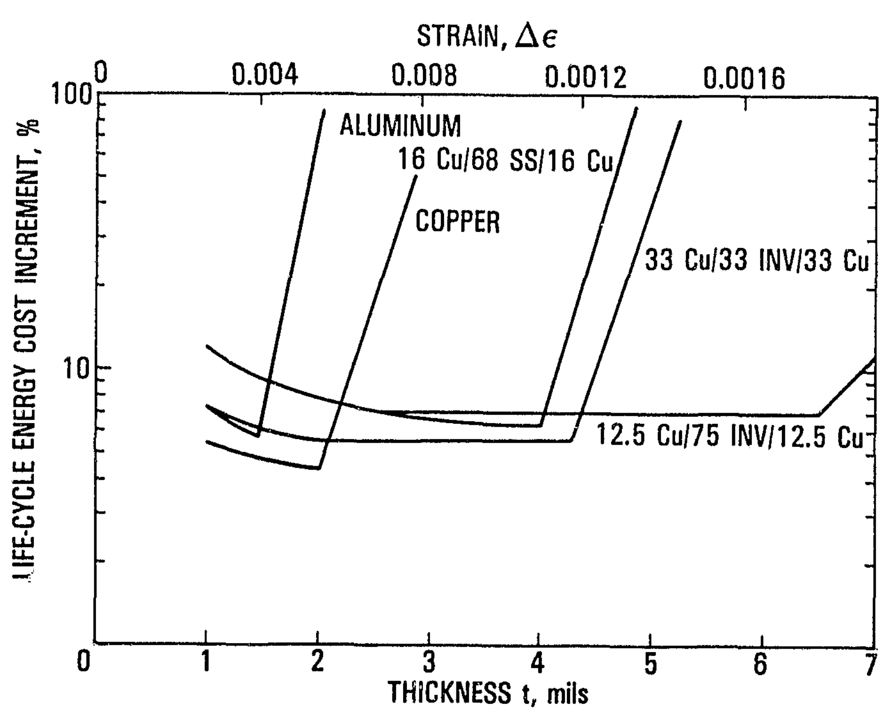

PHOTOVOLTAIC MODULE BYPASS DIODE ENCAPSULATION RESEARCH

GENERAL ELECTRIC CO.

Why Use a Bypass Diode?

- PROVIDES A PARALLEL PATH FOR CURRENT FLOW AROUND CIRCUIT ELEMENTS SO THAT
  - BRANCH CIRCUIT I_{SC} IS NOT LIMITED BY A REDUCTION IN THE I_{SC} CAPABILITY OF ELEMENTS WITHIN THE BYPASSED GROUP
  - REMOVAL OF A MODULE FROM AN ILLUMINATED ARRAY DOES NOT CREATE AN ARC
- LIMITS THE REVERSE VOLTAGE THAT CAN BE DEVELOPED ACROSS THE BYPASSED GROUP TO THE FORWARD VOLTAGE DROP OF THE CONDUCTING BYPASS DIODE

Module Interconnect Options

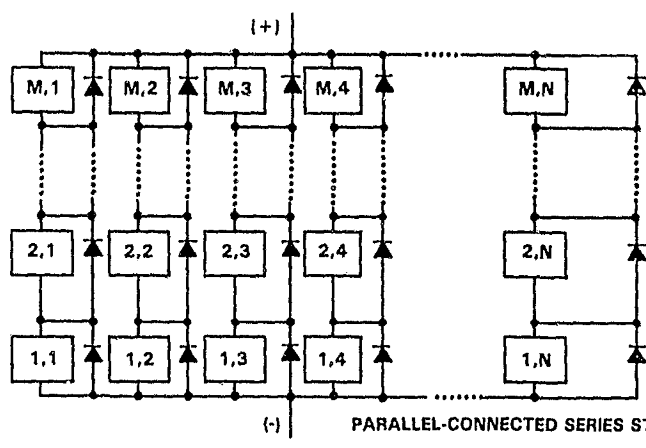

PARALLEL-CONNECTED SERIES STRINGS

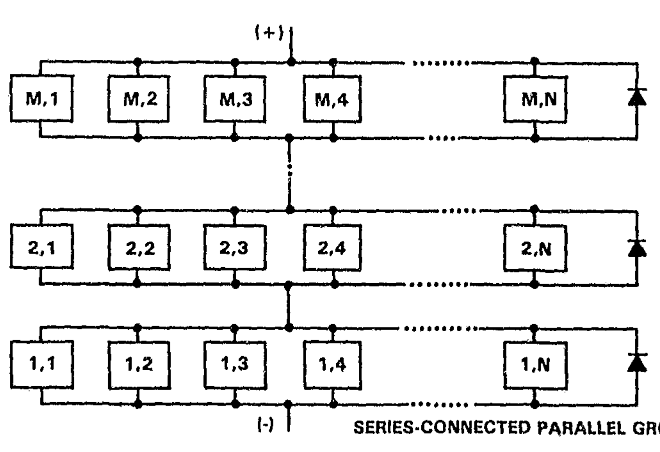

SERIES-CONNECTED PARALLEL GROUPS

Series-Connected Parallel Groups With Multiple Internal Bypass Diodes

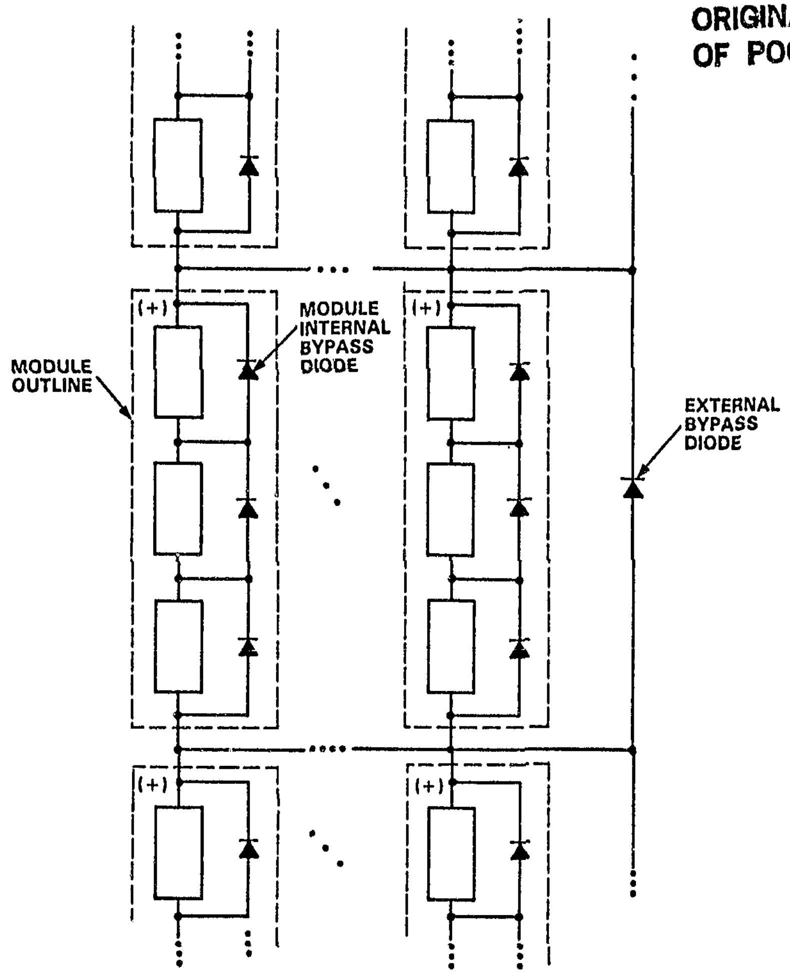

Series-Connected Parallel Groups With a Single Internal Bypass Diode

ORIGINAL PAGE IS OF POOR QUALITY

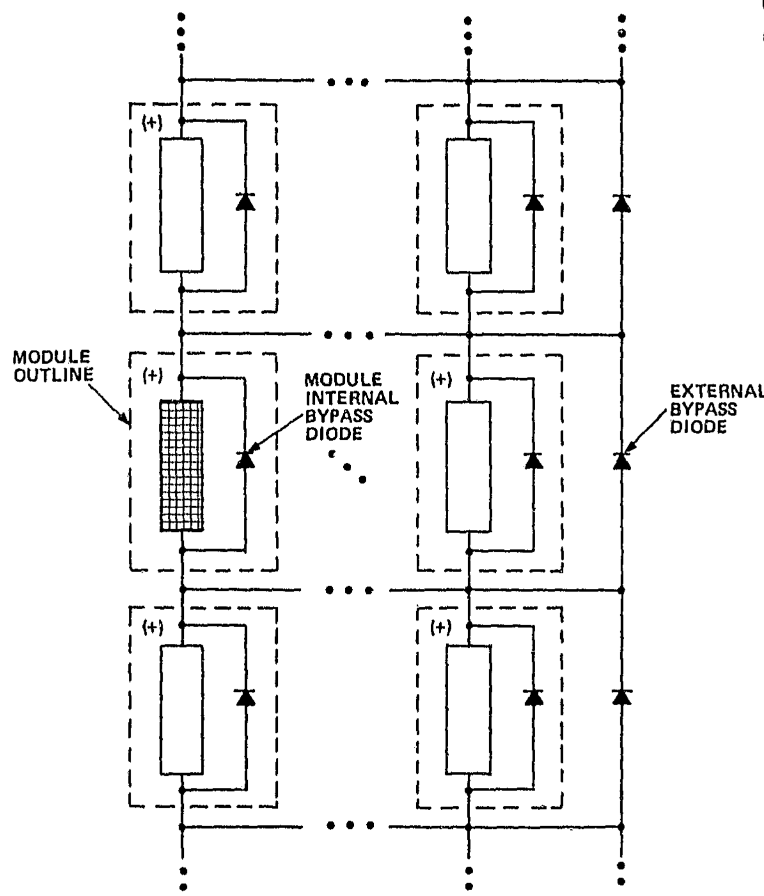

Potential Diode Chip Suppliers

MANUFACTURER	DIODE CHIP TYPE	FORWARD CURRENT RATING (AMPERES)
GENERAL INSTRUMENT	PN JUNCTION	8, 25
INTERNATIONAL RECTIFIER	SCHOTTKY	10, 30, 60
M/ACON (FORMERLY MICROWAVE ASSOCIATES)	SCHOTTKY	5, 15, 30, 60
MOTOROLA	SCHOTTKY	15, 30, 60, 75
SEMICON	PN JUNCTION SCHOTTKY	6, 12, 20, 40, 50 15, 30, 75
TRW	SCHOTTKY	30, 60
UNITRODE	SCHOTTKY	8, 30, 60
VARO	SCHOTTKY	15, 30, 60

ORIGINAL PAGE IS
OF POOR QUALITY

Diode Cell Packaging Configurations

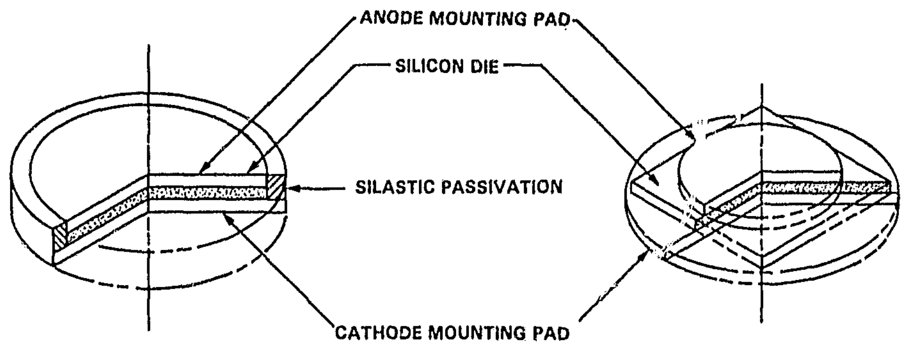

Diode Chip Thermal Resistance Measurements

MANUFACTURER	DIODE TYPE AND RATING	THERMAL RESISTANCE JUNCTION-TO-SINK (°C/WATT) STANDARD PACKAGED UNIT (TYP. PACK. TYPE)	PAD MOUNTED CHIP SOLDERED TO CATHODE PLATE
SEMICON	PN - 12A	2.5 (DO4)	0.97
SEMICON	PN - 20A	1.0 (DO21)	0.95
SEMICON	PN - 40A	1.0 (DO5)	0.61
SEMICON	PN - 50A	1.0 (DO5)	0.50
MOTOROLA	SCHOTTKY - 15A	2.5 (DO4)	0.78
MOTOROLA	SCHOTTKY - 30A	2.0 (DO4)	0.79
MOTOROLA	SCHOTTKY - 60A	1.0 (DO5)	0.79
MOTOROLA	SCHOTTKY - 75A	1.0 (DO5)	0.45
SEMICON	SCHOTTKY - 15A	2.5 (AXIAL)	0.84
SEMICON	SCHOTTKY - 30A	1.5 (DO4)	0.72
SEMICON	SCHOTTKY - 75A	0.65 (DO5)	

Diode/Heat Spreader Assembly

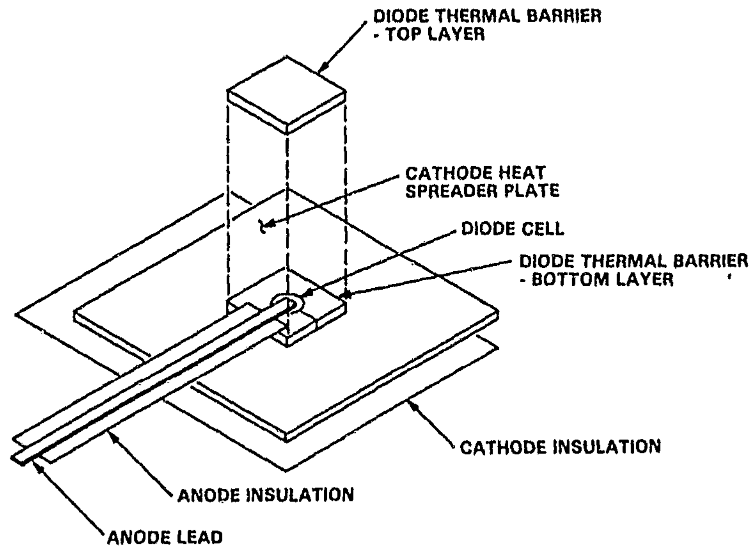

Encapsulation of Diode/Heat Spreader Assembly

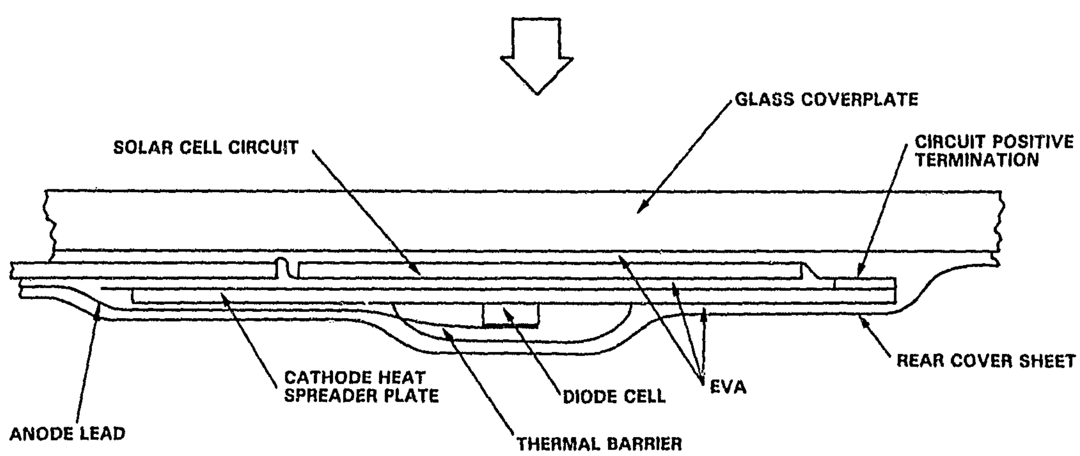

12-amp Experimental Module

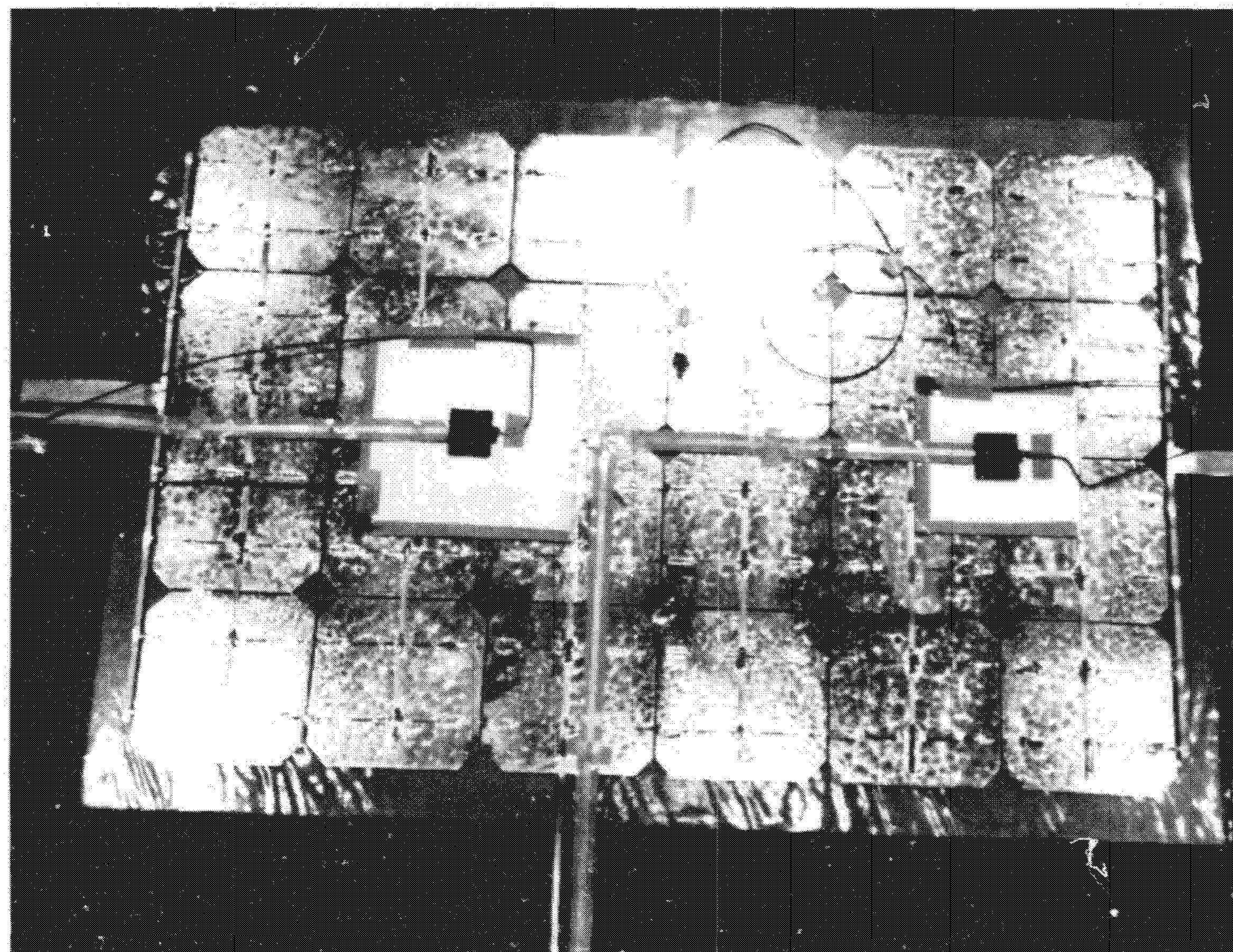

ORIGINAL PAGE IS
OF POOR QUALITY

Comparison of Analytical and Experimental Results

ORIGINAL PAGE IS OF POOR QUALITY

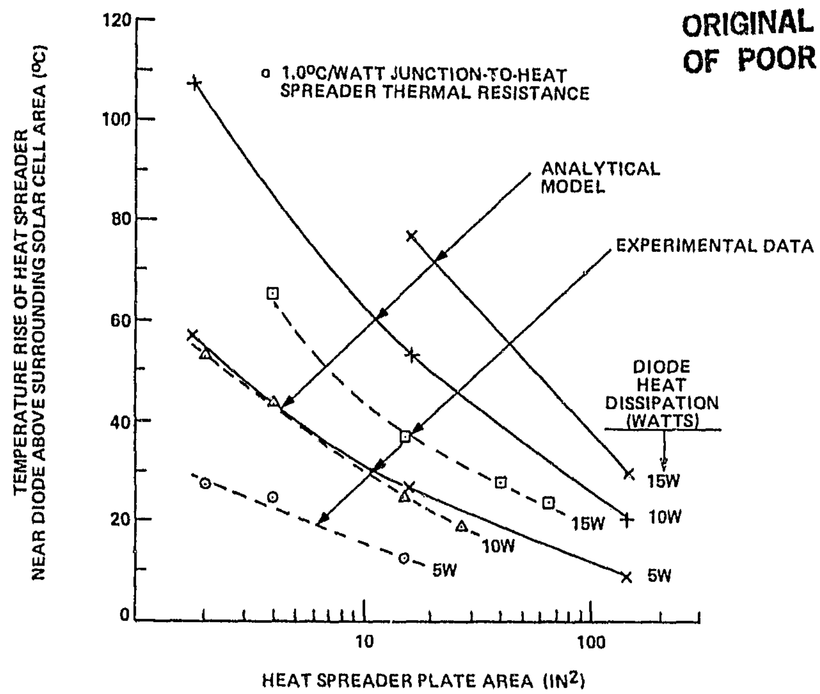

Recommended Encapsulated Diode Heat Spreader Plate Size

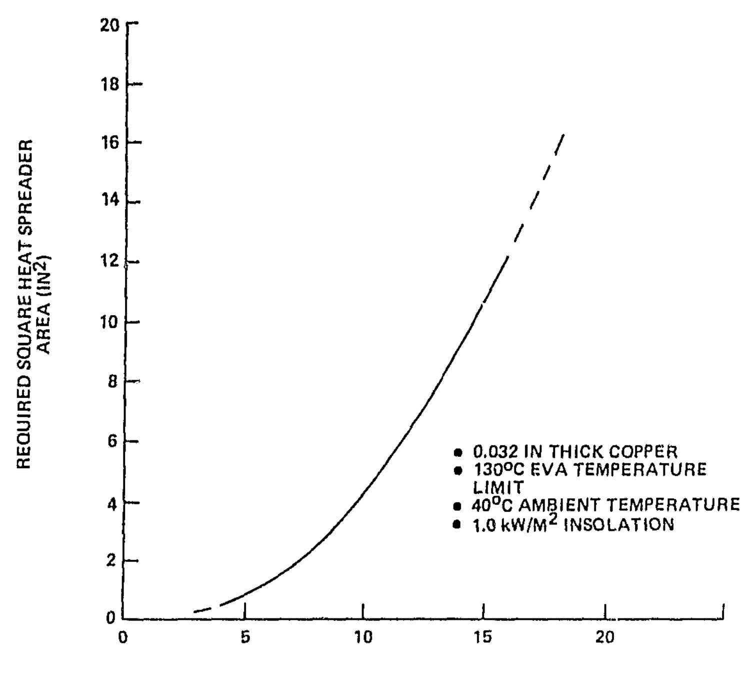

Conclusions

- THE THIN DIODE CELL/HEAT SPREADER ASSEMBLY CAN BE CONVENIENTLY LAMINATED ON THE REAR SIDE OF THE SOLAR CELL CIRCUIT

- THE MODULE ENCAPSULANT PROVIDES THE REQUIRED ELECTRICAL ISOLATION AND ENVIRONMENTAL PROTECTION

- PAD-MOUNTED PN JUNCTION DIODES OF THE TYPE SUPPLIED BY SEMICON AS A COMMERCIAL PRODUCT LINE ARE RECOMMENDED

ARRAY SUBSYSTEM SAFETY CONSIDERATIONS

UNDERWRITERS LABORATORIES, INC.

Allen Levins

Objective

- To research and develop PV safety system concepts as required to reduce hazards associated with PV systems to levels no greater than systems powered by contemporary electrical supplies

Key PV Safety Hazards

Shock hazards

- Parts that are electrically active
- Normally safe, exposed parts that have become energized
  - Insulation failure
  - Cumulative leakage

Fire hazards

- Internally generated
  - Overheated parts
  - Arcing
    - To ground
    - Within a circuit
- Externally generated

Applicable Codes and Standards

- National Electrical Code, proposed Article 690 – Solar Photovoltaic Systems
- Proposed Underwriters Laboratories, Inc, Standards for Safety
  - UL 1703 – Standard for Flat-plate Photovoltaic Modules and Panels
  - Draft Standard for Power-Conditioning Units for Use in Residential Photovoltaic Power Systems

Safety System Research Topics

- Research of individual safety features
  - Circuit grounding — direct, impedance, switched
  - Frame isolation
  - Ground-fault detection circuits
  - Ground sensors
  - Double insulation
  - Bypass diodes
  - Blocking diodes
  - Plug connectors with inaccessible contacts
  - Arc detection circuits
  - Low-voltage arrays (< 30V)
  - Redundant connections
- Integration of features into candidate safety systems

Candidate Safety System Concepts

CONCEPT	HAZARDS AND SOLUTIONS					
	DIRECT PERSONNEL SHOCK	INDIRECT PERSONNEL SHOCK	INSTALLATION SHOCK	GROUND-FAULT ARCS	IN-CIRCUIT ARCS	STATIC CHARGE BUILDUP AND VOLTAGE SURGE
I	Low voltage	Low voltage	Low voltage	GFCI	Low voltage	Solid circuit ground
II	High resistance to ground	Frame grounding	Plug connectors	High resistance to ground	Bypass diodes	High resistance to ground and surge arrestors
III	Switched-in high resistance and DC disconnect	Frame grounding	Plug connectors	Switched-in high resistance and DC disconnect	Bypass diodes	Solid circuit ground and surge arrestors

ORIGINAL PAGE IS
OF POOR QUALITY

Center-Grounded, Transformer-Isolated Strategy

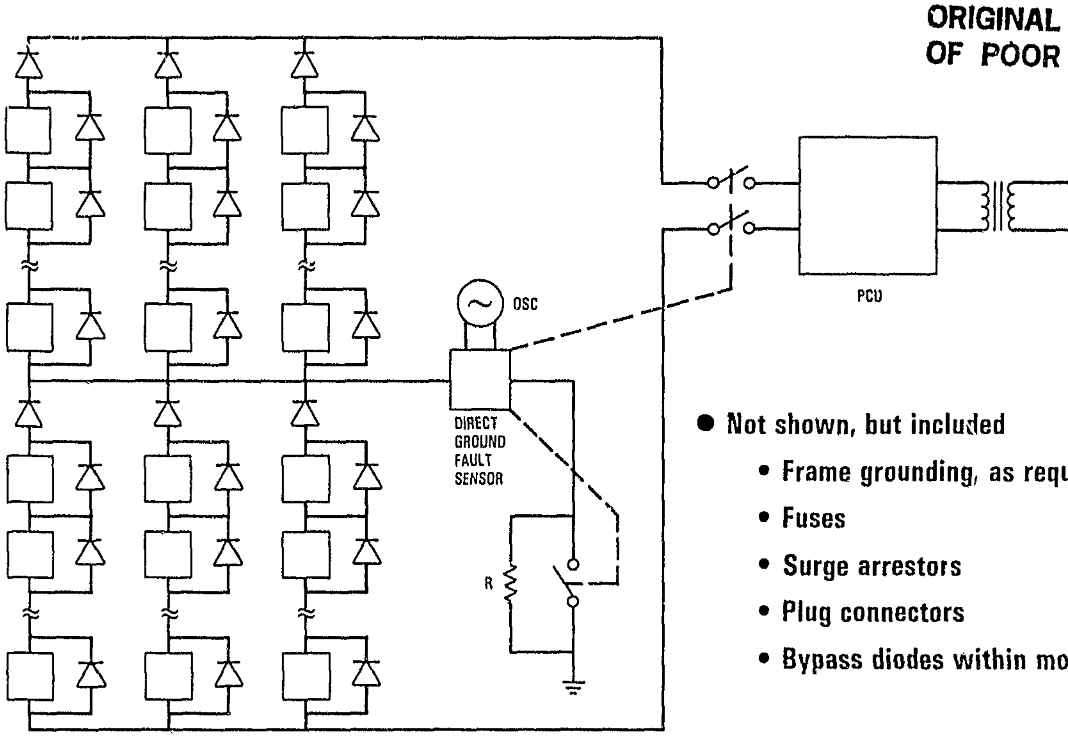

- Not shown, but included
  - Frame grounding, as required
  - Fuses
  - Surge arrestors
  - Plug connectors
  - Bypass diodes within modules

- Center ground restricts voltage between any point of the array and ground to one-half the system voltage
- Direct ground-fault sensor removes load and limits current flow upon ground-fault condition
  - Use of differential ground-fault sensors requires two sensors for each half source circuit – permits partial system operation
  - Oscillator circuit enables operation upon grounding of *grounded* conductor other than through the ground-fault sensor
- Blocking diodes prevent reverse current flow – NEC requires fuses in series with diodes
- Hierarchy of bypass diodes – permits *safe* module removal

Virtual Ground, Transformerless Strategy

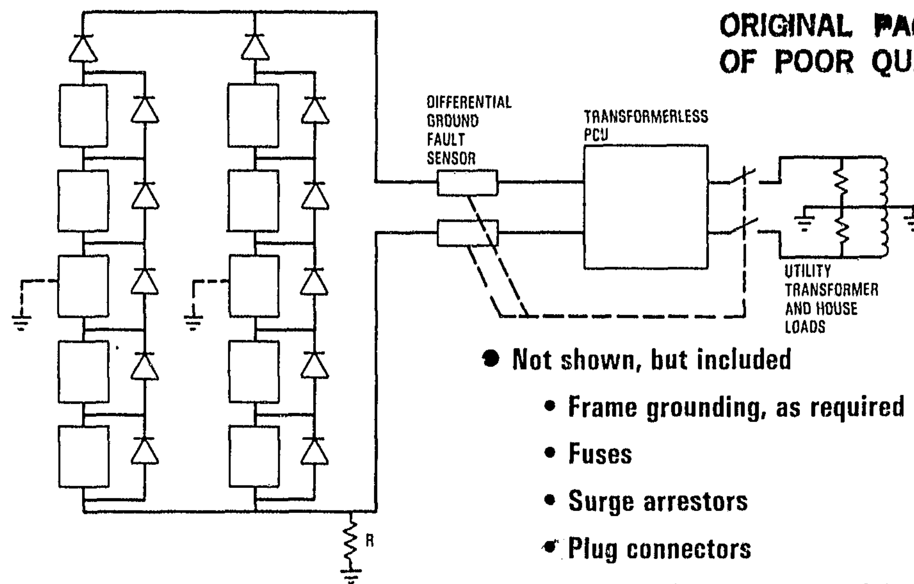

- Not shown, but included
  - Frame grounding, as required
  - Fuses
  - Surge arrestors
  - Plug connectors
  - Bypass diodes within modules

- Virtual ground/center ground restricts voltage between any point of the array and ground to one-half the system voltage
  - Electrically at earth potential, but with no physical connection to earth
  - Should be inaccessible – odd number of modules
- Differential ground-fault sensors removes load and limits current flow upon ground-fault condition
  - Direct ground-fault sensor is not compatible with transformerless, utility-interactive power-conditioning unit
  - Separate sensors for each source circuit permit partial system operation
- Blocking diodes prevent reverse current flow – NEC will require fuses in series with diodes
- Hierarchy of bypass diodes – permits *safe* module removal

Conclusions

- Several candidate safety system concepts that reduce PV safety hazards to acceptable levels have been identified
- Codes and standards addressing safety are nearing reality
- Detailed circuits and safety devices remain to be developed and tested

RESIDENTIAL ARRAY WIRING REQUIREMENTS

UNDERWRITERS LABORATORIES, INC.

T. Lundveit

Objective

To research and develop photovoltaic array wiring concepts for residential arrays

- **Identify wiring and termination requirements**
- **Assess ability of existing wiring systems to satisfy the requirements**
- **Identify candidate wiring system concepts and termination methods**

Proposed NEC Requirement Applicable to PV Wiring Systems

SECTION 690-31 WIRING METHODS PERMITTED

ALL RACEWAY AND CABLE WIRING METHODS INCLUDED IN THIS CODE AND SUCH OTHER WIRING SYSTEMS SPECIFICALLY INTENDED AND APPROVED FOR USE ON PHOTOVOLTAIC ARRAYS SHALL BE PERMITTED WITH APPROVED FITTINGS AND WITH FITTINGS APPROVED SPECIFICALLY FOR PHOTOVOLTAIC ARRAYS.

TO QUALIFY THESE SYSTEMS FOR PV USE, THE FOLLOWING PERFORMANCE SPECIFICATIONS NEED TO BE MET

ORIGINAL PAGE IS
OF POOR QUALITY

Proposed Performance Specification for Evaluation of Solar Photovoltaic Cable

1. Resistance To Mechanical Damage
2. Flexibility
3. Physical Properties of Compounds
4. Tension and Elongation
5. Flammability
6. Sunlight Resistance
7. Dielectric Withstand
8. Drip Test
9. Ease of Stripping
10. Resistance to Water Absorption
11. Direct Burial (optional)

Proposed Performance Specification for Plug and Receptacle Connectors

1. Temperature
2. Strain Relief
3. Dielectric Withstand
4. Accelerated Aging of Gaskets and Seals
5. Impact
6. Exposure to Water Spray
7. Sunlight Resistance
8. Temperature Cycling
9. Water absorption

ORIGINAL PAGE IS OF POOR QUALITY

Wiring Systems Acceptable for Use in Solar PV Array

	Wiring Method	PV Panel Mounting Method: Integral	PV Panel Mounting Method: Direct, Stand-off, Rack
1.	Type MI Cable	A	A
2.	Type AC Cable	A, *	A, *
3.	Type MC Cable	A, *	A, *
4.	Type NM, NMC Cable	A	NA
5.	Types SE, USE Cable	A	A
6.	Type UF Cable	A*	A*
7.	Intermediate Metal Conduit	A	A
8.	Rigid Metal Conduit	A	A
9.	Rigid Nonmetallic Conduit	A	A
10.	Electrical Metallic Tubing	A	A

Code:

A - Applicable
NA - Not Applicable
* - Use Restrictions Per NEC

Installation Methods for PV Wiring Systems

NEC Article 336

Cable Support

Protection From Physical Damage

Through Roof Rafters, Floor Joists

Routing In Accessible Attics

Routing In Unfinished Basements

Wiring Termination Methods Applicable to PV Arrays

1. SPLICES
   - A. CRIMP CONNECTORS
   - B. PRESSURE CABLE CONNECTORS
   - C. BRAZING AND WELDING
   - D. SOLDERING

2. TERMINALS
   - A. WIRE BINDING SCREWS
   - B. STUD-AND-NUT TERMINALS
   - C. PRESSURE CABLE CONNECTORS

3. PLUG AND RECEPTACLE CONNECTORS
   - A. POLARIZATION AND NONINTERCHANGEABILITY
   - B. LIVE PARTS GUARDED
   - C. LATCHING OR LOCKING TYPE
   - D. GROUNDING CONTACT-FIRST MAKE, LAST BREAK
   - E. INTERRUPTING CURRENT RATING

PV Wiring Systems That Do Not Comply With NEC

1. TYPE TC CABLE
   - A. RESTRICTED FOR USE IN CABLE TRAYS AND RACEWAYS
   - B. NOT PERMITTED TO BE INSTALLED AS OPEN CABLE AND SUPPORTED BY BRACKETS OR CLEATS

2. TYPE FCC CABLE
   - A. INTENDED FOR USE UNDER CARPET SQUARES
   - B. GROUNDED METAL TOP SHIELD REQUIRED
   - C. NOT PERMITTED IN WET LOCATIONS
   - D. HARD SMOOTH MOUNTING SURFACE REQUIRED

3. FLEXIBLE CORD
   - A. NOT PERMITTED AS A SUBSTITUTE FOR FIXED WIRING OF A STRUCTURE

Presently Available Cables: Qualification as Solar PV Cable

1. TYPE TC CABLE

   TESTS PER PROPOSED PERFORMANCE SPECIFICATION FOR PV CABLE CONDUCTED ON LISTED TYPE TC CABLE EXCEPT FOR:

   A. RESISTANCE TO MECHANICAL DAMAGE
   B. DRIP TEST
   C. RESISTANCE TO WATER ABSORPTION

2. TYPE FCC CABLE

   SPECIAL INVESTIGATION REQUIRED

Summary

- Proposed NEC Article 690 permits wiring methods and systems that are:
  - Currently accepted within allowed conditions
  - Intended and approved specifically for PV systems
- Wiring and termination requirements for PV arrays have been identified
- Subject to passing additional tests, several existing wiring systems appear to be likely candidates for PV systems

EXPERIENCE WITH THE USE OF THE AIR MASS 1.5 FILTER WITH THE LAPSS

JET PROPULSION LABORATORY

R. Mueller

ORIGINAL PAGE IS OF POOR QUALITY

Spectral Irradiance

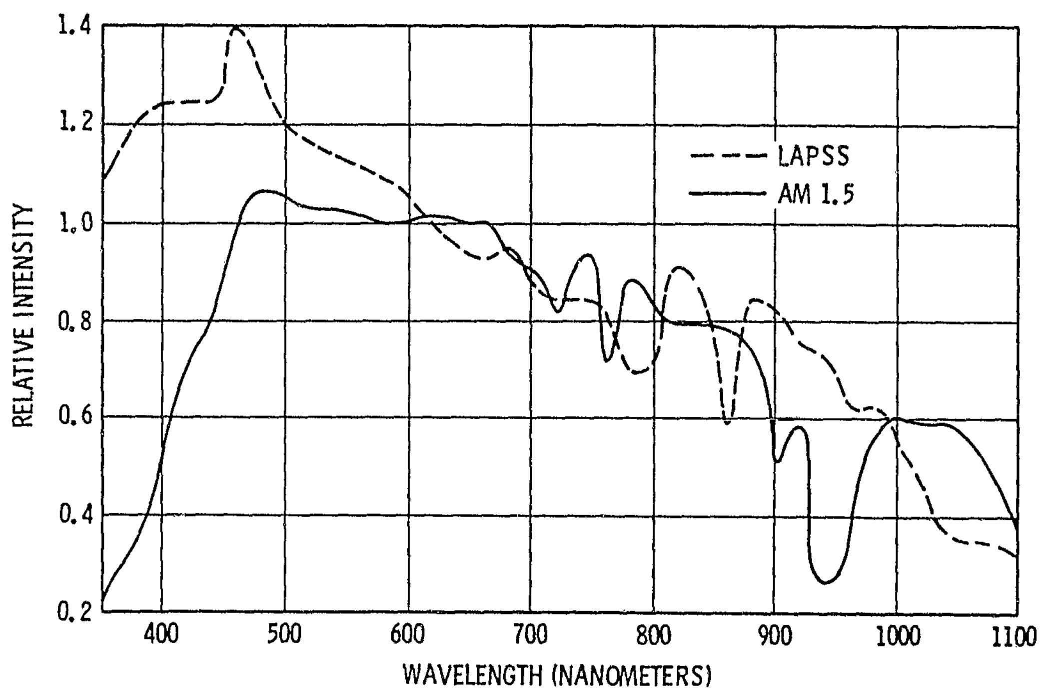

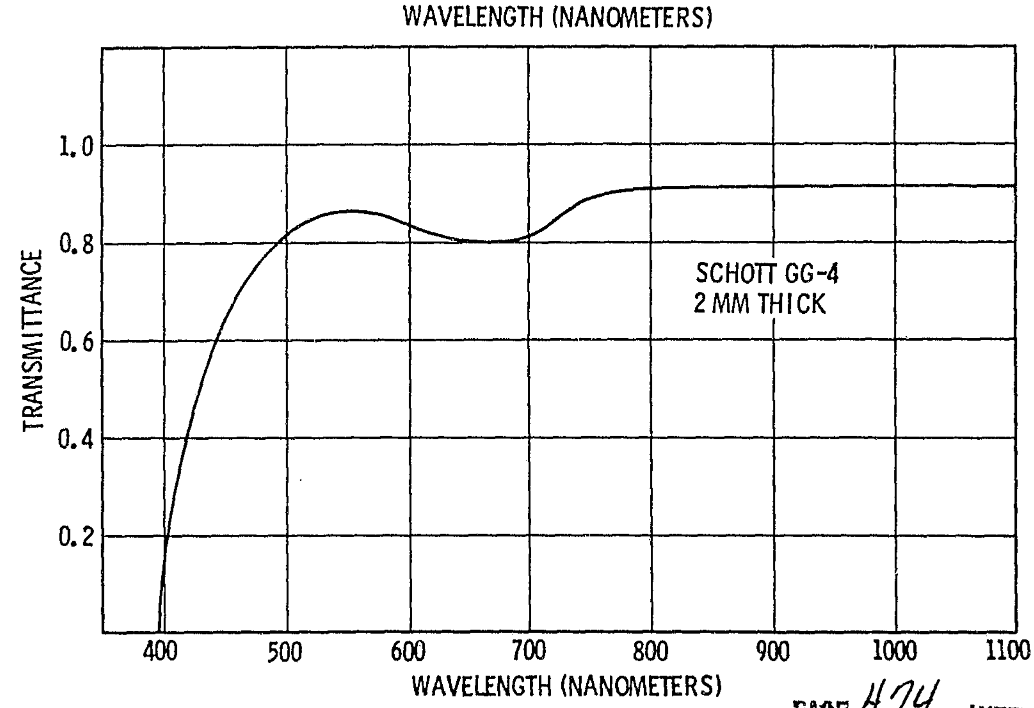

PAGE 474 INTENTIONALLY BLANK

PRECEDING PAGE BLANK NOT FILMED

LAPSS Illuminator Cross-Sectional View

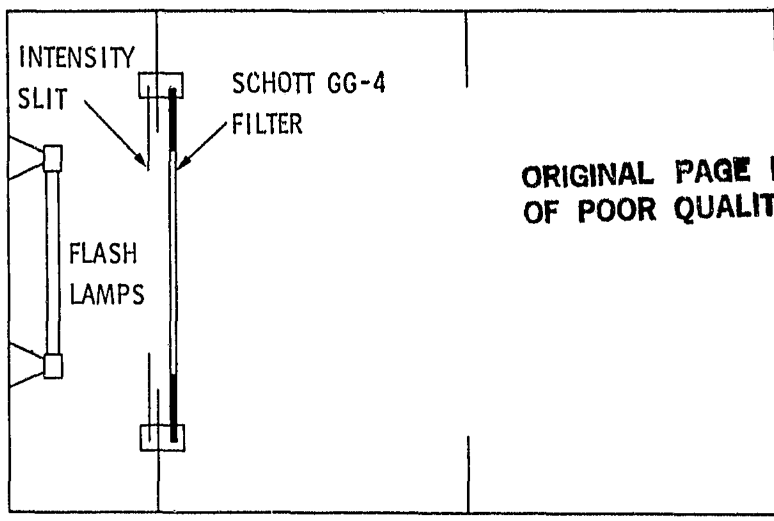

Air Mass 1.5 Filter Holder and Intensity Slit for LAPSS

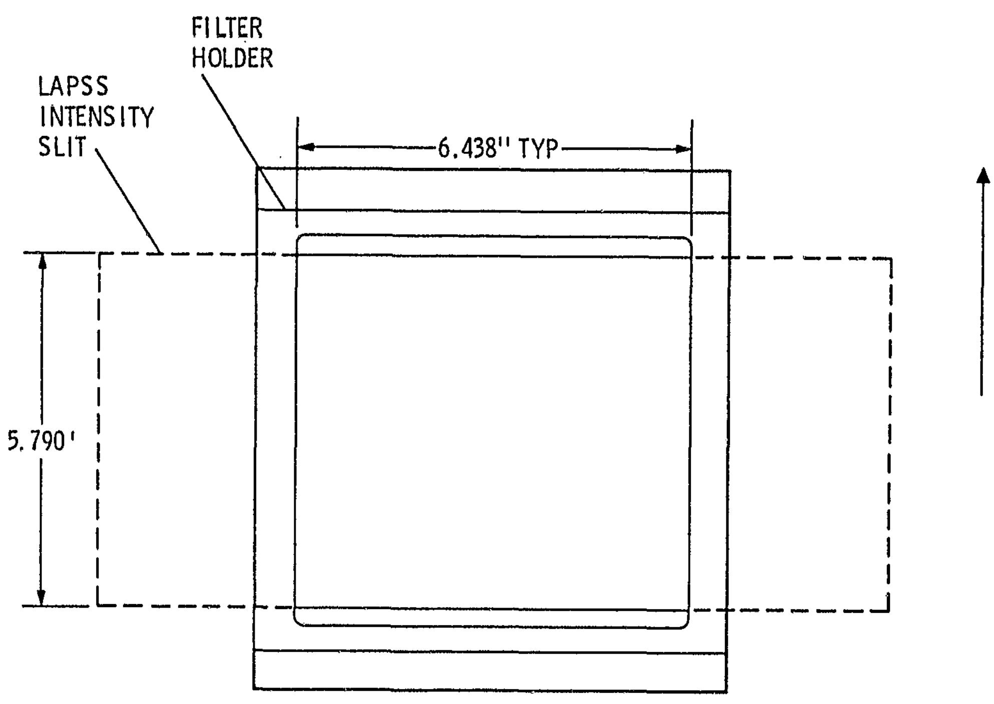

Spectral Irradiance

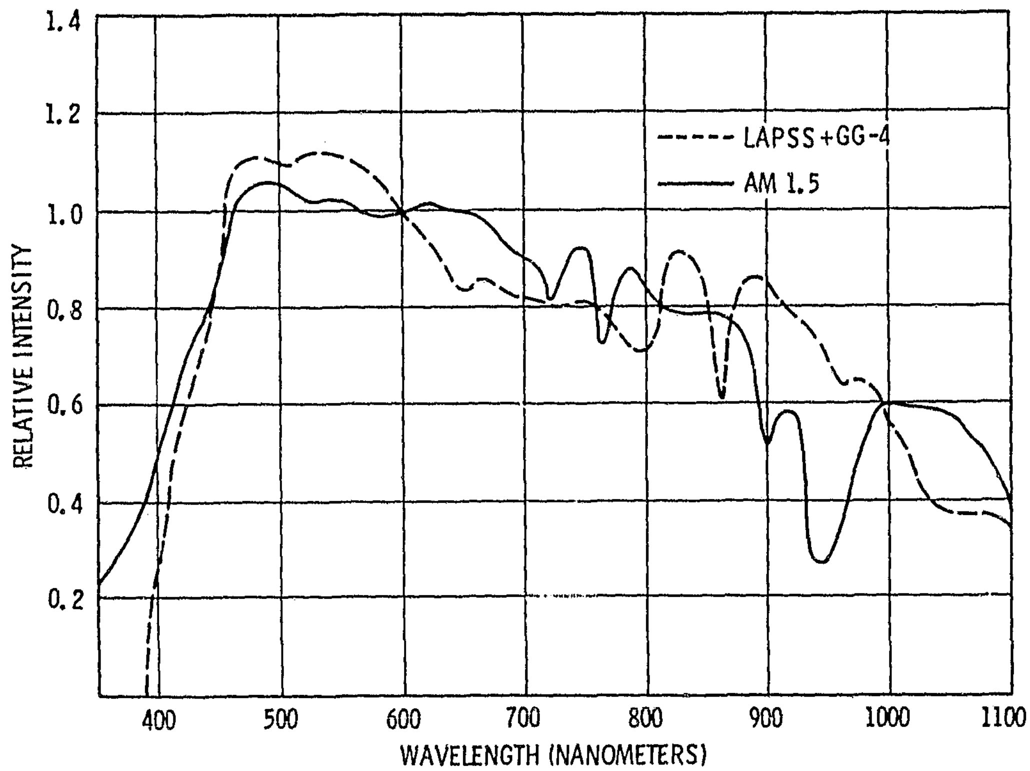

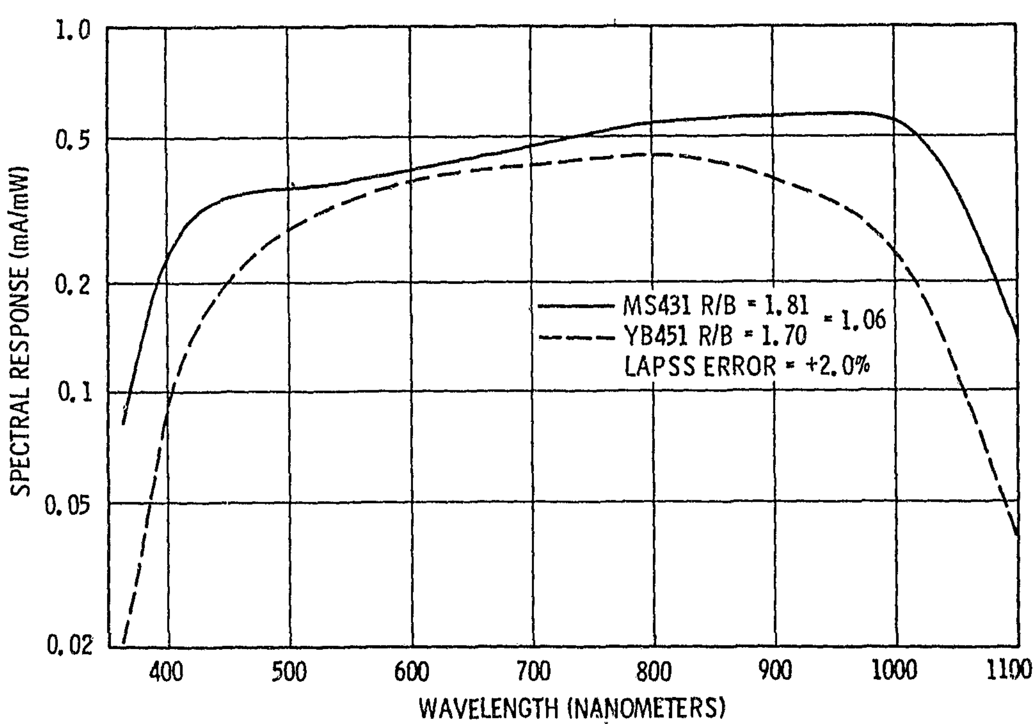

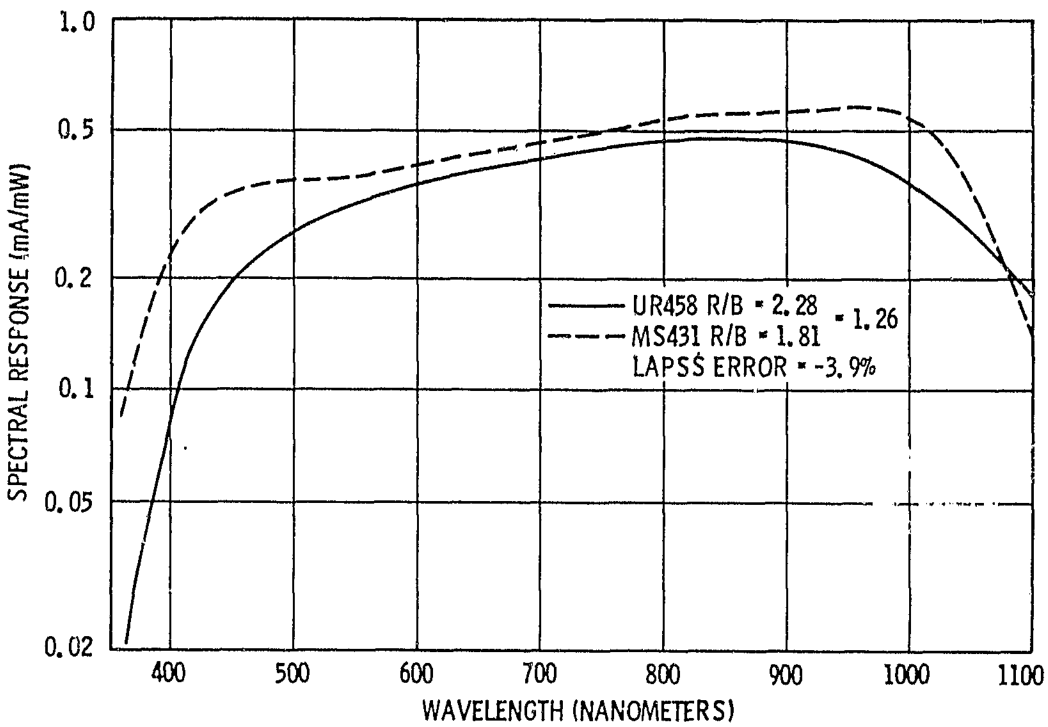
1.0
0.5
0.2
0.1
0.05
0.02
SPECTRAL RESPONSE (mA/mW)
400
500
600
700
800
900
1000
1100
WAVELENGTH (NANOMETERS)
UR458 R/B = 2.28
MS431 R/B = 1.81
= 1.26
LAPSS ERROR = -3.9%

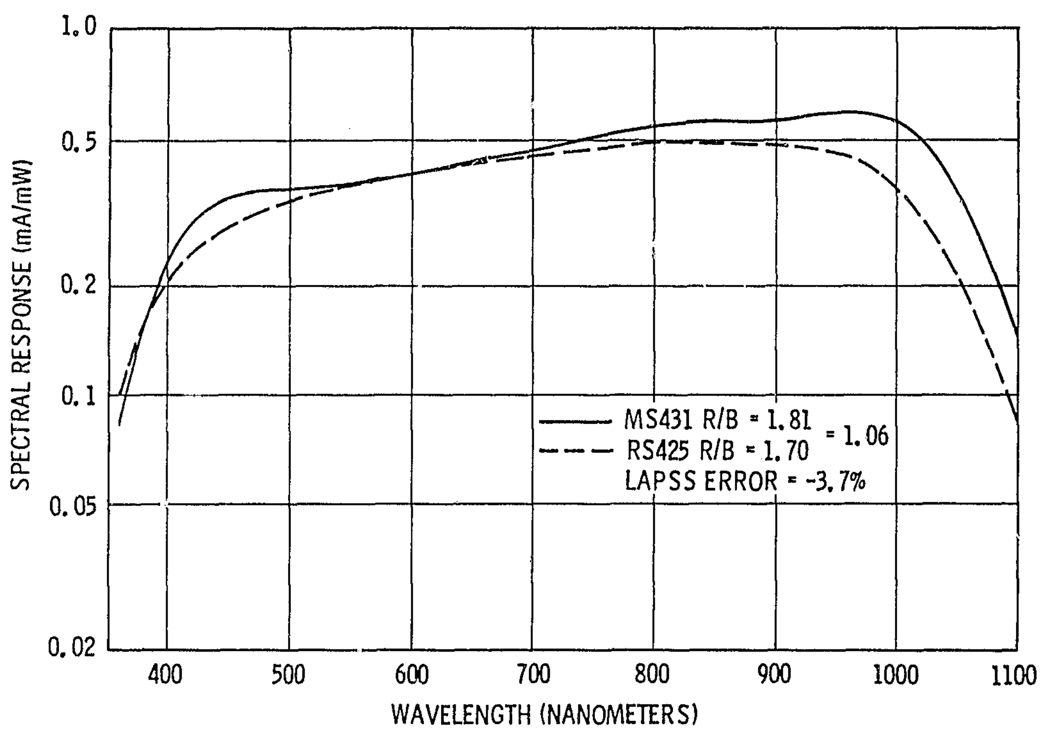
1.0
0.5
0.2
0.1
0.05
0.02
SPECTRAL RESPONSE (mA/mW)
400
500
600
700
800
900
1000
1100
WAVELENGTH (NANOMETERS)
MS431 R/B = 1.81
RS425 R/B = 1.70
= 1.06
LAPSS ERROR = -3.7%

ORIGINAL PAGE IS OF POOR QUALITY

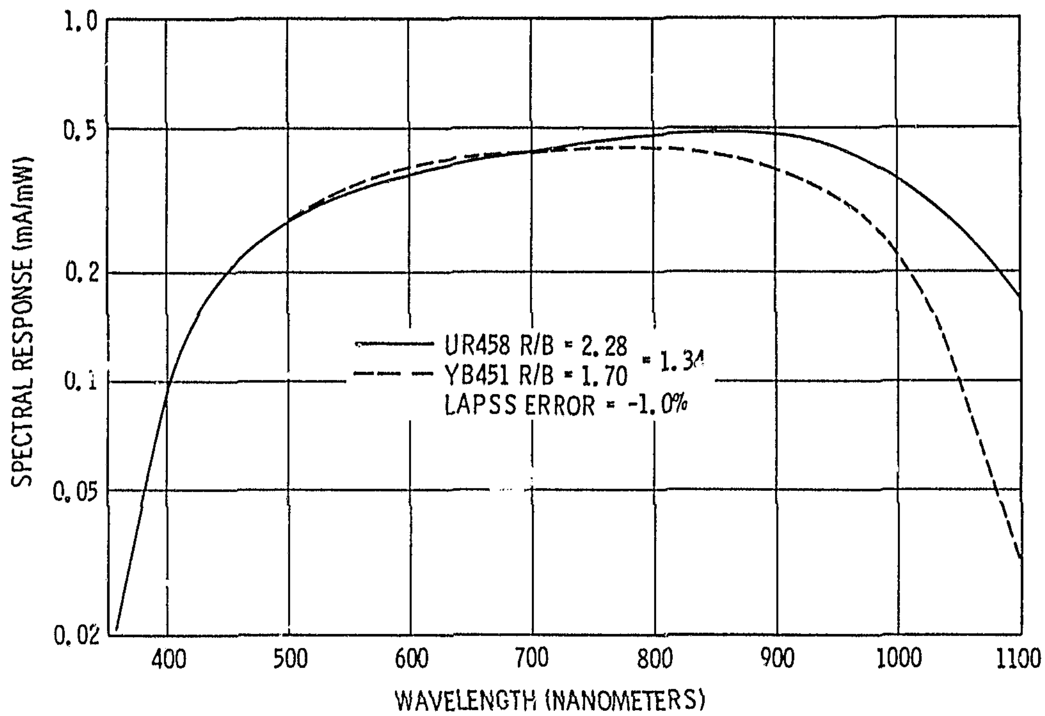

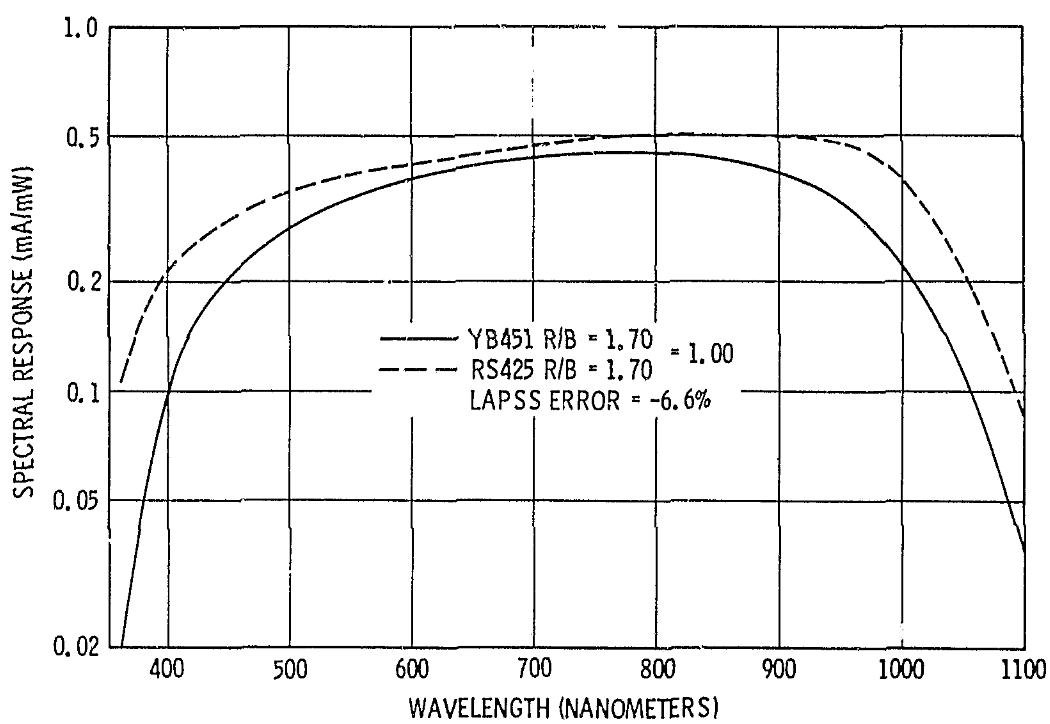

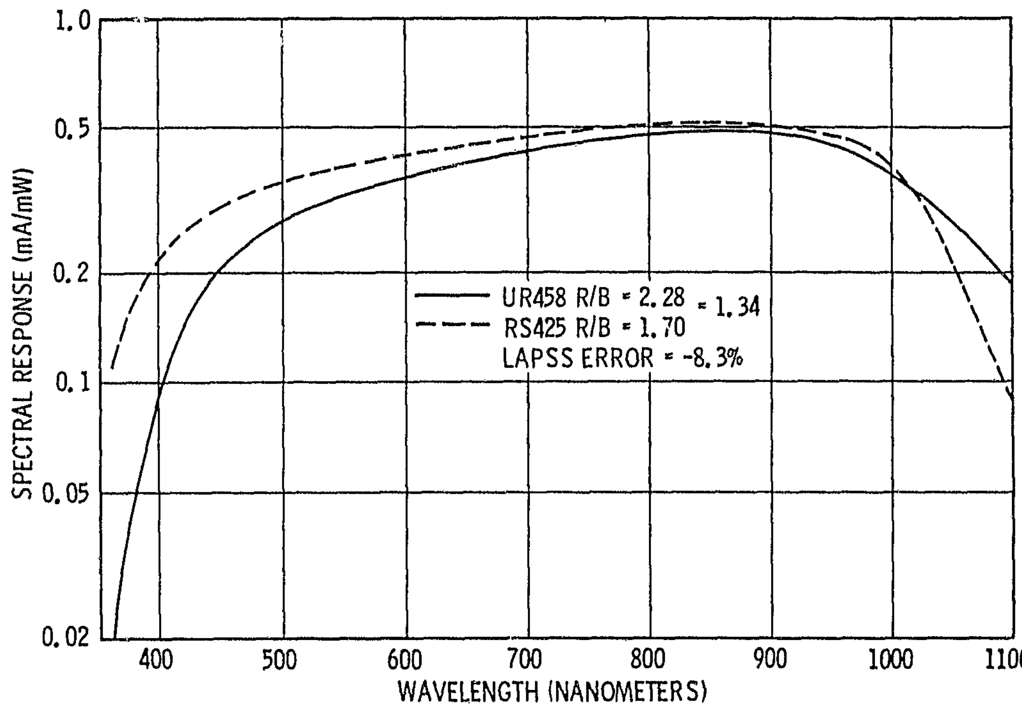

Measured Errors Using LAPSS

	PAIR	R/B	$\frac{(R/B)_C}{(R/B)_R}$		% ERROR NO FILTER	% ERROR FILTER
C	MS 431	1.81	1.06		+2.0	-0.1
R	YB 451	1.70				
C	UR 458	2.28	1.26		-3.9	-0.1
R	MS 431	1.81				
C	MS 431	1.81	1.06		-3.7	+0.2
R	RS 425	1.70				
C	UR 458	2.28	1.34		-1.0	+1.0
R	YB 451	1.70				
C	YB 451	1.70	1.00		-6.6	0.0
R	RS 425	1.70				
C	UR 458	2.28	1.34		-8.3	+0.9
R	RS 425	1.70				
ERROR EXPECTATION VALUE					4.3	0.4

ORIGINAL PAGE IS
OF POOR QUALITY

Red and Blue Filters for LAPSS

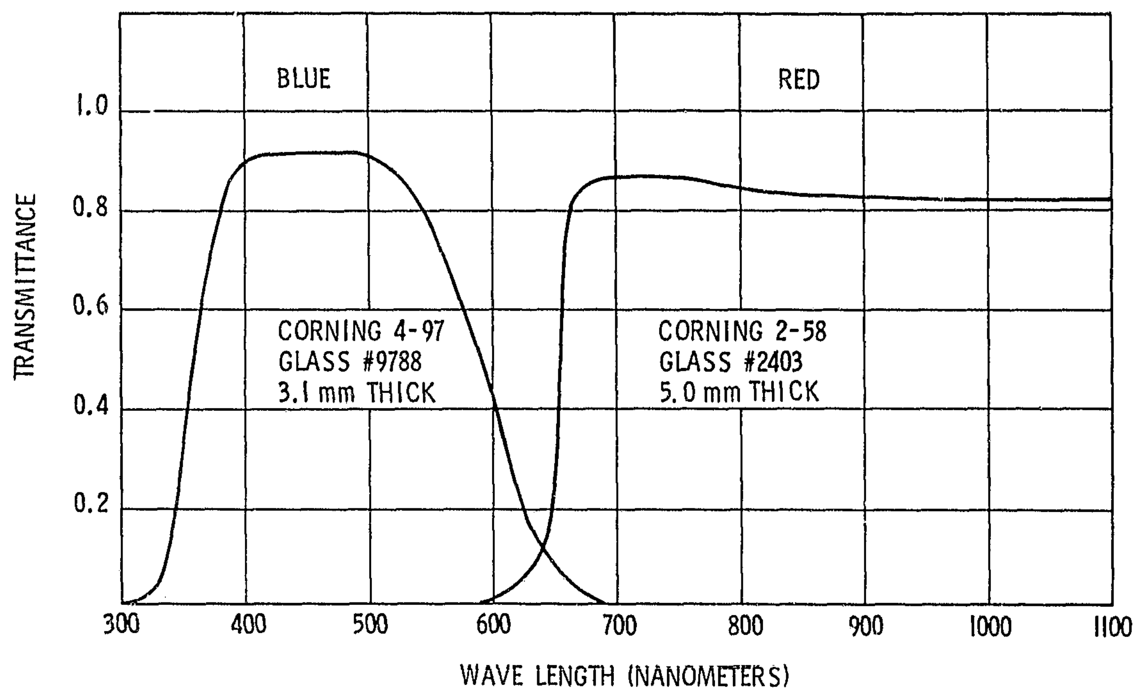

Temporal Stability of Matched Schott GG-4 Filters

TEST: MEASURE THE SHORT CIRCUIT CURRENT (I_{SC}) OF 8 DIFFERENT PV DEVICES USING EACH OF 3 MATCHED FILTERS AND A CONTROL FILTER

HISTORY: FILTER #1 HAS BEEN USED DURING 500 LAMP FLASHES OVER A 3 MONTH PERIOD

FILTER #2 HAS BEEN USED DURING 1500 LAMP FLASHES OVER A 2 MONTH PERIOD

FILTER #3 AND #4 HAVE BEEN USED DURING 20 LAMP FLASHES IN ONE DAY, FOR THIS TEST ONLY

RESULTS: THE AVERAGE I_{SC} OF THE DEVICES TESTED IS < .1% DIFFERENT WHEN USING ANY OF THE FILTERS IN COMPARISON TO THE CONTROL FILTER, #4

Summary

1. THE FILTER SYSTEM IS LOW COST
2. TEMPORAL STABILITY EXCELLENT
3. DOES NOT REQUIRE MATCHED REFERENCE CELL
4. EXPENSIVE SPECTRAL RESPONSE NOT REQUIRED
5. RED-BLUE RATIO NOT REQUIRED
6. MANY NEW REFERENCE CELLS NOT REQUIRED
7. ONLY LIMITED SUN CALIBRATION OF THE SAME REFERENCES IS REQUIRED
8. LOW COST AND TIMELY METHOD OF PROVIDING SECONDARY REFERENCE CELLS
9. POSSIBLY LOWER ERROR THAN SUN CALIBRATED REF CELL USED WITH UNFILTERED LAPSS

EXPERIENCES WITH THE PORTABLE ARRAY DATA LOGGER

JET PROPULSION LABORATORY

R.W. Weaver

- LOGGER WAS DEVELOPED TO ACQUIRE DATA FOR ARRAY PERFORMANCE EVALUATION
- OPERATIONAL IN JULY 1982
- THREE NON-JPL SITES HAVE BEEN TESTED
- FIVE ARRAYS AT JPL TEST SITE ARE TESTED PERIODICALLY

Logger Description

- RANGES:

VOLTAGE	50, 100, 200, 400
CURRENT	5, 10, 20, 40
MAX POWER	16 kW

- ACQUIRES I-V DATA VIA CAPACITOR CHARGING
- DISPLAYS ALL DATA ON COMMAND
- STORES DATA ON EPROM ON COMMAND
- CAN BE PROGRAMMED (BASIC) TO REDUCE AND DISPLAY DATA IN DESIRED FORM

Arrays Tested

JPL SITE:

ARRAY	ISC (AMPS)	VOC (VOLTS)
SOLAREX	4.5	385
ARCO SOLAR	2.4	350
ASEC	5.5	220
MOTOROLA	2.5	360
PHOTOWATT	7.6	68
G E	8.0	200

NON-JPL:

ARRAY	ISC (AMPS)	VOC (VOLTS)
MISSISSIPPI COUNTY COMMUNITY COLLEGE (45 STRINGS)	10-12	400
SDSU - RESIDENTIAL		
5 STRINGS OF	2.2	250
SYSTEM	11.0	250
SDG&E - RESIDENTIAL		
4 STRINGS OF	2.2	250
SYSTEM	8.8	250

Test Results

RESIDENTIALS:
- NO ABNORMALITIES IN THE CURVES BUT PEAK POWER WAS 10-15% BELOW NAME PLATE AT ≈90 mw/cm^2

MCCC:
- FOUND STRINGS WITH BAD CELLS
- THESE WERE CONFIRMED USING IR CAMERA

JPL ARRAYS:
- NO ABNORMALITIES BUT PEAK POWER DOWN 10-15%
- SPECIAL SHADOWING TESTS CONDUCTED

Sample Data: JPL Motorola Array (20 Modules)

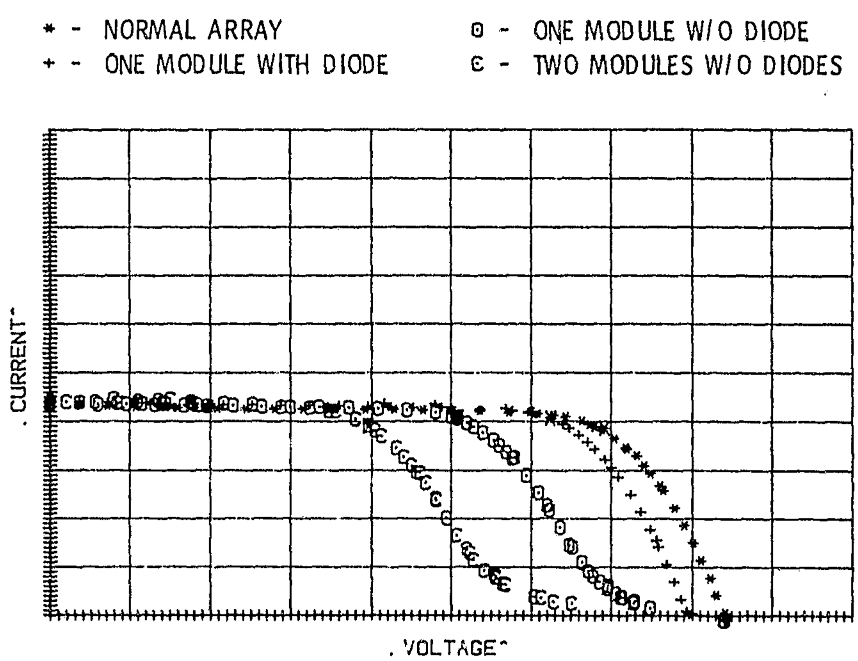

Sample Data: JPL GE Residential Array: 20 Rows of 4 Paralleled Hex Modules

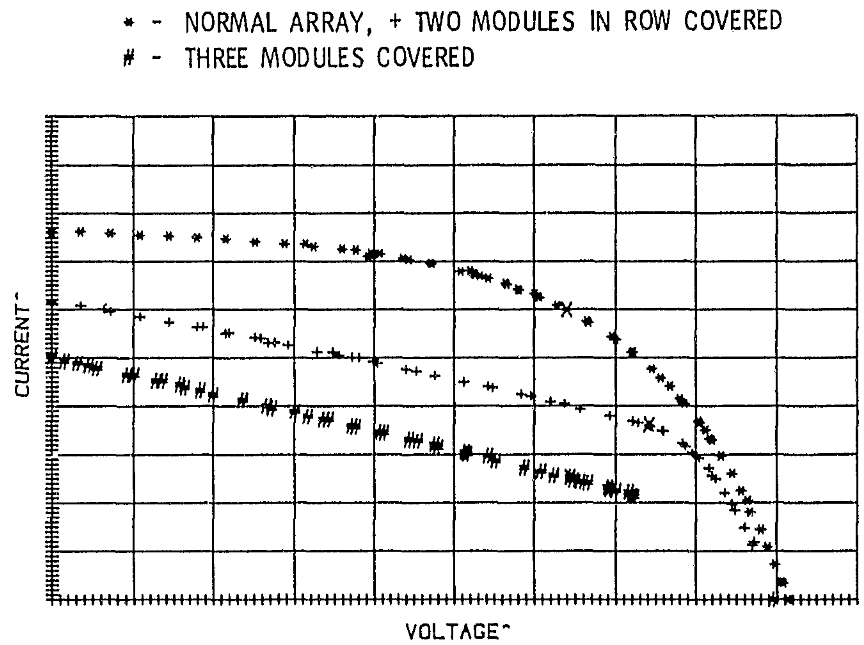

Sample Data: MCCC, One 2-Sided Receiver

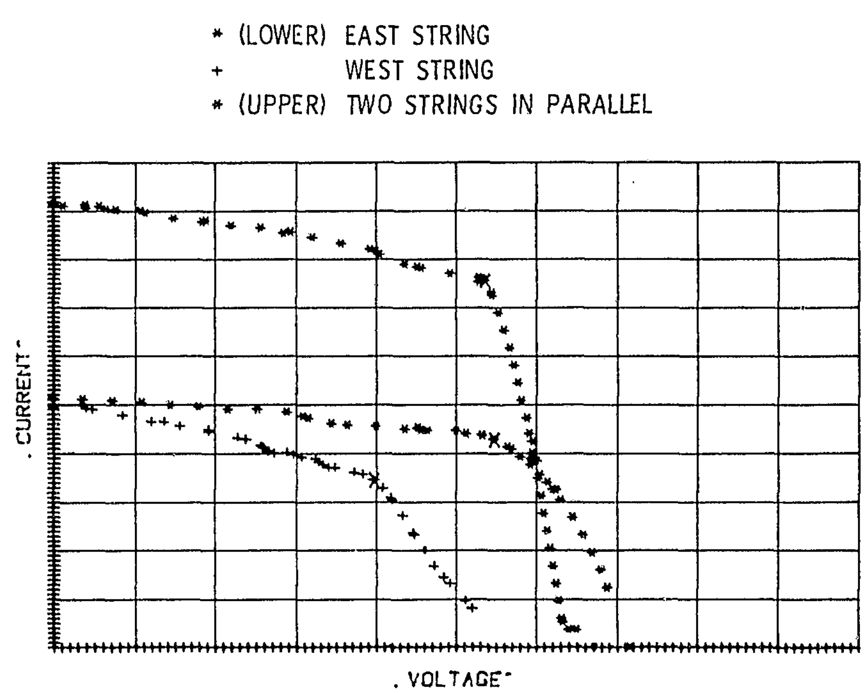

Summary

- THE LOGGER HAS BEEN USEFUL IN ESTABLISHING BASELINE DATA
- ABNORMALITIES ARE READILY DETECTED USING THE SYSTEM
- USEFUL FOR ANALYZING ARRAY PERFORMANCE
- CAN BE USED TO OBTAIN DATA ON ARRAYS WITH KNOWN PROBLEMS OR FOR SPECIAL TESTS

Availability

THE PORTABLE ARRAY DATA LOGGER IS AVAILABLE (WITH OPERATOR) FOR USE ANYWHERE BY MAKING ARRANGEMENTS WITH JPL

PROJECT ANALYSIS AND INTEGRATION

P.K. Henry, Chairman

R.W. Aster of the Project Analysis and Integration Area presented lower-bound cost estimates for encapsulating thin-film PV modules. Module size and design were found to be important: encapsulating costs are largely area-related, with large modules (2 x 4 ft) requiring at least $15/m^2 for materials and processing and small modules (1 x 1 ft) requiring at least $24/m^2. These costs can contribute from 12¢/W to 60¢/W to total module cost. As this does not include all deposition or processing costs, recent thin-film projections of 15¢/W for the entire module seem unreasonable.

Audience response to this presentation was interesting. An RCA representative suggested that the material costs for EVA might be lowered by reducing EVA from 20 to 10 mils thick. The result of adopting the lower EVA thickness is a reduction in cost of $0.60/m^2 in all cases. This is about 4% of the estimated lower bound for large modules. It was pointed out that there are potential low-cost substrate modules and estimates of lower-bound substrate encapsulation costs with conducting metal substrates could be incorporated into the analysis. There was also some audience discussion of the possibility that properties of some thin films may in fact require more stringent encapsulating procedures than were assumed in the analysis.

A new set of Allocation Guidelines (AGs) for FSA were developed recently and presented at at the PIM by R.W. Aster. These guidelines cover all types of flat-plate PV modules, including thin-film modules. The value of increased module efficiency is addressed and allocations for sheet, cell, and module processing are adjusted to provide a constant system cost over a wide range of potential efficiencies.

A stochastic approach to silicon cost analysis using the SIMRAND (SIMulation of Research ANd Development) model and the IPEG costing method was presented. The IPEG approach was validated for the Si manufacturing process. Then, using the capabilities of SIMRAND, stochastic inputs to a step-by-step analysis of the actual manufacturing process of Union Carbide and Hemlock Semiconductor were combined to yield cost probability distributions. The implications of the final results as well as some of the intermediate results and original, encoded distributions were discussed.

Many requests for documentation of the AGs have been received. Unfortunately, new ground rules from DOE and the PV Lead Center will require minor revisions to all of these tables and a new set of allocations for thin films.

The Basic Processing Unit (BPU) methodology for the costing of photovoltaic technologies was presented by J. Glyman. The rationale for the development of generic processes (BPUs) was discussed along with cost data for the technologies assuming a 1990 production environment. Sensitivity analyses of various process cost drivers were also presented. The BPU methodology facilitates rapid estimation and cost comparisons of advanced PV process options.

PROJECT ANALYSIS AND INTEGRATION

A metallization study was presented by R.W. Aster of PA&I at the Cell and Processes technical session. Its purpose was to evaluate the various metallization methods available to the PV industry by comparing them on a cost-and-efficiency basis.

The presentation was well received. A representative of a major PV manufacturer requested viewgraphs and may use this methodology as the basis for recommending changes in a production line. It was also requested that the metallization study be presented at the FSA PV Metallization Research Forum (March 16-18, in Georgia). The metallization forum will provide an opportunity to collect data that should allow expansion of this study, perhaps to the point where it is a definitive analysis of the state of the art in this field. This follow-on work would then be presented at a future PIM.

A poster session describing the analytical models developed by PA&I was conducted. A handout was distributed at the session that provides an overview of: Standard Assembly-Line Manufacturing Industry Simulation (SAMIS); Improved Price Estimation Guidelines (IPEG); SIMRAND, and the Basic Process Unit (BPU) costing methodology.

Economic projections for 1982 single-crystalline technology that were prepared in 1980 have been reviewed and compared with the commercial state of the art. Results of this comparison were presented at the PIM by P.K. Henry, along with projections for ribbon-based technology in the late 1980s and early 1990s. (For a more complete description of these studies, see the PA&I Area Report in this document.)

This presentation was well received, and many requests for additional information on the studies from industry analysts and PV newsletter publishers have been received, as have requests that this presentation be repeated in future PV symposia.

BASIC PROCESS UNIT (BPU) COSTING

JET PROPULSION LABORATORY

J. Glyman

SERI Contract RW-1-9342

- l-yr contract – completion August 1982
- Final report – JPL No. 5030-554
  - Identification and cost of basic process units (BPUs), Phase I and II
- Objective
  - Develop methodology to cost and rate thin-film photovoltaic production processes for 1990 technology
- Tasks
  - Define generic processes
  - Scale process description for 1990 mass production
  - Determine cost drivers using SAMIS/IPEG
  - Run sensitivity analysis on cost drivers

Why Was the Basic Process Unit Concept Developed?

- SERI required a rapid cost estimation method for advanced thin-film process options
- Thirteen SERI process flow sheets were studied including: Poly Si; αSi; CdS; GaAs
- Analysis of typical flow chart showed 44 process options and 776,000 possible combinations
- Cost projections for commercial scale-up of laboratory data requires detailed process design and economic analysis for every manufacturing process
- Therefore, detailed projection for promising options and combinations requires prohibitive cost and time
- A need existed then for a grouping of the many processes studied into generic sets

The Basic Process Unit: What Does it Do?

- **Examination of thin-film processes indicated strong basic similarities across a broad spectrum of cell processing steps**

- **Example: Equipment, labor, facility, and utilities of a production-scale screen printer are similar over a wide variety of cell types and sizes**

- **Therefore: Variations in the cost of the screen-printing process with different cell types are principally a function of variation in material used**

Basic Process Units

- **Described by 16 generic processes**
- **Examples:**
  - **(1) BPU No. 3 – Evaporator, includes processes:**
    - **Sputtering, evaporation, E-beam deposition, resistive evaporation, flash evaporation**
  - **(2) BPU No. 4 – Gaseous furnace, includes processes:**
    - **Anneal, heat treat, open-tube diffusion, thermal oxidation, oxidation with H_2O, thermal diffusion**
  - **(3) BPU No. 9 – CVD reactor, includes processes:**
    - **Chemical vapor deposition, molecular beam epitaxy, epi-reactor, thermal growth**

Basic Process Unit Costing Methodology

- SAMIS and IPEG 4* were both used to generate costs and BPU-specific IPEG equations for sensitivity studies
- SAMIS input – format A, B, and C
- IPEG 4 output – price (value added) and overhead coefficients for EQPT, SQFT, DLAB, MATS, and UTILS generate by SAMIS

---

*IPEG 4 is a computer model that can take SAMIS outputs and then generate process-specific IPEG equations in the general form

$$\text{IPEG price} = [(C_1 \times \text{EQPT}) + (C_2 \times \text{SQFT}) + (C_3 \times \text{DLAB}) + (C_4 \times \text{MATS}) + (C_5 \times \text{UTIL})]/\text{QUAN}$$

Assumptions on Basic Process Unit

- Use 1990 automated factory*
- Factory size: 200 MW/yr
- Use 1.2×2.4 m modules/substrates
- Wafers used: 10×10 cm (where appropriate)
- Some BPU processes are state-of-the-art; data are available on large-scale PV processes
  Examples: screen print, interconnect
- Some BPU processes are laboratory scale; require some R&D for large-scale PV processes
  Examples: laser cut, sprayer
- Most BPU processes are laboratory scale; require extensive R&D for large-scale PV processes
  Examples: Evaporation; plasma glow discharge; chemical vapor deposition

---

*Allows for improved engineering designs but not for major technical breakthroughs

Summary of Basic Process Unit Cost Data

BPU No.	Description	Value Added, $/m²$	Cost Driver, % of Total
1	Plasma Glow Discharge	5.3	EQPT 84.8
2	Sink/Dip in Solution	3.1	MATS 81.4
3	Evaporator	3.8	EQPT 78.5
4	Gaseous Furnace	1.5	DLAB 30.7 MATS 32.9
5	Belt Furnace	3.6	MATS 74.7
6	Printer	20.7	MATS 94.3
7	Sprayer	0.9	MATS 41.7
8	Laminator	14.1	MATS 78.2
9	CVD Reactor	95.9	MATS 91.4
10	Ion Implanter	3.5	UTIL 50.5
11	Electroless Plating	2.0	DLAB 39.6 MATS 29.0
12	Anodic Oxidation	1.7	DLAB 25.9 MATS 38.5
13	Solder Dip	6.5	MATS 88.3
14	Laser Scribing	2.7	UTIL 60.0
15	Interconnect	4.0	DLAB 32.6 MATS 44.1
16	Masking	1.3	DLAB 58.4

ORIGINAL PAGE IS OF POOR QUALITY

Screen Print Process for Major Cost Driver -- MATS

Sensitivity Analysis of Basic Process Unit No. 6

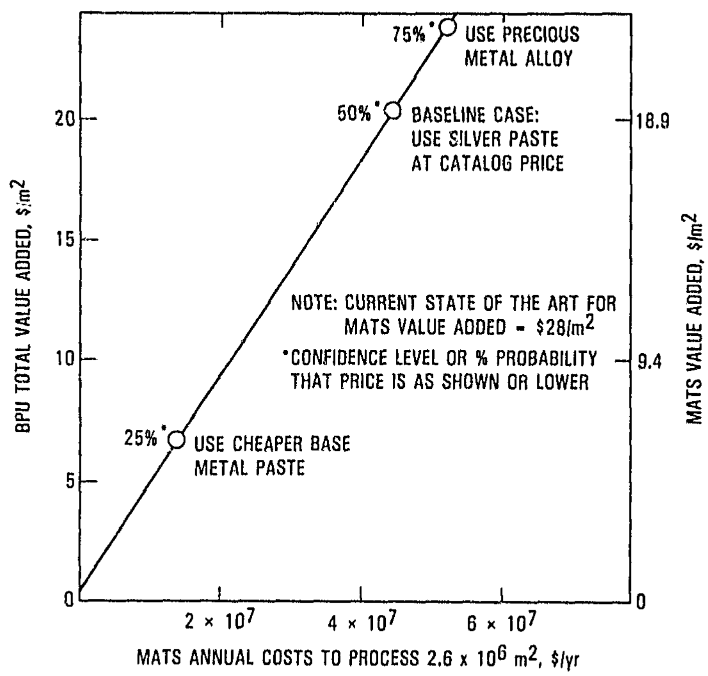

Sink Dip Process for Major Cost Driver -- MATS

Sensitivity Analysis of Basic Process Unit No. 2

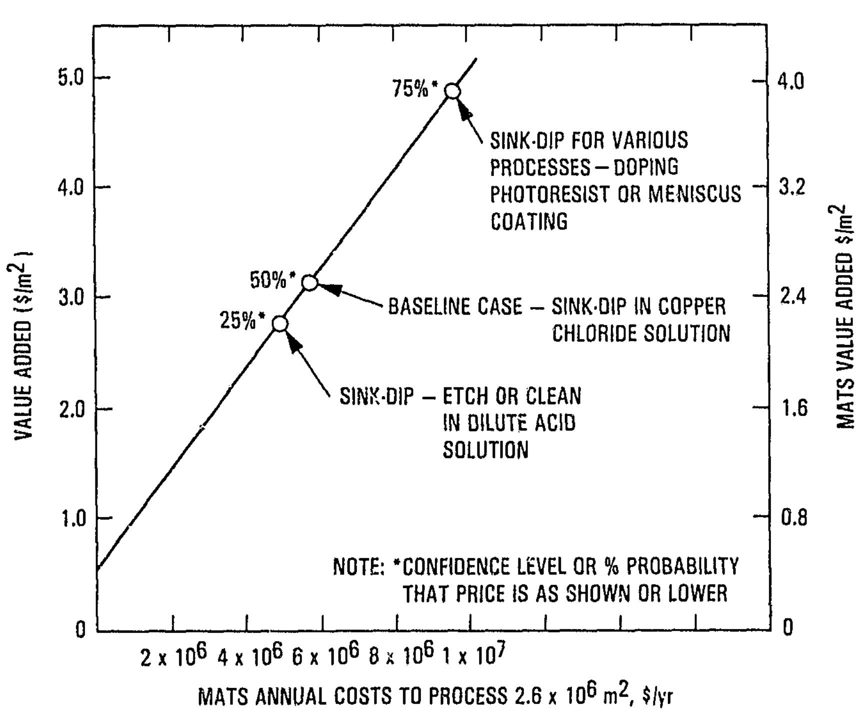

Ion Implant Process for Major Cost Driver -- UTIL

Sensitivity Analysis of Basic Process Unit No. 10

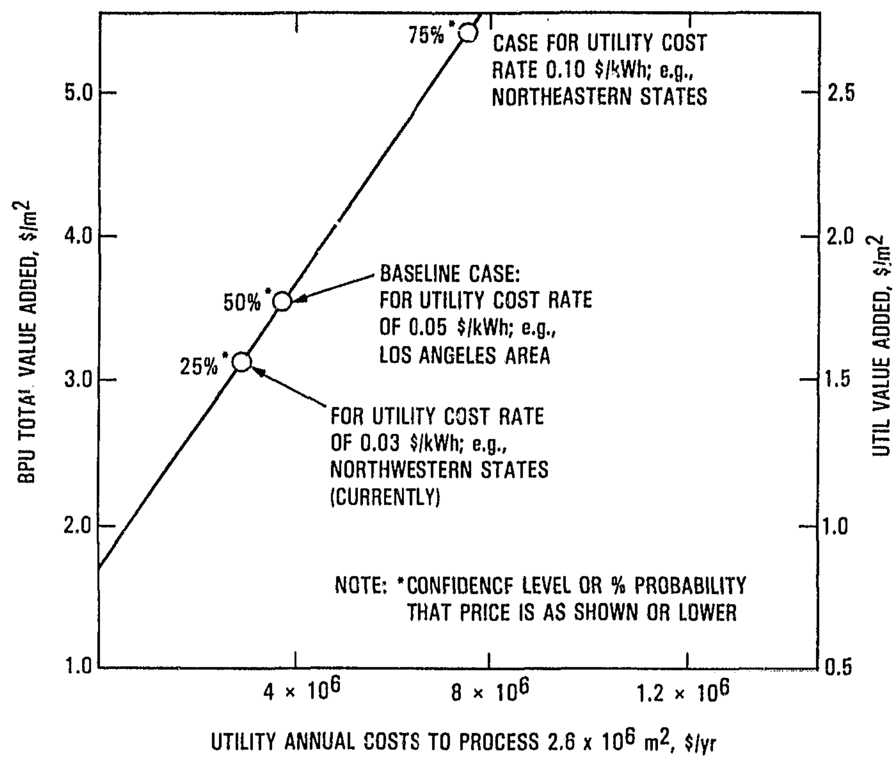

ORIGINAL PAGE IS
OF POOR QUALITY

Glow Discharge Process for Major Cost Driver -- EQPT

Sensitivity Analysis of Basic Process Unit No. 1

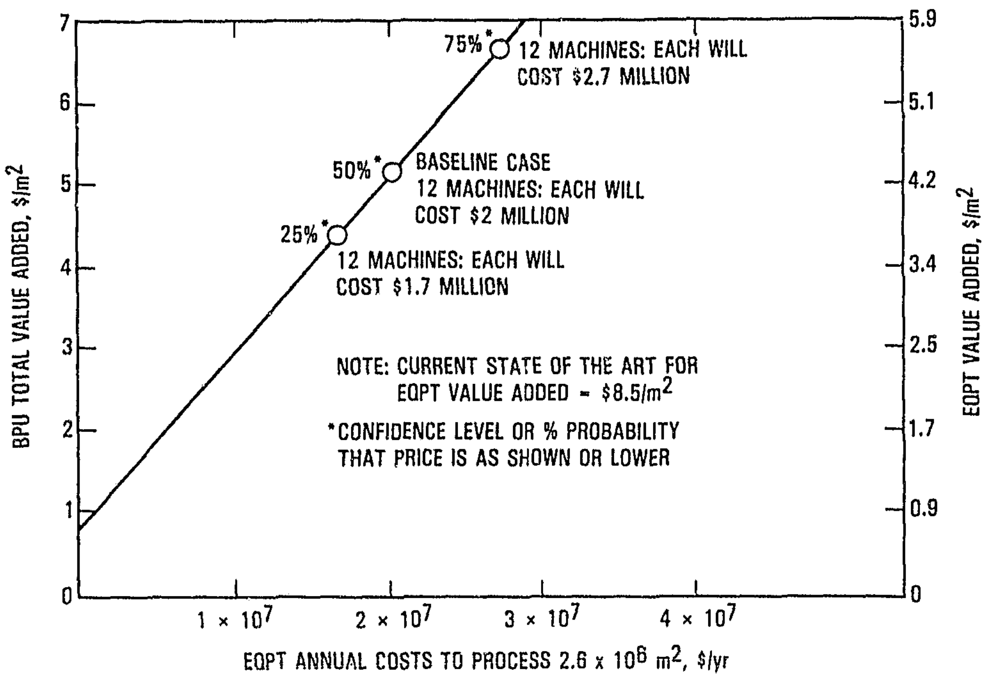

SERI Contract Conclusions

- **BPU concept has been demonstrated as a valuable cost tool to evaluate R&D thin-film PV options**
- **BPU approach can be used for wide spectrum of cell and module processes**
- **Material generally was the major cost driver in a mass-production PV process (1990 technology)**
- **BPU value-added costs are based on assumption that extensive process R&D will be performed**

NEW ALLOCATION GUIDELINES

JET PROPULSION LABORATORY

R.W. Aster

Allocation Guideline Purpose

- Allocation guidelines (AG) are an integrated set of cost and performance targets for several R&D tasks within the Flat-Plate Solar Array Project (FSA)
- Purpose of the new AG is to provide a meaningful set of guidelines for asessing R&D progress toward the FSA objective
- New AG are a working tool of FSA Management. They are used for R&D management purposes only, and should not be interpreted as a prediction of market price for any given year

History

- Guidelines for this Project were first developed in 1976 (see the First Annual Report, ERDA/JPL-1012-76/5, pp. 3-6, 1976)
- As new information has been developed, these guidelines have been modified in the following reports:
  - 1977, JPL-5101-33 (first IEPG document)
  - 1978, JPL-5101-68 (Price Allocation Guidelines)
  - 1980, DOE/JPL-1012-47 (Price Allocation Guidelines)
- New AG are significantly different from these earlier versions; they are expected to be published in 1983

New Features

- Guidelines are for:
  - Near-term ($0.70/W, 11% module baseline
  - Advanced ($0.50/W, 13.5% module baseline
  - Thin-film (equivalent to near-term and advanced)
- Area-related balance of the PV system (Area—BOS) is included
- Guidelines are parametric with module efficiency (high-efficiency sheet and cells have larger allocations)
- Guidelines apply to all silicon sheet technologies

Approach

	NEAR—TERM	ADVANCED
Array subsystem goal	$1.32/W (dc)	$0.87/W (dc)
Subtract: Area—BOS (result is parametric with efficiency)	$50/m^2	$40/m^2
Subtract: Marketing & Distribution (M&D)		
Allocate:		
Silicon	$14/kg	$14/kg
Encapsulant materials	$14/m^2	$12/m^2
Module fabrication	$14/m^2	$12/m^2
Allocate remainder to sheet and cell processing		

- Near-term sheet allocations are based on projections:
  - 9% to 10% modules; e.g., Low-angle sheet; SOC
  - 10% to 12% modules; e.g., EFG; ESP; RTR
  - 12% to 13% modules; e.g., Web; HEM
- Cell processing receives the remainder
- Advanced allocations emphasize high-efficiency approaches and might be met by R&D efforts with Web, ESP, multijunction, or graded-junction devices

Thin-Film Approach

- **Thin-film modules receive the same near-term goals as near-term crystalline modules, and the same long-term goals as advanced crystalline modules**
- **Other system components (M&D, Area—BOS) remain the same**
- **However, the inherent low cost expected from thin-film modules allows them to also have guidelines at lower module efficiencies**
- **For example: A near-term thin film at \$0.40/W, 6.3% (NOC) module efficiency is equivalent to \$0.70/W at 11%. An advanced thin film at \$0.40/W, 10% or \$0.15, 6.1% is equivalent to the advanced \$0.50/W, 13.5% crystalline guideline**

New \$0.70 / W Silicon Allocation Guidelines (1980 \$)

ITEM		MODULE EFFICIENCY (NOC) 9	10	11	12	13
Silicon & Sheet	$\$/m^2$	9	16	24	30	33
	\$/W	0.105	0.168	0.229	0.262	0.266
Cell	\$/W	0.193	0.211	0.215	0.237	0.279
Module:						
Materials, $\$14/m^2$	\$/W	0.156	0.140	0.127	0.117	0.108
Fabrication, $\$14/m^2$	\$/W	0.156	0.140	0.127	0.117	0.108
Module Subtotal	\$/W	0.61	0.66	0.70	0.73	0.76
Marketing & Distribution	\$/W	0.155	0.161	0.167	0.171	0.175
Area—BOS, $\$50/m^2$	\$/W	0.556	0.500	0.455	0.417	0.385
Array Total	\$/W	1.32	1.32	1.32	1.32	1.32

New \$0.50 / W Silicon Allocation Guidelines (1980 \$)

ITEM		MODULE EFFICIENCY (NOC) 10	12	13.5	15	20.5
Silicon & Sheet	$\$/m^2$	8	15	21	26	40
	\$/W	0.084	0.132	0.164	0.183	0.206
Cell	\$/W	0.086	0.142	0.167	0.194	0.283
Module:						
Materials, $\$11/m^2$	\$/W	0.110	0.092	0.082	0.073	0.054
Fabrication, $\$12/m^2$	\$/W	0.120	0.100	0.089	0.080	0.058
Module Subtotal	\$/W	0.40	0.47	0.50	0.53	0.60
Marketing & Distribution	\$/W	0.069	0.071	0.072	0.073	0.074
Area–BOS, $\$40/m^2$	\$/W	0.400	0.333	0.296	0.267	0.195
Array Total	\$/W	0.87	0.87	0.87	0.87	0.87

\$0.70 / W Thin-Film Allocation Guidelines (1980 \$)

ITEM		MODULE EFFICIENCY (NOC) 6.3	9	10	11	12	13
Collector Cost (f.o.b.)	\$/W	0.40	0.61	0.66	0.70	0.73	0.76
Marketing & Distribution:							
Marketing (20% of above)		0.080	0.122	0.132	0.140	0.147	0.152
Distribution	\$/W	0.046	0.033	0.029	0.027	0..024	0.023
Delivered Collector Subtotal	\$/W	0.526	0.765	0.821	0.867	0.901	0.935
Area–BOS, $\$50/m^2$	\$/W	0.794	0.556	0.500	0.455	0.417	0.385
Array Subsystem Total	\$/W	1.32	1.32	1.32	1.32	1.32	1.32

$0.40 / W Thin-Film Allocation Guidelines

(1980 $)

ITEM		MODULE EFFICIENCY (NOC) 6.1	7.9	10	12	13.5	15	20.5
Collector (f.o.b.)	$/W	0.15	0.30	0.40	0.47	0.50	0.53	0.60
Marketing & Distribution								
Marketing (10%)		0.015	0.030	0.040	0.047	0.050	0.053	0.060
Distribution	$/W	0.048	0.037	0.029	0.024	0.022	0.021	0.014
Delivered Collector Subtotal	$/W	0.213	0.367	0.469	0.541	0.572	0.604	0.674
Area–BOS, $40/m^2	$/W	0.656	0.506	0.400	0.333	0.296	0.267	0.195
Array Subsystem Total	$/W	0.87	0.87	0.87	0.87	0.87	0.87	0.87

Status

- The new AG have been reviewed within FSA
- They are consistent with Lead Center guidelines (as they now stand)
- A report will be prepared early in 1983

ECONOMIC PROJECTIONS AND FSA RESEARCH PRIORITIES

JET PROPULSION LABORATORY

P.K. Henry

1. Comparison of economic projections made in 1980 with present practices
2. a. "Where are we now in ribbon-based technology development?"

   b. Recent economic projections for ribbon-based technology

Comparison of \$2.80 / W_p Technical Readiness Projection for 1982 With Present Industrial Practices

	Projection made in 1980 for 1982,* 1980\$/W_p	Present,* 1980\$/W_p	
	30 MW/yr	30 MW/yr	2 MW/yr
Ingot growth (incl. silicon)	1.63	1.53	1.74
Sawing	0.37	0.42	0.77
Cell processing	0.36	0.31	0.84
Module assembly (incl. Encap. Mat'l)	0.34	0.37	0.92
FOB factory dock required price	2.70	2.63	4.27
Marketing and distribution (30%-50%)	0.81-1.35	0.79-1.31	1.28-2.13
Inflation (1980-1982) (14.5% est) (25.4% actual)	0.89-1.03	0.87-1.00	1.41-1.63
Required market price,** 1982\$/W_p	4.40-5.08	4.29-4.94	6.97-8.03

*Assumes 11.4% encapsulated-cell efficiency and 0.78 packing factor
**To convert to \$/m^2 of module, multiply by 89.4

PRECEDING PAGE BLANK NOT FILMED

Factors That Differed From Projections Made in 1980

FACTORS RAISING REQUIRED PRICE

- Interest on corporate debt
  - Projected: 9.25%
  - Actual: ~16%
- Slices/cm of ingot sawing
  - Project: 20 slices/cm
  - Actual: 17 slices/cm
- Saw blade life
  - Projected: 3100 slices
  - Actual: 2500 slices

FACTORS LOWERING REQUIRED PRICE

- Silicon cost (1980$)
  - Projected: $84/kg
  - Actual: $55/kg
- Silver cost (1980$)
  - Projected: $18.40/oz
  - Actual: $9.00/oz
- Cell-processing cumulative yield
  - Projected: 89.1%
  - Actual: 90.0%

Comparison of $2.80 / W_p Technical Readiness Projection for 1982 With Present Industrial Practices: Summary

- All processes, equipment, and module design factors assumed in the projections made in 1980 have been adopted by industry (not all co-located)
- With exception of sawing, all technical and performance parameters have equalled or exceeded the projections made in 1980
- Factors outside the control of the PV Program have had mixed effect on manufacturing costs (market volume, commodity prices, interest rates)

Comparison of State-of-the-Art Ribbon Technology (Scaled Up) With Projections of Ribbon Technology

Ground rule for state-of-the-art ribbon technology scaled up to commercial production in 1985

- **All equipment and processes must be presently in use in the industry or proven to the point that equipment can be ordered for installation and operation by 1985**

Assumptions

	Scaled-up state of the art	Intermediate projection (Late 1980s)	Long-term projection (Early 1990s)
Factory size, MW/yr	25	25	25
Year of production	1985	1988	1990
Ribbon type	Dendritic web	Dendritic web	Dendritic web
Silicon cost, 1980\$/kg	55	14	14
Web growth rate, cm^2/min	10	25	35
Growth machines/operator	6	18	18
Encapsulated-cell efficiency, %	12.3	13.5	15
Packing factor	0.92	0.92	0.92
Module efficiency, %	11.3	12.4	13.8
Cumulative cell process yield	0.77	0.93	0.93

(1980 $) / W_p

	Scaled-up state of the art*	Intermediate projection (Late 1980s)	Long-term projection (Early 1990s)
Sheet growth (incl. silicon)	1.61	0.21	0.14
Cell processing	0.27	0.22	0.19
Module assembly (incl. encap. matl)	0.18	0.16	0.15
FOB factory dock required module price			
(1980$/$W_p$)	2.06	0.59	0.48
(1980$/$m^2$)	233	73.3	66.2

*Technology in existence today but not yet used in full scale commercial production

Summary

- Ribbon growth rates still low due to lack of understanding of thermally induced stresses; high growth rates significantly reduce module price
- Further research and development into process control and equipment parameters would result in higher yeilds and efficiencies sufficient to produce modules at $0.70/$W_p$ or less
- Once $0.70/$W_p$ technology is achieved, modest improvements in ribbon growth rate and cell efficiency can bring $0.50/$W_p$ or less within reach

Plenary Session

Thin-Film Deposition Technologies for PV

E. Christensen, Chairman

PROPERTIES OF AMORPHOUS SILICON USING GLOW DISCHARGE TECHNIQUE

SOLAR ENERGY RESEARCH INSTITUTE

A. Madan

Applications of Amorphous Silicon

* INEXPENSIVE SOLAR CELLS
* THIN FILM TRANSISTORS
  (TO DRIVE LARGE AREA LIQUID
  CRYSTAL DISPLAYS)
* ELECTROPHOTOGRAPHY
* VIDICON TUBES
  ETC.

Preparation Techniques

* GLOW DISCHARGE (SiH_4, SiF_4/H_2)
* REACTIVE SPUTTERING
* CHEMICAL VAPOUR DEPOSITION (SiH_4, Si_2H_6)

Elemental Amorphous Silicon

- EVAPORATION OF Si
- SPUTTERING OF Si in Ar.

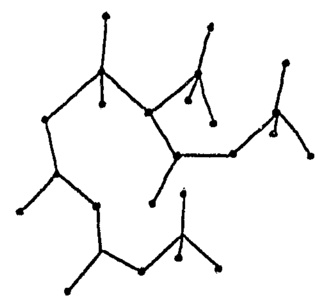

→ LARGE NUMBER OF DANGLING BONDS

→ ACT AS RECOMBINATION CENTRES FOR PHOTOGENERATED CARRIERS

<u>GLOW DISCHARGE</u>

- E.G. SiH_4 GAS

→ H TIES UP DANGLING BONDS

→ LOWERS THE DENSITY OF RECOMBINATION CENTRES (LOCALISED STATES)

→ PRODUCES A USEFUL ELECTRONIC MATERIAL

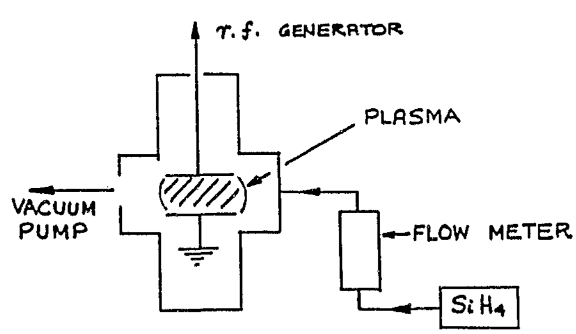

C-6

Electronic Properties of Amorphous Silicon Affected by:

* SUBSTRATE DEPOSITION TEMPERATURE
* GAS COMPOSITION (SiH_4, SiH_4/H_2, SiH_4/Ar...)
* DEPOSITION PRESSURE
* GAS FLOW RATE
* EXCITATION FREQUENCY (R.F., AUDIO, D.C.)
* ANODE-CATHODE DISTANCE
* POWER

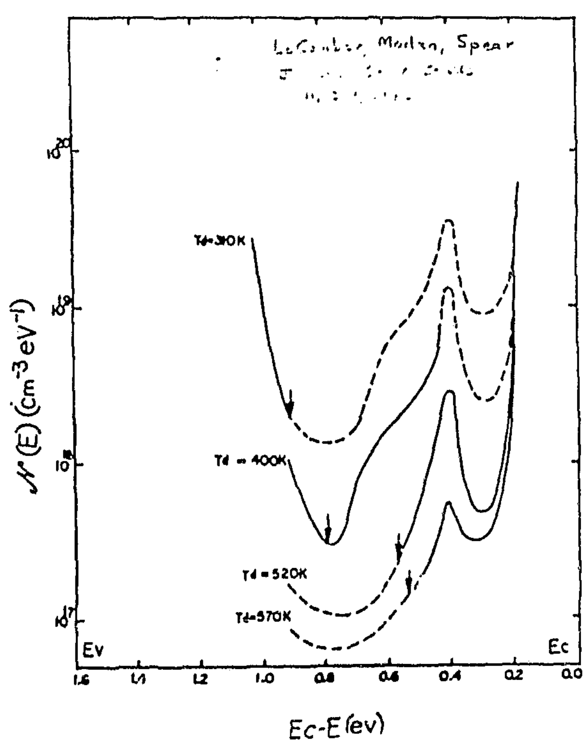

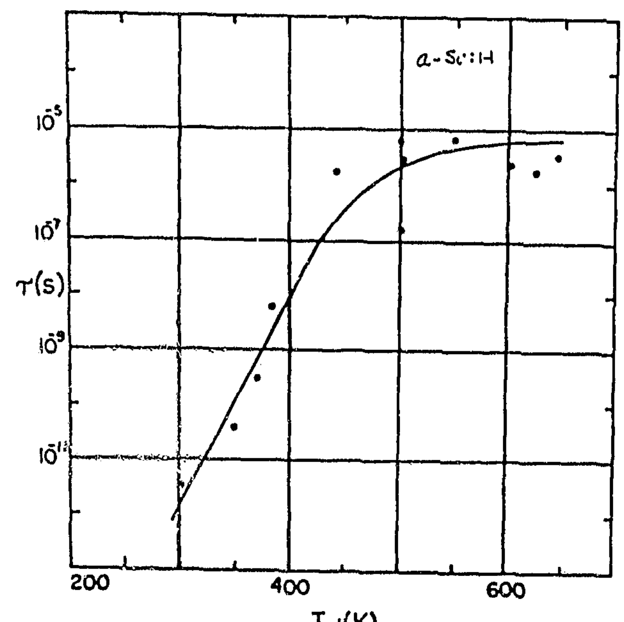

LOVELAND, SPEAR
J. NON CRYST. SOL. 155, 55, 1974.

ORIGINAL PAGE IS
OF POOR QUALITY

Density of States Affected by Substrate Temperature (T_S)

MODEL DUE TO KNIGHTS

* LOW Ts

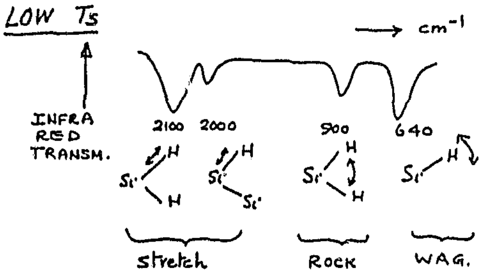

$\longrightarrow$ IMPLIES POLYMERIC CHAINS

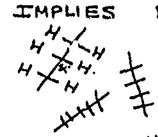

$\longrightarrow$ MATERIAL HAS MICROVOIDS

$\longrightarrow$ LARGE DENSITY OF TRAPPING CENTRES.

* HIGH Ts

NO 2100 cm^{-1} OR 900 cm^{-1} PEAKS

$\longrightarrow$ ELIMINATION OF MICROVOIDS

$\longrightarrow$ IMPLIES RANDOM NETWORK OF Si WITH THE DANGLING BONDS COMPEN. BY H

$\longrightarrow$ LOW DENSITY OF STATES.

Plasma Diagnostics

- OPTICAL EMISSION SPECTROSCOPY
- MASS SPECTROSCOPY

$SiH_4 \longrightarrow SiH,\ SiH_2,\ SiH_3$
$H,\ H_2$
+ EXCITED SPECIES

ORIGINAL PAGE IS OF POOR QUALITY

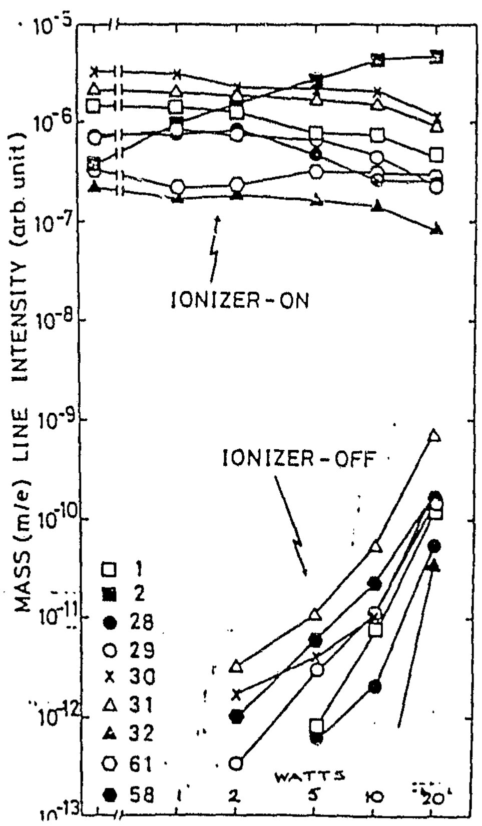

MATSUDA et al (1982)

MATSUMURA et al

- FREE RADICALS ARE PREDOMINANT
- RAPID RISE IN THE POPULATION OF IONS WITH POWER (→ INCREASE IN THE ELECTRON DENSITY)

ORIGINAL PAGE IS OF POOR QUALITY

TURBAN et al

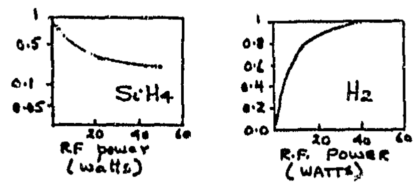

[RELATIVE ABUNDANCE OF SiH_4 and H_2]

- INCREASE OF POWER → INC. OF H_2 ($\therefore e^- + H_2 \rightarrow 2H + e^-$)
- INCREASE OF H FLUX AT THE GROWING SURFACE CAN BREAK BONDS

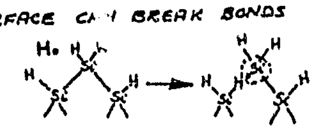

- RESULT CONSISTENT WITH AN INCREASE IN E.S.R. SIGNAL (INCREASE IN THE NUMBER OF TRAPS)

UNDOPED (a-Si:H)	
DARK CONDUCTIVITY	10^{-10}–$10^{-9}(\Omega cm)^{-1}$
LIGHT CONDUCTIVITY (AM-1)	10^{-5}–$10^{-4}(\Omega cm)^{-1}$
BAND GAP	~1.7eV
DENSITY OF LOCALISED STATES	> 10^{15}–$10^{17} cm^{-3} eV^{-1}$
MIN. CARRIER DIFFUSION LENGTH	0.2 – 2 μm

DOPING CHARACTERISTICS			
TYPE	GAS	AMOUNT	CONDUCTIVITY
n^+	PH_3	~5000 vppm	~ $10^{-2} (\Omega cm)^{-1}$
p^+	B_2H_6	~10000 vppm	~ $10^{-3} (\Omega cm)^{-1}$

- A-Si:F:H
(SiF_4/H_2 ~ 8/1) + 500 vppm PH_3
σ_D ~ $10 (\Omega cm)^{-1}$ [MADAN, OVSHINSKY, BENN 1978]

CONDITIONS FOR DEPOSITION	
GAS COMPOSITION	SiH_4
HIGH FLOW RATE	> 40 sccm
LOW POWER	< 0.3 W cm^{-2}
DEPOSITION PRESSURE	~500 m torr
DEPOSITION TEMPERATURE	~250C

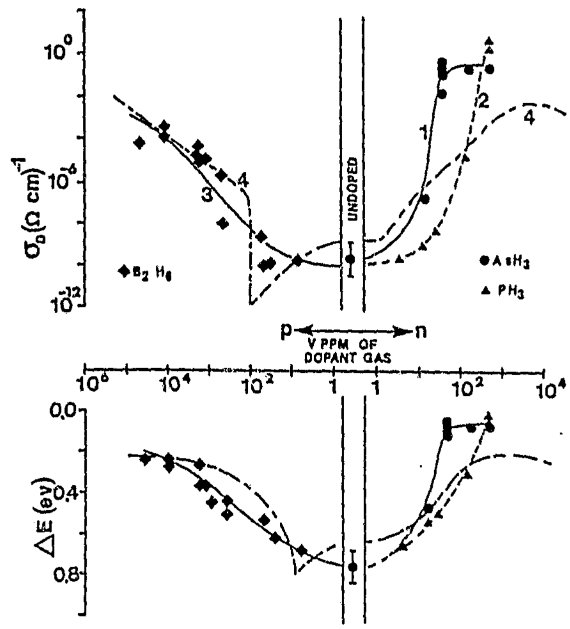
$\sigma_D(\Omega\ cm)^{-1}$
ΔE (ev)
UNDOPED
B_2H_6
AsH_3
PH_3
p ← → n
V PPM OF DOPANT GAS

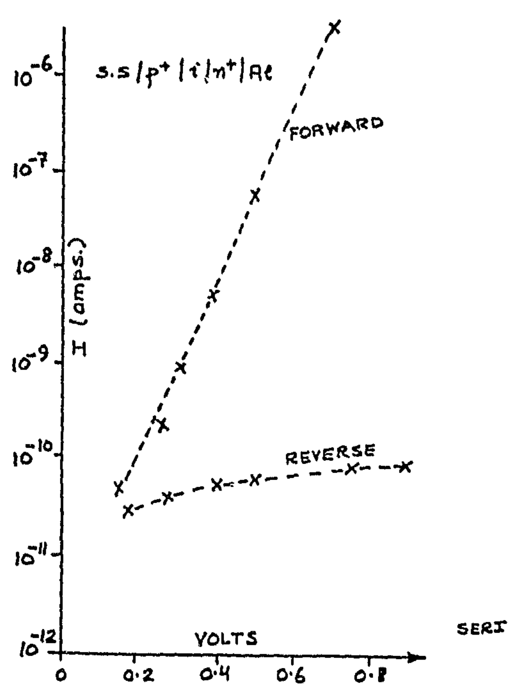
s.s / p+ / i / n+ / Rℓ
FORWARD
REVERSE
I (amps.)
VOLTS
SERI

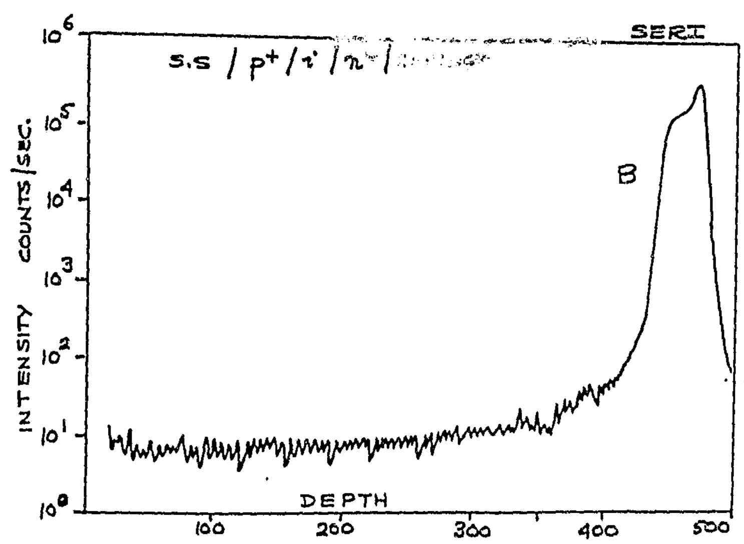
SERI
s.s / p+ / i / n+ /
B
INTENSITY COUNTS / SEC.
DEPTH

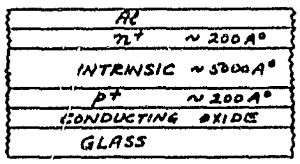

$\eta \simeq 10.1\%$ A ~/cm² CATALANO et al (1982)

* USE OF OPTICAL WINDOW
→ WIDE BAND GAP .. p^+
(Si:C:B:H – HAMAKAWA et al)

* USE OF OPTICAL REFLECTORS
→ Al/Si ~95% for $\lambda \simeq 600\,nm$
[illegible]

* TEXTURED SURFACES
(YABLONOVITCH and CODY)

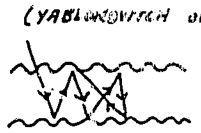

PATH LENGTH INCREASED
≈ 4n² (≃ 50)

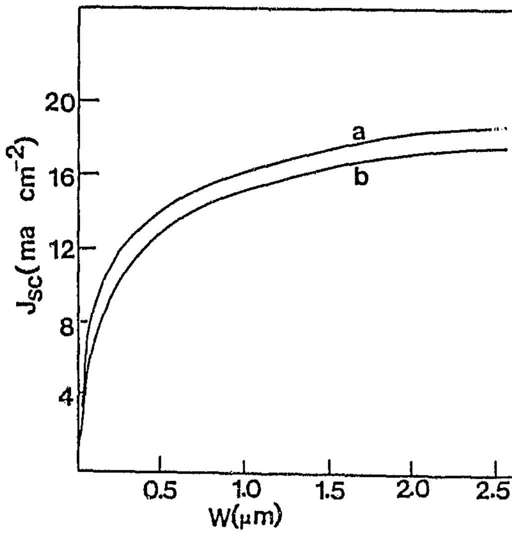

Photovoltaics Market Study -- 1982

Objectives

1. Assess the characteristics and the size of probable future markets for photovoltaics, both in the U. S. and worldwide.
2. Propose ways for Socal to participate profitably in these markets provided they are of sufficient size to be of interest.
3. Develop a realistic timetable and an estimate of the resources required for photovoltaics research, development, demonstration, and commercialization, taking into account current projections on fossil fuel supply and demand, alternative technologies, and competitive activity.

Summary of Requirements for Module/Cell Assembly Performance

	Year 2015 Market Potential, MW	Efficiency, %	Mfg Cost, $/m²
Flat Plate			
Central (Domestic)	40,000	15-25	25-50
Off-Grid DC (International)	10,000	10-15	40-70
Concentrators			
Central (Domestic)	40,000	35-45	35-45

Conclusions from 1982 SoCal PV Market Study

1. Major Advances in Efficiency and Cost Reduction Needed to Generate Large Markets
2. Major U.S. Market: Central Generation
3. Time Frame: 80's, Early 90's - Overseas Markets
   Mid-90's on - Central Generation
4. Long-Range Research Effort Needed Which Merits Continuing Government Support

Efficiency Limit

V_{oc}	$\sim 1.0 - 1.1$ V	BAND TAIL RECOMBINATION (TIEDJE et al)
J_{sc}	$\sim 20 - 22$ mA cm^{-2}	OPTICAL BAND GAP (~ 1.7 eV)
FF	$\sim 0.75 - 0.8$	MIN. CARR. DIFF. LENGTH

$$\eta \simeq 15 - 19\%$$

Future R&D Directions

- CONTROL OF BAND GAP
  - ALLOY WITH GE, SN,...
  - CONTROL OF H CONTENT IN A-SI:H
- INCREASE OF DEPOSITION RATE
  - LABORATORY SCALE DEVICES AT PRESENT $\rightarrow$ 1-3 A°/S
  - REPORTS OF $\sim$10 A°/S ($\eta \sim 6\%$)
  - REQUIRE 50-100 A°/S FOR A VIABLE LARGE SCALE PRODUCTION
- LARGE AREA
  - ELECTRONIC AND PHYSICAL INHOMOGENITIES
  - DEVELOPMENT OF INTEGRATED CELLS (SCRIBING TECHNIQUES)
  - R.F./AUDIO FREQUENCY EXCITATION
- SUBSTRATES
  - GLASS (DEGRADATION OF TCO)
  - STAINLESS STEEL (ENCAPSULANT PROBLEM)
  - PLASTIC (NEED TO LOWER Ts)
- EFFICIENT USE OF GASES
  - RECYCLE - WITHOUT CONTAMINATION
- STABILITY
  - CONTROL OF IMPURITIES
  - STUDY OF DEFECT LEVELS

PHYSICAL VAPOR DEPOSITION

AIRCO TEMESCAL

R. Hill

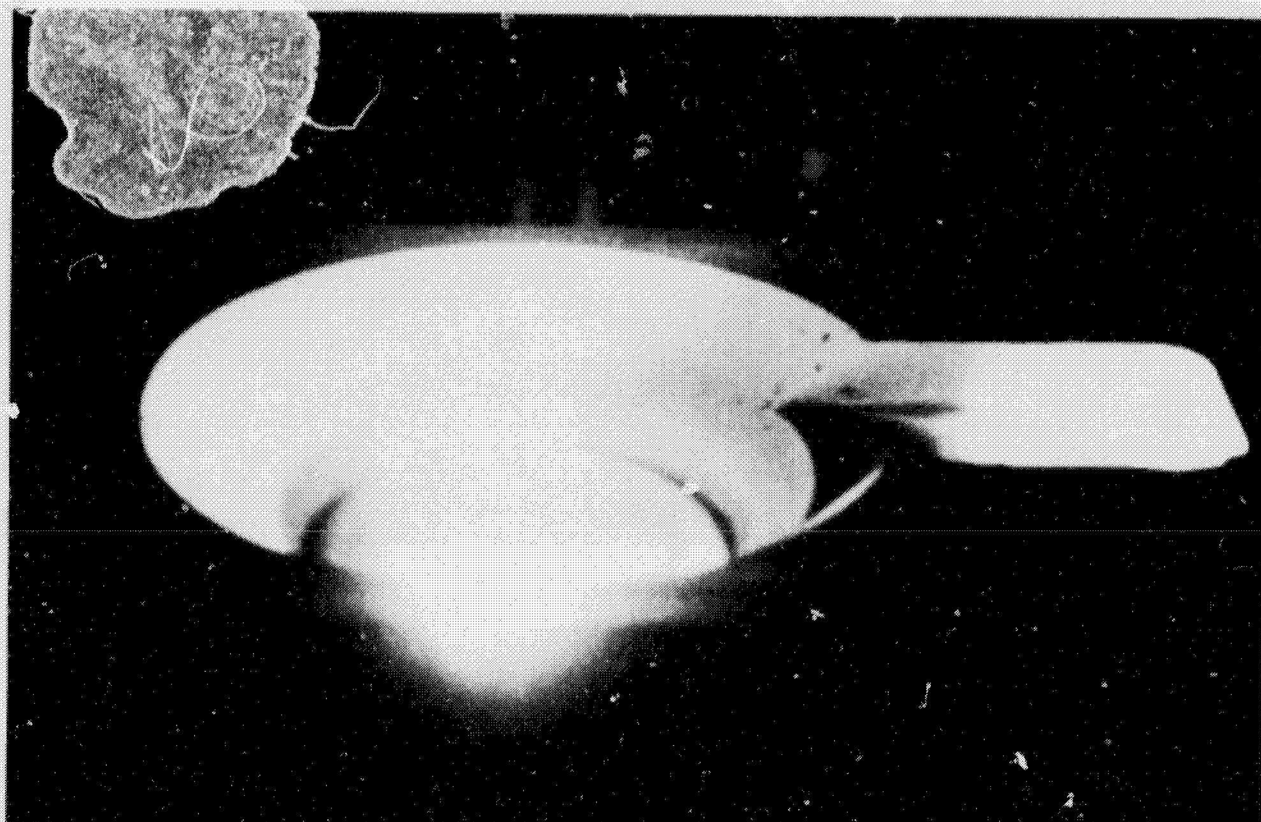

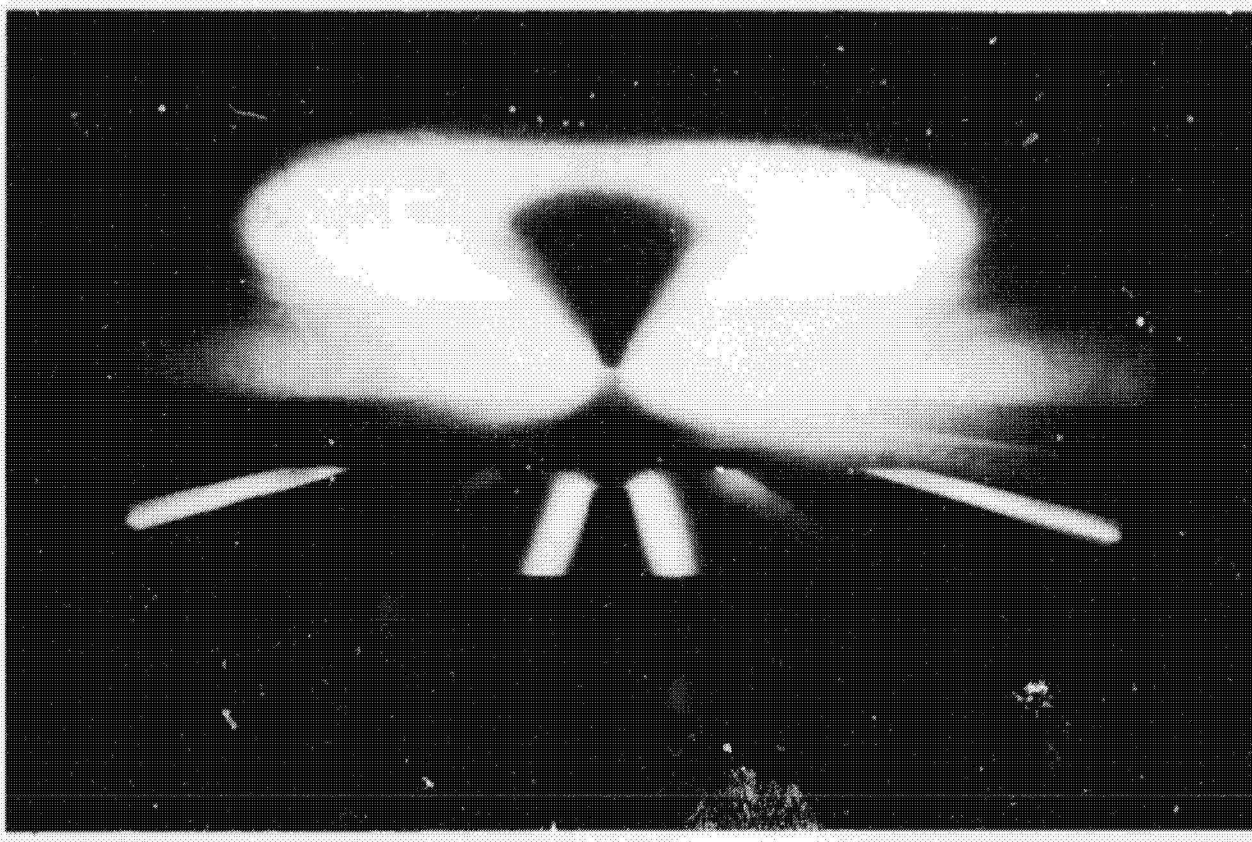

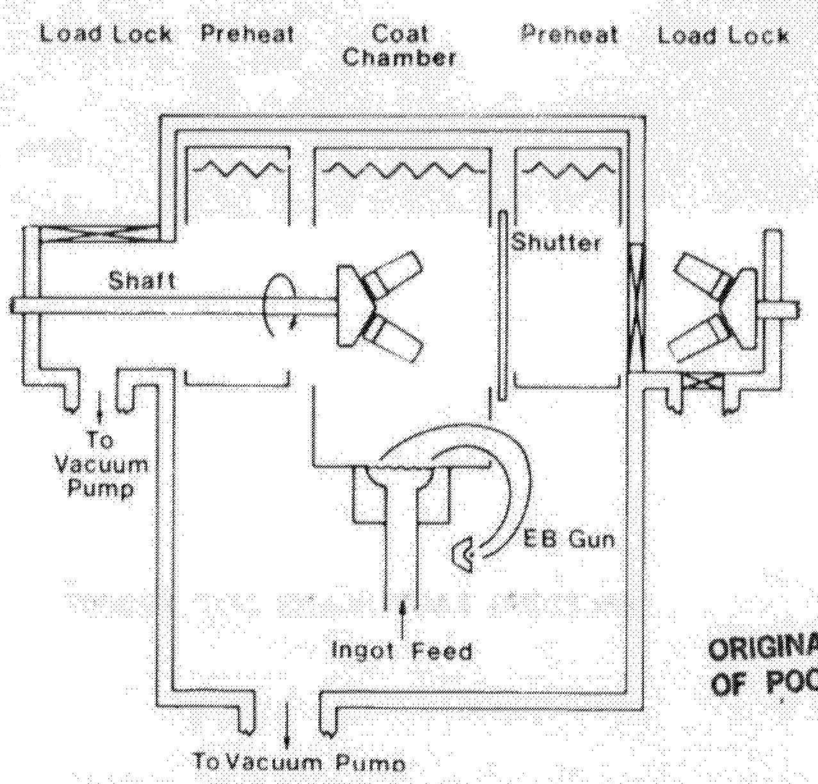

ORIGINAL PAGE IS OF POOR QUALITY

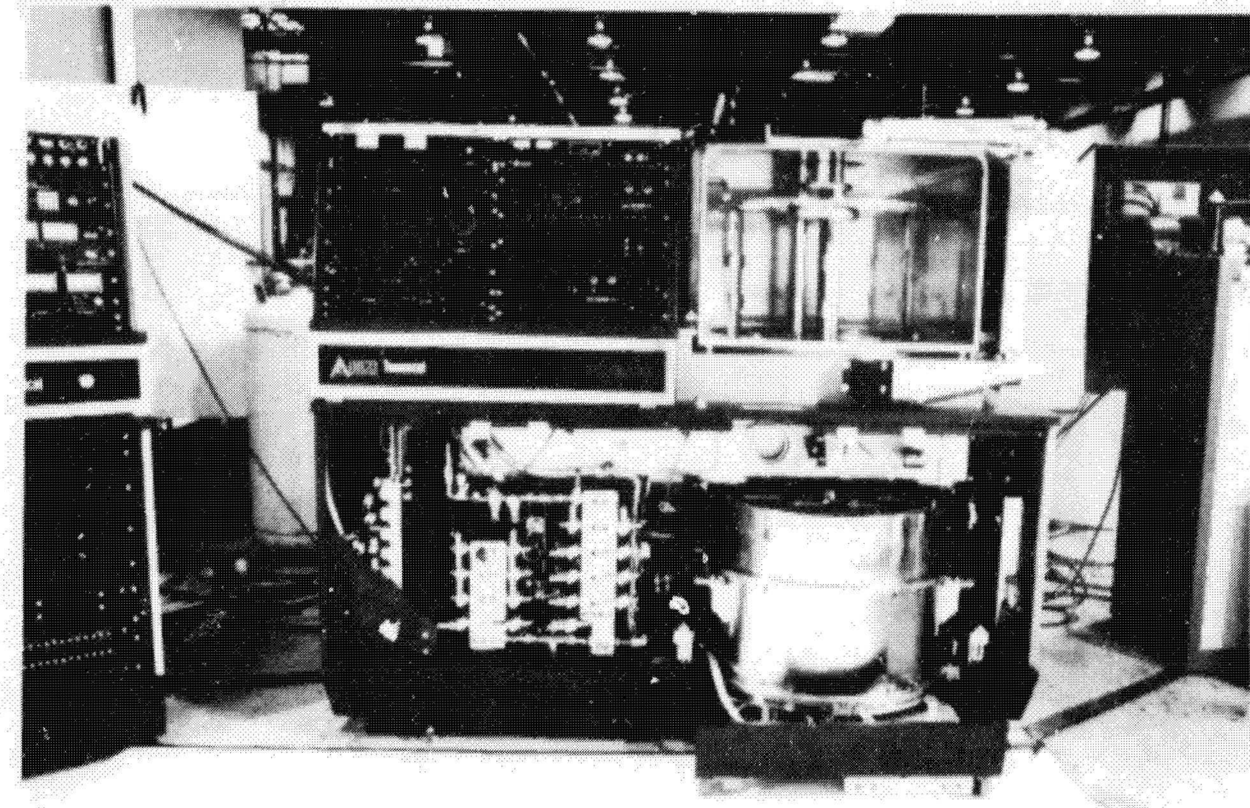

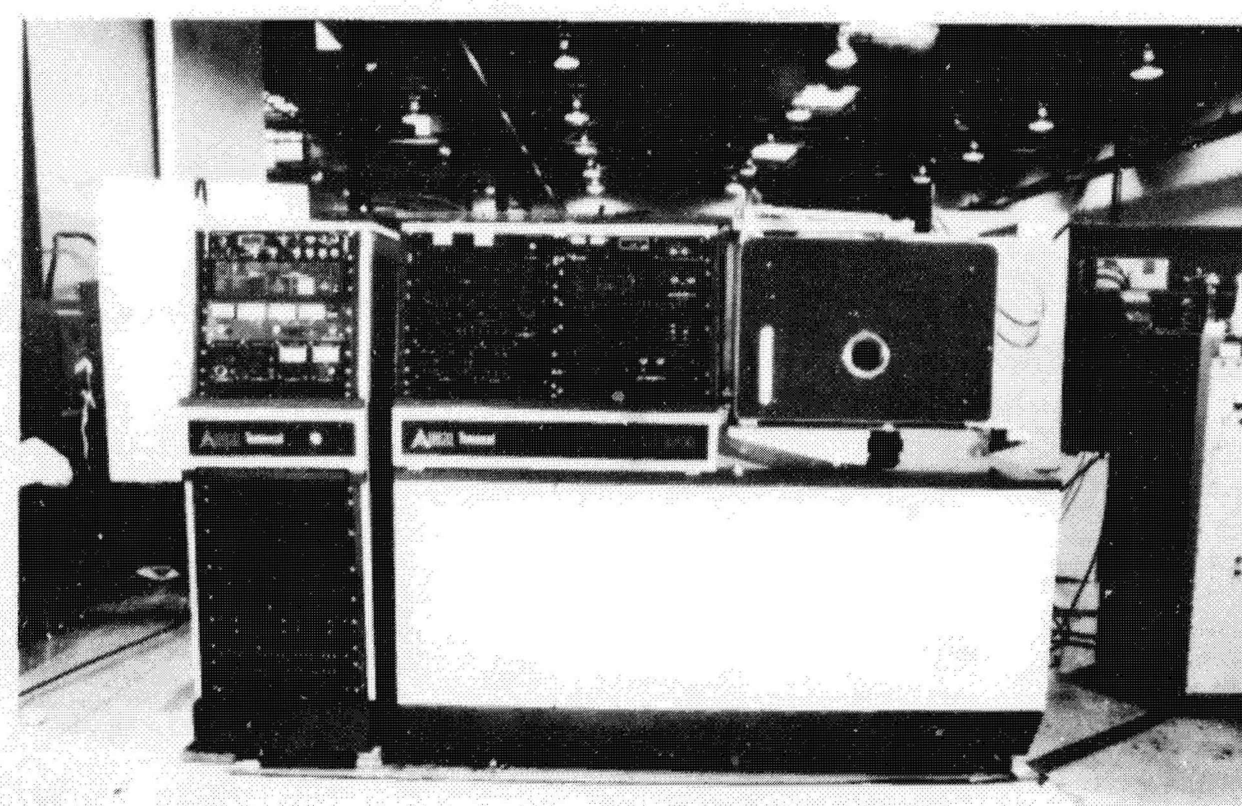

ORIGINAL PAGE IS
OF POOR QUALITY

Schematic of Production Facility Utilizing Electron-Beam Evaporant

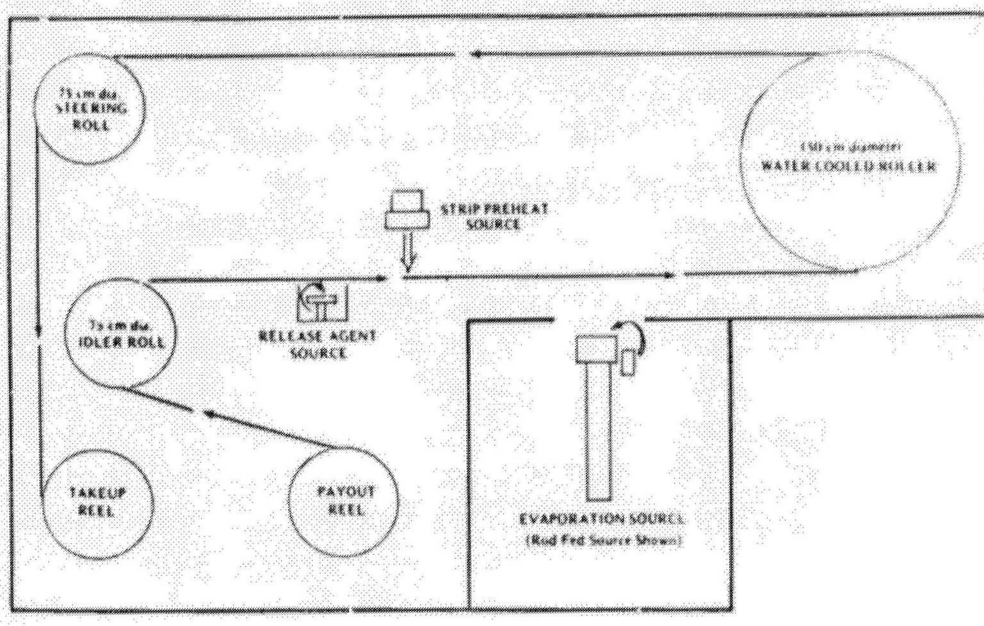

Continuous Strip Line for Vacuum Processing of Metals, Paper and Plastic

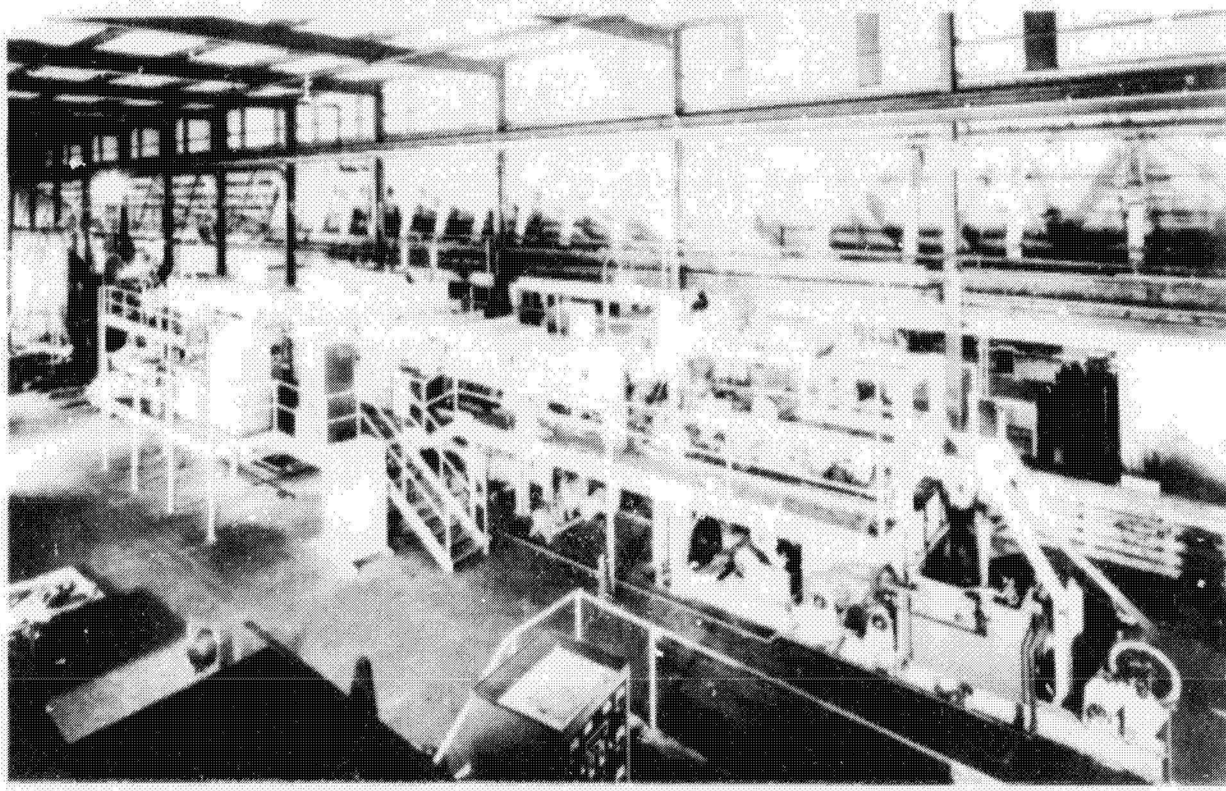

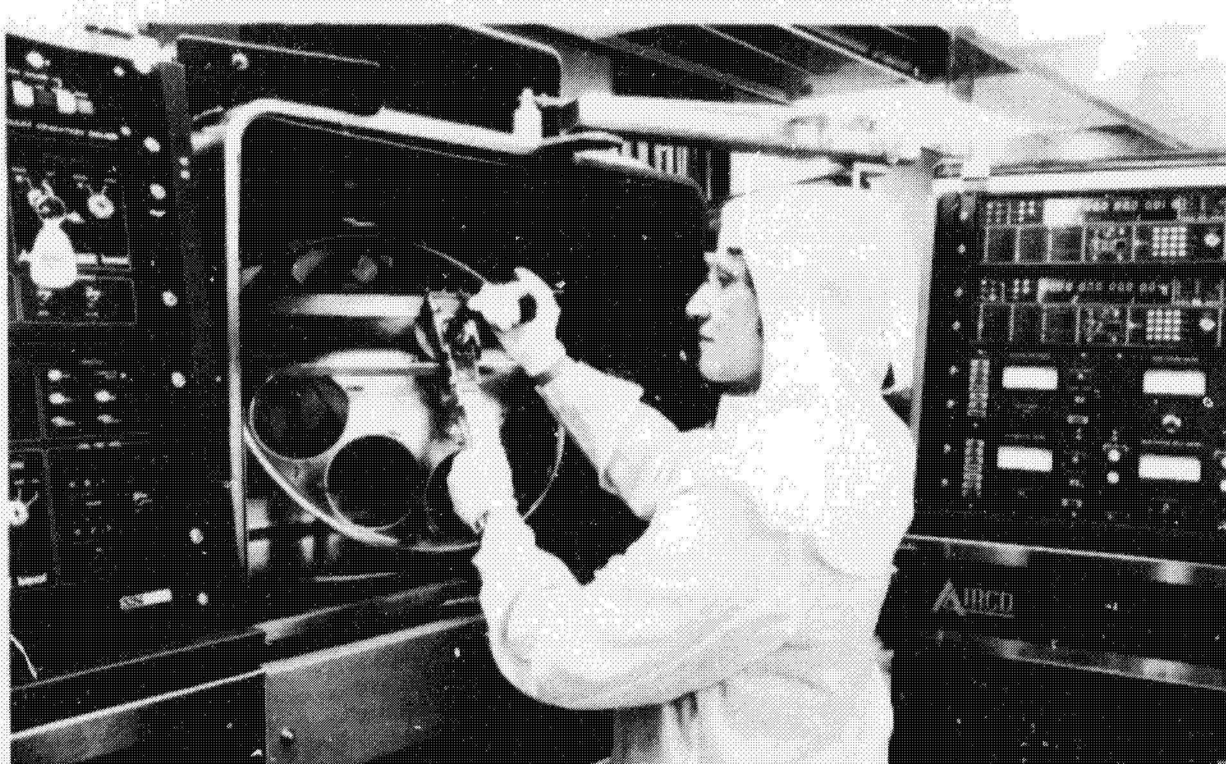

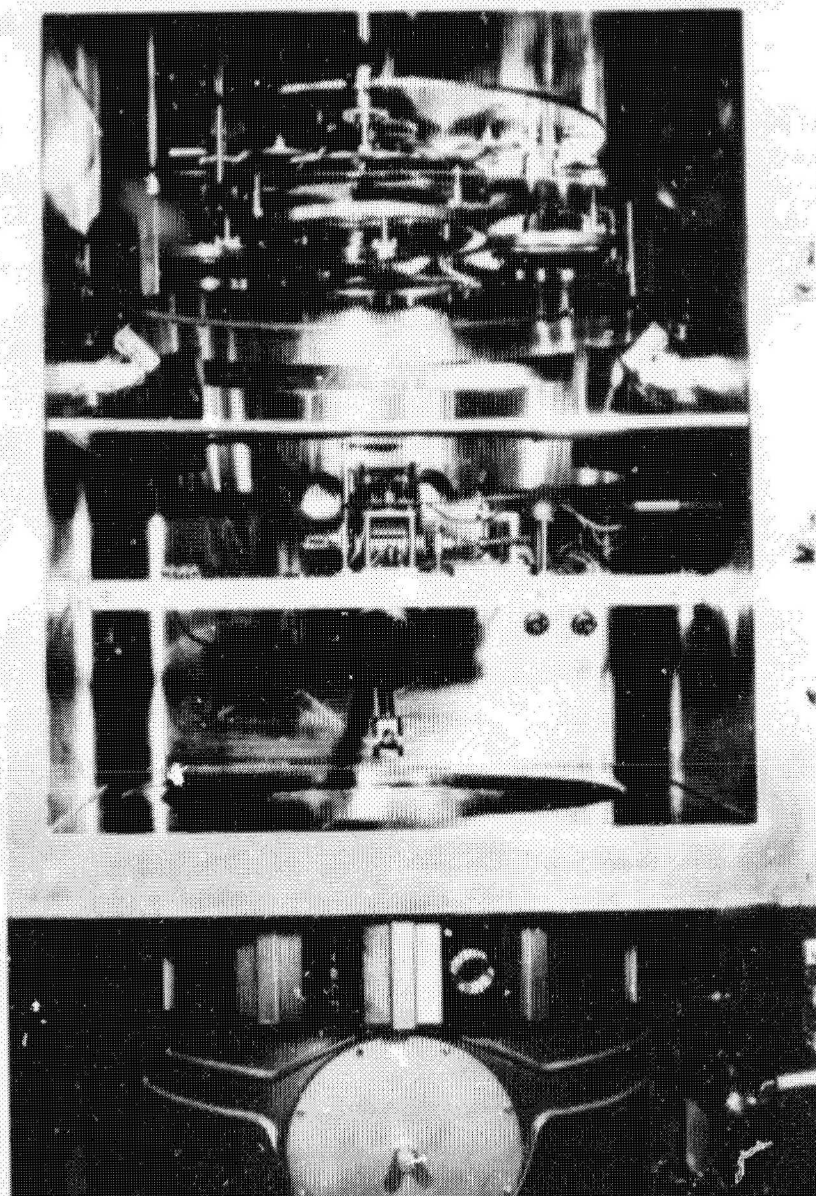

General Features, High-Rate In-Lir ɜ Sputtering System

ORIGINAL PAGE IS
OF POOR QUALITY

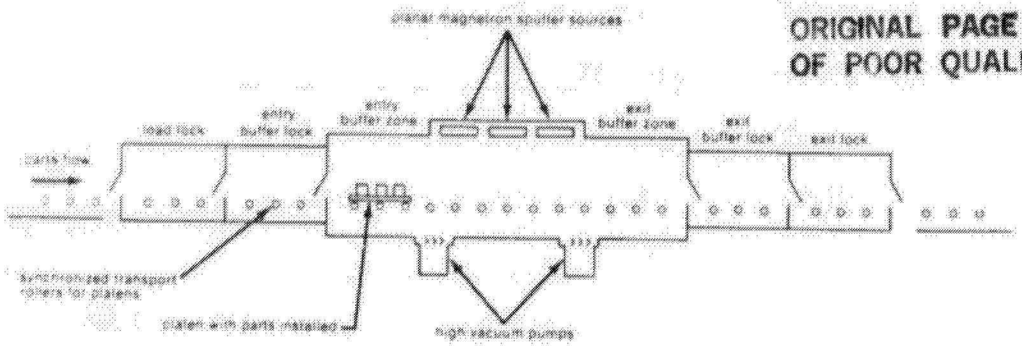

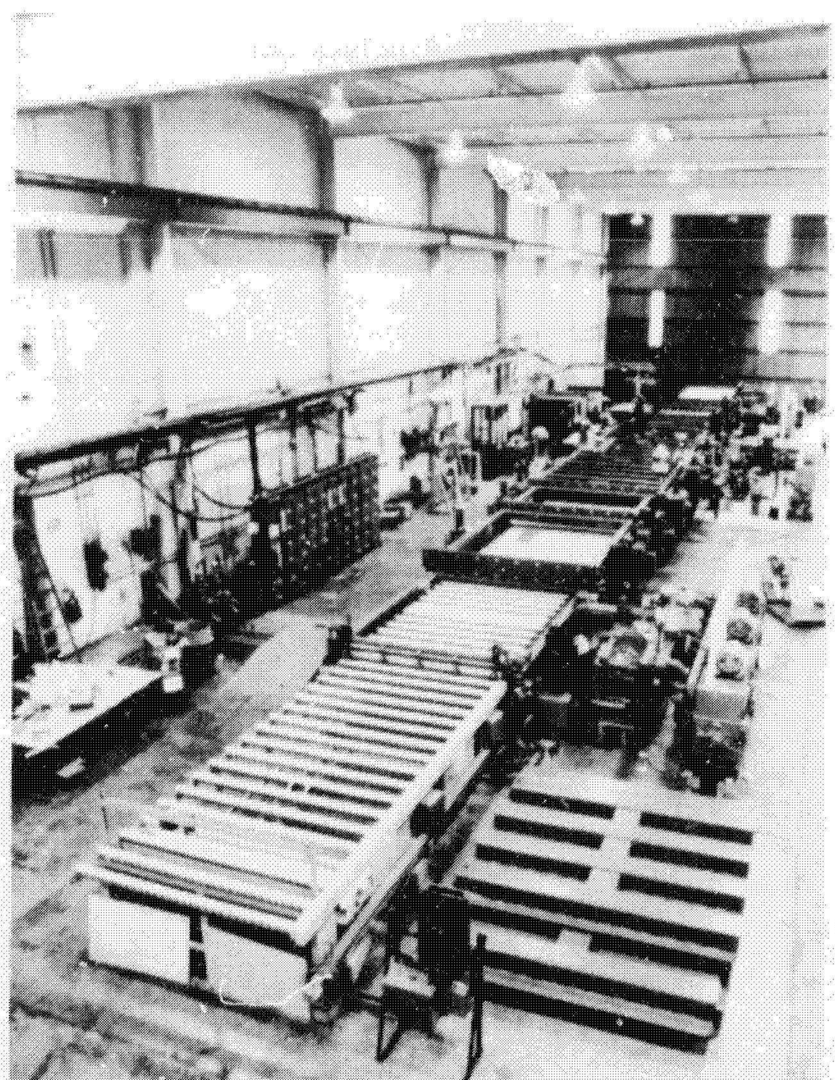

Data Input Worksheet

1) Substrate

   a) substrate material ______________________

   b) substrate thickness (include units ______________

   c) any pre-existing substrate coatings ______________

   ____

   d) any substrate limitations, such as maximum allowable temperature ______________________

2) Substrate shape and size (include units)

   a) circular — diameter ________ ; rectangular — length ________ width ________

   b) substrate shape and size if not circular or rectangular

   ____

3) Total number of film layers to be deposited ____________

4) Number of different film substances to be deposited ______

5) Film layers and thicknesses (include units)

Note: film layer #1 is directly on the substrate; #1 is the first layer to be deposited.

film layer #1	film layer #2
film substance_________	film substance__________
thickness_________	thickness_________

film layer #3	film layer #4
film substance_________	film substance__________
thickness_________	thickness_________

Use additional worksheets for additional layers, numbering the layers in succession as required.

6) Indicate the required degree of film uniformity (± percent); include the dimensions over which the uniformity is specified____

7) Local cost of electrical energy (cost per kilowatt-hour)______

8) Total hourly cost per operator_______________________

9) Number of shifts per day____________________________

10) Number of planned operating hours per shift per year. Example: (40 hours per shift per week) x (50 working weeks per year) = 2000 hours per shift per year._______

____

11) Number of years for equipment amortization____________

12) % yield expected.

Data Generated From Input Information

% coverage (or vapor utilization)
and uniformity expected

Carrier (or line) speed

Coat time

(Sputtering)		(Electron beam evaporation)
Useful target lifetime		Electron beam source material feed rate
Number of parts or feet of line/target	Or	

Throughput

Target or eb feed cost/unit of line length of # parts

Energy cost/unit of line length or # parts

Labor cost/unit of line length of # parts

Equipment cost/unit of line length or # parts

Total cost/unit of line length of # parts

Steps Leading to Production System

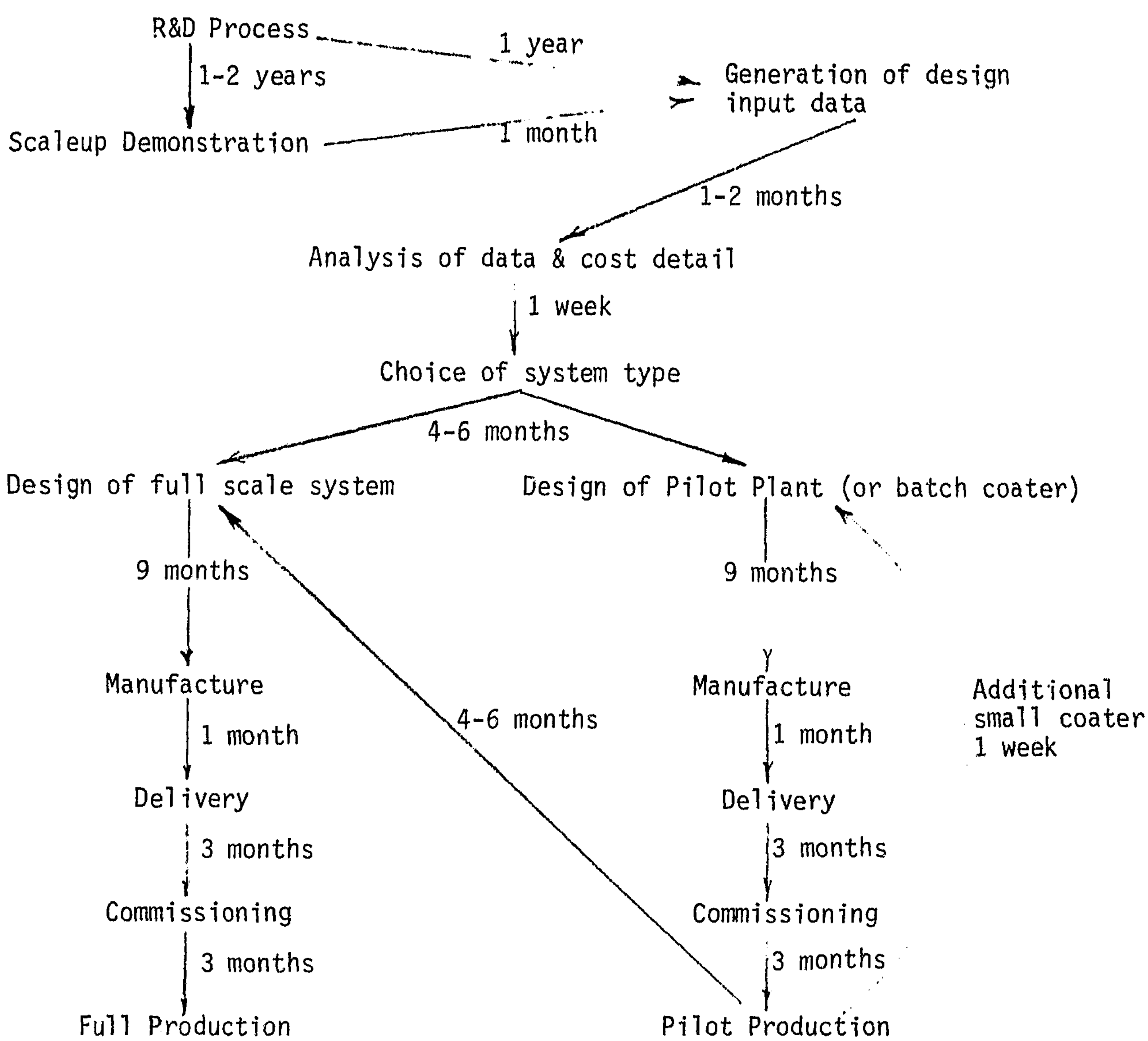

CHARACTERISTICS OF THIN FILMS

TELIC CO.

J. Thornton

- THIN FILMS VERSUS BULK MATERIALS
- PROPERTIES VERSUS DEPOSITION CONDITIONS
- SCALE-UP CONSIDERATIONS

Solar-Cell Thin-Film Requirements

- ABSORPTIVITY
- RESISTIVITY
- MINORITY CARRIER LIFETIME

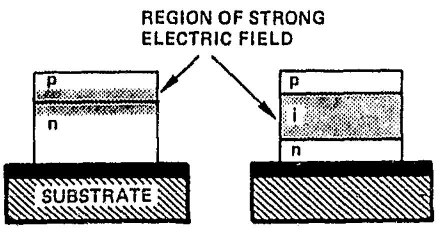

General Character of Thin Films

- COLUMNAR STRUCTURE
  PROPERTIES DIRECTIONAL
- STRUCTURAL FLAWS
  POINT DEFECTS
  GRAIN BOUNDARIES
  GROWTH FLAWS
- DEPARTURES FROM STOICHIOMETRY
- INTERNAL STRESSES

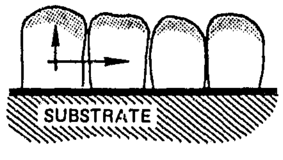

Coating Structure

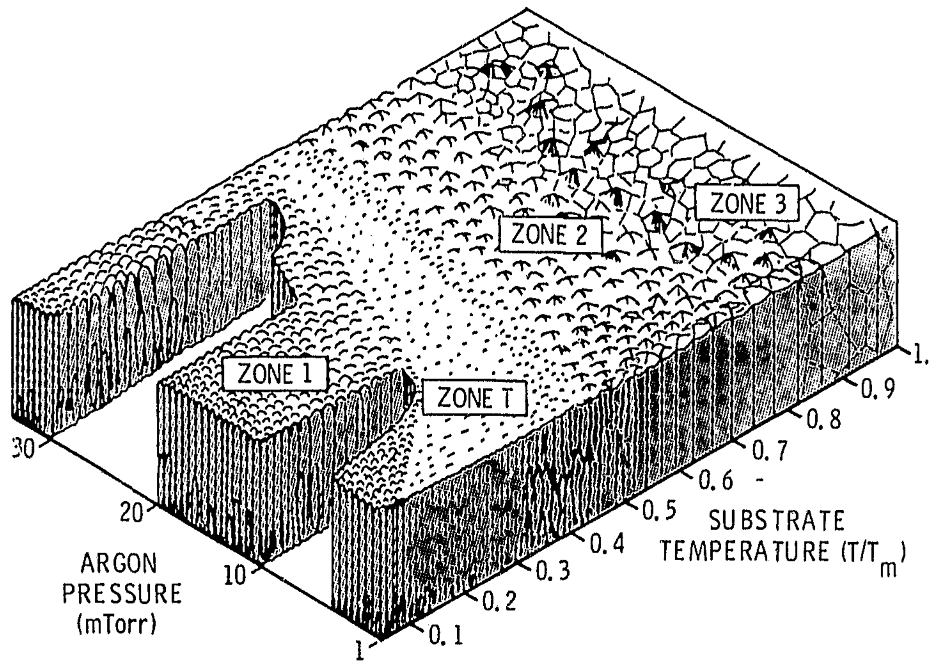

Growth-Hydrogenated Amorphous Silicon

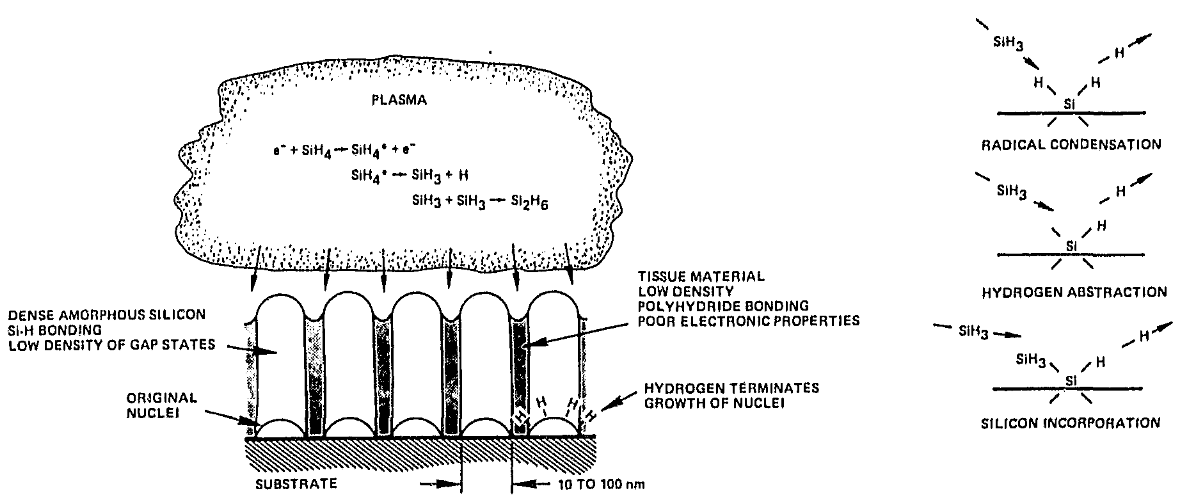

ORIGINAL PAGE IS
OF POOR QUALITY

Coating Phases

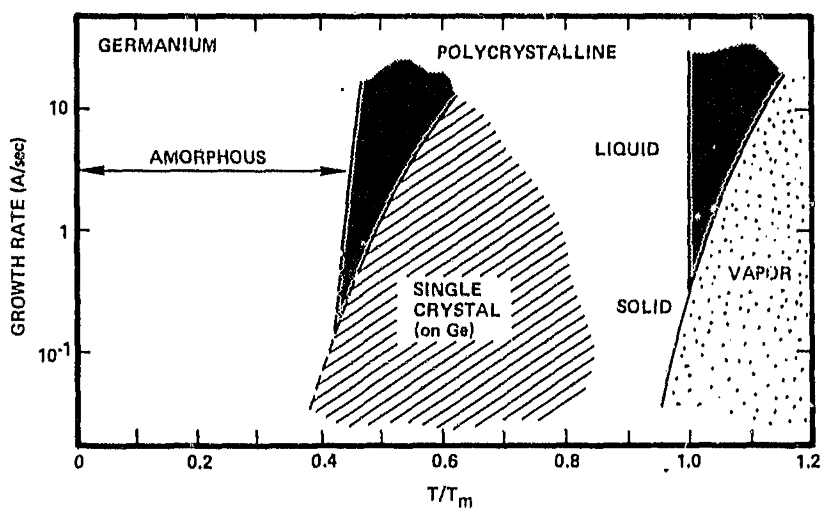

KLAUS BEHRNDT
TECHNIQUES OF METALS RESEARCH, VOL 1.
R.F. BUNSHAH, EDITOR
INTERSCIENCE (1968)

Composition Control

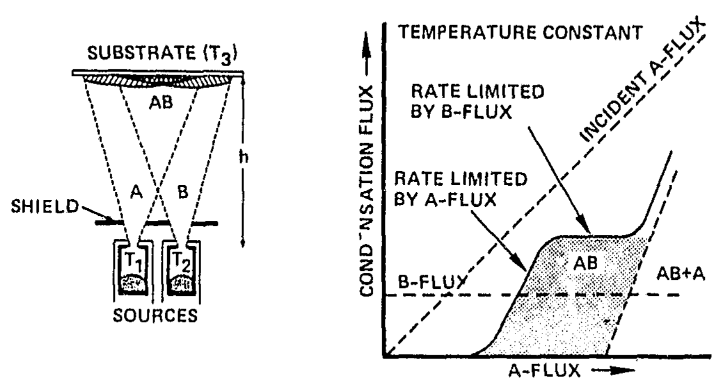

ORIGINAL PAGE IS
OF POOR QUALITY

CdS Resistivity

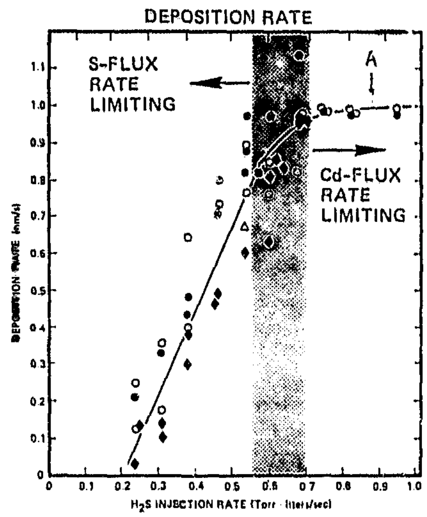

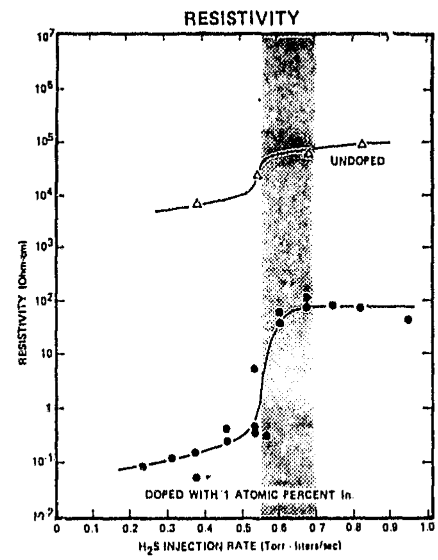

Particle Bombardment Stress

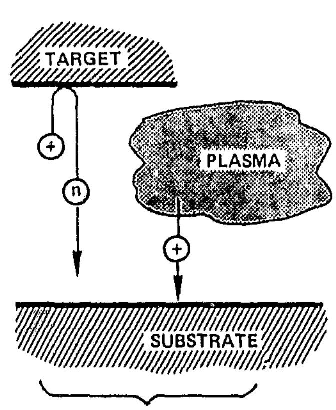

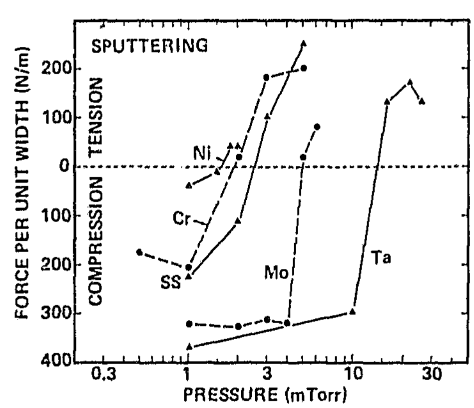

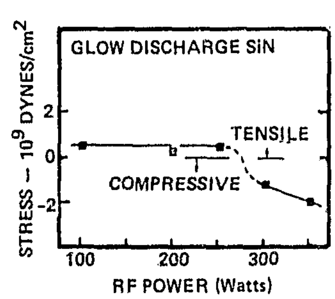

ORIGINAL PAGE IS
OF POOR QUALITY

Geometric Effects

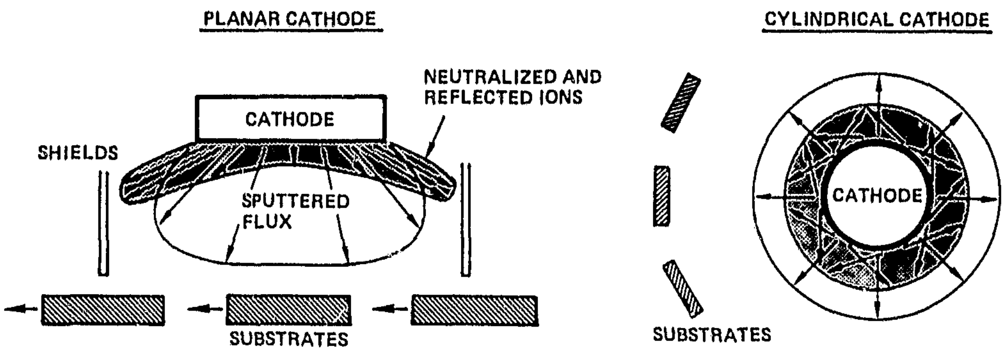

Planar Magnetron Transition Pressure

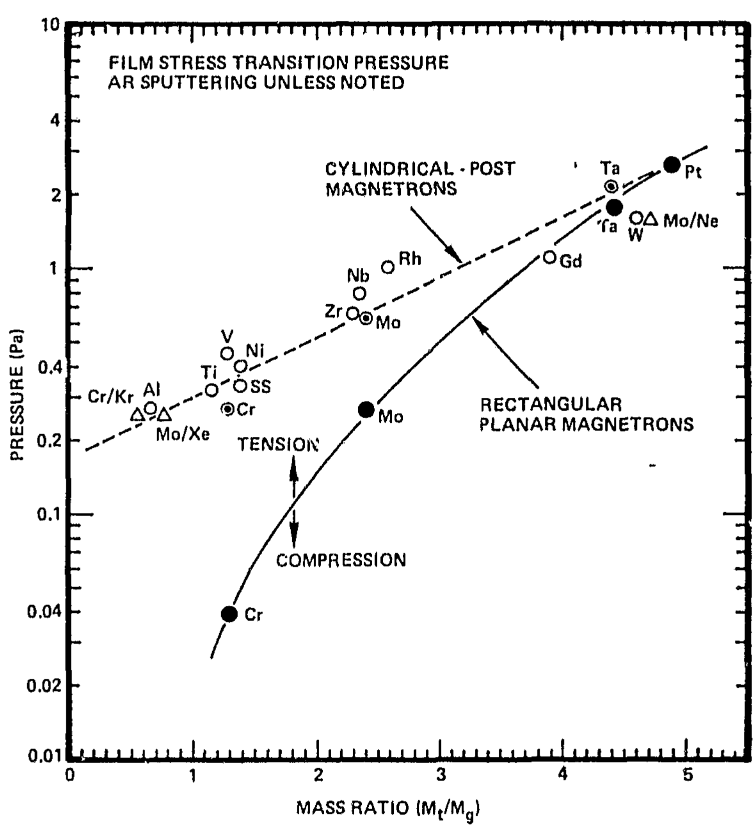

Deposition-Scaling Parameters

- GAS EXCHANGE TIME
- PLASMA SURFACE-TO-VOLUME RATIO
- DEPOSITION FLUX ANGLE OF INCIDENCE
- SUBSTRATE TEMPERATURE CONTROL
- RESIDUAL GAS FLUX
- CONDITION OF WALL SURFACES
- SUBSTRATE BOMBARDMENT

Development Procedures

THEORETICAL DEVELOPMENT

↓

MODELING

↓

SCALING LAWS

↓

BENCH TYPE TESTS

↓

IDENTIFY CRITICAL ISSUES

↓

APPARATUS DESIGN